STRUCTURE OF A RURAL ATMOSPHERIC BOUNDARY LAYER NEAR THE GROUND

A Thesis presented for the Degree of Doctor of Philosophy in Mechanical Engineering in the University of Canterbury, Christchurch, New Zealand

by

R.G.J. FLAY, B.E.(Honours)

University of Canterbury
November, 1978

To my parents,

in appreciation of their interest in my future.

ACKNOWLEDGEMENTS

I would like to thank Dr. D. Lindley for his supervision of this work. His advice and encouragement have been much appreciated.

My sincere thanks are also due to Professor D.C. Stevenson, for his willingness to assume enthusiastic supervision of this research during Dr. D. Lindley's absence, and for the use of the facilities of the Department of Mechanical Engineering.

I would also like to thank Mr. A.J. Bowen for his useful comments, discussion and advice related to this work.

An extensive experimental project of this kind required the assistance of many members of the technical staff in building,servicing, erecting and dismantling the instrumentation. In particular I would like to thank Mr. H. Anink who designed, built and serviced the electronic circuitry associated with the instrumentation and Mr. L. Cheeseman who maintained the equipment in the field, and assisted in all of the field experiments. I would also like to thank the workshop staff, directed by Mr. E.D. Retallick, who assisted in the construction of the anemometers and towers, and the workshop and technical staff who assisted in erecting and dismantling equipment throughout the field experiments.

I would like to thank the Principal, and all of the staff of Lincoln College who helped with this research, especially Dr. N.J. Cherry for the use of his equipment, and Messrs. D. Ower and R. Lamming, Principal Field Officer of the Farm Advisory Service and Farm Manager, respectively, for the use of the site on the research farm, where the measurements were taken.

The care and skill of Mrs. J. Ritchie in handling the large quantity of diagram and photographic reproductions for this thesis, and the willing co-operation and perseverance of Mrs. J. Percival in typing this thesis is gratefully acknowledged.

Finally, I would like to thank the post-graduate students with whom I have worked, not only for the comments related to this work, but also for creating the interesting and stimulating environment in which I have spent the period while undertaking this research.

ABSTRACT

This thesis describes instrumentation and software developed to make detailed measurements of wind structure in the lower part of the planetary boundary layer.

The instrumentation is based on a 190 mm diameter four bladed polystyrene propeller anemometer, designed to give a digital output. Arrays of three such instruments mounted orthogonally are used to measure the instantaneous wind vector as it varies with time. Data from up to 36 of the anemometers i.e. 12 arrays can be recorded simultaneously. The data is recorded onto a 7 track digital magnetic tape compatible with the University's Burroughs 6712 Computer on which the data is analysed using software written in Algol.

The limitations of the propeller anemometer as a sensor of atmospheric turbulence, the data recording method, and the computer analysis system used, are discussed in detail. The complete facility was found to work well.

The results of the two field experiments using the instrumentation and software developed are presented. The first experiment was concerned in investigating the variation of the wind structure to a maximum height of 20 m. The measured results compared favourably with accepted values of the turbulence parameters from the literature. A limitation of the vertical component anemometer was observed as it filtered out high frequency velocity fluctuations when placed near the ground. Correlation functions were also found to be influenced greatly by non-stationarities in the flow.

The second experiment was concerned with investigating the variation of the wind structure properties at a height of 10 m in a line perpendicular to the mean wind direction which had been chosen to study. From the appropriate horizontal space correlations, the integral length scales $^{y}L_{u}$, $^{y}L_{v}$ and $^{y}L_{w}$ were evaluated and found to be in good agreement with other similar full scale field measurements reported in the literature. It was found that $^{y}L_{u} \approx {}^{y}L_{v} \approx$ 20 - 30 m and $^{y}L_{w} \approx$ 4 - 6 m.

LIST OF CONTENTS

LIST OF FIGURES

FIGURES PAGE

FIGURES PAGE

FIGURES PAGE

FIGURES PAGES

FIGURES PAGES

FIGURES PAGES

LIST OF TABLES

LIST OF PLATES

LIST OF SYMBOLS

Unless otherwise specified, the following meaning is given to the symbols used in the text.

A — Amplitude of sinusoidal wind fluctuation, Chapter 3.

A — Ratio of longitudinal component standard deviation to friction velocity, σ_u/U_*.

A_o — Constant in linear trend removal.

A_1 — Constant in linear trend removal.

a — Decay parameter in coherence measurement.

a_j^i — Decay parameter in coherence measurement.

B — Ratio of lateral component standard deviation to friction velocity, σ_v/U_*.

B_0 — Constant in parabolic trend removal.

B_1 — Constant in parabolic trend removal.

B_2 — Constant in parabolic trend removal.

B_e — Resolution bandwidth of a smoothed spectral estimate.

C — Ratio of vertical component standard deviation to friction velocity, σ_w/U_*.

$C_{ii}(\underline{r}, \underline{r}', \tau)$
$C_{ii}(\Delta r, \tau)$
} Cross-covariance function $\overline{i(\underline{r};t).i(\underline{r}';t+\tau)}$.

$C_{ij}(\tau)$ $i \neq j$) Reynolds stress.

D — Side of lattice structure tower.

d — Number of degrees of freedom in χ^2 distribution, Chapter 5, average roughness element height.

$f(t)$ — Applied disturbance to first order system.

f — Frequency cycles per second, and dimensionless frequency in spectral equations, sampling frequency $\frac{1}{\Delta t}$.

f_m — Frequency of peak of Busch and Panofsky spectral equation.

f_U — Upper cut-off frequency.

f_L — lower cut-off frequency.

Δf_j — Reduced frequency, $n\Delta x_j/\bar{U}$.

$G(j)$ — Power spectral density at frequency, j/T.

g — Gravitational constant.

$H_o/\rho_a C_p$ Surface heat flux.

$I(j)$ Imaginary part of a function in the frequency domain.

i $\sqrt{-1}$, integer used as an index.

$i(t)$, $i(k)$, $i(\ell)$ Sample time histories. i may be replaced by any combination of letters, upper and lower case.

i_ℓ Largest velocity.

i_s Smallest velocity.

$i(\underline{r};t)$ Signal at position $\underline{r}$ and time t.

$i(t;n,\delta n)$ Signal in the bandwidth δn centered at frequency n.

$i(f)$, $i(j)$ Sample function in frequency domain. i may be replaced by any combination of letters, upper and lower case.

j Integer used as an index.

K_{10} Surface drag coefficient with reference to a height of 10 m.

k The von Kármán constant, taken as .4.

L Length constant of anemometer with mean wind vector parallel to its axis.

L_θ Length constant of anemometer with mean wind vector at angle θ to its axis.

L_a Length constant related to ideal anemometer rotational speed with the angle θ between itself and the mean wind vector.

L' Monin-Obukhov length scale.

$^{x}L_u, ^{y}L_v, ^{z}L_w$ Principal longitudinal length scales of turbulence measured along r = x, y or z axes respectively.

$^{x}L_v, ^{x}L_w, ^{y}L_u, ^{y}L_w, ^{z}L_u, ^{z}L_v$ Principal lateral length scales measured along r = x, y or z axes respectively.

ℓ Number of frequency estimates averaged over in power spectral density smoothing.

ℓ_m Mixing length in Prandtl's mixing length theory.

M Amplitude ratio.

m Maximum lag number.

N Number of samples.

N_c Number of classes in probability density distribution calculation.

N_k Number of samples in class k, in probability density distribution calculation.

n	Rotational speed, frequency.
n_o	Initial rotational speed.
n_1	Final rotational speed.
$\tilde{n}_u$	Reduced frequency for ESDU (1974b) spectrum.
$\tilde{n}_v$	Reduced frequency for ESDU (1974b) spectrum.
$\tilde{n}_w$	Reduced frequency for ESDU (1974b) spectrum.
n_p	Frequency at which the peak in the measured spectrum occurs.
P	Period of fluctuation.
$P_{ii}(\Delta r,n)$	Co-spectral density.
$p(i)$	Measurement of probability of i velocity component.
Q	Position of sensor.
$Q_{ii}(\Delta r,n)$	Quad-spectral density.
q	Number of independent sample records for ensemble averaging spectral components.
R	Response of anemometer to sinusoidal wind velocity fluctuation.
R	Distance of sensor from tower, Chapter 3.
Ri	Richardson number.
$R(r\Delta t)$	Autocorrelation function.
$R^C(r\Delta t)$	Circular autocorrelation function.
$R(j)$	Real part of a function in the frequency domain.
r	Radius to blade element.
$\underline{r}$, $\underline{r}'$	Position vectors.
r_m	Measured correlation.
r_∞	Correlation at large time delays.
r_t	Correlation due to rapid velocity fluctuation.
Δr	Separation distance between sensors.
$S_{ii}(n)$	Single point power spectral density function.
$S_{ii}(\underline{r},\underline{r}',n)$, $S_{ii}(\Delta r,n)$	Cross-spectral density function, r = X,Y,Z.

$\hat{S}_{ii}(n)$ Measured spectral estimate.

SR Scan rate.

T Length of data file.

T Period over which anemometer counters integrate, Chapter 3.

T_t Time constant of anemometer.

$T_{x\theta}$ Time constant of anemometer aligned in the x_1 direction.

$T_{y\theta}$ Time constant of anemometer aligned in the y_1 direction.

T_θ' Equivalent time constant for paired horizontal component anemometers.

T_u Longitudinal component integral length scale.

T_v Lateral component integral length scale.

T_w Vertical component integral length scale.

T_θ Time constant with the mean wind at an angle θ with the anemometer axis.

T_{pi} Time for which i(t) lies within the range i to i + Δi.

T_Z Absolute temperature at height Z.

T_0 Absolute temperature at the surface.

T_a Ambient temperature.

T_E Time for correlation function to fall to $\frac{1}{e}$.

t Time.

t_o File start time.

Δt Time between consecutive samples.

U_o Upstream velocity.

U_* Friction velocity.

$\bar{U}$ Mean wind speed.

U Mean wind speed.

U_p Velocity of section of blade at radius r.

U_{rel} Relative velocity of air over blade element.

U(t) Longitudinal component velocity, u(t) + $\bar{V}_Z$.

u,u(t) Longitudinal component velocity fluctuation.

Δu Step change in wind velocity, amplitude of sinusoidal fluctuation.

u_{ms} Longitudinal component mean square velocity.

u' Paired anemometer response to step change in wind velocity Δu.

$\bar{V}$ Mean velocity.

$\bar{V}_Z$, $\bar{V}_{\tilde{Z}}$ Mean velocity at height Z.

V_{ref} Mean velocity at reference height Z_{ref}.

v, $v(t)$ Lateral component velocity fluctuations.

w, $w(t)$ Vertical component velocity fluctuations.

$x(t)$, $x(k)$, $x(j)$ Sample time histories.

x Direction parallel to the mean wind direction.

x_1 Direction parallel to a horizontal component anemometer in a right handed system.

$X(j)$ Fourier transform of $x(k)$.

$X(f)$ $(\sin(f))/f$ function.

XR, XI Data arrays in program PSAUTCORS.

Δx Quantising increment.

ΔX Separation between sensors in mean wind direction.

y Direction perpendicular to the mean wind sector.

y_1 Direction parallel to a horizontal component anemometer, in a right handed system.

ΔY Separation perpendicular to the mean wind direction.

$Z, \tilde{Z}$ Effective height above ground.

z Vertical direction.

z_1 Co-ordinate direction of vertical component anemometer.

Z_1, Z_2 Reference heights.

Z_o Roughness length.

Z_{ref} Reference height.

Z_G Gradient height.

ΔZ Separation in the vertical direction.

α Exponent in power law velocity profile.

$(1 - \alpha)$ Probability that an estimate lies within the particular range required.

α, β, γ Angles between co-ordinate systems in Chapter 9.

γ Change in absolute temperature with height.

ε_r Random error.

θ Angle between mean wind vector and the anemometer aligned in the x_1 direction, angle between mean wind vector and tower line in Chapter 13.

λ Gust wavelength.

$\gamma_{ii}^2(\underline{r},\underline{r}',n)$, $\gamma_{ii}^2(\Delta r,n)$ Coherence function of i velocity component.

ν Kinematic viscosity.

ξ Angle of inclination of the wind vector.

$\rho_{ii}(\tau)$ Autocorrelation function of the i velocity component.

$\rho_{ii}(\underline{r},\underline{r}';\tau)$, $\rho_{ii}(\Delta r,\tau)$ Cross correlation function, $C_{ii}(r,r';\tau)/\sigma_i\sigma_i'$

$\rho_{ij}(\tau), i \neq j$ Normalised Reynolds stress.

ρ_a Air density.

σ_i Standard deviation of i velocity component.

τ_m Time delay when maximum correlation occurs.

τ Time delay of one data stream with respect to the other in a correlation measurement.

τ_o Surface shear stress.

ϕ Angle between anemometer axis and section of blade at radius r.

ω Frequency, radians per second.

Γ Dry adiabatic lapse rate.

$\Delta_o(f)$, $\Delta_o(t)$, $\Delta_1(t)$ Dirac functions.

ψ Universal function in non-neutral stability velocity profile equation, phase lag angle.

CHAPTER 1

INTRODUCTION

1.1 RATIONALE FOR THIS RESEARCH

Research was initiated into the structure of the atmospheric boundary layer by the Wind Engineering Group in the Department of Mechanical Engineering of the University of Canterbury, Christchurch, in 1969 as it had been recognised that there was a scarcity of data relating to the wind loading of structures.

The need for this work partially resulted from the New Zealand Electricity Department who had had pylons supporting electrical conductors fail during severe storms. It had been found that there was little data available in the relevant New Zealand design codes on the loading of such structures by the wind. The design method suggested used a peak static wind load applied to the structure. No dynamic effects were considered.

It was found that there was very little information available on the horizontal spatial structure of the wind useful for wind loading. Some useful work had been done by Shiotani and Arai (1967) which was reported at the Wind Effects on Buildings and Structures Conference in Ottawa.

In view of the above, Raine (1974) reviewed the relevant literature in preparation to building a wind tunnel modelling the rural neutrally stable atmospheric boundary layer. It was found by Raine that further full scale field measurements were required to use as a framework for modelling the rural boundary layer. In particular, measurements of the $\overline{uw}$ Reynolds stress variation with height as well as of cross-correlations needed to be made.

Thus the decision to make full scale measurements of the detailed wind structure in the micrometeorological range of the total wind spectrum, given in Fig. 1.1. It was considered also that a worthwhile contribution to this area of research would be to make comparisons between full scale measurements and similar measurements of models in the boundary layer wind tunnel. The comparisons would serve to justify or otherwise the wind tunnel modelling techniques used. It had been noted that very few full scale field experiments in a rural boundary layer had been compared with scaled models in a representative rural boundary layer wind tunnel.

1.2 PREVIOUS RESEARCH IN THE DEPARTMENT OF MECHANICAL ENGINEERING

Comparisons between the wind flow over windbreaks in both full scale and wind tunnel model experiments have been reported by Raine (1974). In addition, full scale, wind tunnel model comparisons have been made in investigating the wind flow over cliffs and escarpments. The results of some of this work has already been reported by Bowen and Lindley (1974, 1977). However these early full scale field experiments were compromised somewhat because cup anemometers were used so that only comparisons of average velocities could be made.

The latter aspect of the research has been extended recently into investigating the flow over complex terrain from the standpoint of selection of the best wind turbine sites. The results of a comparison between an extensive wind tunnel and full scale measurement programme of the Rakaia Gorge, New Zealand, has been reported by Meroney et al (1978).

1.3 SCOPE OF THIS WORK

This thesis describes the development of instrumentation and software for the measurement of wind structure and also the results of

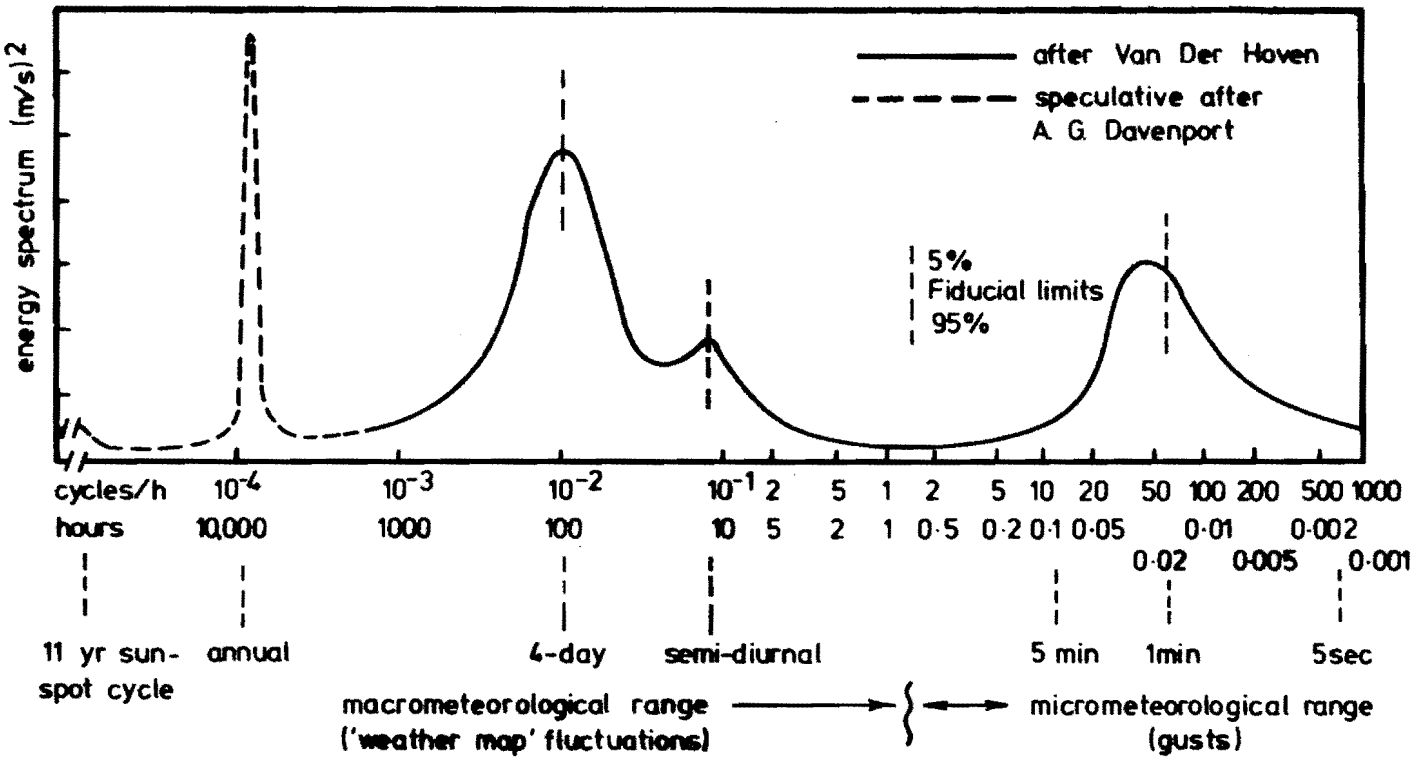

FIG. 1·1 SPECTRUM OF HORIZONTAL WIND SPEED NEAR THE GROUND FOR AN EXTENSIVE FREQUENCY RANGE (FROM MEASUREMENTS AT 100m HEIGHT BY VAN DER HOVEN AT BROOKLYN, NY, USA).

two experiments undertaken to measure the detailed structure of the wind in the lowest 20 m of a rural neutrally stable atmospheric boundary layer. The measurements were taken in terrain typical of Canterbury, on a research farm at Lincoln College, 16 km south-west of Christchurch.

Winds from only a very small range of directions, close to the north-west direction were studied. The winds studied were thus influenced by virtually the same upstream terrain.

This particular wind direction was chosen because examination of long term meteorological records at the nearby Christchurch International Airport showed that there was a high probability of strong winds from this direction during the period for which it was proposed to record the data. A recent examination of the less extensive wind data from Lincoln College by Cherry (1977) had shown that the wind directions at Christchurch International Airport and Lincoln College were very similar, although the average velocity at Lincoln College tended to be the higher. Thus the information from Christchurch International Airport could be extrapolated to Lincoln College.

Strong winds were required because it was desired to study winds in a neutrally stable atmospheric boundary layer. No temperature measuring instrumentation was available with which to determine the lapse rate, so to ensure neutral stability, data was recorded only when the wind velocity at 10 m height above ground was close to or greater than 10 m/s.

The first experiment, which investigated the vertical variation of the wind structure, used seven orthogonal arrays, each of three propeller anemometers attached to a 20 m tower. For this experiment many runs of data were recorded, of which finally four were analysed in detail and the results presented here.

The second experiment which investigated the horizontal spatial, structure of the wind used orthogonal arrays of three propeller anemometers mounted on the top of each of eight 10 m towers. The towers were arranged in a line almost perpendicular to the wind direction under investigation. For this particular experiment, again many runs of data were recorded of which two have been analysed and the results presented here.

As well as providing wind structure data, the first experiment was used to check on the reliability of the instrumentation, and the data analysis technique which had been developed in this work and had not been used previously.

The purpose of the second experiment was to provide specifically horizontal spatial cross-correlations to enable the integral length scales $^{y}L_{u}$, $^{y}L_{v}$, $^{y}L_{w}$ to be evaluated, as well as providing other turbulence characteristics. This information is required by engineers to determine the wind loading on pylons supporting electrical conductors, suspension bridges and other long, slender, horizontal structures. Previous reviews of the literature had found that there was a weak data base from which to obtain values for these particular parameters.

CHAPTER 2

LITERATURE SURVEY AND BACKGROUND

This chapter is a brief survey of the relevant literature on full scale field measurements of wind structure. Recent comprehensive reviews have been given by Teunissen (1970), ESDU (1972, 1974b, 1975), Raine (1974) and Counihan (1975). The literature cited attempts to put this work in perspective compared with other full scale field measurements.

By the early 1950's the general properties of the lower part of the atmosphere were reasonably well understood as discussed by Sutton (1953, 1955). In the lower atmosphere, under neutrally stable conditions, the velocity variation with height was found to agree with a fully developed aerodynamic rough flat plate boundary layer, with the leading edge of the "plate" an infinite distance upstream of the point of observation. Estimates of the roughness length Z_o had been made, and the velocity variation was found to be a function of stability, as typified by the Richardson number, Ri, (Deacon, 1949).

The motion of the air was observed to be turbulent with the lateral component variations measured to be similar to the longitudinal component variations. Field measurements of wind structure were difficult to make at this time as sensitive instruments were difficult to build and use. Recording the data with sufficient fidelity and analysis of analogue velocity-time signals, often a pen trace on paper, meant that parameters other than average velocities were difficult to determine from the data.

Examination of the power spectrum for horizontal winds at a height of 100 m by van der Hoven (1957) revealed the presence of an energy gap. There was little energy in the wind from those spectral components having

periods ranging from about five minutes to two hours. Van der Hoven's work showed that the total horizontal velocity spectrum, given in Fig.1.1, could be conveniently broken into two parts, separated by the energy gap. Hence the high frequency portion of the spectrum, the micrometeorological part, could be conveniently measured with sensitive instruments over periods of five minutes to one hour. This meant that the wind speed averaging periods of ten minutes each hour or one hour, commonly used for long term meteorological records, gave stable estimates of the average velocity for the micrometeorological range of the velocity fluctuations. The macrometeorological range consisting of the longer time scale changes, was due to climatical and weather map variations.

The International Symposium on Atmospheric Diffusion and Air Pollution in 1958, the proceedings of which were given in Advances in Geophysics (1959), summarised much of the earlier work on wind structure. Panofsky and Deland (1959) gave a paper titled "One-dimensional Spectra of Atmospheric Turbulence in the Lowest 100 Metres". It was stated that it had been found that Taylor's hypothesis was well satisfied in homogeneous turbulence. It was also found that the longitudinal and lateral velocity component spectra were affected by convection in the low frequency regions, and turbulence of mechanical origin in the high frequency portion. The lateral component spectrum was found to be particularly sensitive to the lapse rate. The vertical component spectrum, although maintaining the same shape, shifted to lower frequencies at greater heights from the ground. The main interest in measuring the fine structure of the turbulence at the time was to obtain diffusion data.

Cramer (1959), at the same conference, discussed measurements of turbulence structure made during Project Prairie Grass, which studied diffusion processes in the atmosphere. The sensors consisted of bivanes with heated thermocouple anemometers. Spectra were calculated in a manner due to Tukey (1949), involving Fourier transforming the auto-

covariance and cross-covariance functions. Integral length scales were calculated from data from the same experiment and this was later reported by Panofsky (1961).

At this stage engineers were not particularly interested in the wind structure for design purposes. Design was conservative and structures were usually made from materials with a large amount of internal damping, e.g. stone, wood, concrete and low strength steels. Recent developments changed this. The use of new structural designs and materials resulted in structures and buildings which were light in weight, tall or of large areal extent and having low mechanical damping. Glass was used to form large surfaces.

These trends stimulated efforts to describe wind characteristics for engineering purposes; to understand the nature of flow over bluff bodies, and to develop adequate design procedures which would result in the low probability of failure.

There was increased attention being given by architects, city planners and engineers to the matter of human comfort. This led to concern about wind-excited accelerations of tall buildings and towers, wind generated noise, buffeting of pedestrians by gusty winds at street level etc. Increasing population density and concern regarding the environment resulted in work regarding stack location relative to air-conditioning intakes, population centres etc. The above reasons led to a requirement for engineers to know more about the structure of the wind.

In 1958 the Second National Conference on Applied Meteorology: Engineering was held at Ann Arbor, Michigan. Blackader (1960) gave a paper titled "A Survey of Wind Characteristics Below 1500 ft.", which summarised work by Prandtl, Deacon, Monin and Obukhov, and Ellison. Cramer (1960) stated that the conventional civil engineering practice where wind forces were treated as static loads was clearly unsatisfactory.

Ultimate resolution of the problem of predicting the wind forces on structures depended on the improved knowledge of spectra and co-spectra of velocity fluctuations. Cramer then went on to state how wind velocity spectra could be used to determine loads on civil engineering structures, using the same approach which was widely used by aeronautical engineers at the time.

Davenport (1960, 1961a, 1961b, 1963, 1964, 1967) closed the gap between micrometeorology and the wind loading of structures through a series of papers written in the 1960's. Davenport (1960) proposed a spectrum for the longitudinal velocity component variation derived from a series of spectral measurements from all over the world. In the same paper he proposed a formula for the coherence of the longitudinal velocity components with a vertical separation. This was another way of defining the cross-correlation of the components. Later papers by Davenport gave examples of how to use the longitudinal component spectrum in determining the forces on, and the displacements of structures.

In a similar vain to Davenport, Harris (1963) outlined the similarity of communication theory to the description of turbulence, and its usefulness for describing the response of structures to buffeting by the wind. Harris also described a tower at the G.P.O. Rugby Radio Station which was instrumented with an array of wind velocity sensors. At the Electrical Research Association's (ERA) Cranfield Field Station a line of six 10 m towers with anemometers atop them, perpendicular to the prevailing wind, were described. Measurements from these sensors were intended to describe the horizontal spatial characteristics of the turbulent wind structure.

Lumley and Panofsky (1964) summarised the statistical description of turbulence at the time, and went on to describe the structure of the atmospheric boundary layer as it was known.

Throughout the 1950's and 1960's, increasing use was being made of wind tunnels to determine the interaction of wind structure on scale models. However in the 1940's and early 1950's, laboratory studies in aeronautical wind tunnels showed little resemblance between field and wind tunnel results. It was found that the turbulence in the earth's boundary layer had to be accurately modelled in the wind tunnel to get comparable results with full scale. Researchers using wind tunnels required therefore accurate full scale wind structure measurements as a framework on which to model their wind tunnels.

Throughout the late 1960's results from more full scale field measurements of wind structure were published. Harris (1968a) discussed some results of measurements made at Rugby. Later papers by Harris (1971, 1972) discussed further results and comparisons with theoretical predictions.

The 1968 Air Force Cambridge Research Laboratories (AFCRL) (Haugen et al, 1971) experiment in Kansas was an attempt to obtain a comprehensive set of data on wind and temperature fluctuations over a flat uniform site. Instrumentation was becoming increasingly sophisticated and three-axis sonic anemometers, hot-wire anemometers and five platinum wire thermometers were mounted at three levels on a 32 m tower. Surface shear stress measurements were obtained from two CSIRO drag plates (Bradley, 1968). Data storage was on digital magnetic tape. The analysis of this data giving spectral characteristics of surface-layer turbulence by Kaimal et al (1972) represents probably the most comprehensive spectral measurements to date.

Work was also instigated at the Physical Sciences Laboratories, Nikon University, Japan, during the early 1960's to look at the spatial characteristics of surface-layer turbulence. In this work a row of five 40 m towers with Aerovane anemometers atop them were positioned on the north-east coast of Shikoku Island. Horizontal spatial correlations,

and other turbulence characteristics have been discussed for a variety of wind velocities and directions. The vertical variation of wind structure was measured near the same site, on the coast, using Aerovane anemometers mounted on a 150 m tower. In particular, data has been recorded during typhoons and monsoons. The results of this work have been published in e.g. Shiotani and Arai (1967), Shiotani and Iwatani (1971, 1976), Shiotani (1975), Iwatani (1977) and Shiotani et al (1978).

The requirement for increasing knowledge of the wind structure in relation to launching space vehicles, VTOL and STOL aircraft promoted further work in the United States. Fichtl (1968) and Fichtl and McVehil (1969) discuss an engineering spectral model of turbulence and turbulence characteristics obtained from the NASA 150 m tower at Cape Kennedy.

Elderkin (1966) discusses extensive measurements of the turbulence structure in the lower atmosphere from a single tower for the United States Atomic Energy Commission.

Research was also being done to try to fit mathematical models of the atmospheric boundary layer to field experiments. The most recent of these was a report by Deaves and Harris (1976) titled "A Mathematical Model of the Structure of Strong Winds". This work had been based on earlier research carried out by the Environmental Sciences Research Unit (ESRU) at Cranfield Institute of Technology during 1960-1974. Use was also made of data published by other workers in Europe, North America and Australia, notably the measurements carried out at Nantes, France, (Duchêne-Marullaz, 1974, 1975, 1976). The aim of the report was to provide an adequate description for the purposes of wind engineering, of the nature of strong winds.

Teunissen (1977a) has presented a recent description of a facility for taking full scale field measurements which was found to be similar to the one under development at the University of Canterbury at the same time. Teunissen (1977b) also presents the results of some wind structure

measurements made over a small suburban airport. Results of helicopter and tower data are discussed and compared. A series of towers were positioned at various locations around the airport which enabled comparisons of different terrains and fetch to be made for given wind directions. However no horizontal spatial cross-correlation measurements were made. Field measurements are to be compared with model data in a boundary layer wind tunnel. This work represents one of the few full scale, model comparisons.

From the above discussion it can be seen that throughout the late 1960's and 1970's, the lower part of the earth's boundary layer was being measured extensively. Very little work was being done measuring correlations from rows of tower mounted anemometers however.

Significant work in this area has been done by Shiotani, (Shiotani et al, 1978 etc.), Powell and Elderkin (1974), who investigated Taylor's hypothesis by comparing horizontal space correlations with autocorrelations, Piekle and Panofsky (1970), Ropelewski et al (1973) and Panofsky (1961). Research involving calculations of cross-correlations and integral length scales from several tower mounted anemometers is currently being done by Teunissen and Harris, but to date, none of these recent results have been published.

ESDU (1975) represented the most up to date summary of the characteristics of atmospheric turbulence near the ground as it varied in space and time for strong winds in a neutrally stable atmosphere when it was published. It is probably still the best summary of this work at present. ESDU (1975) have the following comments to make on the reliability of their data:

> *"...In general, reliable data for cross-correlations or coherence functions for strong winds (neutral atmosphere) are sparcely reported in the literature and many show*

considerable variations from each other due to the large number of variables involved..."

"...it is not possible to assess precisely the accuracy of the data presented in this Item; furthermore there are comparatively few detailed measurements in strong winds (neutral atmosphere), for a wide variety of terrains and heights, with which comparisons can be made..."

"...The majority of available measurements are for relatively smooth terrains..."

In the light of the above, it thus seemed that a contribution to the wind structure data base could be made by analysing results from a full scale field experiment involving a row of tower mounted anemometers. Results from several anemometers mounted on a single tower could serve as a check of the equipment and data analysis procedure, since there was a host of field measurements of this kind, with which to make comparisons.

CHAPTER 3

INSTRUMENTATION

3.1 INTRODUCTION

Early field experiments reported by Bowen and Lindley (1974,1977) used cup anemometers (Rimco models ASI and AMI 6-5373) as these experiments required the measurement of average wind speeds only. However for the more detailed measurements of the wind structure envisaged, it was realised that these instruments were unsuitable. A sensor was required that measured the instantaneous wind vector, was robust, and was sensitive enough to measure all of the predominant energy containing eddies in the micrometeorological range of the total wind velocity spectrum, i.e. could measure accurately up to frequencies of 1 Hz. A further requirement, dictated by the limited financial resources of the Department was that it had to be relatively inexpensive. This latter requirement in fact eliminated all commercially available sensors, and so the instrumentation had to be capable of manufacture within the Departmental workshops.

It was also realised that the velocity signals from each sensor needed to be recorded for subsequent analysis to extract the detailed wind structure parameters. For this requirement it seemed obvious that the data should be recorded on a magnetic tape. Recent advances in electronics suggested that a digital magnetic tape recorder should be used in conjunction with a computer.

Since the sensor was required to be selected first, before the ancilliary equipment, a survey was made of meteorological wind speed and direction sensors that had the desired specifications.

Cup anemometers were unsuitable as they had a relatively slow response to gusts and were omni-directional. They thus needed to be used in conjunction with wind vanes which had a second order response

which was not desirable, and they were therefore regarded as unsuitable. Sonic anemometers were expensive, were then unreliable, had an analogue output which was difficult to handle from many channels in the field at the time, and their manufacture was considered to be beyond the capabilities of the Department. Hot wire and hot film anemometers were considered unsuitable for field work because of their relatively fragile construction, requirement for short cables between the probe and the control circuitry, analogue output, calibration and linearisation requirements, and expence, since many sensors were required. Strain gauged cantilevered spheres gave a non-linear analogue output which like the sonic anemometer was undesirable. Vanes directing a propeller into the wind had a relatively complicated response to wind gusts, and their response was rather slow.

The survey indicated that a propeller anemometer, similar to the Gill UVW anemometer, used in orthogonal arrays of three propeller anemometers at each point was the most suitable. It offered the possibilities of yielding the components of the instantaneous wind vector. Furthermore, the literature at the time, e.g. (Holmes et al, 1964, MacCready and Jex, 1964, MacCready, 1965, Gill, 1967), indicated that it had the desired frequency response. Commercial models of the Gill UVW propeller anemometer gave an analogue output from a D.C. generator and were relatively expensive so it was proposed, therefore, to build a propeller anemometer similar to the Gill UVW anemometer, but with a digital output.

The final design evolved out of some years of development within the Department, (Omar and Ow, 1972, Ng, 1973, Ong and Dien, 1974, Lindley and Bowen, 1974, Lindley et al, 1974). In the final design, the four bladed polystyrene propeller drives a slotted disc which rotates between two pairs of photo diodes and receivers. Two square waves are generated, one from each photo receiver, obtained from the slots passing through

each light beam. This enables the velocity and rotational direction of each anemometer to be determined.

By scanning each of three such sensors arranged in an orthogonal array it is thus possible to obtain the components of the instantaneous velocity vector as a function of time.

Wind tunnel tests of the Gill UVW propeller anemometer had previously indicated that it had a response length or distance constant of about 1 m (Camp et al, 1970, Hicks, 1972, Gill, 1975). This was later confirmed by wind tunnel tests on our own instruments (Lindley et al, 1974, Omar and Ow, 1972, Ong and Dien, 1974) which gave a response length of approximately .95 m when the wind direction was parallel to the anemometer axis. This result meant that the sensor would have a suitable frequency response.

Because of the large range of frequencies of interest in the natural wind, data needs to be recorded over a long time period. Also, because the wind varies in space as well as in time, the data from a large number of sensors is required in order to be able to define the spatial characteristics of the wind environment being measured.

This meant that an enormous amount of data needed to be recorded. Consequently the data was recorded onto digital magnetic tape because it had the capability of being able to store the amount of data required and could be used in conjunction with a digital computer.

The polystyrene propellers and all other electro-mechanical component assemblies and circuitry were made within the Department.

This chapter details the various aspects of the design of the anemometers and their limitations. The additional equipment necessary for a full scale field experiment is also described. The final section outlines the experimental arrangement used in the two experiments, the results of which are discussed in Chapters 7 to 15.

3.2 THE PROPELLER ANEMOMETER

3.2.1 The Anemometer Body

A cross-section of the propeller anemometer body giving the overall dimensions, is given in Fig.3.1. Plate 3.1 shows the anemometer with the electronic circuitry exposed.

The part of the body housing the electronic circuitry and slotted disc is 38 mm in diameter and 210 mm long. The body tapers to a 15 mm diameter propeller shaft housing which is 150 mm long. The propeller is easily removed from the bearing supported propeller shaft after unscrewing a nut from the shaft.

The fine tolerance between the two flanges on the rotating propeller shaft and the housing, which can be seen at the right hand end of Fig.3.1, was initially thought to be sufficient to prevent moisture ingress to the inside of the anemometer. During initial field tests this was found to be an unsatisfactory arrangement as the electronic circuits corroded and then malfunctioned. The problem was later cured by purging the anemometer body with nitrogen.

The anemometers were mounted in orthogonal arrays by attaching three of them to the appropriate brackets using the screws shown at the left hand end of the anemometer in Fig.3.1.

3.2.2 Purge System

Since moisture ingress could only occur through the gap between the propeller shaft flange and the propeller shaft housing, an obvious solution to prevent this was to purge the anemometer with nitrogen, expelling the gas through the gap. To achieve this objective, nitrogen was bled into the body through a small nipple located at the opposite end from the propeller, and is shown in Plate 3.1.

The nitrogen flow-rate required to purge each anemometer adequately obviously was very low. As the anemometers were required to be in

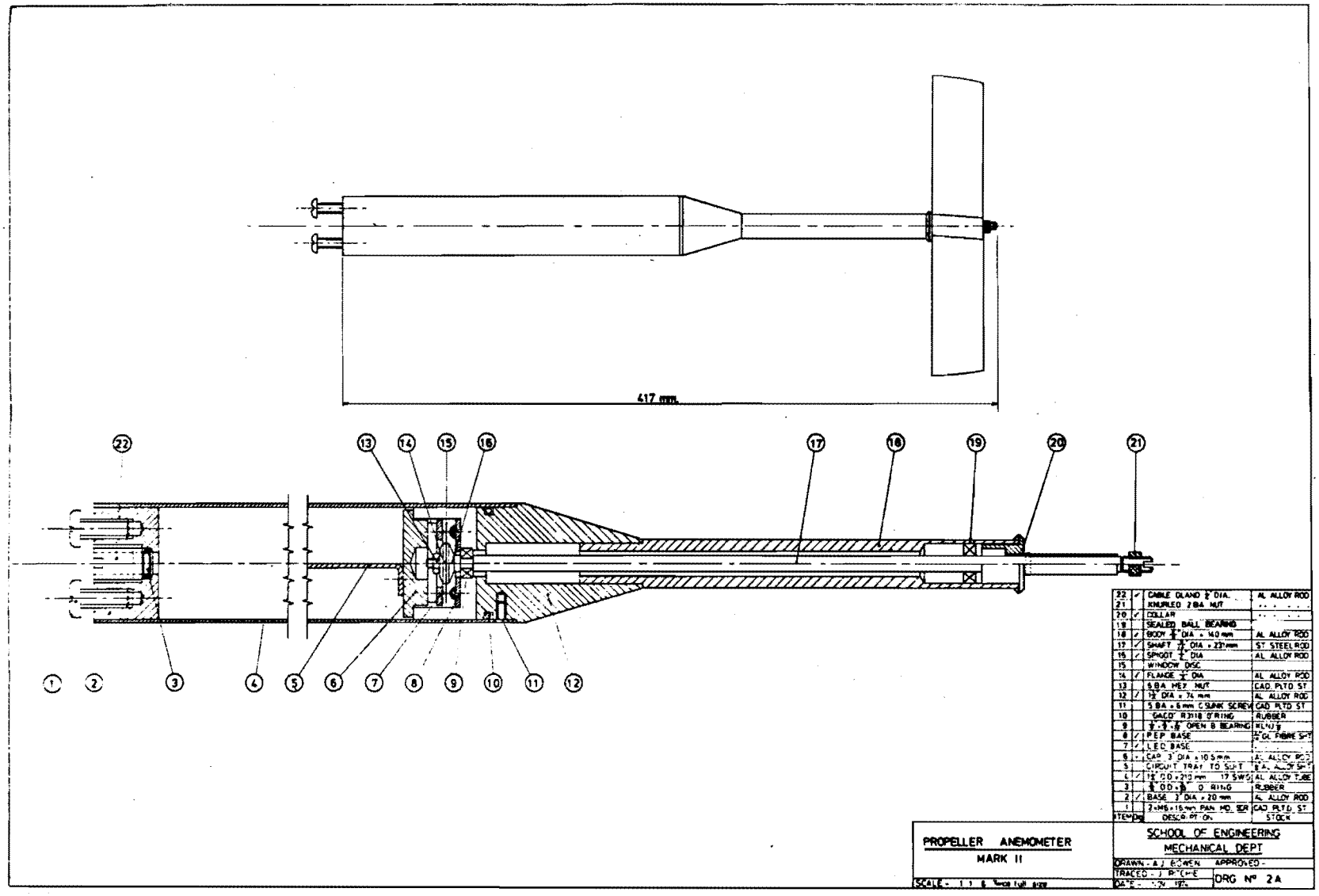

FIG. 3·1. PROPELLER ANEMOMETER BODY

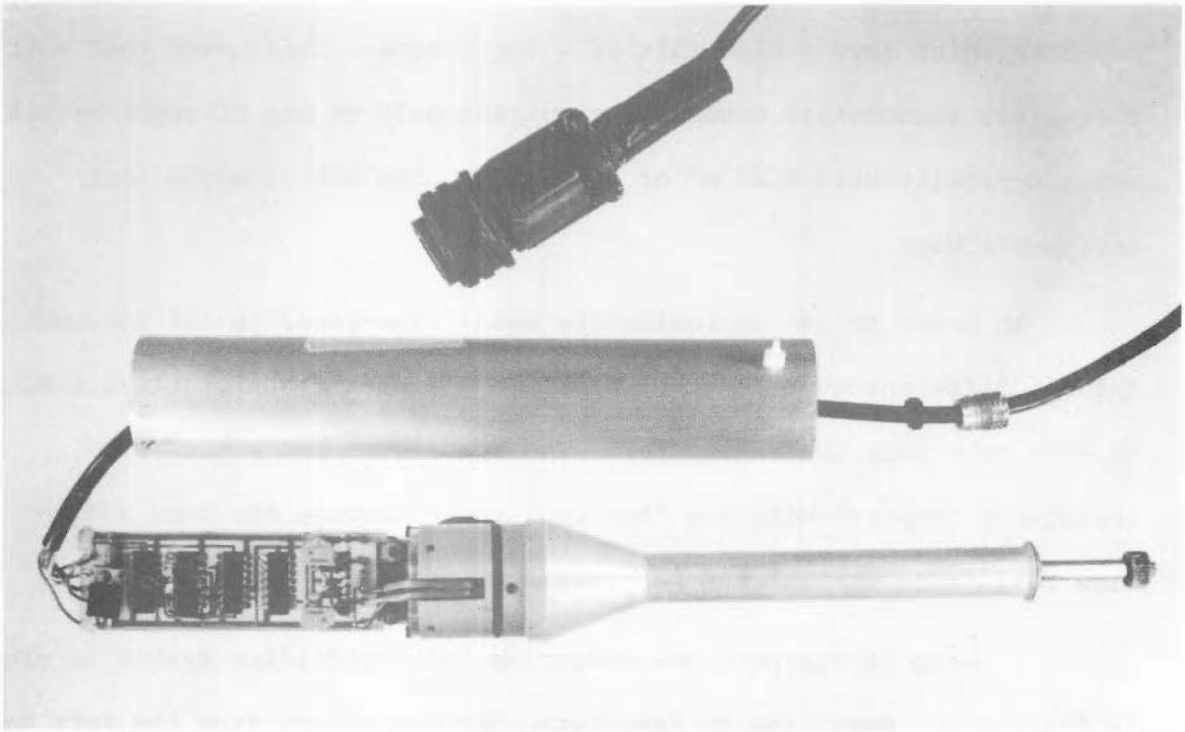

PLATE 3.1 THE ANEMOMETER BODY

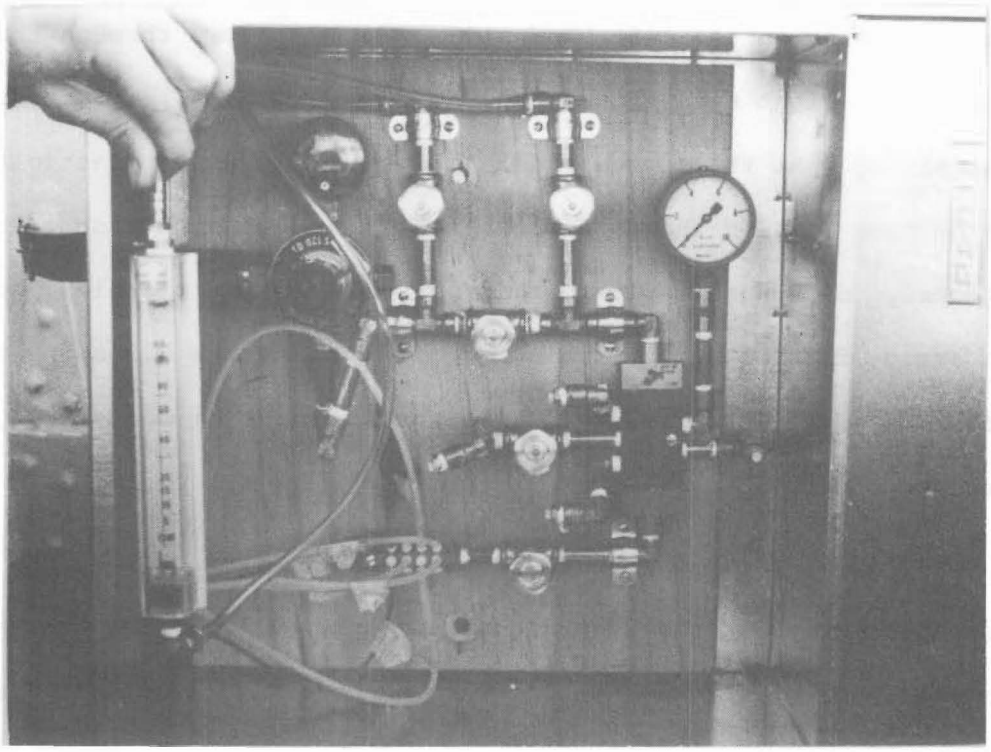

PLATE 3.2 ANEMOMETER PURGE SYSTEM CUPBOARD

the field for several months at a time, for the practical reason of minimising nitrogen bottle changes, the flow-rate was required to be low also. The flow-rate was thus calculated for one complete gas change per hour which gave a flow-rate of ~ 3cc/minute. This meant that with thirty-six anemometers connected simultaneously to one nitrogen bottle, which typically held 6.27 m^3 of gas at STP, the bottle would last thirty-six days.

In order to get approximately equal flow-rates to all anemometers through different tube lengths, a 0.1 mm diameter restrictor was placed in each tube near the anemometer. The restrictor had a high flow resistance compared with the flow resistance through the tube and the flow resistance through the bearings supporting the propeller shaft.

A photo of the pressure reduction and manifolding system is given in Plate 3.2. Referring to the Plate, the gas enters from the left hand side and goes into a pressure reducing valve which reduces the pressure to about 2.5 kN/m^2. In the Plate, the flow-rate is being checked with the flow meter on the left hand side. The gas flows through the brass tube to the right hand side where there is provision for further manifolding. At the bottom middle of the Plate, seven plastic tubes can be seen leaving the manifold through the left hand side of the cupboard. Each tube taped to the required instrument cables, goes to one array of anemometers. This can be seen in Plate 3.3 and Plate 3.4 shows the single tube manifolded to three restrictors and tubes, one for each anemometer.

Since the tubes were taped to the instrument cables, the inconvenience of setting up the instruments with the purge system tube attached was small. The nitrogen bottles were placed conveniently at the base of the towers. A schematic representation of the purge system layout is given in Fig.3.2.

Purging the anemometers reduced their failure rate, due to moisture ingress, considerably.

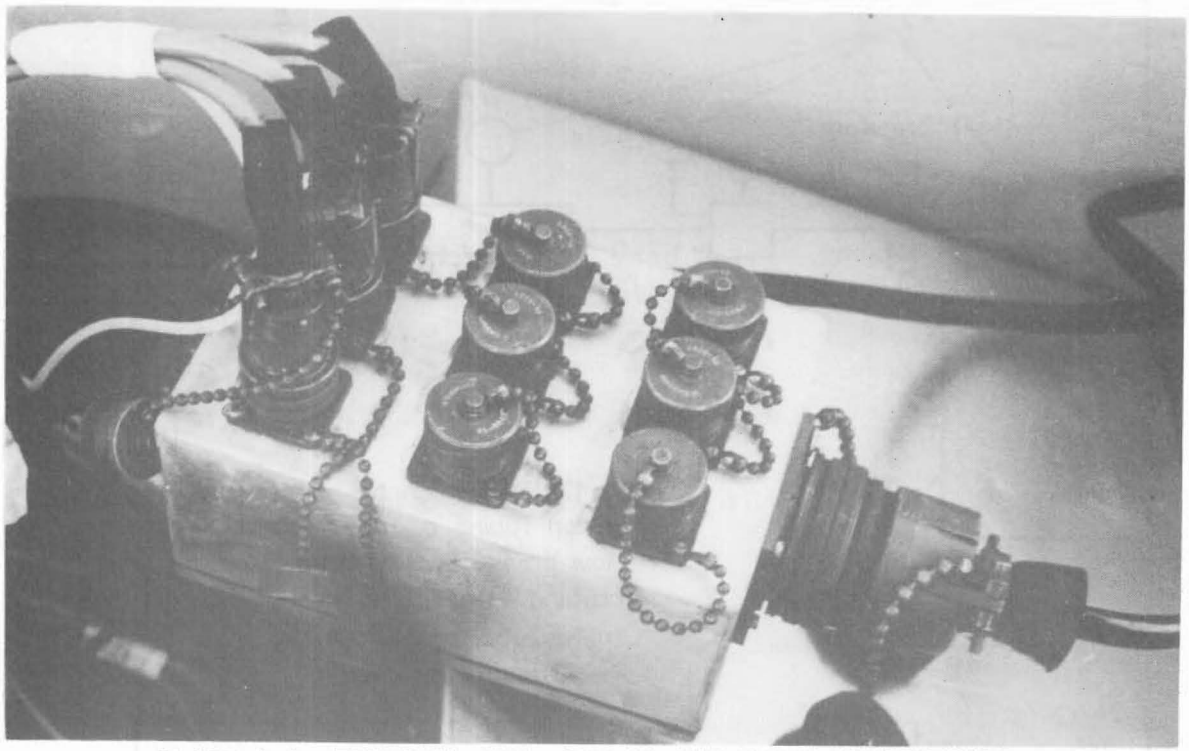

PLATE 3.3 TERMINAL BOX, CABLES AND PURGE SYSTEM TUBE

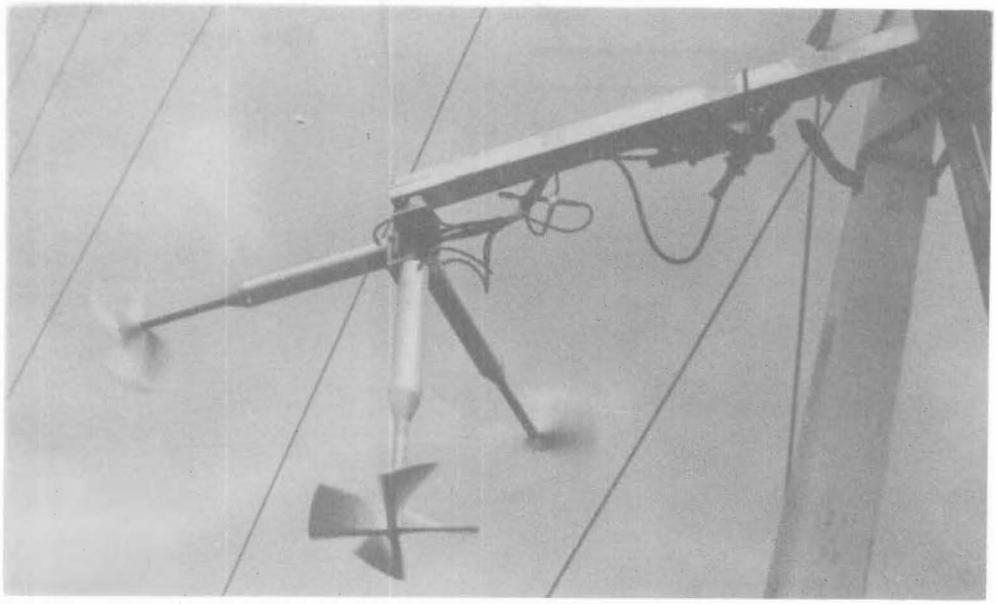

PLATE 3.4 ANEMOMETER ORTHOGONAL ARRAY

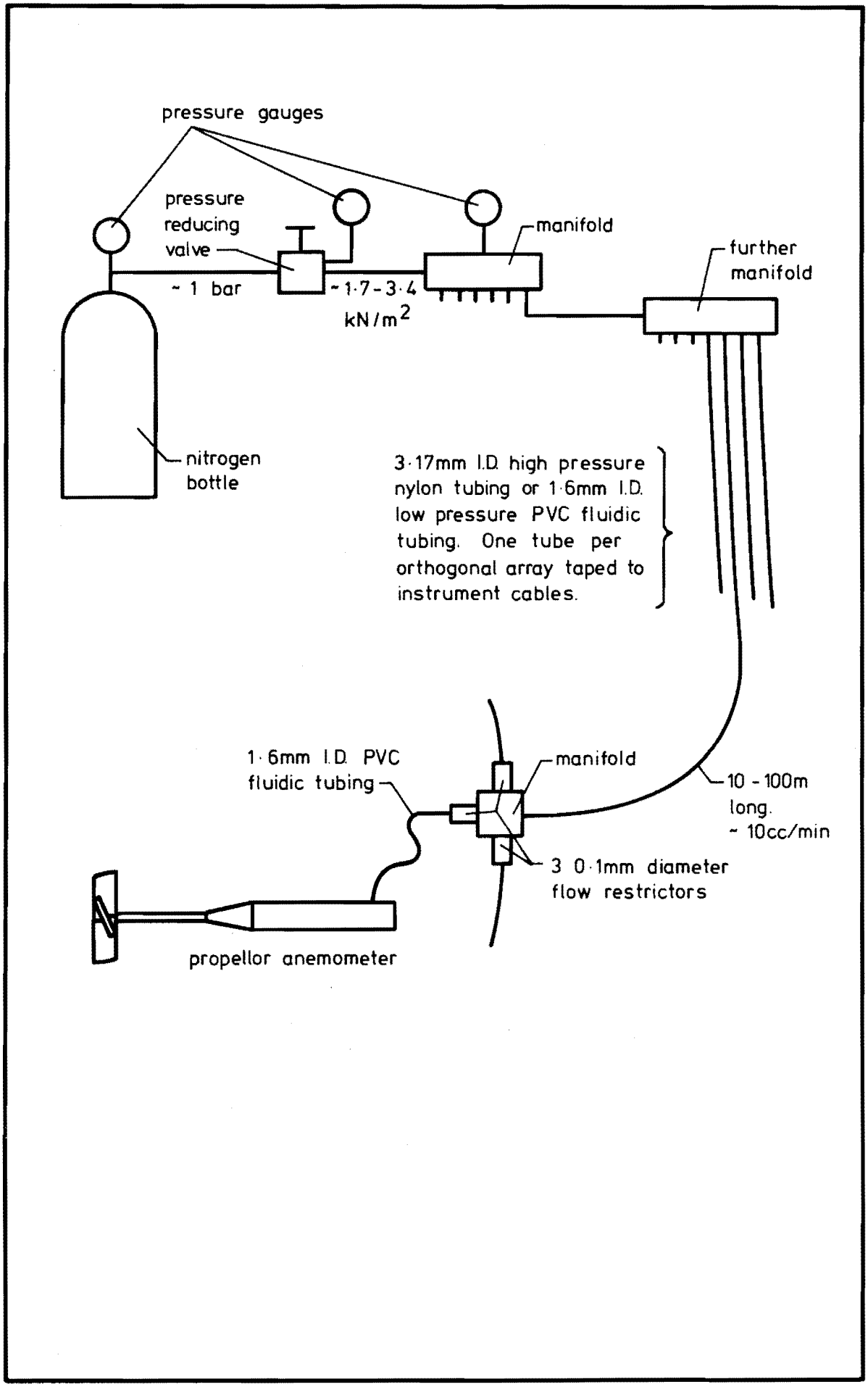

FIG 3·2 PURGE SYSTEM LAYOUT

3.2.3 Signal Generation

The propeller is directly coupled to a thin brass disc 25 mm in diameter containing thirty-two equally spaced sector shaped slots. The disc rotates between two pairs of photo diodes and receivers, mounted almost on a diameter, so that each photo receiver produces a square wave with a frequency proportional to the rotational speed,when the propeller rotates. The shaft mounted disc can be seen in Plate 3.5 with the photo diodes to the right and the receivers to the left of the disc. The disc can also be seen in Plate 3.6 which also shows the photo receivers. The propeller thus has to exert no torque to obtain an output and therefore has a very sensitive response.

The photo diode, receiver pairs are mounted such that when one pair is in the centre of a hole in the disc, the other pair is on the edge of a hole. This means that when the disc rotates the photo receivers generate square waves 90 degrees out of phase. The frequency of the square waves thus determines the rotational speed and decoding which square wave leads the other determines the direction of rotation. This is shown in Fig.3.3

The power supply to and the output from each anemometer is via a multi-core twisted pair cable. The output from each anemometer to the data recording instrumentation is transmitted via differential line drivers in two twisted pairs, thus eliminating cross-coupling effects between different signals over lengths of cables which may be up to 1000 m long. The velocity signal from each anemometer is a square wave from one photo diode, receiver pair as shown in Fig.3.3. The direction signal is a positive or negative voltage difference in the other twisted pair, depending on the rotational direction.

The system was found to work very well providing the disc was mounted concentrically on the propeller shaft and the photo diode, receivers pairs were positioned accurately. However it was found that

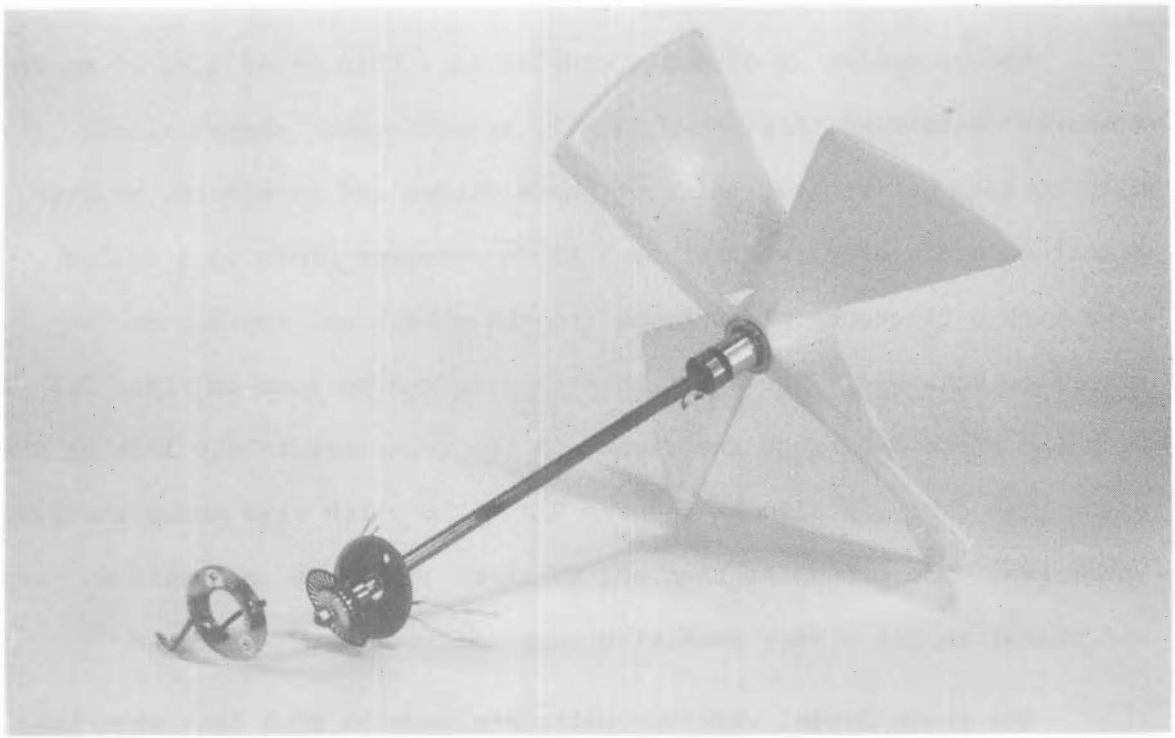

PLATE 3.5 PROPELLER SHAFT MOUNTED DISC

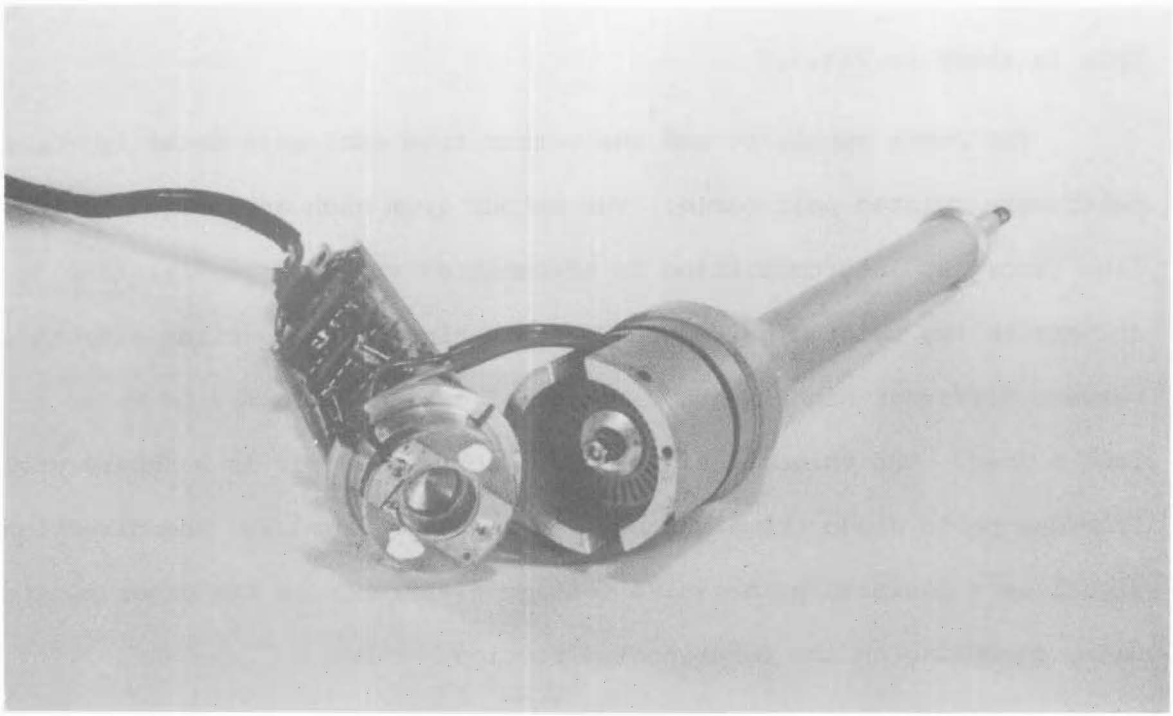

PLATE 3.6 SLOTTED DISC AND PHOTO RECEIVERS

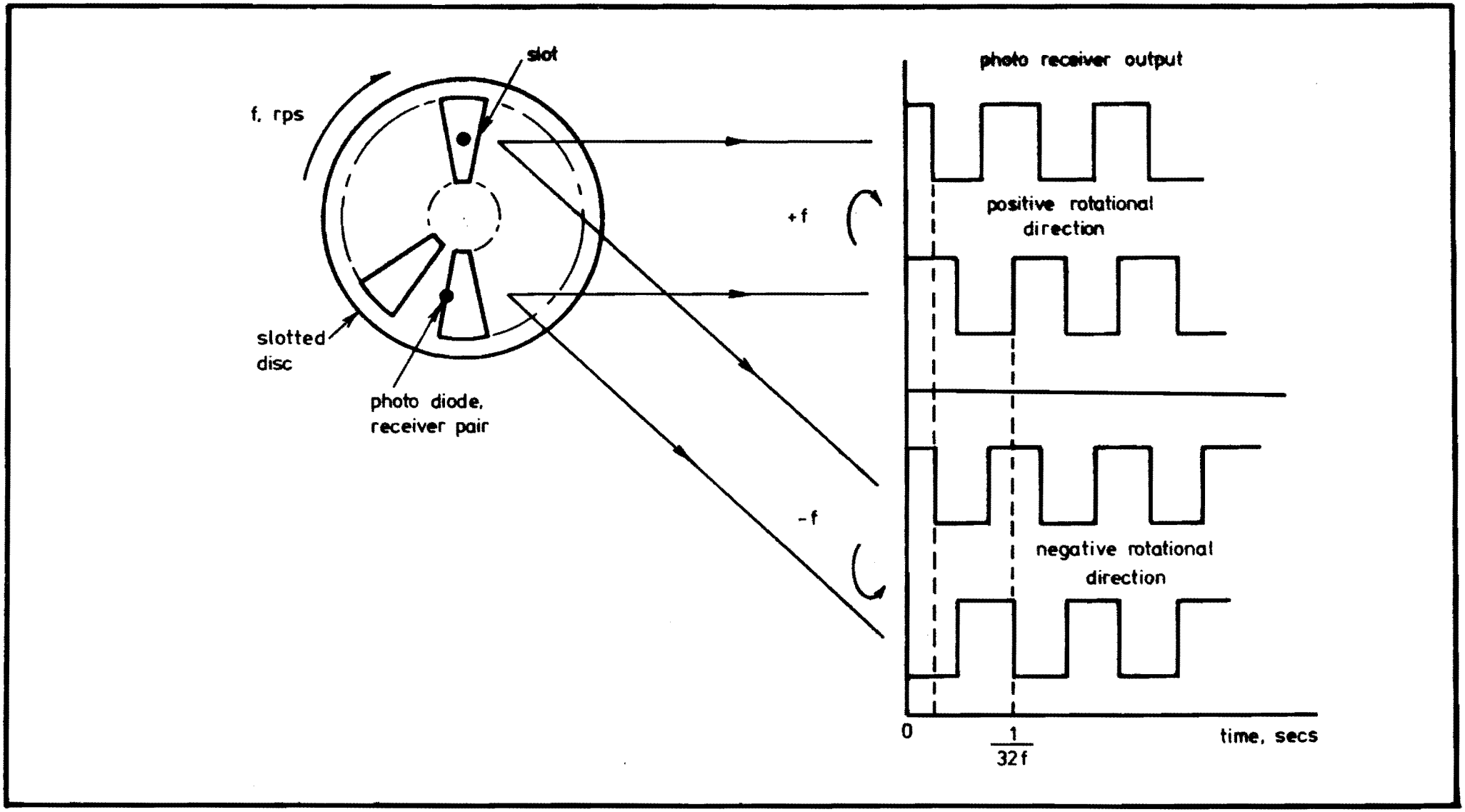

FIG 3·3. SIGNALS GENERATED FROM PHOTO RECEIVERS

in practice, the signal reliability was very strongly dependent on the slotted disc. It had to be made with extreme precision, having equally sized slots. The disc had to be mounted exactly concentrically on the shaft, which had to be supported by the bearings with no lateral movement between it and the housing.

The two photo diode receiver pairs being mounted almost on a diameter meant that small errors in misalignment and assembly, particularly the disc not being mounted concentrically on the shaft, made the phase of the two square waves vary markedly. Had the two photo diode, receiver pairs been mounted as near as possible to each other, tolerancing of the mechanical parts could have been less severe, and setting the equipment up initially could have been done much more quickly.

3.2.4 Propeller Design and Construction

A propeller was desired which had the following characteristics:

(1) Light, i.e. of low rotational inertia.

(2) Strong, i.e. could survive wind speeds up to 150 kmph.

(3) A calibration coefficient which did not change with wind speed.

(4) Rotated at a speed of $\bar{U} \cos\theta$ where $\bar{U}$ is the wind velocity and θ the angle it makes with the anemometer axis.

(5) Could be made within the Departmental workshops.

(6) Were stalled for only a small range of angles near $\theta = 90$ degrees.

It appeared that the alternative which came closest to satisfying the above criteria was to make the propeller blades by expanding polystyrene beads in a mould of the propeller.

Following Holmes et al (1964), two and four bladed helicoid section propellers were designed to rotate one revolution for .305 m of passing wind. Fig.3.4 shows a section through the propeller at radius r and making the usual assumptions, it follows that the propeller speed at

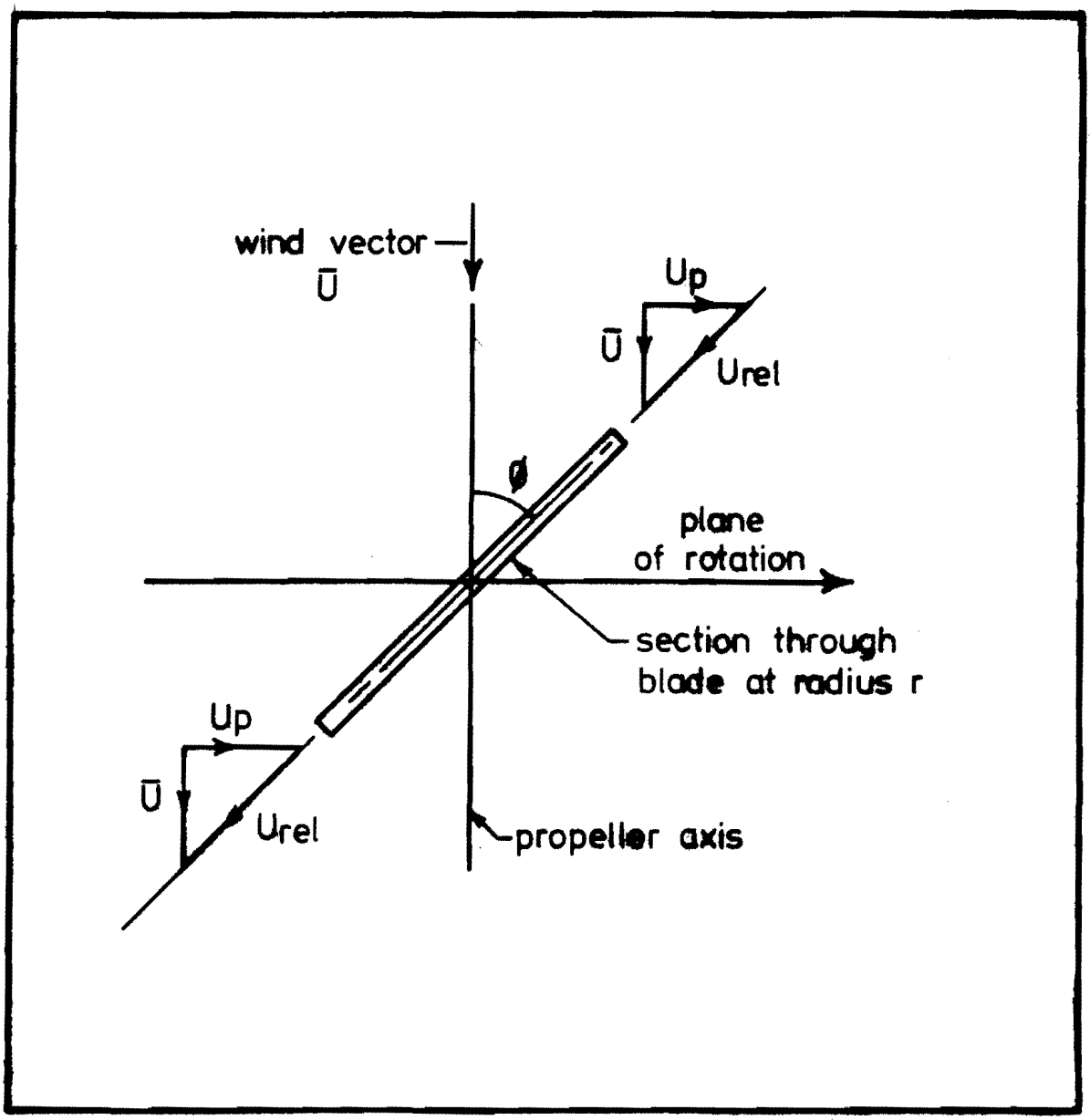

FIG. 3·4. PROPELLER BLADE GEOMETRY

this radius, $U_p = \bar{U} \tan\phi = 2\pi rN$, where N is the rotational speed and ϕ the angle between the wind vector $\bar{U}$ and the blade surface at radius r. Assuming frictionless flow, then in order to maintain the velocity U_{rel} parallel to the blade surface for all r, $\tan\phi$ varies with radius according to the relation $\phi = \tan^{-1}(\frac{2\pi rN}{\bar{U}})$. An angular distribution ϕ was chosen therefore to make the propeller rotate 1 rps when $\bar{U}$ was .305 m/s.

An aluminium mould was built which made two bladed propellers with a diameter of 200 mm to the above specifications. The propellers were steam injection moulded from .08 mm diameter polystyrene beads which were first partially expanded by allowing steam to pass through them until their diameter had increased to approximately .16 mm. These partially expanded beads were then expanded again in the aluminium mould surrounded by steam jackets. The steam at 276 kPa and 130°C was injected via forty-four .05 mm diameter holes, positioned in each half of the propeller mould. These were essential to ensure even expansion of the polystyrene beads. The time of steam injection into the mould varied between two and three minutes. Four bladed propellers were manufactured by splicing, with Araldite, two two bladed propellers that had been moulded with a dovetail joint at the central boss.

The four bladed propellers which were used in this work were cut to a diameter of 190.5 mm with a hot wire. The surface finish was improved and the propellers made more resilient by covering them with paint or polyurethane. Finally the blades were balanced with pins.

Plate 3.7 shows a propeller blade which is just about to be removed from the mould. At the centre of the propeller it can be seen that half of the boss is not formed with polystyrene as this blade, in conjunction with another, is to be made into a four bladed propeller. Plate 3.8 shows two blades, similar to the one in Plate 3.7, before being glued together. The top four bladed propeller is being trimmed to size and the four bladed propeller on the left is the finished product.

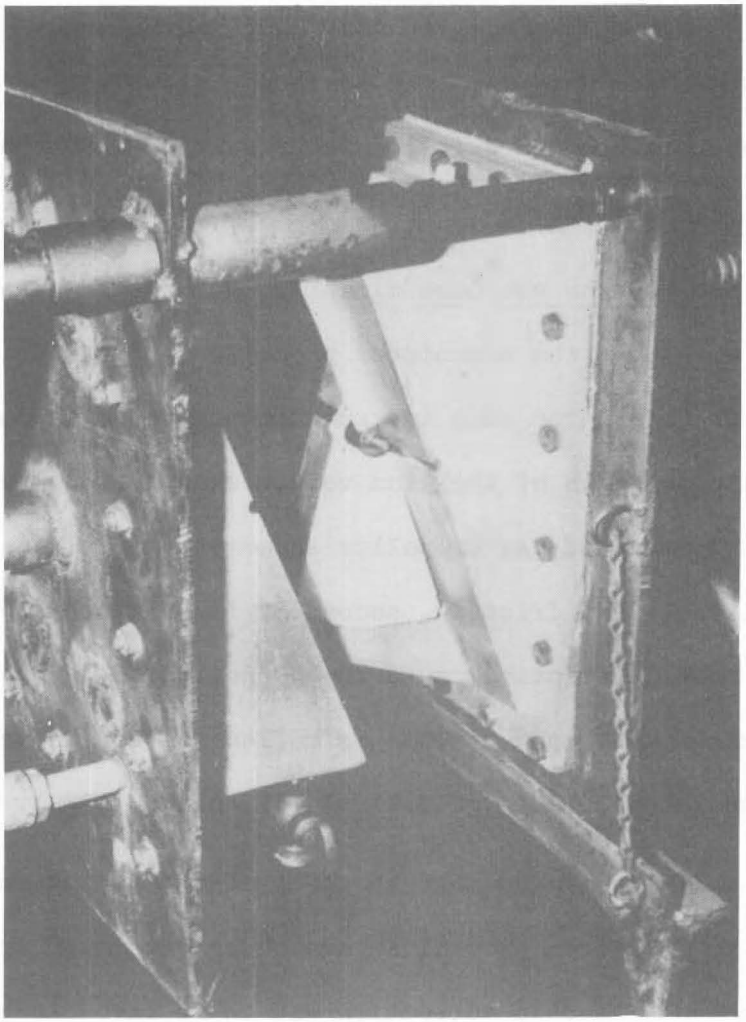

PLATE 3.7 PROPELLER MOULD

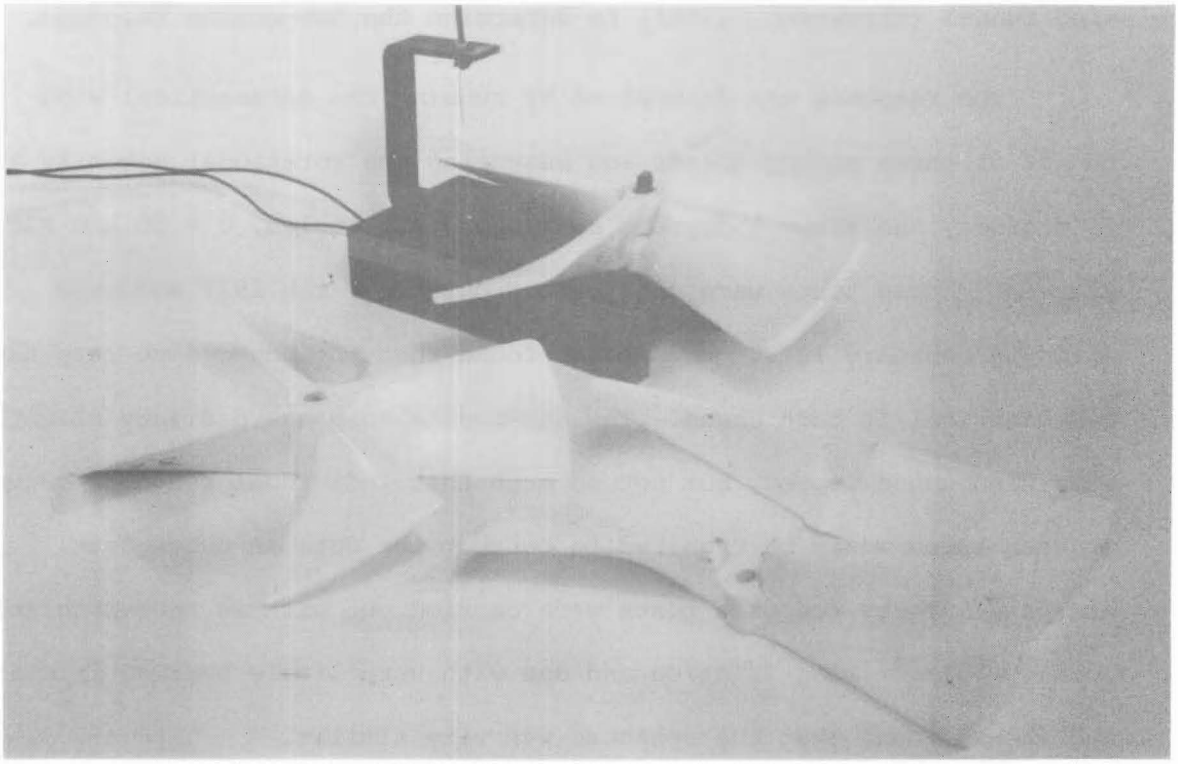

PLATE 3.8 FOUR BLADED PROPELLER CONSTRUCTION

3.2.5 Performance of the Propeller Anemometer

This section describes the various limitations of the anemometer to measuring the turbulence in the lower part of the atmospheric boundary layer.

3.2.5.1 Cosine Response Ideally, as stated in Section 3.2.4, it is desirable that the anemometer propeller rotates at a speed equal to $\bar{U} \cos\theta$ as then three such instruments mounted orthogonally would measure the components of the wind vector exactly. However in practice, it has been found that the propeller anemometer does not behave ideally. In the real case skin friction, secondary flows caused by centrifugal forces,and bearing friction cause the propeller to rotate at a speed somewhat less than $\bar{U} \cos\theta$. This is called non-cosine response and has been observed elsewhere, e.g. Gill (1975), Hicks (1972), Horst (1973a).

Horst (1973a) found that the most effective correction that could be applied to data from propeller anemometer orthogonal arrays was that for non-cosine response. As this correction was to be investigated in this work, wind tunnel tests were performed in the Departmental aeronautical wind tunnel (Stevenson, 1968), to determine the non-cosine response.

The response was determined by running the aeronautical wind tunnel at three steady speeds and measuring the rotational velocity every 10 degrees, and every 5 degrees near the stall angles, θ = 90 and 270 degrees. These tests were done twice, once in March 1977 and once again in February 1978, and it was found that the non-cosine response was identical in both cases. The non-cosine response did vary slightly with wind tunnel speed, but not so much that individual response curves at each speed would be required to correct the data in subsequent analysis. These response tests were carried out with an anemometer with considerable bearing friction and one with very little bearing friction, and it was found that the response was very similar.

In these tests, the wind tunnel speed was determined using a

pitot-static tube, and the anemometer rotational speed was determined by observing the visual display on the control panel of the Field Data Acquisition System (FDAS). The rotational speed was checked periodically with a Dawe Straboflash Unit (Straboscope 1290C). The results of these tests have been plotted in Fig.3.5.

Previous investigations into the non-cosine response of the propeller anemometers have been done by Omar and Ow (1972), and Ong and Dien (1974). The previous results agree with the results presented here.

The correction factors, obtained from these results for use in an iterative scheme, modified from Horst (1973b), for correcting for the non-cosine response in the data analysis computer programs, are given in Appendix A.

3.2.5.2 Response of the Propeller Anemometer to a Step Change in Wind Velocity. It is usual to assume that propeller anemometers are first order sensors, (MacCready, 1965, 1966, 1970, Gill, 1966, 1967), i.e. that the sensor's change towards a final equilibrium value depends on the difference between the final value and its present value, and the sensor's rate of change.

A first order sensor can be represented by

$$T_t \frac{dn}{dt} + n = f(t), \qquad (3.1)$$

where t denotes time, f(t) an applied disturbance or forcing function, T_t is the time for the sensor to change to $1 - \frac{1}{e}$ of a step change in f(t) and is called the time constant and n is the sensor response which in this case of a propeller anemometer is the rotational speed in rps.

It can be shown that if an anemometer is rotating at n_o rps, and there is a step change in wind velocity such that the new equilibrium rotational speed for the anemometer is n_1 rps, the response will be

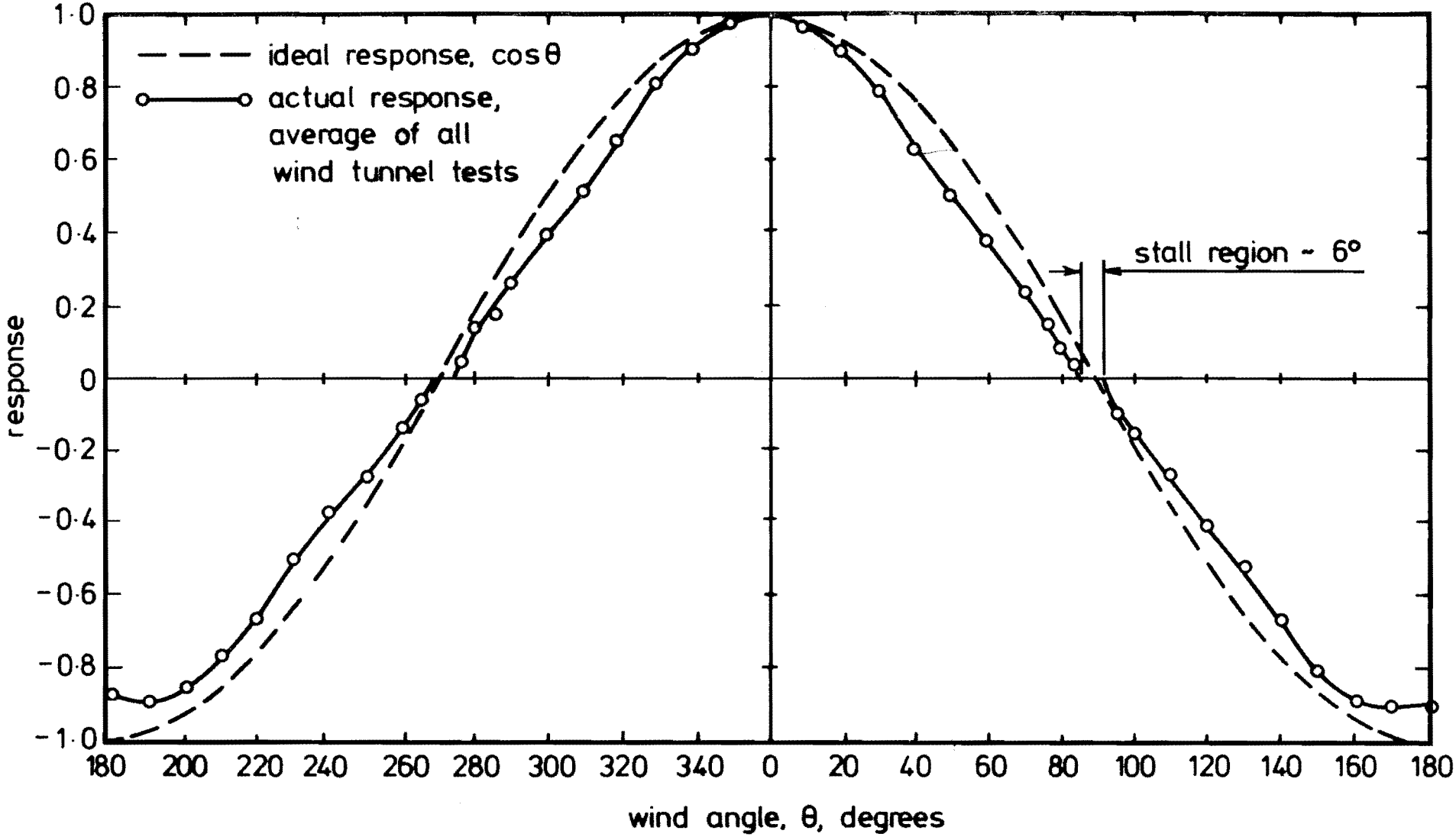

FIG. 3·5 NORMALISED ROTATIONAL SPEED AS A FUNCTION OF ANGLE BETWEEN WIND VECTOR AND ANEMOMETER AXIS.

governed by the following equation :

$$n = n_1 + (n_o - n_1)e^{-t/T_t}$$

In the special case where $n_o = 0$ then

$$n = n_1(1 - e^{-t/T_t}) \tag{3.2}$$

For rotating mechanical type speed sensors, T_t has been found to increase inversely with the wind speed U providing that friction is negligible, (MacCready, 1970). Thus a response distance, length constant, distance constant, or response length, L can be defined which is more convenient to use.

$$L = UT_t \tag{3.3}$$

L is the same at all wind speeds and is the length of the air column that passes the propeller in order for it to change by 63.2% to its new equilibrium value from a step change in wind velocity.

The length constant L is an important parameter to know because it determines the anemometer's sensitivity to measuring the velocity fluctuations. It was required therefore to determine L for this work to investigate how the anemometer's finite response time would compromise the results.

The response distance L was determined in a manner suggested by Gill (1967). The anemometer, positioned with its axis parallel to the flow, was allowed to accelerate from rest in the aeronautical wind tunnel which was running at a predetermined steady speed. The digital signal from the anemometer was integrated to yield an analogue output which was displayed on a Hewlett Packard Type 141B Storage Oscilloscope. The trace, similar to the one shown in Fig.3.6, was then photographed with a Hewlett Packard Polaroid camera. The trace was analysed in the manner shown in Fig.3.6 but usually the first part of the trace was ignored as the propeller was stalled in this region.

Wind tunnel tests of the distance constant by Omar and Ow (1972) and Ong and Dien (1974) showed that the length constant L was equal to

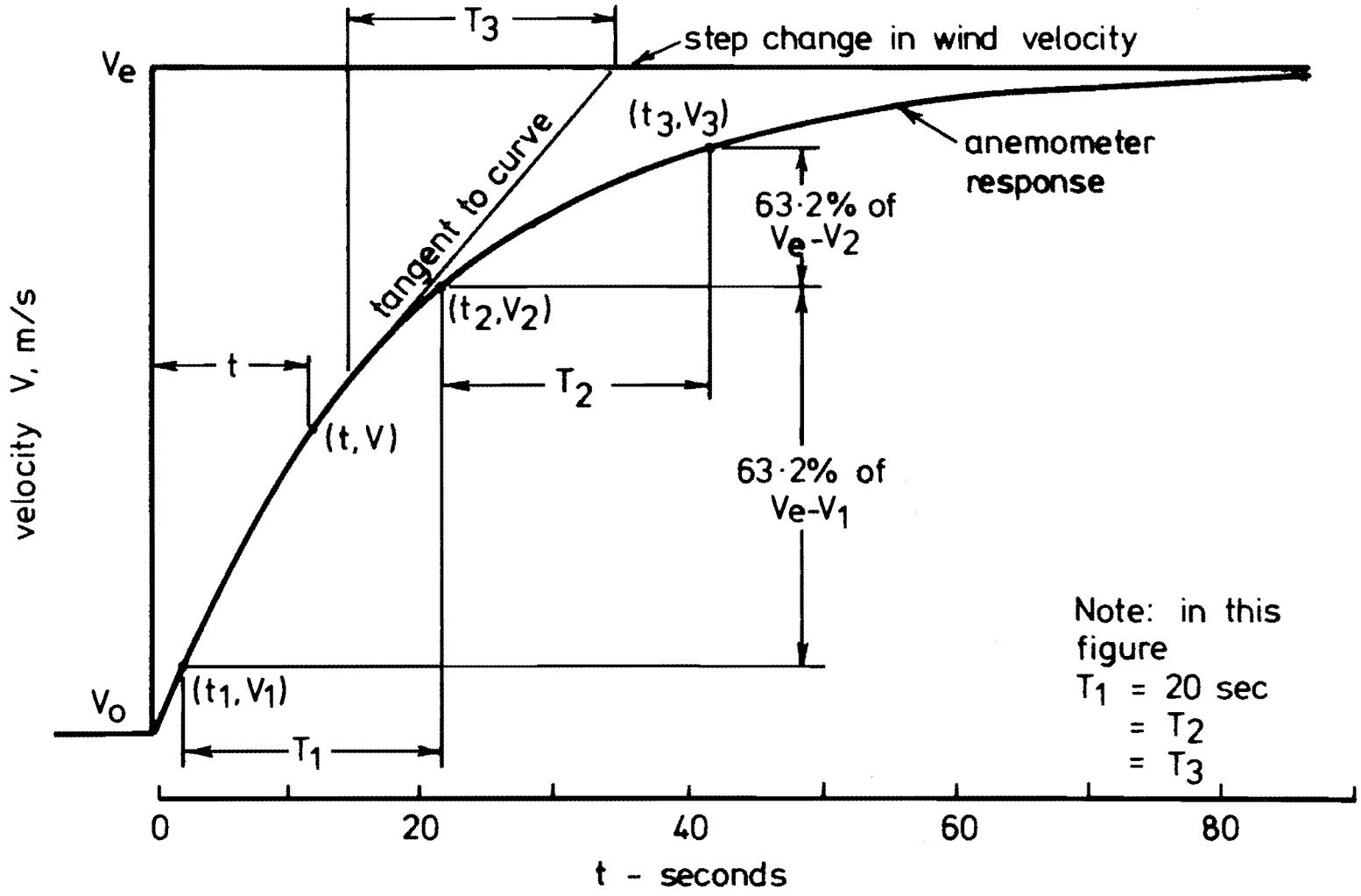

FIG 3·6 RESPONSE OF A PROPELLER ANEMOMETER WITH A TIME CONSTANT T, TO A STEP CHANGE IN WIND VELOCITY, FROM V_o TO V_e.

.95 mm with an error of ±10%, which is similar to the value reported for the Gill UVW propeller anemometer length constant.

3.2.5.3 Effect of Angle Between Anemometer Axis and Wind Vector on the Length Constant. Previous work by Hicks (1972), Garratt (1974), Gill (1975) and Brook (1976) has shown that the propeller anemometer responds more slowly to changes in wind speed when the wind is not directed along the propeller axis. Fig.3.7 from Garratt (1974), shows che increase in the length constant, L_θ with increase in the angle between the anemometer axis and the wind vector. The figure shows that the anemometer is least sensitive when the flow is almost perpendicular to the anemometer axis, and this is precisely the attitude of the vertical component anemometer.

Following the definition given in Equation 3.3, a series of length and time constants can be defined and evaluated for various angles of the wind direction, θ. The ones commonly used are

$$L_\theta = T_\theta U \ , \tag{3.4}$$

where L_θ is the length constant for the instrument for wind angle θ, referred to the wind velocity U, and T_θ is the time constant at angle θ. A parameter L_a, with the dimensions length, can also be defined, related to the ideal rotational anemometer speed for U and θ, by

$$L_a = T_\theta U \cos\theta \ . \tag{3.5}$$

Wind tunnel tests by Hicks (1972) and Gill, (1975) have shown that to a reasonable approximation,

$$L_a = L \cos^{\frac{1}{2}} \theta \ . \tag{3.6}$$

This has been further verified by tests on our own instruments, (Ong and Dien, 1974).

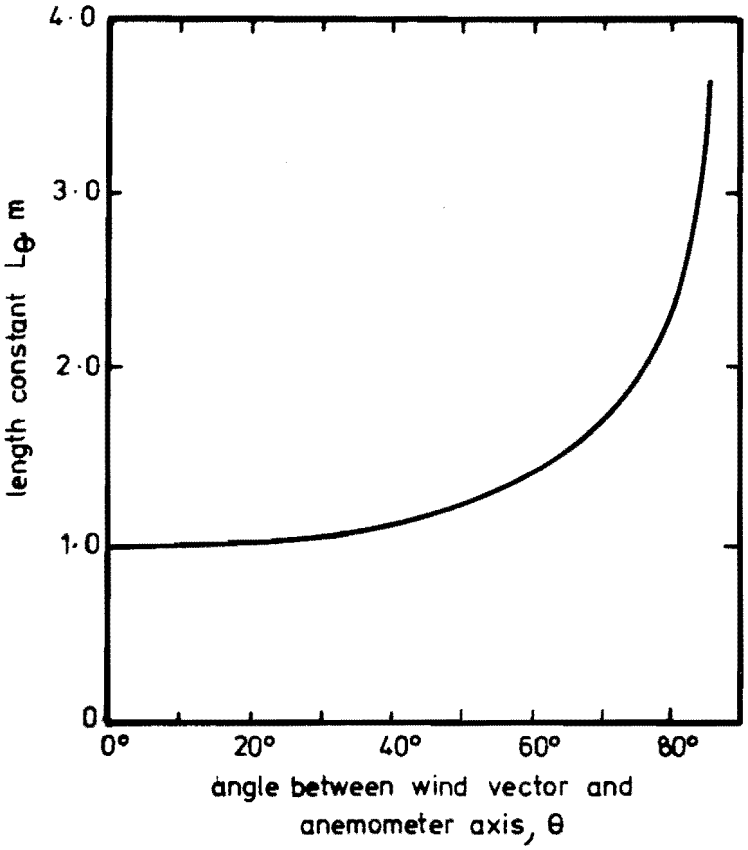

FIG 3·7 DEPENDENCE OF THE LENGTH CONSTANT L_θ ON THE ANGLE BETWEEN THE WIND VECTOR AND THE PROPELLER ANEMOMETER AXIS.

Brook (1976) has examined the effective response of paired Gill anemometers, in the configuration used for the two horizontal component anemometers in an orthogonal array. Brook calculated the response length of the two anemometers combined, thus giving the response length as a function of the angle between the wind vector and the two anemometers, mounted at 90 degrees.

Following the analysis of Brook, the effects of the response characteristics of an orthogonal pair of anemometers on the measured values of u and v are examined by considering step changes in u and v. This analysis assumes that the data has been already corrected for non-cosine response.

Consider the anemometers to lie along conventional x_1 - y_1 axes with the mean wind, and therefore u, making an angle θ with the x_1 axis. Then from Equations (3.5) and (3.6), two time constants can be defined for the x_1 and y_1 anemometers respectively.

$$T_{x\theta} = L/U \cos^{\frac{1}{2}} \theta$$
$$T_{y\theta} = L/U \sin^{\frac{1}{2}} \theta \qquad (3.7)$$

If the step change in u is

$$u = 0 \qquad t < 0$$
$$u = \Delta u \qquad t > 0$$

then u_x and u_y the components of u measured by the x_1 and y_1 anemometers respectively are, from Equation (3.2).

$$u_x = \Delta u \cos\theta(1 - \exp(-tU \cos^{\frac{1}{2}} \theta/L))$$
$$u_y = \Delta u \sin\theta(1 - \exp(-tU \sin^{\frac{1}{2}} \theta/L)) \qquad (3.8)$$

Then the observed longitudinal component u' is

$$u' = (u_x^2 + u_y^2)^{\frac{1}{2}}$$
$$= \Delta u \left\{\cos^2\theta(1 - \exp(-tU \cos^{\frac{1}{2}} \theta/L))^2 + \sin^2\theta(1 - \exp(-tU \sin^{\frac{1}{2}} \theta/L))^2\right\}^{\frac{1}{2}} \qquad (3.9)$$

Brook has shown by plotting $\ell n(1 - \frac{u'}{\Delta u})$ against tU/L that it is very close to linear for all θ, thus implying that even with the wind not directed along the anemometer axes, the response is still very close to first order. An equivalent time constant T_θ' was determined by valuating the time for u' to reach $(1 - \frac{1}{e})\ \Delta u$. Brook approximates this by

$$T_\theta' \ U/L = 1.093 + .093 \sin\ (4\theta - 90) \qquad (3.10)$$

Because of the symmetry of the problem an exactly similar analysis can be made for the v component obtaining the same results.

Equation (3.10) thus allows T_θ' to be evaluated for a given mean wind angle θ and enables the extent of the data compromisation by the instruments to be evaluated when the wind is at any angle to the horizontal component anemometers. This is discussed further in the following section.

3.2.5.4 Response of the Propeller Anemometer to a Sinusoidally Fluctuating Input. Consider initially a single propeller anemometer with its axis aligned parallel to the wind flow. An analysis using first order theory then enables the response of the instrument to be determined for a fluctuating wind speed. This theory is later extended to include more than one anemometer with the wind not aligned along the anemometer axis.

If the applied disturbance f(t) in Equation (3.1) is sinusoidal, i.e. the wind velocity fluctuations are governed by the following equation,

$$f(t) = A\sin\omega t\ , \qquad (3.11)$$

where A is the velocity fluctuation amplitude and ω the frequency in radians per second, the response of the anemometer is found to be a function of A and ω. By substituting Equation (3.11) into Equation (3.1), the response n can be shown to be

$$n = A(1 + (T_t\omega)^2)^{-\frac{1}{2}} \sin(\omega t - \psi) \ , \tag{3.12}$$

where ψ, the phase lag angle is equal to $\tan^{-1}(T_t\omega)$. At the time when $\sin(\omega t - \psi) = 1$, the amplitude of the response, R is given by

$$\frac{R}{A} = (1 + (T_t\omega)^2)^{-\frac{1}{2}} = M \tag{3.13}$$

The term $(1 + (T_t\omega)^2)^{-\frac{1}{2}}$, M, is called the "dynamic gain" or "amplitude ratio", and is the ratio of the amplitude of the output response, R to the amplitude of the applied disturbance, A, the wind velocity fluctuation amplitude.

A sinusoidal wind velocity fluctuation with a frequency ω radians per second or

$$f = 2\pi\omega \quad \text{Hz} \ , \tag{3.14}$$

has a period

$$P = \frac{1}{f} \quad \text{seconds.} \tag{3.15}$$

If the fluctuation is convected along at velocity U, then the gust wavelength λ is given by

$$\lambda = PU \quad \text{metres} \ . \tag{3.16}$$

Substituting Equations (3.3), (3.14), (3.15) and (3.16) into Equation (3.13) allows the interrelationship between the various parameters to be determined giving

$$\frac{L}{\lambda} = \frac{T_t}{P} = \frac{\left(\left(\frac{A}{R}\right)^2 - 1\right)^{\frac{1}{2}}}{2\pi} \tag{3.17}$$

Following Gill (1967), Equation (3.17) has been evaluated and plotted in Fig.3.8 for various ranges of $\frac{T_t}{P}$, $\frac{L}{\lambda}$ and $\frac{R}{A}$.

The relationship given in Equation (3.17) is useful because it allows the ratio $\frac{R}{A}$ to be calculated from the physical characteristics of the sensor, the wind speed, and the gust frequency. Following Gill (1967), the amplitude ratio of several instruments with different response lengths is given as a function of gust wavelength in Fig.3.9. It is

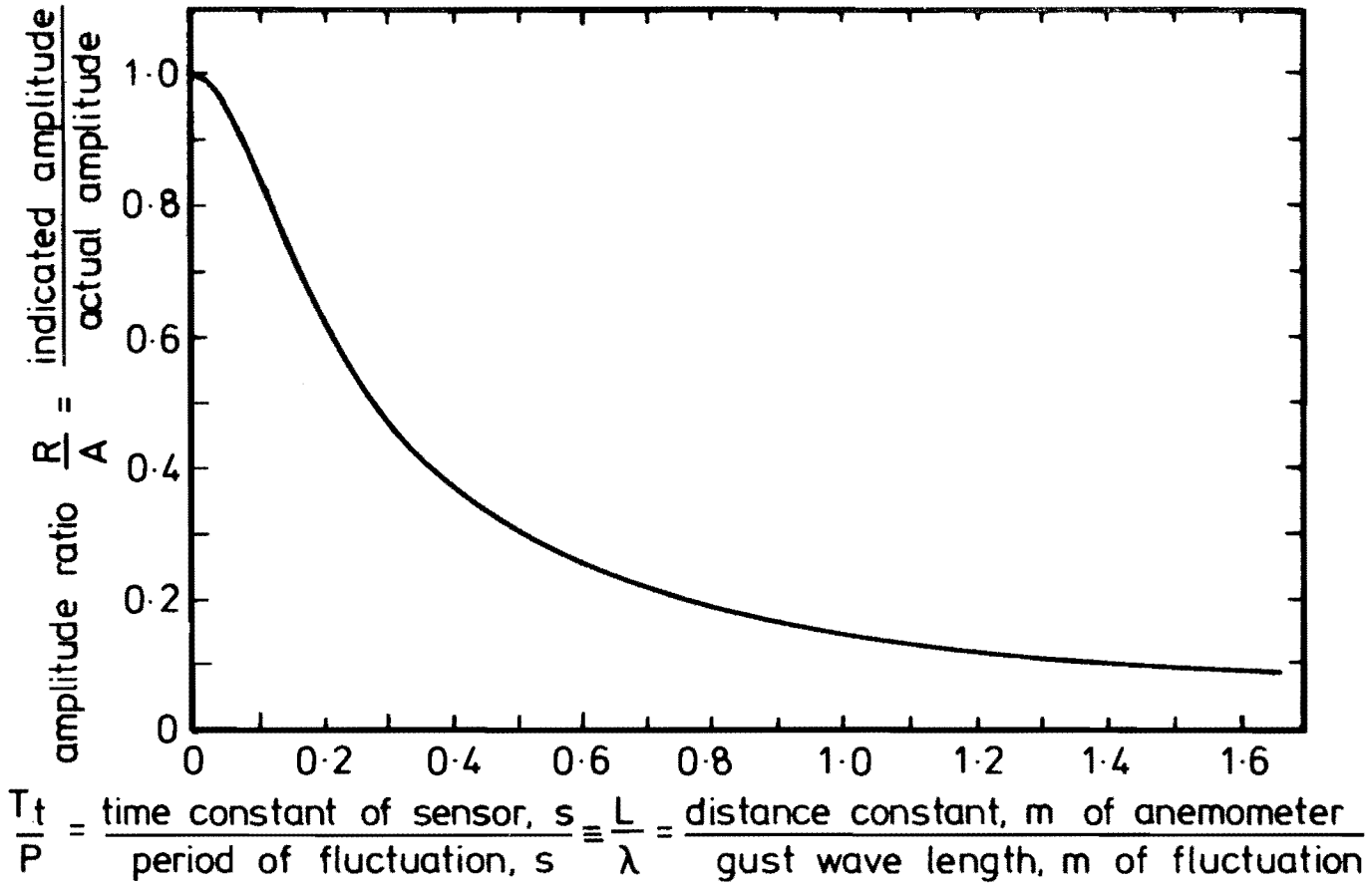

FIG. 3·8 RELATIONSHIP BETWEEN THE TIME CONSTANT, Tt, OF A PROPELLER ANEMOMETER, THE PERIOD, P, OF A SINUSOIDAL VELOCITY FLUCTUATION, THE DISTANCE CONSTANT, L, OF A PROPELLER ANEMOMETER, THE GUST WAVE LENGTH, λ, OF A SINUSOIDAL SPEED FLUCTUATION, AND THE FIDELITY OF RECORDING THIS FLUCTUATION.

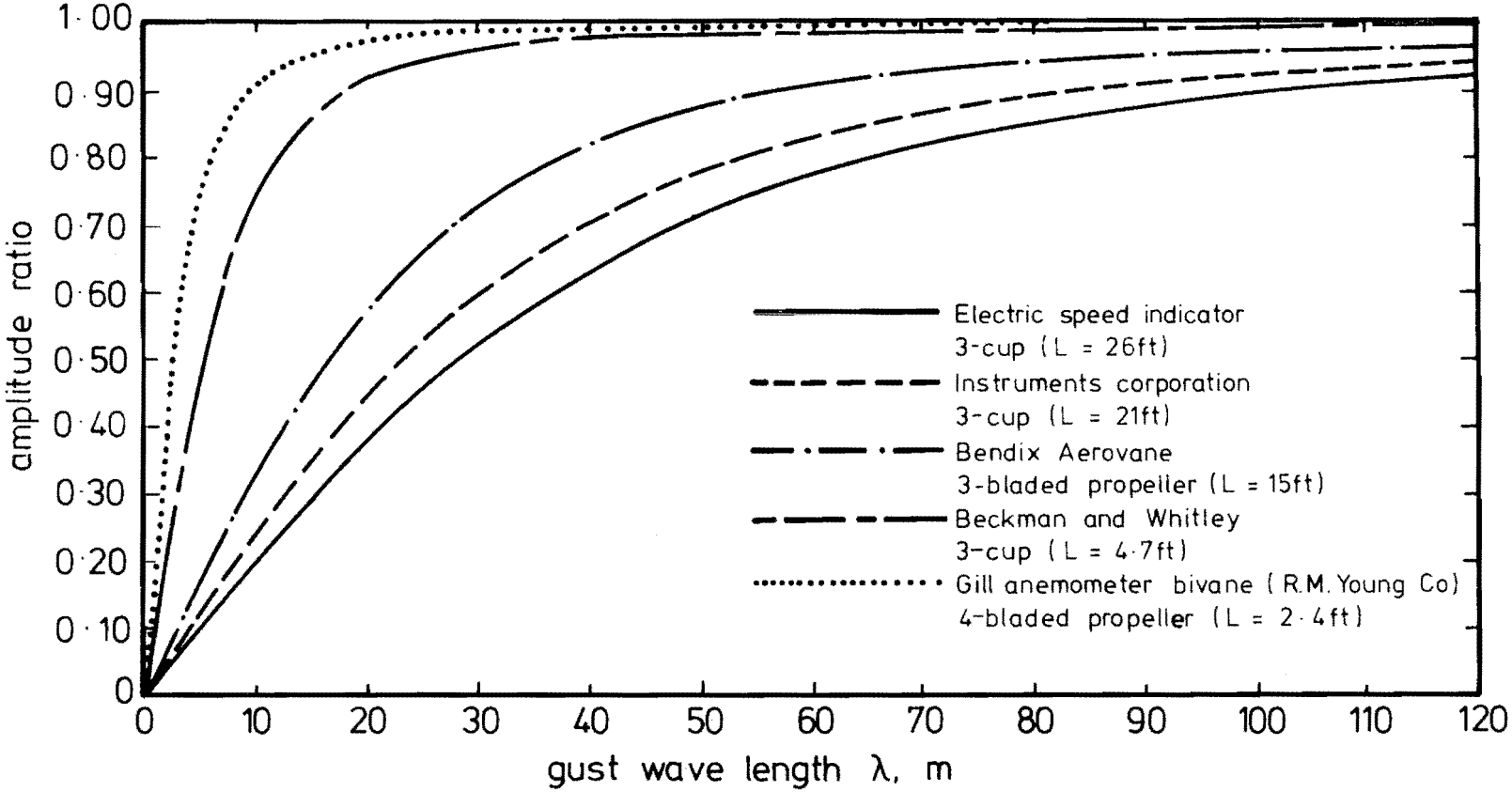

FIG 3·9 RESPONSE OF SEVERAL TYPICAL WIND SPEED SENSORS TO SINUSOIDAL WIND SPEED FLUCTUATIONS OF VARYING GUST WAVE LENGTH.

shown quite dramatically that the instruments become less sensitive to small wavelengths when the response length is increased.

For our own particular instrument with L = .95 m, the gust wavelength can be calculated at which it measures $(\frac{1}{2})^{\frac{1}{2}}$ of the amplitude, or only half of the energy at that particular frequency, by putting $(\frac{R}{A})^2 = \frac{1}{2}$ in Equation (3.17). This gives λ = 6 m. For wind with an average velocity of 10 m/s, this gives the frequency at which this occurs as 1.7 Hz. At a frequency of 1 Hz and for the same wind velocity, $(\frac{R}{A})^2$ = .74.

The two examples above show that the anemometers theoretically measure frequencies up to 1 Hz quite well when the average wind speed is 10 m/s and is directed along the propeller axis. However by using Equation (3.10) in conjunction with Equation (3.17), the response can be evaluated for any angle θ for the horizontal anemometers. Using Fig.3.7 to give a value of L_θ for the vertical component anemometer also allows the effect of its response on the measured results to be evaluated. The problem then becomes one of evaluating θ for which to determine L_θ. MacCready (1970) discusses a method by which the spectrum curve can be corrected to the true atmospheric spectrum by multiplying by $(\frac{1}{M})^2$ at each frequency, where M is defined in Equation (3.13).

In this work no account was taken of the response length in determining the power spectral densities. The longitudinal and lateral component spectra are probably therefore reliable up to .3 - .5 Hz, and the vertical component spectra accurate to slightly less than this.

3.2.5.5 Over-estimation of the Mean Velocity. Lindley (1975) and others have shown that cup and propeller anemometers over-estimate the average wind speed when placed in unsteady flow. After Lindley (1975), it can be seen in Fig.3.10 that Gill type four bladed propeller anemometers over-estimate the mean velocity by less than the other types of sensor in the figure.

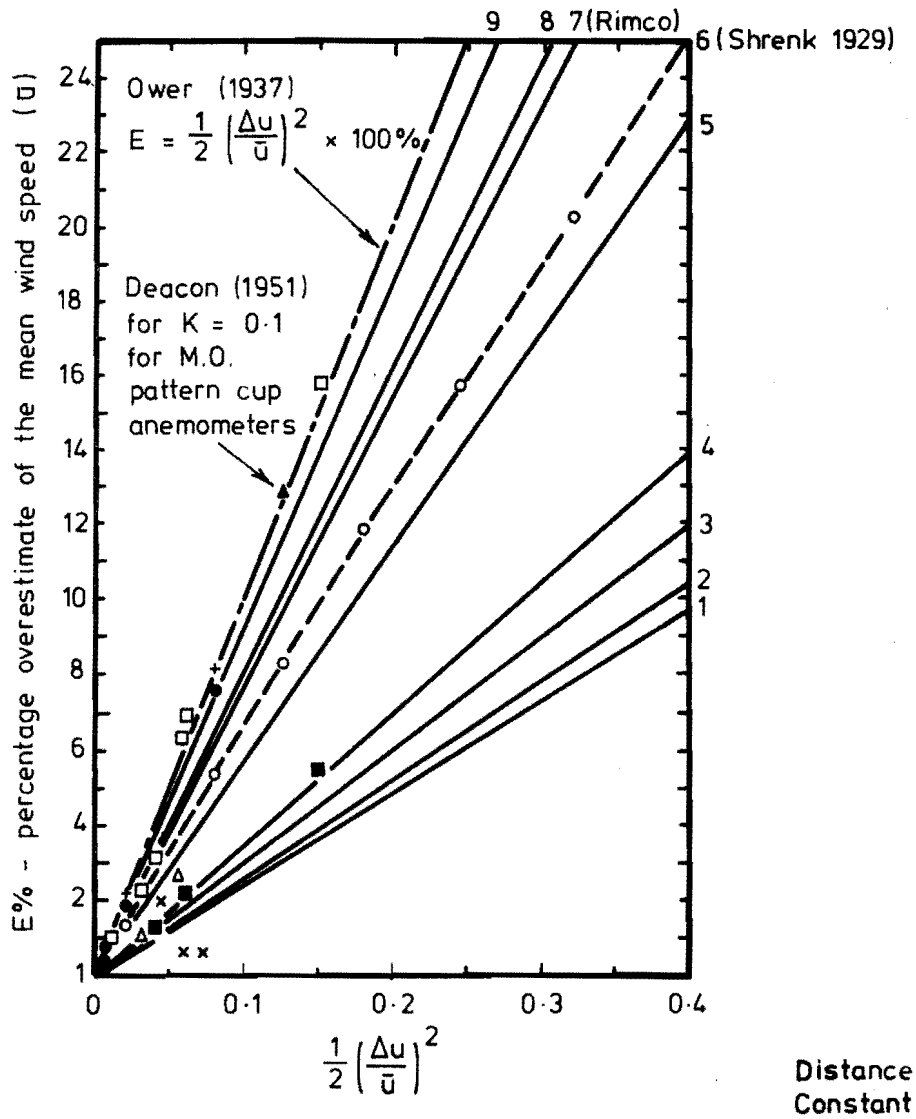

	Key:-	Distance Constant m
1	Gill 4-bladed propeller	0·94
2	6-cup polystyrene arm (4·76mm lip)	0·62
3	6-cup " " (1·58mm lip)	0·5
4	Gill 2-bladed propeller	0·77
5	6-cup polystyrene arm (lipless)	0·59
6	Shrenk (1929), K = 0·1, 4 hemispherical cups	—
7	Rimco (3ins) cup	1·77
8	3-cup metal arm (lipless)	1·02
9	3-cup polystyrene arm (lipless)	0·49
●	Hyson (1972) for n = 1·3Hz	1·42
+	Hyson (1972) for n = 2Hz	1·42
□	3-cup cassella (lipless) Frenzen (1966, 1967)	2·2
△	3-cup cassella (9·53mm lip) " " "	—
■	6-cup polystyrene arm (lipless) " " "	0·4
×	6-cup " " (2·38mm lip) " " "	—

FIG 3·10 PERCENTAGE OVERESTIMATION OF CUP AND PROPELLER ANEMOMETERS IN A FLUCTUATING WIND OF AMPLITUDE Δu AND MEAN SPEED $\bar{u}$.

Using wind structure turbulence parameters already well verified, an analysis can be made showing the amount of over-estimation likely with the four bladed propeller anemometers.

From ESDU (1974b) the value of the turbulence intensity $\frac{\sigma u}{\bar{V}_Z}$ is found to be not usually greater than .22 in a rural atmospheric boundary layer. In Fig.3.10, Δu is given as the amplitude of a fluctuating wind. If σu is considered to be made up of a sinusoid of a single frequency being equivalent to Δu, then

$$\frac{\Delta u}{2^{\frac{1}{2}}} = \sigma u$$

$$\text{or} \quad \Delta u = \bar{V}_Z \times .22 \times 1.414 = .31 \bar{V}_Z$$

This gives $\frac{\Delta u}{\bar{u}} = .31$ or $\frac{1}{2}\left(\frac{\Delta u}{\bar{u}}\right)^2 = .05$, using the nomenclature of Fig.3.10. From the same figure it can be seen that the over-estimation error is negligible. It was thus not considered further in this work as other sources of error were far more significant.

3.2.6 Calibration of the Propeller Anemometer

The calibration of the anemometers was carried out in a closed-return subsonic wind tunnel of .914 m x 1.22 m cross-section described by Stevenson (1968). The individual anemometers were aligned with their axes parallel to the wind direction, and then the wind tunnel run at a variety of steady speeds. The wind tunnel speed was determined by a pitot-static tube located in the tunnel working section, and the propeller rotational speed by observing the visual read-out display on the control panel of the field data recording system. The rotational speed was periodically cross checked using a Dawe Straboflash Unit (Straboscope 1290C). A calibration coefficient was then determined from the slope of a line obtained from plotting the rotational speed against the wind speed. The calibration was not performed for wind velocities less than 2 m/s where the behaviour is non-linear, as it was proposed to conduct field experiments in strong winds.

When the anemometers were calibrated in March 1977 and in February 1978, it was observed that the latter calibration tests yielded coefficients which indicated that the anemometers were rotating at a slightly greater rate for a given wind speed than observed in the former tests. This was probably because bearing friction reduced with use. The average over all anemometers for the former calibration gave $U = .2774\ n$, and the latter gave $U = .2707\ n$, where U is the wind speed in m/s and n the rotational speed in rps.

During the first calibration before the field experiments, it was decided to use one particular propeller for each individual anemometer body. The calibrations were thus performed with pairs of propellers and anemometer bodies, and were to be applied to the pairs individually during subsequent computer runs. This was because it was found that the calibrations were not identical, but varied by about ±5% around the mean. However, while the field tests were in progress individual anemometer component circuitry failed, and propellers were broken during erection and maintenance of the instruments, thus the original calibration factors for the individual anemometer-propeller pairs became superseded. It was thus proposed that a practical alternative was to use a common calibration factor for all anemometer-propeller combinations. This was taken as the average of the March 1977 and February 1978 calibration data tests and was

$$U = .2744\ n \tag{3.18}$$

It was estimated from the calibration curves that this would introduce a maximum error at 10 m/s of approximately ±5% in the velocity.

During the calibration tests it was noted that the calibration factor varied more with a change of propeller than with a change of anemometer body. It is thus concluded that more consistent calibrations could be obtained through greater attention to the moulding technique used during propeller manufacture.

3.3 FIELD DATA ACQUISITION SYSTEM AND TAPE RECORDER

This section discusses the hardware and the data recording method, followed by an appraisal of the limitations of the data recording method.

3.3.1 Data Recording Method

The output from the anemometers, a square wave indicating rotational speed, and a high or low voltage depending on the rotational direction,needed to be processed before it could be recorded onto digital magnetic tape.

The square wave from each anemometer indicating rotational speed and with a frequency of 32 x the rotational speed in revolutions per second was connected to an 8 bit counter which integrated the counts over selected time periods. Depending upon the direction signal from the anemometer, the counters either counted up from 0 to 127 for a positive rotational direction or down from 256 to 129 for a negative direction. Thus the counting period had to be selected so that the maximum count remained within the above limits.

The data was recorded onto a digital seven track tape using a rugged seven track industrial compatible magnetic tape transport, a Kennedy Model 8107, via a Kennedy 8230C Buffered Formatter. The tape deck used one track internally for parity checking thus leaving six tracks for data storage.

To have efficient utilisation of the tape for data storage, the contents from three 8 bit counters, i.e. counters from three anemometers, were grouped together thus giving 24 bits. The 24 bits were then transferred to the buffered formatter via four 6 bit characters. This created the situation where three channels were gated together, thus having identical counting periods. For consistency in subsequent computer programming,the three anemometers grouped together were always

from a single orthogonal array (triplet) aligned along the x_1,y_1 and z_1 axes and the data was recorded from the x_1,y_1 and z_1 anemometers respectively for all triplets. This is shown diagrammatically in Fig.3.11.

To provide capacity for large numbers of anemometers,a time division multiplexor with switch selectable counting periods and with variable channel capacity was developed. Thus a scanning output was obtained.

Data from a maximum number of twelve triplets, i.e. thirty-six anemometers was able to be recorded simultaneously. There was also provision for input to a further 3 x 24 bits in the three special channels reserved for other equipment if required, but this facility has never been used. A schematic representation of the multiplexor address system is given in Fig.3.12.

The operation of the multiplexor is such that when the multiplexor address is at position (1) in Fig.3.12, the contents of the three counters from triplet 1 are locked, and their values transfered to the buffered formatter. The counters are then reset to zero. When the multiplexor address advances to position (2), triplet 1 counters resume counting and the counters from triplet 2 are locked etc.

Referring to the same figure, the counting period T is switch selectable and has values of $T = \frac{1}{8}, \frac{1}{16}, \frac{1}{32}, \frac{1}{64}, \frac{1}{128}$ seconds. The inverse of the counting period, called the scan rate, has values of $SR = 8, 16, 32, 64, 128\ s^{-1}$. Since it took $\frac{T}{16}$ seconds for the counters' contents to be transferred to the buffered formatter, and then reset to zero, the sampling frequencies corresponding to the above scan rates are respectively 7.5, 15, 30, 60, 120, Hz. This is the inverse of the time it took the multiplexor address to go from position (2) say, back to position (2) in Fig.3.12 after one scan.

To obtain the highest tape utilisation, the number of triplets

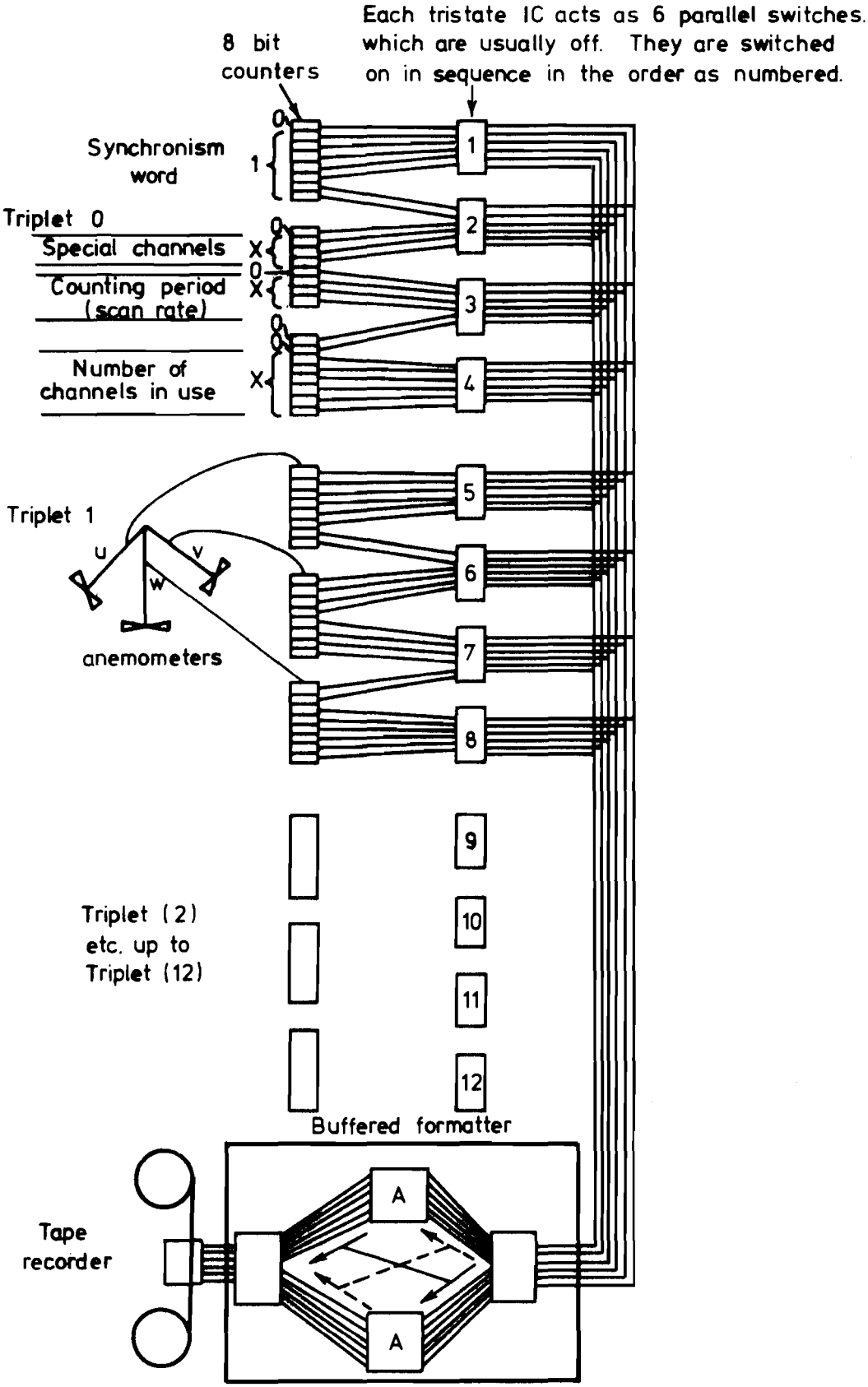

A - 512 x6 bit word buffer, one of which is being filled while the other is having its contents written to tape.
x - denotes a bit which can be 0 or 1.

FIG 3·11 MAIN FEATURES OF THE DATA PATH - FROM ANEMOMETERS TO TAPE STORAGE.

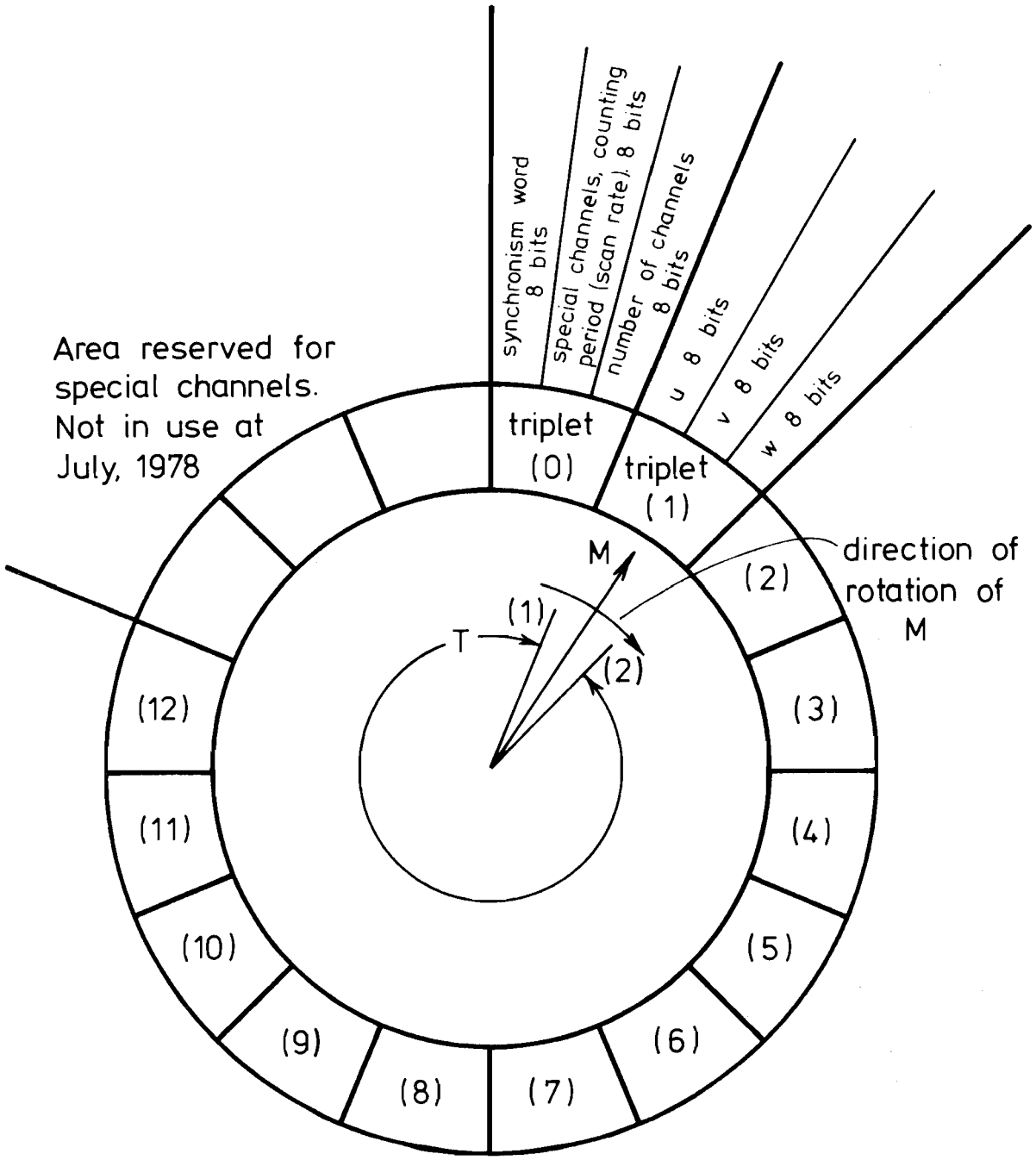

M – multiplexor address
T – counting period, seconds

FIG 3·12 SCHEMATIC REPRESENTATION OF MULTIPLEXOR ADDRESS SYSTEM

recorded was switch selectable from 1 to 12, i.e. the number of channels recorded was 3 to 36 in 3's. Depending on the value of the number of triplets to be recorded, data from triplets 1 up to the number of triplets to be recorded only was transferred to tape. The special channels were also switch selectable in 3's independently.

Since the scan was basically continuous, the start of a scan was identified by placing scanning information in the first address of the multiplexor. The first address, which consists of 24 bits, had a synchronism character placed in the first 8 bits. The synchronism character was the bit pattern 01111111, which as a binary number is 127. In the next group of 8 bits, bits 4, 5, and 6 were used to indicate whether the special channels were on. Bits 4, 5 or 6 on meant that the special channels 1, 2 or 3 were on respectively. Bits 0, 1 and 2 were used to indicate what counting period had been selected, bit patterns 001, 010, 011, 100 and 101 indicating counting periods of $\frac{1}{8}$, $\frac{1}{16}$, $\frac{1}{32}$, $\frac{1}{64}$, and $\frac{1}{128}$ seconds respectively. The final 8 bits of the first address of the multiplexor indicated how many channels were in use. Bits 0 to 5 were used, a binary number indicating the number of channels, which was of course a multiple of 3. E.g. three triplets in use gave the bit pattern 00001001, which as a binary number is 9.

The time division multiplexed data was sent via six parallel lines to the buffered formatter. The buffered formatter had two buffers, each containing five hundred and twelve 6 bit characters. Incoming data was automatically switched from one buffer to the other so that while one buffer was being filled, the other was being written to tape. This is shown in Fig.3.11. Writing to tape was therefore not continuous but in records of five hundred and twelve 6 bit characters separated by a gap of 19 mm. This allowed high tape utilisation factors because the multiplexor could operate completely asynchronously from the tape transport, without having to maintain a continuous data flow.

The tape deck did a read after write check to see that there was no parity error. If there was one it rewrote that particular record until there was no error.

3.3.2 Limitations of the Field Data Acquisition System

If a high scan rate was being used, e.g. 64 or 128, and data from all triplets was being recorded, then it was possible for multiple number of 6 bits to be lost between the multiplexor and the buffered formatter. This only occurred when the tape deck had to rewrite a tape record, which meant that the buffer receiving the incoming data could become full before the contents of the other buffer had been written to tape. Decoding the data after loss of multiple numbers of 6 bits is discussed in Section 5.2, and can be quite difficult.

In practice this limitation is not very serious because usually the scan rate selected is 8, 16 or 32 which allows the tape deck plenty of time to rewrite the occasional record of incorrectly written data. In this work, multiple numbers of 6 bits at no time were lost.

Referring to Fig.3.13, it can be seen that each triplet does not have identical counting times, but that triplet 1 starts counting before triplet 2 etc. The greatest time lag occurs between triplet 1 and triplet 12, where the time lag is $\frac{11}{15}$ T. In this work, the scan rate used was 16, which meant that the time lag between triplet 1 and triplet 12 was $\frac{11}{15} \times \frac{1}{16} = .046$ seconds. This time lag is small compared with the time lags of interest for instance in cross-correlation measurements, and is also small compared with the resolution of any graphical output. This time lag is of even smaller significance when it is considered that in this work, usually eight consecutive samples from each channel were added together to reduce the sampling frequency to 1.875 Hz. It is thus reasonable to assume that the data from each triplet is simultaneous.

A more significant problem is that of selecting the best scan rate so that the counters driven from each anemometer do not count past

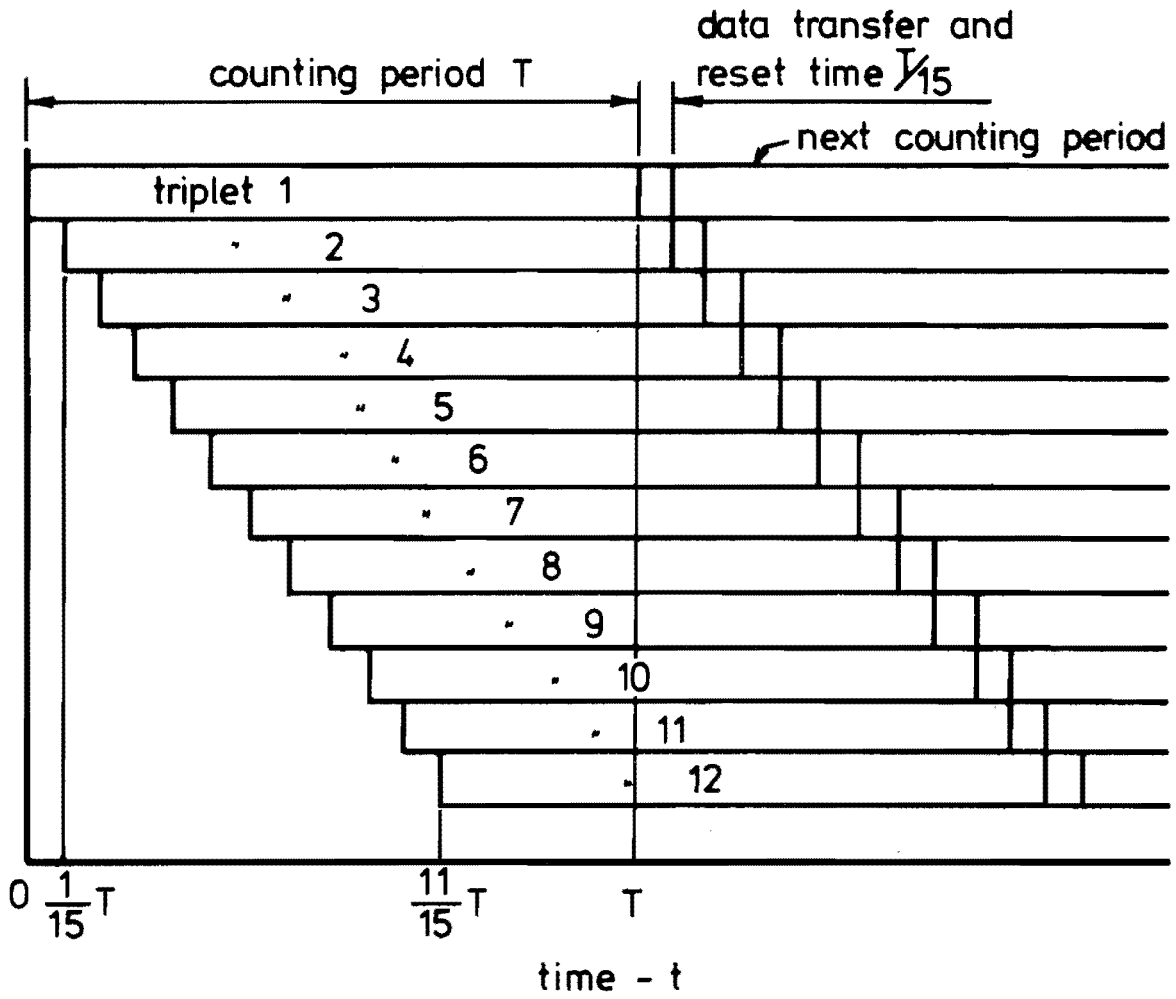

FIG 3·13 RELATIVE START AND FINISH COUNTING TIMES FOR EACH TRIPLET OF ANEMOMETERS

their limits and thus cause the data to be difficult to decode. When this happens, negative rotational directions are automatically decoded as positive, and vice versa.

An obvious solution to this problem at first glance is to select a high scan rate so that the counters always count to a value much less than their maximums. This is not however the ideal solution as it increases the quantisation error, particularly for the vertical component anemometer, and is discussed later in this section. The best alternative was to select the lowest scan rate so that the counters did not quite overflow.

Wind at a point is inherently variable in both speed and direction, but some of its characteristics have been measured. This enables a characteristic "peak gust" to be determined from an average velocity $\bar{U}$.

The peak gust can be defined as

$$U_{peak} = \bar{U} + b\sigma_u \ , \tag{3.19}$$

where U_{peak} is the peak gust averaged over three seconds, $\bar{U}$ is the average wind speed, σ_u the standard deviation of the longitudinal component, and b is a constant.

Panofsky (1977) suggests that $b \approx 3$ and ESDU (1974b) gives $\frac{\sigma_u}{\bar{U}} = .22$ near the ground. Thus an estimate of U_{peak} is

$$\begin{aligned} U_{peak} &= \bar{U}\ (1 + 3 \times .22) \\ &= 1.66\ \bar{U} \end{aligned} \tag{3.20}$$

However the propeller anemometers respond to much smaller sized gusts than the so-called three second peak gust so that Equation (3.20) is an under-estimate. In order to contain the peak gusts within the counter limits it is necessary that the scan rate be selected so that the average velocity gives a count no more than half of the total count of 127.

The relationship between the propeller rotational speed, the maximum number of counts possible and the scan rate can be used to select a suitable scan rate. The relationship is

number of counts in one scan

$$= 32 \times n \times T \qquad (3.21)$$

The maximum wind speed and the average wind speed for each scan rate, required to record the data accurately, have been tabulated in Table 3.1. The relationship between propeller rotational speed and wind speed used is Equation (3.18), namely U = .2744 n, the calibration coefficient. The maximum velocity is obtained by using the maximum count of 127, and the average velocity by using the count of 63.

T seconds	MAXIMUM VALUES		AVERAGE VALUES	
	rotational speed rps	velocity m/s	rotational speed rps	velocity m/s
$\frac{1}{8}$	31.75	8.7	15.8	4.4
$\frac{1}{16}$	63.5	17.4	31.7	8.8
$\frac{1}{32}$	127	34.8	63.5	17.4
$\frac{1}{64}$	254	69.7	127	34.8
$\frac{1}{128}$	508	139.4	254	69.7

TABLE 3.1 RELATIONSHIP BETWEEN WIND SPEED AND SCAN RATE

From Table 3.1 it can be seen that for these particular instruments, the highest scan rate is redundant as the wind speeds corresponding to it are extremely large. The most useful scan rates are 16 and 32.

The quantisation error results from the fact that the magnitude of

the rotational speed has to be expressed by a fixed set of levels, which is an approximation to the infinite set of levels in the continuous change in wind velocity. An illustration of quantisation error is given in Fig.3.14.

Following Bendat and Piersol (1971), assuming ideal conversion of a signal to the fixed set of levels, the quantisation error has a uniform probability distribution with a standard deviation of ~ $.29\Delta x$ where Δx is the quantising increment. For this particular data using $T = \frac{1}{16}$, Table 3.1 gives

$$\Delta x = \frac{17.4}{127} = .137 \text{ m/s.}$$

Thus the standard deviation of the quantisation error is .29 x .137 = .04. The quantisation error can be considered as a noise on the desired signal. When the count is say 60, the signal to quantisation noise is

$$\frac{60\Delta x}{.29\Delta x} = 207 \text{ or } 46 \text{ dB}$$

i.e. very large.

The quantisation error is however more significant in the data from the vertical component anemometer which typically has counts of 10% of the horizontal component anemometers. Thus for a count of 6 on the vertical component anemometer, the signal to noise ratio is

$$\frac{6\Delta x}{.29\Delta x} = 21 = 26 \text{ dB}$$

Thus even for the vertical component anemometer the quantisation error is small. Its significance is reduced by using as low a scan rate as possible.

3.4 DESCRIPTION OF CARAVAN

A caravan was used to house the data recording equipment and other items required during a field experiment to measure wind structure.

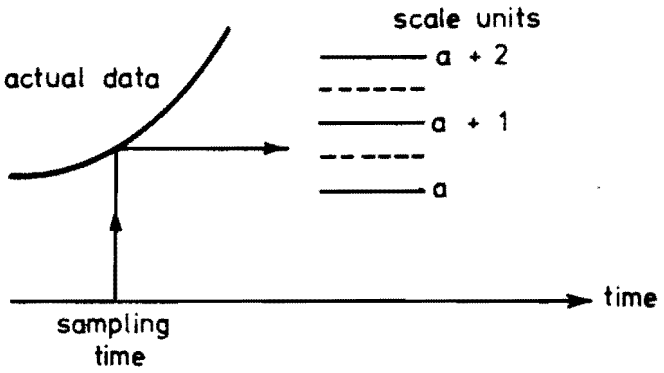

FIG 3·14 ILLUSTRATION OF QUANTIZATION ERROR

The signal multiplexer, control panel and tape recorder were mounted in a vertical stand on small wheels so that it could be taken out of the caravan's expecially large door easily. When the caravan was being towed, the stand was bolted to the caravan wall, and in this position was also convenient to use when data was being recorded. The data recording equipment in the stand is shown in Plate 3.9,bolted to the caravan wall.

The anemometer cables entered the caravan through a small hole in the floor so that they could be connected to the recording equipment permanently when the caravan was left locked. Provision was also made for 12 volt battery lighting in case the caravan was required for temporary accommodation when the unit was being used in remote areas. A portable diesel-electric generator could also be housed in the caravan when field experiments were required in remote areas where there was no mains electric power available. The generator was not used for these field experiments as mains power was available.

The caravan can be seen in Plate 3.10 which also shows the instrument cables from the anemometers on the 20 m tower.

3.5 DESCRIPTION OF TOWERS

Two types of towers to support the anemometer arrays were used in this work. To investigate the variation of wind structure with height, a 20 m crank-up Weather Measure Tower was used and this is shown in Plate 3.10. It is a three-sided relatively open lattice-type structure. The side of the triangular section varies from .4 m at the base to .05 m at the uppermost pipe section. The pipe diameter of the lattice structure is 32 mm and is connected by horizontal straps 40 mm wide at the bottom. At the top the 25 mm diameter pipe is connected by 30 mm wide straps. The horizontal straps were connected approximately every .4 m apart all the way up the tower. At the end of one telescope

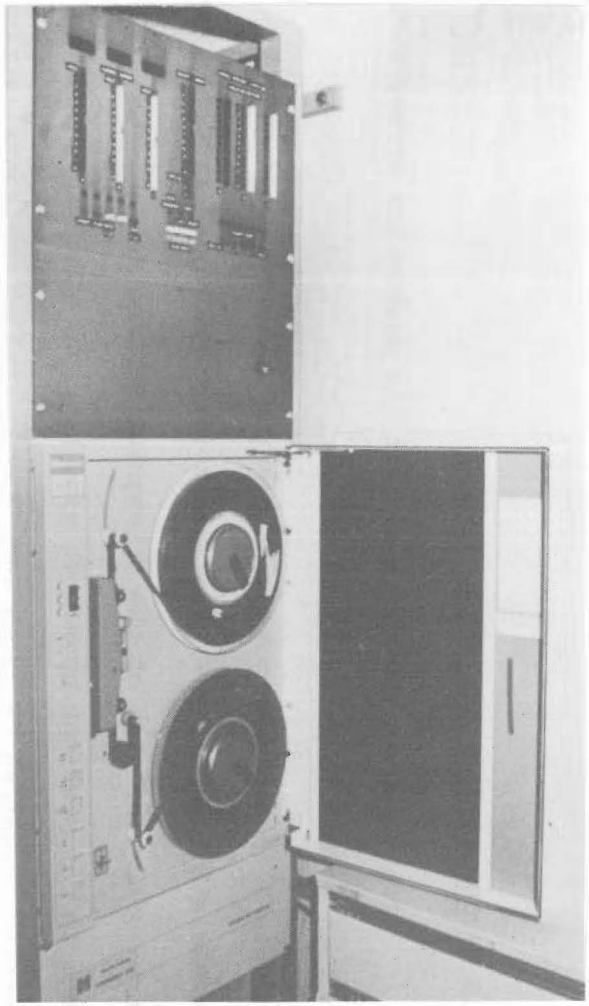

PLATE 3.9 DATA ACQUISITION SYSTEM CONTROL PANEL AND TAPE RECORDER

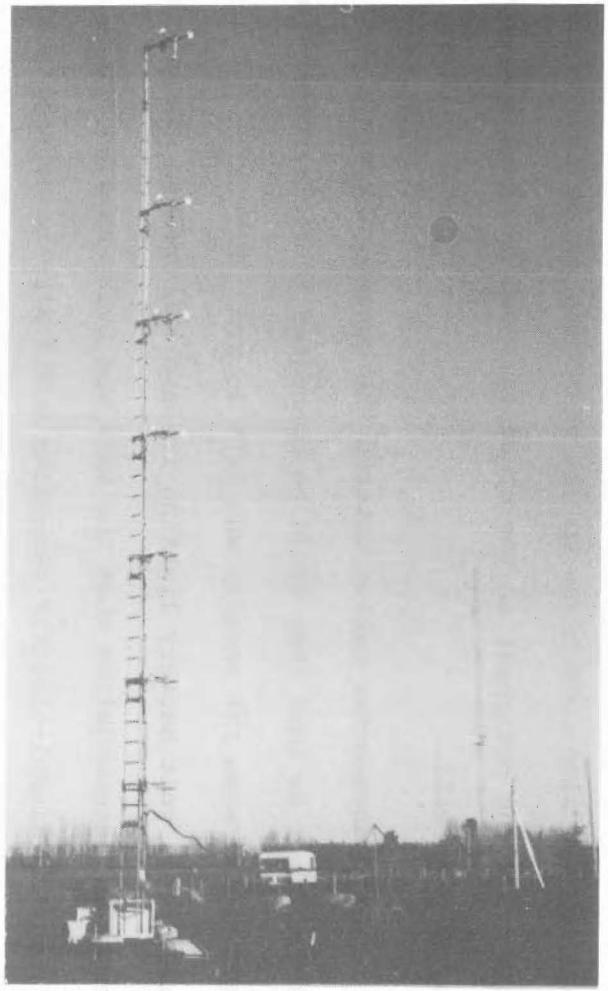

PLATE 3.10 CARAVAN, CABLES, TRAILER, 20 m TOWER AND ANEMOMETERS

type section and the beginning of the next, there was an overlap of about .4 m.

The other types of tower used were 10 m long, 57 mm diameter alloy pipes. These towers consisted of either two or three sections of pipe which fitted together making 10 m in total. Three or four guys were fixed half way up and at approximately .5 m from the top.

In all experimental runs with both types of tower, the anemometer arrays were mounted on the ends of arms 900 mm long facing into the wind direction to be measured. Each anemometer array was mounted with its open aspect to the north-west so that the horizontal component anemometers would not interfere with each other for winds from the north-west. In addition, all data runs were taken when the wind direction was approximately north-west so that the anemometers were never in the lee of the tower.

Gill et al (1967) has performed wind tunnel tests on towers similar to the 20 m tower used in this work. Fig.3.15, from Gill et al (1967), gives the wind velocity reduction at Q where the sensor is mounted for all wind directions.

Reductions in velocity are given for various values of $\frac{R}{D}$, the ratio of the arm length to the side of the triangular tower.

In the work here involving the 20 m tower, the arms were 900 m long from the centre of the tower side to the anemometer fastening bracket, thus R as defined in Fig.3.15 increased as D reduced. The values of R and D for the 20 m tower at the seven positions where the anemometer arrays were mounted are given in Table 3.2.

Data was collected only when the wind direction was in the range 270 - 360 degrees in Fig.3.15 which indicates from the same figure that tower shadow effects were negligible at all heights. The bottom anemometer array might be somewhat affected by the blockage effect of

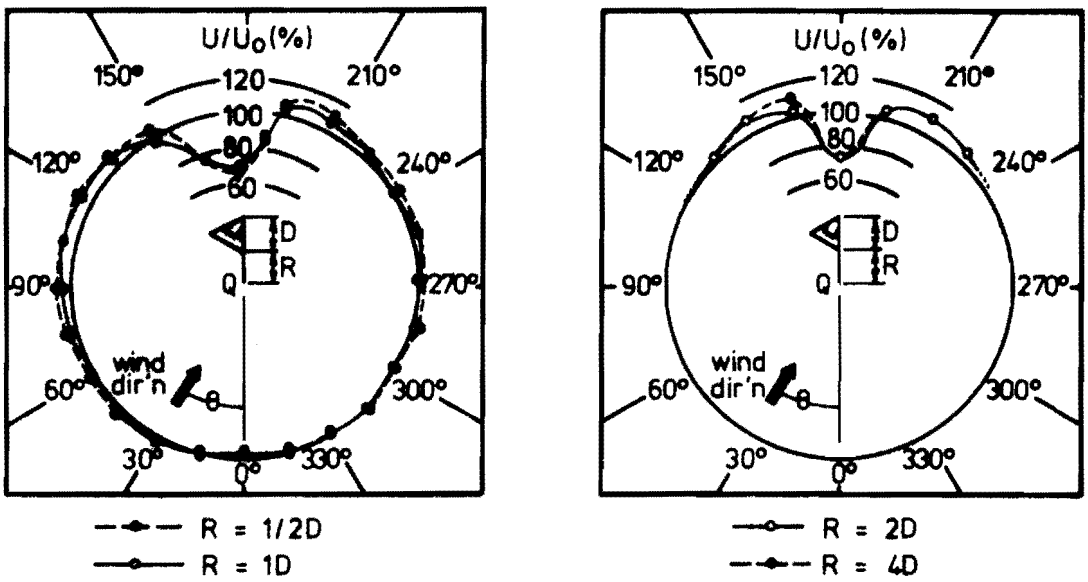

U = measured velocity
U_0 = upstream velocity
Field data collected for wind directions in the range 270°-360° only.

FIG 3·15 WIND SPEED PROFILE AT SENSOR Q, LOCATED A DISTANCE R FROM A TRIANGULAR OPEN LATTICE STRUCTURE TOWER, OF SIDE D.

the trailer on which the tower was mounted. Figure 3.15 also suggests that tower shadow effects are negligible for the 10 m towers as well, since $\frac{R}{D}$ for them is extremely large.

Side of Tower D , mm		Length of arm R , mm	$\frac{R}{D}$
bottom anemometer array	415	690	1.7
	345	730	2.0
	290	755	2.6
	235	780	3.3
	125	837	6.7
	113	843	7.5
top anemometer array	52	874	17.0

TABLE 3.2 20 m TOWER MOUNTING ARM LENGTH AND TOWER SIDE DIMENSIONS

3.6 EXPERIMENTAL ARRANGEMENT IN THE FIELD

In the first experiment which involved measuring the vertical variation of wind structure, seven anemometer arrays were mounted on the 20 m tower as described in Section 3.5. Two theodolites at right angles were used to align the tower vertically and to measure the height of each anemometer array. They were also used to check that the alignment of the vertical component anemometer was within 3 degrees of vertical.

Cables to each of the seven arrays, as well as the nitrogen purge tubes,were taped to the tower. At the base of the tower the single cables were connected to a junction box, one of which is shown in Plate 3.3. Each junction box could be connected to a maximum of nine anemometers. The junction boxes were further connected to a thicker multi-core multi-strand twisted pair cable which transmitted the power

and signals from and to the data recording equipment in the caravan.

A maximum of four of the larger type cables were available, three being 325 m in length and one being 75 m. These cables have suitable amphenol connectors at each end so that they can be connected in series if required, but this limits the total number of anemometers which can be used simultaneously.

To reduce the current required in the long thicker cables, the power supply wires in it supplied power at 100 volts which was regulated down to 12 volts at the junction box for transmission through the shorter cables to individual anemometers. These individual anemometer cables were shorter than the four larger ones, and had lengths of 7, 15, 22 and 25 m.

Particular note had to be taken of the connections between the anemometers, cables, and terminal boxes as mistakes made during initial equipment installation were difficult and time consuming to find without first running some data through the computer. Note also had to be made of the anemometer and propeller code numbers to facilitate maintenance of the correct anemometer if failure occurred. As stated in Section 3.3.1 the cables were always connected so that data from anemometers aligned in the x_1, y_1 and z_1 directions was recorded in the first, second, and third groups of 8 bits in a single triplet respectively.

In this experiment the most economical use of tape space was made by connecting the seven anemometer arrays into the first seven triplets of the multiplexer addresses, and recording data from only these triplets to tape.

The second experiment used a series of eight 10 m towers whose layout is described in Chapter 4. The same precautions regarding setting up this experiment had to be made as in the former one.

The main difference between this experiment and the former in

actual cable connections was that this experiment made full use of all the cables and terminal boxes in order to achieve the desired span of 315 m. In fact limitations in the number of cables and terminal boxes meant that data from all twelve triplets had to be written to tape, although four of them, interspersed between the others had no anemometers connected.

In both experiments, before a data recording was taken the wind direction was checked visually by observing a nearby wind vane, and the wind velocity was checked by observing the visual display on the control panel of the data acquisition system. A check was also made of the amount of insolation, and depending upon the results of these observations, a data recording was made.

3.7 CONCLUSIONS

This chapter has discussed various aspects of the instrumentation which has been developed to measure the structure of the wind, and was later used in two field experiments.

A survey was made of possible sensors which could have been used for this work. It was found that the most suitable sensor was the Gill UVW propeller anemometer. This was however too expensive considering the large number required for the field measurements envisaged.

Following the decision to build a digital propeller anemometer, the design and main features of the anemometer and propellers were discussed and described.

A detailed study of the performance of propeller anemometers was made which indicated that its main disadvantages were a lack of ideal cosine response, and a finite length constant which limited it to measuring spectral components with a frequency less than about .3 - .5 Hz if no correction for its length constant was made.

The method by which the data from anemometers is recorded onto 7-track magentic tape was discussed,which indicated that providing the correct scan rate i s selected, the motion of the propeller is faithfully recorded onto the tape.

By mounting the anemometers on arms at least 900 mm long and pointing towards the approach wind direction, it has been shown that the 20 m lattice-type tower does not affect the wind velocity measured significantly. The 10 m towers also have negligible effect.

The final section states that care needs to be exercised in connecting the equipment so that it may be processed with the least amount of trouble on a computer.

The instrumentation is able to faithfully sense and record the wind velocity fluctuations, so that the data may be processed to yield reliable wind structure parameters. The results of the vertical component anemometer have to be interpreted in the light of its length constant at its operating region.

CHAPTER 4

SITE DESCRIPTION

4.1 REASONS FOR THE CHOICE OF THE SITE

A site, to conduct the field measurements of wind structure, was required which was reasonably close to the University of Canterbury to enable regular inspections of the instrumentation to be made easily. It had to be representative of typical rural terrain in Canterbury and with the approach terrain roughness as near homogeneous as possible. It was also necessary to have easy car access to the caravan housing the data recording equipment and to the towers, to facilitate installation and maintenance of the instrumentation.

The site selected for the wind structure measurements satisfied all of the above criteria. It was on a research farm situated at Lincoln Agricultural College about 16 km south-west of Christchurch, in the South Island of New Zealand.

4.2 THE APPROACH TERRAIN

Plate 4.1 shows the type of terrain typical for the area. This type of terrain of level plains of short grass with occasional trees, sparcely distributed shelter belts and farm buildings extends for a distance of about 100 km in the north-west direction towards the Southern Alps. It also extends for about the same distance to the north and west. To the east of the site lie the hills of Banks Peninsula, and to the north-east, the city of Christchurch.

The immediate area of the site is described in Fig. 4.1, and also by Plate 4.2. 200 m to the south of the 20 m tower, Number 2 in Fig. 4.1, a shelter belt of fir trees is situated. There is also another shelter belt at the south-west end of the line of towers. Since only winds from

PLATE 4.1 TERRAIN SURROUNDING MEASUREMENT SITE

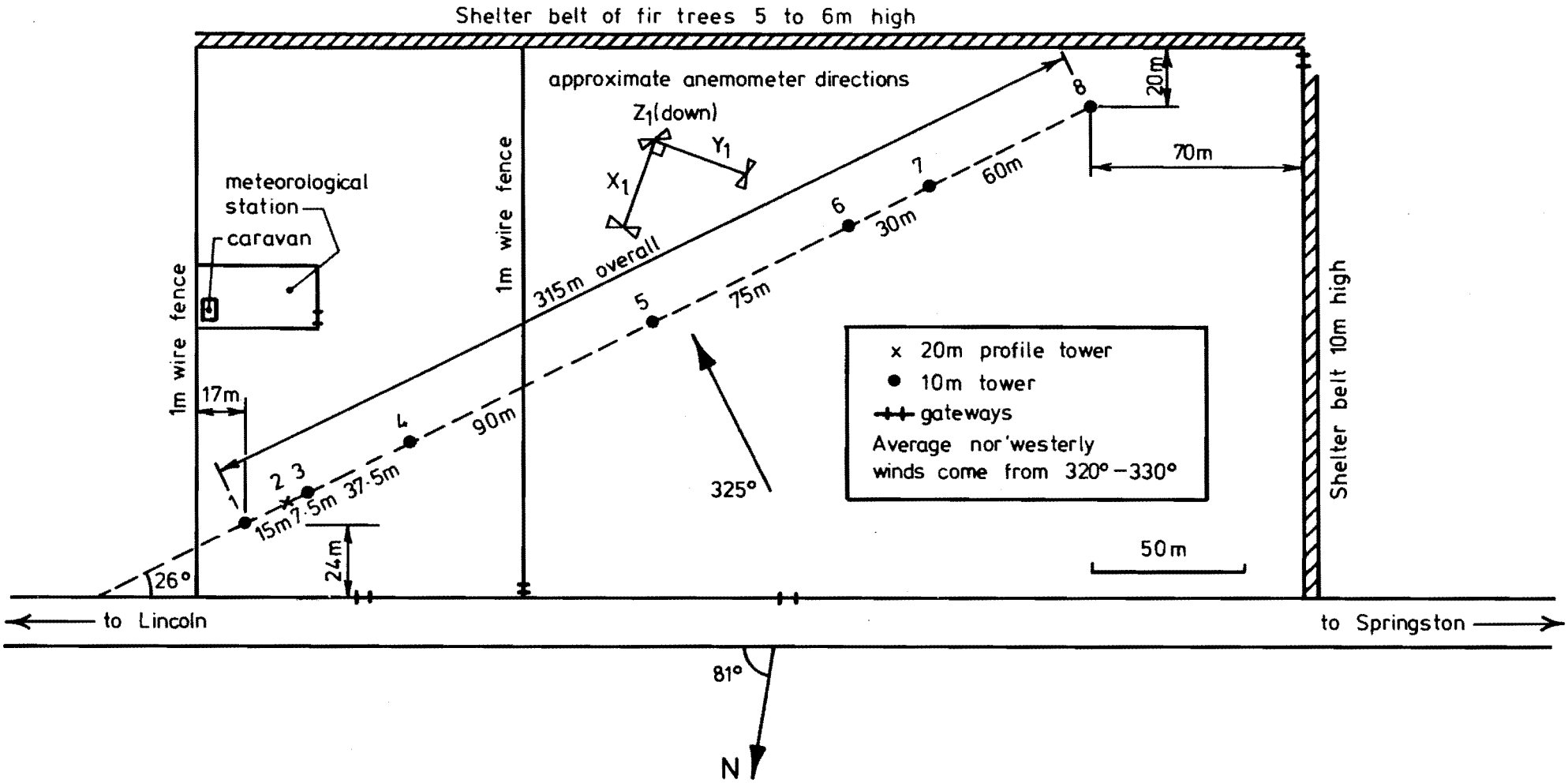

FIG 4.1 MEASUREMENT SITE

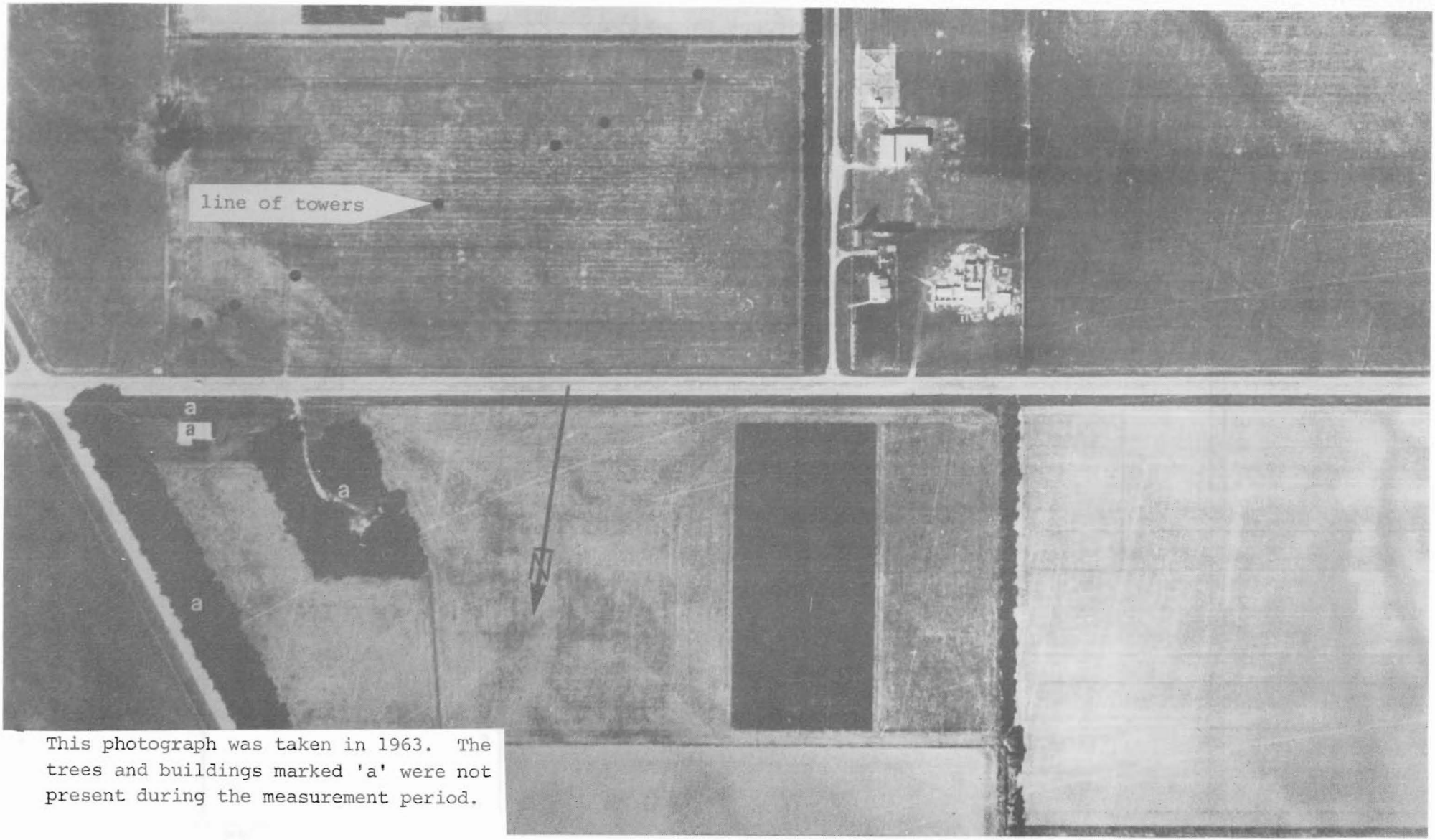

This photograph was taken in 1963. The trees and buildings marked 'a' were not present during the measurement period.

PLATE 4.2 IMMEDIATE SURROUNDINGS OF THE MEASUREMENT SITE

the nor'westerly quarter were to be analysed in this study, neither shelter belt was of any concern for measurements to be made on the 20 m tower. However wind from the nor'westerly quarter, impinging on tower Number 8 used during horizontal spatial cross-correlation measurements, had to pass over the south-west shelter belt. Tower Numbers 6 and 7 were also somewhat in the lee of the same shelter belt.

Plate 4.3 shows the terrain looking from the base of the 20 m tower towards the north-west, i.e. the terrain immediately upstream of the 20 m tower, and Plate 4.4 shows the row of eight tower mounted orthogonal arrays of anemometers from the north-east end of the tower line.

At various times sheep grazed in paddocks upstream from the towers, and in the paddocks in which the towers were situated. This can be seen in Plate 3.10 which also shows the 20 m tower, the caravan and the instrument cables hanging from poles out of reach of the sheep.

Previous work has meant that the vertical variation of velocity, turbulence intensities, longitudinal and vertical component power spectral densities, and autocorrelation functions is now fairly well known for this type of terrain. ESDU (1974b) gives terrain of this type, which corresponds to between "few trees" and "many trees, hedges, few buildings" in its classification, a value of the roughness length Z_o in the range between .02 m and .2 m. Davenport (1963) suggests that for flat open country a power law velocity profile of the form

$$\frac{\bar{V}_Z}{\bar{V}_{ref}} = \left(\frac{Z}{Z_{ref}}\right)^{\alpha}$$

should have a value of $\alpha = .16$, where

$\bar{V}_Z$ is the average velocity of height Z, and

$\bar{V}_{ref}$ is the average velocity at the reference height Z_{ref}.

Davenport also suggests that the gradient height Z_G should be 300 m, and the drag coefficient, K_{10} should be .005. The drag coefficient at 10 m

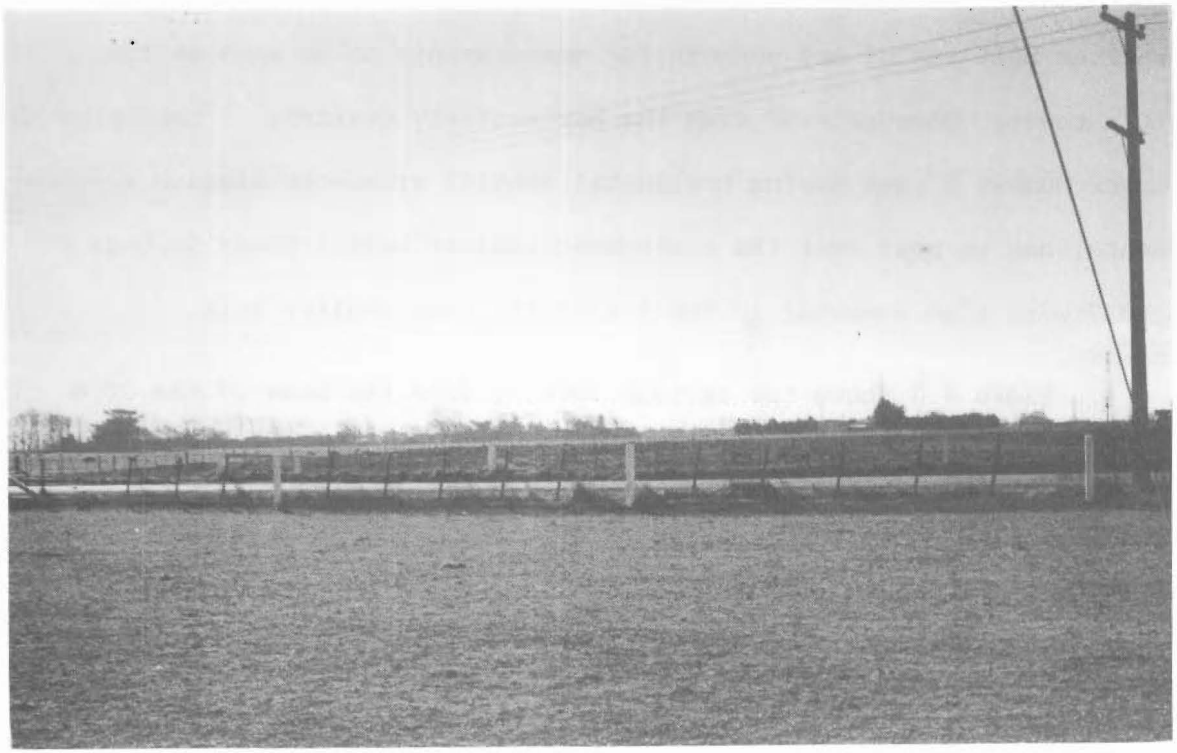

PLATE 4.3 TERRAIN TO THE NORTH-WEST OF THE 20 m TOWER

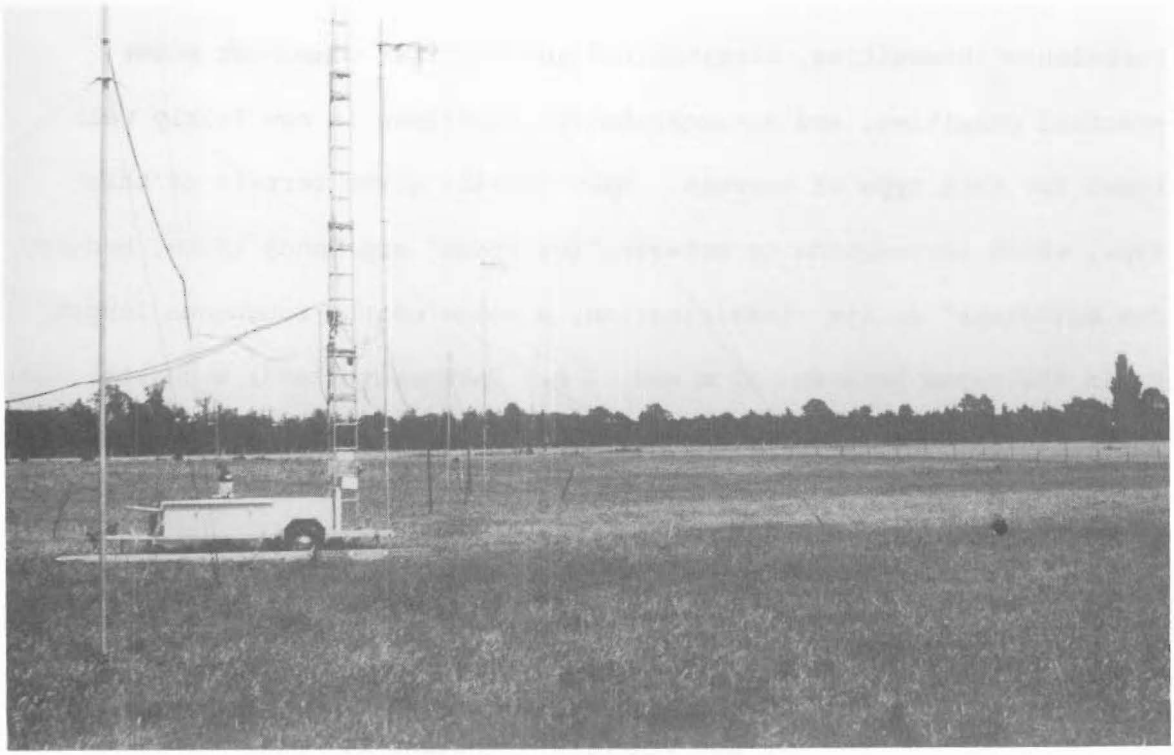

FIG.4.4 TOWER MOUNTED ANEMOMETER LINE FROM THE NORTH-EAST END

is defined as

$$K_{10} = \left(\frac{U_*}{\bar{V}_{10}}\right)^2 \quad , \text{ and } U_* \text{ is the friction velocity.}$$

This type of terrain also lies in Counihan's (1975) Category 2 of Moderately Rough. Counihan thus suggests Z_o in the range .001 to .2 m, and α in the range .13 to .16.

4.3 LAYOUT OF TOWERS

The measurements of wind structure consisted of two separate experiments with different tower layouts. In the first experiment, which examined the vertical variation of the wind structure, the single 20 m tower only was used, i.e. tower Number 2 in Fig.4.1. Seven orthogonal arrays of anemometers were attached to the 20 m tower and measured the wind velocity from the nor'westerly direction, the only wind direction for which data was recorded. The position of the 20 m tower was selected so that it had good exposure for winds from the north-west.

The second experiment was concerned in obtaining horizontal spatial cross-correlation measurements. Eight 10 m towers, with orthogonal arrays of propeller anemometers atop them, were thus arranged in a straight line perpendicular to the direction of the average nor'westerly wind expected, the only wind direction for which data was recorded for this experiment as well. The horizontal distance between towers was calculated such that a large number of spatial separation distances could be obtained from the minimum number of towers. The number of different distances between towers was twenty-four.

The minimum separation of 7.5 m was selected to yield a high correlation between the velocity components, and the total span of 315 m, so that the correlations would fall completely to zero well within it.

CHAPTER 5

DATA PROCESSING

5.1 INTRODUCTION

The nature of this research and the method by which data was recorded meant that a large amount of effort was involved in data processing.

The instrumentation used in this research has been discussed in detail in Chapter 3. A line diagram of the path of the data from the anemometer to the 7-track digital magnetic tape is given in Fig.5.1, and the physical layout of one tape record of data is given in Fig.5.2

The data was written sequentially to the tape in the order that the anemometers were scanned. At the beginning of each scan 24 bits were used to provide scanning information, not only to locate the beginning of a scan but also to provide information on details of the data recording parameters. This is shown in Figs.3.11 and 3.12.

The wind velocity data written to the tape was simply the numbers contained in each 8 bit counter. These numbers were obtained from integrating the pulses from the square waves output from each anemometer for a selected time period, taking due account of the rotational direction. Thus the numbers 0 to 127 indicated increasing positive rotational speeds and numbers 256 to 129 indicated increasing negative rotational speeds. In some cases selected channels were "failed" manually by the operator during a data recording by operating a switch on the data acquisition system control panel. When this occurred the number 128 was written to the tape in the selected channel for all future scans.

A channel might be failed if the counters were observed to count past their limits above or "over flow". This occurred when the scan

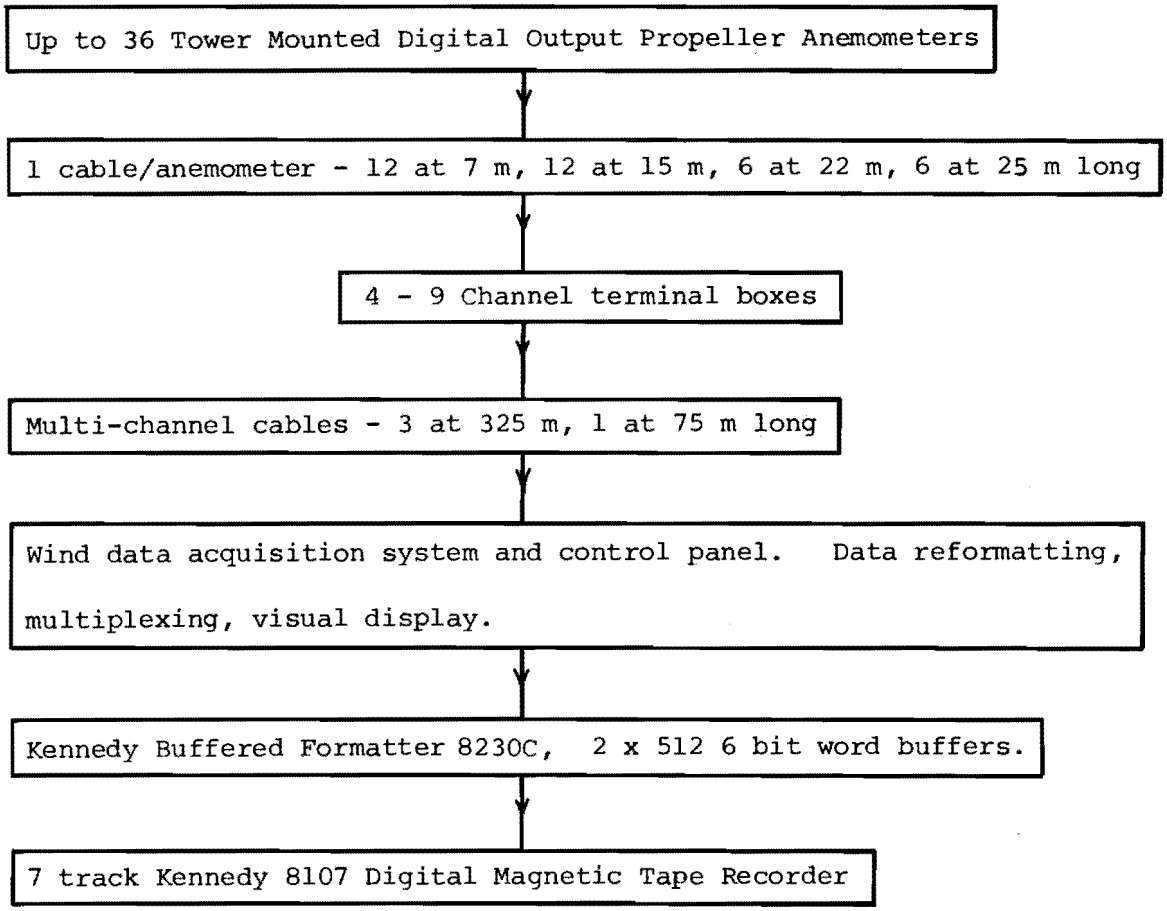

Fig. 5.1 Data Path - Anemometers to Magnetic Tape.

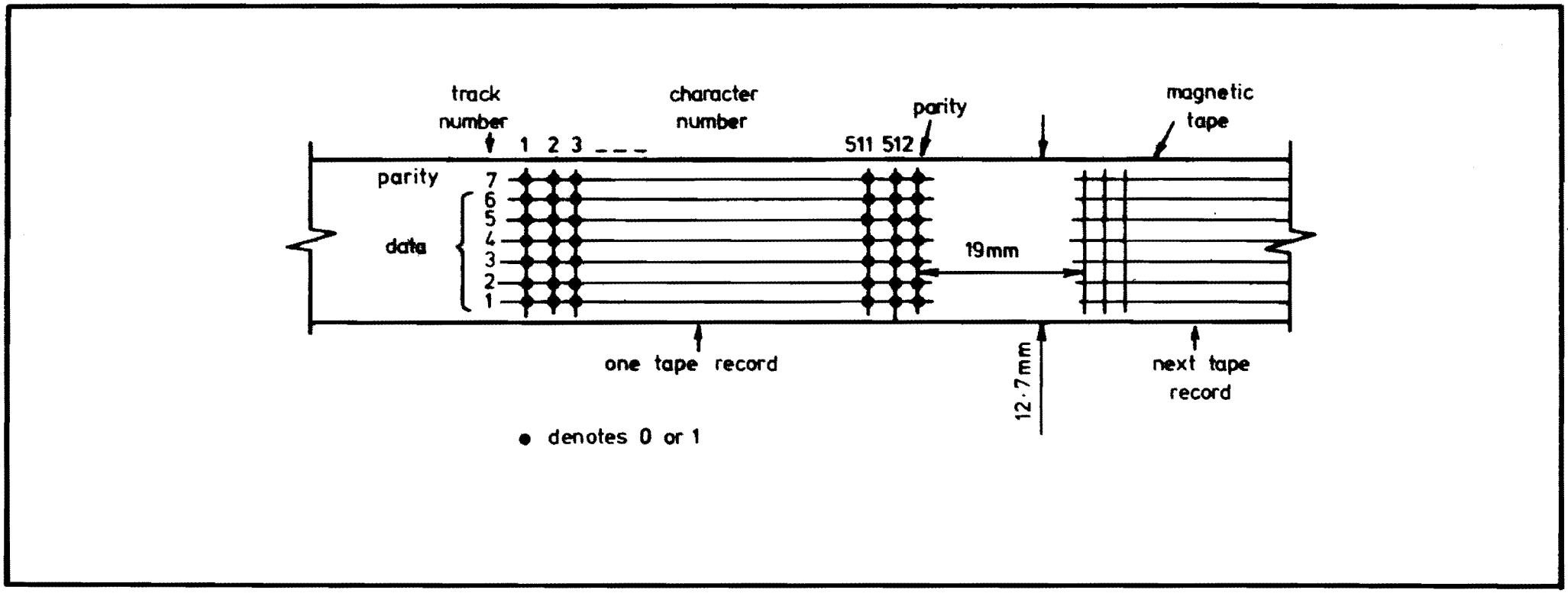

FIG 5·2 DATA LAYOUT OF ONE TAPE RECORD

rate selected was too low. A channel might also be failed if an anemometer was observed to malfunction. However, data from channels which were observed to overflow were not always necessarily failed as sometimes the data could still be analysed. It could only be analysed if the anemometers concerned were observed to rotate only in one direction throughout the entire data recording. In this case the program COPYDATA, discussed in Section 5.3, could be directed to override its normal assumptions regarding anemometer rotational direction. This is discussed further in Section 5.3.

In order to process the data most efficiently, a suite of computer programs were written in Algol and run on the University of Canterbury's B6712 computer. The order in which the programs were run and their main features of interest are given in Fig.5.3.

Some of the programs were written to investigate the effect of various processing methods on the final result of the turbulence parameters. Now that these effects are known, this flexibility in the programs is virtually redundant. However, it is described here for completeness. Other programs were written to find hardware errors during commissioning of the instrumentation. These have not been included, nor have the many programs written to check the accuracy of certain parts of the software used, e.g. Fourier transforms of square waves to see that library procedures worked correctly etc.

The final set of programs has evolved over a period of about three years, each updated version of a program being better than the previous version. For example, the references Bendat and Piersol (1971), Akins and Peterka (1975) and Bergland (1969) each give slightly different methods of computing autocorrelation functions by fast Fourier transform (FFT) techniques. Several of these were tried before the one used in this work was adopted.

At the outset of this work it was considered that the best way

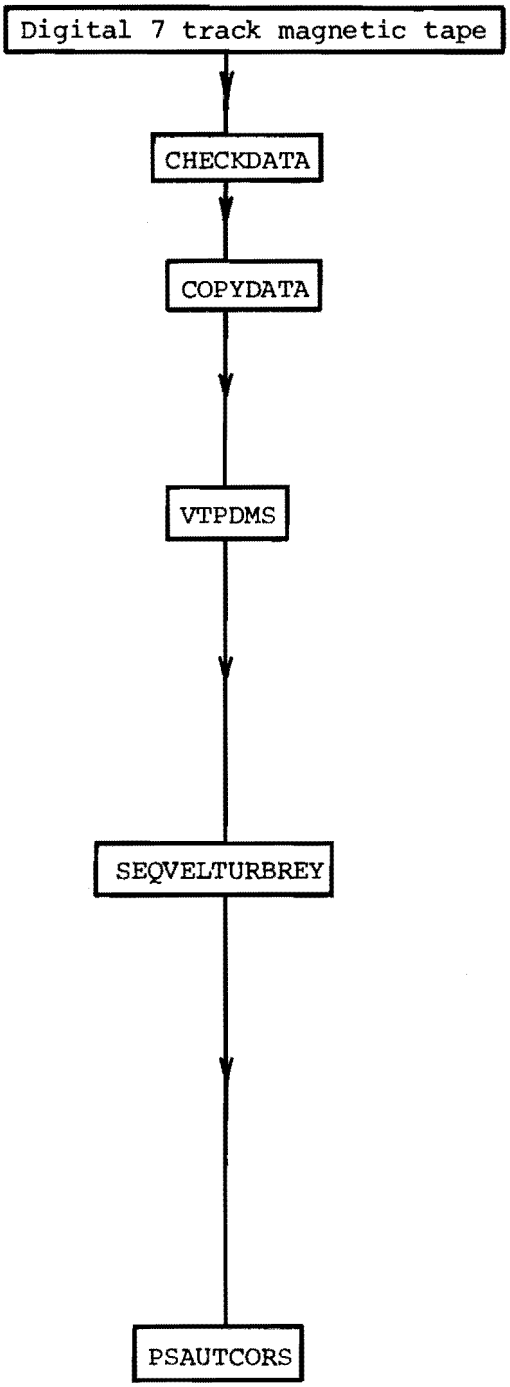

- hardware errors

- reformatting, data compression data copied to computer library tape

- Velocity time, probability density distribution and mean squares graphical output - enables data to be checked visually

- Average velocities, directions, turbulence intensities and Reynolds stresses calculated for selected file lengths, sampling frequencies, and both with and without correcting for non-cosine response

- Power spectral densities, autocorrelation functions, cross-correlations, with selected trend removal type, file length, sampling frequency etc.

Fig. 5.3 Sequence For Running Programs

to process the data would be to estimate the reliability of the data on the actual tape used in the field experiment. This would involve checking for system hardware errors, and also making comparisons between simple parameters such as average velocities and wind directions, with observations made at the time the data was being recorded. If the data at this stage looked reliable, it would then be copied to a Computer Centre library tape which is easier to handle under the Burroughs system. Subsequent programs used to calculate the wind structure parameters required,would use the data as it was stored on the library tape. The programs developed to achieve these objectives are briefly outlined below.

The program CHECKDATA was designed to analyse data directly off the field experiment data tape. It checked for a variety of hardware errors and errors which could occur during a data recording such as the scan rate selected being too low. Providing the data still appeared to be useful after program CHECKDATA was run on it, program COPYDATA was used to copy the data to a library tape. The data was reformatted in the process and only the desired anemometer channels were copied to the library tape.

The program VTPDMS was used to plot a velocity time graph of the longitudinal velocity component from all anemometer arrays. The probability density distribution was also plotted and compared with the Gaussian distribution for the three orthogonal directions-longitudinal, lateral and vertical for all anemometer arrays. The mean squares of the longitudinal velocity component,averaged over 2.28 minutes were also plotted as a function of time.

This program was thus used to inspect the data visually for errors and trends. It was also capable of removing a linear and a parabolic trend before the above output was plotted.

Providing that the data still appeared to be error free, the two programs SEQVELTURBREY and PSAUTCORS were run, using this data as input, to calculate the turbulence parameters required.

5.2 PROGRAM 'CHECKDATA'

This program was always the first to be run with new data. It was written so that it read data sequentially off the 7-track field data storage tape,a record at a time (see Fig.5.2), whereas the other programs, except for COPYDATA, read the data from a 9-track Computer Centre library tape.

There were a variety of errors which could and did occur when data was being recorded in the field. This program was written so as to anticipate these likely errors so that the data could be recovered if this was possible. It also gave useful error messages for future program runs to recover the data,in case this was necessary. Consequently the program was developed as these errors occurred, and now in its final form is more sophisticated than it was at the beginning of the field tests.

It has already been stated in Section 5.1 and detailed in Section 3.3.1 that each scan of data on the tape is preceded by 24 bits containing scanning information. The first group of 8 bits contains the bit pattern 01111111 which as a binary number is 127 and indicates the very beginning of a scan. The next group of 8 bits contains information on the special channels and the scan rate. The final group of 8 bits uses bits 0 to 5 to give the number of channels of data which have been recorded onto the tape. For further details, Section 3.3.1 should be consulted.

In order to decode the information on the tape, the program uses the fact that three anemometer channels are grouped together to give

3 x 8 bits of information. For consistency in the analysis of data in later programs, these three channels which form one triplet are usually connected to the anemometers aligned in the x_1, y_1 and z_1 directions from a single orthogonal array of anemometers, which then have identical counting times. The 24 bits from a single triplet is then multiplexed into four 6 bit characters for storage on the tape in records of 512 6 bit characters.

Burroughs 6712 Algol allows 6 and 8 bit pointers which can be used to extract characters of 6 or 8 bits from one Burrough's word which is 48 bits. Hence the first record of data on the 7-track tape is read into 64 words of a one dimensional array. This follows because

512 x 6 bits = 384 x 8 bits = 64 x 48 bits.

Each word of the array therefore contains six 8 bit characters. Normally an 8 bit pointer is scanned along the array which extracts each 8 bit character and puts it into one word of an array, or into an integer or real variable.

Finding the first scan involves finding the first 127. Since this may be a data sample, more than the first 127 must be found. By using an 8 bit pointer, the program looks for the first group of 8 bits yielding the number 127. It then assumes that the next group of 8 bits contains information on the special channels and the scan rate, and the third group of 8 bits contains a number indicating the number of channels in use. It then uses this value to locate the 8 bit character which should correspond to the beginning of the next scan by assuming that it occurs at 3 + (the number of channels) 8 bit characters after the first 127. Finding 127 in this location it goes to the beginning of the next scan. If this value is 127 it knows that it has correctly found the beginning of the data file. The program then returns to the first 127 and starts decoding each channel of anemometer data separately.

If 127 does not appear where it should, the program returns to the character immediately following the first 127 and works along the record until it finds the next 127, after which it repeats the steps outlined above. In order to satisfy the test for the data beginning, the program will look for 127 right along the tape record. If the data file beginning test is still not satisfied, the program assumes that a 6 bit slip has occurred, i.e. multiple numbers of 6 bits have been lost between the multiplexer and the buffered formatter, as described in Section 3.3.2. This is easily appreciated after observing Fig.3.11.

This test for the beginning of the data file corresponds to the statement "Positively identify the beginning of the file" in Fig.5.4.

6 bit slip only occurs however,when a high scan rate has been selected and a large number of channels are being recorded. It appears not to occur when a realistic scan rate of 16 or 32 is selected, and did not occur in this work, although it may also possibly occur when the tape recorder heads are dirty. When it has occurred, scanning along a record in groups of 8 bits will mean that the test for the beginning of the data stream will never be satisfied.

When it is required to, the program copes with 6 bit slip in the following way. It assumes firstly a 6 then 12 then 18 bit slip has occurred. If the data file beginning is still not found the record is rejected and the next record is read off the tape and processed in the same way. To extract the information after a 6 bit slip, a feature of Burrough's Algol called "Bit Concatenation" is used. In this, the pointer is positioned to the second character, character 1, in the first word of the array, and a combination of bits from character 1 and character 0 are merged into another variable. This is shown in Fig.5.5

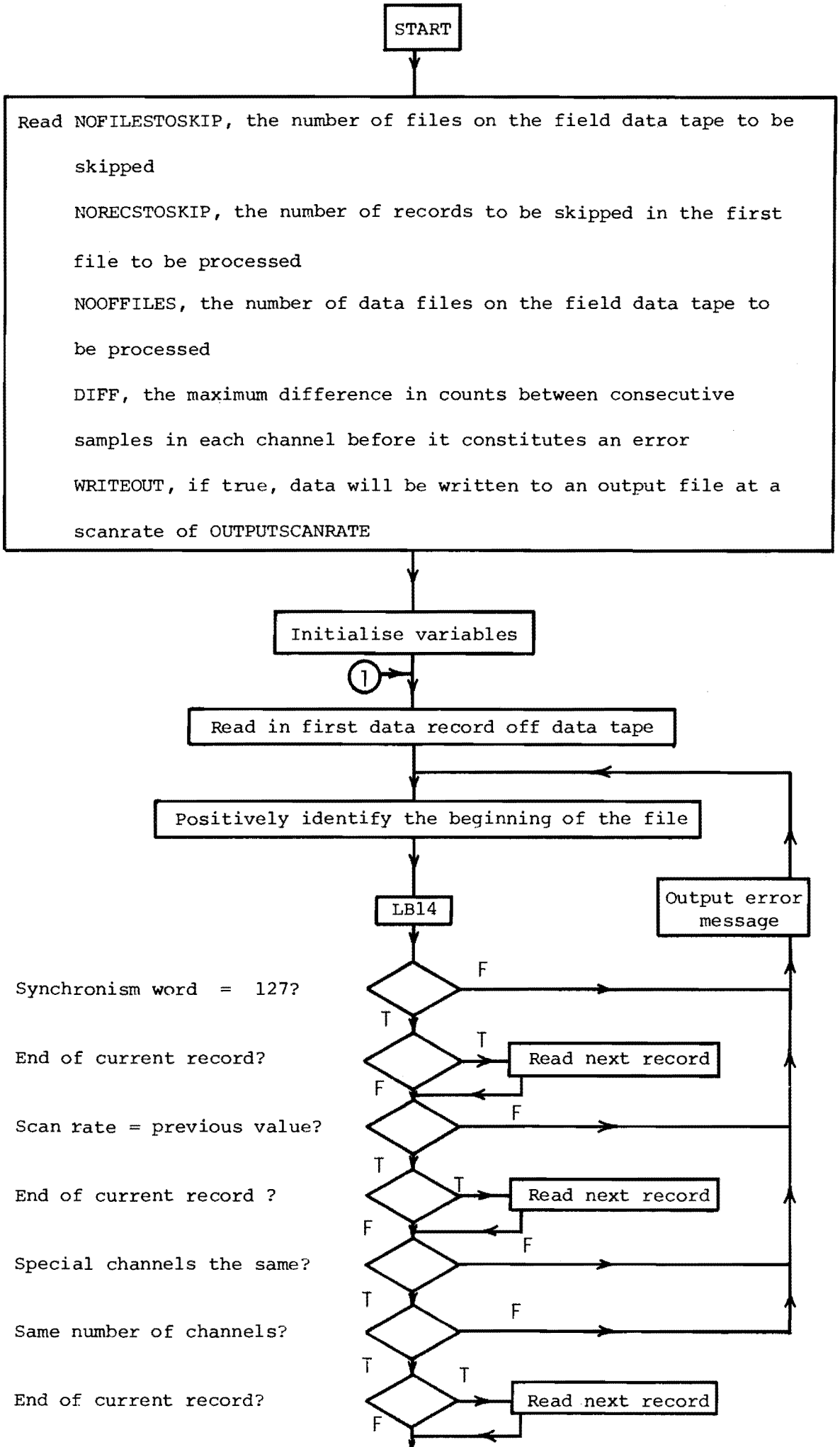

Fig. 5.4 Flowchart of Program CHECKDATA (Continued)

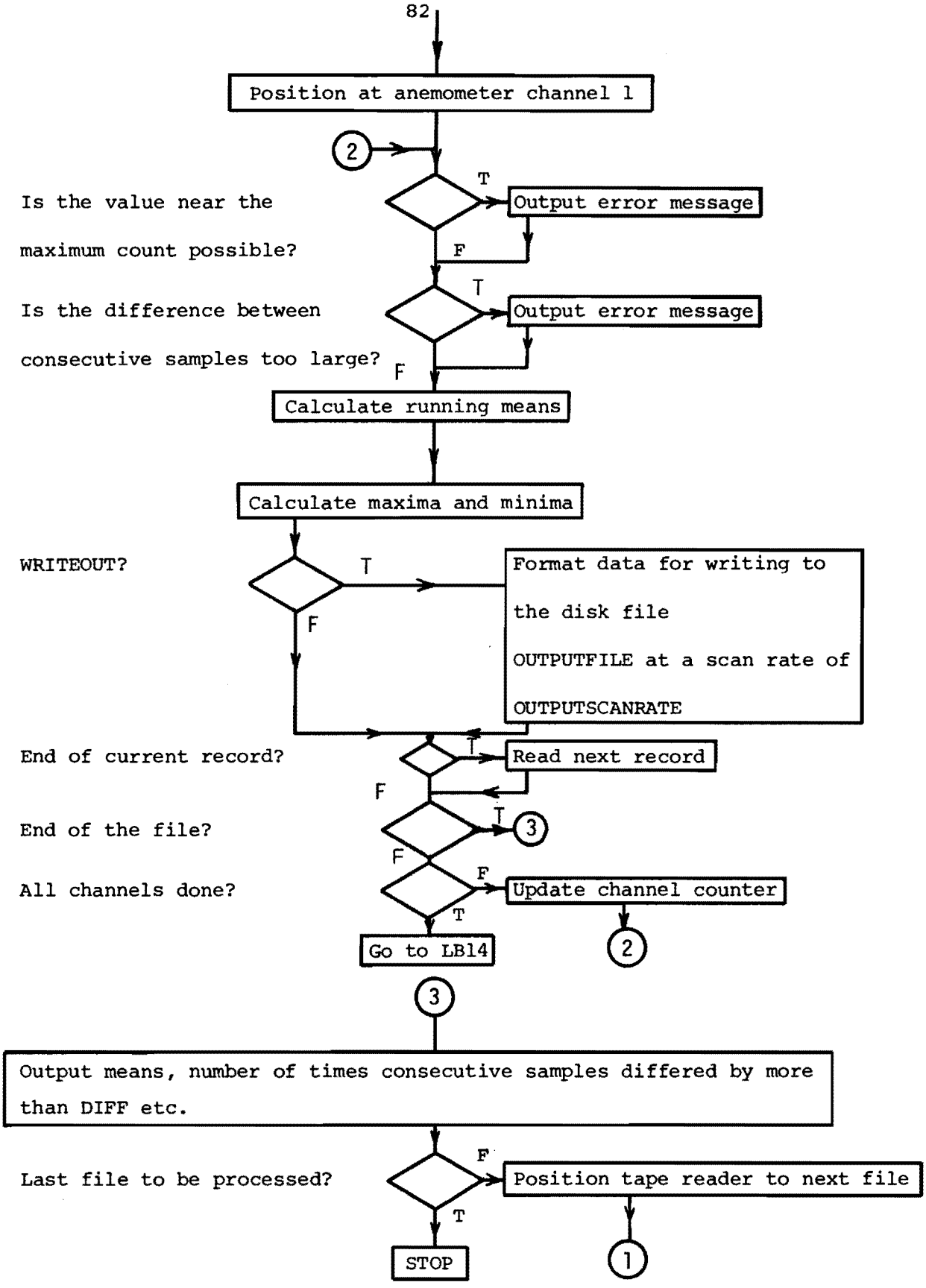

Fig. 5.4 Flowchart of Program CHECKDATA

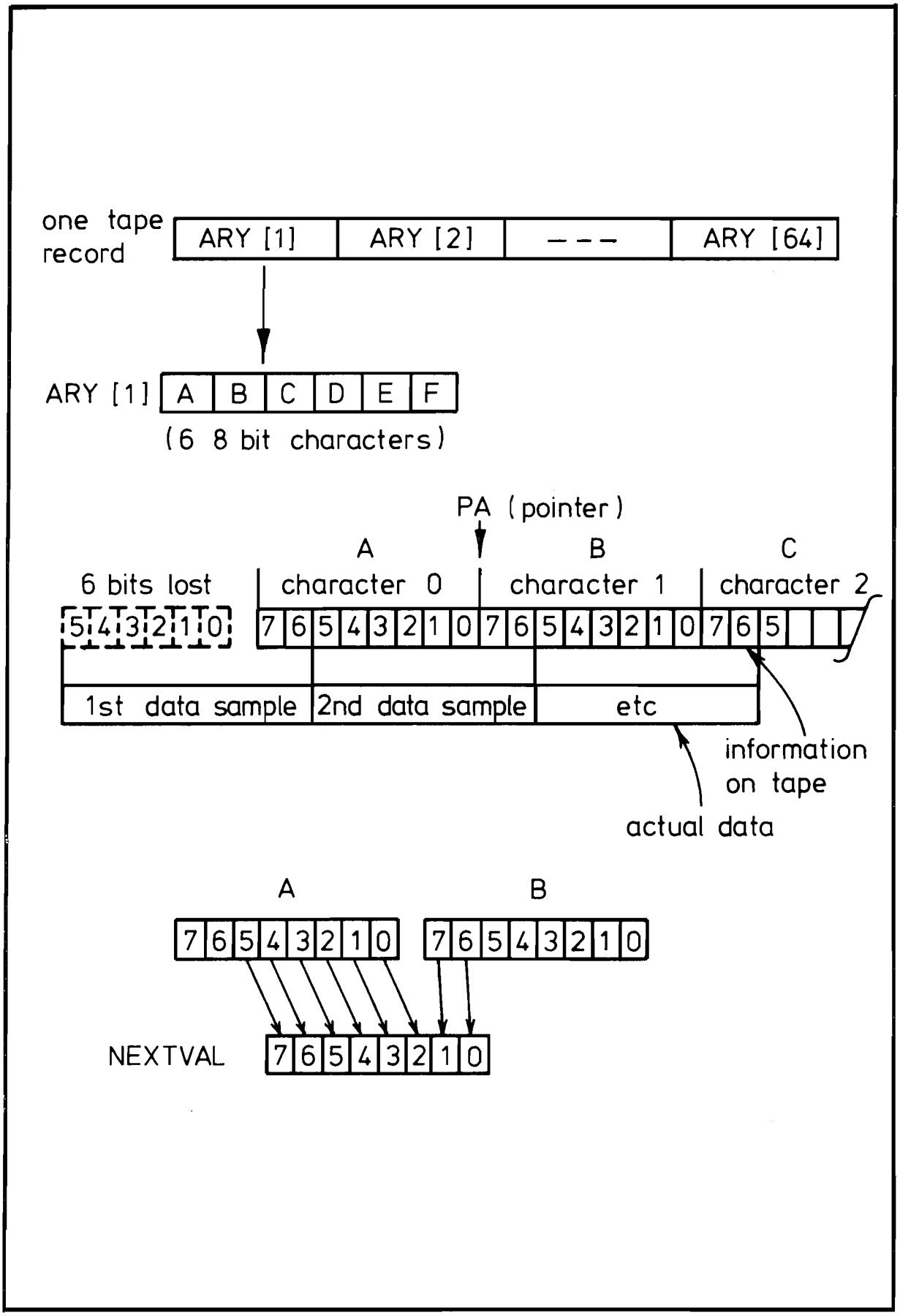

FIG 5·5 6 BIT SLIP

For a 6 bit slip,the statement (see program listing in Appendix B)

NEXTVAL: = 0 & REAL (PA,1)[1:7:2] & REAL (PA-1,1)[7:5:6]

is used.

This can be interpreted as setting NEXTVAL to zero, then merging two bits into NEXTVAL starting at bit 1, from character B starting at bit 7. Then merging 6 bits into NEXTVAL starting at bit 7, from character A starting at bit 5.

The pointer is positioned along the array, being updated by 8 bits at a time, and the data extracted by the above technique. A similar type of statement is used for 12 and 18 bit slip. When the end of the current record is reached, the last 8 bits of the current record are positioned at the beginning of the next record to facilitate decoding the next record. Referring to Fig.5.4, coping with 6 bit slip is performed automatically in the statements "Read next record".

Providing the bit pattern on the tape can be decoded into data as above, various tests as outlined in the flow chart in Fig.5.4 are made to see that errors did not occur during the recording.

The beginning of every scan is checked to see that it is equal to 127. The bits used for the special channels and the scan rate values are checked to see that they are still equal to their values from the previous scan, as are the bits indicating the number of channels in use. If any are different, an error message is printed and decoding starts again from this position. In practice, this should not occur as the end of each file should be finished with an end of file mark before another file, perhaps at a different scan rate, is started.

Each sample from the anemometer channels is checked firstly to see that it is not near the maximum count possible, which occurs when the scan rate selected is too low. The value is then checked to see that

it is not equal to 128, which would indicate that the channel had been failed manually by the operator during the data recording, by operating a switch on the data acquisition system control panel. Consecutive samples from each channel are compared,as malfunctioning anemometers cause the difference between consecutive samples to be much larger than they should be,considering the physical characteristics of the anemometer. Bits incorrectly changing state and other hardware errors may cause this to happen also. When the difference is greater than a predetermined value, an error message is printed which enables the faulty channels to be easily identified and the data from them ignored.

A running mean from each channel is calculated using two methods. Firstly a mean of the actual numbers from the counters is calculated, and secondly a mean is calculated taking account of the sign of each data sample. In the same way, the maximums and minimums from each channel are calculated also. The output from the program can then be used along with observations made at the time the data was recorded to see if the values are reasonably near those expected. Depending on the result of this comparison, the data file may be rejected or accepted.

The program also contains the facility for writing the anemometer data to an output disk file. This is a feature which is not normally used but is available if required. It is required only when a 6, 12 or 18 bit slip has occurred because the program COPYDATA cannot cope in this case. This facility is only rarely required because 6, 12 and 18 bit slip occur very infrequently in practice.

A flow chart of the program, detailed with comment statements is given in Appendix B.

5.3 PROGRAM 'COPYDATA'

This is used to read the data off the 7-track tape used in the field and writes the data from it to a library tape.

The field data tape contains scanning information and the format is unwieldy for most computing. Consequently, COPYDATA reformats the data into a form which is more suited for subsequent programs, and also removes unwanted data, e.g. scanning information and data from channels which may have been recorded but have had no anemometer connected, or may have malfunctioned.

During the series of field experiments, some faults were experienced with the 7-track Kennedy Tape Deck. Sometimes when data was being recorded it would suddenly run in reverse. When this happened, either the tape would be removed and another one fitted, or the tape deck would be taken off line from the multiplexer and a new file started near where the tape started to go in reverse. Usually the latter alternative was the one taken as it wasted less tape space and was quicker.

This fault meant that COPYDATA had to have the facility of being able to join files from both different tapes, and from different files on the one tape, or combinations of these.

The scan rate used when data was being recorded was set by the system hardware and the wind speed, and is rather high when compared with the response of the propeller anemometer. A scan rate somewhat less could have been used if the counters servicing the anemometers had been larger, without losing any resolution in the data.

The data is written onto the 7-track tape in a very compact form, i.e. 8 bits per data sample. However, for storage on a library tape, it is most convenient to have one word allocated to one data sample, so what originally took 8 bits on the 7-track tape takes 48 bits on library tape. This six-fold increase in tape space means that input/output time and cost during computing is high if the data is stored directly at the same scan rate. The program thus was designed so that sequential samples from each channel could be added together in multiples of two's to reduce

the scan rate. If 8 consecutive samples from a channel with a scan rate of 16 are added together the scan rate is reduced to 2.

The minimum scan rate which could be used, and which gave values of the turbulence parameters very close to those calculated from data at a higher scan rate is discussed in detail in Section 6.3.

The program could be directed to the channels which contained the data required, missing those channels which were faulty, or which had no anemometer connected. This facility was particularly useful when the second experiment was being performed because some channels in the middle triplets had no anemometers connected. These channels were ignored when the data was subsequently copied to library tape.

The program operation is such that data is read off the 7-track tape and put into a two dimensional array. One dimension is used as the channel number and the other dimension, 256 words long, contains the data from each channel. When this array is full, the required number of samples from each channel are added together to achieve the desired scan rate. These values are then written into another two dimensional array again with the data dimension 256 words long. When this array is full, its contents are written to a disk file.

On the Burrough's system, this is a temporary file which may be lost as soon as the program finishes executing. The data is written to the file in records of 256 words from a particular channel in the order - channel 1, channel 2, ..., channel N, channel 1, channel 2.. etc., where N is the number of anemometer channels containing data to be written to library tape, and has to be a multiple of 3. When the 7-track tape is finished, the temporary disk file is copied to the 9-track library tape for permanent storage.

A flow chart showing the main features of this program is given in Fig.5.6, and the program listing is given in Appendix C.

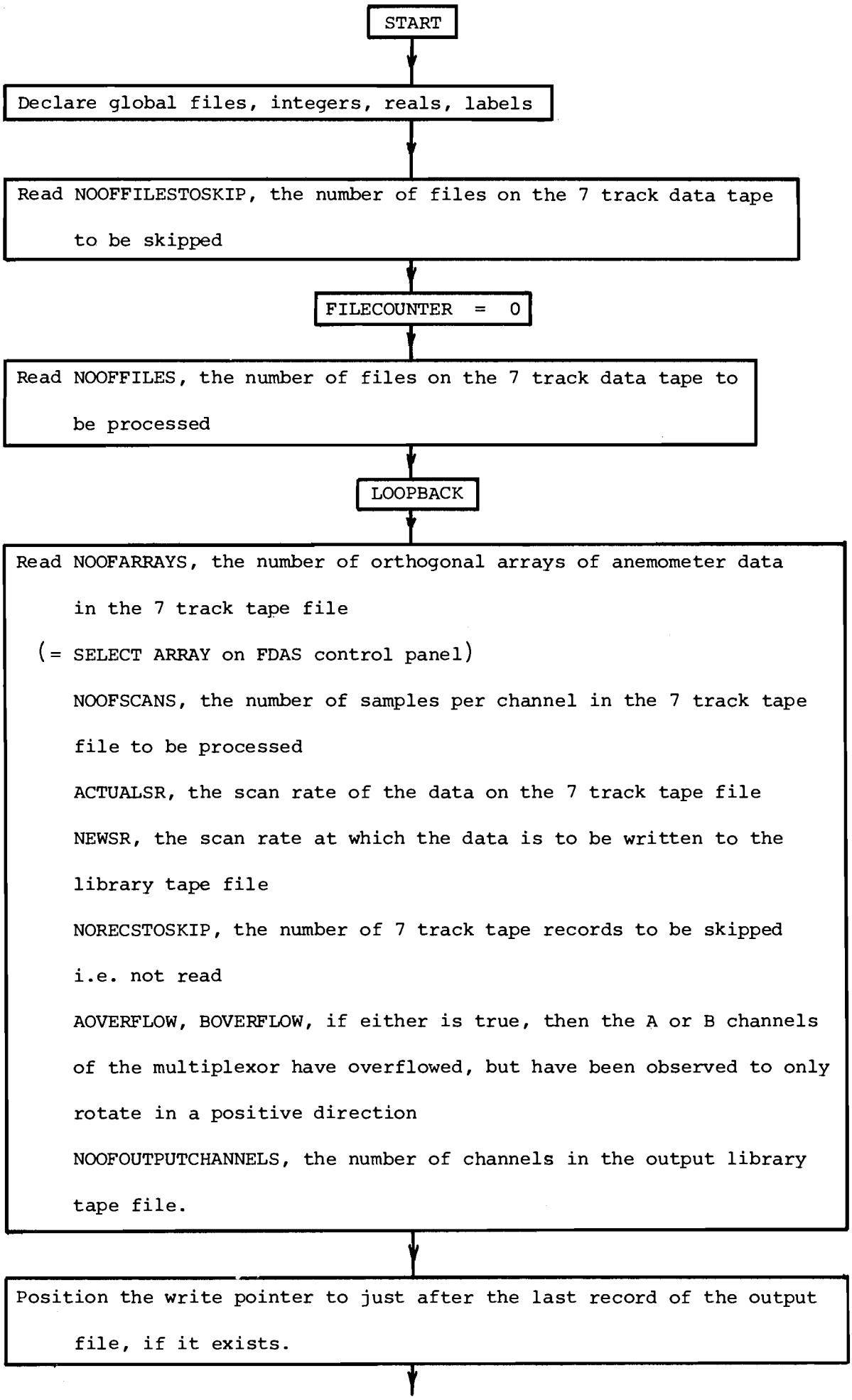

Fig. 5.6 Flowchart of Program COPYDATA. (Continued)

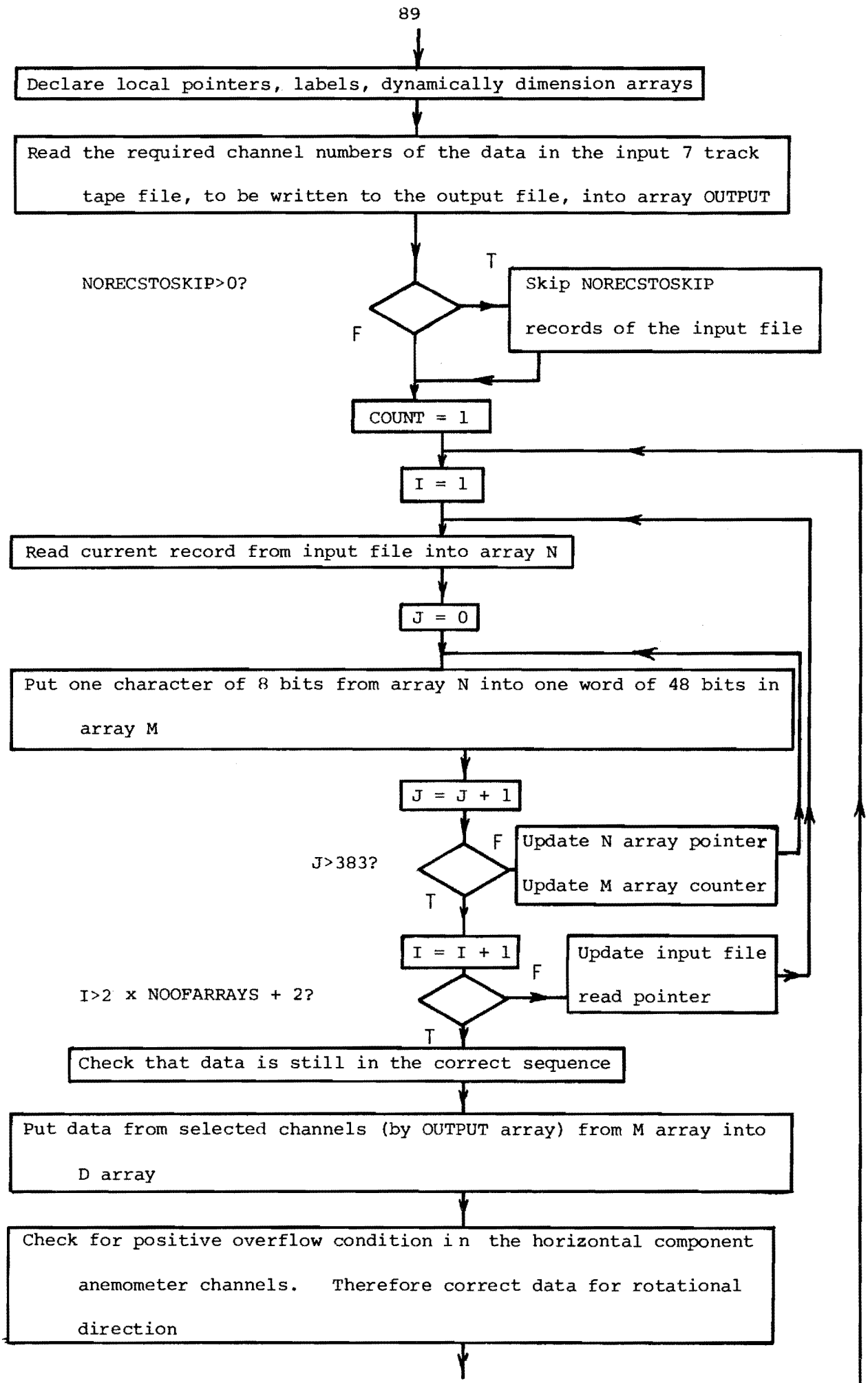

Fig. 5.6 Flowchart of Program COPYDATA (Continued)

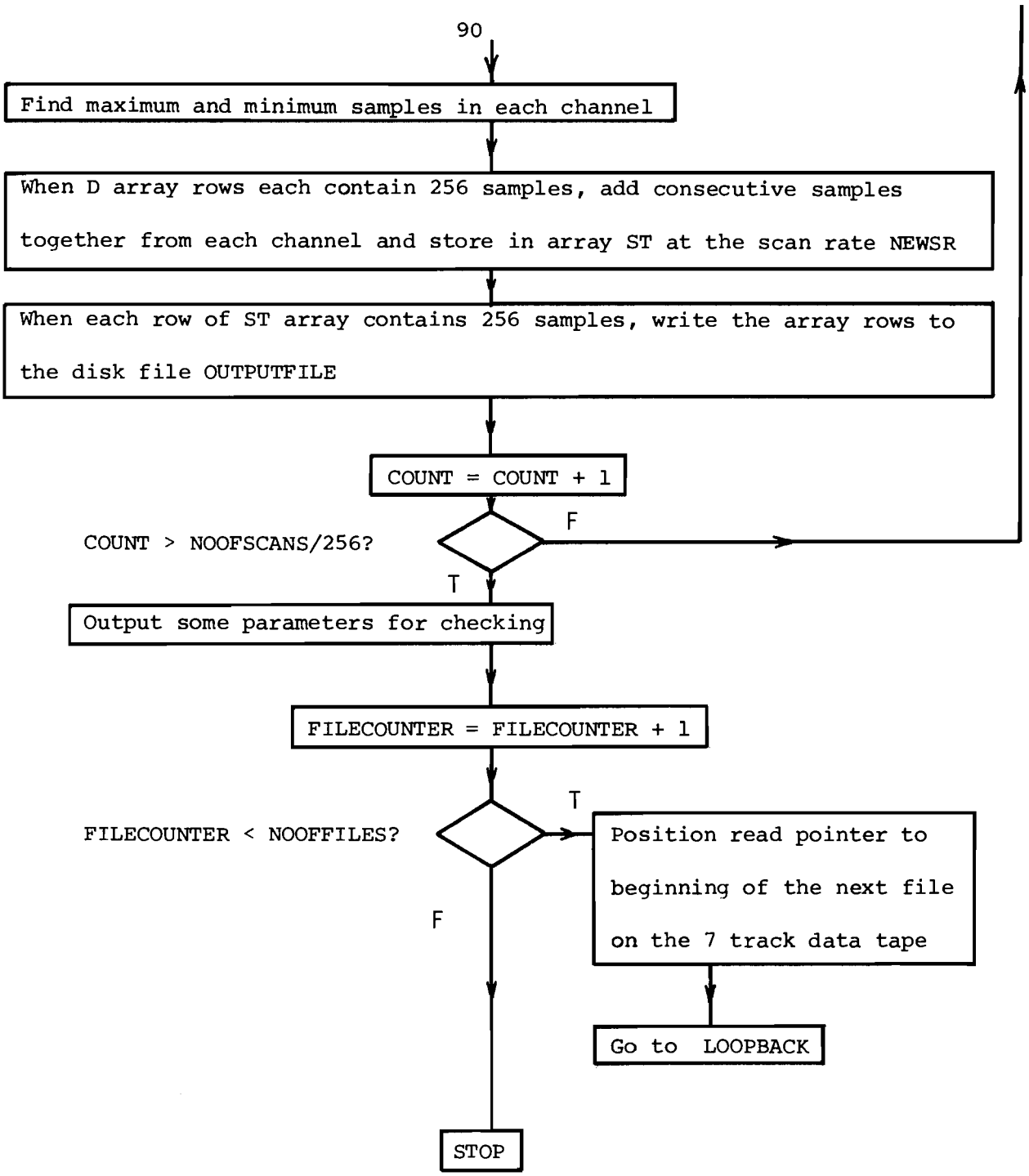

Fig. 5.6 Flowchart of Program COPYDATA

Care has to be exercised when this program is used when several files are being created. If the program is run more than once with the same physical file equated to the internal output file, then the program will join the two files, i.e. the second file will be added to the end of the first one. If however, two different output files are required, then the appropriate work flow language must be used to equate the internal file to a different physical file each time.

The different physical files may then be written to a library tape and saved as different files.

5.4 PROGRAM 'VTPDMS'

This program is used to check the data once again. It is run using data which the program CHECKDATA has indicated is free from obvious hardware errors and COPYDATA has copied to library tape. The program has been written to give graphical output of three kinds :

(1) A longitudinal component velocity - time graph.

(2) Probability density function graphs from all components.

(3) Graph of the short term longitudinal component mean square averages as a function of time.

Much of the coding for all of this output is identical, hence the fact that they have been incorporated into one program.

Each triplet of anemometers is processed in turn. The scan rate at which the data is processed may be changed to a lower value before detailed processing is performed. It is done by adding consecutive samples from each channel together. The horizontal anemometer data is resolved into components parallel and perpendicular to the average wind direction for the period. It is not corrected for the non-cosine response of the anemometers but the counts are converted to m/s using a single calibration coefficient.

As the data is resolved, totals are accumulated to give the data for the graphical output. Thus sufficient samples of longitudinal component data are added together to give eight second averages for the velocity-time graph, and similarly, sufficient values of the longitudinal component mean squares are added together to give 2.28 minute averages. At the same time the highest and lowest velocities in each channel are determined. These values are required because the probability density function part of the program has the number of classes determined by an input parameter. The class widths are all equal and their values are determined such that the highest and lowest samples in each channel are just contained in the highest and lowest classes respectively.

After the class boundaries have been calculated, the number of samples which fall into each class is determined. This is then normalised to give unit standard deviation, and a total area under the curve of 1. Thus the curves can quickly be compared with data from other orthogonal arrays and also with the Gaussian distribution.

The program has provision for removing linear and parabolic trend lines, by least squares, from the data. The form of the output is the same as above, but the scales of the plots are altered to give a useful output.

Each probability density graph has curves for one type of trend removal and for one of the orthogonal directions, but from all of the orthogonal arrays. Thus curves from the three different orthogonal directions and with different types of trends removed are plotted on separate graphs. Comparisons between the same components with the same types of trends removed but from different orthogonal arrays can therefore easily be made, because they are on the same graph.

The type of graphical output has been determined by observations made using different scales. The velocity-time curve was found to be visually acceptable when averages over eight seconds were determined for

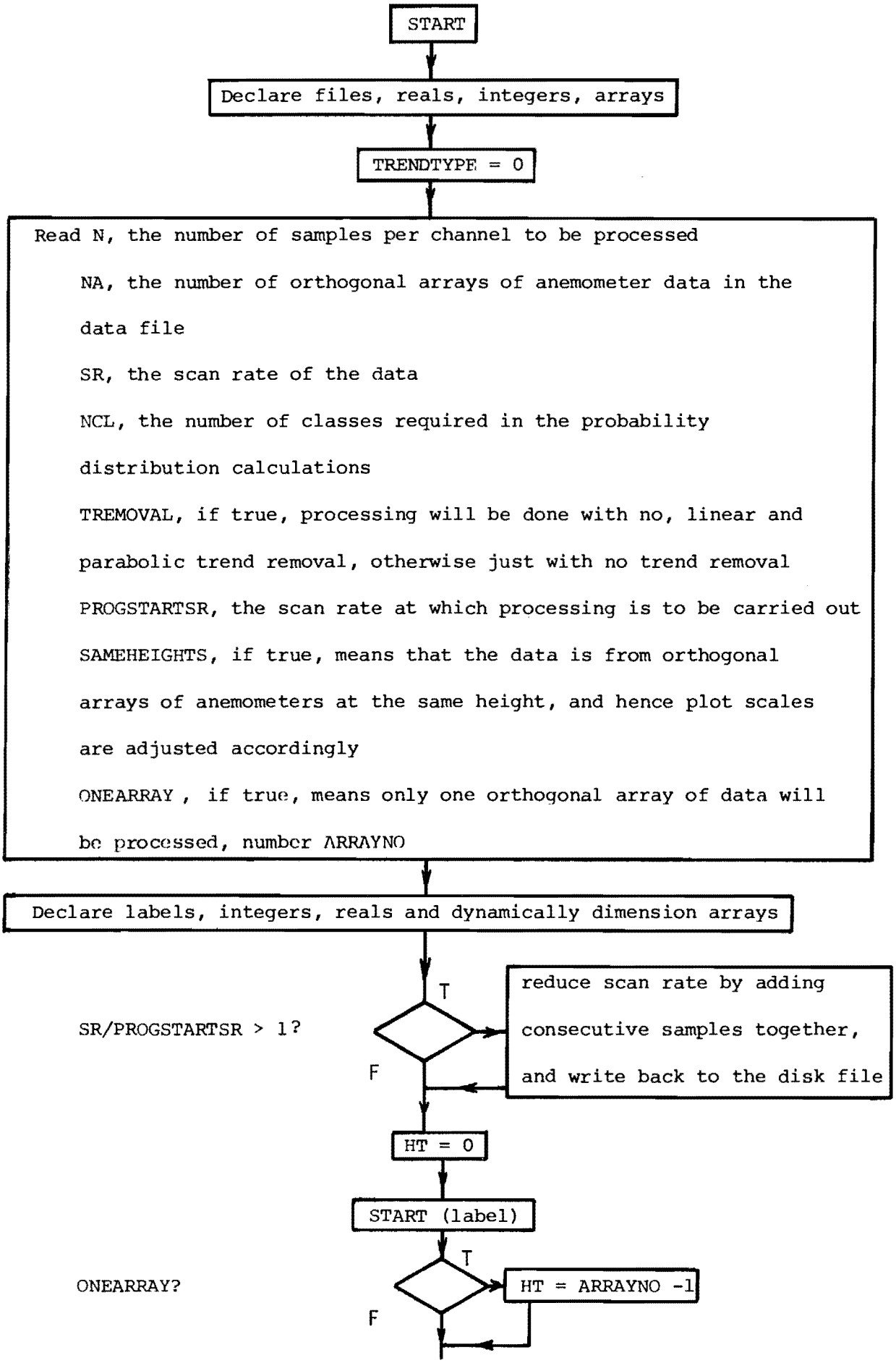

Fig. 5.7 Flowchart of Program VTPDMS (Continued.....)

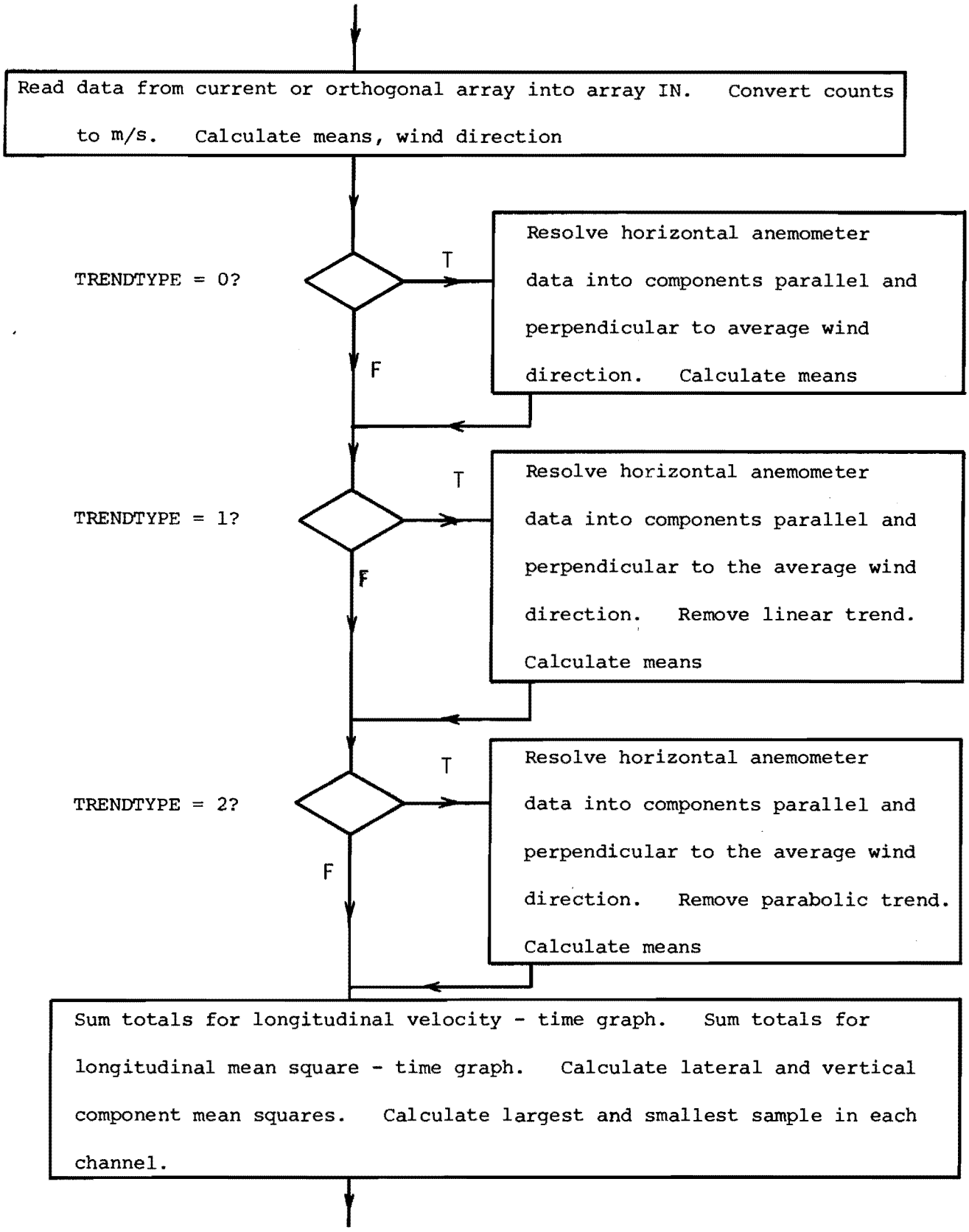

Fig. 5.7 Flowchart of Program VTPDMS (Continued.....)

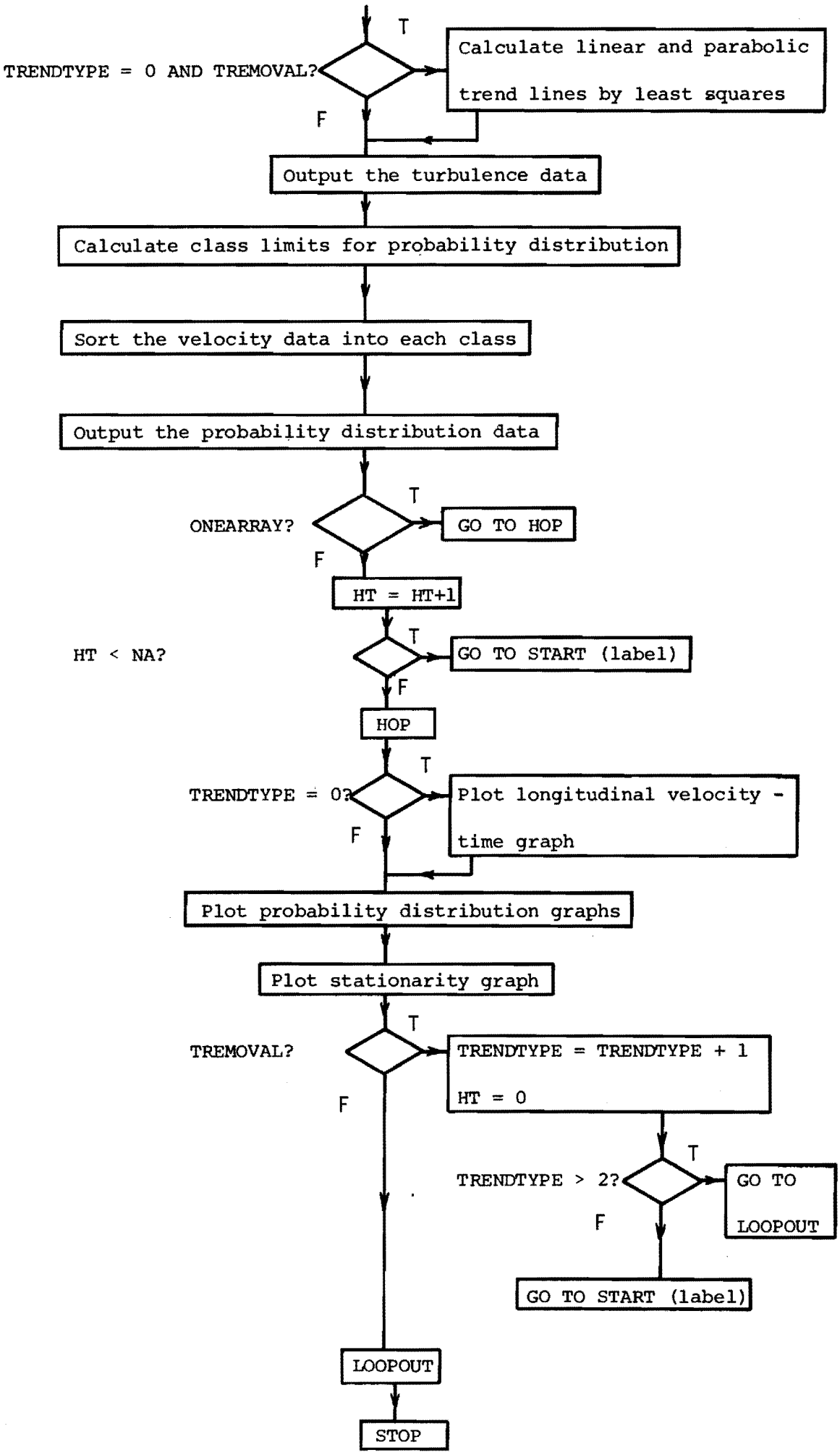

Fig. 5.7 Flowchart of Program VTPDMS

each point. Shorter averaging times gave much increased fluctuation, and the trace became smeared. However, longer averaging times reduced the resolution of the data. The curves produced from eight second velocity averages from all orthogonal arrays could be plotted on one graph. Thus the amount of correlation between arrays could be seen at a glance.

The averaging period of 2.28 minutes for the longitudinal mean squares was determined from two criteria :

(1) The time was sufficiently long enough for the autocorrelation to drop to zero, meaning each period was independent of the others.

(2) It was sufficiently short so that a reasonable number of mean square averages could be determined for a data file of typically 30 - 60 minutes duration.

The number of classes in the probability distribution curve was a variable which was read in from a data card during program execution. Thus it could then be varied to enable a suitable value to be determined. It was found that twenty classes gave a reasonable output.

A flow chart of the program is given in Fig.5.7. A program listing well described by comment statements is given in Appendix D.

5.5 PROGRAM 'SEQVELTURBREY'

This program was initially written to look at the effect of different processing techniques, and data file constraints on the turbulence parameters calculated. The data file constraints to be considered were the length of the file and the sampling frequency at which the data was collected.

The major processing technique to be investigated was the effect of correcting for the non-cosine response of the propeller anemometers.

Another less significant correction to be investigated was the effect of small misalignments from the vertical direction of the vertical component anemometer, on the $\overline{uw}/\sigma_u\sigma_w$ Reynolds stress.

In order for direct comparisons to be made easily between turbulence parameters which had been calculated from data processed in slightly different ways, it was decided that the output should be graphical.

The data file length and the sampling frequency used are important parameters to be considered, because between them they determine the amount of data to be processed. Only the data file length could be determined when a data recording was being made because the sampling frequency was constrained to high values by the system hardware. However, when the data was read off the field tape, written to a library tape and reformatted, the data could be written to the library tape at a reduced sampling frequency. Subsequent programs using the data on the library tape would thus require to process less data.

The program was developed so that it reads data sequentially from the data file. The values of the turbulence parameters for each orthogonal array are determined from running totals of products and summations obtained from the anemometer data. It was decided to calculate the parameters in this manner because all of them could be calculated from the totals without having to re-read any previous data. The derivation of the equations to calculate the turbulence parameters in this manner is given in Appendix E, along with the program listing.

After each block of 4.551 minutes of data has been read, the turbulence parameters are determined for all the data processed up to that time. At that time the values of the turbulence parameters - average longitudinal velocity, average wind direction, average turbulence intensities in the x, y, and z directions, and the three

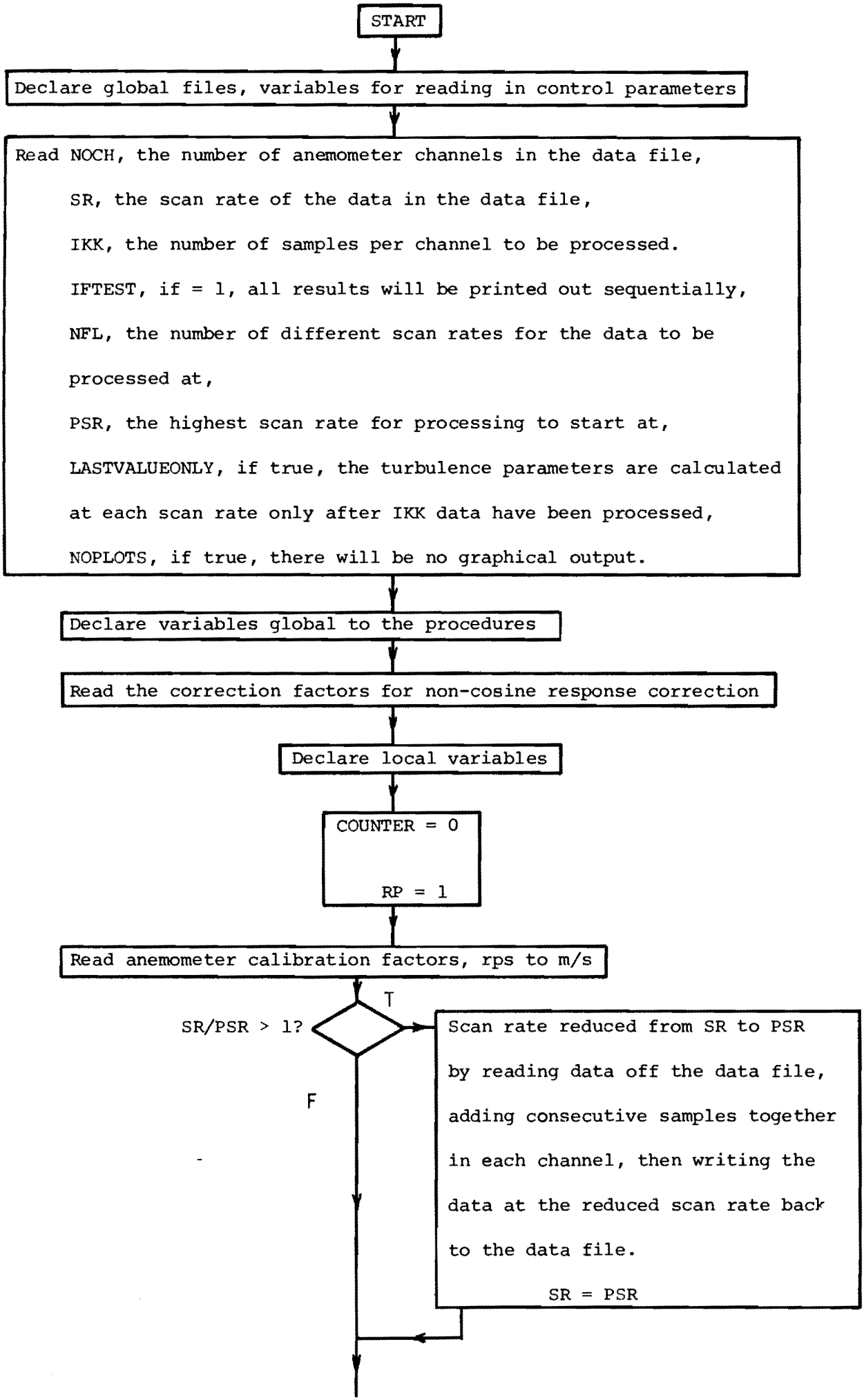

Fig. 5.8 Flowchart of Program SEQVELTURBREY (Continued.....)

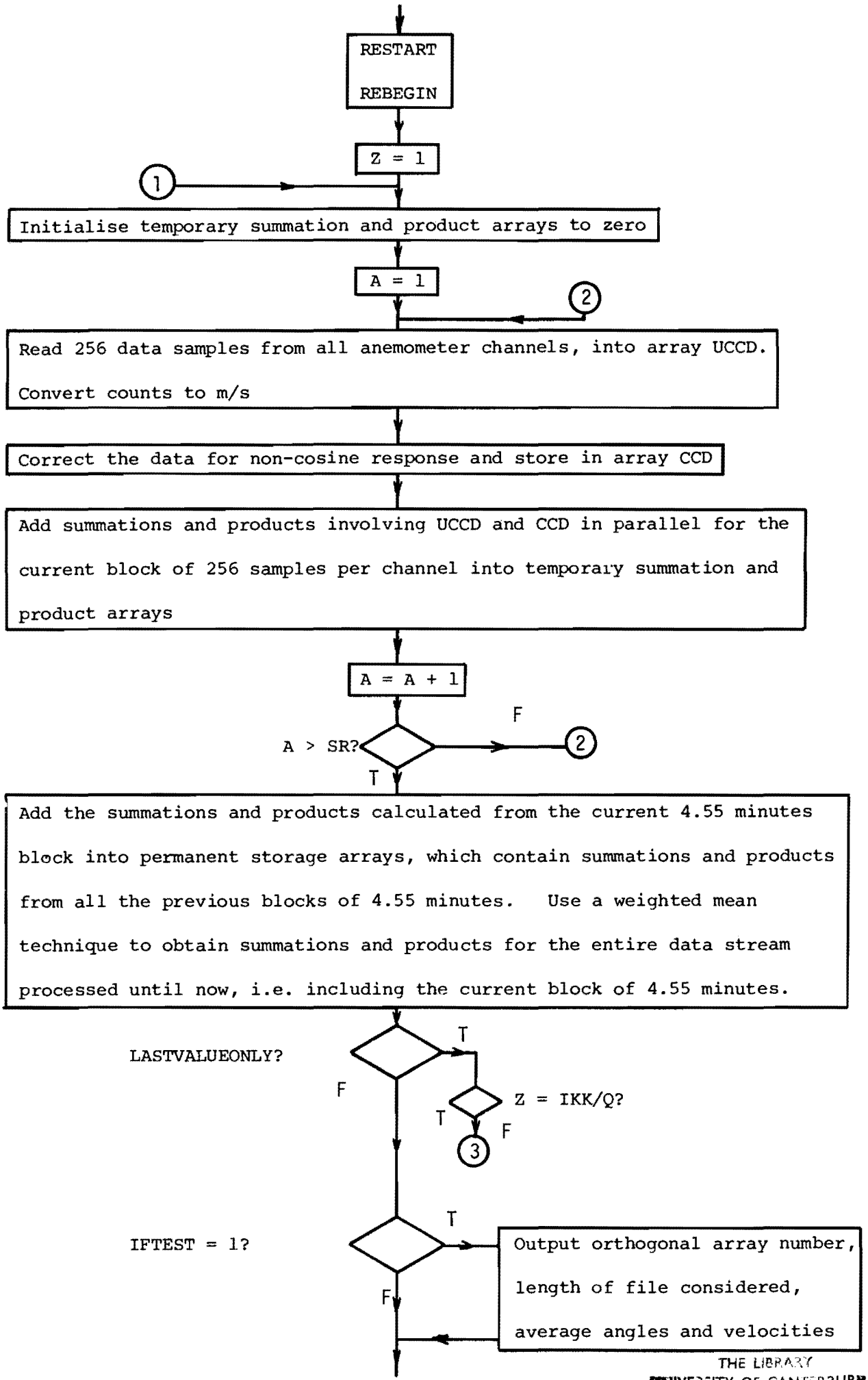

Fig. 5.8 Flowchart of Program SEQVELTURBREY (Continued....)

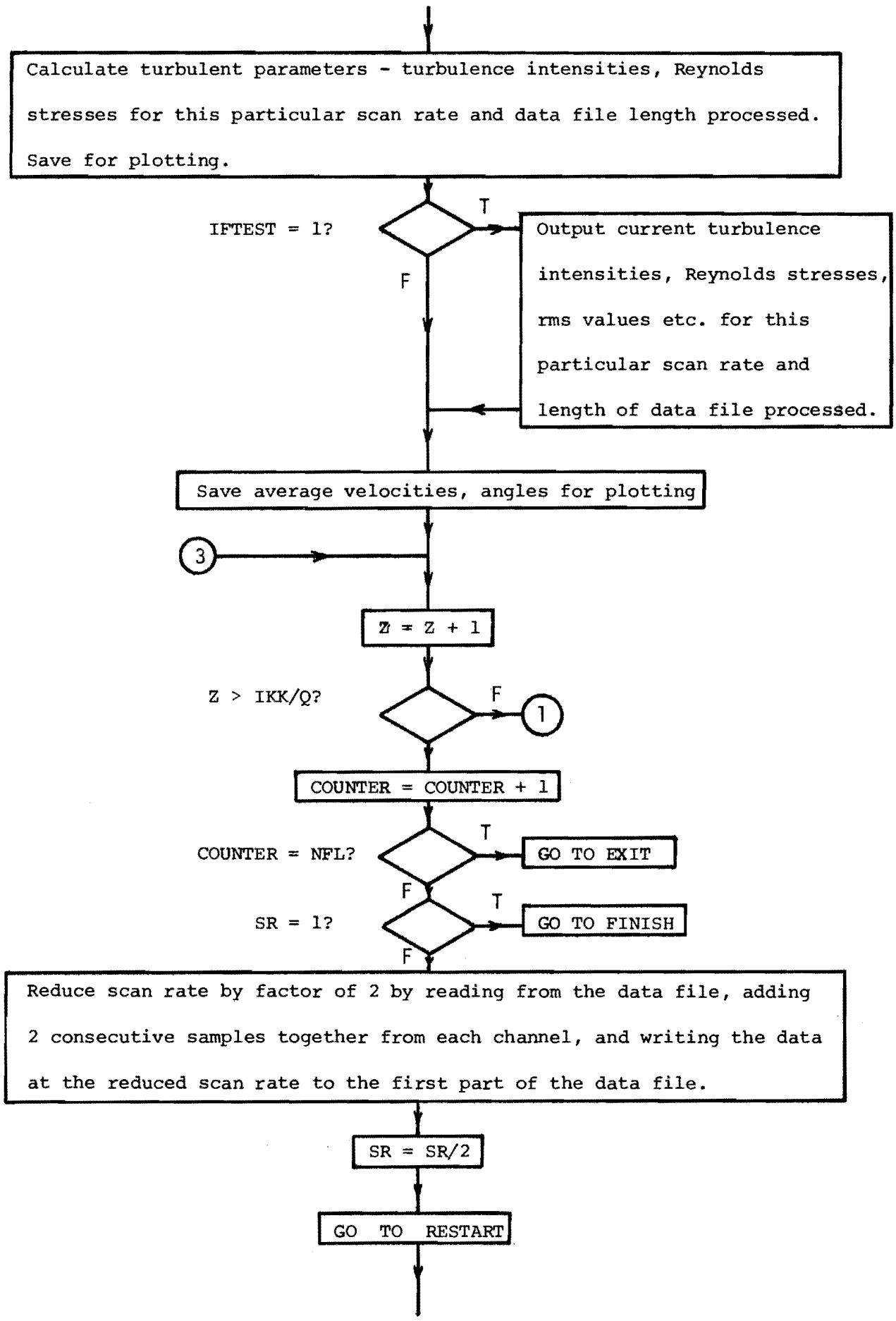

Fig. 5.8 Flowchart of Program SEQVELTURBREY (Continued.....)

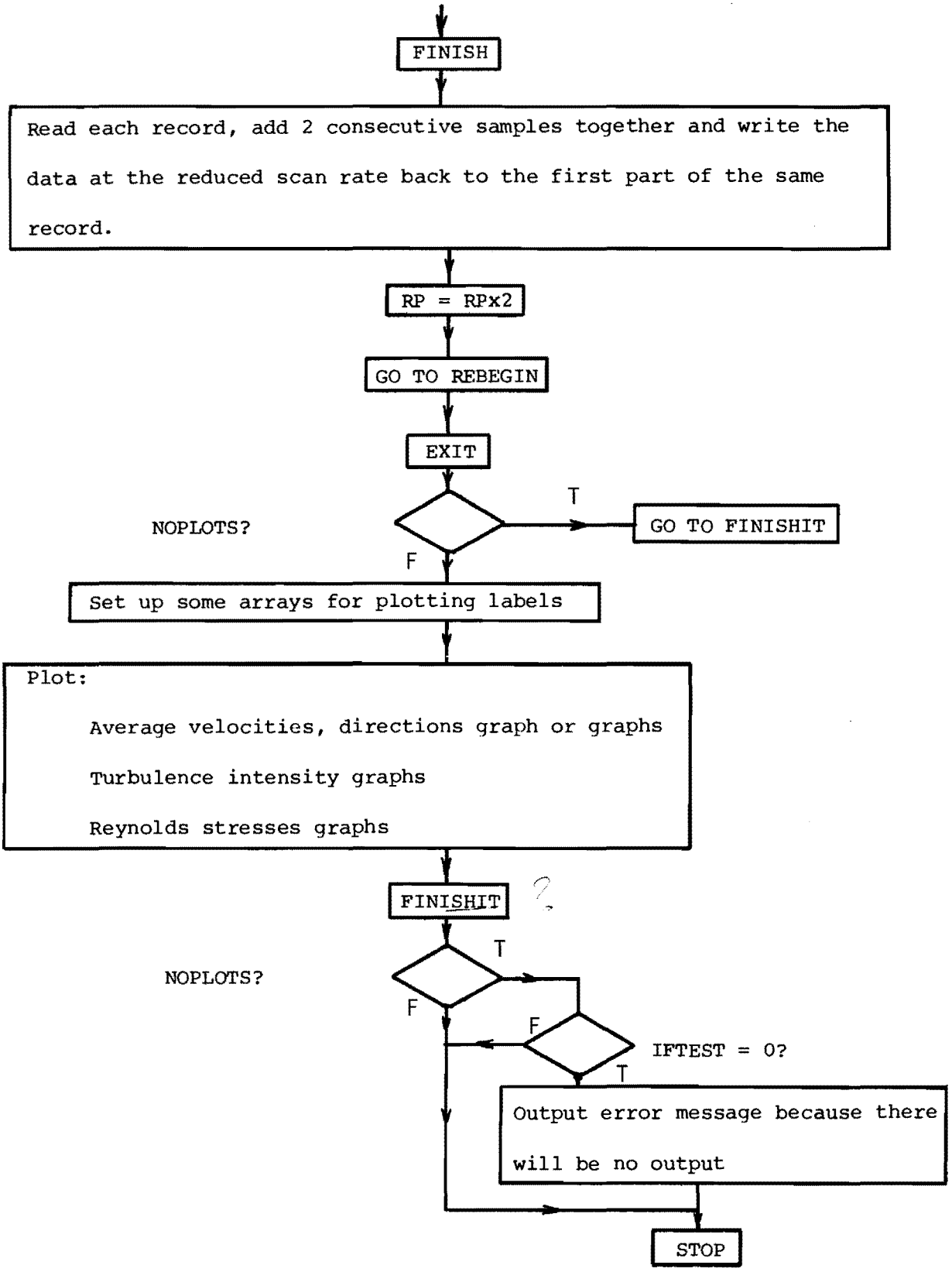

Fig. 5.8 Flowchart of Program SEQVELTURBREY.

Reynolds stresses $\overline{uw}/\sigma_u\sigma_w$, $\overline{uv}/\sigma_u\sigma_v$, and $\overline{vw}/\sigma_v\sigma_w$ are saved for plotting at a later stage.

Data corrected for non-cosine response and data not corrected for non-cosine response is calculated in parallel so that for each of the turbulence parameters mentioned above, corrected and uncorrected values are saved. This process is repeated until the end of the data file is reached.

However, at this stage, only one sampling frequency has been considered. Since one of the objectives was to find the minimum sampling frequency of the data, the program has not finished.

In order to reduce the scan rate, the data file, a temporary disk file, is read and for each channel, two consecutive samples are added together. The data is then written back to the file, but this time the file is only half as long.

The program then repeats itself, calculating the turbulence parameters at every multiple of 4.551 minutes and saving them for plotting, but using the data which is now at half the initial sampling frequency, as input.

The above process is continued until the sampling frequency is as low as the desired value which is read in from a data card.

Thus for example, the turbulence intensity $\frac{\sigma_u}{V_z}$ may be calculated for sampling frequencies of 15, 7.5, 3.75, 1.875, .94, .47, .23 Hz, for data file lengths of 4.551, 9.10, 13.65, 18.20, 22.76, 27.31, 31.86, 36.41, 40.96, 45.51, 50.06, 54.61, 59.16, 63.72, 68.27, 72.82 minutes, and for the data corrected and not corrected for the non-cosine response of the anemometers.

Hence for the single variable of turbulence intensity $\frac{\sigma_u}{V_z}$, this gives a total of 7 x 2 x 16 = 224 values.

The three turbulence intensities are plotted on the same graph,

and thus the effects of either of the data file length, sampling frequency and correction for non-cosine response can be observed easily. One graph only is required per orthogonal array of anemometers for the turbulence intensity.

Because the average velocity is not a function of the sampling frequency, it is a simple average, all the velocity data from all orthogonal arrays is plotted on the same graph.

The $\overline{uw}/\sigma_u\sigma_w$, $\overline{uv}/\sigma_u\sigma_v$ and $\overline{vw}/\sigma_v\sigma_w$ Reynolds stresses are plotted on the same graph so one graph is required per orthogonal array of anemometers.

In order to compare the changes in the turbulence parameters directly, the pairs of values obtained for a given record length and sampling frequency, but with one corrected and one not corrected for the non-cosine response of the anemometers, are plotted slightly displaced on the time axis, e.g. for the values obtained for a data stream of 4.551 minutes duration, the uncorrected result is plotted at 4.5 minutes, and the corrected result at 4.6 minutes.

The minimum file length required for the parameter was determined by the length of time the variable took to attain a steady value, i.e. a value similar to values for a longer file length.

The minimum sampling frequency required was determined from the graphs, because the minimum sampling frequency gave values of the variable which were the same as for higher sampling frequencies. A sampling frequency which was too low gave different values of the variables from those at higher sampling frequencies.

The program was thus very useful for determining whether correcting for the non-cosine response was necessary for the velocity, turbulence intensity, and Reynolds stress values. It also showed the minimum sampling frequency and file length necessary to give results

similar to those obtained at a higher sampling frequency and for a longer file length.

A flow chart is given in Fig.5.8 showing the main features of the program and a program listing with detailed comment statements is given in Appendix E. The comments are sufficiently detailed within the listing to enable program changes to be made, but the overall operation is reasonably straightforward as shown by Fig.5.8.

The effect of trying to correct for the misalignment of the vertical anemometer on the $\overline{uw}/\sigma_u\sigma_w$ Reynolds stress was also investigated. This correction is described in detail in Chapter 9. The two values of the Reynolds stress obtained by correcting the data and not correcting the data for the misalignment of the vertical anemometer were not plotted, but the two results printed.

It was found that the effect of the correction was small, but reduced the variation of the value between runs and orthogonal arrays. To reduce the error in calculating this Reynolds stress, the most important one physically, it was decided to incorporate the correction always.

5.6 PROGRAM 'PSAUTCORS'

5.6.1 Introduction

This program is the largest and most complicated developed to analyse the wind velocity data. It was developed as a separate program because the method of processing used in it has certain features which differ from the programs SEQVELTURBREY and VTPDMS. The most significant difference is that the program PSAUTCORS computes Fourier transforms (FT) of the velocity data. The fast Fourier transform (FFT) procedures used required all the velocity data to be present in two arrays, and then the FFT was taken of the data in these arrays.

This meant that instead of working sequentially along a data file and accumulating various totals which would enable the turbulence parameters to be calculated, all the data from an anemometer channel had to be in core memory at one time. This reason alone meant that a separate program had to be written.

This program has been written so that it calculates:

(1) Power spectral densities.

(2) Autocorrelations.

(3) Cross-correlations.

At the outset of this work it was desired to look at the effects of file length, sampling frequency, trend removal and correcting for non-cosine response on the above turbulence parameters, and also to look at the effect of "data windows" on the power spectral densities. This program therefore allows for lots of flexibility in its processing operation. There are so many combinations of the above processing constraints, coupled with the many anemometer channels, that initially the output was so vast that it was unwieldly. Thus a series of different types of plotting output was developed to make analysis of the graphical output more streamlined, and to reduce to the minimum, the amount of output required for a given set of data conditions and processing techniques.

A detailed discussion of the effect of different data conditions and processing techniques is given in Chapter 6. The flexibility of the program and the large number of combinations of methods for processing was required mainly for Chapter 6. Now that these effects are known, after many runs on different data streams, the flexibility is not required. However the program has been written such that sections of it which are not required are by-passed. The only additional expense of running such a large program is in compiling it.

5.6.2 Brief Description of the Theory behind the Processing Methods

5.6.2.1 Calculation of Power Spectral Densities. The variation of wind velocity with time at a point can be assumed to be the fluctuation of a random variable, with time as the independent variable. The velocity time trace can be considered to be the superposition of many sine waves of different frequencies from 0 to ∞, with different amplitudes, and phases.

Analysis of the frequency and amplitude or amplitude squared of the sine waves contributing to a particular wind trace provide a great deal of information on the wind properties.

Much has been written on the subject of spectral analysis, so the equations and discussion presented here are those which apply specifically to analysis of wind data.

The fast Fourier transform package used here for spectral analysis had provision for complex input/output. Data was placed in two one dimensional arrays which were used as the data input to the FFT procedure. On output, the original data in the two arrays was written over with the Fourier transform of the original data.

The fast Fourier transform is a fast way of performing a discrete Fourier transform (DFT), and a discrete Fourier transform is a special case of the continuous Fourier transform (CFT). The method used to compute the power spectra in this work involving the FFT therefore obtains values which are different from those which would be obtained by a CFT from an ideally continuous and infinitely long time record of data.

The FFT method used to calculate the power spectral density of the velocity data is given below.

Consider a time series with N samples collected every Δt seconds apart, and recorded over a total time T. Then $T = N\Delta t$ and f, the sampling frequency $= \frac{1}{\Delta t}$.

The sequence of operations on the original time series is to :

(1) Truncate it so that it contains N samples where N is a power of 2.

(2) Remove the mean and divide by the standard deviation of the time series.

(3) Taper it if required with a data window, e.g. a cosine taper.

(4) Compute the FT of the series using an FFT procedure, i.e. compute

$$X(j) = \sum_{k=0}^{N-1} x(k)\exp(-i2\pi jk/N) \qquad (5.1)$$

$$\text{for } j = 0,1,..N-1.$$

where x(k) is the original time series, X(j) is the Fourier transform of the original series, $i = (-1)^{\frac{1}{2}}$.

(5) Calculate $G(j) = \frac{2\Delta t}{N}\left|X(j)\right|^2$ (5.2)

for $j = 0,1...\frac{N}{2} - 1$, where G(j) is the power spectral estimate.

(6) Multiply G(j) by some factor, e.g. by $\frac{1}{.875}$ if a cosine taper has been used on the first and last 10% of the time series to normalise the output so that the area under the spectrum is equal to one.

(7) Smooth G(j) using either frequency or segment averaging. Frequency smoothing is averaging spectral components across several raw spectral estimates in one power spectrum and placing the averaged value at the centre of the frequencies averaged over. Segment averaging is averaging each spectral component across several power spectra obtained from different time series to obtain one averaged spectra.

5.6.2.2 Difficulties in Calculating the Power Spectral Density. The DFT transform is only an approximation to the CFT because of several reasons :

(1) Only a finite portion of the signal is considered of a theoretically infinitely long signal, i.e. this is like looking at the signal through a unity amplitude data window.

(2) The continuous time history is sampled at discrete time instances.

(3) The frequency domain function contains discrete frequencies.

The above three reasons can lead to errors in calculating the Fourier transform. This is best understood by developing the DFT graphically, based on CFT theory. Fig.5.9 shows several functions each with their Fourier transforms in the time and frequency domains. If the function h(t) is considered, then it has a FT given by H(f). Graphically it can be shown how the DFT gives an approximation to H(f).

Firstly, the time series h(t) has to have discrete samples. This is obtained by multiplying it with an infinite Dirac "comb"which is shown in Fig.5.9(b). Multiplying h(t) by the Dirac comb in the time domain is equivalent to convolving H(f) with $\Delta_o(f)$ in the frequency domain. This will cause aliasing if h(t) is not sampled at a frequency higher than twice the highest component in h(t). However, there will be no loss of information if the signal is sampled at least twice the highest frequency component in h(f). If the function H(f) is not band limited, i.e. H(f) = 0 for some $|f| > f_c$, then sampling will cause aliasing as illustrated in Fig.5.9(c).

For digital computation, only a finite number of points say N can be considered, i.e. the time series must be multiplied by a truncation function, e.g. the unity amplitude box-car window in Fig.5.4(d). However this function has a Fourier transformer of the form X(f), a $\frac{\sin(f)}{f}$

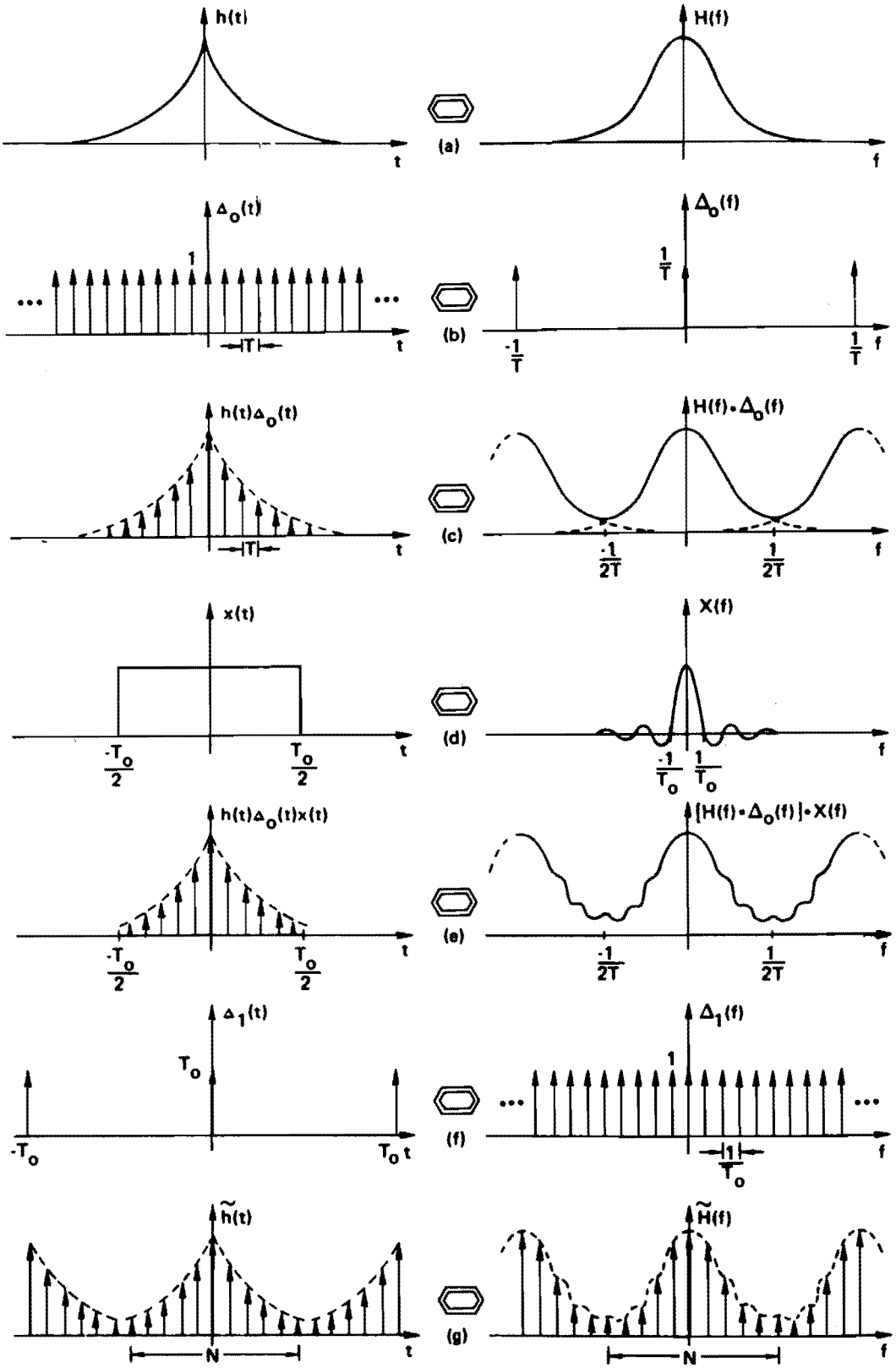

FIG. 5·9 GRAPHICAL DEVELOPMENT OF THE DISCRETE FOURIER TRANSFORM.

function. Multiplication in the time domain is like a convolution in the frequency domain, and the effect of the truncation is to introduce a ripple to the Fourier transformed result. For machine computation, the frequency domain result cannot be continuous, but must only contain sample values, i.e. it needs to be multiplied by a Dirac comb. Multiplying by this comb in the frequency domain is the same as convolving the time series with $\Delta_1(t)$, which means that the time series is assumed to be periodic, as is the function in the frequency domain.

With care good approximations can be obtained. The two most important requirements are :

(1) Use a sampling frequency which is at least twice the highest frequency in the time series - this stops aliasing.

(2) Use as large a number of samples as possible - providing the data is still stationary, as this makes the sin f/f function in Fig.5.9(d) become more like an impulse function, and will reduce leakage and the picket fence effect (Bergland, 1969).

A good summary of digital analysis theory to calculate power spectra is given by Teunissen (1977a). Teunissen also includes the effect of averaging samples after digitisation, and retaining only the average value, therefore reducing the amount of data to be subsequently Fourier transformed.

5.6.2.3 Methods for Computing Spectra and Correlations using FFT Procedures Designed for Complex Input/Output. Many FFT packages are written for complex input/output. They may use two one dimensional data arrays, one two dimensional array, or just one one dimensional array with real and imaginary components in consecutive elements.

The FFT library package used in this work used two one dimensional arrays. The discussion following will be limited to this type of input/output.

Savings in computing time can be made if real data is being Fourier transformed. It is wasteful to set all the imaginary array element coefficients to zero. This is because not only is there no imaginary data input, but the output is Hermitian, i.e. the real component coefficients of the Fourier transformed real time series are even, and the imaginary component coefficients are odd. Hence for N real data input and N imaginary coefficients set to zero, the Fourier transformed data can be fully defined by the first $\frac{N}{2} + 1$ pairs of complex coefficients as output.

Since the output is Hermitian, when the power spectrum is obtained by squaring and adding the complex coefficients at each frequency, it is real and even. The autocorrelation is obtained by taking the inverse Fourier transform of the power spectrum and again it is real and even, hence the autocorrelation function and the power spectrum do not require 2N values to define them.

Often when performing Fourier transforms, a limit imposed by the computer is the maximum array length. It is therefore desirable to make as much use of data arrays as possible and not to fill them out with zeros unnecessarily.

Consequently a separate procedure was written to recover the spectral data after a forward transform involving 2N real data had been obtained from a FFT procedure with N pairs of complex coefficients input/output. The relevant theory is given in Brigham (1974).

Assume that a real time series x(k) is described by 2N samples, and its Fourier transform is desired. The method is to :

(1) Divide x(k) up as

$$\begin{aligned} h(k) &= x(2k) \\ g(k) &= x(2k+1),\ k = 0,1,\ldots N-1 \end{aligned} \tag{5.3}$$

(2) Form the function

$$y(k) = h(k) + ig(k), k = 0,1,\ldots N-1 \tag{5.4}$$

(3) Compute the Fourier transform of y(k)

$$\begin{aligned} Y(j) &= \sum_{k=0}^{N-1} y(k)\exp(-i2\pi jk/N) \\ &= R(j) + iI(j), \qquad j = 0,1,\ldots N-1 \end{aligned} \tag{5.5}$$

where R(j) and I(j) are the real and imaginary parts of Y(j) respectively.

(4) Compute

$$\begin{aligned} X_r(j) &= \left[\frac{R(j)}{2} + \frac{R(N-j)}{2}\right] + \cos\frac{\pi j}{N}\left[\frac{I(j)}{2} + \frac{I(N-j)}{2}\right] \\ &\quad - \sin\frac{\pi j}{N}\left[\frac{R(j)}{2} - \frac{R(N-j)}{2}\right] \\ X_i(j) &= \left[\frac{I(j)}{2} - \frac{I(N-j)}{2}\right] - \sin\frac{\pi j}{N}\left[\frac{I(j)}{2} + \frac{I(N-j)}{2}\right] \\ &\quad - \cos\frac{\pi j}{N}\left[\frac{R(j)}{2} - \frac{R(N-j)}{2}\right] \\ &\qquad j = 0,1,\ldots N-1. \end{aligned} \tag{5.6}$$

where $X_r(j)$, $X_i(j)$ are respectively the real and imaginary parts of the 2N point discrete Fourier transform of x(k).

The processing in Equation (5.6) above is calculated by procedure RRDR in the program PSAUTCORS which is given in Appendix F along with a detailed flow chart of its method of operation.

Use of this condensed method can be further extended to cross-spectral density and cross-correlation analysis. The normal method of calculating these is as follows :

Consider two time series x(k) and y(k), k = 0,1,...N-1 and it is desired to calculate their cross-correlation.

(1) Compute $X(j) = FT \text{ of } x(k)$

$Y(j) = FT \text{ of } y(k)$ (5.7)

$k,j = 0,1,...N-1$

both X(j) and Y(j) are Hermitian.

(2) Perform the multiplication

$Z(j) = X(j)Y(j)^*$ (* denotes complex conjugate)

$j = 0,1,...N-1$ (5.8)

again Z(j) is Hermitian.

(3) Compute

$z(k) = \text{inverse FT of } Z(j)$

$k,j = 0,1...N-1$ (5.9)

since Z(j) is Hermitian, z(k) is real.

To perform the above calculations using the condensed method, the following process is performed.

Consider x(k), y(k) to be defined by 2N samples, i.e. k = 0,1,...2N-1

(1) form $h(k) = x(2k)$

$g(k) = x(2k+1)$

$c(k) = y(2k)$

$d(k) = y(2k+1)$ $\quad k = 0,1,...N-1$

(2) form the functions

$a(k) = h(k) + ig(k)$

$b(k) = c(k) + id(k)$ $\quad k = 0,1,...N-1$

(3) Compute the Fourier transforms of a(k) and b(k) using Equation (5.5) yielding

$$A(j) = R_a(j) + i\, I_a(j)$$

$$B(j) = R_b(j) + i\, I_b(j) \quad , \; j = 0,1,\ldots N-1.$$

(4) Obtain the actual complex coefficients of both A(j) and B(j) using Equation (5.6) obtaining

$$AA(j) = A_r(j) + i\, A_i(j)$$

$$BB(j) = B_r(j) + i\, B_i(j) \quad , \; j = 0,1,\ldots N-1.$$

(5) Perform the complex multiplication

$$Z(j) = AA(j)\; BB(j)^*$$

$$= Z_r(j) + i\, Z_i(j) \quad , \; j = 0,1,\ldots N-1.$$

(6) Form the functions

$$ZZ(j) = R_z(j) + i\, I_z(j) \quad , \; j = 0,1,\ldots N-1$$

using the inverse of Equation (5.6).

(7) Compute the inverse Fourier transform of ZZ(j)

$$z(k) = \frac{1}{N} \sum_{j=0}^{N-1} ZZ(j) \exp(i2\pi jk/N) \qquad k = 0,1,\ldots N-1$$

The array z(k) then contains the cross-correlation data with consecutive time lags in the real and imaginary parts of the two output arrays. This method therefore requires half of the storage allocation required than if no use is made of the imaginary data array for input.

In the program PSAUTCORS contained in Appendix F, the method outlined below is used to calculate the forward and inverse transforms.

Consider a time series of 2N samples,

$$x(k) \quad , \; k = 0,1,\ldots 2N-1$$

Then the time series is put into the arrays XR and XI in the program by

XR[k] = x(2k)

XI[k] = (2k+1) k = 0,1,...N-1

M is defined by $N = 2^M$.

The pairs of spectral coefficients from zero frequency to the folding frequency, i.e. half the sampling frequency, are obtained by the following sequence of procedure calls :

```
DIRN = 1
FFTF(XR,XI,S,C,M)
BITREV2(XR,XI,M)
RRDR(XR,XI,M,DIRN)
```

To obtain 2N real coefficients from N + 1 pairs of Hermitian coefficients, the following calls are made :

```
DIRN = -1
RRDR(XR,XI,M,DIRN)
BITREV2(XR,XI,M)
FFTR(XR,XI,S,C,M)
```

The real time series will then be found in XR and XI such that consecutive time series samples are contained alternately in XR and XI, viz,

x(2k) =XR[k]

x(2k+1) = XI[k] , k = 0,1,...N-1.

5.6.3 Assumptions made when Going Between Spectra and Correlations

If a time series of N samples is Fourier transformed, then a spectrum may be obtained which is quite adequate, providing considerations of sampling frequencies, data windows etc. are taken into account.

The "roundabout" Fourier transform method of producing auto-correlations however, i.e. to take a Fourier transform of the time series,

square and add the coefficients and then to take the inverse Fourier transform, obtains not the correlation function defined by

$$R(r\Delta t) + \frac{1}{N}\sum_{k=0}^{N-r} x(k).x(k+r) \quad , \quad r = 0,1,\ldots m \ .$$

r is the lag number, Δt the time between consecutive samples, m is the maximum lag number, $R(r\Delta t)$ is the autocorrelation at a lag of $r\Delta t$ seconds and x(k) is a time series. Instead, the "circular" correlation function defined by

$$R^{C}(r\Delta t) = \frac{1}{N}\left[\sum_{k=0}^{N-r} x(k).x\ (k+r) + \sum_{k=0}^{r} x(k)\ .x(N-r+k)\right]$$

$$r = 0,1,\ldots m$$

is obtained. There is an extra contribution due to the end of the time series being folded back and correlated with the beginning of the series. This effect is of no concern when the autocorrelation falls to zero quickly, and for time lags less than say 20% of the file length. This is because the ends of the file will be uncorrelated and hence integrate to zero. The problem can be avoided by adding N zeros to a data stream of N samples which then spreads apart the two portions of the circular correlation function.

It has not been necessary to add zeros to this data because the autocorrelations dropped to zero quickly, and short time lags, compared with the file length have been considered. When the data appeared to contain a trend, it was found during comparison tests that there was little change between the autocorrelation obtained from a time series with zeros added or with no zeros added. For short time lags the circular correlation had very little effect.

Providing the autocorrelation falls to zero quickly, the FFT roundabout method of producing autocorrelations, with no additions of

zeros, obtains values which can be considered to have been calculated by the following formula :

$$R(r\Delta t) = \frac{1}{N}\sum_{k=0}^{N-r} x(k).x(k+r) \qquad r = 0,1,...m$$

This gives a biased estimate of the autocorrelation which has to be corrected. The traditional method of defining the autocorrelation is

$$R(r\Delta t) = \frac{1}{N-r}\sum_{k=0}^{N-r} x(k).x(k+r) \qquad r = 0,1,...m$$

Therefore the estimate obtained by the FFT method needs to be multiplied by $\frac{N}{N-r}$, r = 0,1,2...m to obtain an unbiased estimate.

If some kind of data window is applied to the time series data in order to get a "better" spectrum, then this spectrum cannot be used to obtain the autocorrelation. This means that transformations from the time to the frequency domain have to be made more often if a data window is used to obtain a power spectrum, and the autocorrelation is also required.

The most efficient method for obtaining the autocorrelation function then is to :

(1) From a real time series of N samples where N is a power of 2, remove the mean and divide by the standard deviation. This will make the autocorrelation have a correlation of 1 at zero time lag, and to tend to zero for large time lags.

(2) Compute the N point Fourier transform using a $^{N}/2$ complex FFT package.

(3) Calculate

$$XR[I] = (XR[I]^2 + XI[I]^2)/N \ , \ XI[I] = 0 \ ,$$

$$I = 0,1,...^{N}/2$$

(4) Take the inverse FT of XR,XI.

(5) Multiply the result by $\frac{N}{N-r}$ for r = 0,1,...m to obtain an unbiased estimate of the autocorrelation function.

5.6.4 Description of Program PSAUTCORS

The program listing is given in Appendix F along with a detailed flow chart. Comment statements have been included throughout the program listing to identify its operation. Because the program is rather long, only a very simplified flow chart has been given here in Fig.5.10.

The basic operation of the program is that it calculates power spectral densities, autocorrelation functions, and cross-correlations with as few FFT calls as possible. Throughout the program, booleans are checked to see what type of results are required. The state of the booleans are determined by data cards, read in as control parameters during program execution. Fourier transformed data is always saved in temporary disk files if it is needed later on in the program for another calculation. Results to be plotted are saved in other temporary disk files.

Cross-correlation plots occur throughout the program but power spectral density and autocorrelation plots occur only after all of the required data has been analysed.

Provision has been made for applying a data window to the time series data. When this is done and correlations are required, the respective time series have been Fourier transformed twice, once for each spectrum and once for each correlation. No zeros have been added to the data to spread apart the circular autocorrelation, since the autocorrelations fell to zero quickly, and larger data arrays increased the computing cost and execution time. A FFT package designed for complex input/output was used in conjunction with a procedure to do analysis on real and Hermitian data with half the storage usually necessary. This has been explained in Section 5.6.2.3.

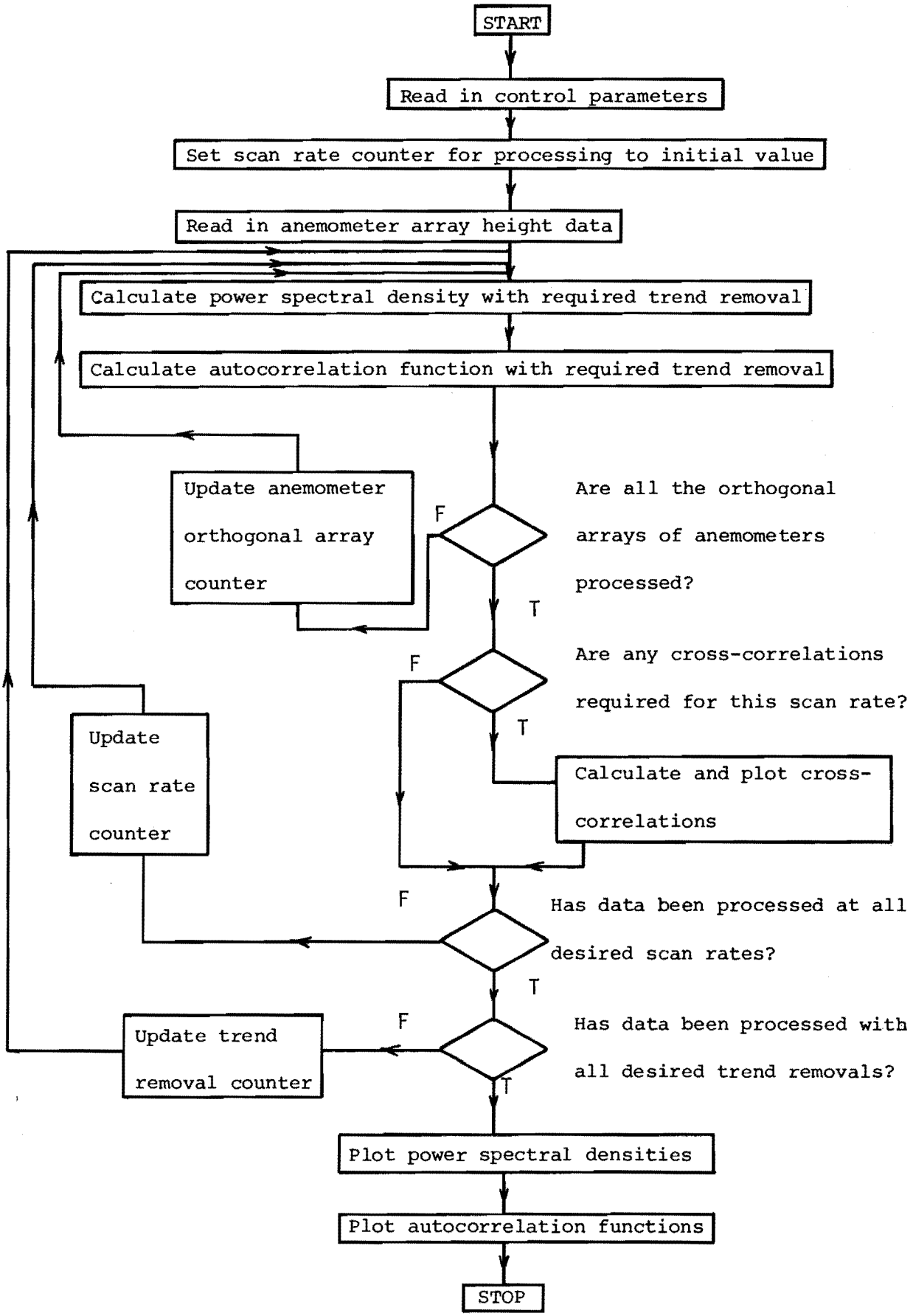

Fig. 5.10 Simplified flowchart of program PSAUTCORS

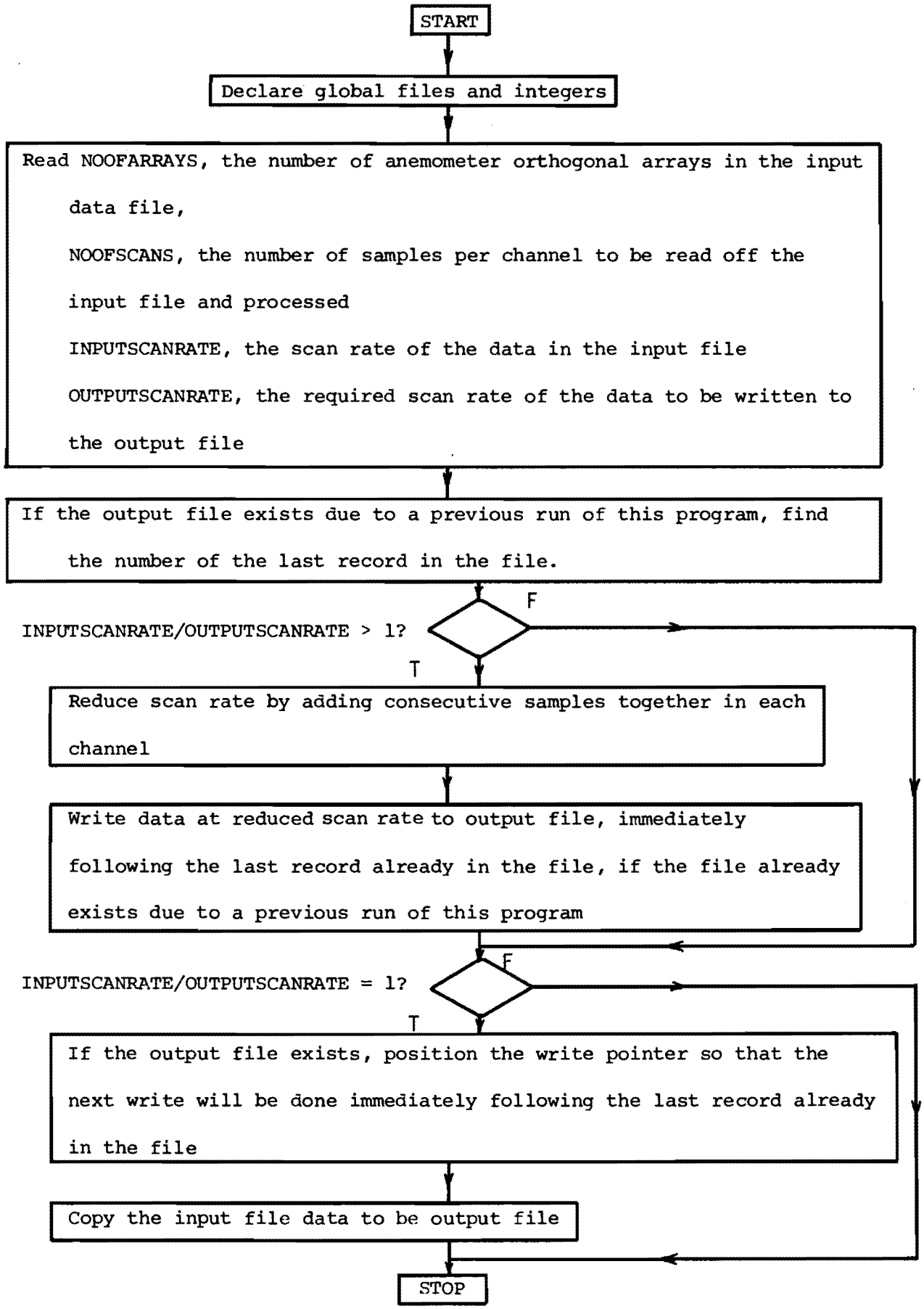

Fig. 5.11 Flowchart of program JOINFILES

5.7 PROGRAM 'JOINFILES'

This program, the flowchart of which is given in Fig.5.11 and whose listing is given in Appendix G, was written not to calculate turbulence parameters, but to manipulate data files.

Sometimes when data was being recorded in the field, the tape recorder malfunctioned and different parts of a data recording were written to different tapes, and as different files onto the same tape. Subsequently some of these different files were written as different files to library tapes. This program can be used to join these separate files into one file.

The program can also read a data file and then write the data at a reduced scan rate to another file, both being library tape files. This feature is useful for reducing the data required to be stored permanently, and to reduce computing costs.

It might appear that there has been some duplication with this program because the others also have the feature of being able to reduce the scan rate. However, if data has been stored on a library tape at a scan rate which is higher than necessary, for subsequent processing, it is most efficient to run this program and to copy the data at a reduced scan rate to another file. This file may then be processed in the usual way to obtain the turbulence parameters.

5.8 CONCLUSIONS

Programs have been described which :

(1) Read data off 7-track field data tape and check it for hardware and other errors. The program may also copy the data to a library tape if a 6 bit slip has occurred.

(2) Copy data free from hardware and other obvious errors to a library tape at a desired scan rate.

(3) Plot longitudinal velocity-time and mean squares graphs. Plot velocity probability density function graphs for each anemometer channel. This allows a visual check to be made on the data.

(4) Calculate average velocities and directions, turbulence intensities, and Reynolds stresses with and without correcting for non-cosine response, for any desired file length, and for any desired scan rate.

(5) Calculate the power spectral density and autocorrelation function for all components, and calculate cross-correlations for any pairs of data streams.

(6) Handle library tape files so that they may be joined together, or the scan rate reduced.

The programs if used carefully, enable a detailed description of the wind environment, measured by orthogonal arrays of propeller anemometers, to be made.

CHAPTER 6

THE EFFECT OF THE TYPE OF ANALYSIS ON THE TURBULENCE PARAMETERS

This chapter deals with the effects of non-cosine response correction, the length of the period for which data is recorded, the sampling frequency, and trend removal,on turbulence parameters computed from data streams generated by orthogonal arrays of propeller anemometers. The last sub-section of the chapter concerns itself with the effect of a cosine taper data window on power spectra computed from such data streams.

6.1 THE EFFECT OF THE CORRECTION FOR NON-COSINE RESPONSE

It has already been mentioned in Chapter 3 that the propeller anemometer has a response to wind velocity which is less than the ideal value of $\bar{U}\cos\theta$. The effect is well documented in the literature, (Gill, 1975, Drinkrow, 1972, Horst, 1973a, Hicks, 1972). There is a paucity of data obtained from comparisons of results from data streams corrected and not corrected for the sensor's non-cosine response, although Horst (1973a) states that the most effective correction that can be applied to Gill UVW anemometers is that for non-cosine response.

The effect of this non-ideal response is to cause the wind to be underestimated if three such sensors are assumed to rotate at $\bar{U}\cos\theta$ in an orthogonal array. Thus the turbulence parameters calculated from an uncorrected data stream would be in error. The magnitude of this error has been investigated by computing the various turbulence parameters from uncorrected and corrected data streams. One set of computations assumes that the sensor behaves ideally, i.e. each sensor is assumed to rotate at exactly $\bar{U}\cos\theta$, the other set uses cosine response data obtained from aeronautical wind tunnel tests on the instruments to "correct" every sample of u_1, v_1 and w_1 from each orthogonal array for the sensors non-cosine response.

The correction procedure uses correction factors, which have been obtained by the method given in Section 3.2.5.1 from the response curve given in Fig.3.5 . The correction factors obtained from this curve are given in Appendix A. These values have been modified slightly from the original ones obtained directly from Fig.3.5 so that their change from one angle to the next is more continuous. This proved necessary to ensure that the correction procedure converged quickly to a solution.

The iterative correction procedure used was one suggested by Horst (1973b), rewritten in Algol to run on a Burroughs 6712 computer and to use real variables. It works by using the wind direction from a previous scan as a first trial to locate the correction factors for the next scan. Using the first trial correction factors it multiplies u_1, v_1 and w_1 by them. These first trial corrected velocities are used to obtain a new wind direction which is then used to obtain the next trial correction factors. If the agreement between consecutive trials is less than 2% the values are assumed to have been corrected and iteration ceases. Failing that, the procedure is exited after six iterations have been done. Usually less than three iterations have been found to be sufficient to correct the data. Subsequently in the analysis the response of each anemometer is assumed to be equal to $\bar{U}\cos\theta$ for every scan.

Two computer programs were used to investigate the effect of correcting for non-cosine response. SEQVELTURBREY was used and has been discussed in Section 5.5. This program investigated the effect of the correction on the average velocity, the three orthogonal turbulence intensities and the three Reynolds stresses $\frac{\overline{uw}}{\sigma_u \sigma_w}$, $\frac{\overline{uv}}{\sigma_u \sigma_v}$ and $\frac{\overline{vw}}{\sigma_v \sigma_w}$. The program PSAUTCORS was used to investigate the effect on power spectral densities, autocorrelation functions and the three Reynolds stresses with time lag. The operation of this program has been discussed in Section 5.6. A flow chart and program listing are also given in Appendix F.

The comparison between the two sets of results has made it quite clear that it is necessary to correct the data for the anemometer's non-ideal response when used in orthogonal arrays.

6.1.1 Variation of Wind Speed and Direction

Fig.6.1 shows the variation with time of the average velocity and direction from a data file 73 minutes long. The uncorrected longitudinal component velocity values are generally about 10% less than the corrected values. This is as expected because the anemometers always underestimate the actual velocity. The angle between the wind vector and the anemometer aligned along the x_1 axis can be seen to have reduced by about 4° for the entire period. This again is as expected because the x_1 anemometer had approximately 60° between itself and the wind vector and the data needed greater correction than data from the y_1 anemometer which had 30° between itself and the wind vector. Consequently the velocity from the x_1 anemometer is increased by a greater percentage than that on the y_1 anemometer, thereby reducing the angle between the x_1 anemometer and the wind vector.

6.1.2 Variation of Turbulence Intensity

The effect of the non-cosine response correction on the computation of the three component turbulence intensities is somewhat less obvious. The same data stream used to produce Fig.6.1 has been manipulated to yield the turbulence intensity components shown in Fig.6.2. Correcting the data increases the average velocity as shown in Fig.6.1. Since the three turbulence intensities $\frac{\sigma_u}{\bar{V}_Z}$, $\frac{\sigma_v}{\bar{V}_Z}$ and $\frac{\sigma_w}{\bar{V}_Z}$ are normalised by the average velocity, this effect alone would tend to reduce the turbulence intensities. However the correction increases the magnitude of the variation of the velocity components about their mean values when compared with uncorrected data. The relative amount of both of these effects thus determine the amount by which the three turbulence intensities vary.

The points plotted in Fig.6.2 show that $\sigma_w/\bar{V}_Z$ has increased from

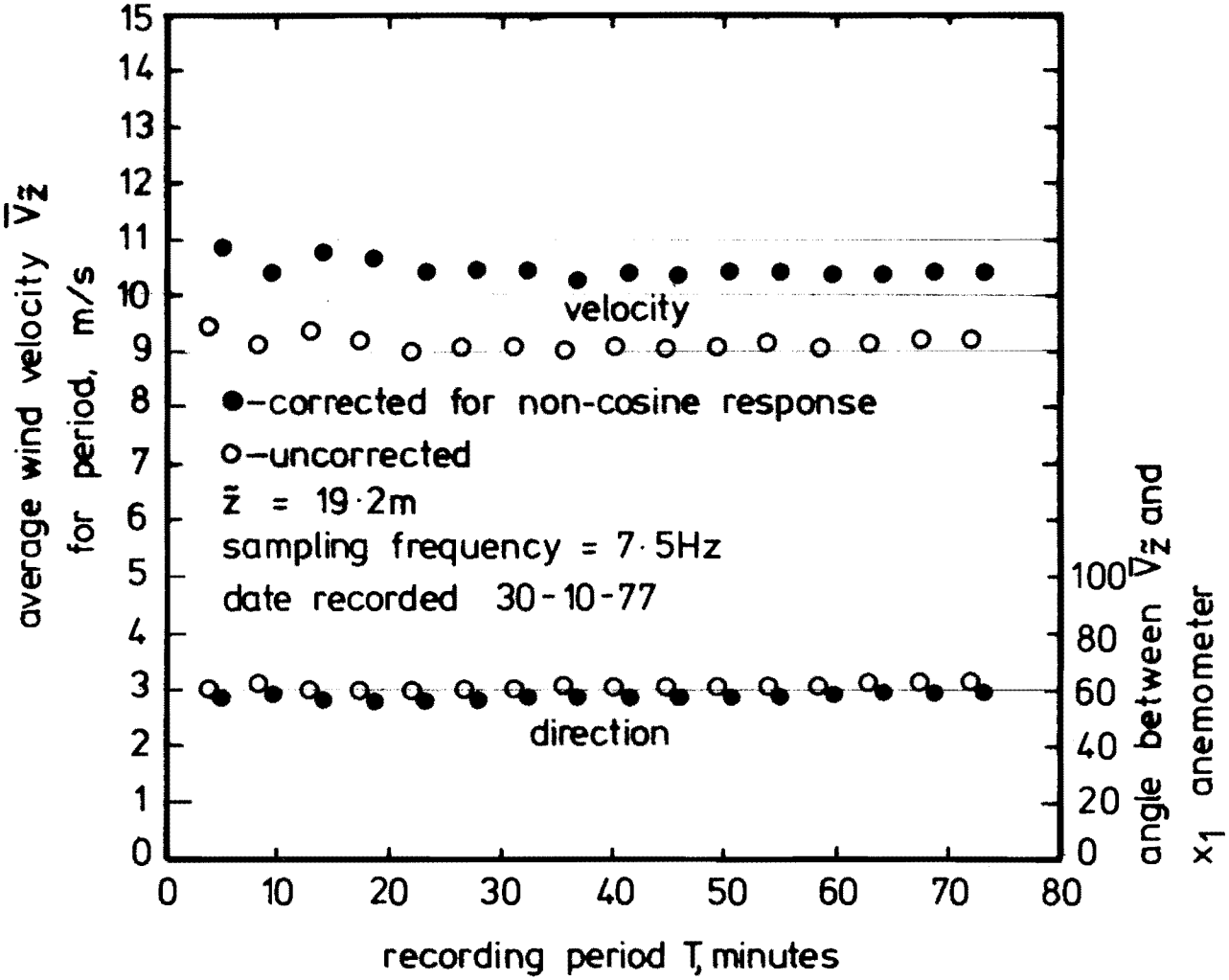

FIG. 6·1 AVERAGE WIND SPEED AND DIRECTION VARIATION WITH LENGTH OF DATA FILE AND CORRECTION FOR NON-COSINE RESPONSE OF THE ANEMOMETER

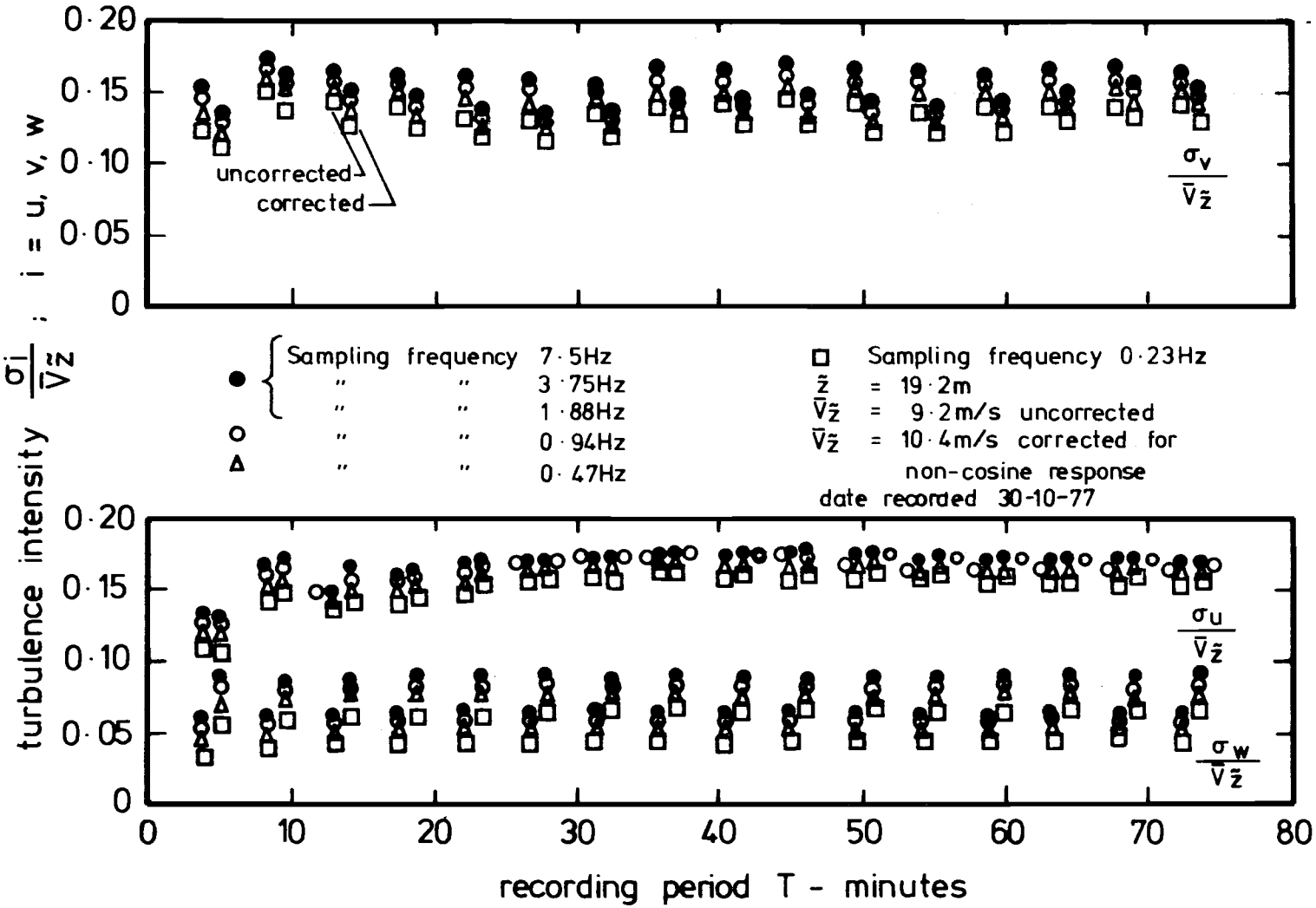

FIG. 6·2 TURBULENCE INTENSITY VARIATION WITH SAMPLING FREQUENCY, CORRECTION FOR NON-COSINE RESPONSE OF THE ANEMOMETER AND LENGTH OF DATA FILE.

about .06 to .08, an increase of about 30%. The amount of increase in $\sigma_u/\bar{V}_Z$ is virtually nil, whilst $\sigma_v/\bar{V}_Z$ levels have been reduced by the correction. Thus σ_u has been increased by the correction but σ_v may have been increased by a much smaller amount, or not at all.

The reason for the large increase in $\sigma_w/\bar{V}_Z$ is apparent if the correction procedure is studied in detail. In most cases the rotational speed of the vertical component anemometer is small compared with the horizontal component anemometers. This means that the wind vector is frequently around θ = 90 degrees for the vertical component anemometer where its non-cosine response is worst. Consequently the correction factors for this region are correspondingly larger meaning that w_1 and therefore σ_w are increased by a much greater amount than $\bar{V}_Z$, thus increasing the value of $\sigma_w/\bar{V}_Z$. For the two horizontal component turbulence intensities the effects of this correction on σ_u and σ_v are of similar size to the corrections on $\bar{V}_Z$.

6.1.3 Variation of Reynolds Stresses

Fig.6.3 reveals that correcting the data stream for non-cosine response has caused a slight reduction in magnitude of the $\overline{uw}/\sigma_u\sigma_w$ or $\rho_{uw}(0)$ Reynolds stress from about -0.38 to -0.37. The $\rho_{vw}(0)$ Reynolds stress is near zero, i.e. virtually no correlation exists, and there is little or no effect of the non-cosine response correction. A large change in $\rho_{uv}(0)$ is shown in the same figure however. It reduces from about 0.1 to about -0.2. Correcting the velocity data for non-cosine response has made it much more negatively correlated.

Figs. 6.4, 6.5 and 6.6 show the three Reynolds stresses calculated from 72.8 minutes of the same data stream used in the previous figures. These figures have been calculated with the program PSAUTCORS using the roundabout fact Fourier transform method whereas Figs.6.1, 6.2 and 6.3 were derived using the program SEQVELTURBREY which used a simple product

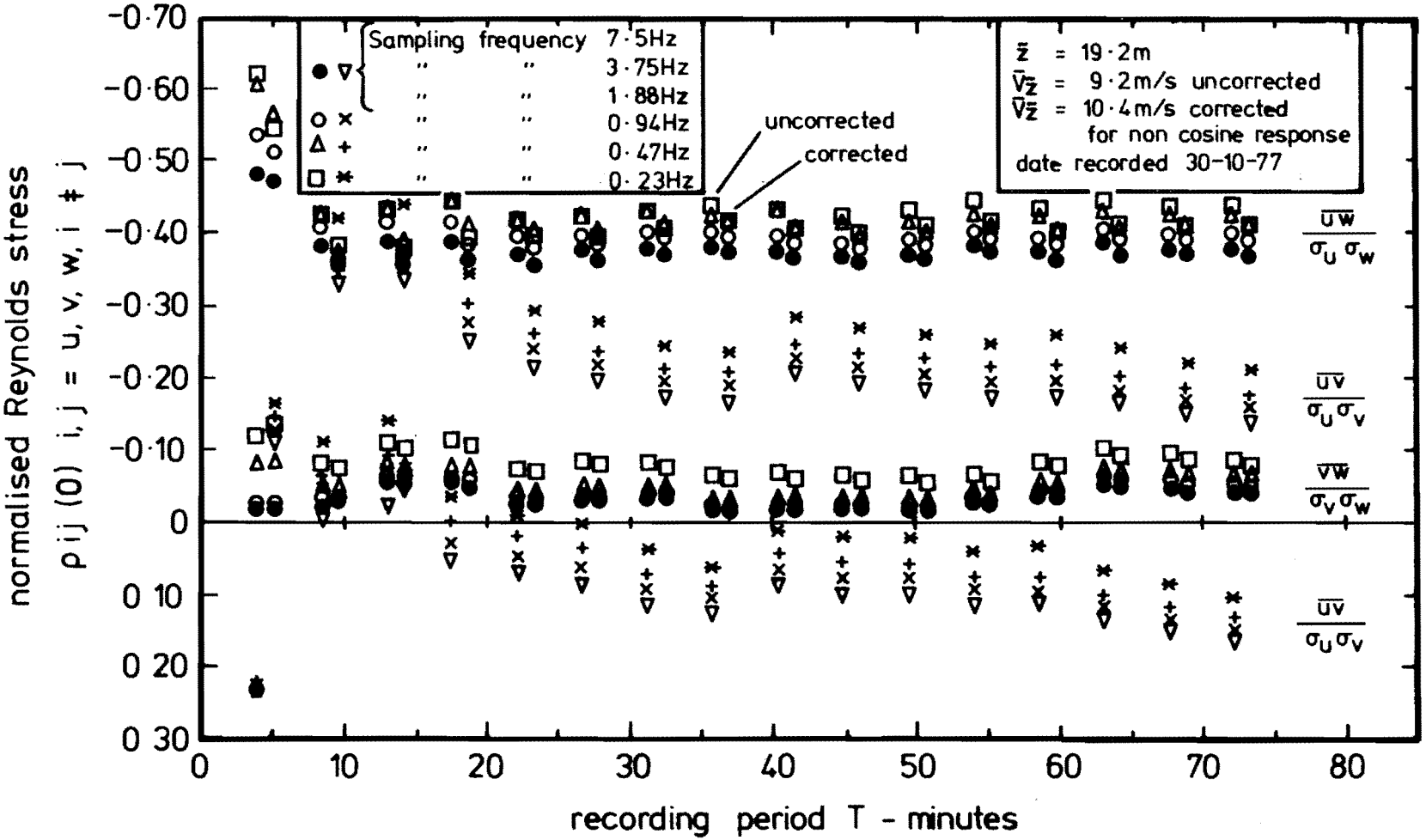

FIG. 6·3 REYNOLDS STRESS VARIATION WITH SAMPLING FREQUENCY, CORRECTION FOR NON-COSINE RESPONSE OF THE ANEMOMETER AND LENGTH OF DATA FILE.

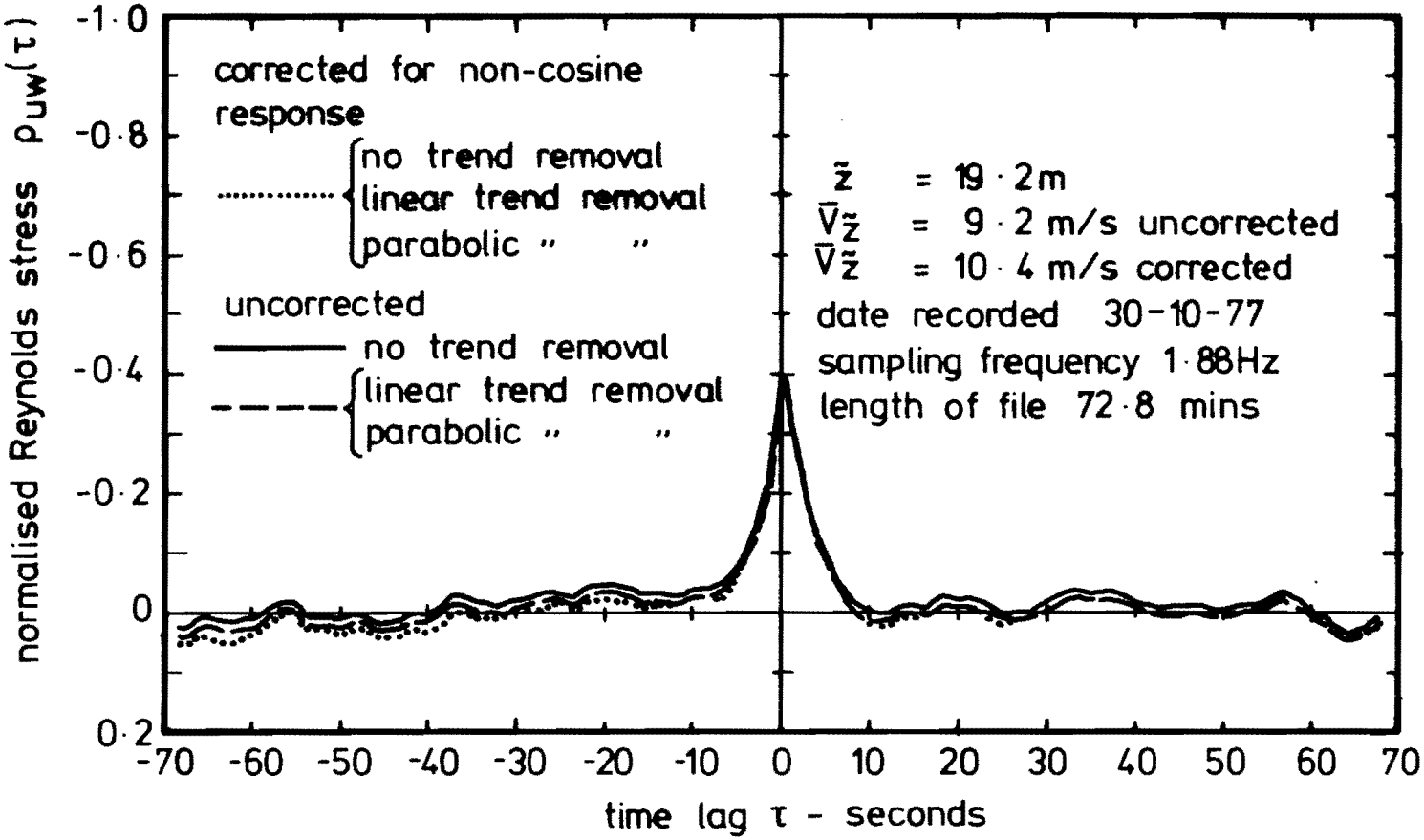

FIG. 6·4 VARIATION OF $\frac{\overline{uw}}{\sigma_u \sigma_w}$ NORMALISED REYNOLDS STRESS WITH TIME LAG, TREND REMOVAL AND CORRECTION FOR NON-COSINE RESPONSE.

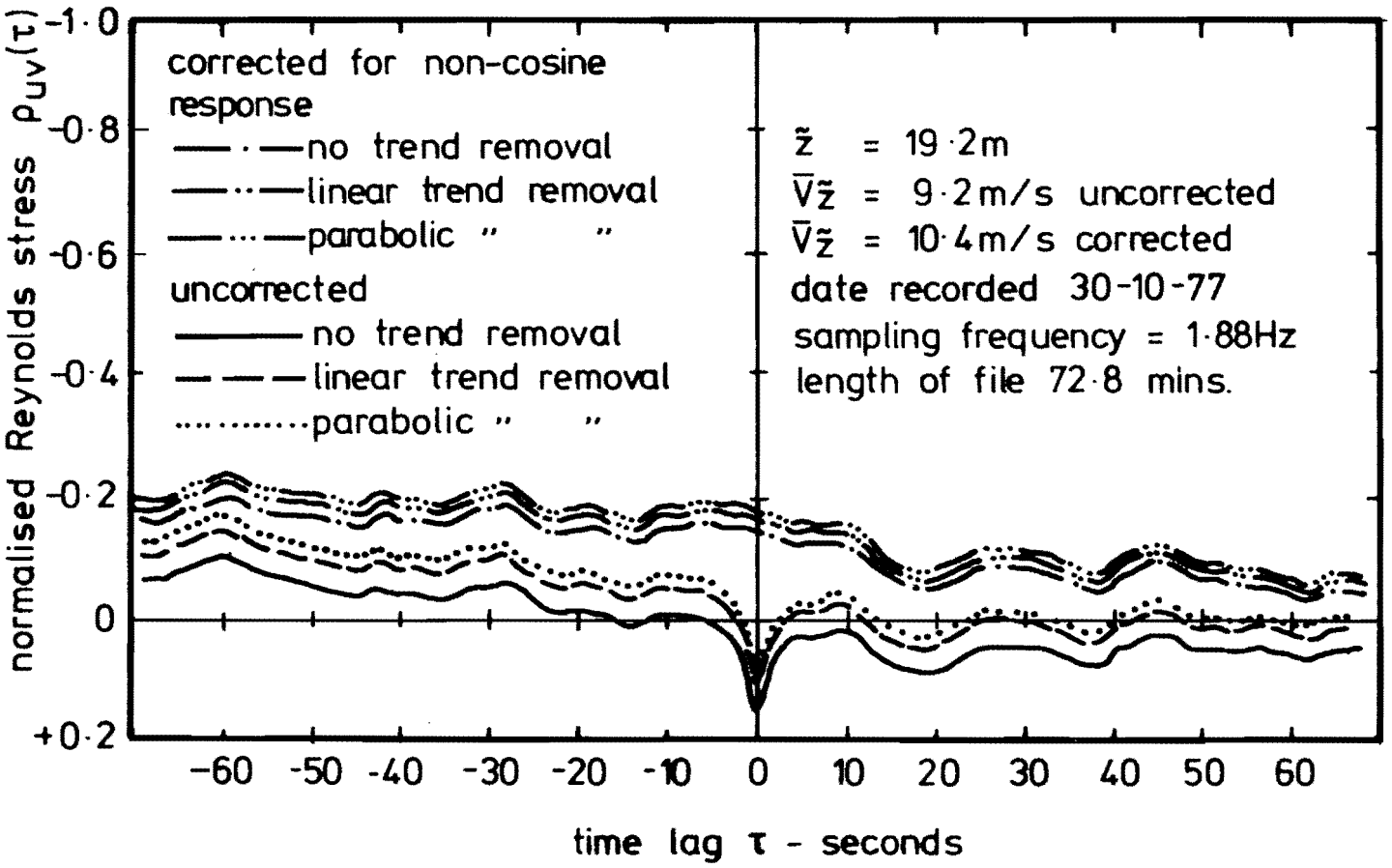

FIG. 6·5 VARIATION OF $\frac{\overline{uv}}{\sigma_u \sigma_v}$ NORMALISED REYNOLDS STRESS WITH TIME LAG, TREND REMOVAL AND CORRECTION FOR NON-COSINE RESPONSE.

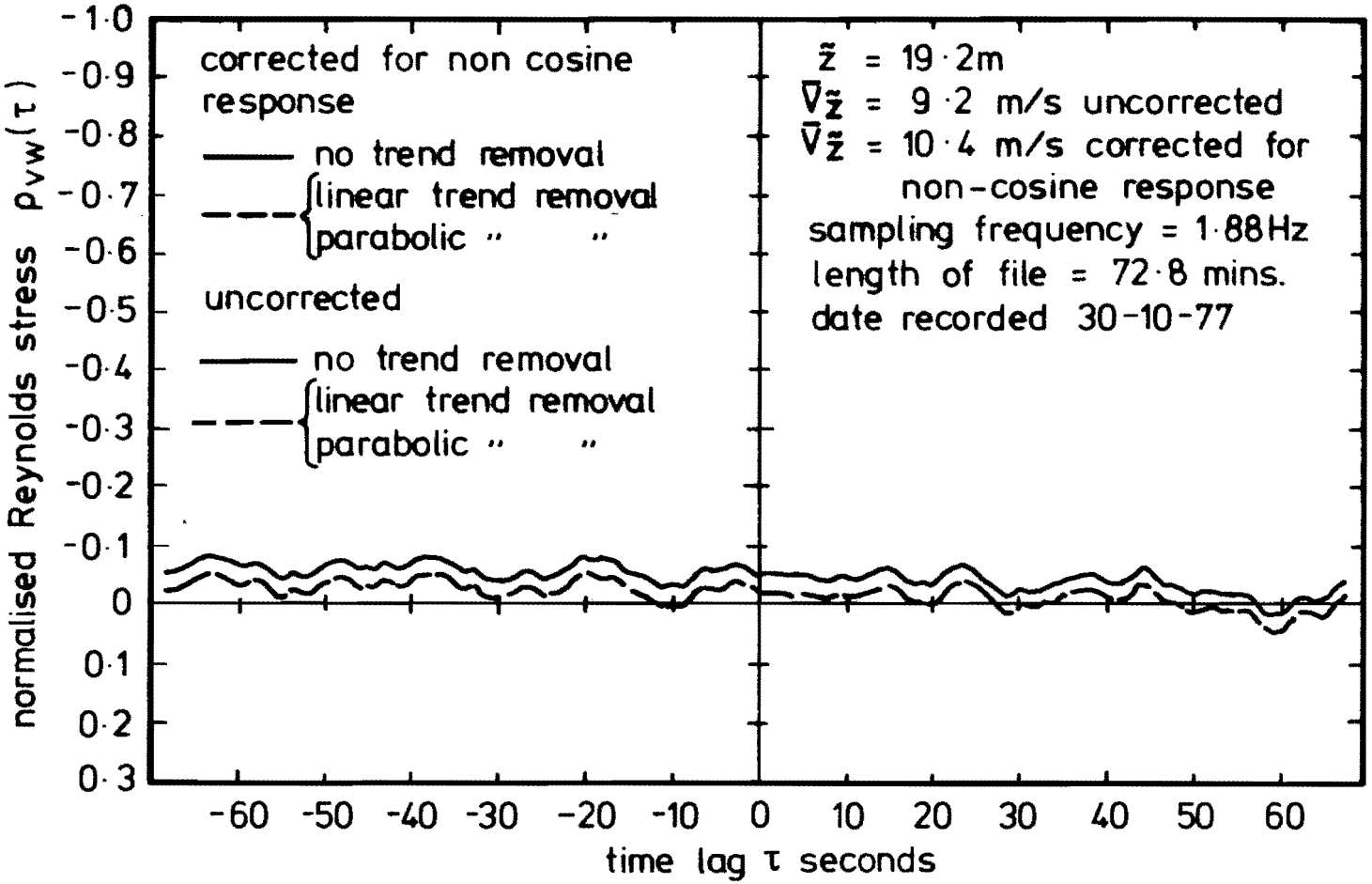

FIG. 6·6 VARIATION OF $\frac{\overline{vw}}{\sigma_v \sigma_w}$ NORMALISED REYNOLDS STRESS WITH TIME LAG, TREND REMOVAL AND CORRECTION FOR NON-COSINE RESPONSE.

summation technique. The results from the two programs at a time lag τ of zero can thus be used as a check on their accuracy, providing account is taken of one feature which the program SEQVELTURBREY incorporates and which PSAUTCORS does not. This is a correction for $\rho_{uw}(0)$, discussed in Section 5.5 and Appendix E, resulting from misalignments from vertical of the vertical component anemometers. It has generally been observed that the effect of this correction is to make $\rho_{uw}(0)$ closer to zero. It can be seen by comparing Figs.6.3, 6.4, 6.5 and 6.6 that the agreement is good for all of the three Reynolds stresses.

In addition Fig.6.5 shows the large change in $\rho_{uv}(\tau)$ with correcting for non-cosine response. It is shown to extend for all time lags and appears to be caused by the correction procedure introducing a correlation between the u and v data streams.

Further investigation of the correction procedure indicates that the correction factors are indeed slightly correlated. The vertical component velocity is usually small which means that the value of the vertical component velocity has only a small effect in determining the correction factors for the x_1 and y_1 anemometers. Extending this further and neglecting the contribution of the vertical component anemometer in determining the correction factor for the two horizontal component anemometers means that for every given wind direction, the correction factors applied to the horizontal component anemometers correspond to the same pair, i.e. the correction factors applied to the x_1 and y_1 anemometers are related. This is probably how the correlation is introduced. The same effect does not occur with Reynolds stresses involving the vertical component because the correction factor applied to the vertical component data is not affected greatly by the individual velocities measured by the x_1 or y_1 anemometers.

6.1.4 Variation of Power Spectral Density

Normalised power spectral densities for the longitudinal, lateral, and vertical components have been plotted in Figs.6.7, 6.8 and 6.9 respectively for the same data streams used for Figs.6.1 to 6.6, showing the effect of correcting for the non-cosine response of the anemometer. Fig.6.7 shows for the longitudinal component spectrum there is comparatively more energy at low frequencies and less at higher frequencies after correcting for non-cosine response, than without the correction. Horst (1973a) found that the general level of the $nS_{uu}(n)$ spectrum was increased slightly by correcting for non-cosine response. Note that the results of Horst are not normalised by σ_u^2. Horst found that correcting for non-cosine response made the propeller anemometer spectra agree well with spectra obtained from nearby sonic anemometers. The most significant difference was at frequencies above 0.3 Hz where the propeller anemometers underestimated the sonic anemometer spectrum due to the propellers' inertial lag.

Fig.6.8 shows the lateral component power spectral density $nS_{vv}(n)/\sigma_v^2$ which is identical both with and without the correction. Since σ_v has been shown in Fig.6.2 to have been reduced by correcting, the general level of $nS_{vv}(n)$ has been reduced by the correction.

In Fig.6.9 the vertical component spectrum is shown to have increased slightly at high frequencies and to have reduced slightly at low frequencies compared with uncorrected results, following the correction. Since σ_w has been shown to be increased by the correction in Fig.6.2, this means that the general level of $nS_{ww}(n)$, particularly at high frequencies, has been increased by the correction also.

6.1.5 Variation of Autocorrelation Functions

The autocorrelation functions, corresponding to the power spectral densities in Fig.6.7, 6.8 and 6.9, have been plotted in Figs.6.10, 6.11

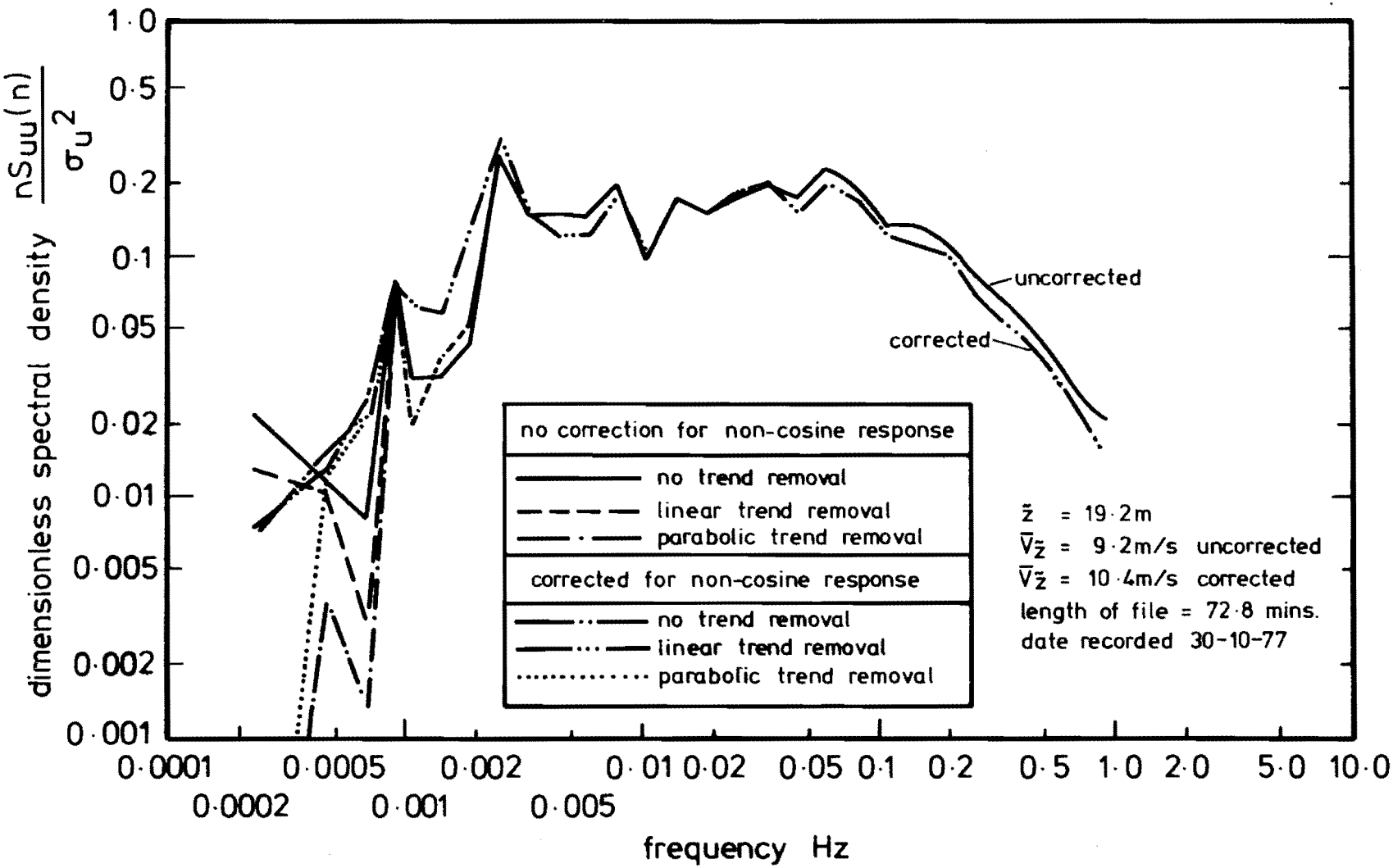

FIG. 6·7 LONGITUDINAL COMPONENT u POWER SPECTRAL DENSITY VARIATION WITH TREND REMOVAL AND CORRECTION FOR NON-COSINE RESPONSE.

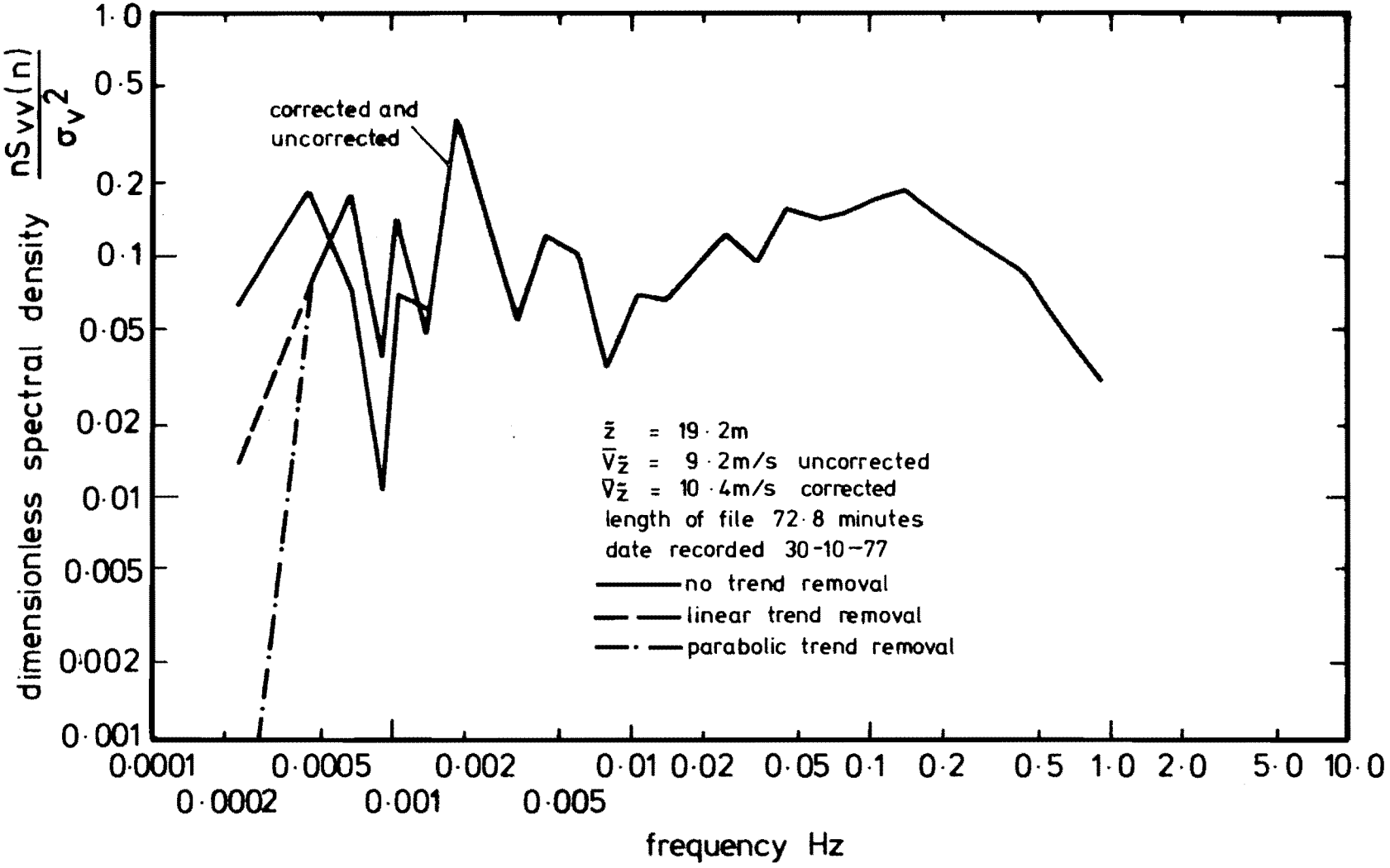

FIG. 6·8 LATERAL COMPONENT v POWER SPECTRAL DENSITY VARIATION WITH TREND REMOVAL AND CORRECTION FOR NON-COSINE RESPONSE.

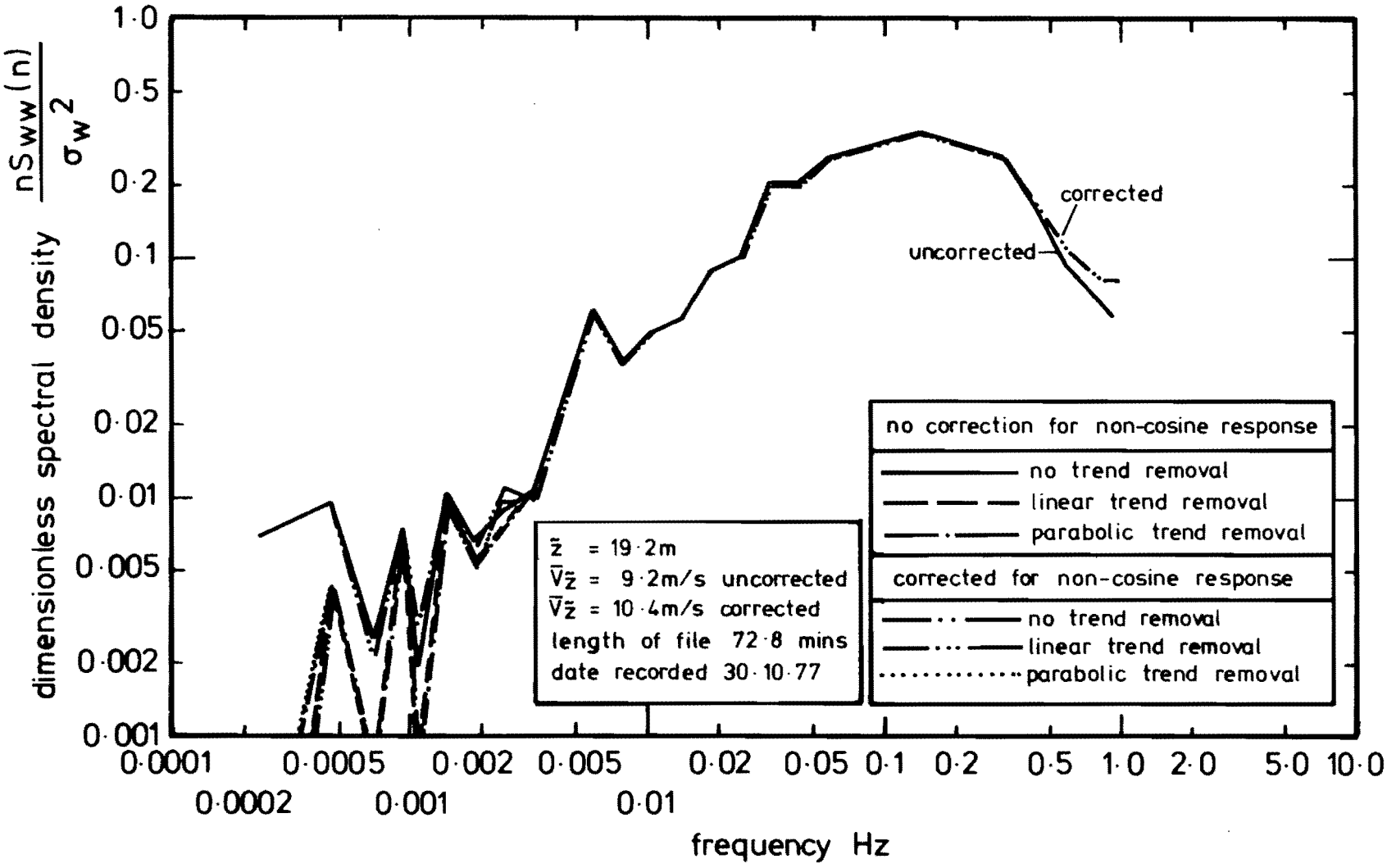

FIG 6·9 VERTICAL COMPONENT w POWER SPECTRAL DENSITY VARIATION WITH TREND REMOVAL AND CORRECTION FOR NON-COSINE RESPONSE.

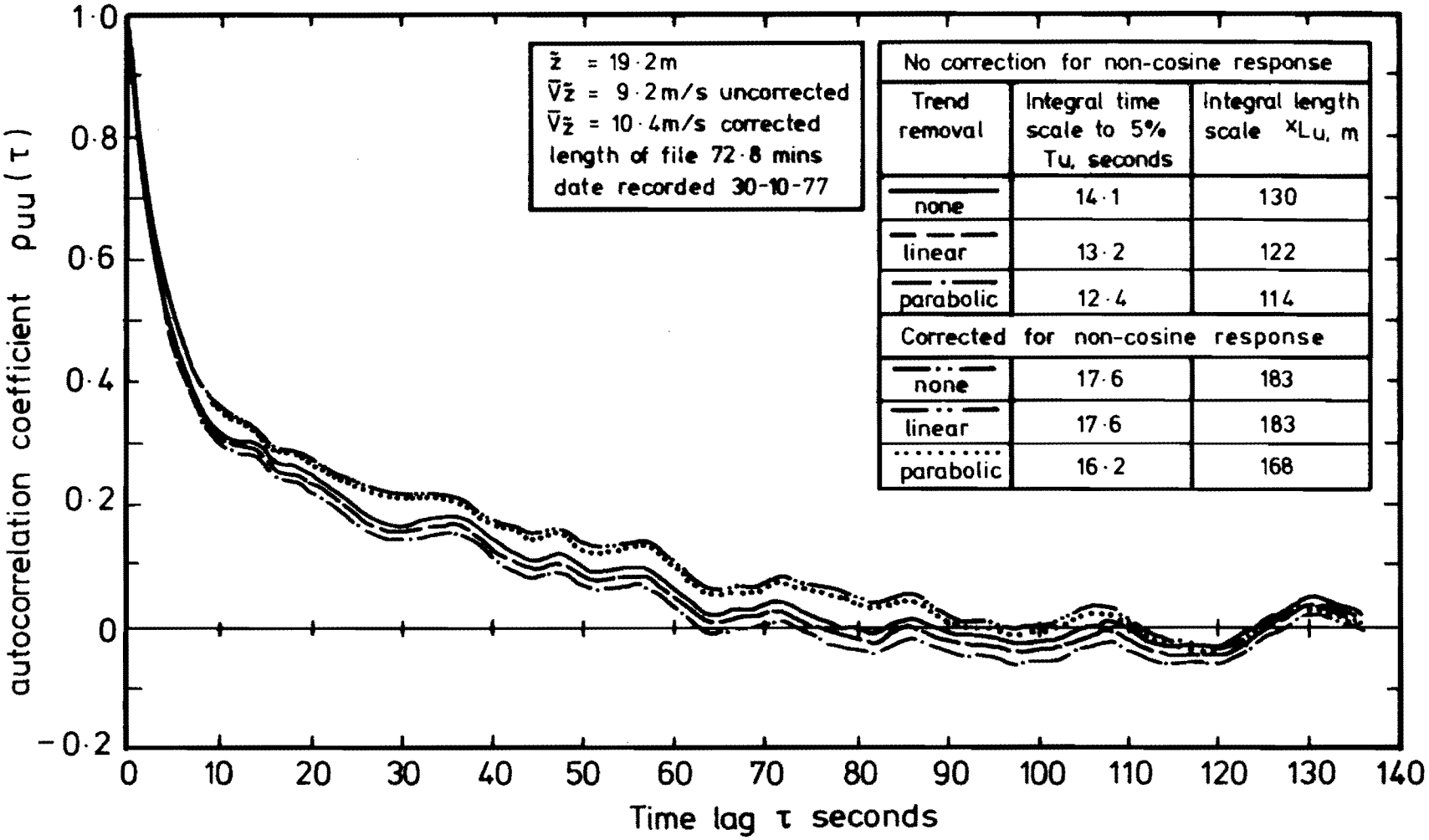

FIG. 6·10 LONGITUDINAL COMPONENT u AUTOCORRELATION FUNCTION VARIATION WITH TREND REMOVAL AND CORRECTION FOR NON-COSINE RESPONSE.

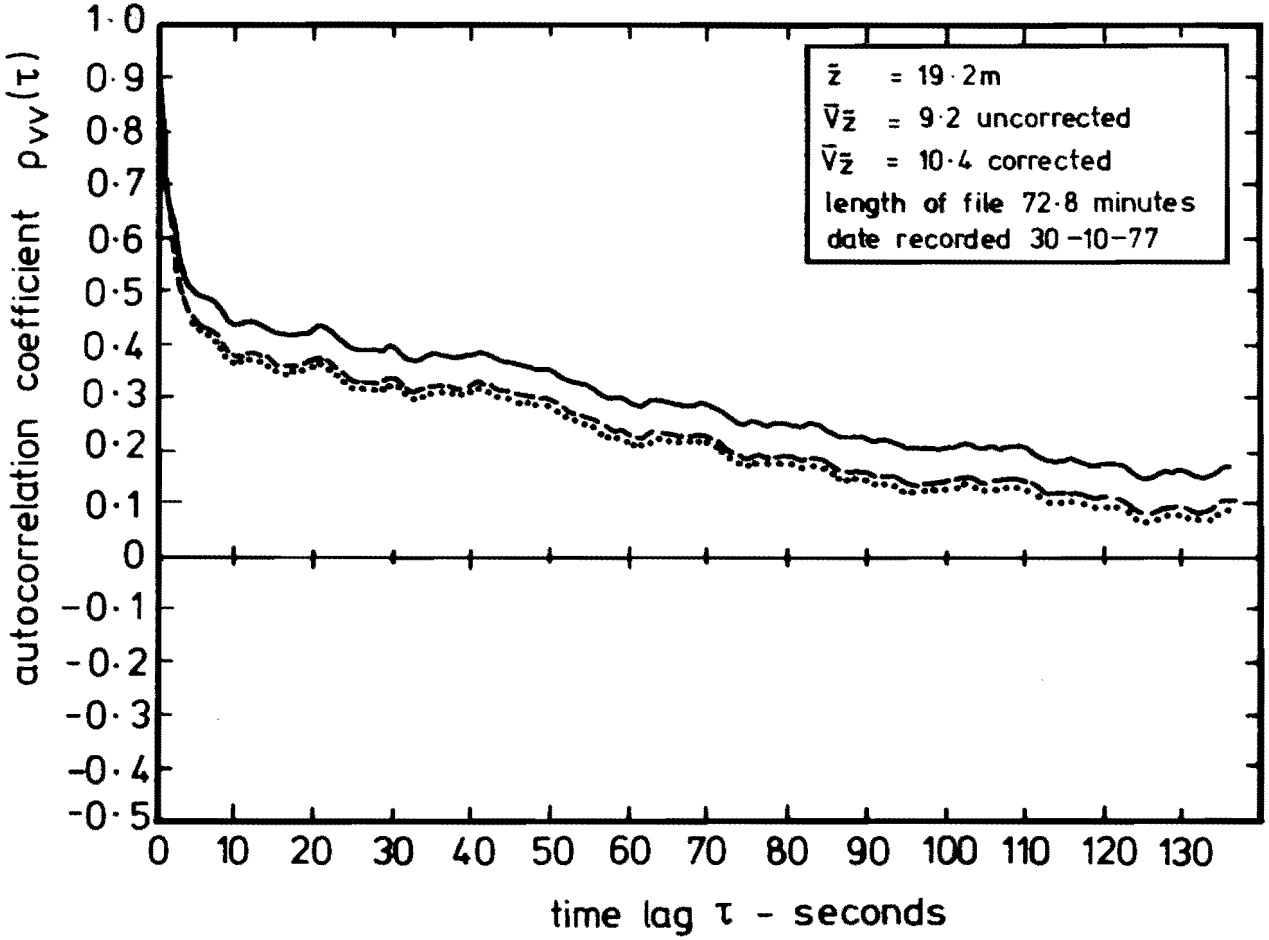

no correction for non-cosine response		
trend removal	integral time scale to 5% T_v, seconds	integral length scale $^{x}L_v$, metres
none	50·5	466
linear	34·7	320
parabolic	31·5	290
corrected for non-cosine response		
none	51·3	534
linear	35·5	369
parabolic	32·0	333

FIG. 6·11 LATERAL COMPONENT v AUTOCORRELATION FUNCTION VARIATION WITH TREND REMOVAL AND CORRECTION FOR NON-COSINE RESPONSE

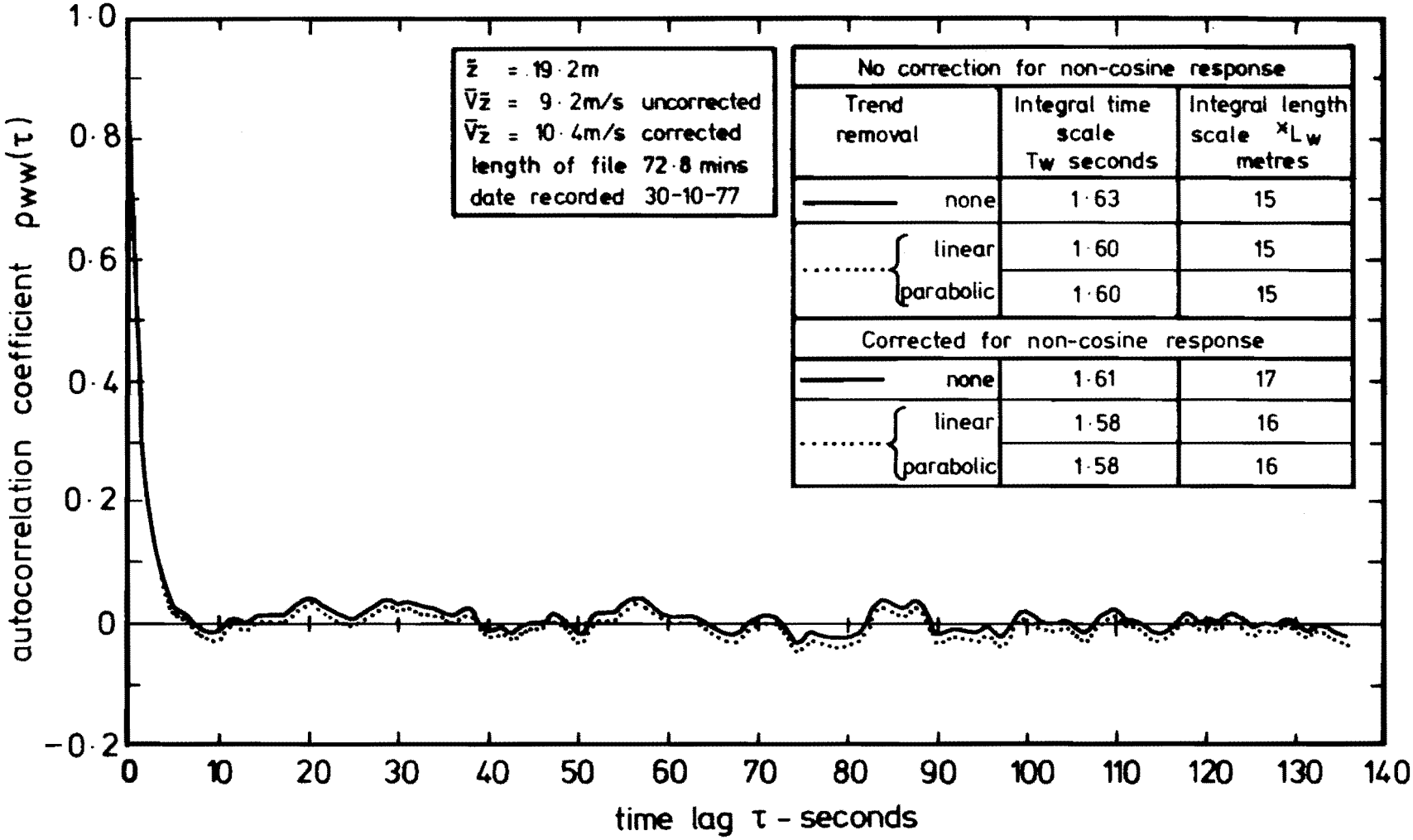

FIG. 6·12 VERTICAL COMPONENT w AUTOCORRELATION FUNCTION VARIATION WITH TREND REMOVAL AND CORRECTION FOR NON-COSINE RESPONSE.

and 6.12. Fig.6.10 shows that the longitudinal component autocorrelation function has a higher correlation for all time lags when corrected for non-cosine response. This means that the integral time scale obtained by integrating the curve (until it drops to a correlation of 5%), has been increased from 14.1 to 17.6 seconds. With the additional increase in the average velocity caused by the correction, the integral length scale $^{x}L_{u}$ has been increased from 130 to 183 m, a considerable amount.

The lateral component autocorrelation function shown in Fig.6.11 is virtually identical both with and without the correction, meaning that the integral time scale T_{v} is virtually identical in both cases. However through the increase in the average longitudinal velocity, the integral length scale $^{x}L_{v}$ has been increased from 466 to 534 m after the correction was applied. This length scale is somewhat corrupted however because Fig.6.11 indicates that the lateral component data contains a trend. This makes estimation of $^{x}L_{v}$ unreliable by the method of integrating the area under the autocorrelation curve.

The vertical component autocorrelation function in Fig.6.12 shows little difference calculated either from corrected or uncorrected data. In fact the integral time scale T_{w} has been reduced from 1.63 to 1.61 seconds by the correction. The larger increase in the average velocity due to the correction, has meant however,that the integral length scale computed from the data streams increased from 15 to 17 m.

These comparisons have served to illustrate that correcting for the anemometers' non-cosine response is necessary when they are used in orthogonal arrays.

6.2 THE EFFECT OF THE LENGTH OF THE DATA RECORDING

A detailed study has been carried out to investigate the effect of the length of the period for which data was recorded on the derived

turbulence parameters. Some of the results have been plotted in the figures which have been discussed in the previous section.

The effect on the average longitudinal velocity and direction, the three component turbulence intensities and the three Reynolds stresses were analysed by plotting out the values as they varied with time for one particular orthogonal array. These values have been plotted at discrete multiples of 4.55 minutes because this was a convenient time length to observe any changes and because it corresponded to numbers of samples which gave an integral number of records of the data file, and hence made programming more straightforward.

The effect of different lengths of the data file on the power spectral densities and autocorrelation functions was observed by calculating these for file lengths of 4.55, 9.10, 18.20, 36.41 and 72.82 minutes. Similar data streams were used as for the previous results discussed in Section 6.1.

Fig.6.1 shows that the average velocity is steady after approximately 25 minutes. Fig.6.2 shows that $\sigma_w/\bar{V}_Z$ is steady after 4.5 minutes and that values of $\sigma_u/\bar{V}_Z$ and $\sigma_v/\bar{V}_Z$ are steady after about 30 minutes. However, even for shorter time periods than these, the fluctuations are small. Fluctuations in the Reynolds stresses shown in Fig.6.3 can be seen to extend for rather longer time periods than the turbulence intensities. However, all three Reynolds stresses do not vary very much for recording periods greater than 30 minutes.

Figs.6.13 and 6.14 show the longitudinal component power spectral densities and the corresponding autocorrelation functions for a variety of recording periods. It is quite apparent in both figures that the longer lengths of the recording reduce the amount of scatter in the derived result. There is not much variation in the power spatial densities and the autocorrelation functions derived from either 72.8

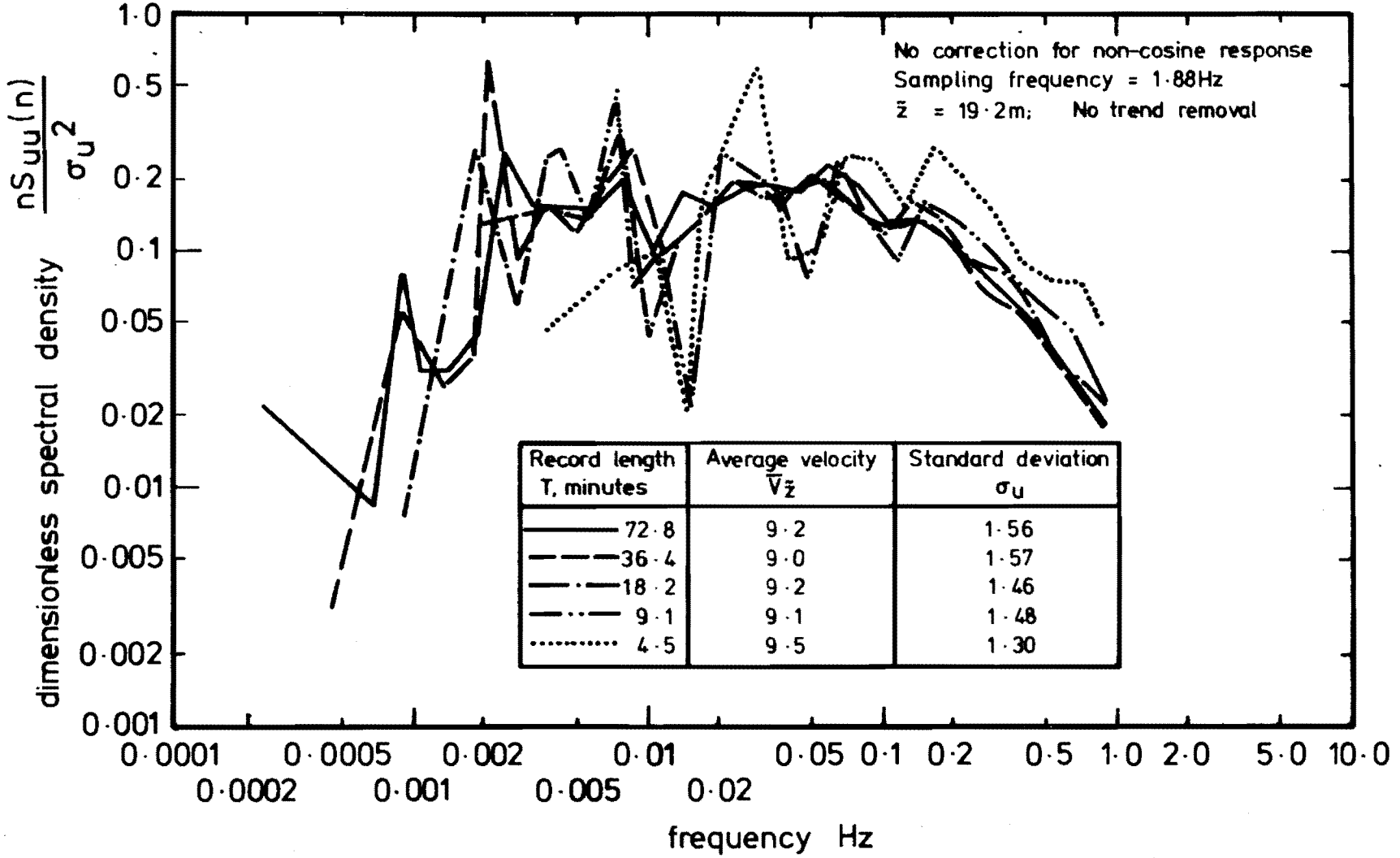

FIG 6·13 LONGITUDINAL COMPONENT u POWER SPECTRAL DENSITY VARIATION WITH LENGTH OF DATA FILE.

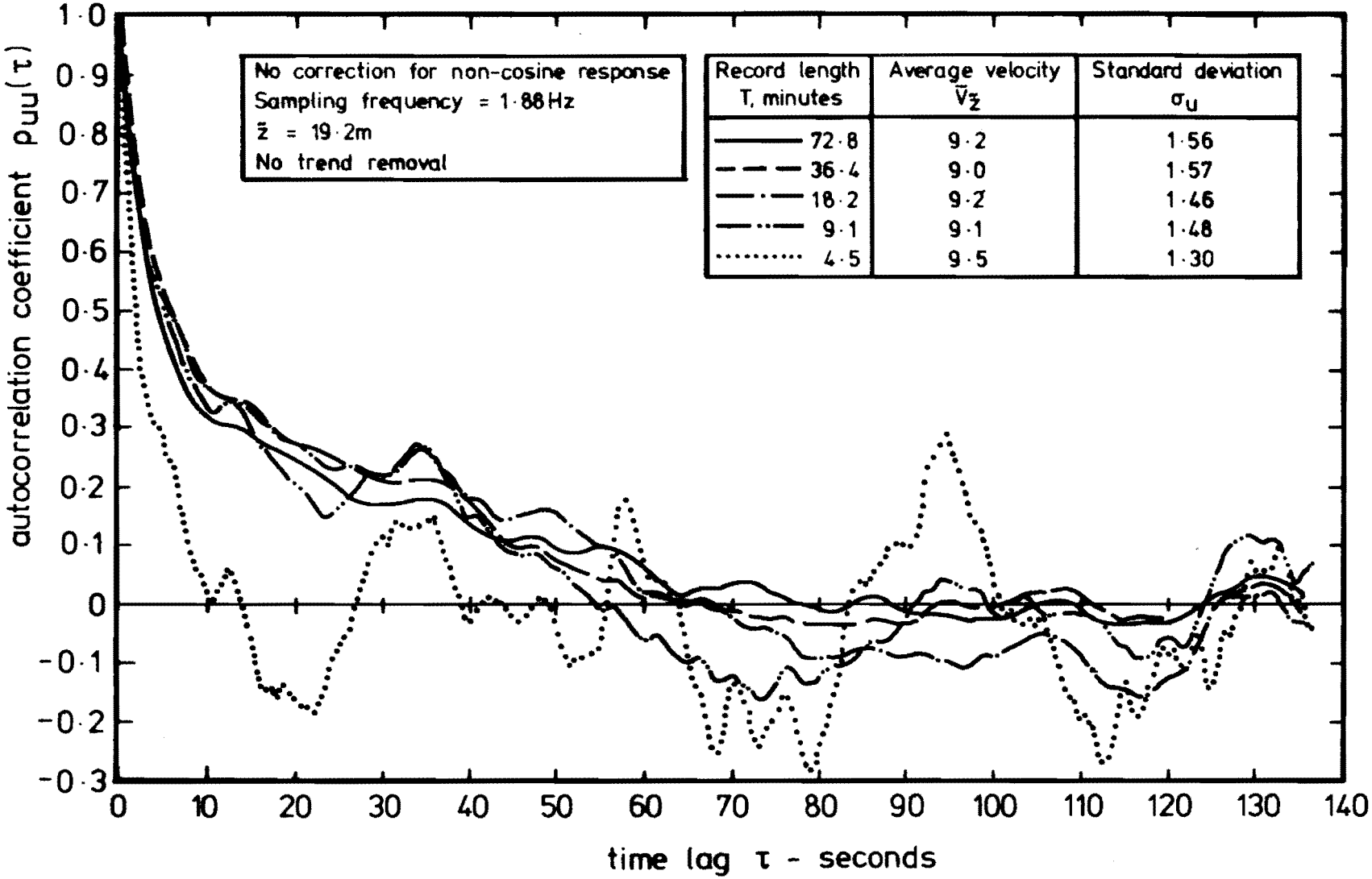

FIG. 6·14 LONGITUDINAL COMPONENT u AUTOCORRELATION FUNCTION VARIATION WITH LENGTH OF DATA FILE.

or 36.4 minutes of data. Shorter data file lengths show a much greater variation.

From the above discussion it has been shown that all of the turbulence parameters investigated appear to be reasonably steady after approximately 30 minutes of data has been analysed. Hence 30 minutes of data could be considered to be the minimum amount of data which should be analysed to give steady, representative results. Larger data file lengths would give better power spectral density estimates at low frequencies, providing the data was still stationary, i.e. the overall wind pattern had not changed.

6.3 THE EFFECT OF SAMPLING FREQUENCY

The effect of the data sampling frequency on the derived turbulence parameter has been investigated to determine the minimum sampling frequency necessary to get results which compare well with results obtained from a higher sampling frequency. It is desirable to use the minimum sampling frequency necessary as this minimises the amount of data to be analysed.

To achieve the objective, the turbulence parameters were calculated from a single data stream, but at a variety of sampling frequencies. The turbulence parameters were then plotted to enable comparisons between sampling frequencies to be made easily.

The sampling frequency was altered by adding consecutive samples together, the number of samples always being a power of 2. Hence the sampling frequency is halved each time from the initial highest sampling frequency which was determined by the scan rate used when the data was recorded. This method of reducing the sampling frequency is therefore equivalent to letting the anemometers drive larger counters which are allowed to integrate over a longer time period (see Section 3.3).

Another method of altering the sampling frequency would have been

to take every nth sample, n being a power of 2. The former method was used because it has a low pass filtering effect, (Teunissen, 1977a), whereas taking every nth sample would have been more prone to cause aliasing.

The average velocity measured at all sampling frequencies was, of course, identical because the same data points were averaged at all frequencies. Fig.6.2, which plots the three turbulence intensities shows that these are affected by the sampling frequency. Sampling frequencies of 7.5, 3.75 and 1.88 Hz are shown to all yield the same result but with further reduction in the sampling frequency the values of all three turbulence intensities is reduced. This figure suggests that a sampling frequency of 1.88 Hz is the lowest for reliable measurements of the three turbulence intensities. The three Reynolds stresses shown plotted in Fig.6.3 also indicate that a sampling frequency of 1.88 Hz is the lowest for reliable measurements. Reductions in the sampling frequency below 1.88 Hz show that for all three Reynolds stresses, the values become more negative, i.e. positive correlations tend towards zero, and negative correlations tend to larger negative values. Since the three Reynolds stresses are normalised by their corresponding standard deviations, in fact they are simply correlations; a decrease in the standard deviations alone will tend to increase the magnitude of the normalised Reynolds stress $\frac{\overline{uw}}{\sigma_u \sigma_w}$ for example.

The frequency at which a continuous signal is sampled is determined by the frequencies in the signal. This in turn is determined by the frequency response of the sensor itself. It has been shown in Section 5.6.2.2 that the sampling frequency is required to be at least twice the highest frequency component in the signal. The digital data is then a true representation of the continuous signal. Sampling at a frequency which is too low causes aliasing. This causes frequency components in the continuous signal with a frequency above half of the sampling

frequency to be interpreted as frequencies less than half of the sampling frequency in the digital data. This effect has been discussed in detail by Bendat and Piersol (1971), Brigham (1974) and Bergland (1969) etc.

Sometimes it may prove to be impossible to sample at a high enough frequency to eliminate aliasing. In that situation an alternative might be to analogue low pass filter the continuous signal before digitisation, as once the signal has been digitised it is impossible to remove the effects of aliasing.

Although the neutral atmospheric boundary layer contains a small amount of energy in eddies even up to 10 Hz, the amount of energy is small above 1 Hz. Also, the propeller anemometer used in this work has a length constant of about .95 m which means that it responds poorly to frequencies above about 1 Hz when the wind speed is about 10 m/s. This would indicate that the rotational velocity should be sampled approximately at 2 to 3 Hz.

The action of the counter which services each anemometer is to integrate the velocity over the period for which it is allowed to count. It thus gives an average velocity for that period. The method of reducing the sampling frequency by averaging consecutive counts acts as a low pass filter with its first zero at $\frac{1}{\text{averaging time}}$ and thus is beneficial from the point of view of aliasing.

To investigate the effect of sampling frequency on the power spectral density, it was calculated for a variety of sampling frequencies and is shown plotted in Fig.6.15. It is immediately apparent that all the curves obtained at different sampling frequencies are all remarkably similar. Lowering the sampling frequency shifts the maximum frequency end of each curve to lower frequencies. The low frequency end is virtually unchanged. The curve obtained from a sampling frequency of 1.88 Hz is probably a good compromise because σ_u is not reduced by much compared with the value at 7.5 Hz and this frequency gives results only where the anemometer response is useful i.e. up to about 1 Hz.

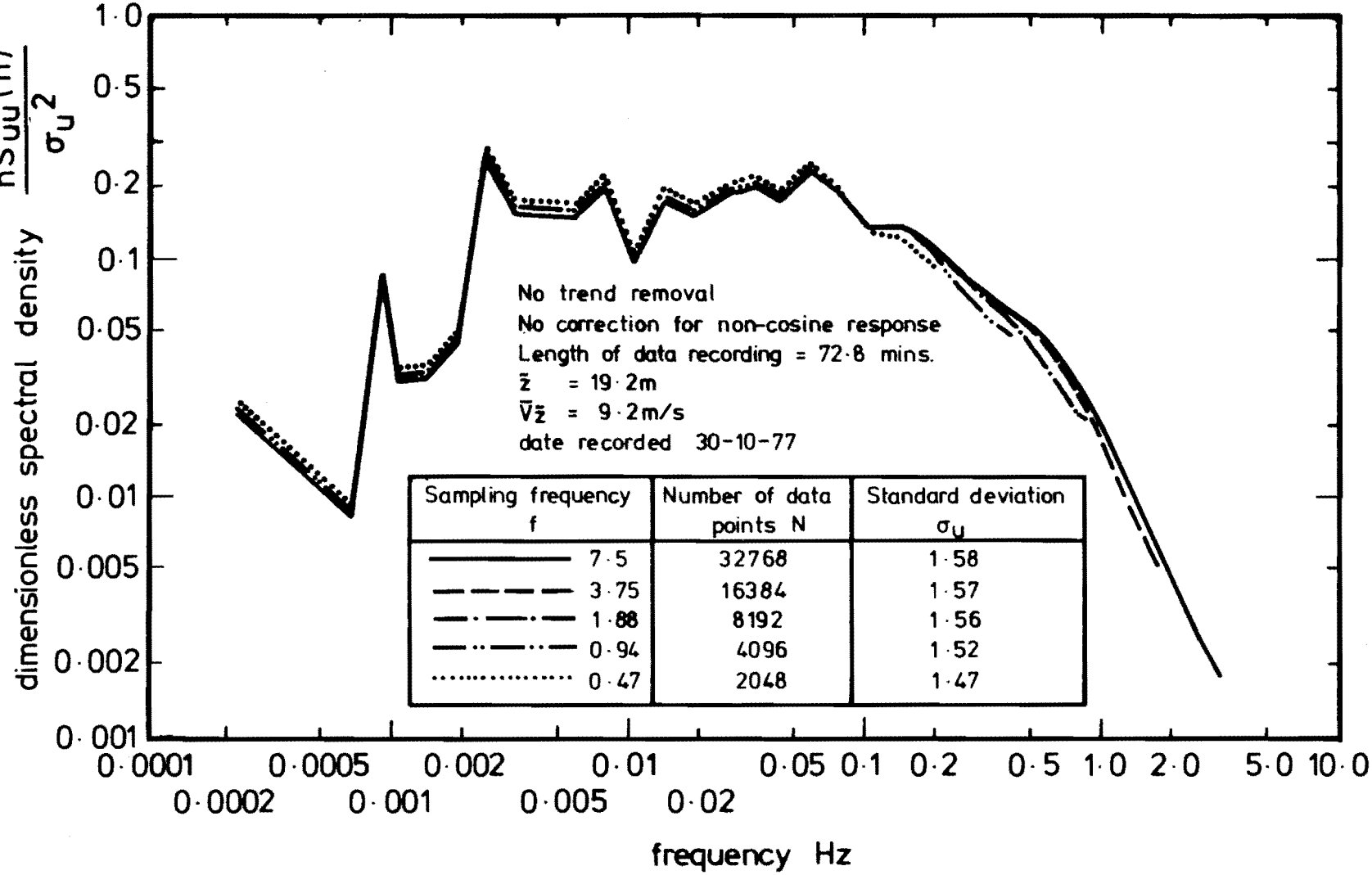

FIG 6·15 LONGITUDINAL COMPONENT u POWER SPECTRAL DENSITY VARIATION WITH SAMPLING FREQUENCY.

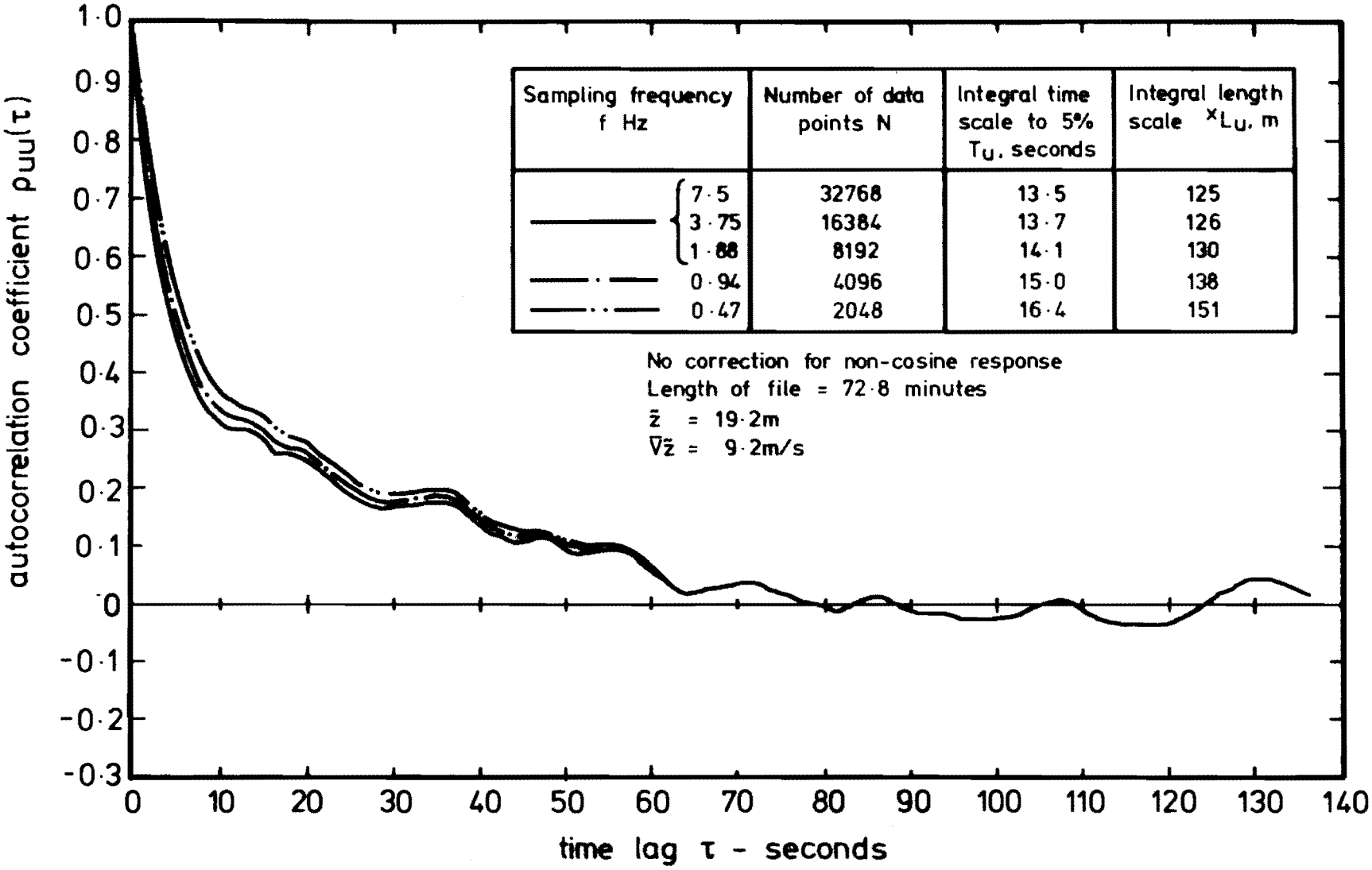

FIG 6·16 LONGITUDINAL COMPONENT u AUTOCORRELATION FUNCTION VARIATION WITH SAMPLING FREQUENCY

Fig.6.16, which shows the corresponding autocorrelation functions, suggests that 1.88 Hz is the lowest permissible because for reduced sampling frequencies, the integral time scale T_u and the integral length scale ^xL_u are both increased significantly.

It is also useful to note that above .5 Hz the power spectra curves in Fig.6.15 show a more rapid decrease than the theoretical decrease which is a $-\frac{2}{3}$ slope. The spectra could be improved by correcting for inertial lag of the anemometer, as suggested by Horst (1973a) and MacCready (1970). This can be done by determining the effective length constant as described in Section 3.2.5.

The analysis of the figures in the discussion above would point at a sampling frequency of 1.88 Hz as being an acceptable compromise between reliable results and minimum data to analyse. This frequency is also physically justifiable considering the sensor's frequency response. This frequency would allow one hour of data to be stored in one array of most computers and would therefore enable power spectral densities and autocorrelations to be calculated easily.

6.4 THE EFFECT OF TREND REMOVAL

A trend in the data is defined as any frequency component whose period is longer than the time for which data was recorded. In particular, this type of component cannot be removed by highpass digital filtering, (Bendat and Piersol, 1971). Hence a special trend removal technique must be applied. In the data presented here, least squares procedures were employed for the removal of a linear and a parabolic trend.

Trend removal is an important intermediate step in the digital processing of random data. If trends are not eliminated from the data, large distortions can occur in the later processing of correlation and spectral quantities. Trends in the data can completely nullify the

estimation of low frequency spectral content.

Slow drifts in the average velocity, or trends, are not uncommon in wind records of 10 to 60 minutes duration and are the result of the inherent nature of atmospheric winds. They are low frequency variations in wind speed and/or direction caused by long term weather pattern changes and can be intepreted as a manifestation of the fact that the so-called "spectral gap" hypothesis is not always a perfect one. There is often significant energy in spectral components with periods between 10 to 60 minutes, (van der Hoven, 1957). These low frequency variations tend to make integral length and time scales calculated from correlation curves very difficult to determine because the low frequency variations tend to prevent the correlations from approaching zero at large time lags. Trends in the data indicate what the wind is actually doing but are required to be removed to make the process ergodic. The ergodic process can then be analysed using conventional statistical theory.

The propeller anemometers used in this work were aligned so that the wind vector lay between the two horizontal component anemometers so that they did not shelter each other at all. The terrain was reasonably horizontal, so that average wind vector was assumed to lie in the horizontal plane. This meant that the components measured by the horizontal component anemometers could be resolved in some way to obtain the longitudinal and lateral component variation of the mean wind vector.

A trend in the wind behaviour, either a change in velocity or direction would manifest itself as a trend like behaviour on anemometers aligned in both the x_1 and y_1 directions. Thus the trends could be removed either before component rotation into longitudinal and lateral components, or after component rotation. The former method considers that the mean wind vector varies in a trend like manner in both magnitude and direction throughout the data recording. Both methods have been discussed by Teunissen (1977a) who found that either method produced equivalent

results but that the latter was a better alternative computationally because it was easier to express the mean by a fixed value rather than a trend line.

In this work the mean values on anemometers aligned in the x_1 and y_1 directions were calculated, and then the angle between the mean wind vector and the x_1 anemometer was found. The data was subsequently resolved into longitudinal and lateral components in the following manner. Assume that the velocity data on the x_1 and y_1 anemometers is u_1 and v_1 respectively, and that the time between consecutive samples, of a total of N, is Δt seconds. u and v are the longitudinal and lateral components at each scan respectively. Then, neglecting subscripts,

$$\theta = \tan^{-1} \frac{\sum_{0}^{N-1} v_1}{\sum_{0}^{N-1} u_1}$$

θ is constant for the entire data file.

$$u = u_1 \cos\theta + v_1 \sin\theta$$

$$v = v_1 \cos\theta - u_1 \sin\theta \quad \text{for all samples.}$$

From the resolved data, u and v, linear and parabolic trend lines have been fitted by least squares. The linear trend line is defined by

$$A_0 + A_1.j.\Delta t \qquad j = 0,1,\ldots N-1$$

and the parabolic trend line by :

$$B_0 + B_1.j.\Delta t + B_2(.j.\Delta t)^2$$

where A_0, A_1, B_0, B_1 and B_2 have been found via least squares. These have subsequently been removed from the data by forming new variables without these trends. For linear trend removal, and for the longitudinal component this is,

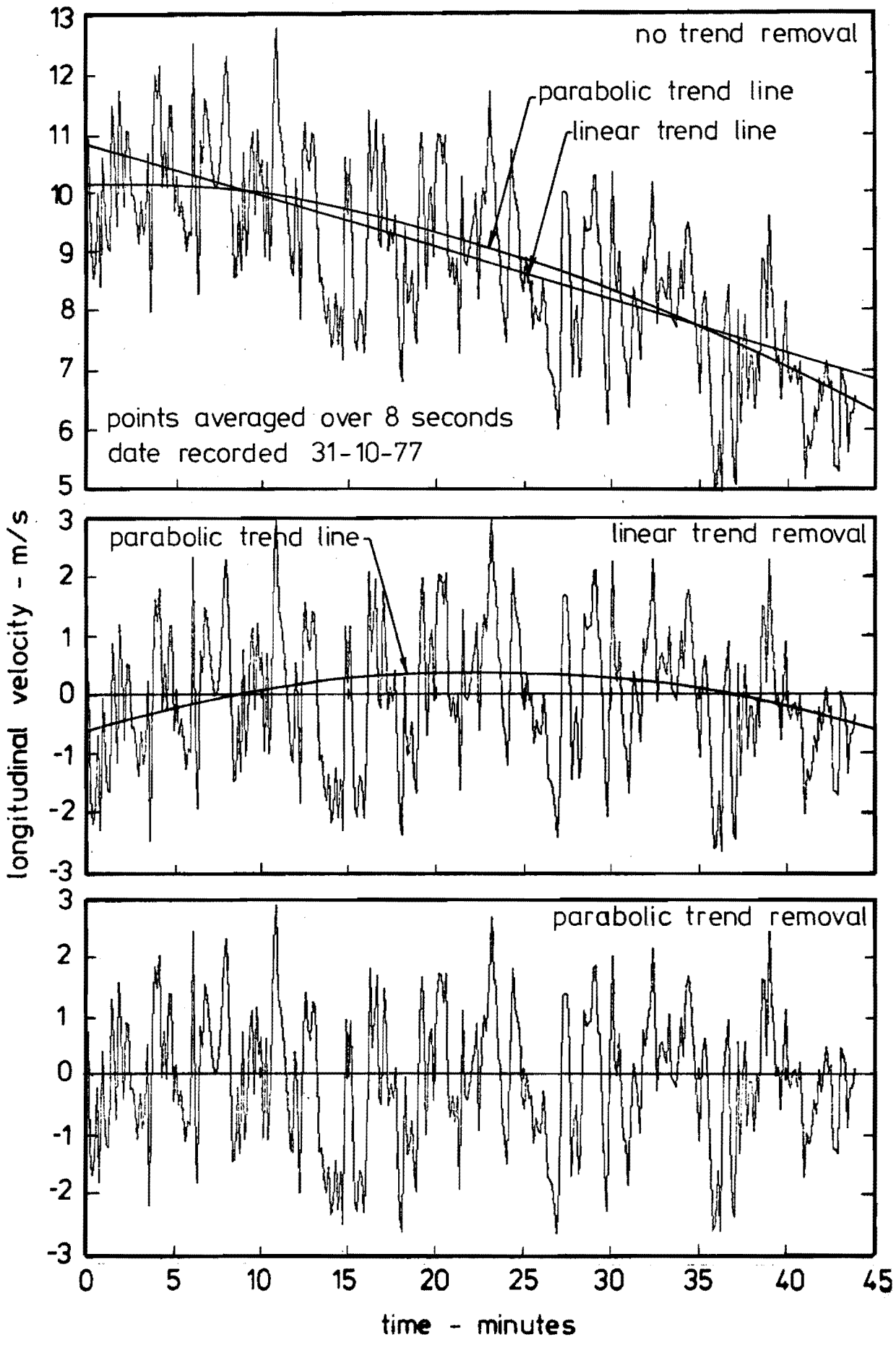

FIG. 6·17 VELOCITY TIME TRACES AFTER VARIOUS TYPES OF TREND REMOVAL

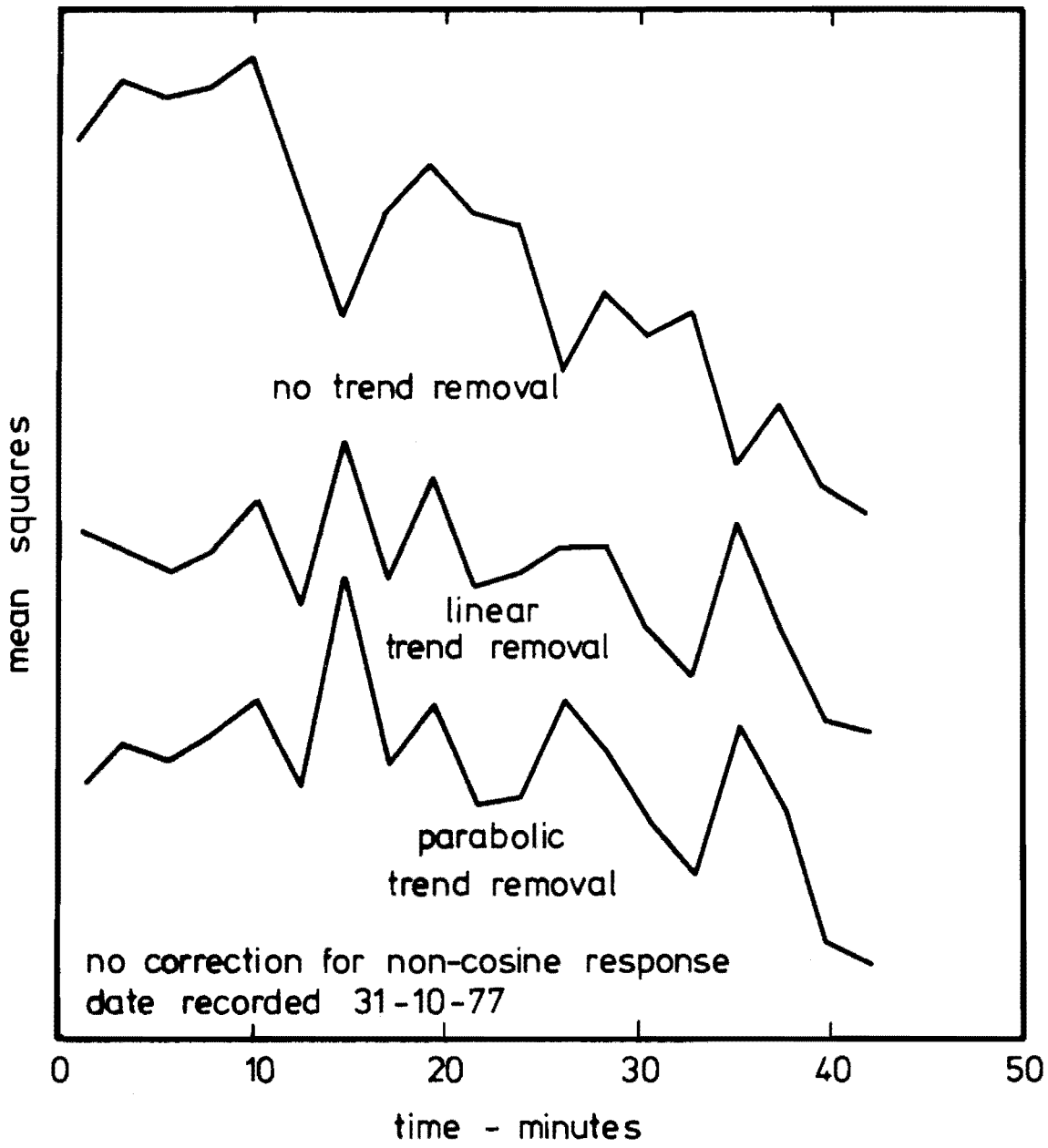

FIG. 6·18 LONGITUDINAL COMPONENT u MEAN SQUARES AVERAGED OVER 2·28 MINUTES, VARIATION WITH TREND REMOVAL.

$$u_{\ell_j} = u_j - A_0 - A_1.j.\Delta t \ , \quad j = 0,1,...N-1$$

and for parabolic trend removal,

$$u_{p_j} = u_j - B_0 - B_1.j.\Delta t - B_2(.j.\Delta t)^2 \ , \ j = 0,1,...N-1$$

where u_{ℓ_j} and u_{p_j} are data with a linear and a parabolic trend removed respectively. The same results hold for the lateral component. The vertical component is easier to deal with since no resolving is involved and the trend lines are removed simply from the data stream w_1 to form trend free data.

Fig.6.17 shows a velocity time trace of the longitudinal component of data collected from one orthogonal array. The marked improvement in the constancy of the mean is quite obvious after linear and parabolic trend lines have been removed from it compared with the data before a trend removal. Fig.6.18 shows the mean squares averaged over 2.28 minutes of the same data used in Fig.6.17. It can be seen that the values vary less after a linear trend line has been removed, although there appears to be little change between parabolic and linear trend removal.

The mean squares averaged over short time periods throughout the recording have been calculated because they are useful in trying to determine whether the data is stationary. This is because a time history can be considered to be stationary if its properties do not vary "significantly" from one independent time interval to the next. The word significantly means that the observed variations are greater than would be expected due to normal statistical sampling variations. This is discussed in greater detail in Section 8.2.

The effect of trend removal on the three orthogonal turbulence intensities can be seen in Fig.6.19 and for this particular data file is not particularly large. It has generally been found that it has little effect on the vertical component, but can have a significant effect on the longitudinal and lateral velocity components.

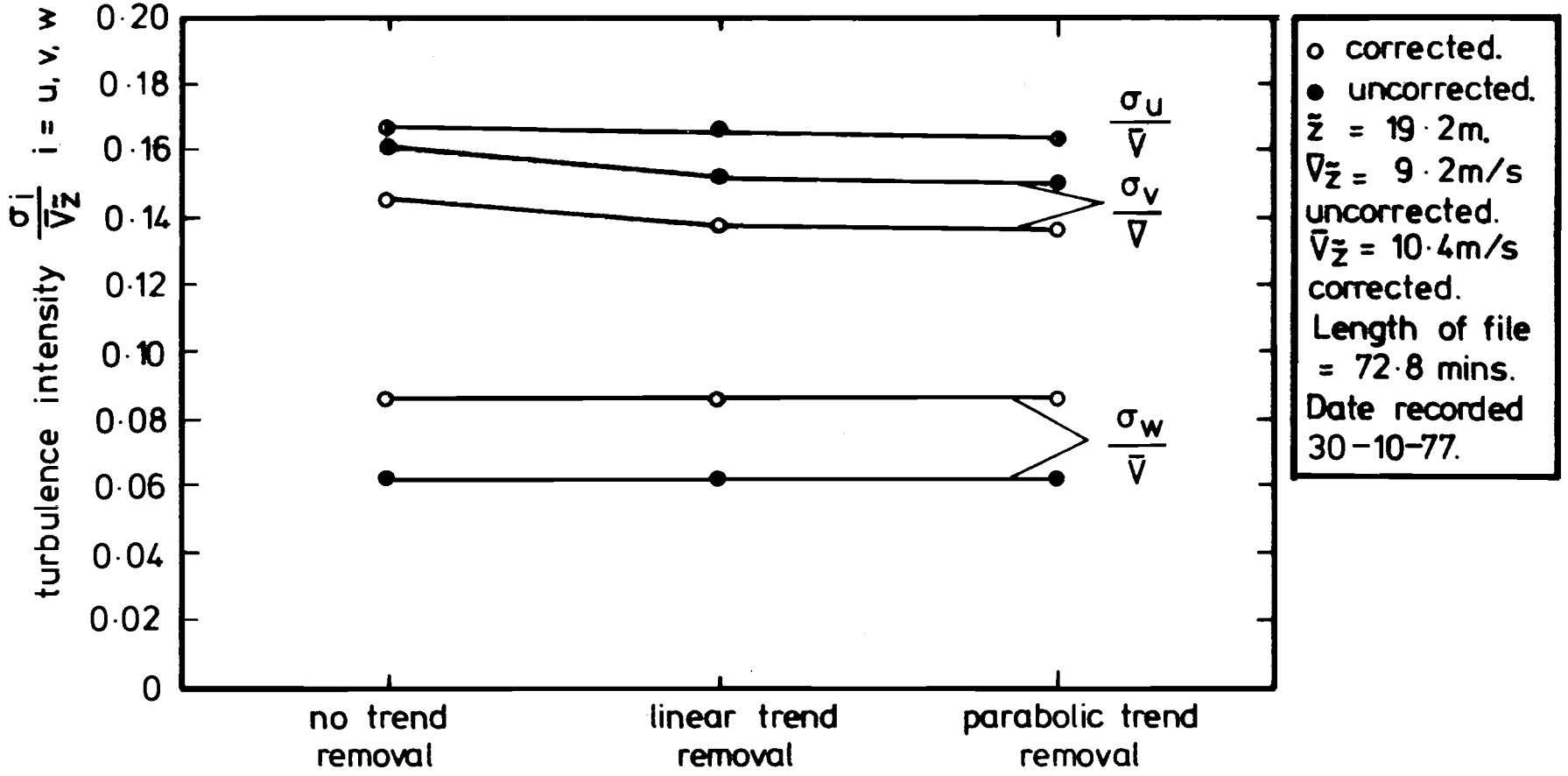

FIG. 6·19 TURBULENCE INTENSITY VARIATION WITH TREND REMOVAL AND CORRECTION FOR NON-COSINE RESPONSE.

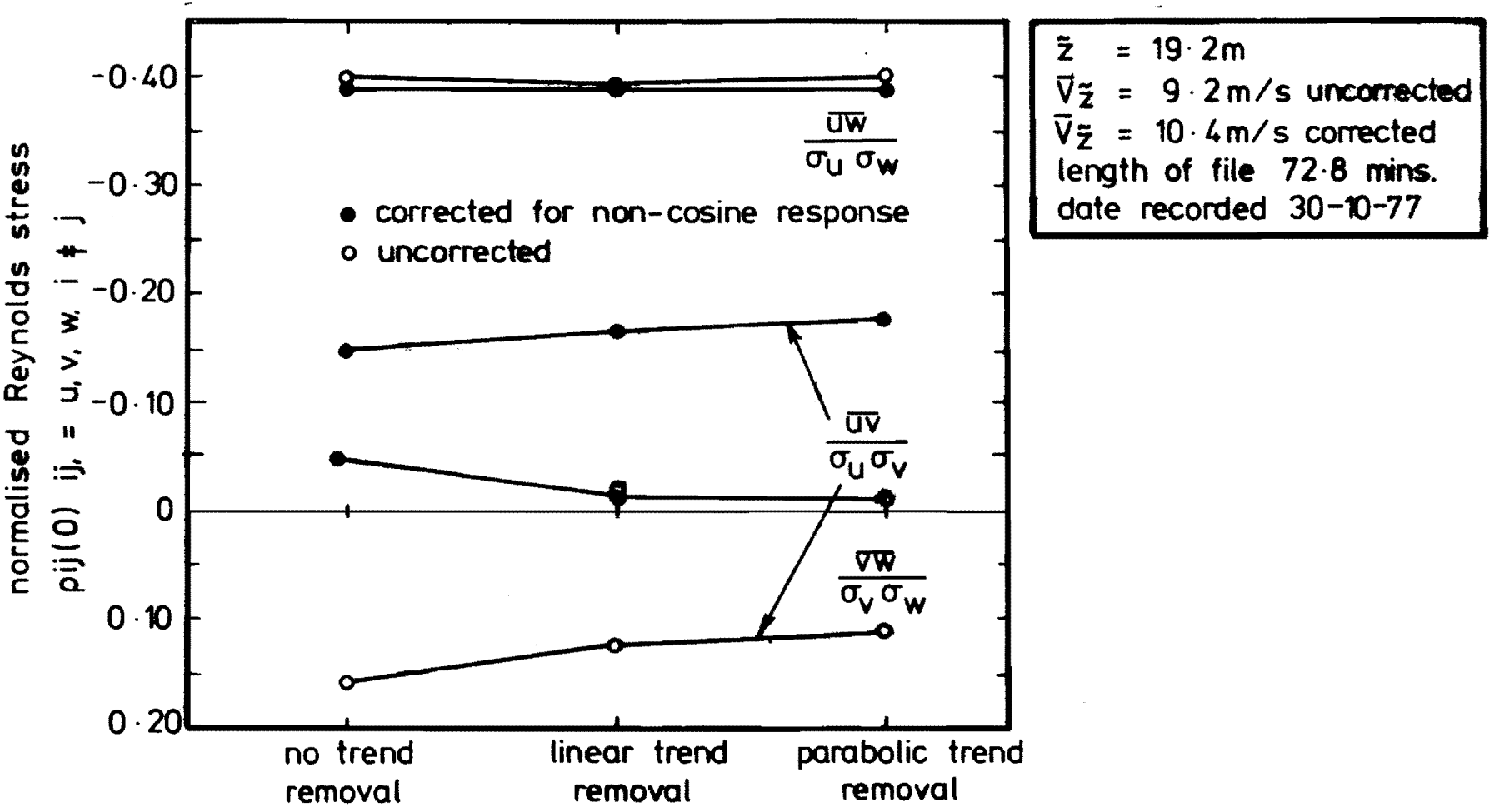

FIG 6·20 NORMALISED REYNOLDS STRESS VARIATION WITH TREND REMOVAL AND CORRECTION FOR NON-COSINE RESPONSE.

The Reynolds stress in Fig.6.4 is shown to approach zero more rapidly following a trend removal, although no effect is noticed on the data which has been corrected for non-cosine response. Removing a trend from the $\rho_{uv}(\tau)$ Reynolds stress in Fig.6.5 is shown in all cases to make the correlation tend towards a more negative correlation, i.e. positive correlations approach closer to zero and negative correlations became more negatively correlated. $\rho_{vw}(\tau)$ is shown in Fig.6.6 to be less well correlated after a trend removal and the same feature can be observed in Fig.6.20 which also shows the change in $\rho_{uw}(0)$ and $\rho_{uv}(0)$ with trend removal.

The effect of trend removal on the longitudinal, lateral and vertical component power spectral densities can be observed in Figs. 6.7,6.8 and 6.9 respectively. In the three figures it can be observed that the effect of removing trends is to influence the low frequency spectral components only. These components are generally reduced in magnitude and have less fluctuation after a trend line is removed. Generally the effect of a parabolic trend line removal is greater than a linear trend line removal.

The effect of trend removal on the three orthogonal autocorrelations from a single anemometer array can be observed in Figs.6.10,6.11 and 6.12. In all cases the effect is to make the correlation approach zero more rapidly than the correlation curve with no trend removal. The parabolic trend line has a greater effect than the linear trend line.

The figures discussed above have shown that various turbulence parameters are influenced by differing amounts by trend removal Sometimes the effect of a linear or a parabolic trend removal is similar and sometimes a parabolic trend removal has much more effect than a linear trend removal. The results have shown that it is an important consideration in data analysis. In this work it was decided to remove a parabolic trend from all data streams regardless of whether they appeared to need

it or not. In fact later results have tended to show that perhaps a higher order polynomial trend line should have been removed from the data.

6.5 THE EFFECT OF A COSINE TAPER DATA WINDOW ON POWER SPECTRA

Power spectra were calculated from data which had a simple "box-car" truncation of the data stream, and also from data which had a "cosine taper" applied to the first and last 10% of the data, as suggested by Bendat and Piersol (1971). These two data windows are shown in Fig.6.21.

Windowing is discussed in, e.g. Yuen and Fraser (1976), Brigham (1974), Bendat and Piersol (1971), Teunissen (1977a), Brook (1974) and Bergland (1969). It is used to reduce the amount of leakage from one frequency component into another. This results from the fact that a time domain truncation of a sampled waveform, (i.e. taking a finite length of data), results in a frequency domain convolution with a $\frac{\sin(f)}{f}$ function. This convolution introduces additional components into the frequency domain because of the side lobe characteristics of this function.

To reduce leakage of one spectral component into another, it has been suggested that it is necessary to employ a time domain truncation function which has side lobe characteristics which are of a smaller magnitude than those of the $\frac{\sin(f)}{f}$ function. The cosine taper is one of these.

Brook (1974) has noted that the advantages in using a more sophisticated window than the box-car are not immediately obvious. Akins and Peterka (1975) suggest the use of a cosine taper but do not discuss it in detail.

Because of the inconsistency of evidence in the wind structure literature on the use of such windows, spectra were calculated using both a box-car and a cosine taper data window, and the spectra obtained

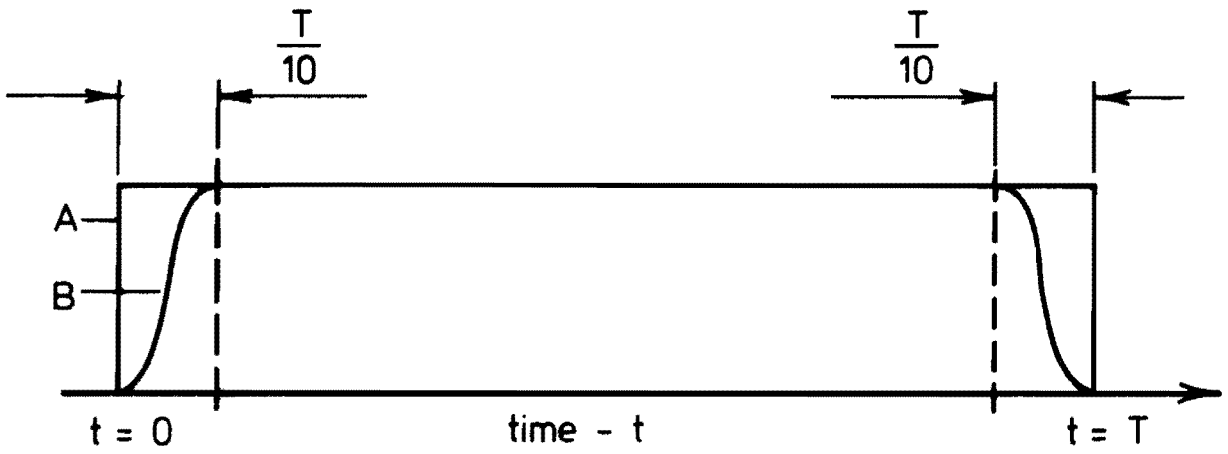

A - Boxcar data window

$x(t) = x(t)\ ,\ 0 \leq t < T$

$= 0$ otherwise

B - Cosine taper data window

$x(t) = x(t) \times [0{\cdot}5 - 0{\cdot}5 \cos(\frac{10\,t\pi}{T})], 0 \leq t < \frac{T}{10}$

$x(t) = x(t), \frac{T}{10} \leq t < \frac{9T}{10}$

$x(t) = x(t) \times [0{\cdot}5 + 0{\cdot}5 \cos(\frac{10\pi}{T}\{t - \frac{9T}{10}\})]$

$\frac{9T}{10} \leq t < T$

$x(t) = 0$, otherwise

FIG 6·21 BOXCAR AND COSINE TAPER DATA WINDOWS

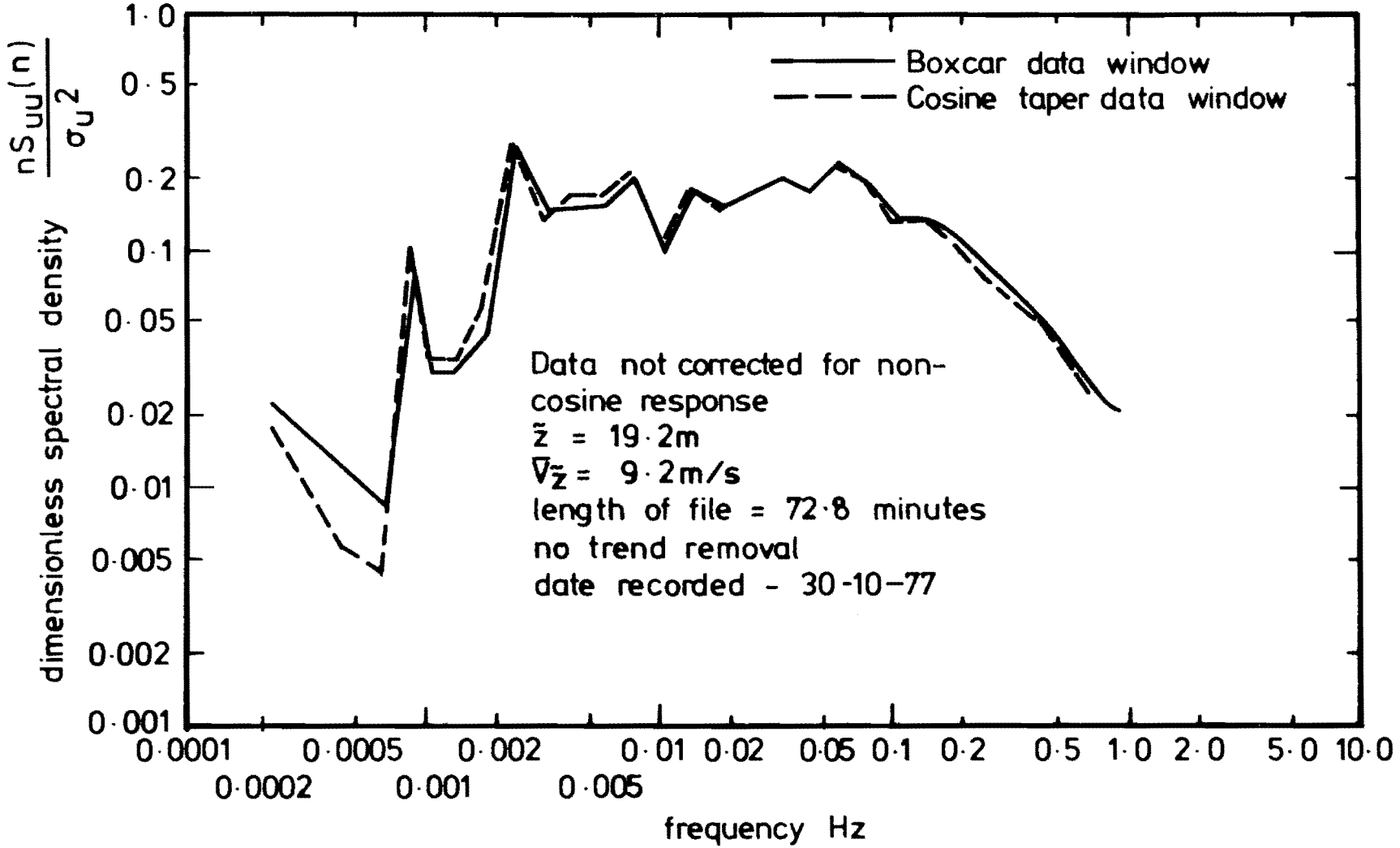

FIG. 6·22 LONGITUDINAL COMPONENT u POWER SPECTRAL DENSITY VARIATION WITH A BOXCAR AND A COSINE TAPER DATA WINDOW.

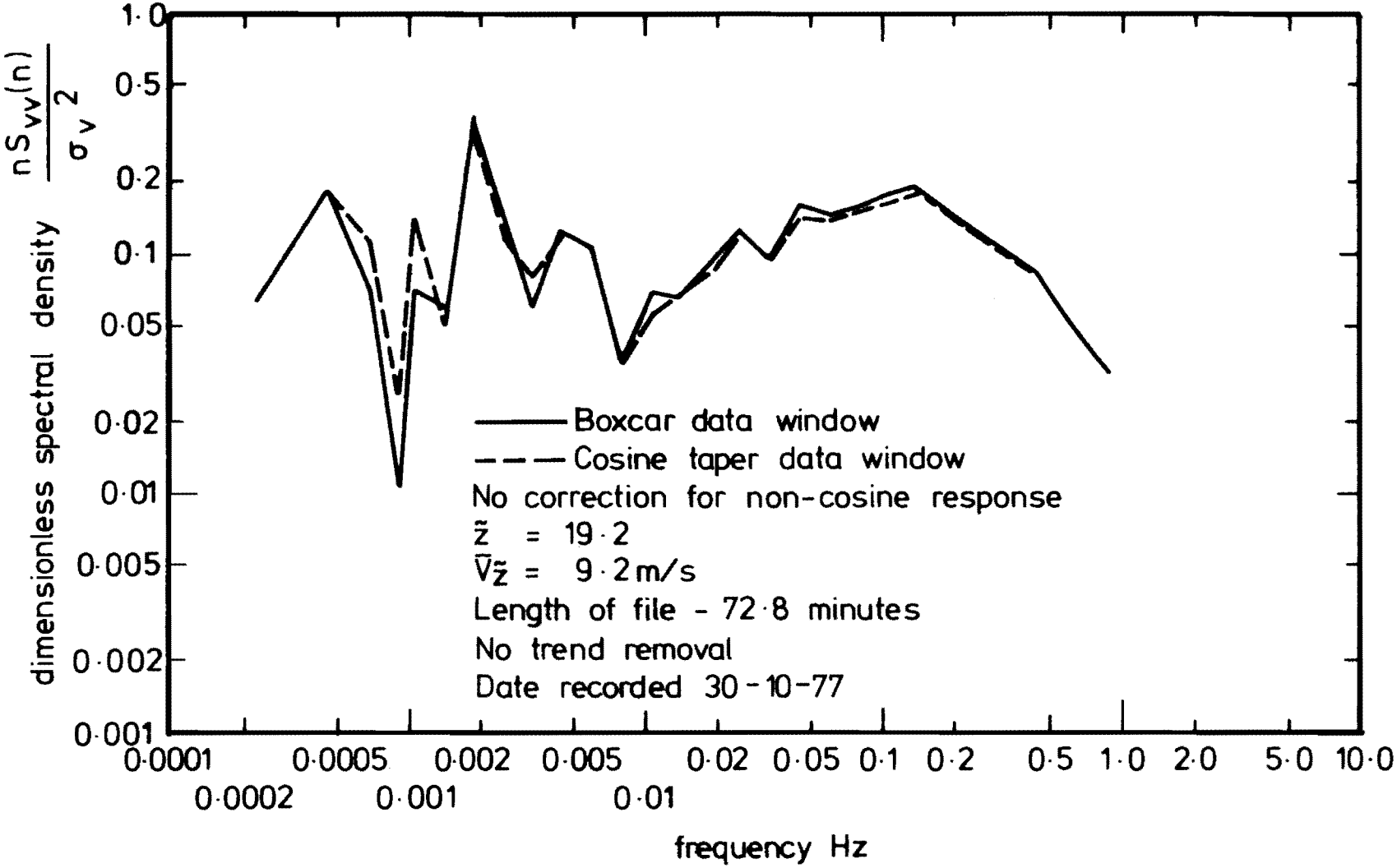

FIG 6·23 LATERAL COMPONENT v POWER SPECTRAL DENSITY VARIATION WITH A BOXCAR AND A COSINE TAPER DATA WINDOW.

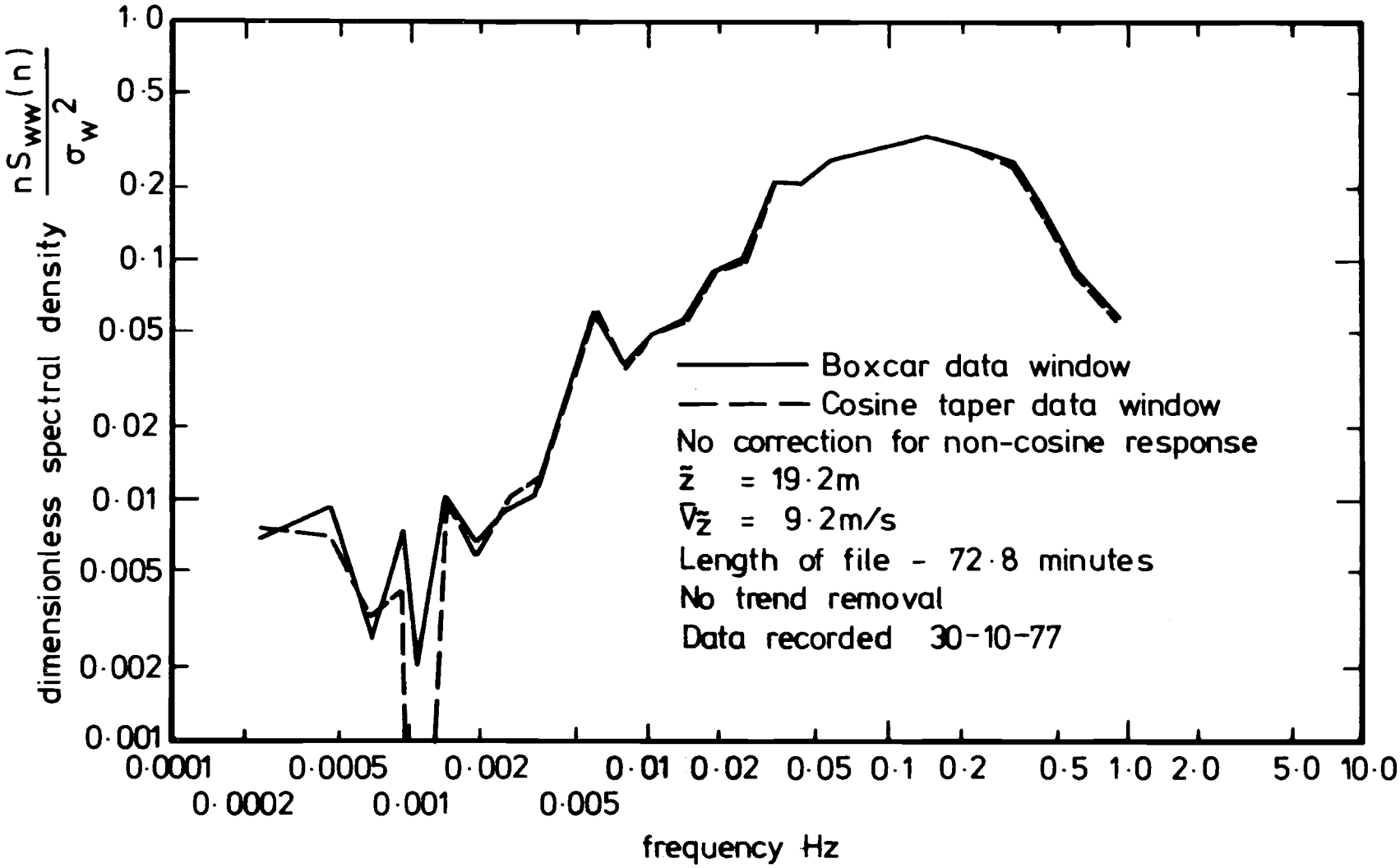

FIG 6·24 VERTICAL COMPONENT w POWER SPECTRAL DENSITY VARIATION WITH A BOXCAR AND A COSINE TAPER DATA WINDOW

compared directly. Figs.6.22,6.23 and 6.24 show the comparison in the result for the longitudinal, lateral and vertical components respectively from a single orthogonal array.

The three figures show significant variation only for the very low frequency spectral estimates. These estimates are subject to a large amount of random error and therefore are not very reliable, so small changes in their values are not very significant. Since there is very little change in the spectral estimates at intermediate and high frequencies, the advantages in cosine tapering the data are not immediately obvious. The results suggest that a simple box-car data window would not appear to compromise the spectra compared with using a cosine taper.

For subsequent analysis it was decided to use a box-car data window to simplify processing. This also has the advantage that the autocorrelation functions can be calculated directly by an inverse Fourier transform of their corresponding power spectral densities, whereas this is not possible when a data window is used in the time domain, (Brigham, 1974).

6.6 CONCLUSIONS

Correcting the data for non-cosine response has been shown to be important. Average velocity values are considerably underestimated otherwise. Turbulence intensities are changed in value. The effect on the longitudinal and lateral component turbulence intensities appear to be dependent on the average angle of the wind vector to the orthogonal array. However, the vertical component turbulence intensity value is always underestimated without the correction.

The $\rho_{uw}(\tau)$ and $\rho_{vw}(\tau)$ Reynolds stresses are not affected very much by the correction, although $\rho_{uv}(\tau)$ is considerably changed. The large change in $\rho_{uv}(\tau)$ after correcting it for non-cosine response makes

its reliability suspect, particularly when the size of the change is compared with the very minor change in the other two Reynolds stresses.

The shape of the spectral curves is not altered much by the correction. These results showed that the longitudinal component spectrum in Fig.6.7 was changed slightly in shape whereas the lateral and vertical component spectra in Figs.6.8 and 6.9 were changed by a much lesser amount.

The longitudinal autocorrelation function has been shown to exhibit a higher correlation in Fig.6.10 after the correction whereas the lateral and vertical component autocorrelations in Figs.6.11 and 6.12 respectively are virtually unchanged.

Like the turbulence intensities, it would appear that changes in the horizontal component power spectral densities and autocorrelation functions after correcting for non-cosine response, are functions of the average wind direction with respect to the orthogonal array of anemometers, and are therefore not very predictable.

It has been shown to be important to record data for as long a period as possible in order to get reliable power spectral density estimates, especially at low frequencies. Longer data recordings also reduce the magnitude of the fluctuations of the autocorrelation functions. A minimum file length of 30 minutes would appear to be indicated by the results of the power spectral density, autocorrelation and Reynolds stress plots presented. The length of the data file required for steady average velocities and turbulence intensities appear not to be quite as stringent, but here again 30 minutes would be a suitable minimum file length. However, long data files without trends are difficult to obtain in practice. Thus the increase in accuracy through using a longer data file could be thwarted by contributions due to trends in the data.

The minimum sampling frequency which gives uncompromised results compared with sampling at a higher frequency is 1.875 Hz. This is in

agreement with the sensor's response limitations and with the large drop off in energy in the surface layer at frequencies above .5 Hz.

Trend removal has been shown to be a very important aspect of the overall analysis. It is a particularly important feature in obtaining reliable spectra and correlation functions. It is therefore important in obtaining reliable integral length scales if these are to be obtained from correlation functions. Even slight trends in the data alter the correlation function estimates by significant amounts, and this introduces errors into the integral time scales computed from the correlations and consequently into the integral length scales.

It can be seen in Fig.6.11 that the autocorrelation function does not approach zero until quite a long time lag has elapsed, even with a parabolic trend removed from the data. This feature has been observed with other data as well, and would indicate that perhaps higher order polynomial trend lines should be removed from the data. This point is worth further investigation. An alternative method to investigate would be to include a high pass digital filter with a suitable cut-off frequency. The problem would then become one of determining where the trend like behaviour in the mean stopped, and the low frequency behaviour of interest in the data started.

Usually the difference in the derived parameter calculated from data with a parabolic trend removed or a linear trend removed was smaller than the difference between parameters calculated from data with a linear trend removed or no trend removed. However, since there usually was some effect, it was decided to remove a parabolic trend line from all data streams analysed in this research.

Cosine tapering the data in order to produce more reliable power spectral density estimates has not been shown to give significantly improved results. The data window tended to alter the low frequency estimates which have a large amount of random error. Since a more complex data window did not appear to be warranted, the simple box-car truncation function was used for all subsequent data analysis.

CHAPTER 7

THE VELOCITY PROFILE

7.1 INTRODUCTION

7.1.1 Data Analysed

Chapters 7 to 12 discuss the turbulence parameters measured using the single 20 m tower at the site shown in Fig.4.1.

The 20 m tower was initially erected in April 1977 at a position between the meteorological station and the shelter belt to the south shown in Fig.4.1. For a period of several months, very little useful data was recorded for a variety of reasons. During this period it was found that the anemometers needed to be purged because their life in the field was extremely short. A variety of other hardware faults in the instrumentation were found at this stage and corrected. A final reason for the lack of useful data recorded was that the wind did not blow from the direction from which data was to have been recorded. Consequently a lot of this early data was compromised because the anemometers sheltered each other or were in the lee of the tower.

In September 1977 the 20 m tower was moved to the position number 2 in Fig.4.1 and the anemometers were aligned, as detailed in Section 3.5, to accept wind from the north-west quarter. It was expected, as outlined in Section 1.3, that strong nor'westerly winds would blow during the period for which it was proposed to record the wind velocity data.

Wind data was only recorded when the wind direction lay between the horizontal component anemometer axes so neither sheltered the other. This constituted a restriction on the amount of data which was recorded. However, between the period 14-9-77 and 31-10-77, data was collected on five days, of which data from four days has been extensively analysed and the results presented here. Details regarding each data recording

have been given in Table 7.1. When the data collected on these four days is referred to subsequently, it is called Run 1,2,3 and 4 respectively.

Run 3 has been extensively analysed in Chapter 6 and data from Run 4 has been briefly discussed in Section 6.4.

At all times data was attempted to be recorded for at least 73 minutes as this period gave a number of samples which whilst still being a power of 2 was closest to being one hour long. Shorter data file lengths were recorded only through instrumentation failure.

Run number	Date data recorded	Start time	File length, minutes	Sampling frequency, Hz	Number of triplets	Weather conditions
1	14.9.77	2.40pm	73	15	7	moderately cloudy
2	23.10.77	3.40pm	37	15	7	moderately cloudy
3	30.10.77	6.20pm	73	15	7	moderately cloudy
4	31.10.77	5.50pm	37	15	7	moderately cloudy

TABLE 7.1 SINGLE 20 m TOWER DATA RECORDINGS

7.1.2 Definitions

The mean wind speed in the longitudinal direction, for a given averaging time, where the wind speed varies continuously with time is defined as :

$$\bar{V}_Z = \lim_{T \to \infty} \int_{t_o}^{T+t_o} U(t)\, dt \,. \qquad (7.1)$$

where U(t) is the wind speed in the longitudinal direction for the period over which data is recorded. If the wind speed variation with time is stationary, $\bar{V}_Z$ is not a function of t_o. It has also been found that T in the range 10 to 60 minutes gives stable averages.

Since the velocity data is recorded digitally, the digital form

of the mean equation for a time series with N samples is :

$$\bar{V}_Z = \frac{1}{N} \sum_{k=0}^{N-1} U(k) \tag{7.2}$$

Defining the x and y component axes parallel and perpendicular to the average wind direction, and the z axis vertically means that the component velocities u,v, and w along each of these axes respectively will be such that $\bar{v} = 0$. Also $\bar{w} = 0$ for homogeneous horizontal terrain.

The fluctuation u is found by,

$$u(k) = U(k) - \bar{V}_Z \ , \ k = 0,1,...N-1 \tag{7.3}$$

so $\bar{u} = 0$. Thus the velocities u,v, and w can be considered as the turbulent fluctuations superimposed on the mean flow $\bar{V}_Z$ at each height.

The anemometers were not aligned parallel to the x,y, and z axes, so some manipulation of the data streams was required to calculate the longitudinal, lateral and vertical components for each scan. Although the details vary slightly, the following technique can be considered to have been used in the programs VTPDMS, SEQVELTURBREY and PSAUTCORS to calculate the longitudinal, lateral and vertical components. The technique outlined assumes that the anemometers are aligned along x_1,y_1 and z_1 orthogonal axes measuring values u_1,v_1 and w_1 respectively at each scan for a total of N samples.

(1) Apply anemometer calibration coefficient to u_1,v_1 and w_1 data streams.

(2) Use an iterative procedure to correct for sensor non-cosine response if this is required.

(3) Form

$$\bar{u}_1 = \frac{1}{N} \sum_{k=0}^{N-1} u_1(k) \ , \tag{7.4}$$

$$\bar{v}_1 = \frac{1}{N} \sum_{k=0}^{N-1} v_1(k) \ , \tag{7.5}$$

$$\bar{w}_1 = \frac{1}{N}\sum_{k=0}^{N-1} w_1(k) \tag{7.6}$$

$$\bar{V}_Z = (\bar{u}_1^{\,2} + \bar{v}_1^{\,2})^{\frac{1}{2}} \tag{7.7}$$

(4) Assume that the wind velocity for the period is horizontal. Find the angle between the average wind vector and the x_1 anemometer.

$$\theta = \tan^{-1}\left(\frac{\bar{v}_1}{\bar{u}_1}\right) \tag{7.8}$$

(5) Rotate the samples from the horizontal component anemometers into components parallel and perpendicular to the average wind vector.

$$u(k) = u_1(k)\cos\theta + v_1(k)\sin\theta - \bar{V}_Z \tag{7.9}$$

$$v(k) = v_1(k)\cos\theta - u_1(k)\sin\theta \ . \tag{7.10}$$

$$k = 0,1,\ldots N-1$$

(6) Assume that $\bar{w}_1$ is not equal to zero only because of anemometer misalignment, therefore form :

$$w(k) = w_1(k) - \bar{w}_1 \ , \quad k = 0,1,\ldots N-1 \ . \tag{7.11}$$

The values u, v and w are then amenable to analysis giving

$$\bar{u} = \bar{v} = \bar{w} = 0, \text{ and } \bar{V}_Z = \bar{u}_1\cos\theta + \bar{v}_1\sin\theta \ . \tag{7.12}$$

7.1.3 Boundary Layer Description

The total atmospheric boundary layer can conveniently be divided into three regions. These regions are the free atmosphere, the planetary boundary layer and the surface layer.

In the free atmosphere there is no effect of the earth's surface

friction, viscosity is negligible and only inertial, Coriolis and pressure gradient forces act on the air. Sutton (1953) shows that the air is at equilibrium when it flows along the isobars, and is called the gradient wind. In the special case when the isobars are straight, the gradient wind is called the geostrophic wind.

The least height at which the gradient height is obtained is called the gradient height, Z_G. Davenport (1963) suggests that Z_G varies from about 300 m over rural terrain to 600 m over urban terrain, but Counihan (1975) suggests that for strong wind conditions, when the atmosphere is neutrally stable, a value of Z_G = 600 m represents the average gradient height of both rural and urban boundary layers. The planetary boundary layer extends between the earth's surface and the gradient height and the surface layer is a sub-layer of the planetary boundary layer.

In the surface layer, Coriolis forces are assumed negligible, and the wind characteristics are determined by surface roughness conditions, thermal stability, and height. The extent of the surface layer is defined as the layer where the shear stress remains virtually constant. It is sometimes called the constant shear stress layer.

Early data suggested that the constant shear stress layer extended only to heights of 30-50 m, however more recent measurements have suggested a greater height. Counihan (1975) after reviewing considerable data suggests that the average height of the constant shear stress layer is 100 m. Panofsky (1977) states that in strong wind conditions, the surface layer extends up to around 150 m height.

7.1.4 Historical Development of Velocity Profile Theory

Nikuradse's experiments on the flow of water through smooth and rough pipes showed that the flow was independent of Reynolds number and dependent only on surface roughness in the third regime, i.e. fully aerodynamic rough flow when $U_* Z_o/\nu > 2.5$, where ν is the kinematic

viscosity, (Schlichting, 1960).

It was found by Nikuradse that in this regime, when the results were plotted in a dimensionless form, the distribution fitted a simple power law.

The form was

$$\frac{u}{U} = \left(\frac{r}{R}\right)^{\alpha} \tag{7.13}$$

where U was the velocity at the pipe centre, R the pipe radius, and u the velocity at radius r. The exponent α was found to have various values lying approximately within the range $\frac{1}{7}$ to $\frac{1}{4}$.

This same law was applied to velocity readings in the planetary boundary layer. A form of the type

$$\frac{\bar{V}_Z}{V_{ref}} = \left(\frac{Z}{Z_{ref}}\right)^{\alpha} \tag{7.14}$$

was used. α was then observed to vary depending on the roughness of the terrain, having values as high as $\frac{1}{4}$ to $\frac{1}{2}$ for urban terrain and $\frac{1}{7}$ for rural terrain.

Concurrently a logrithmic velocity profile law was developed and tested in the atmosphere. The logrithmic law (log law) for the mean velocity variation with height in neutrally stable air can be derived from Prandtl's mixing length or from von Kármán's similarity hypothesis, e.g. see Schlichting (1960).

The log law is only applicable in the constant shear stress layer, the lower 10 - 15% of the planetary boundary layer, and assumes that :

(1) viscous stress is negligible,

(2) mixing length is proportional to height, i.e. $\ell_m = kZ$, k being von Kármán's constant which is usually taken to be .4, although this value is disputed, (Tennekes, 1973),

(3) shearing stress is constant and equal to the surface shear stress τ_o.

Since the shear stress in the surface layer is equal to $-\rho_a \overline{uw}$, where ρ_a is the air density, a friction velocity can be defined such that

$$-\rho_a U_*^2 = -\rho_a \overline{uw} = \tau_o .$$

The log law profile can then be defined as :

$$\bar{V}_Z = \frac{U_*}{k} \ln \left(\frac{Z}{Z_o}\right) , \quad \text{where } \bar{V}_Z = 0 \text{ at } Z_o \tag{7.15}$$

and $Z_o << Z$.

Equation (7.15) is only applicable in a neutrally stable atmosphere. It is not very representative of the measured data when the terrain is very rough as in the centres of large cities, consequently there are two major variations on the simple log law profile given in Equation (7.15). These are discussed in the following two sections.

7.1.4.1 Zero Plane Displacement Form. Equation (7.15) is modified to :

$$\bar{V}_Z = \frac{U_*}{k} \ln \left(\frac{Z-d}{Z_o}\right) \tag{7.16}$$

d is sometimes taken as the average roughness element height. It effectively lifts the log law profile up above the roughness elements, above which normal turbulent exchange occurs. Sutton (1953) suggests that Equation (7.16) is valid for $Z >> d + Z_o$, and Cermak and Arya (1970) state that it has been verified for flow over tall crops and forest canopies.

7.1.4.2 Form for Non-neutral Stability. Under non-neutral stability conditions, Equation (7.15) is modified to :

$$\bar{V}_Z = \frac{U_*}{k} \left[\ln\left(\frac{Z}{Z_o}\right) - \psi\left(\frac{Z}{L'}\right)\right] \tag{7.17}$$

where L' is the Monin-Obukhov length and ψ is a universal function depending

only on $(\frac{Z}{L'})$. The usefulness of Equation(7.17) is discussed below.

The behaviour of wind profiles in non-neutral stratification has been clarified by Monin-Obukhov similarity theory, e.g. as discussed by Calder (1966) and Panofsky (1977). In this theory, a length L' is defined which depends both on the surface heat flux and surface stress, and is independent of height. L' is defined to be negative with upward heat flux, and is therefore negative in the daytime and positive at night. Also L' is positive in stable stratification and negative in unstable stratification. At heights much below $|L'|$ i.e. when $|\frac{Z}{L'}|$ is small, mechanical turbulence dominates. At heights of order $|L'|$ or larger, i.e. $\left(|\frac{Z}{L'}|\right) \gtrsim .1$, convection dominates. Thus $\frac{Z}{L'}$ is a measure of the relative importance of heat convection and mechanical turbulence.

A neutrally stable atmosphere has a temperature-height variation described by

$$T_Z = T_o - \Gamma Z \ , \tag{7.18}$$

where T_o is the absolute temperature at the surface, T_Z is the absolute temperature at height Z and Γ is the "dry adiabatic lapse rate". In dry air $\Gamma \approx 1°C/100$ m and if $\gamma \equiv \frac{dT}{dZ} > \Gamma$, the atmosphere will be unstable - superadiabatic and if $\gamma < \Gamma$ the air will be stable - an inversion period. The atmosphere is neutrally stable when $\Gamma - .03 \lesssim \gamma < \Gamma$.

When the atmosphere is unstable, a parcel of air which has moved upwards say, will feel a resultant force upwards due to its lower density and will continue to rise. In a neutrally stable atmosphere, parcels of air moving vertically,instantaneously take up the density of the surrounding air and hence feel no resultant force, whereas under stable conditions a moving parcel of air upwards for example will feel a restoring force downwards.

The Richardson Number Ri is defined as :

$$Ri = \frac{\text{mean rate of work done against gravity/unit vol.}}{\text{work done by Reynolds stress/unit vol.}}$$

$$= \frac{g\,(\Gamma - \gamma)}{T_Z \left(\frac{\partial \bar{v}_Z}{\partial Z}\right)^2} \qquad (7.19)$$

where g is the gravitational constant, and T_Z is the absolute temperature at height Z. It can be used to determine whether heat convection can be neglected.

Panofsky (1977) states that it is probably legitimate to neglect the effect of heat convection provided $|Ri| < .01$. This condition is often satisfied at low heights under strong wind conditions, but the wind shear decreases rapidly with increase of height so that heat convection becomes progressively more important. Above 50 m or so, convective turbulence can no longer be neglected even with strong winds.

In stable air, i.e. $\gamma < \Gamma$, ψ, the universal function in Equation (7.17) is given by

$$\psi\left(\frac{Z}{L'}\right) = -5\,\frac{Z}{L'}\,. \qquad (7.20)$$

In unstable air the expression is complex so is given in Table 7.2 from Panofsky (1977) :

$\frac{Z}{L'}$	-.01	-.02	-.05	-.1	-.2	-.5	-1.0	-2.0	-5.0
ψ	.05	.10	.20	.37	.60	1.01	1.40	1.85	2.52

TABLE 7.2 VARIATION OF ψ WITH $\frac{Z}{L'}$ FOR UNSTABLE AIR

L' the Monin-Obukhov length is very hard to measure as it is defined as

$$L' = -U_*^3 \,/\left(\frac{kg\,H_o}{T_a \rho_a C_p}\right) \qquad (7.21)$$

$H_o/\rho_a C_p$ = surface heat flux

k = von Kármán Constant

T_a = ambient temperature.

It requires temperature-velocity correlation measurements in order to determine the surface heat flux.

However, Monin-Obukhov theory predicts that $\frac{Z}{L'}$ should only depend on Ri and measurements have shown that very nearly,

$$\frac{Z}{L'} = Ri \quad , Ri \leqslant 0, \text{ i.e. unstable,} \tag{7.22}$$

and

$$\frac{Z}{L'} = \frac{Ri}{1 - 5Ri} \quad , 0 \leqslant Ri < .2 \text{ i.e. stable} \tag{7.23}$$

For Ri $>$ .2, turbulence is essentially damped out by the stable temperature distribution, and winds at different heights become uncoupled. Equations (7.22) and (7.23) become inaccurate for $\frac{Z}{L'}$, Ri very close to zero, but for small values, corrections to the wind profiles are small and great accuracy is not required.

Ri can be determined much more simply than L' as it requires only average temperature and velocity readings at a minimum of two heights. It can hence be used with Equations (7.20), (7.22) and (7.23), and Table 7.2 to determine $\psi(\frac{Z}{L'})$which can then be used in Equation (7.17) to determine the theoretical profile.

An alternative, even simpler, method of obtaining an approximate value of L' for wind data collected under a certain set of meteorological conditions is outlined by Panofsky (1977). It relies on estimating a "Pasquill class" from observations of the average wind velocity and incoming solar radiation from Table 7.3. With this class, an approximate estimate of $\frac{1}{L'}$ can be made from Fig.7.1 which can then be used with Equation (7.20) and Table 7.2 to determine $\psi(\frac{Z}{L'})$. This value can then be used in Equation (7.17) to determine the theoretical profile.

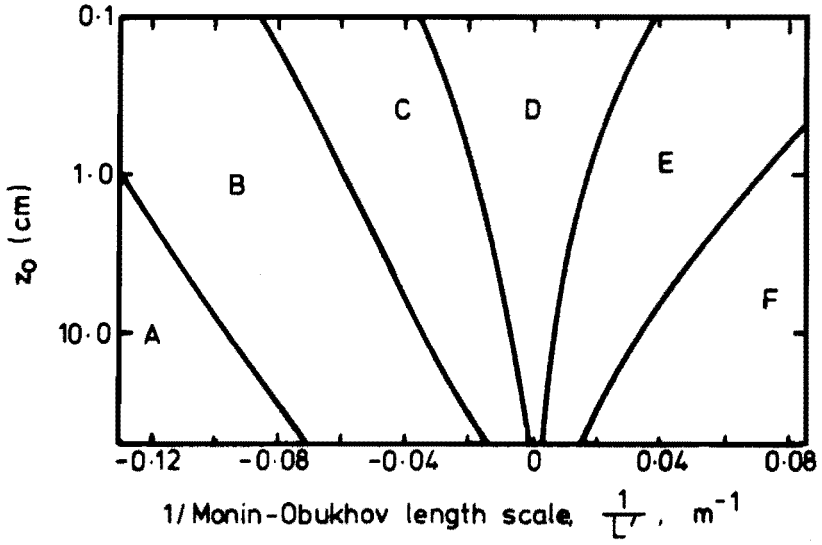

FIG 7·1 RELATIONS OF MONIN-OBUKHOV L' TO PASQUILL CLASS AND ROUGHNESS LENGTH.

Surface Wind Speed (at 10 m) m/s	Day			Night	
	Incoming Solar Radiation			Thinly Overcast or $\geqslant \frac{4}{8}$ low cloud	$< \frac{3}{8}$ cloud
	Strong	Moderate	Light		
< 2	A	A - B	B		
2 - 3	A - B	B	C	E	F
3 - 5	B	B - C	C	D	E
5 - 6	C	C - D	D	D	D
> 6	C	D	D	D	D

TABLE 7.3 PASQUILL CLASSES

7.2 THE MEASURED PROFILES

The measurements described in this research were taken in strong wind conditions when the wind velocity at 10 m height was at least approximately equal to 10 m/s. Also, since only the lower 20 m of the surface layer was observed, the simple log law profile of Equation(7.15) should describe the profile shape because the results under these conditions would be from a neutrally stable region of the planetary boundary layer.

A power law profile might equally be fitted to the data but the exponent α in Equation(7.14)fitted to the data would not be appropriate to the whole planetary boundary layer. α depends on the roughness length and the height interval over which the law is applied as described by Panofsky (1977) and Counihan (1975). A fit of α to results from a small height range results in a value of α which is too large to be used for the whole planetary boundary layer.

Lines joining points which are the longitudinal velocity component averaged over 8 seconds have been plotted in Figs. 7.2, 7.3, 7.4 and 7.5 for Runs 1, 2, 3 and 4 respectively. Thus these figures show the relatively long term fluctuations in velocity, as well as giving a visual appreciation

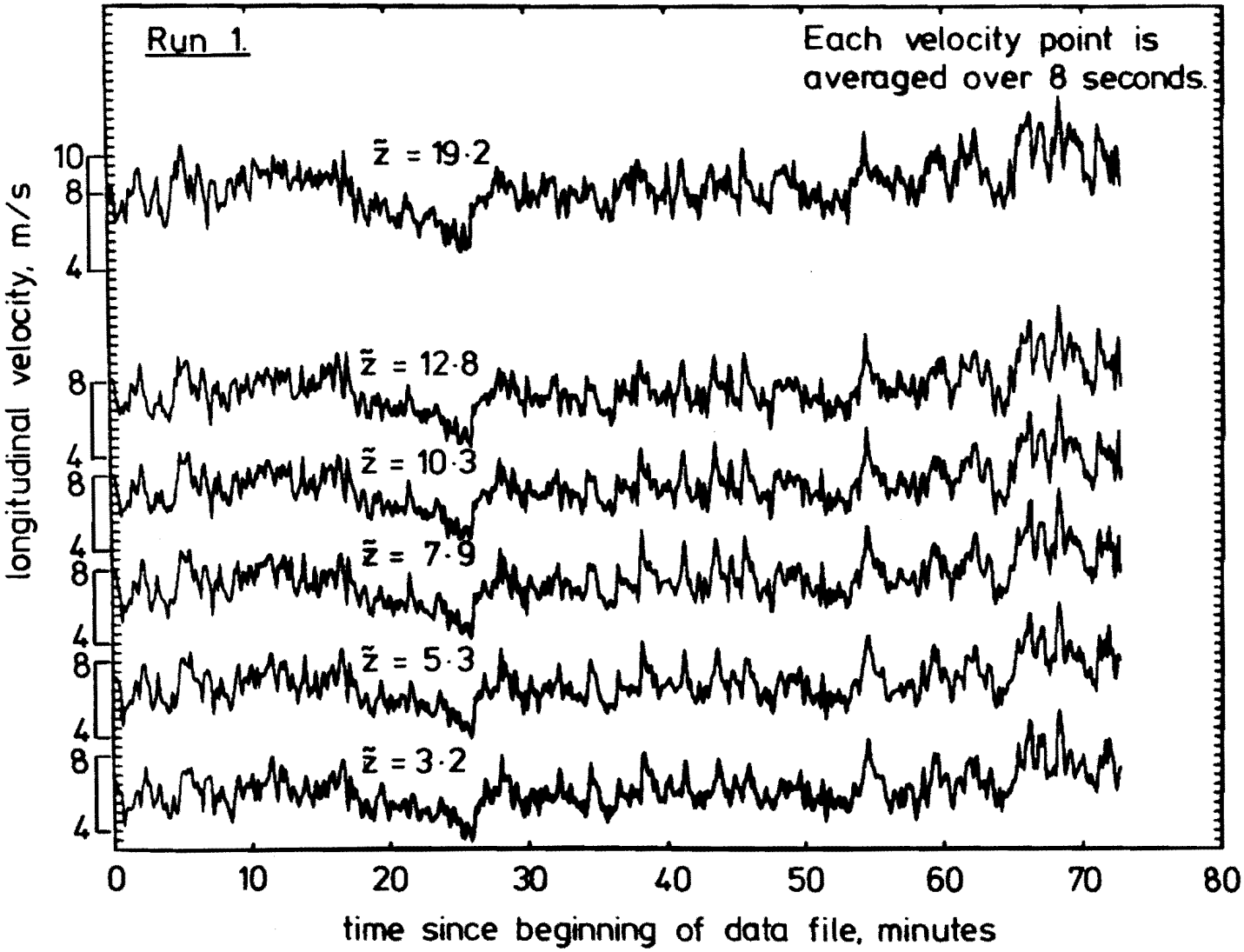

FIG. 7·2 VELOCITY AS A FUNCTION OF TIME OVER MEASURED PERIOD FOR RUN 1.

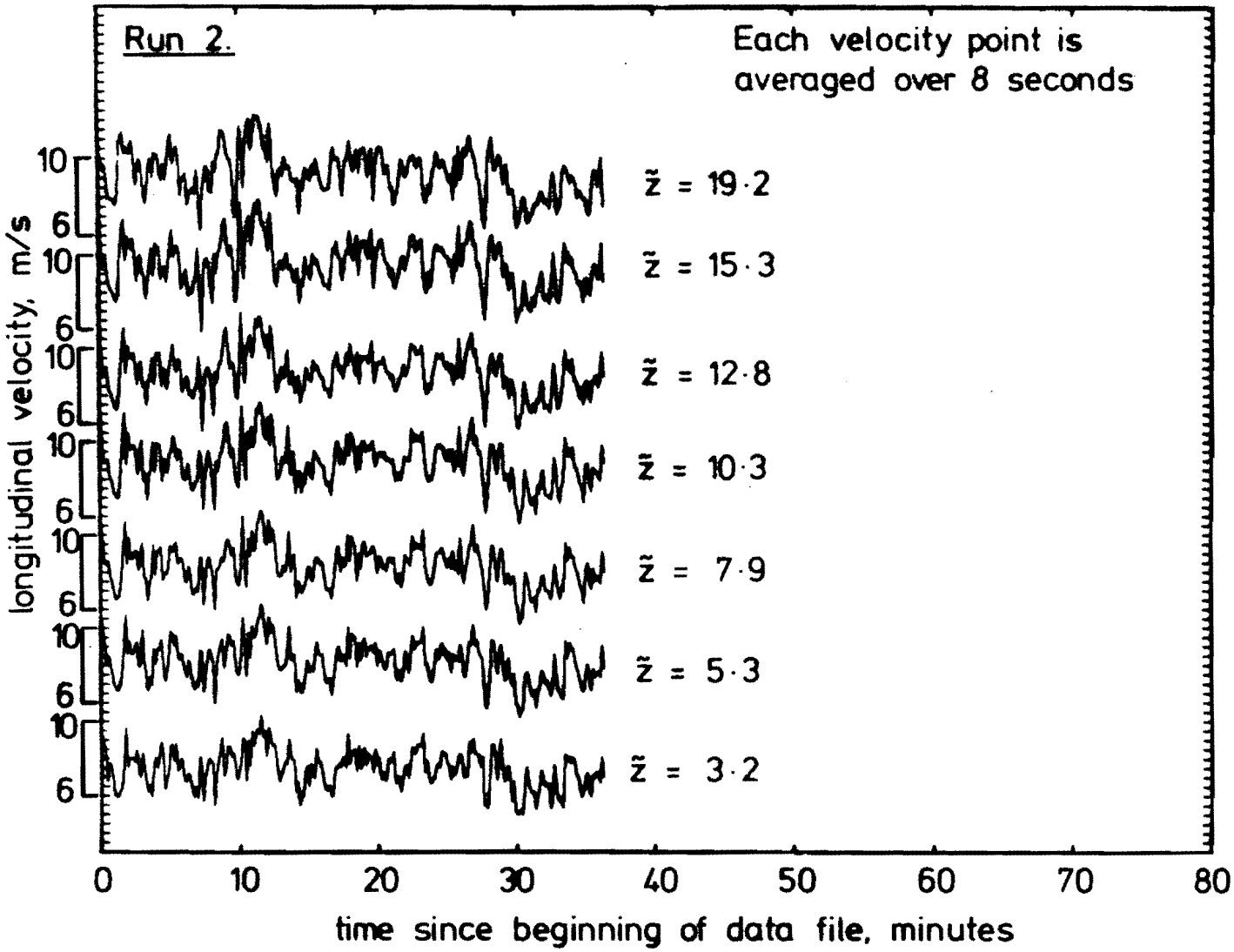

FIG. 7·3 VELOCITY AS A FUNCTION OF TIME OVER MEASURED PERIOD FOR RUN 2.

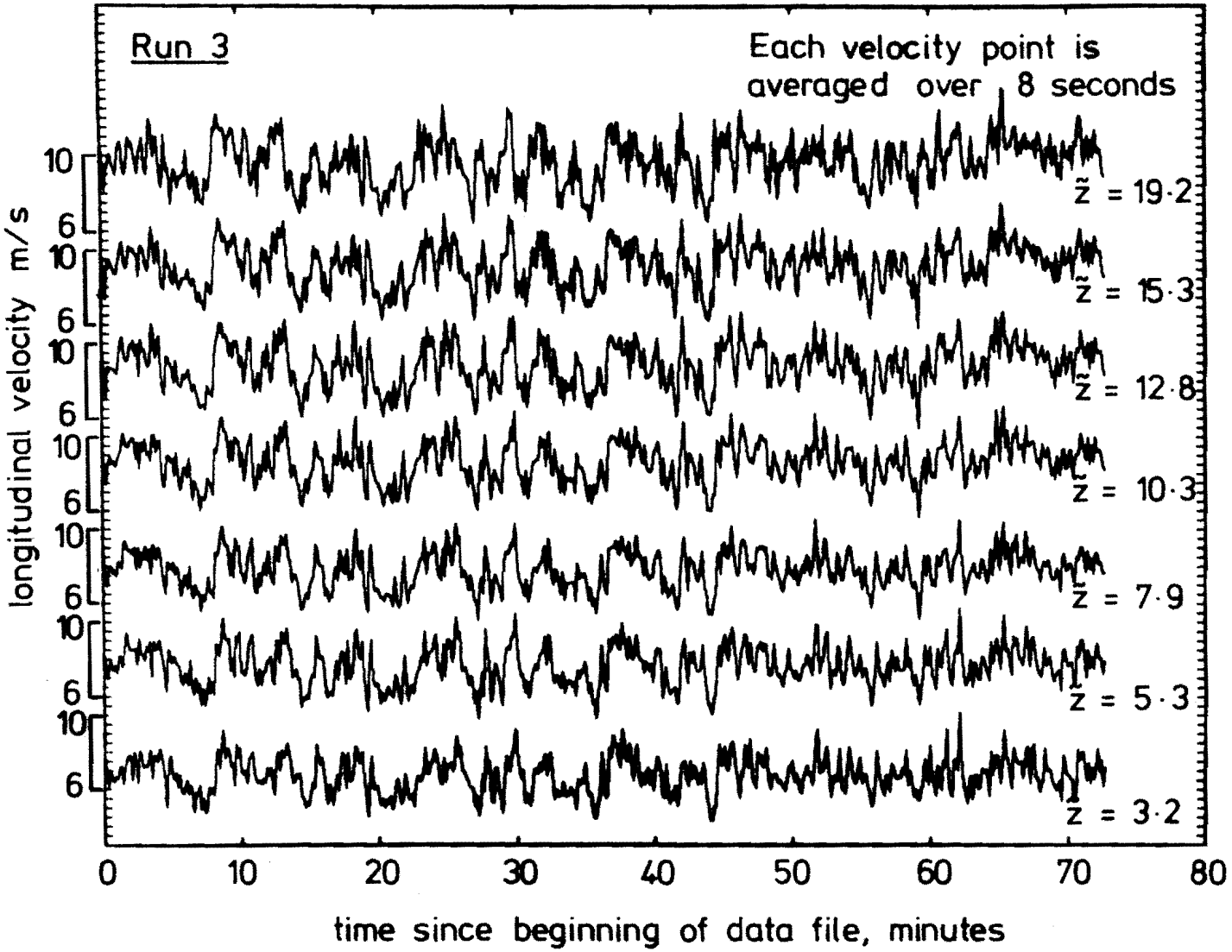

FIG. 7·4 VELOCITY AS A FUNCTION OF TIME OVER MEASURED PERIOD FOR RUN 3.

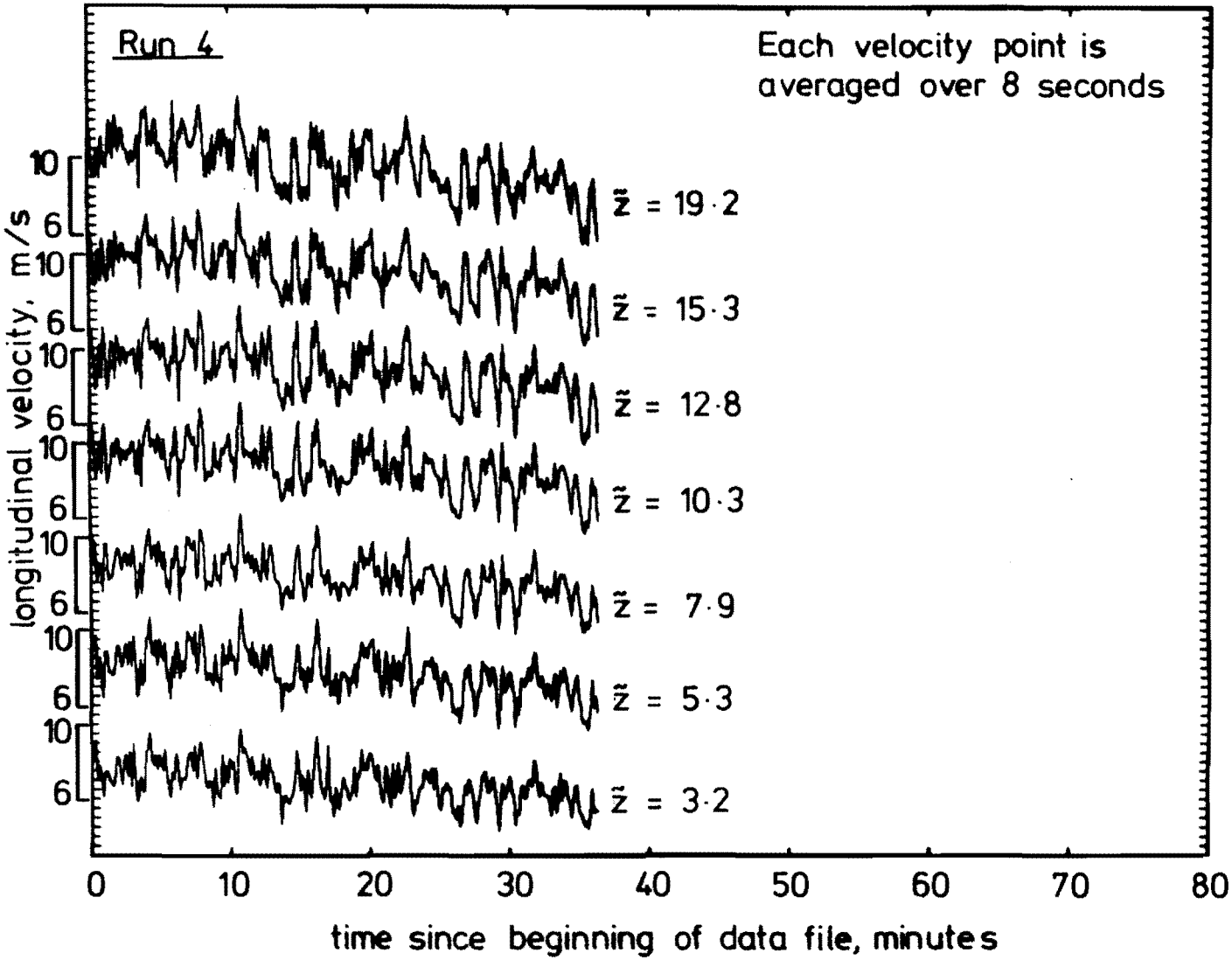

FIG. 7·5 VELOCITY AS A FUNCTION OF TIME OVER MEASURED PERIOD FOR RUN 4.

for the amount of correlation between the orthogonal anemometer arrays mounted vertically up the tower.

The four profiles are plotted in Fig.7.6, and show the comparison between Runs. The velocity has been measured at seven heights, although one point at 15.3 m height for Run 1 is missing due to a malfunctioning anemometer. The curves drawn through the points in Fig.7.6 have been taken from Fig.7.7 where a straight line was fitted to the velocity-height data, from each Run, thus giving a log law velocity profile. The slope of each of these lines in Fig.7.7 was obtained from values of $\rho_{uw}(0)$ calculated by the eddy correlation technique. For each Run, the average Reynolds stress value over all levels was used. The agreement between the slopes obtained from the average $\rho_{uw}(0)$ Reynolds stress values using the eddy correlation technique, and also from the positions of the actual data points in Fig.7.7 is good. It indicates that the velocity profile method and the eddy correlation method produce virtually equivalent values of $\rho_{uw}(0)$. This is discussed in more detail in Chapter 9.

The average wind direction measured to the anemometer aligned in the x_1 direction is shown in Fig.7.8. There is some variation in the wind direction up the tower but this however is rather small and is probably the result of anemometer misalignments and slight differences in the response characteristics of individual anemometers.

From Fig.7.7, Z_o has been found to have values of .032, .02, .029 and .027 m for Runs 1,2,3 and 4 respectively. Taking the average to be .03 m agrees with values in Table 7.4 from ESDU(1974b), as it falls in the "farmland" range. It also agrees with Table 7.5, from Counihan (1975), by falling in category number 2 of moderately rough.

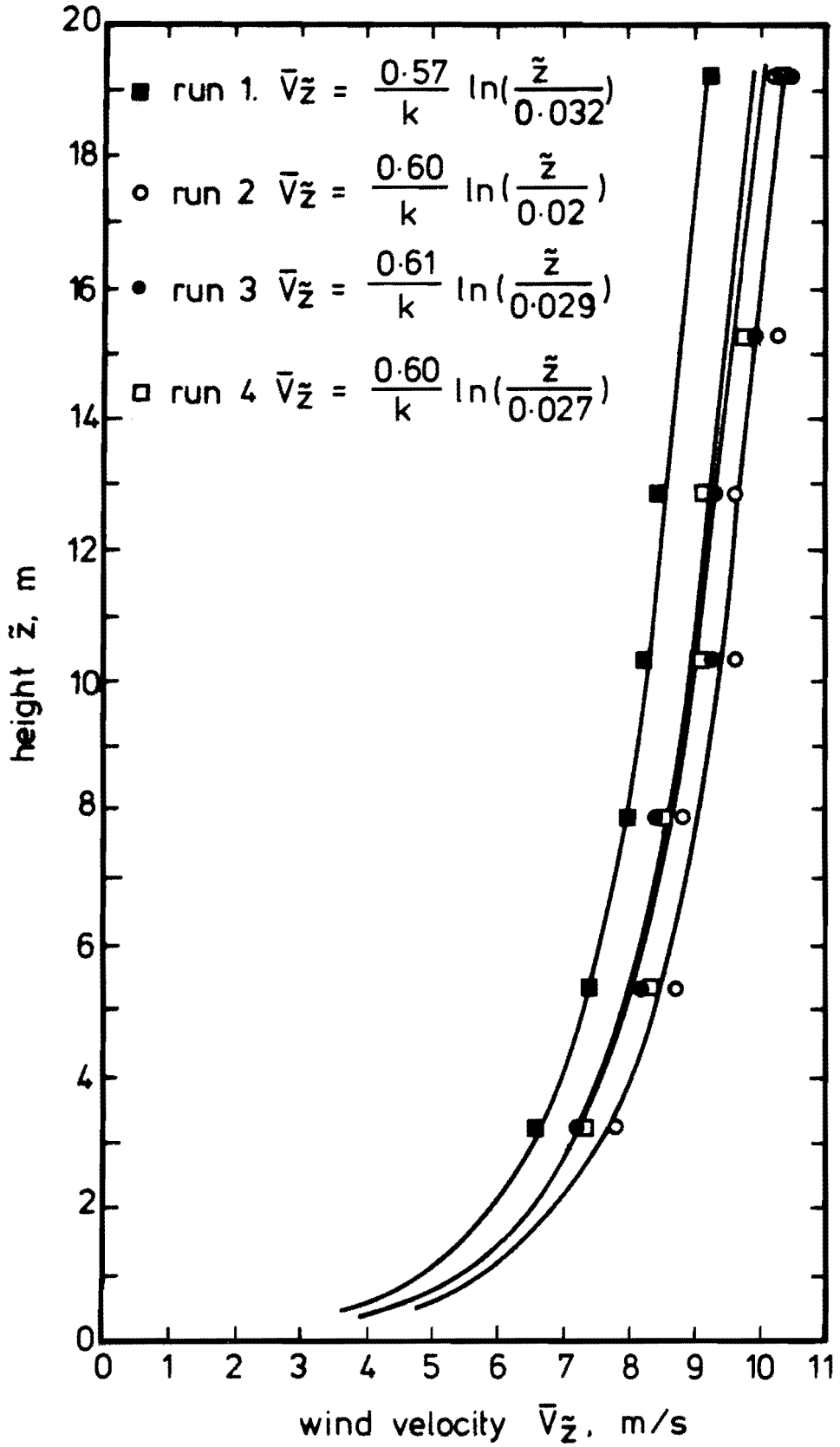

FIG. 7·6 MEASURED VELOCITY PROFILES, WITH LOG PROFILES FITTED TO THE MEASURED DATA.

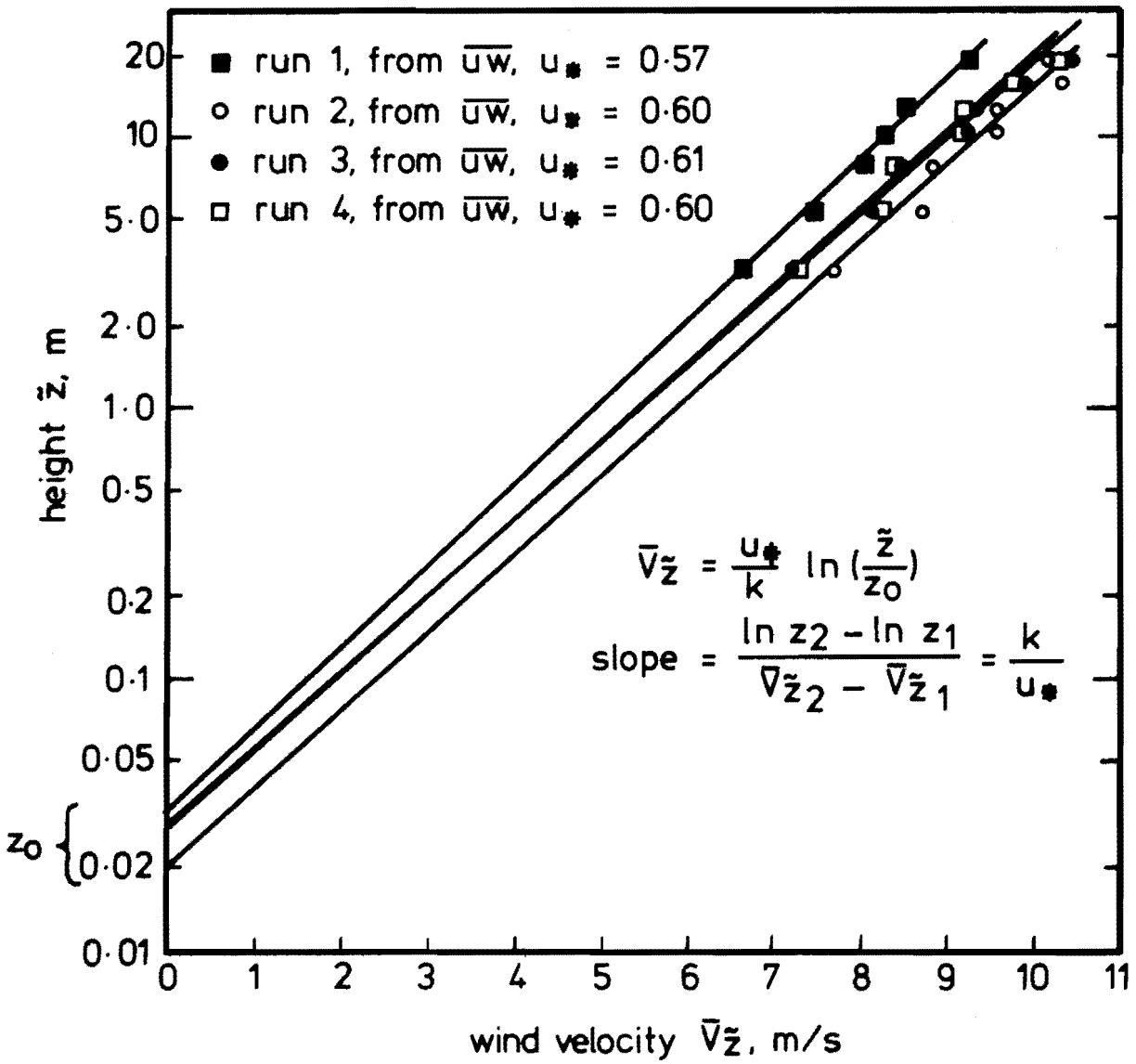

FIG. 7·7 VELOCITY PROFILES PLOTTED ON SEMI-LOG PAPER TO OBTAIN z_0 AND u_*.

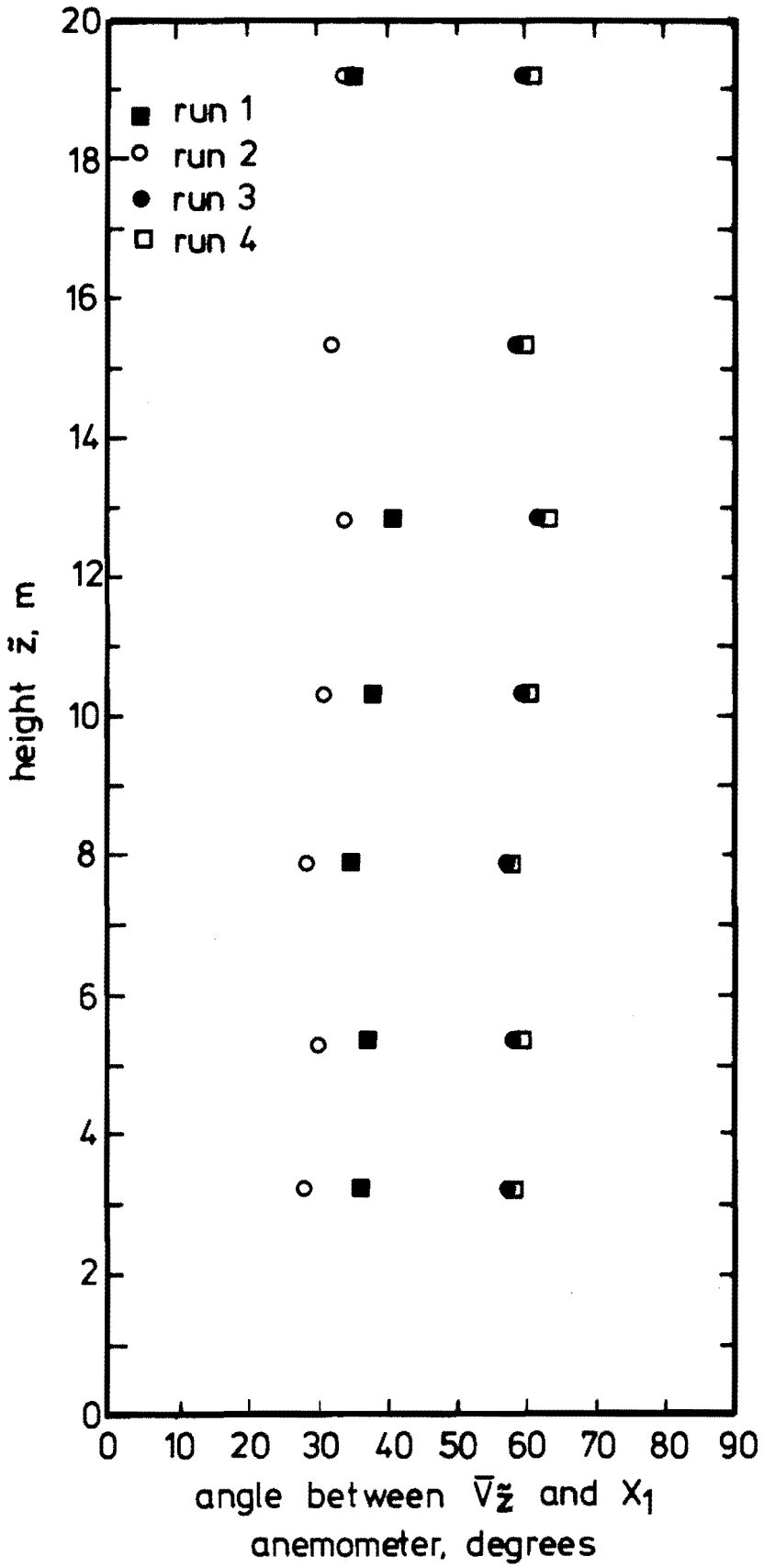

FIG. 7·8 ANGLES BETWEEN MEAN WIND VECTOR $\bar{V}_{\tilde{z}}$ AND A REFERENCE ANEMOMETER.

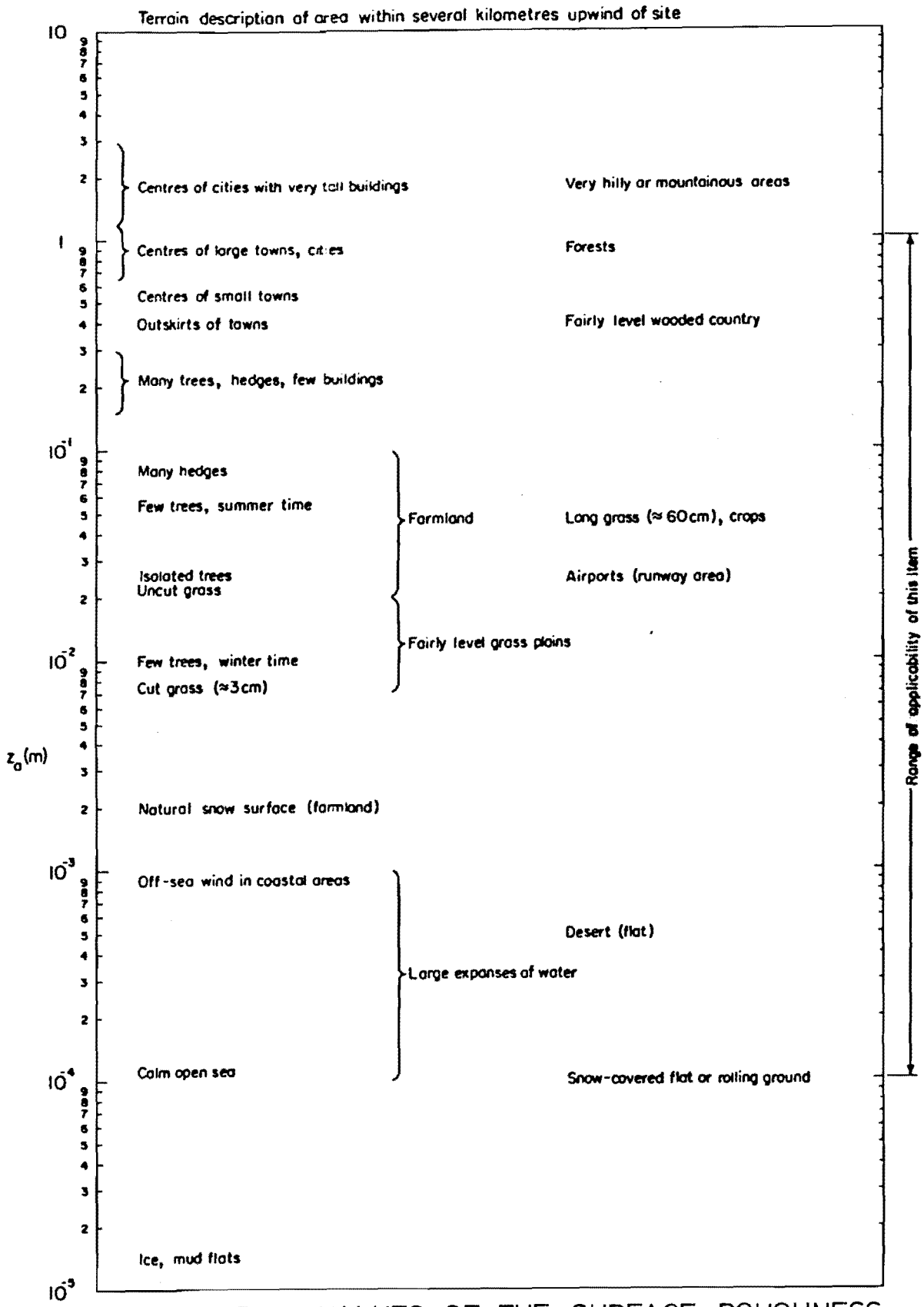

TABLE 7·4 VALUES OF THE SURFACE ROUGHNESS PARAMETER Z_O

TERRAIN TYPE / QUANTITY	1 SMOOTH ICE - MUD - SNOW - SEA	2 MODERATELY ROUGH SHORT GRASS GRASS - CROPS - RURAL	3 ROUGH RURAL WOODS - WOODS - SUBURBS	4 VERY ROUGH URBAN
z_o cm	0.001 - 0.04 - 0.1 - 2.0	0.1 -3 ∿ 7 - 20	100 - - 150	100 - 300 - 400
$\overline{uw}/\bar{V}_G^2$	0.0004-0.006 - 0.001	0.0014 -0.0020 - 0.0040	-	-
α	0.08 - 0.11 - 0.12	0.13 - 0.143 - 0.16	0.20 - 0.23	0.25 - 0.40
$\sigma_u/\bar{V}_z$, $0 \leq z \leq 30$	0.10 - 0.12	0.13 - 0.20	- 0.20 -	0.30 - 0.48

TABLE 7.5 DEFINITION OF MAIN TERRAIN TYPES

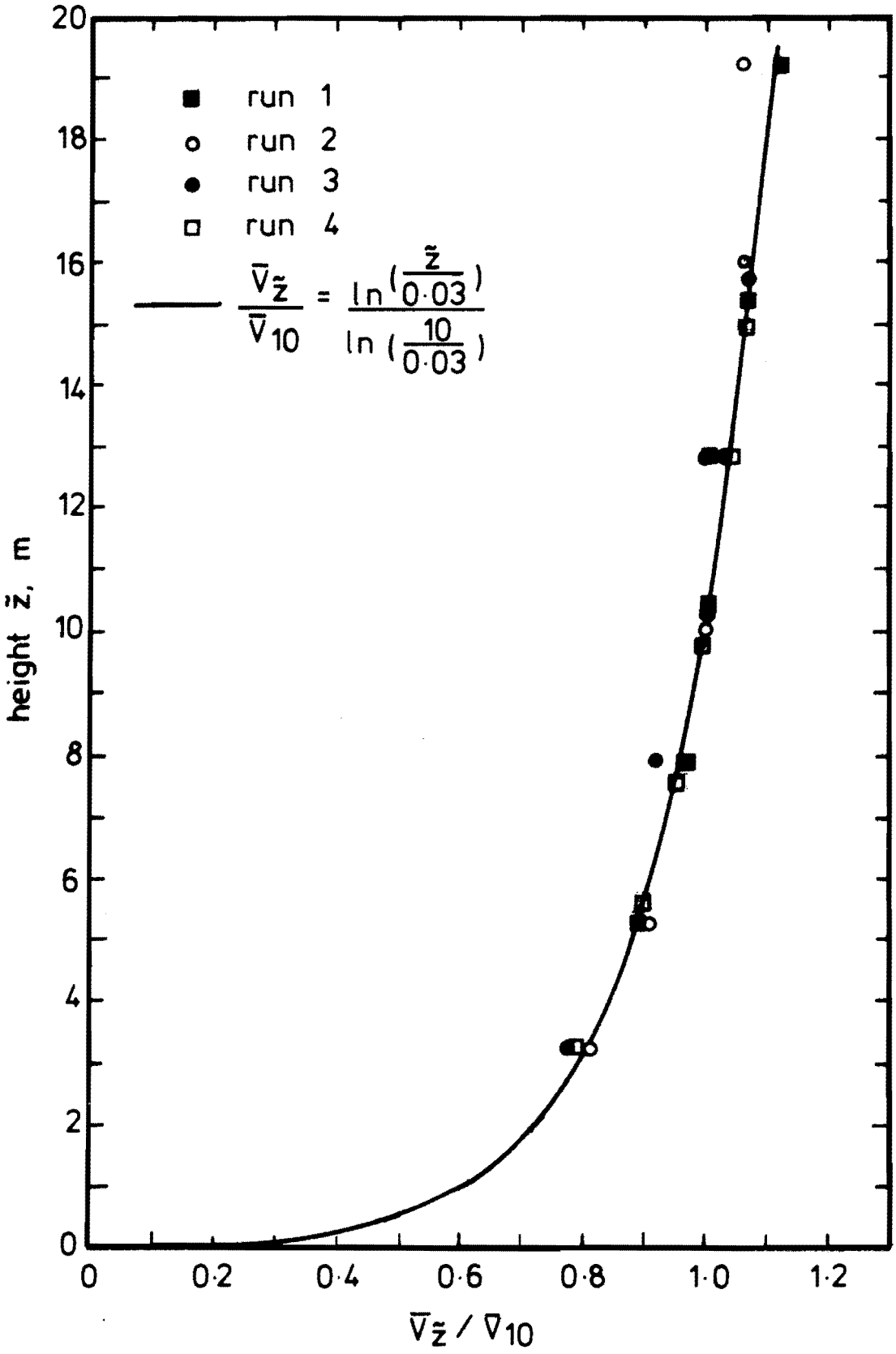

FIG. 7·9 VELOCITY PROFILES FROM ALL RUNS NORMALISED BY $\bar{V}_{10}$ WITH A NORMALISED LOG PROFILE FITTED TO ALL OF THE DATA.

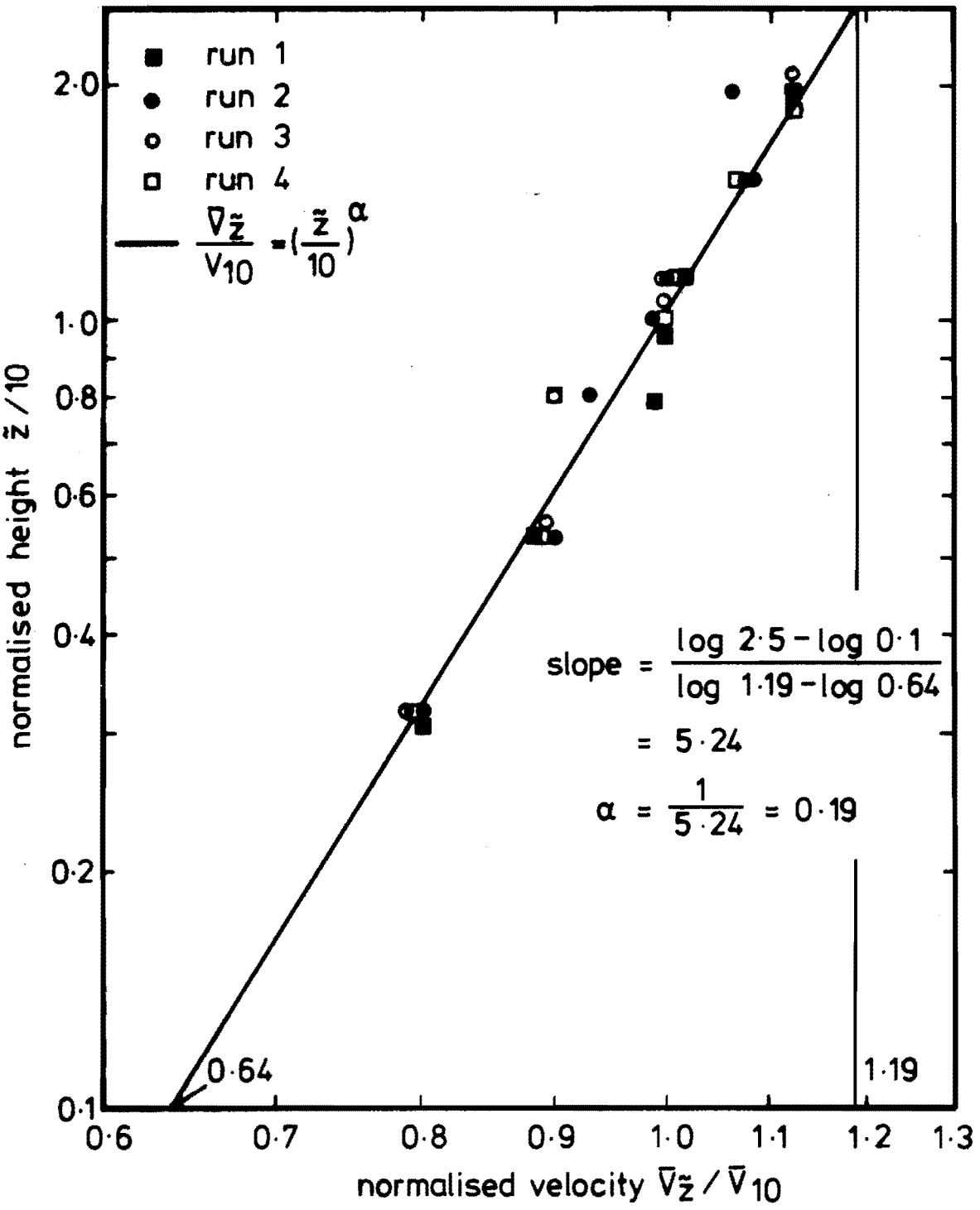

FIG 7·10 POWER LAW VELOCITY PLOT

The data has been plotted again in Fig.7.9 normalised by the velocity at 10.3 m height for each Run. Also shown is a curve obtained by assuming a log profile, with a roughness length of .03 m, and normalised by the velocity at 10.3 m. It can be seen that this line is a good fit to all of the measured data. The deviations from this line will probably be due to calibration differences, and slight differencesin individual anemometer non-cosine response.

A log - log plot of data, normalised by the velocity at a height of 10.3 m is shown in Fig.7.10. A line was fitted to the data and although there is some scatter, is seen to fit reasonably well. The power law exponent obtained from this curve is α = .19 which is high for rural terrain. However the exponent of a power law profile is a function of the roughness length and the geometric mean height range over which the profile is required to fit the data. Consequently this power law exponent could not be used to extrapolate velocities up to heights of say 100 m.

Panofsky (1977) provides an equation derived from the log law for determining α for a desired height range which is

$$\alpha = \frac{1}{\ell n\left(\frac{\sqrt{z_1 z_2}}{z_o}\right)} \qquad (7.24)$$

Thus for Z_1 = 10 m, Z_2 = 100 m and Z_o = .03 m α is found to be .143 or $\frac{1}{7}$. This value is of course much smaller than .19. Counihan (1975) also provides a method to obtain the exponent in the power law directly from the roughness length. The equation provided is :

$$\alpha = .096 \log_{10} Z_o + .016 (\log_{10} Z_o)^2 + .24 \qquad (7.25)$$

which applies for $0.001 \leqslant Z_o, m \leqslant 5.0$ m

using Z_o = .03 m gives

$$\alpha = .131 = \frac{1}{7.6} .$$

This data agrees with the observation made by others that the power law exponent is usually overestimated from data obtained from a small height range above the ground.

7.3 CONCLUSION

The results obtained compare well with the velocity profile predicted by the log law for the constant shear stress layer. There is some variation between Runs, but the average roughness length obtained for the site appears to be approximately .03 m. This is in agreement with ESDU (1974b) in Table 7.4 as it corresponds to the region of farmland, and is also in agreement with Counihan (1975) as the measured roughness length lies in Category 2 of moderately rough in Table 7.5.

The exponent α obtained by fitting a power law to the measured data was rather high. However this was not unexpected. In fact, for a height range of 2 to 20 m, substituting into Equation (7.24) gives $\alpha = .19$ which is the same value as was measured at the site.

CHAPTER 8

TURBULENCE CHARACTERISTICS

8.1 INTRODUCTION

8.1.1. Definitions

Following the definition of the mean velocity given in Section 7.1.2, the degree of turbulence can be defined in much the same way. The usual method of measuring the degree of turbulence existing in a flow situation is to calculate the standard deviations of the fluctuating components, u, v and w which are superimposed on the mean flow $\bar{V}_Z$. Thus the standard deviation of the u fluctuation, where u varies continuously with time is

$$\sigma_u = \left[\frac{1}{T}\int_{t_o}^{T+t_o} (u(t))^2 \, dt\right]^{\frac{1}{2}} \tag{8.1}$$

T is normally taken as 10 to 60 minutes, and for stationary conditions σ_u is not a function of t_o. σ_v and σ_w are defined in a similar manner.

If u(t) is the wind speed in the longitudinal direction for the period over which data is recorded, then the mean square velocity fluctuation in the longitudinal direction is :

$$\begin{aligned} u_{ms} &= \frac{1}{T}\int_0^T U(t)^2 \, dt \\ &= \frac{1}{T}\int_0^T (\bar{V}_Z + u(t))^2 \, dt \\ &= \bar{V}_Z^{\,2} + \frac{1}{T}\int_0^T (u(t))^2 \, dt \\ &= \bar{V}_Z^{\,2} + \sigma_u^{\,2} \, . \end{aligned} \tag{8.2}$$

The mean square velocity fluctuation in the longitudinal direction is thus the sum of the mean velocity squared and the longitudinal component variance.

The form of the equation to compute the longitudinal component standard deviation from a discrete time series with N samples is :

$$\sigma_u = \left[\frac{1}{N} \sum_{k=0}^{N-1} u(k)^2 \right]^{\frac{1}{2}} \qquad (8.3)$$

σ_v and σ_w are formed in a similar manner.

The power spectral density of each component is usually defined such that the contributions from all positive frequencies making up the turbulence, sum to the variance,

$$\text{i.e.} \quad \int_0^\infty S_{ii}(n)\,dn = \sigma_i^2 \quad , \quad i = u,v,w \qquad (8.4)$$

where $S_{ii}(n)$ is the power spectral density of the i component at frequency n.

The turbulence intensity is a measure of the relative magnitude of the turbulent fluctuations, compared with the mean flow velocity. It is thus defined as the ratio of the standard deviation of the fluctuating velocity components to the mean wind speed for the averaging period chosen.

$$\text{turbulence intensity} = \frac{\sigma_i}{\bar{V}_Z} \quad , \quad i = u,v,w. \qquad (8.5)$$

Another useful function to describe velocity fluctuations is the probability density function. The probability density function of random wind velocity fluctuations describes the probability that the velocity data will assume a value within some defined range of velocities at any instant of time. For example, consider the sample time history record i(t) illustrated in Fig.8.1.

The probability that i(t) assumes a value within the range i and (i + Δi) is the ratio T_{pi}/T, where T_{pi} is the total amount of time that i(t) falls inside the range i to (i + Δi), during the period T

seconds. This ratio approaches an exact probability distribution as T approaches infinity. This is shown below.

$$\text{Prob}\,[i < i(t) \leqslant i + \Delta i] = \lim_{T\to\infty} \frac{T_{pi}}{T} \tag{8.6}$$

The probability density function p(i) is defined as

$$p(i) = \lim_{\Delta i \to 0} \frac{\text{Prob}\,[i < i(t) \leqslant i + \Delta i]}{\Delta i}$$

$$= \lim_{\Delta i \to 0} \frac{1}{\Delta i}\left[\lim_{T\to\infty} \frac{T_{pi}}{T}\right], \quad i = u,v,w. \tag{8.7}$$

$$T_{pi} = \sum_{j=1}^{k} \Delta t_j$$

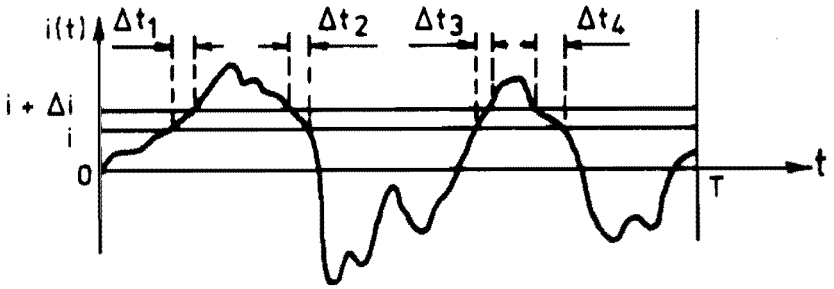

FIG. 8·1 MEASUREMENT OF PROBABILITY FOR A SINGLE DATA STREAM

To calculate the probability density function from a time history of N discrete samples of wind velocity data, Equation (8.7) is compromised somewhat. A series of "classes" are formed such that each velocity value in i(k), k = 0,1,...N-1, will fall into one of the classes. The number of samples which fall into each class are then summed and is then used to calculate the probability.

For example, if there are N_c classes covering a range of velocities from i_ℓ to i_s, then for each sample the class number is found from the following formula:

$$\text{Class number} = \text{absolute value of} \left[\frac{i(k)-i_s}{\left(\frac{i_\ell - i_s}{N_c}\right)} \right], \quad k = 0,1,\ldots N-1. \qquad (8.8)$$

The numbers of samples in each class have been normalised in this work so that they may be compared directly with a Gaussian distribution. Thus, the values have been normalised to have unit standard deviation, and so that the area under each probability density function curve is equal to 1. Thus if there are N_k samples in class number k, this value is normalised to the probability

$$p(i) = \frac{N_k \times \sigma_i}{N \times \left[\frac{i_\ell - i_s}{N_c}\right]} \qquad \begin{matrix} k = 0,1,\ldots N_c - 1, \\ i = u,v,w \end{matrix} \qquad (8.9)$$

8.1.2 Historical Development

It was recognised in the early literature that the degree of turbulence in the planetary boundary layer was a function of both the surface roughness and the height above ground level. This is because the rate of production of turbulence and its intensity is a function of both the Reynolds stresses and the mean velocity profile of the flow being considered.

Counihan (1975) states that Scrase (1930) showed that the ratio of the three component standard deviations were as follows :

$$\sigma_u : \sigma_v : \sigma_w = 1 : 0.73 : 0.46 \qquad (8.10)$$

for the height range considered from ground level up to 20 m. Typical flat plate data gave 1 : 0.75 : 0.54. Later work has mainly verified that these ratios are quite close to typical values in the atmosphere.

Best (1935) established that the longitudinal component turbulence intensity was .15 - .16 over rural terrain, which meant that the other two components could be found by using Equation (8.10).

Early turbulence measurements were difficult because of the scarcity of suitable instruments which were sensitive enough. Recording and analysing data were also difficult and time consuming. Estimates of the longitudinal component standard deviation were sometimes made by using the width of an ink velocity trace on paper. The fact that these early results agree as well as they do with more recent measurements using more responsive instruments, with better data recording and analysis techniques, is unexpected.

8.1.3 Current Turbulence Intensity Values

More recently the turbulence in the surface layer has been measured at many places over various types of terrain and by a large number of researchers. The longitudinal and vertical component turbulence have been studied in greater detail than the lateral component turbulence.

It was shown that variations in turbulence intensity with height were comparable to those of fully developed aerodynamic flat plate boundary layers. Swanson and Cramer (1965) showed that both the longitudinal and lateral component turbulence intensities decreased with increase of height up to 100 m above ground level. Pritchard (1966) showed that the vertical component turbulence intensity was approximately constant, with increase of height up to about 370 m. Harris (1972) showed that σ_u was not invariant with height in the 180 m range considered. This is particularly relevant when the ratios

$$A = \frac{\sigma_u}{U_*} \tag{8.11}$$

$$B = \frac{\sigma_v}{U_*} \tag{8.12}$$

and

$$C = \frac{\sigma_w}{U_*} \tag{8.13}$$

are considered. These ratios are used extensively to obtain estimates of turbulence intensities and assume invariance of U_*, σ_u, σ_v and σ_w with

height. They are based on the assumption of proportionality between the turbulent energy and the friction velocity squared.

When Equation (8.11) is combined with the log law velocity profile equation for neutral stability, the longitudinal component turbulence intensity can be related to the height and roughness length viz,

$$\frac{\sigma_u}{\bar{V}_Z} = \frac{A\ k}{\ell n(\frac{Z}{Z_o})} \tag{8.14}$$

where k is the von Kármán constant.

Counihan (1975) gives mean values of A, B and C from all of the data consdered in the review, which are respectively 2.5, 1.875 and 1.25. These values thus give :

$$\sigma_v/\sigma_u = 0.75 \text{ and } \sigma_w/\sigma_u = 0.50 \tag{8.15}$$

Teunissen (1970) presents values which are slightly different, and are :

$$A : B : C : U_* = 2.5 : 2.0 : 1.3 : 1 \text{ , giving}$$

$$\sigma_v/\sigma_u = 0.80 \text{ and } \sigma_w/\sigma_u = .52 \tag{8.16}$$

Using the value of A from either Teunissen or Counihan in Equation (8.14) with von Kármán's constant k = 0.4 gives :

$$\frac{\sigma_u}{\bar{V}_Z} = \frac{1}{\ell n\ (\frac{Z}{Z_o})} \tag{8.17}$$

ESDU (1974b) presents values of the three component turbulence intensities as functions of the height considered and the roughness length.

Davenport (1963) on the basis of integrating his invariant gust spectrum, suggested that ,

$$\sigma_u = 2.46\ (K_{10})^{\frac{1}{2}}\ \bar{V}_{10} = 2.46\ U_* \tag{8.18}$$

This was later modified by Harris (1971) who proposed a slightly different gust spectrum. Harris suggested that ,

$$\sigma_u = 2.58 \, (K_{10})^{\frac{1}{2}} \, \bar{V}_{10} = 2.58 \, U_* \tag{8.19}$$

Both Harris and Davenport later used ,

$$\frac{\sigma_u}{\bar{V}_Z} = 2.5 \, (K_{10})^{\frac{1}{2}} \left(\frac{\bar{V}_{10}}{\bar{V}_Z} \right) , \tag{8.20}$$

in conjunction with a power law profile to obtain values of the turbulence intensity at various heights. K_{10} was estimated using data provided by Davenport (1964) and given here in Table 8.1.

Ground Roughness Condition	K_{10}
Rough open water	.001 - .002
Open grassland	.003 - .005
Woodland, forests, suburbs	.015 - .030
Urban centres	.030 - .050

TABLE 8.1 VALUES OF THE SURFACE DRAG COEFFICIENT AT A HEIGHT OF 10 m.

Thus there is a considerable data base of turbulence information with which to make comparisons.

8.2 VARIATION OF THE LONGITUDINAL COMPONENT MEAN SQUARE VALUES WITH TIME

8.2.1 Test for Stationarity

To assess the stationarity of the data, the mean squares over short time intervals of the longitudinal velocity component were calculated. This was done for all levels of anemometers for all four Runs using program VTPDMS. The program is described in Section 5.4 and the listing is given in Appendix D.

A random process is said to be strongly stationary if all possible moments and joint moments computed from it are time invariant. It is said to be weakly stationary if the mean and autocorrelation functions are identical when computed from ensemble averages from different records or from time averages. When an individual time history is said to be stationary, a slightly different interpretation of stationarity is involved. A individual time history is stationary if its properties computed over short time intervals do not vary "significantly" from one interval to the next. This means that the observed variations must not be greater than those due to normal sampling variations,in order for it to be stationary.

Since the data recorded in each Run could be considered as an individual time history, it was the latter definition of stationary which was used to assess the stationarity of the data. The method used follows Bendat and Piersol (1971). The several assumptions involved in using this method are briefly discussed below.

The given sample data record must properly reflect the nonstationary character of the random process in question. It has to be long compared with the lowest frequency component in the data excluding a nonstationary mean. This is to allow the nonstationary trends to be differentiated from the random fluctuations in the time history. The assumption is then made that any nonstationarity of interest will be revealed by time trends in the mean square value of data (i.e. the zero time lag value of the autocovariance function).

Bendat and Piersol (1971) thus suggest dividing the sample record into N equal time intervals where the data in each interval can be considered independent, and then to calculate the mean squares for that interval. The sequence of mean squares is then tested for underlying trends or variations other than those due to normal sampling variations.

The mean squares were therefore calculated over averaging periods of 2.28 minutes. This was selected as a suitable averaging period because

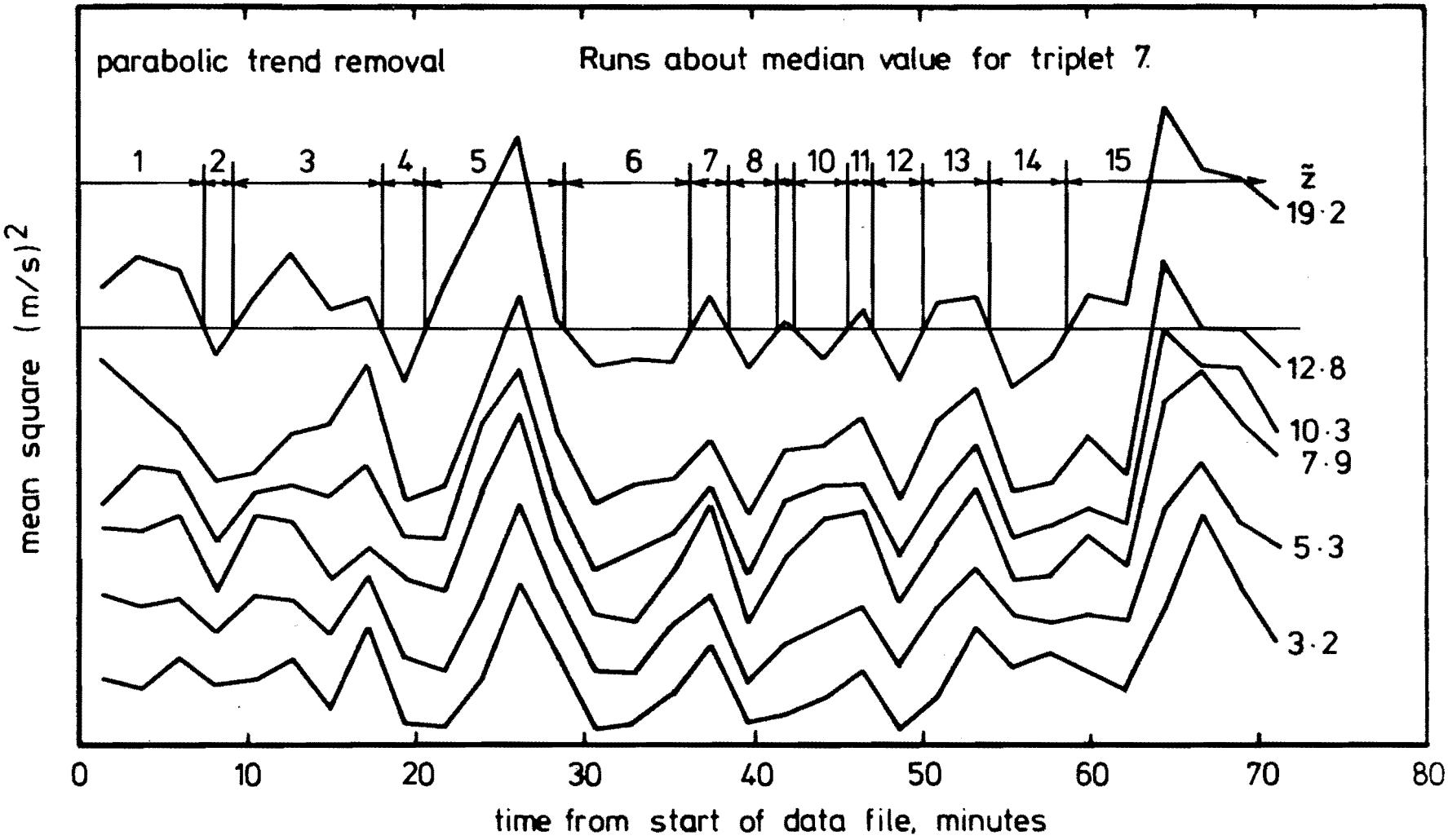

FIG 8·2 VARIATION OF THE LONGITUDINAL COMPONENT MEAN SQUARE VALUE, AVERAGED OVER 2·28 MINUTES, OVER THE MEASUREMENT PERIOD, FOR RUN 1.

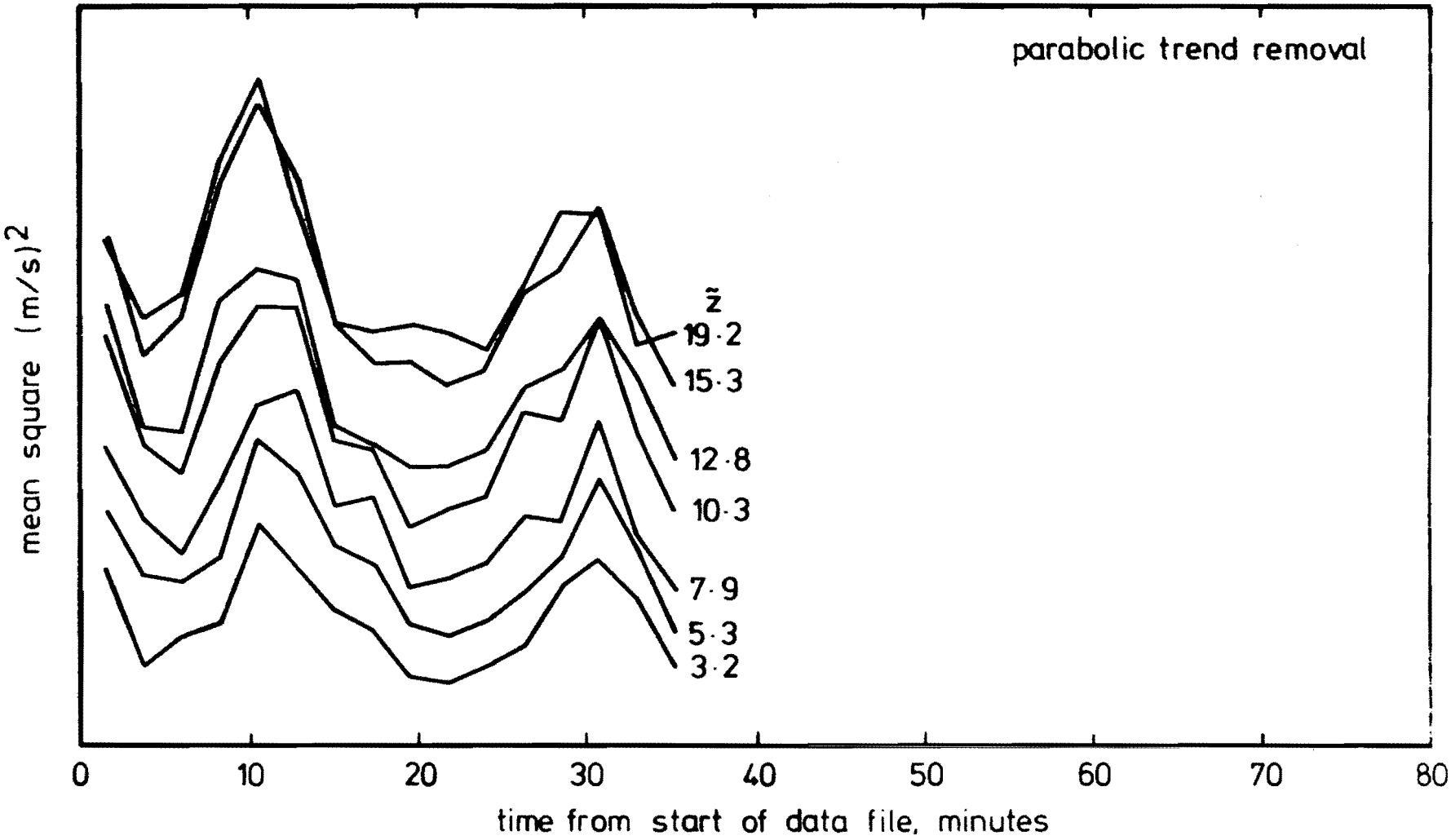

FIG 8·3 VARIATION OF THE LONGITUDINAL COMPONENT MEAN SQUARE VALUE, AVERAGED OVER 2·28 MINUTES, OVER THE MEASUREMENT PERIOD, FOR RUN 2.

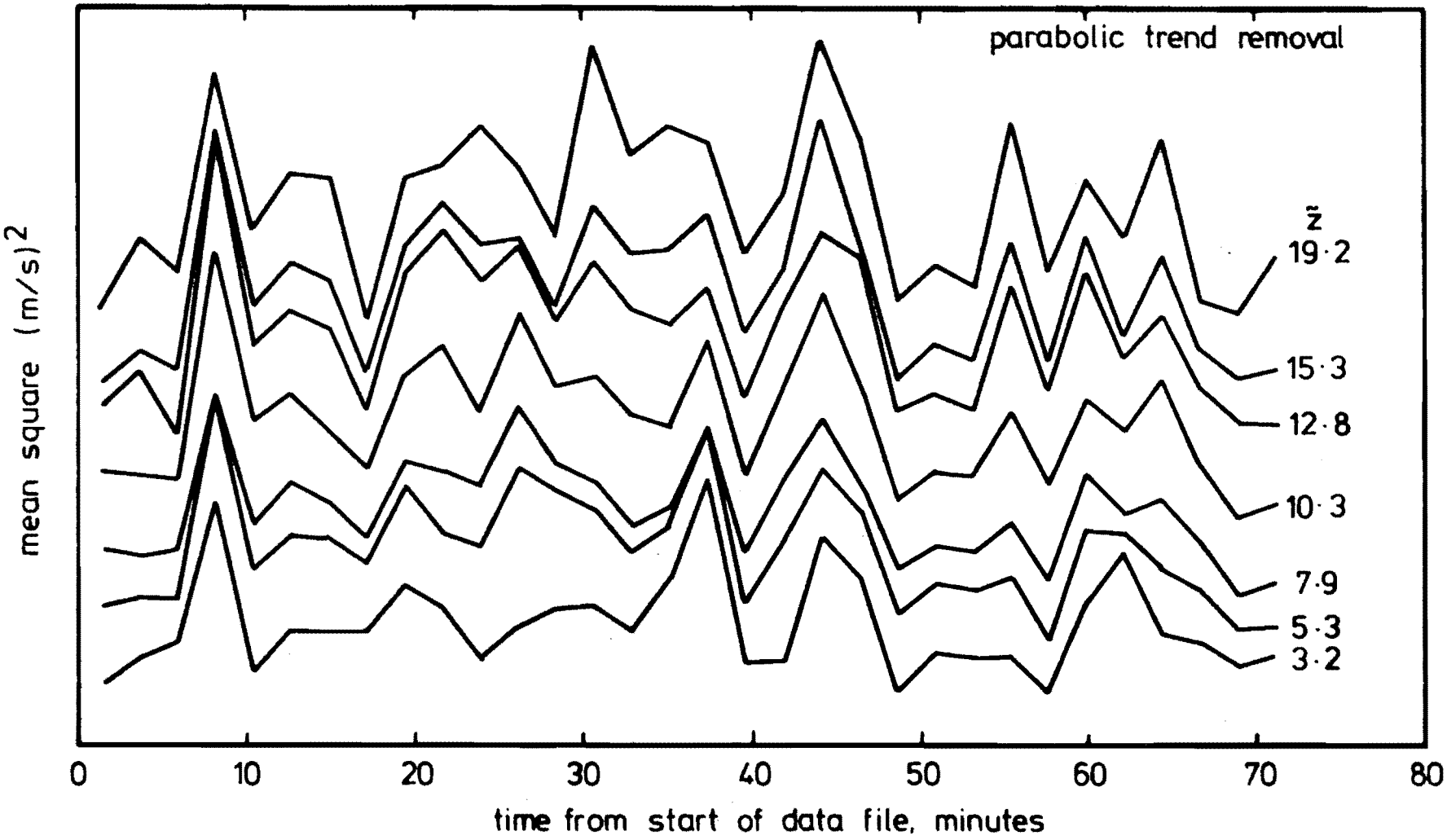

FIG 8·4 VARIATION OF THE LONGITUDINAL COMPONENT MEAN SQUARE VALUE, AVERAGED OVER 2·28 MINUTES, OVER THE MEASUREMENT PERIOD, FOR RUN 3.

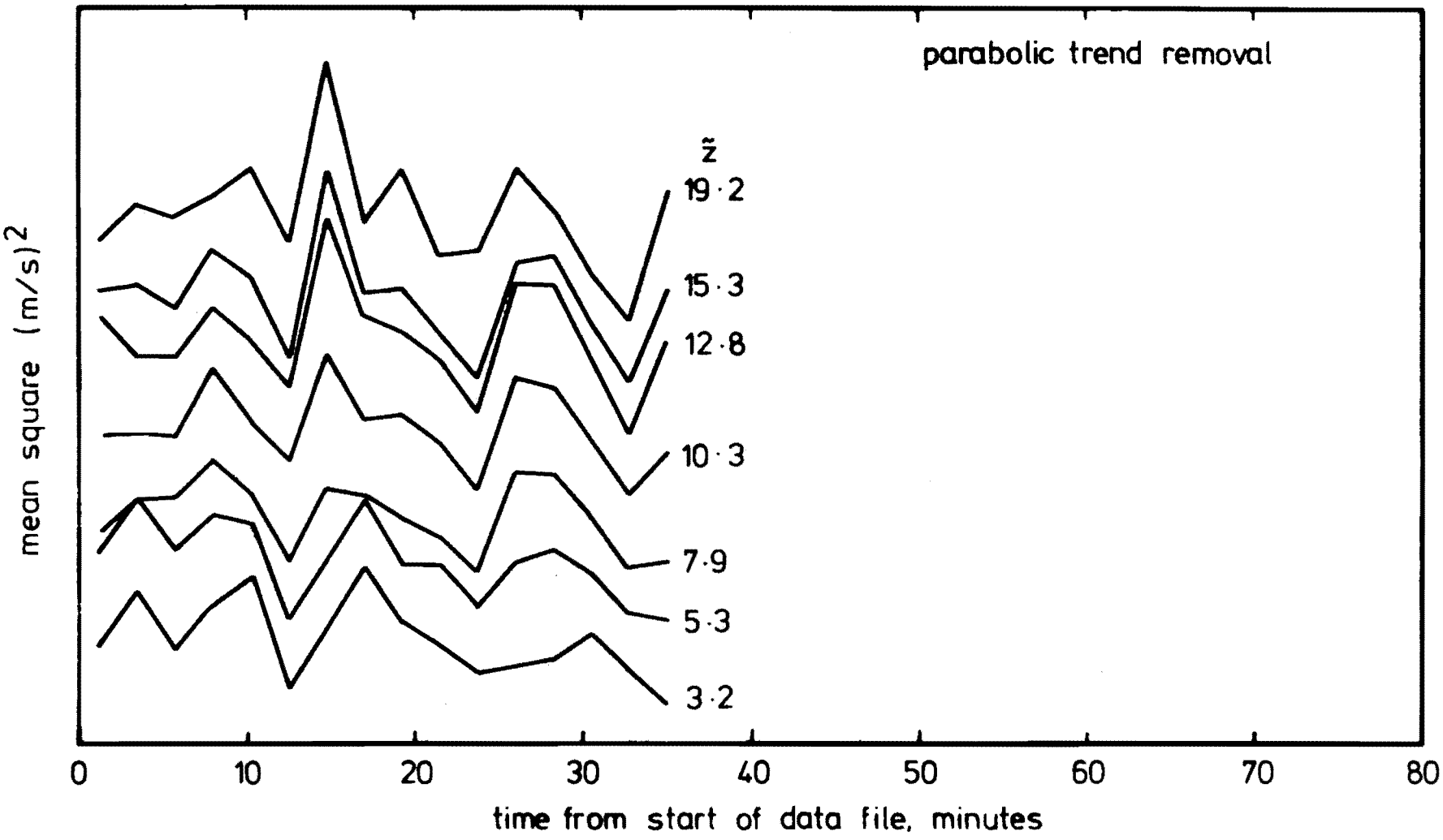

FIG 8·5 VARIATION OF THE LONGITUDINAL COMPONENT MEAN SQUARE VALUE, AVERAGED OVER 2 28 MINUTES, OVER THE MEASUREMENT PERIOD, FOR RUN 4.

the longitudinal component autocorrelation function fell to zero generally after about one minute. This meant that separate samples in the sequence of mean squares could be considered independent.

A parabolic trend line was removed from the data before the mean squares were calculated. The sequence of mean squares from Runs 1,2,3 and 4 have been plotted in Figs. 8.2, 8.3, 8.4 and 8.5 respectively.

The sequence of mean squares was checked for underlying trends using the *Run Test*. A *Run* is defined as 1 plus the number of times a line joining consecutive samples of the sequence of mean squares, crosses the line of the average mean square value for the entire sample record. The number of *Runs* is then tested to see if it is significantly different from that of a random variable.

Fig.8.2 shows the number of *Runs* for the longitudinal component data stream from the orthogonal array at 19.2 m from Run 1. The number of *Runs* is 15. Bendat and Piersol (1971) tabulate the number of *Runs* which are acceptable for several levels of significance, and for different numbers of samples in a sequence. For the sequences shown in Fig.8.2, there are 32 samples. For a .05 level of significance, the number of *Runs* should lie between 11 and 22. This means that there is a probability of .05 that the data is stationary and the number of *Runs* will lie outside the 11 to 22 range.

The data tested had 15 *Runs* and therefore can be considered stationary. For the shorter sequences shown in Figs.8.3 and 8.5, the number of samples is 16. Bendat and Piersol (1971) state that in this case the number of *Runs* should lie in the range 4 - 13 for a .05 level of significance. This means that according to the *Run Test* all of the data analysed here is stationary at the .05 level of significance.

Since the data with a parabolic trend line removed from it appears to be stationary according to the *Run Test*, analysis of the data by conventional statistical theory is valid.

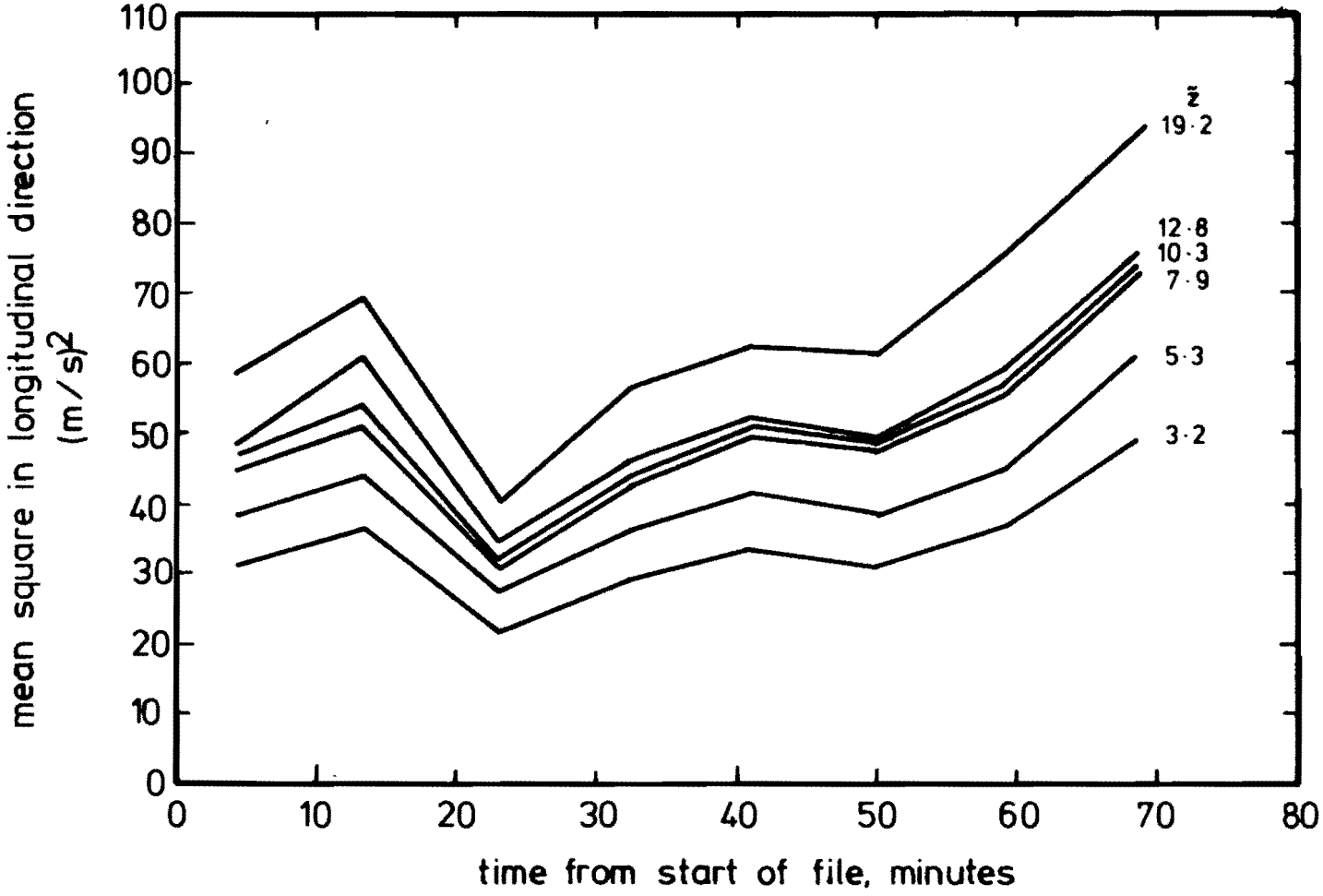

FIG. 8·6 VARIATION OF THE LONGITUDINAL COMPONENT MEAN SQUARE VALUE, AVERAGED OVER 9·1 MINUTES, OVER THE MEASUREMENT PERIOD, FROM RUN 1.

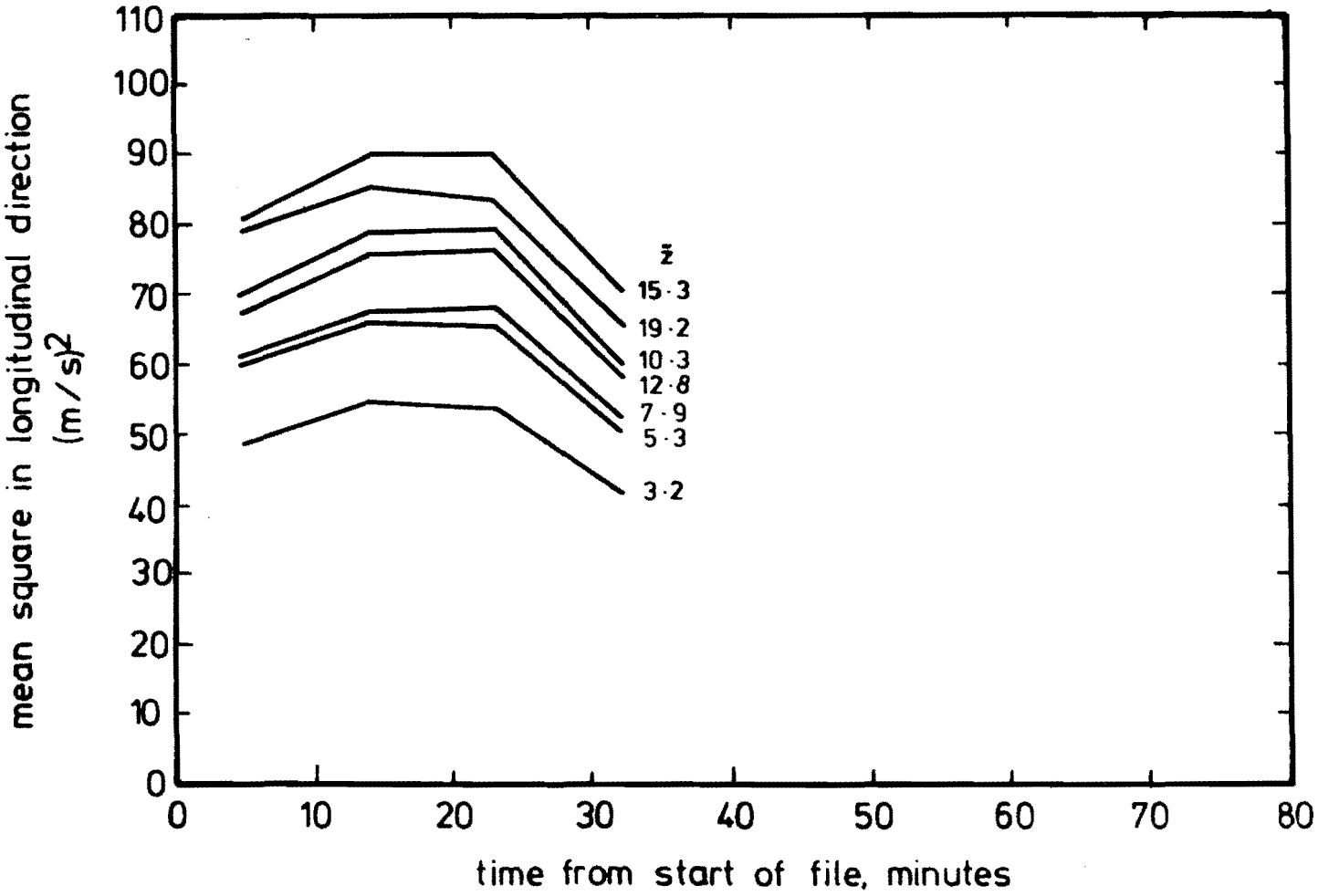

FIG. 8·7 VARIATION OF THE LONGITUDINAL COMPONENT MEAN SQUARE VALUE, AVERAGED OVER 9·1 MINUTES, OVER THE MEASUREMENT PERIOD, FROM RUN 2.

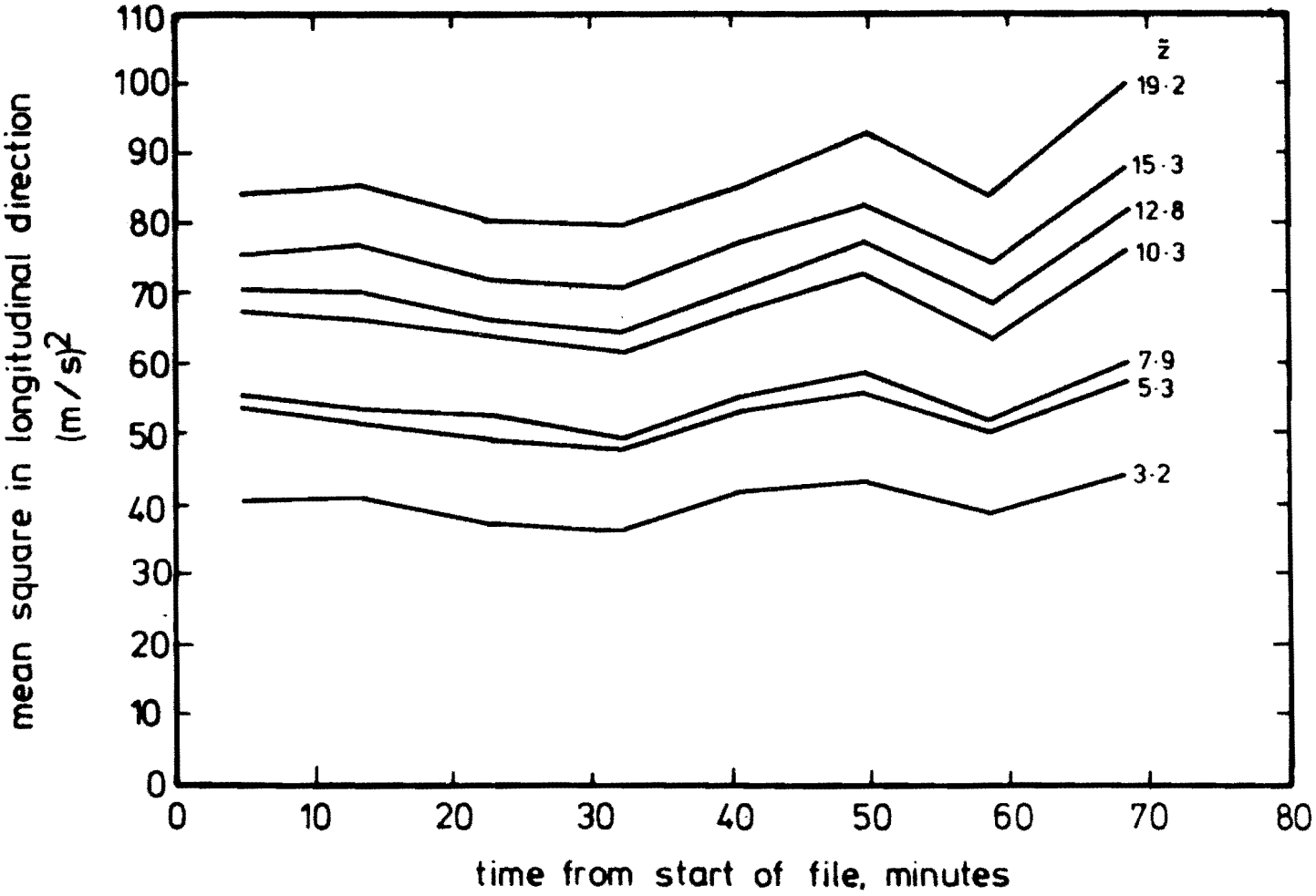

FIG. 8·8 VARIATION OF THE LONGITUDINAL COMPONENT MEAN SQUARE VALUE, AVERAGED OVER 9·1 MINUTES, OVER THE MEASUREMENT PERIOD, FROM RUN 3.

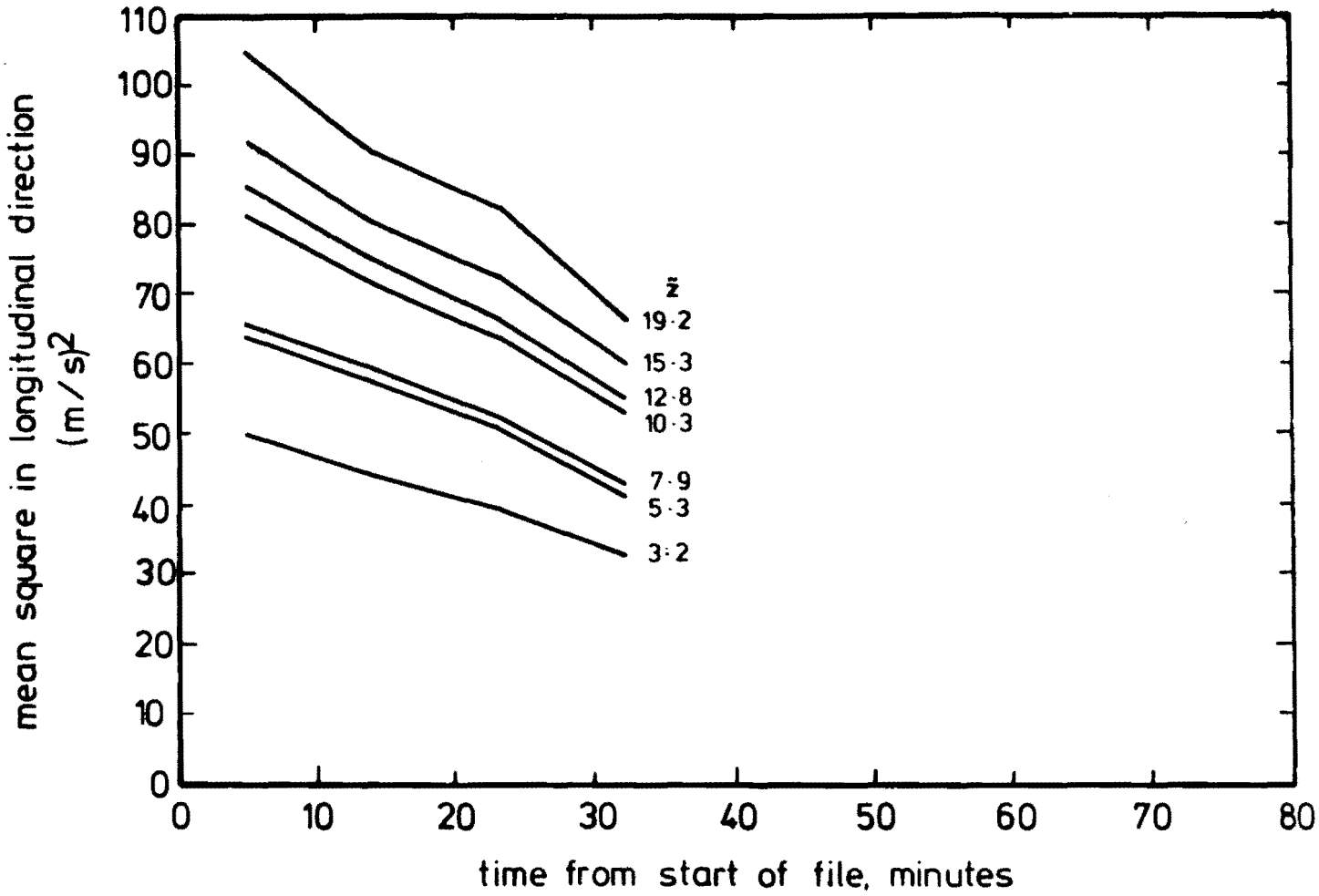

FIG. 8·9 VARIATION OF THE LONGITUDINAL COMPONENT MEAN SQUARE VALUE, AVERAGED OVER 9·1 MINUTES, OVER THE MEASUREMENT PERIOD, FROM RUN 4.

8.2.2 Mean Square Values Averaged over 9.1 Minutes

The variations in the mean square values averaged over 9.1 minutes have been plotted for the 4 Runs, and are given in Figs.8.6,8.7,8.8 and 8.9. This time no trend has been removed from the data. These values have been presented because an averaging period of ten minutes, (which is quite close to 9.1 minutes), has often been used to characterise wind structure parameters at a site. Figs.8.6, 8.7, 8.8 and 8.9 illustrate the variation in the wind structure parameters with time, even over quite short periods. The figures show the different values of the mean square which would have been obtained had the duration of the period for which data was recorded been limited to any one of the 9.1 minute periods. It is also interesting to note that the removal of the parabolic trend lines from the data presented in Figs.8.2,8.3,8.4 and 8.5 has made it appear much more stationary than the same data which is displayed in Figs.8.6, 8.7,8.8 and 8.9.

8.3 PROBABILITY DENSITY FUNCTIONS

It has often been assumed that wind velocity fluctuations over periods of between ten minutes and two hours have a probability distribution which is Gaussian. Thus the probability densities were calculated to see if this was the case for this data also. The probability distributions are plotted in Figs.8.10,8.11,8.12 and 8.13 for Runs 1,2,3 and 4 respectively.

It was found, although it is not presented here, that where a trend existed in the data, the comparison with the Gaussian distribution was better after a parabolic trend line had been removed from the data than without a trend line removed.

Figs.8.10,8.11,8.12 and 8.13 show that the measured data probability distributions compare very well with the Gaussian distribution, particularly in the longitudinal and lateral directions. It is not

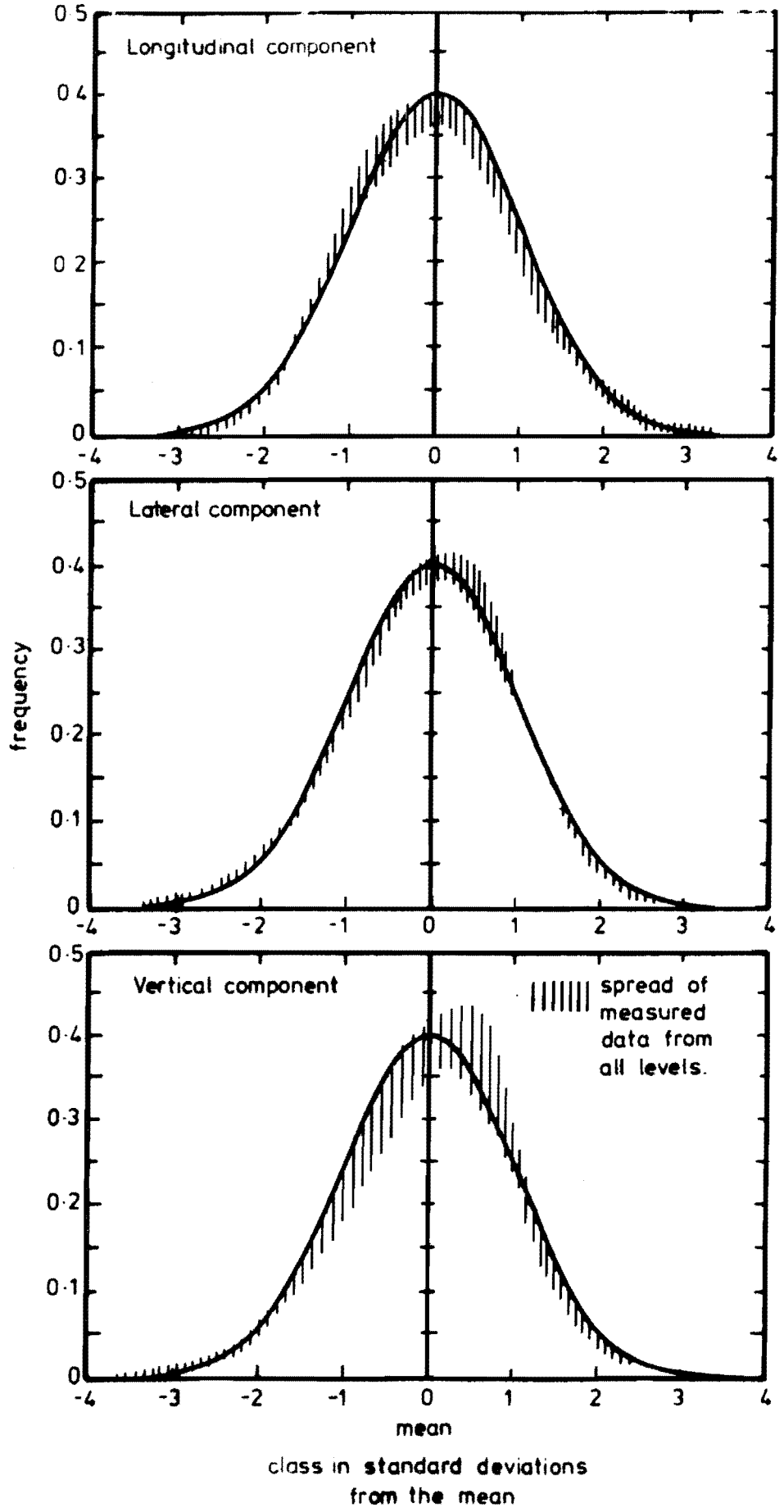

FIG. 8 · 10 WIND VELOCITY PROBABILITY DENSITY DISTRIBUTION FOR RUN 1

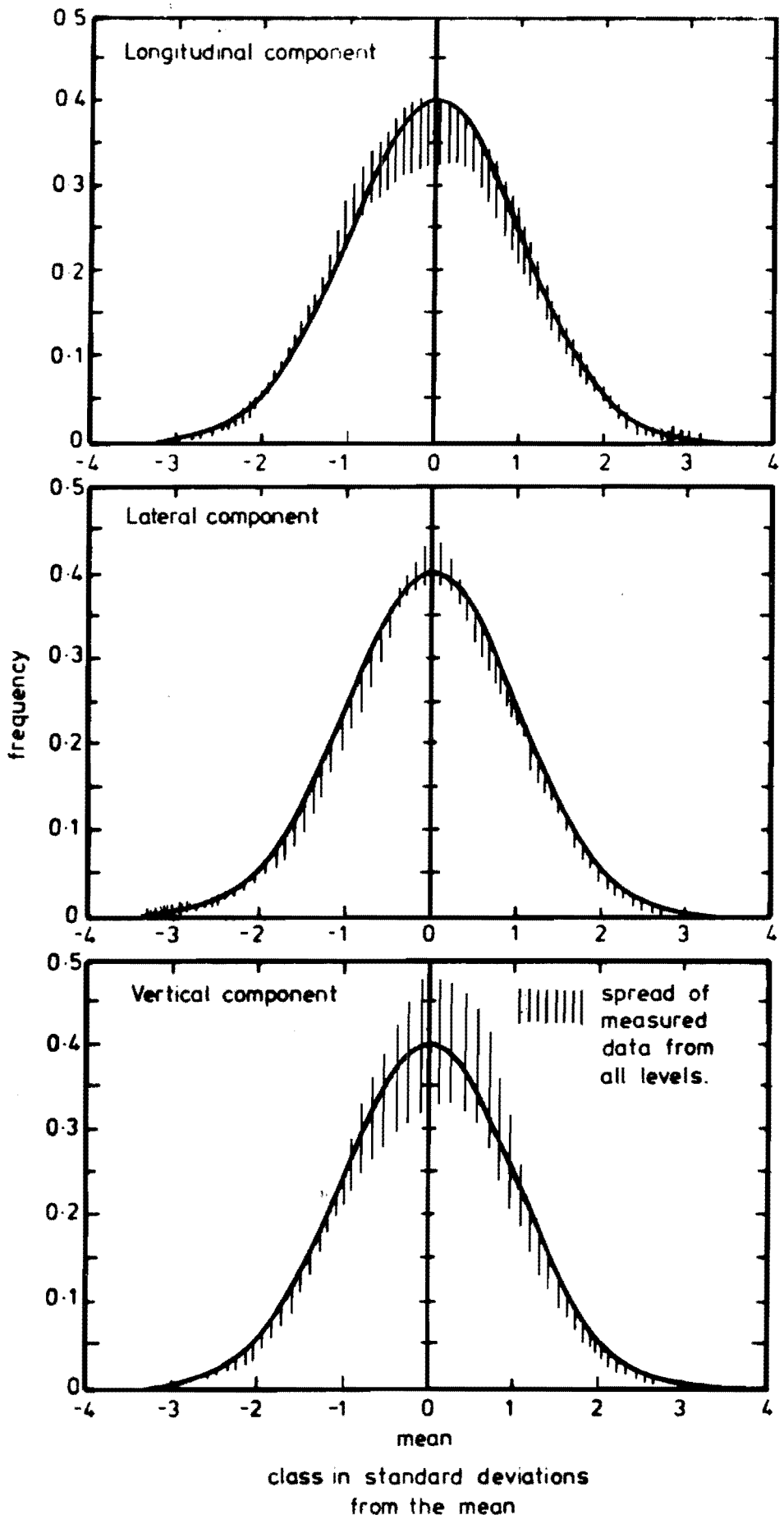

FIG. 8·11 WIND VELOCITY PROBABILITY DENSITY DISTRIBUTION FOR RUN 2

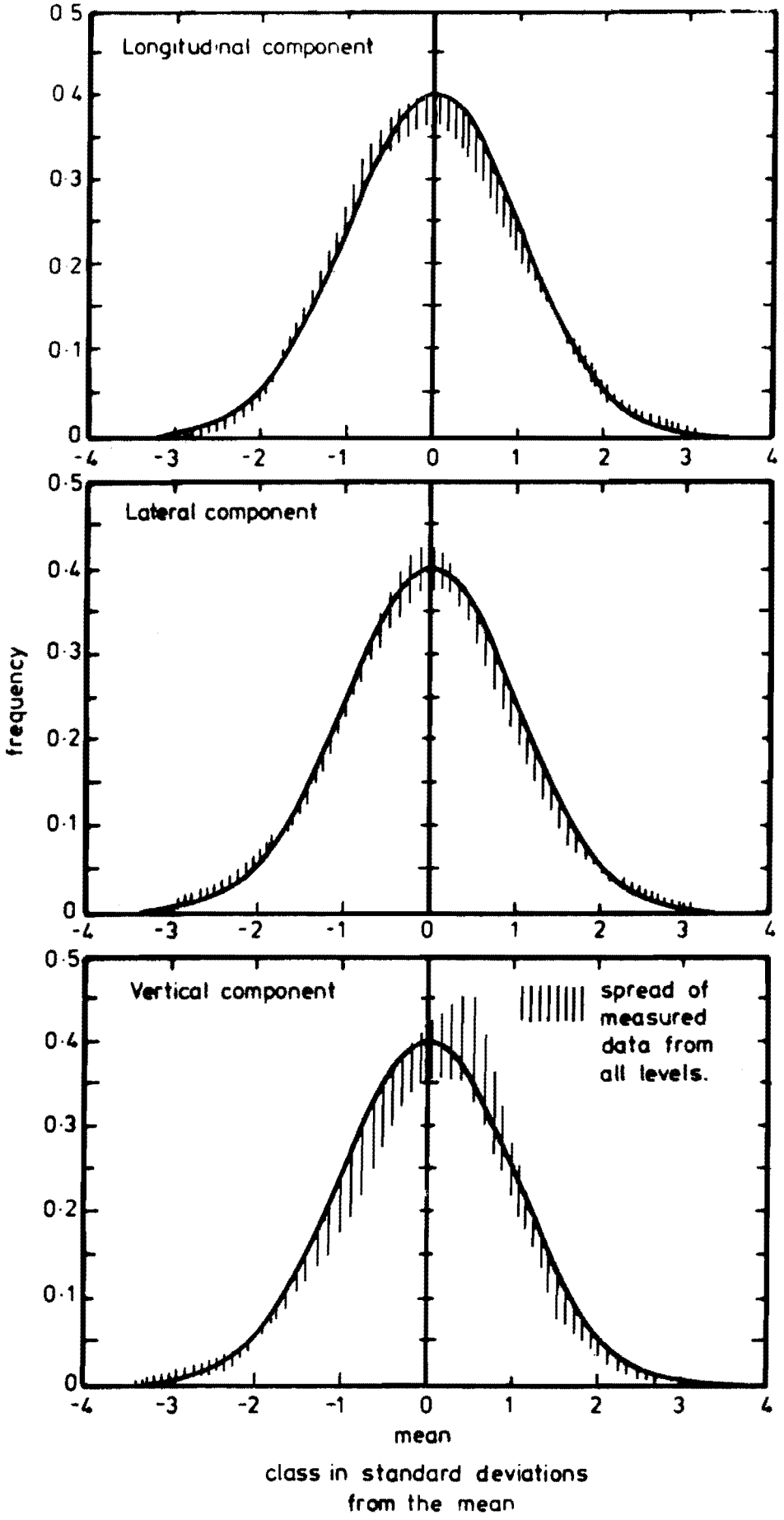

FIG. 8·12 WIND VELOCITY PROBABILITY DENSITY DISTRIBUTION FOR RUN 3

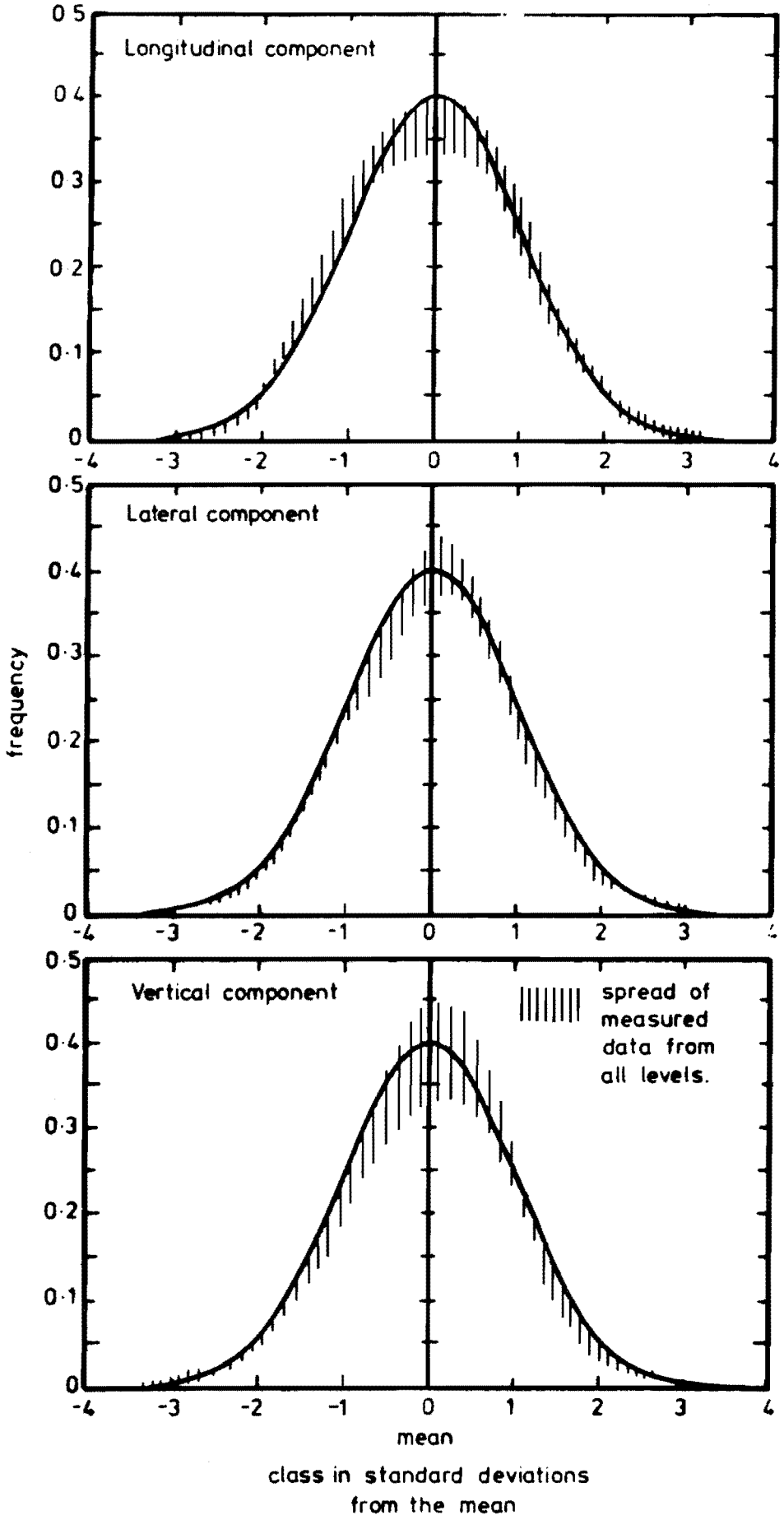

FIG. 8·13 WIND VELOCITY PROBABILITY DENSITY DISTRIBUTION FOR RUN 4

obvious in this data that it tends to have larger gusts and longer lulls than predicted by the Gaussian distribution,as suggested by ESDU (1974b).

Counihan (1975) also states that the Gaussian distribution is probably reasonable for velocity fluctuations up to about ±3 standard deviations. Outside this the Gaussian distribution is not satisfactory, as there is reported to be a larger number of gusts than indicated by the Gaussian distribution.

The longitudinal component has longer "tails" in some of the probability distribution plots for some Runs, and shorter tails in others compared with the Gaussian distribution. For the longitudinal and lateral velocity components, the Gaussian distribution is a very good model.

The vertical component probability density function shows the most significant variation from the Gaussian distribution, but even so is surprisingly good considering that the propeller is stalled a lot of the time. A general feature of the vertical component probability density function apparent in Figs.8.10,8.11,8.12 and 8.13 is the high peak near the mean. The peak frequency value probably occurs when the anemometer is not rotating which would occur more often than it should. This is because it is unresponsive to small vertical component fluctuations due to its large length constant in this mode and because it is stalled for about ±3° either side of $\theta = 90°$. It is likely that a certain threshold vertical velocity is required to make it start rotating, after which it accelerates quite quickly. The peak frequency does not in general occur at the mean because it is again likely that the vertical component anemometer is not aligned exactly vertically. However, the measured probability distribution is quite good near the tails of the distribution which correspond to larger vertical motions of the air.

The probability distribution of this data was calculated to further ensure that the data processing had been done correctly, and that the data had a probability density function which compared reasonably well

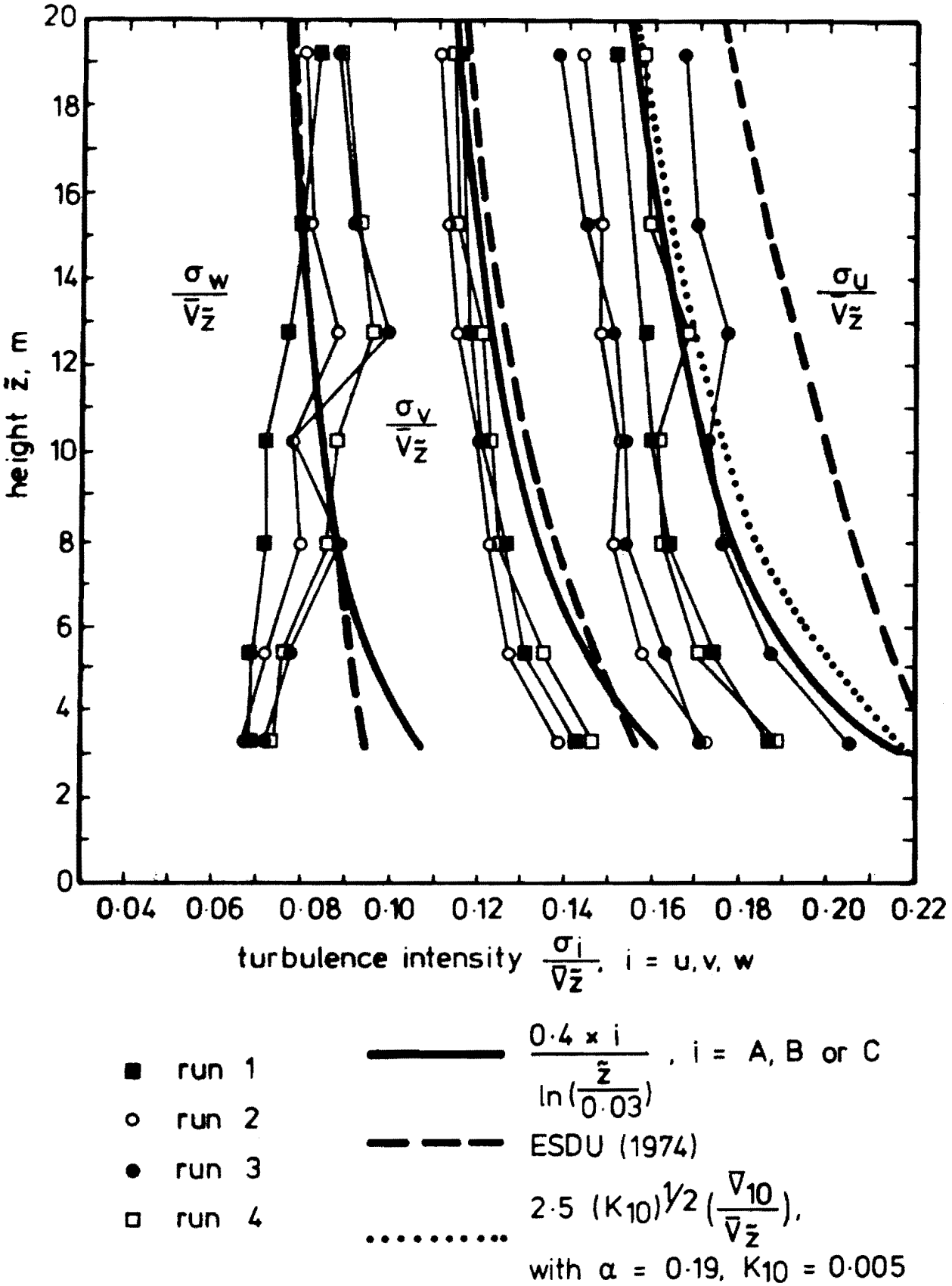

FIG. 8·14 TURBULENCE INTENSITY OF ALL COMPONENTS VARIATION WITH HEIGHT.

with the Gaussian distribution. It was more of a qualitative test than a quantitative one.

The data agreed well with the Gaussian distribution so that other turbulence parameters calculated with this data should be representative of surface layer atmospheric turbulence.

8.4 THE TURBULENCE INTENSITIES MEASURED

The turbulence intensities measured with data obtained from the 4 Runs have been plotted in Fig.8.14 as a function of height above the ground. Plotted in the same figure are several theoretical curves as a comparison. These are curves obtained from ESDU (1974b) for the three component turbulence intensities using Z_o = .03 m, from Counihan (1975), using $\frac{\sigma_u}{\bar{V}_Z} = \frac{1}{\ell n(\frac{Z}{.03})}$, and also assuming σ_v/σ_u = .75 and σ_w/σ_u = .50, thus giving the lateral and vertical component turbulence intensities. Finally, the longitudinal component turbulence intensity used by Davenport and Harris, namely $\frac{\sigma_u}{\bar{V}_Z} = 2.5\ (K_{10})^{\frac{1}{2}} \left[\frac{\bar{V}_{10}}{\bar{V}_Z}\right]$ has been plotted using α = .19, and K_{10} = .005 obtained from Table 8.1.

Some variation between Runs is apparent, but generally the measured results agree quite well with the theoretical curves. There is one exception however. The longitudinal component turbulence intensity given by ESDU (1974b) for Z_o = .03 m is significantly higher than both the measured values and the two other theoretical curves.

The vertical component turbulence intensity values show a systematic increase up to a height of approximately 13 m, above which they decrease slightly. The decrease then follows the trend indicated by both ESDU (1974b) and Counihan (1975).

The lateral component turbulence intensities are slightly smaller than the theoretical values, except for Run 3 where the measured value is higher than the theoretical values. A possible explanation for this is

that the data was not trend free, even after a parabolic trend removal. This is discussed in greater detail in Chapter 11.

The longitudinal component turbulence intensities measured agree well with the theoretical predictions, except for ESDU (1974b).

8.5 THE STANDARD DEVIATIONS OF THE VELOCITY FLUCTUATIONS

The standard deviations of the three components have been plotted in Fig.8.15 for the four Runs. These are compared with theoretical values obtained from the commonly accepted ratios of

$$\sigma_u = 2.5U_*$$

$$\sigma_v = 1.875U_*$$

$$\sigma_w = 1.25U_*$$

and $U_* = 0.60$ m/s is the average from the four Runs, from point Reynolds stress measurements. The value of U_* is discussed in more detail in Chapter 9.

There is reasonable agreement between the measured values and the theoretical curves for all three components, except that σ_v from Run 3 appears particularly high. σ_w values show an increase up to a height of approximately 13 m, above which the values are virtually invariant.

The decrease in σ_w measured near the ground is quite likely due to the lack of response of the anemometer at high frequencies, as the turbulence near to the ground has a greater contribution from the higher frequency spectral components than further away from the ground. The vertical component propeller anemometer is not particularly sensitive in this mode as discussed in Sections 3.2.5 and 8.3. Hicks (1972) has discussed this in some detail and gives recommendations as to their siting. Garratt (1974) also has suggested that for reasonable operation, vertical

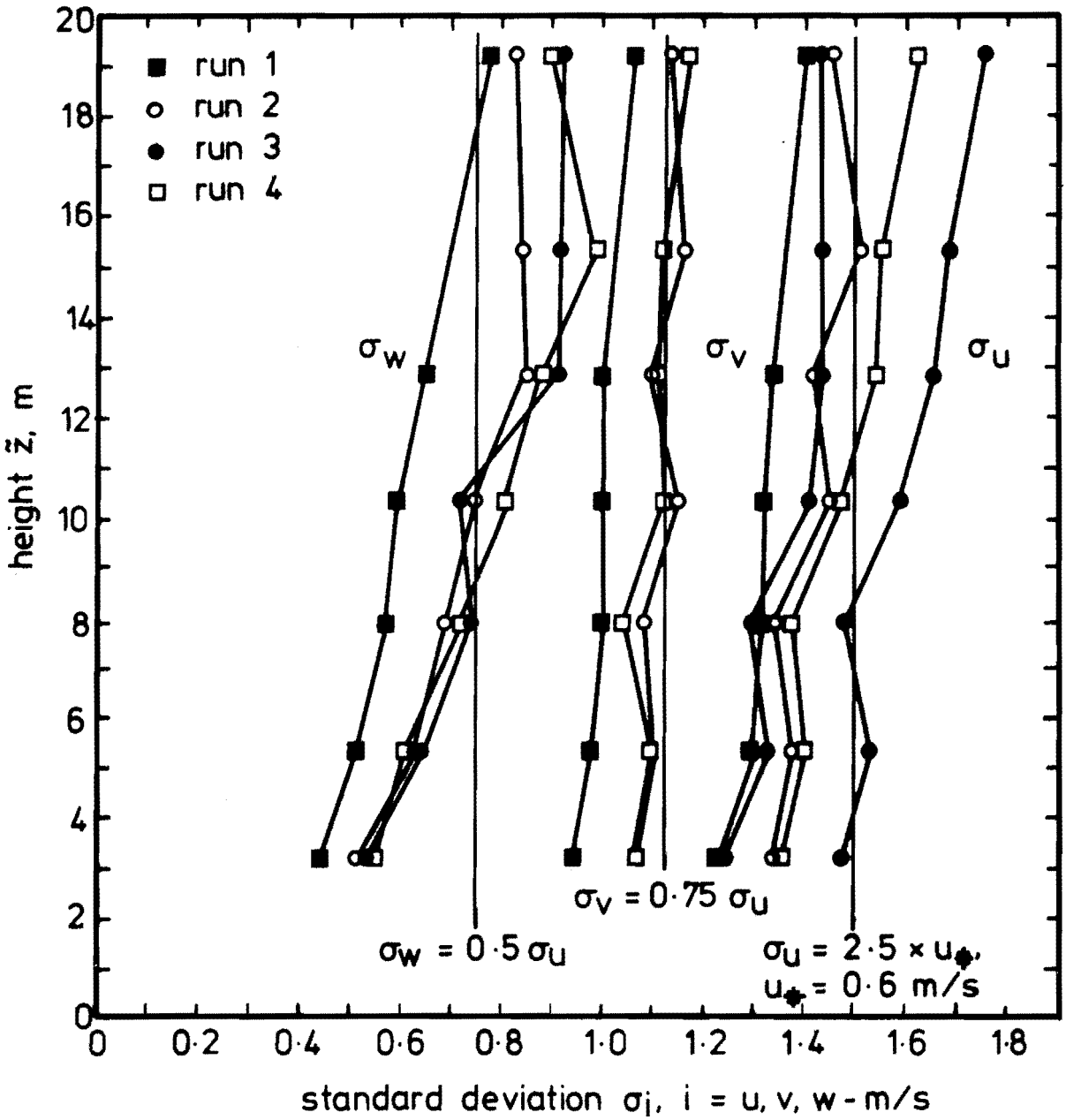

FIG. 8·15 STANDARD DEVIATION OF ALL COMPONENTS VARIATION WITH HEIGHT.

component propeller anemometers should be positioned at a height of at least 10 m above the sea, and at least 5 m above the ground for neutral stability conditions. It is apparent in Fig.8.15 that σ_w at levels 3.2 m and 5.3 m are the worst affected which agrees with the observations made by Garratt.

The ratios of the standard deviations of the three components with their respective friction velocities for each Run have been tabulated in Table 8.2. The ratios for all three components, when averaged over the four Runs, show an increase with height. The average for all levels and Runs is

$$\sigma_v : \sigma_v : \sigma_w : U_* = 2.43 : 1.93 : 1.20 : 1.$$

This is in good agreement with Counihan (1975) who proposes :

$$2.5 : 1.875 : 1.25 : 1 ,$$

and Teunissen (1970) who proposes :

$$2.5 : 2.0 : 1.3 : 1 .$$

The vertical component standard deviation is slightly lower than both values proposed by Counihan and Teunissen and may, as mentioned previously, be due to the low pass filtering effect of the vertical component anemometer.

The ratios of the standard deviation with respect to σ_u at each level and for each Run have been given in Table 8.3.

The ratio σ_w/σ_u averaged over all Runs shows an increase with height whereas σ_v/σ_u is virtually invariant. The averages over all levels and Runs are :

$$\sigma_u : \sigma_v : \sigma_w = 1 : 0.79 : 0.49 ,$$

which compares well with Teunissen

$$1 : 0.8 : 0.52 ,$$

and Counihan

$$1 : 0.75 : .50 .$$

Height Z , m	Run 1			Run 2			Run 3			Run 4			Average at each height			
	$\frac{\sigma_u}{U_*}$	$\frac{\sigma_v}{U_*}$	$\frac{\sigma_w}{U_*}$	$\frac{\sigma_u}{U_*}$	$\frac{\sigma_v}{U_*}$	$\frac{\sigma_w}{U_*}$	$\frac{\sigma_u}{U_*}$	$\frac{\sigma_v}{U_*}$	$\frac{\sigma_w}{U_*}$	$\frac{\sigma_u}{U_*}$	$\frac{\sigma_v}{U_*}$	$\frac{\sigma_w}{U_*}$	$\frac{\sigma_u}{U_*}$	$\frac{\sigma_v}{U_*}$	$\frac{\sigma_w}{U_*}$	$\frac{U_*}{U_*}$
3.2	2.16	1.66	.78	2.22	2.06	.86	2.40	1.99	.84	2.26	1.77	.87	2.26	1.87	.84	1
5.3	2.27	1.71	.90	2.29	1.84	1.04	2.49	2.17	1.05	2.34	1.85	1.04	2.35	1.89	1.01	1
7.9	2.30	1.76	1.00	2.22	1.79	1.16	2.41	2.11	1.20	2.28	1.74	1.19	2.30	1.85	1.14	1
10.3	2.31	1.75	1.04	2.42	1.91	1.24	2.60	2.30	1.17	2.46	1.87	1.34	2.45	1.96	1.20	1
12.8	2.36	1.76	1.14	2.36	1.83	1.41	2.69	2.29	1.48	2.56	1.84	1.47	2.49	1.93	1.38	1
15.3	Instrumentation Failure			2.51	1.94	1.40	2.75	2.32	1.49	2.58	1.86	1.49	2.61	2.04	1.46	1
19.2	2.45	1.86	1.37	2.42	1.88	1.37	2.84	2.35	1.50	2.69	1.95	1.50	2.60	2.01	1.44	1
Average	2.31	1.75	1.04	2.35	1.89	1.21	2.60	2.22	1.25	2.45	1.84	1.27	2.43	1.93	1.20	1

TABLE 8.2 RATIOS OF STANDARD DEVIATIONS TO THE FRICTION VELOCITIES FOR EACH RUN

Height Z , m	Run 1		Run 2		Run 3		Run 4		Average at each height		
	$\frac{\sigma_v}{\sigma_u}$	$\frac{\sigma_w}{\sigma_u}$	$\frac{\sigma_v}{\sigma_u}$	$\frac{\sigma_w}{\sigma_u}$	$\frac{\sigma_v}{\sigma_u}$	$\frac{\sigma_w}{\sigma_u}$	$\frac{\sigma_v}{\sigma_u}$	$\frac{\sigma_w}{\sigma_u}$	$\frac{\sigma_u}{\sigma_u}$	$\frac{\sigma_v}{\sigma_u}$	$\frac{\sigma_w}{\sigma_u}$
3.2	.76	.36	.81	.39	.83	.35	.78	.38	1	.80	.37
5.3	.75	.40	.80	.46	.87	.42	.79	.44	1	.80	.44
7.9	.77	.44	.81	.52	.88	.50	.76	.52	1	.81	.50
10.3	.76	.45	.79	.51	.88	.45	.76	.55	1	.80	.49
12.8	.75	.49	.78	.59	.85	.55	.72	.57	1	.78	.55
15.3	Instrumentation Failure		.77	.56	.85	.54	.75	.59	1	.79	.56
19.2	.76	.56	.78	.57	.82	.53	.73	.56	1	.77	.56
Average	.76	.45	.79	.51	.86	.48	.76	.52	1	.79	.49

TABLE 8.3 RATIOS OF ORTHOGONAL COMPONENT STANDARD DEVIATIONS FOR EACH RUN

8.6 CONCLUSIONS

This chapter described various measures of the turbulence characteristics of the data analysed. The turbulence values measured have been compared with generally accepted values from the current literature. Agreement has been found to be good. The variations in the values are no more significant than the variation in the accepted values themselves, quoted from different sources, e.g. Counihan (1975) and ESDU (1974b) for $\frac{\sigma_u}{\bar{V}_Z}$.

The probability density functions from the data streams compare well with a Gaussian distribution, particularly for the longitudinal and lateral components. This is in agreement with previous observations, (ESDU, 1974b). The vertical component probability density function compares least well with the Gaussian distribution, although even this data compares surprisingly well. The wider spread of the data for the vertical component is probably due to the fact that the vertical component anemometer is stalled an appreciable amount of the time. Also, small differences in the alignment of the vertical component anemometers at different levels up the tower cause different anemometers to have a peak frequency at different distances from the mean. This contributes to the relatively large amount of "spread" in the measured data shown in Figs.8.10,8.11,8.12 and 8.13 for each particular Run.

The data streams were checked for stationarity and were found to be stationary by the *Run Test* at the .05 level of significance.

The good agreement with the Gaussian distribution and the fact that the data appears to be stationary means that the data can be analysed using conventional statistical theory.

CHAPTER 9

REYNOLDS STRESSES

9.1 INTRODUCTION

9.1.1 Definitions

The Reynolds stresses are the non-diagonal terms of the tensor formed when pairs of the three velocity components at a single point are correlated with each other, or the non-diagonal terms of the covariance function. Using the nomenclature of ESDU (1974a), the covariance function is formed by the mean product of two fluctuating velocity components measured at times t and t + τ, and is shown diagrammatically in Fig.9.1. When the velocity components are at the same point, this can be expressed as

$$C_{ij}(\tau) = \overline{i(t).j(t+\tau)} = \lim_{T\to\infty} \frac{1}{T} \int_0^T i(t).j(t+\tau)\, dt. \qquad (9.1)$$

$$i,j = u,v,w.$$

When i = j the products are called autocovariances and when τ = 0, the autocovariances reduce to the variances, namely σ_u^2, σ_v^2 and σ_w^2. The three Reynolds stresses are :

$$C_{uw}(\tau) = \overline{u(t).w(t+\tau)} \ ,$$

$$C_{vw}(\tau) = \overline{v(t).w(t+\tau)} \ , \quad \text{and} \qquad (9.2)$$

$$C_{uv}(\tau) = \overline{u(t).v(t+\tau)} \ .$$

Normally the Reynolds stresses are normalised by the appropriate standard deviations of the constituent velocity components to form correlation functions, i.e.

$$\rho_{ij}(\tau) = C_{ij}(\tau)/\sigma_i\sigma_j \ . \qquad (9.3)$$

When $i = j$, e.g. $\rho_{uu}(\tau) = \overline{u(t).u(t+\tau)}/\sigma_u^2$ (9.4)

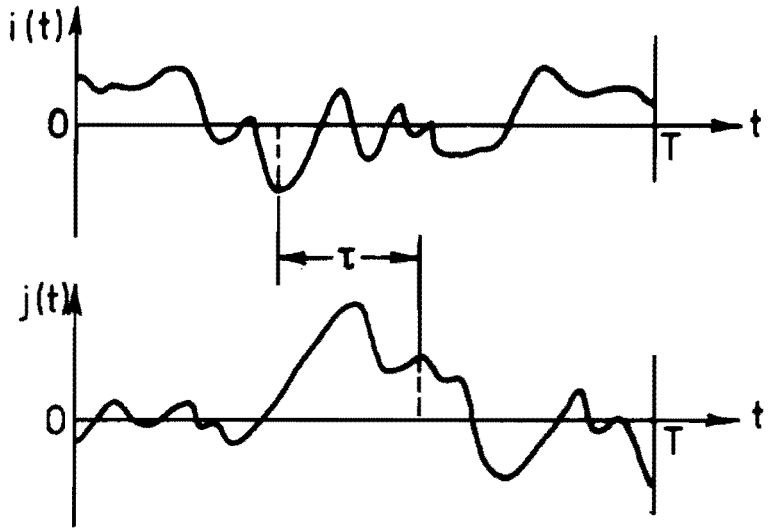

FIG. 9·1 ILLUSTRATION OF A CROSS-CORRELATION MEASUREMENT.

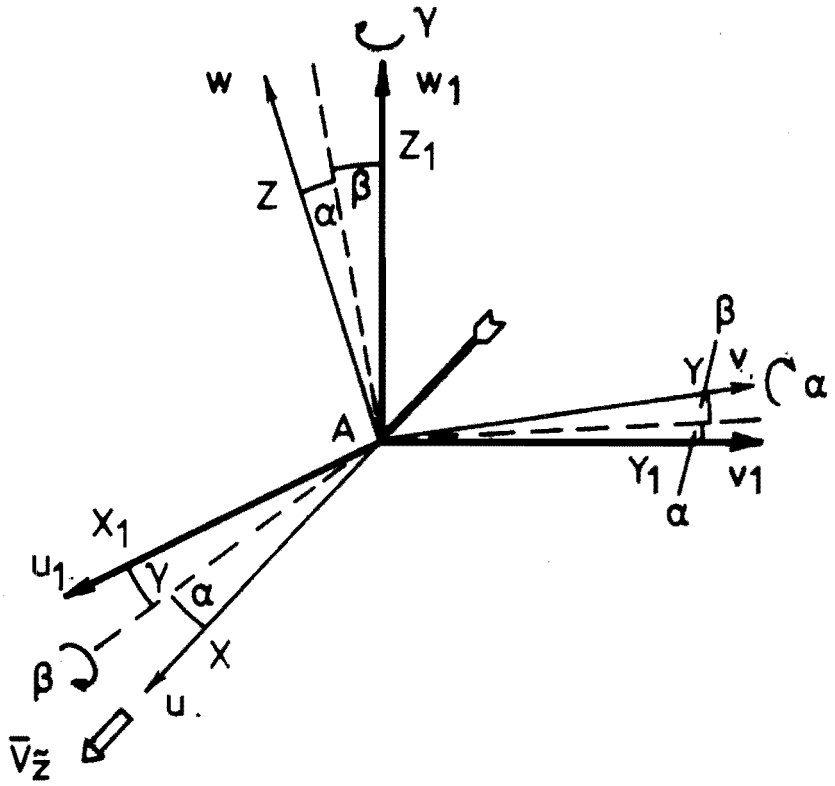

FIG. 9·2 COORDINATE SYSTEMS. α, β, γ ARE ROTATION ANGLES RELATING TRUE WIND COMPONENTS u, v, w, TO MEASURED WIND COMPONENTS BY A SENSOR AT A. u IS DEFINED PARALLEL TO THE MEAN WIND VECTOR $\bar{V}_{\tilde{z}}$.

the correlations $\rho_{uu}(\tau)$, $\rho_{vv}(\tau)$ and $\rho_{ww}(\tau)$ are called autocorrelation functions.

The discrete form of the above functions is obtained by changing the integral sign to a sigma and summing terms for a finite sample record length. Consider time histories with N samples, and Δt seconds between consecutive samples. Then if r is the lag number,

$$\rho_{uw}(r\Delta t) = \frac{1}{N}\sum_{k=0}^{N-1} u(k).\, w(k+r)/\sigma_u\sigma_w \qquad r = 0,1,\ldots m \tag{9.5}$$

In practice, because the N samples are from records of a finite length, in order to obtain unbiased estimates of the correlation functions, the following formula is used :

$$\rho_{ij}(r\Delta t) = \frac{1}{N-r}\sum_{k=0}^{N-r-1} i(k).j(k+r)/\sigma_i\sigma_j \qquad r = 0,1,\ldots m \qquad i,j = u,v,w. \tag{9.6}$$

m is the maximum lag number, and is normally limited to less than N/10.

The zero time delay Reynolds stresses are :

$$\rho_{uw}(0) = \frac{1}{N}\sum_{k=0}^{N-1} u(k).w(k)\ , \tag{9.7}$$

$$\rho_{uv}(0) = \frac{1}{N}\sum_{k=0}^{N-1} u(k).v(k)\ , \qquad \text{and} \tag{9.8}$$

$$\rho_{vw}(0) = \frac{1}{N}\sum_{k=0}^{N-1} v(k).w(k)\ . \tag{9.9}$$

9.1.2 Errors in Reynolds Stress Measurements Due to Misalignment of the Anemometers.

The errors discussed in this Section are those caused in particular by the non-vertical alignment of the vertical component anemometer. This misalignment causes errors in the computation of Reynolds stresses at a single point when the eddy correlation method is used. The discussion is limited to errors in the measurement of $\rho_{uw}(0)$ as this is the most

important Reynolds stress physically. The theory follows Hyson et al (1977), but is adapted for orthogonal arrays of propeller anemometers.

Consider the two coordinate systems shown in Fig.9.2. A turbulence sensor (one orthogonal array of propeller anemometers), is fixed at point A in space with orthogonal sensing elements measuring wind components u_1,v_1 and w_1. In practice the three propeller anemometers are mounted rigidly on a bracket so that they are orthogonal. When the array is fixed to a tower the z_1 axis will be close to the vertical with the x_1 and y_1 axes close to the horizontal plane. At A the wind vector consists of the mean velocity $\bar{V}_Z$ with the turbulent fluctuations u,v and w superimposed on it. u is parallel to $\bar{V}_Z$, w is normal to the surface so that $\bar{u} = \bar{v} = \bar{w} = 0$.

The equations which transform one set of velocity components measured on one coordinate system to velocity components measured on the other coordinate system are :

$$u_1 = (\cos\gamma\cos\alpha - \sin\gamma\sin\beta\sin\alpha)U' - (\sin\gamma\cos\beta)v + (\cos\gamma\sin\alpha + \sin\gamma\sin\beta\cos\alpha)w \ , \tag{9.10}$$

$$v_1 = (\sin\gamma\cos\alpha + \cos\gamma\sin\beta\sin\alpha)U' + (\cos\gamma\cos\beta)v + (\sin\gamma\sin\alpha - \cos\gamma\sin\beta\cos\alpha)w \ , \tag{9.11}$$

$$w = (-\cos\beta\sin\alpha)U' + (\sin\beta)v + (\cos\beta\cos\alpha)w \ . \tag{9.12}$$

where $U' = \bar{V}_Z + u$.

When orthogonal arrays of three propeller anemometers are used to measure atmospheric turbulence, some of the misalignment angles α, β and γ are more or less important for the different components measured.

To calculate $\rho_{uw}(0)$, the data off the orthogonal triplet is corrected for non-cosine response. Misalignments do not affect the correction procedure because all three components are considered simultaneously. This correction has been discussed in Section 6.1. The next manipulation required is to resolve the horizontal component data measured

on the axes x_1,y_1 and z_1 into components parallel and perpendicular to the average wind direction. It was assumed in this work that since the terrain was horizontal and reasonably homogenous, the flow averaged over 10 minutes to 1 hour would be horizontal.

The horizontal component anemometers are relatively insensitive to small angles of α and β so the data from the anemometers aligned in the x_1 and y_1 directions was resolved through the angle γ to obtain the longitudinal and lateral components. The details of this resolving, i.e. whether it is done for every component or whether totals are accumulated such as described in Section 5.5 and Appendix E, do not matter because the correction for misalignment is applied to $\rho_{uw}(0)$ after the value assuming no misalignment has been obtained.

The vertical component anemometer is sensitive to both α and β. Consequently $w \neq w_1$ and $\bar{w}_1 \neq 0$. The vertical component anemometer measures w_1 which consists of a mean and a fluctuating part. Thus

$$w_1 = \bar{w}_1 + w_1' \tag{9.13}$$

Note the slight change in nomenclature here from Section 7.1.2. In Equation (9.13) $\bar{w}_1$ is the mean of the fluctuations measured by the vertical component anemometer and w_1' is the fluctuating part. The fluctuating part has been called w in e.g. Sections 7.1.2. w_1' is found simply by removing the mean from w_1 for all samples.

To calculate $\rho_{uw}(0)$, computationally $\overline{w_1'u}$ is formed, i.e. the summation of the products of the vertical component fluctuations with the horizontal component fluctuations.

From Equation (9.12), this is really :

$$\overline{w_1'u} = (-\cos\beta \sin\alpha)\ \sigma_u^2 + \sin\beta\ \overline{vu} + (\cos\beta \cos\alpha)\ \overline{uw} \tag{9.14}$$

which can be rewritten as :

$$\overline{w_1'u} = \overline{uw}\cos\alpha\cos\beta\left[1 + \left(\frac{\sigma_u^2}{-\overline{uw}}\right)\tan\alpha + \frac{\overline{uv}}{\overline{uw}}\frac{\tan\beta}{\cos\alpha}\right] \qquad (9.15)$$

Typically in the surface layer, in neutrally stable conditions,

$$\frac{\sigma_u^2}{(-\overline{uw})} = 6.25, \text{ (Lumley and Panofsky, 1964, Counihan, 1975).}$$

Hyson et al (1977) suggest that $|\overline{uv}| \approx |\overline{uw}|$ from Bernstein (1966) and Cramer et al (1962). However Teunissen (1970) suggests that in the surface layer both $|\overline{uv}|$ and $|\overline{vw}|$ are considerably smaller than $|\overline{uw}|$. ESDU (1974b) also suggest that $|\overline{uv}|$ and $|\overline{vw}|$ are small and can be ignored. Assuming then for the worst case $|\overline{uv}| \approx |\overline{uw}|$, after Hyson et al, means that Equation (9.15) can be expressed as

$$\overline{w_1'u} = \overline{uw}\cos\alpha\cos\beta\left[1 + 6.25\tan\alpha \pm \tan\beta/\cos\alpha\right] \qquad (9.16)$$

Expressing $\cos\alpha\cos\beta = \cos\phi$, where ϕ is the angle between AZ_1 and AZ, shows that for $\phi \leqslant 8°$, the effect on $\cos\alpha\cos\beta$ is less than 1%. However the term in square brackets implies a difference in $\overline{w_1'u}$ and $\overline{uw}$ of about 11% per degree of α. Since the sign of $\overline{uv}$ is undetermined, the effect of β on the measured $\rho_{uw}(0)$ can be of either sign but is of the order of 1.7% per degree of β, and is of course even smaller if $|\overline{uv}| < |\overline{uw}|$.

From equation (9.12),

$$\overline{w_1} = -\cos\beta\sin\alpha\,\bar{V}_Z \text{ , or}$$

$$\cos\beta\sin\alpha = -\frac{\overline{w_1}}{\bar{V}_Z} \qquad (9.17)$$

Substituting Equation (9.17) into Equation (9.14) and setting $\cos\beta\cos\alpha = 1$ gives,

$$\overline{w_1'u} = \overline{uw} - \sigma_u^2\left[\frac{-\overline{w_1}}{\bar{V}_Z}\right] + \overline{uv}\sin\beta \qquad (9.18)$$

or $$\overline{uw} = \overline{w_1'u} - \sigma_u^2\left(\frac{\overline{w_1}}{\bar{V}_Z}\right) - \overline{uv}\sin\beta \qquad (9.19)$$

Neglecting the last term in Equation (9.19) means that $\overline{uw}$ will be in error up to ±1.7% per degree of β when $\alpha = 0$ and ±1.8% per degree when $\alpha = 10°$. Equation (9.19) then becomes

$$\overline{uw} = \overline{w_1'u} - \sigma_u^2 \left(\frac{\overline{w_1}}{\bar{V}_W} \right) \tag{9.20}$$

In Equation (9.20), all the values can be calculated. $\overline{w_1'u}$ is the product of the longitudinal component fluctuations about the mean velocity, and the vertical component fluctuations about the mean velocity, $\overline{w_1}$ is the average on the vertical component anemometer, and σ_u^2 and $\bar{V}_Z$ are respectively the longitudinal component variance and the mean velocity for that particular height. Consequently, in processing, $\overline{w_1'u}$ is formed and then $\sigma_u^2 \left(\frac{\overline{w1}}{\bar{V}_Z} \right)$ removed from it to give $\overline{uw}$ with the error reduced from about 11% to about 2% per degree of misalignment of β.

9.1.3 Methods of Measuring the Reynolds Stresses

The most common method of determining $\rho_{uw}(0)$ is to plot velocity-height data on log-linear graph paper. Provided the atmosphere is neutrally stable, the theoretical equation relating velocity and height,

$$\bar{V}_Z = \frac{U_*}{k} \ln \left(\frac{Z}{Z_o} \right) \tag{9.21}$$

may be fitted to the data. From the slope of the velocity profile, the value of U_* may be found, and consequently $\overline{uw}$ since,

$$U_*^2 = - \overline{uw} \, . \tag{9.22}$$

The velocity profile may only be used to find $\rho_{uw}(0)$, not the two other Reynolds stresses.

If the horizontal and vertical components are measured simultaneously with sensitive instruments, the three Reynolds stresses can be measured directly via the eddy correlation technique, i.e. using Equation (9.6).

This method also enables the Reynolds stresses to be evaluated as a function of the time delay between the two signals.

Other methods have also been used to determine $\rho_{uw}(0)$, e.g. drag plates (Bradley, 1968), and Brook (1974) discusses some of these.

In this research $\rho_{uw}(0)$ was determined from the velocity profile, and was compared with $\rho_{uw}(0)$ calculated directly by summing the product $u(k).w(k)$ $k = 0,1,...N-1$. The value obtained was then corrected for anemometer misalignment as discussed in the previous Section. The progam used to do this was SEQVELTURBREY, discussed in Section 5.5.

Equation (9.6) was also evaluated by the roundabout fast Fourier transform technique discussed in Section 5.6.2.3. This enabled the three stresses $\rho_{uw}(\tau)$, $\rho_{uv}(\tau)$ and $\rho_{vw}(\tau)$ to be evaluated to see how dependent they were on τ. Typical variations in the stresses with τ are shown in Figs.9.3 and 9.4. Note that $\rho_{uw}(\tau)$ shown in Fig.9.3 has not had the correction for misalignment discussed in Section 9.1.2 applied to it. A biased value of $\rho_{uw}(\tau)$ was thus evaluated from the following equation

$$\rho_{uw}(r\Delta t) = \frac{1}{N} \sum_{k=0}^{N-1} w_1'(k).u(k+r) \qquad (9.23)$$

where w_1' is defined by Equation (9.13), which was assumed to be a good approximation to the unbiased estimate because $r < 1\text{-}5\%$ of N.

9.1.4 Measurements of Reynolds Stresses in the Literature

Measurements of the three Reynolds stresses are reported infrequently in the literature. Counihan (1975) states that it is very difficult to assess this quantity since the available data are not very extensive, and in the case of urban areas are particularly sparce. Teunissen (1970) also states that there is not sufficient data to make significant conclusions about the assumption of constant stress in the surface layer.

However, Counihan concludes that $\overline{uw}$ increases with increase in

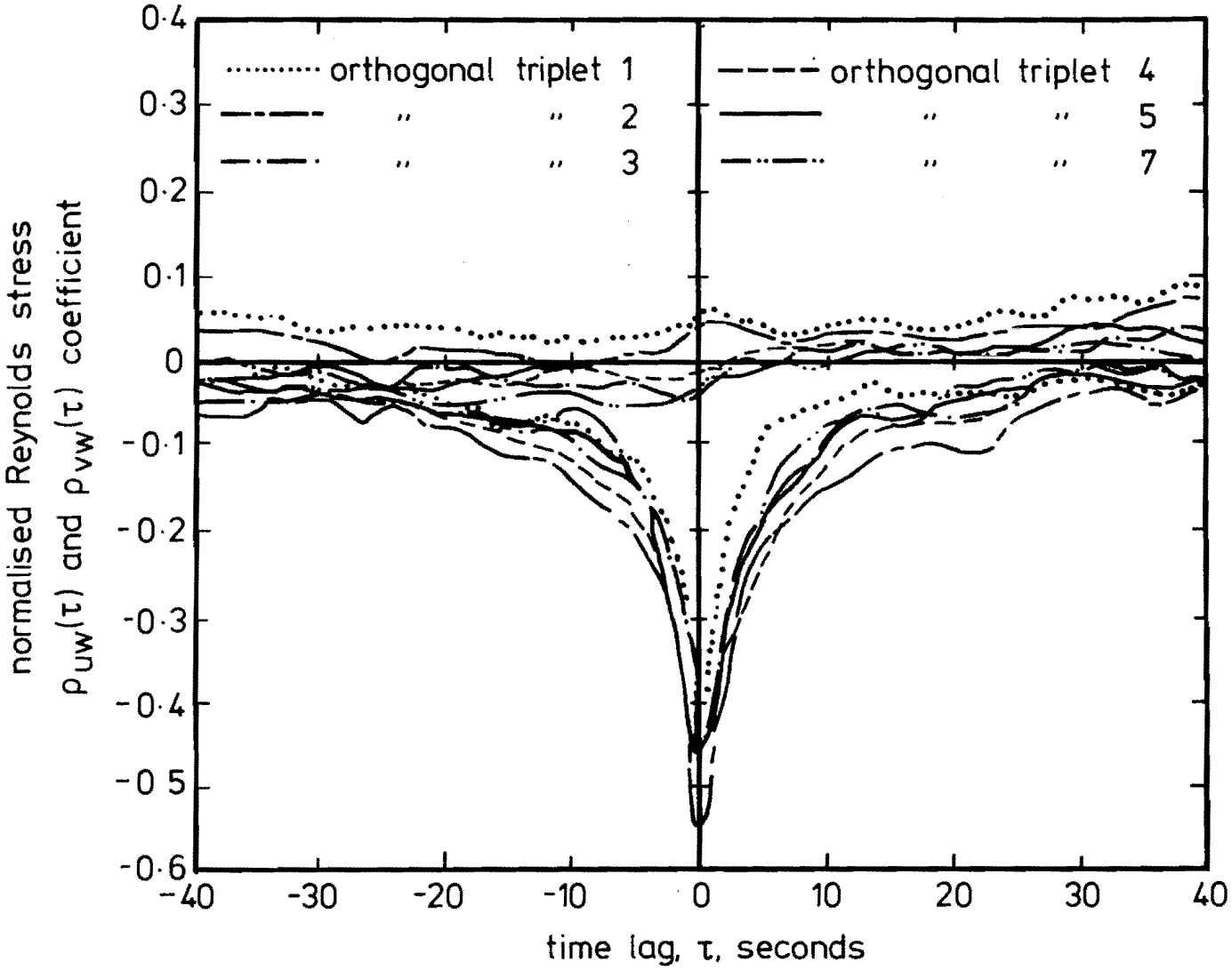

FIG. 9·3 NORMALISED REYNOLDS STRESS $\rho_{uw}(\tau)$ AND $\rho_{uv}(\tau)$ VARIATION WITH TIME LAG FOR RUN 1 DATA.

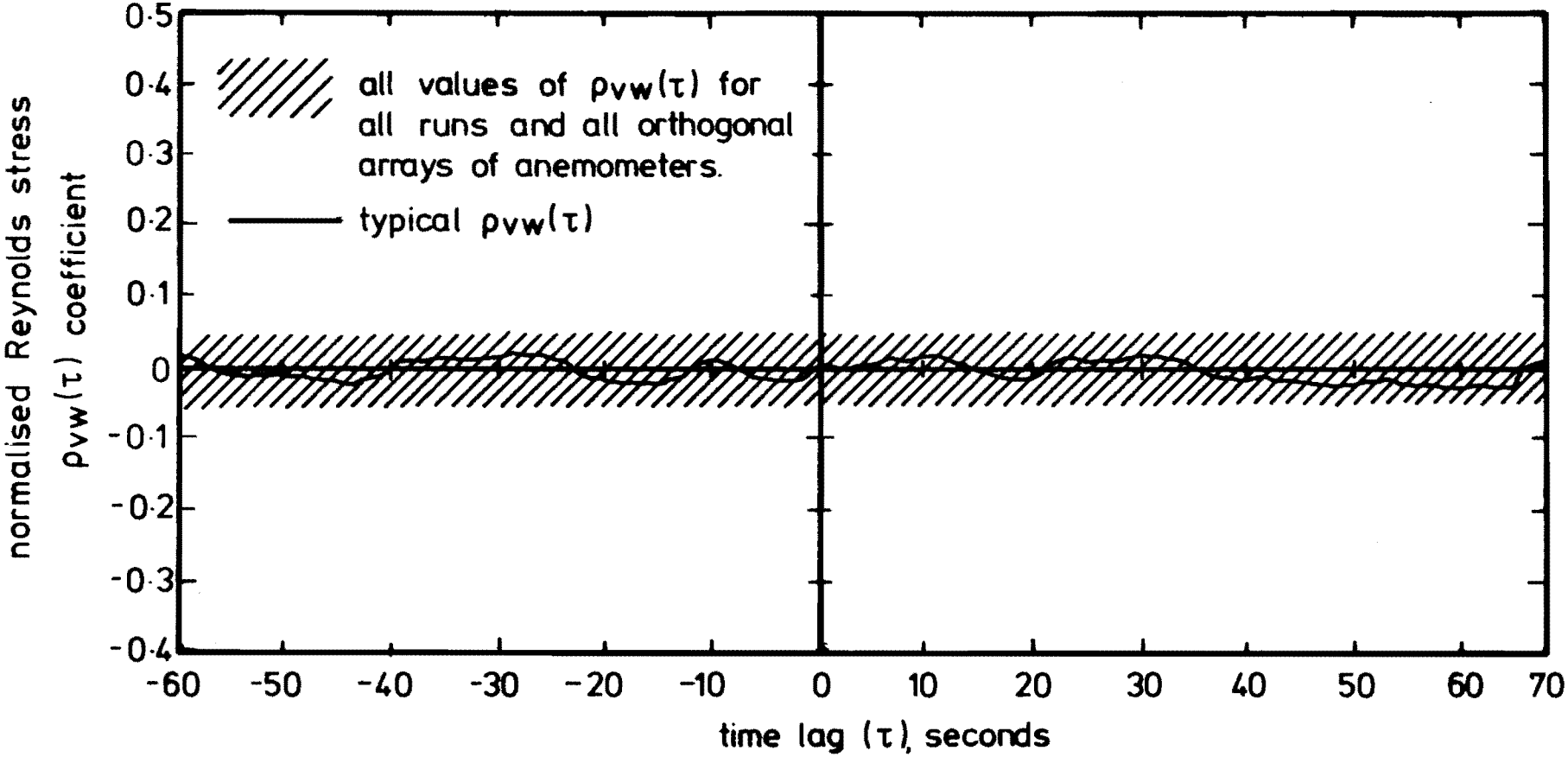

FIG 9·4 NORMALISED REYNOLDS STRESS $\rho_{vw}(\tau)$ VARIATION WITH TIME LAG FOR ALL DATA.

the roughness length up to at least Z_o = 1 m, and is not very sensitive to variations in the gradient velocity $\bar{V}_G$. For rural areas

$$.002 \leqslant - \overline{uw}/\bar{V}_G^{\,2} \leqslant .0025 \ , \tag{9.24}$$

is recommended and $\bar{V}_G$ is assumed to occur at Z = 600 m. An equation is also provided, relating the $\overline{uw}$ covariance, normalised by the gradient velocity squared, to the roughness length. The equation is :

$$\overline{uw}/\bar{V}_G^{\,2} = - (2.25 \times 10^{-3} + 6 \times 10^{-4} \times \log_{10} Z_o) \tag{9.25}$$

This Equation gives values of $\overline{uw}/\bar{V}_G^{\,2}$ rather larger in magnitude than Davenport (1964) and Pasquill (1971) but Counihan states that the values from Davenport and Pasquill are biased towards the lower range of all the available data.

Under neutrally stable stratification and assuming the ratios of the component standard deviations with the friction velocity are those of Teunissen (1970), $\dfrac{\overline{uw}}{\sigma_u \sigma_w}$ can be evaluated. This gives

$$\frac{\overline{uw}}{\sigma_u \sigma_w} = \frac{- U_*^{\,2}}{2.5U_* 1.3U_*} = - .31 \tag{9.26}$$

This is slightly larger in magnitude than the value of $\rho_{uw}(0)$ recommended by ESDU (1974b) for Z_o = .03 m, which is $\rho_{uw}(0)$ - .27 . (9.27)

There is very little data available for $\overline{uv}$ and $\overline{vw}$. ESDU (1974b) states that both are small and can be ignored. Elderkin (1966) found that

$$\overline{uw} \ > > \ \overline{uv} \ > > \ \overline{vw} \tag{9.28}$$

It is probably reasonable to assume that both $\overline{uv}$ and $\overline{vw}$ are significantly smaller than $\overline{uw}$.

9.2 THE REYNOLDS STRESSES MEASURED

The Reynolds stresses shown in Figs.9.5 and 9.6 have been calculated by a simple zero time delay product summation of the [illegible]uent velocity

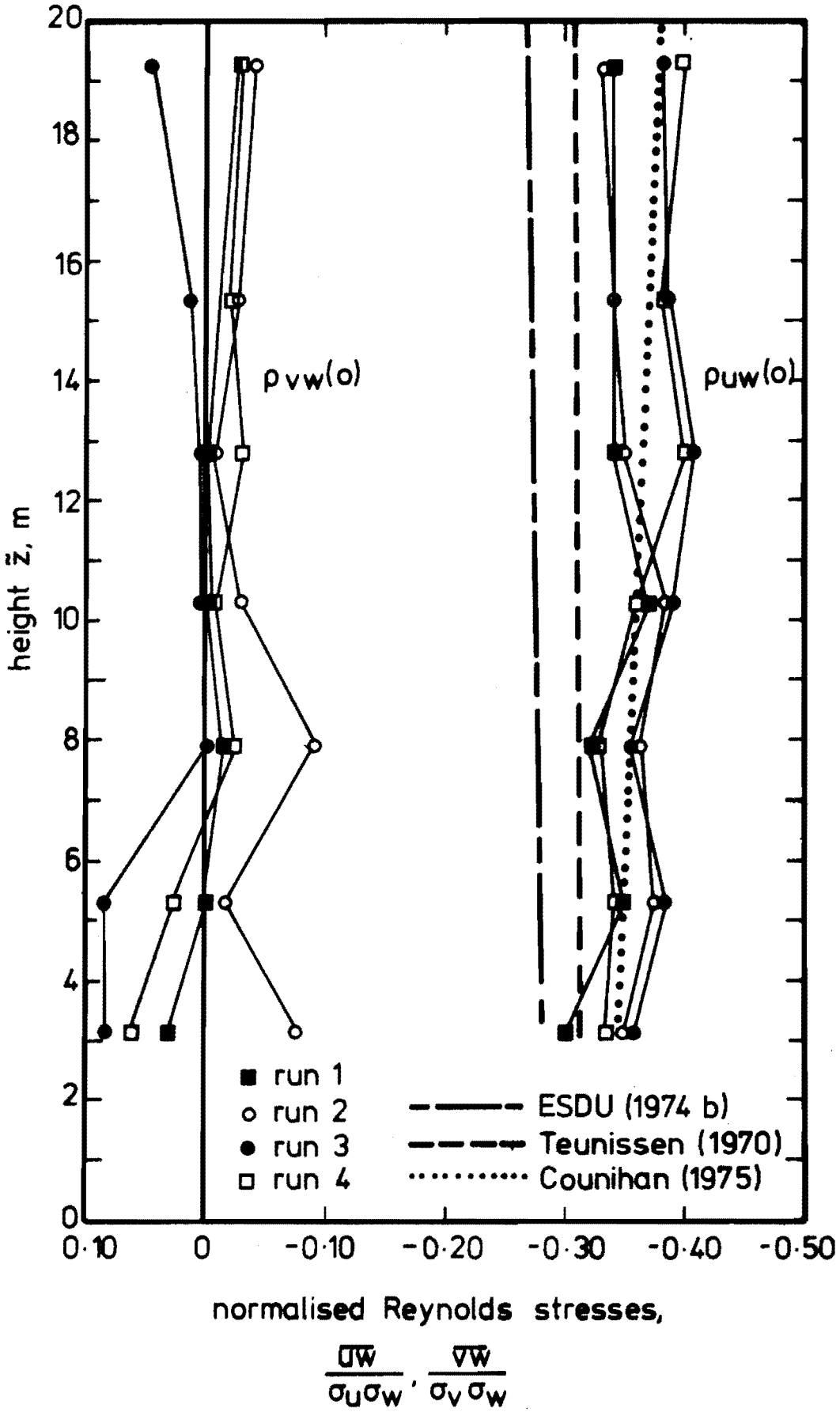

FIG 9·5 NORMALISED REYNOLDS STRESSES $\rho_{uw}(o)$, $\rho_{vw}(o)$ VARIATION WITH HEIGHT.

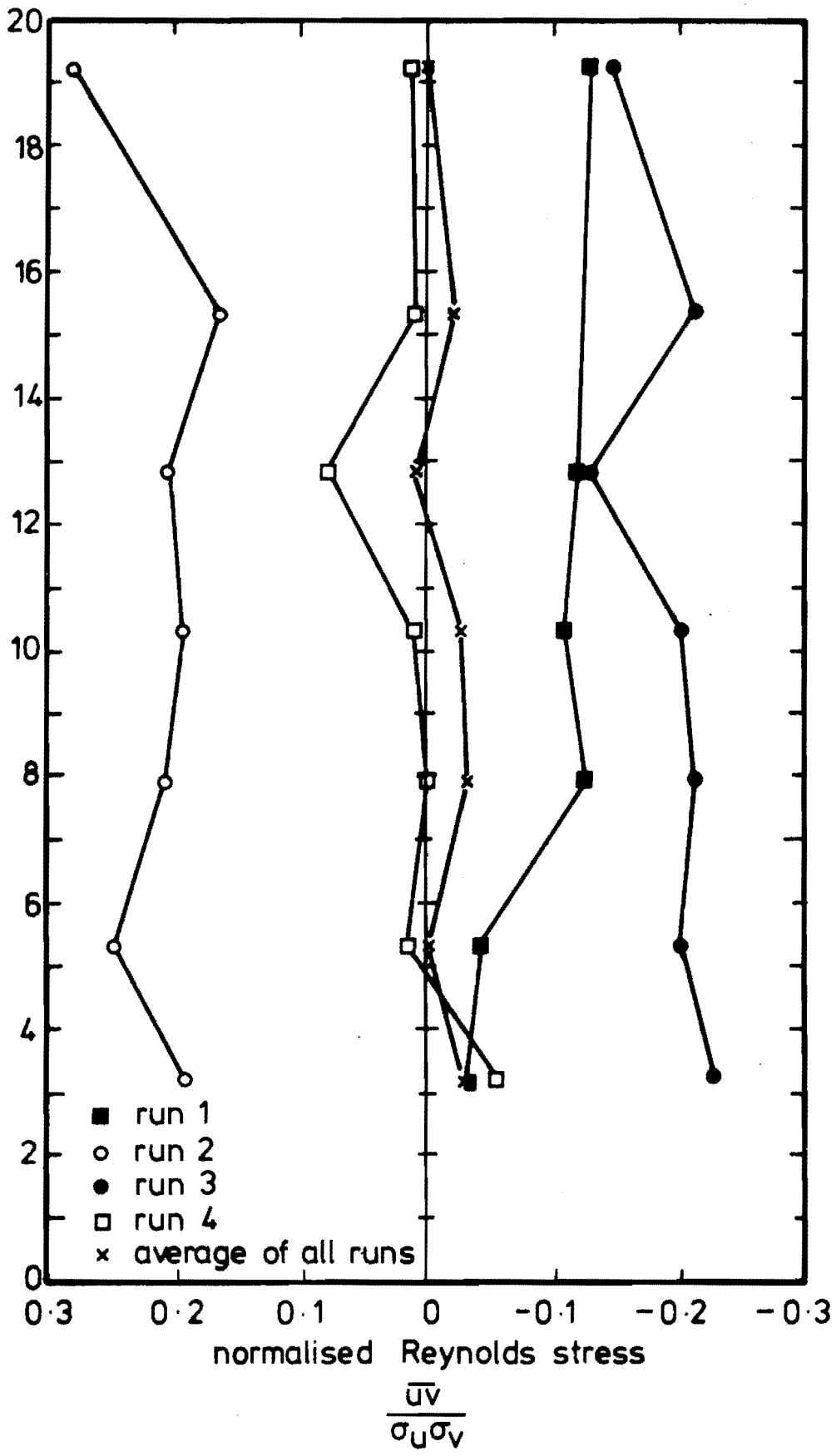

FIG. 9·6 NORMALISED REYNOLDS STRESS $\rho_{uv}(o)$ VARIATION WITH HEIGHT.

components. The values have been normalised by their respective standard deviations. $\rho_{uw}(0)$ has been corrected for anemometer misalignment. No trends were removed from the data before the Reynolds stresses were calculated.

$\rho_{uw}(0)$ is shown in Fig.9.5 to be almost invariant with height, although the average value at each level does show a slight move towards more negative values with increase of height. The average for all levels and Runs appears to be about -.36. This stress, which determines the wind profile and the shear stress on the ground has been compared with the values in the literature discussed in Section 9.1.4.

The measured values are clearly more negative than both the value of -.27 suggested by ESDU (1974b) for Z_o = .03 m and the height range considered, and the value of -.31 suggested by Teunissen (1970). The values recommended by Counihan (1975) are contained in a formula, Equation (9.25) and are in a different format from the results presented here.

Substituting Z_o = .03 m into Equation 9.25 gives

$$\frac{\overline{uw}}{\bar{V}_G^2} = -1.84 \times 10^{-3} \tag{9.29}$$

$\bar{V}_G$ is assumed to occur at Z = 600 m. Thus a power law can be used to extrapolate downwards from the gradient height. Using α = .131 as obtained in Section 7.2 gives

$$\frac{\bar{V}_Z}{\bar{V}_{600}} = \left(\frac{Z}{600}\right)^{.131} \tag{9.30}$$

Further assuming that $$\frac{\sigma_u}{\bar{V}_Z} = \frac{1}{\ell n\left(\frac{Z}{Z_o}\right)}, \tag{9.31}$$

and $$\sigma_w = .5\sigma_u \tag{9.32}$$

means that Equation (9.29) can be put in a form similar to the measured results presented. Squaring Equation (9.30) and substituting for $\bar{V}_Z$ from

Equations (9.31) and (9.32) into Equation (9.30) gives

$$\frac{2\sigma_u\sigma_w\left(\ell n\left(\frac{Z}{Z_o}\right)\right)^2}{\bar{V}_{600}^{\,2}} = \left(\frac{Z}{600}\right)^{.262} \tag{9.33}$$

Substituting for $\bar{V}_{600}^{\,2}$ from Equation (9.33) into Equation (9.29) gives

$$\frac{\overline{uw}}{\sigma_u\sigma_w} = \frac{-.00184.2.\left(\ell n\left(\frac{Z}{Z_o}\right)\right)^2}{\left(\frac{Z}{600}\right)^{.262}} \tag{9.34}$$

Equation (9.34) thus allows the evaluation of $\rho_{uw}(0)$ from the required values of Z and Z_o. For Z_o = .03 m and Z = 20 m, Equation (9.34) yields $\rho_{uw}(0)$ = -.38 and for Z = 10 m yields $\rho_{uw}(0)$ = -.36.

A straight line drawn through these two values is shown in Fig.9.5. It can be seen that it agrees extremely well with the spread of measured data at all levels.

In the same Figure, $\rho_{vw}(0)$ is plotted for all four Runs and for all levels. All values are near zero and the average for all Runs is very near zero.

The values of $\rho_{uv}(0)$ have been given separately in Fig.9.6. This Reynolds stress shows much more scatter between Runs than the other two, although the variation between levels for each Run is about the same as the two other Reynolds stresses. However, the average value at each level has been plotted and can be seen to be very near zero. The large amount of variation in $\rho_{vw}(0)$ between Runs compared with both the variation in $\rho_{uw}(0)$ and $\rho_{vw}(0)$ tends to make its reliability suspect. It has already been stated in Section 6.1.3 that the correction for non-cosine response appears to introduce a correlation between the two horizontal component velocities because all values were changed considerably by the correction. Note also that in Fig.6.5 which shows the data from Run 3, that the "peak" of the correlation at τ = 0 when the data

is uncorrected is lost when the data is corrected. Similar data shown in Fig.9.3 also show that for Run 1, which has been corrected for non-cosine response, there is no significant peak in $\rho_{uv}(0)$.

Very little can be concluded from the results analysed here with regard to $\rho_{uv}(0)$ and $\rho_{uv}(\tau)$.

The results presented in Figs.9.3 and 9.4 have been obtained from data streams with parabolic trend lines removed from them. The results have been calculated by Equation (9.6), but using the fast Fourier transform method.

Since the values in Figs. 9.3 and 9.4, and in Figs.9.5 and 9.6 have been obtained by slightly different methods, the zero time delay values in Figs.9.3 and 9.4 do not correspond exactly with values in Figs.9.5 and 9.6. However, some interesting features are highlighted.

In Fig.9.3 the maximum value of $|\rho_{uw}(\tau)|$ occurs when $\tau = 0$, and drops rapidly towards zero for $|\tau| > 0$. This suggests that the fluctuations in the u and w components, contributing to the $\overline{uw}$ Reynolds stress, occur simultaneously. In the same Figure, $\rho_{uv}(\tau)$ is shown to be not very dependent on τ and the same feature can be observed in Fig.9.4 for $\rho_{vw}(\tau)$. It is also interesting to note that $\rho_{uv}(0)$ in Fig.9.3 is somewhat less than $\rho_{uv}(0)$ in Fig.9.5. This difference suggests that the parabolic trend removal from the data presented in Fig.9.3 has tended to reduce the corrrelation of $\rho_{uv}(0)$ compared with the data with no trend removal shown in Fig.9.6.

The value of $\rho_{uw}(0)$ in Fig.9.3 is also significantly higher than $\rho_{uw}(0)$ shown in Fig.9.5 which shows the importance for correcting for anemometer misalignment.

Since the surface layer could be assumed to be neutrally stable when the data was recorded, the point Reynolds stress values were used to obtain the friction velocity. Thus for each Run, the average Reynolds

stress over the height range was evaluated. From this average value the friction velocity was obtained using Equation (9.22).

The value of the friction velocity obtained for each Run was used in Chapter 7 to determine the velocity profile using the slope obtained from U_*. A log law profile was assumed and then this was fitted to the velocity-height data. The value of Z_o obtained at the same time was a further check on the reliability of both the velocity measurements and the Reynolds stress measurements.

The value of U_* from each Run was also compared with the standard deviations of the velocity fluctuations in Chapter 8. The good agreement with accepted ratios further suggested that U_* and consequently $\frac{\overline{uw}}{\sigma_u \sigma_w}$ values obtained were reliable.

9.3 CONCLUSIONS

The values obtained for $\rho_{uw}(0)$ have been shown to compare well with the sparcely reported values in the literature. Cross checking U_*, evaluated from point Reynolds stress measurements by the eddy correlation method, with the velocity profiles measured and the component standard deviations further indicated the reliability of the estimates of $\rho_{uw}(0)$.

The co-spectrum of the $\overline{uw}$ Reynolds stress has been observed to decrease by a $-^7/3$ power law in the inertial subrange with an increase in frequency. This compares with a $-^5/3$ power law for the three velocity component power spectral densities (Kaimal et al, 1972). Thus there is very little contribution to $\overline{uw}$ from the higher frequencies. It is assumed that the small eddies are approximately isotropic and thus do not contribute to $\overline{uw}$. This is fortunate because it means that at the higher frequencies where the anemometers become less responsive, there is very little contribution. The larger anisotropic eddies which contribute to $\overline{uw}$ can be measured by the anemometers.

The results indicate that orthogonal arrays of propeller anemometers

can be used to make reliable single point $\rho_{uw}(0)$ Reynolds stress measurements. However, for reliable results, precautions have to be taken when recording and analysing the data. These are :

(1) The vertical component anemometer must be aligned as close to vertical as possible.

(2) The orthogonal array should not be placed closer than 5 m from the ground under neutrally stable conditions.

(3) The anemometers should be mounted, upwind of the tower, well away from any protuberances

(4) The vertical component anemometer must have very low friction bearings.

(5) The value of $\rho_{uw}(0)$ obtained has to be corrected for anemometer misalignment.

The values of $\rho_{vw}(\tau)$ were always near zero for all Runs, orthogonal arrays, and the range of τ considered. This is in agreement with previous observations.

The results of $\rho_{uv}(\tau)$ obtained appear inconclusive. There was a lot of scatter in the results between different Runs, although it was always smaller than $\rho_{uw}(\tau)$. The average of all Runs was near zero. Trends in the u and v data streams also appear to affect the correlations obtained. The data displayed in Fig.9.6 with no trend removal for Run 1 has a higher correlation than the zero time delay correlation in Fig.9.3.

The data generally appears to confirm the observations of ESDU (1974b) that

$$|\overline{uw}| > |\overline{uv}| >> |\overline{vw}| .$$

CHAPTER 10

POWER SPECTRAL DENSITIES

10.1 INTRODUCTION

10.1.1 Definitions

Each fluctuating wind velocity component can be regarded as being compounded of oscillations of cosine and sine form of varying amplitude and frequency, and in the general case can be represented by the sum of a Fourier cosine and sine series. A one dimensional power spectral density function can be defined so that the total energy, or variance, associated with each gust component over the frequency range $0 \leqslant n \leqslant \infty$ can be represented by

$$\sigma_i^2 = \int_0^\infty S_{ii}(n)\, dn \quad , \quad i = u,v,w \ . \tag{10.1}$$

$S_{ii}(n)$ is the power spectral density at frequency n, Hz, and this is the definition used for this work.

The quantity $S_{ii}(n).\delta n$ is a measure of the energy associated with that component over the narrow frequency band n and $n + \delta n$. In practice, one way of obtaining a power spectral density $S_{ii}(n)$ at frequency n is as follows. A signal i(t) is put through a narrow band pass filter so that only those parts of the signal i(t) corresponding to a frequency bandwidth of δn centred about frequency n remain; the average mean square of the filtered signal $i(t;n,\delta n)$ is then given by :

$$\frac{1}{T} \int_0^T i^2(t;n,\delta n)dt \ , \tag{10.2}$$

and the power spectral density at frequency n is defined as :

$$S_{ii}(n) = \lim_{\substack{T \to \infty \\ \delta n \to 0}} \frac{1}{T.\delta n} \int_0^T i^2(t;n,\delta n)dt \ . \tag{10.3}$$

The details of performing this continuous Fourier transform on a digital computer are given in Section 5.6.

10.1.2 Analysis Procedure

Since the technique used to calculate power spectral densities is discussed fully in Chapter 5, only a brief resume of the main points will be given here.

All the spectra presented here have been calculated in the following manner.

(1) The data was read off the field data tape, checked, reformatted and written to a Computer Centre library tape.

(2) The data was corrected for non-cosine response using correction factors obtained from wind tunnel tests in the Departmental Aeronautical Wind tunnel.

(3) If the sampling frequency of the data on the library tape was greater than 1.875 Hz, the sampling frequency was reduced to this value by adding the required number of consecutive samples together.

(4) The horizontal component data was resolved into components parallel and perpendicular to the average wind direction for the averaging period chosen.

(5) A parabolic trend line was removed from the data streams as discussed in Section 6.4.

(6) A box-car data window was used to truncate the velocity data.

(7) The number of velocity samples Fourier transformed was 4096 when the data file was 37 minutes long or 8192 when the data file was 73 minutes long.

(8) A forward discrete Fourier transform was taken of the velocity data using a fast Fourier transform library procedure to obtain the spectral components. The data was manipulated so that a N point complex input/output FFT library procedure

was used to Fourier transform 2N points.

(9) The spectral estimates were averaged over frequency by the following regime. The first four estimates were not averaged. All higher frequency estimates were averaged in bands between f_u and f_L, where $f_u/f_L = 10^{.125} = 2^{.4152} = 1.333$. f_u is the upper cut-off frequency and f_L is the lower cut-off frequency.

(10) The spectra were plotted as :

$$\log \frac{nS_{ii}(n)}{\sigma_i^2} \text{ versus } \log n \text{ , } i = u,v,w.$$

and n is frequency in Hz.

10.1.3 Statistical Errors in Power Spectral Density Estimation

The statistical errors in power spectral density estimation are discussed because they are significantly larger than the statistical errors involved in any of the other turbulence parameter estimation.

Following Bendat and Piersol (1971), it can be shown that the real and imaginary parts of the complex number, obtained from a Fourier transform of real data, are uncorrelated random variables with zero means and equal variances. The power spectral density which is formed at each frequency by squaring and adding the real and imaginary components of the complex number can be shown to have a sampling distribution given by

$$\frac{\hat{S}_{ii}(n)}{S_{ii}(n)} = \frac{\chi_2^2}{2} \qquad (10.4)$$

$\hat{S}_{ii}(n)$ is the estimate of the true value $S_{ii}(n)$ and χ_2^2 is the chi-square variable with d = 2 degrees of freedom. The random error of this estimate is substantial. The normalised standard error, which defines the random portion of the estimation error is , $\varepsilon_r = \frac{\text{standard deviation}}{\text{mean}}$, of the chi-square variable,

$$= \frac{\sqrt{2d}}{d} = \sqrt{\frac{2}{d}}, \tag{10.5}$$

where d is the number of degrees of freedom.

When d = 2, as in the case of no averaging over different spectral estimates, $\varepsilon_r = 1$, which means that the standard deviation of the estimate is as large as the quantity being measured. This is unacceptable, consequently the random error is required to be reduced. This is done by smoothing the estimate further.

There are two methods of smoothing the estimates. The first way is to smooth over an ensemble of estimates. This can be done by computing individual spectra from q independent sample records. The smoothed estimate is then obtained by averaging over the q estimates of each spectral component from the different records. This method is often used in wind tunnel work where the boundary layer conditions are usually stationary for relatively long periods of time compared with the period of the lowest frequency component of interest. The second method of smoothing is to average over frequency. This can be done by averaging together the results for ℓ contiguous spectral components from a single sample record. If ℓ spectral estimates are averaged over frequency, the number of degrees of freedom in the estimate is increased to $d = 2\ell$ and the normalised random error becomes

$$\varepsilon_r = \sqrt{\frac{2}{d}} = \frac{1}{\sqrt{\ell}} \tag{10.6}$$

The sampling distribution of the smoothed estimate is approximately chi-square with $d = 2B_eT$ degrees of freedom. B_e is the resolution bandwidth of the smoothed estimate and is equal to $\frac{\ell}{T}$ for frequency smoothing. A $(1-\alpha)$ confidence interval for a power spectral density function $S_{ii}(n)$, $i = u,v,w$, based on an estimate $\hat{S}_{ii}(n)$ is given by

$$\frac{d.\hat{S}_{ii}(n)}{\chi^2_{d;\alpha/2}} \leqslant S_{ii}(n) < \frac{d.\hat{S}_{ii}(n)}{\chi^2_{d;1-\alpha/2}} \tag{10.7}$$

$$i = u,v,w.$$

since the distribution of $S_{ii}(n)$ is chi-square. Also, $d = 2B_eT = 2\ell$ and $B_e = \frac{\ell}{T}$.

This means that Equation (10.7) can be used to estimate the range of $S_{ii}(n)$ for a desired confidence interval, i.e. probability that the estimate will be within the range, and from the number of degrees of freedom, which is obtained from the number of spectral estimates averaged over.

As has been stated in Section 10.1.2, all except the first four spectral estimates of the spectral data presented here have been averaged over frequency. The number of estimates ℓ in each band increases as n the frequency increases. Thus the normalised random error ε_r decreases as n increases. This is obvious from the spectra displayed in Figs.10.1 to 10.12 as it can be seen that the magnitude of the fluctuations in the power spectral density estimates decreases as n increases. The low frequency spectral estimates show a large amount of variation which is consistent with their standard error being equal to 1.

10.2 THE LONGITUDINAL COMPONENT POWER SPECTRAL DENSITIES

The longitudinal component power spectral densities obtained from Runs 1,2,3 and 4 have been plotted in Figs. 10.1,10.2,10.3 and 10.4 respectively. Each plot consists of measured data from all levels and three empirical curves obtained from previous research. Since the measured spectral densities were very similar at all levels, they have been defined simply by two edge lines indicating the spread of the measured data.

The common longitudinal component spectral equations which the measured data were compared with are given below.

$$\frac{nS_{uu}(n)}{\sigma_u^2} = \frac{\frac{2}{3}\frac{n\ell}{\bar{V}_{10}}}{\left(2+\left(\frac{n\ell}{\bar{V}_{10}}\right)^2\right)^{5/6}} \quad \text{, where} \quad = 1800 \text{ m,} \tag{10.8}$$

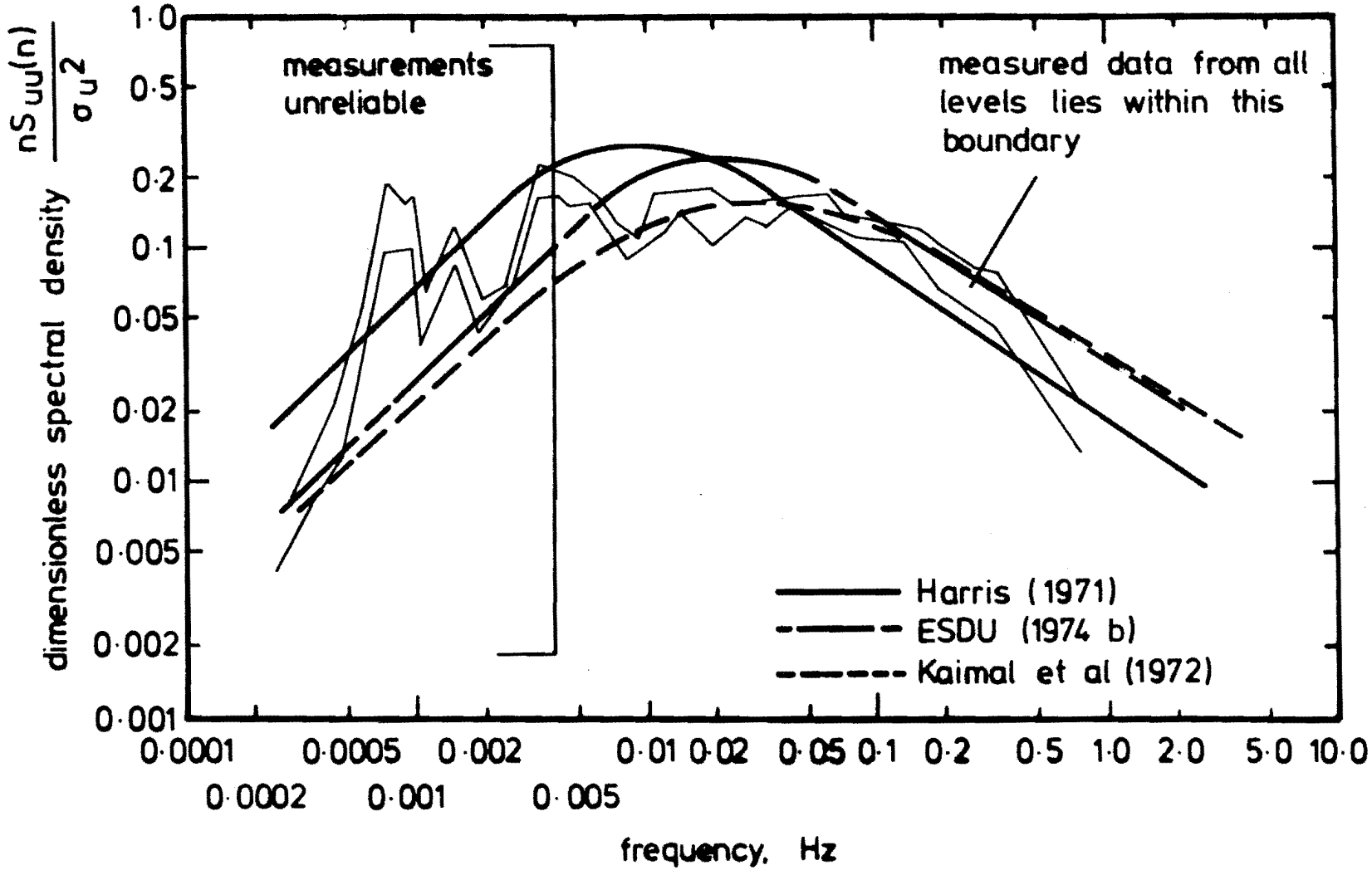

FIG. 10·1 LONGITUDINAL COMPONENT u POWER SPECTRAL DENSITY FOR RUN 1.

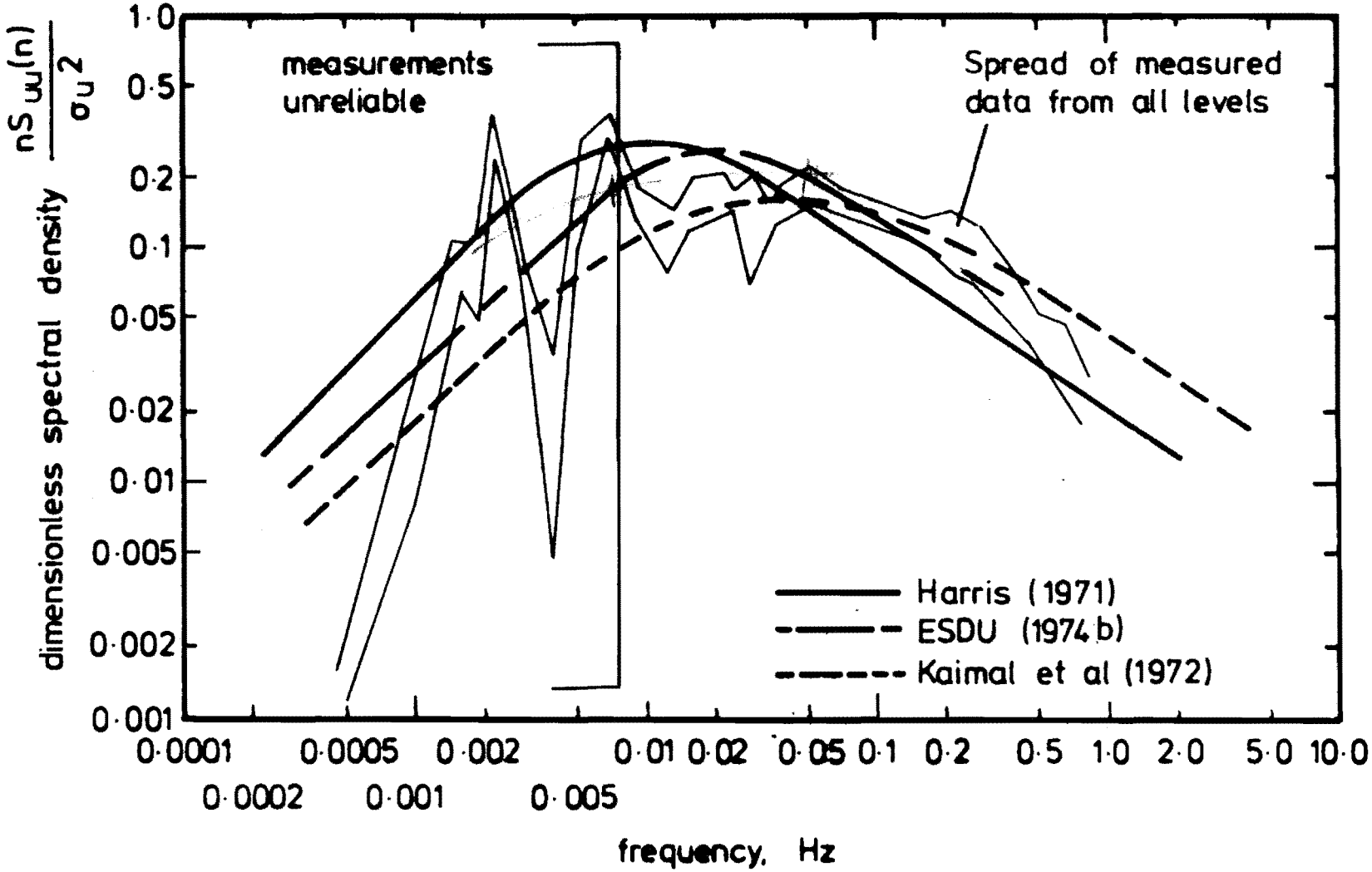

FIG. 10·2 LONGITUDINAL COMPONENT u POWER SPECTRAL DENSITY FOR RUN 2.

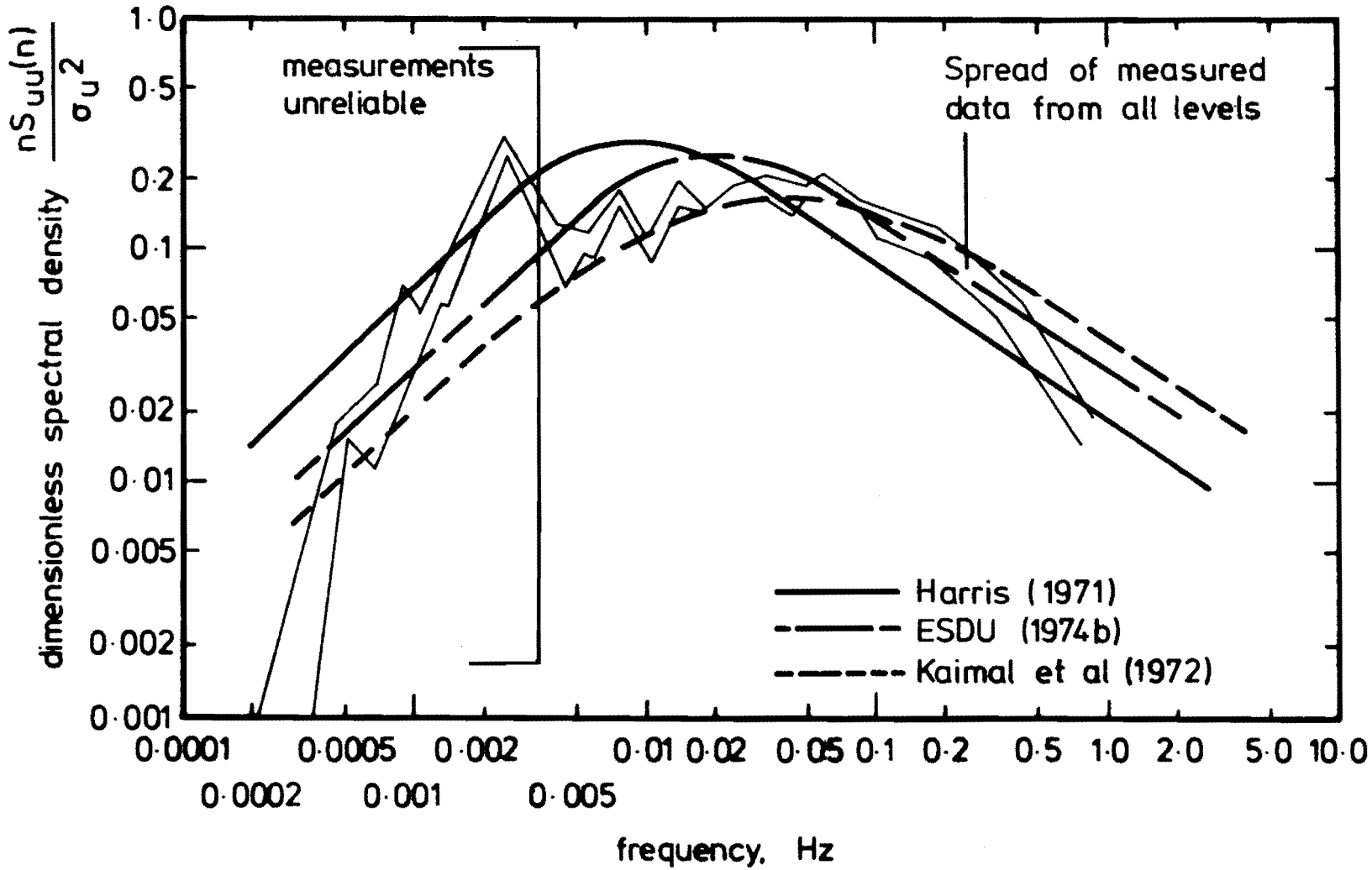

FIG. 10·3 LONGITUDINAL COMPONENT u POWER SPECTRAL DENSITY FOR RUN 3.

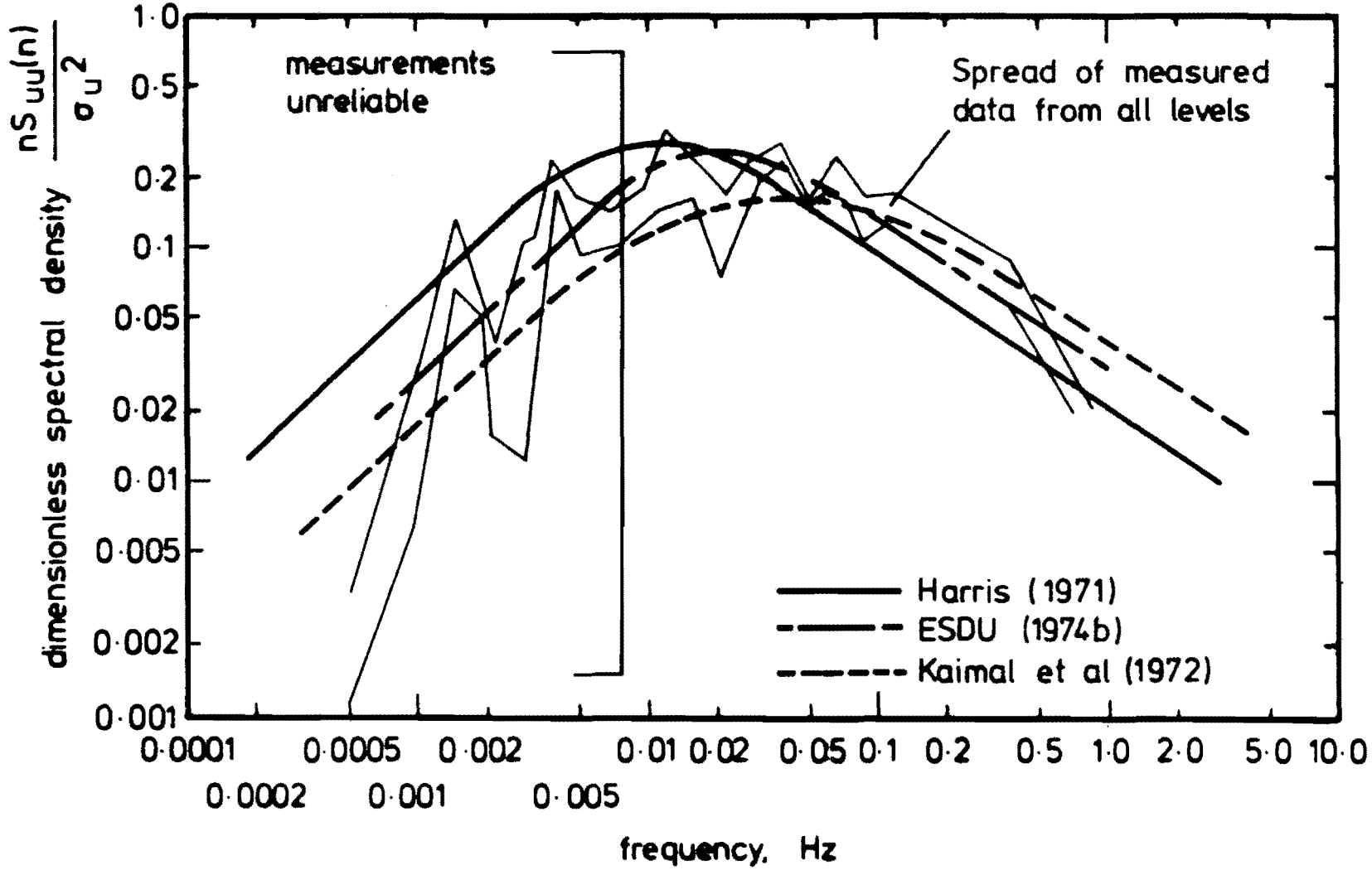

FIG. 10·4 LONGITUDINAL COMPONENT u POWER SPECTRAL DENSITY FOR RUN 4.

has been obtained from Harris (1971) .

$$\frac{nS_{uu}(n)}{\sigma_u^2} = \frac{4\,\tilde{n}_u}{(1 + 70.8\,\tilde{n}_u^2)^{5/6}} \qquad (10.9)$$

where $\tilde{n}_u = \frac{x_{L_u}\, n}{\bar{V}_Z}$,

is the von Kármán form and has been taken from ESDU (1974b).

$$\frac{nS_{uu}(n)}{U_*^2} = \frac{105\,f}{(1 + 33f)^{\frac{5}{3}}} \text{ , where } f = \frac{nZ}{\bar{V}_Z} \text{ ,} \qquad (10.10)$$

has been obtained from Kaimal et al (1972). In Equation (10.10), the relationship $\sigma_u^2 = 6.25\, U_*^2$ has been assumed, to transform the left hand side of the Equation into a format similar to Equations (10.8) and (10.9).

The three spectral equations given above have been plotted for $\bar{V}_Z$ measured at Z = 10.3 m for each Run in Figs.10.1,10.2,10.3 and 10.4. The similarity between the measured spectra at all levels means that the theoretical spectral equations describe all levels approximately equally.

In Figs.10.1,10.2,10.3 and 10.4 it can be observed that the measured data has a slope of approximately $-\frac{2}{3}$ between the frequencies of .1 and .3 Hz. At frequencies greater than .3 to .5 Hz, the measured spectral densities drop away at a rate higher than the $-\frac{2}{3}$ slope. This is presumably due to the low pass filtering effect of the anemometers.

A vertical line has been drawn through the spectral curves, and it corresponds to a frequency of 16 times the fundamental frequency, i.e. if the length of the data file is T seconds, the vertical line corresponds to a frequency of $\frac{16}{T}$. It can be seen that in all Runs, the random variation in the measured spectral densities increases significantly to the left of each vertical line. Also, the spectral densities to the right of the line are very similar for the four Runs. To the left of the line, the agreement between the measured data from different Runs is extremely poor.

The line corresponding to the spectral equation from Harris (1971), consistently underestimates the high frequency spectral components. The Harris spectral curve also has its peak at a much lower frequency than the measured data, and the peak is much higher than that of the measured data. To the left of the peak this spectral equation fits the measured data no worse than the two other spectral equations.

The spectral equation from ESDU (1974b) has been fitted to the data from each Run at the height of 10.3 m and Z_o = .03 m has been used. This gives ${}^{x}L_u$ = 70 m from ESDU (1974b). It is shown to fit the measured data from Runs 1,2, and 3 quite well in the region .1 to .3 Hz but it overestimates the peak which it gives at a lower frequency than the measured data. For Run 4 however, it fits the data quite well. For all Runs it fits the measured data much better than the Harris (1971) spectral equation.

The spectral equation obtained from Kaimal et al (1972) undoubtedly fits the measured data the best of the three spectral equations. It was derived from extensive full scale measurements below a height of 32 m. This spectral equation was developed to fit the measured data for neutrally stable atmospheric conditions. It is therefore not surprising that it fits the data better than the Harris and ESDU spectral equations, as these latter two were developed for isotropic turbulence. Atmospheric turbulence is very anisotropic near the ground.

It has been noted by Raine (1974) that the spectral peak is often ill-defined, particularly near the ground, where it tends to be flat. This statement applies directly to the measured data displayed in Figs.10.1, 10.2,10.3 and 10.4. Thus the spectral equation from Kaimal et al (1972), with its smoother shape and lower peak is a much better fit to Runs 1,2, and 3 especially, although it is not quite so good for Run 4.

The large amount of variation in the measured spectral densities to the left of the vertical line in the figures indicates that perhaps

the averaged spectrum should have been obtained from averaging over more spectral estimates at these low frequencies. This would of course increase the bandwidth B_e and also increase the lowest frequency at which an estimate was obtained. In this work they were plotted as shown in the figures to determine how much variation there was between spectral estimates with little or no averaging, and also to allow an estimate to be made for the very lowest frequency possible.

Yuen and Fraser (1976) state that to be usable, a spectral estimate must have at least 16 degrees of freedom, preferably more. This corresponds to averaging over at least eight contiguous frequencies. The measured data discussed here certainly displays that the random error is large for a spectral estimate with less than sixteen degrees of freedom.

10.3 THE LATERAL COMPONENT POWER SPECTRAL DENSITIES

Lateral component spectra have been measured less frequently than longitudinal and vertical component spectra in full scale atmospheric boundary layer measurements. It is essentially the spectrum of the wind direction multiplied by the mean wind speed.

The lateral component spectrum is not very dependent on the height in neutral stability conditions, however, the low frequency part of the spectrum is very dependent on stability, much more so than the vertical or longitudinal component spectra. The high frequency portion of the lateral component spectrum is dependent on the mechanical stirring of the air like the vertical and longitudinal component spectra.

The lateral component spectrum is usually compared with the von Kármán model for isotropic turbulence. Obtained from ESDU (1974b), this is :

$$\frac{nS_{vv}(n)}{\sigma_v^2} = \frac{4\tilde{n}_v(1 + 755.2\,\tilde{n}_v^2)}{(1 + 283.2\,\tilde{n}_v^2)^{\frac{11}{6}}} \qquad (10.11)$$

with $\tilde{n}_v = {}^{x}L_v/\bar{V}_Z$.

To account for the departure from isotropic turbulence near the ground, ESDU recommends that σ_v and ${}^{x}L_v$ be allowed to vary since they typify the intensity and size of eddies constituting turbulence. ESDU therefore provides graphs to obtain σ_v and ${}^{x}L_v$ for various values of Z and Z_o.

The lateral component spectra for Runs 1,2,3 and 4 have been plotted in Figs.10.5,10.6,10.7 and 10.8 respectively. Since the measured spectral curves for all levels for each Run were very similar in shape, again, as for the longitudinal component measured data, two edges lines have been given which determine the width of the spread of measured data. For comparison purposes, three curves from theoretical spectral equations for the lateral component have also been given. These are :

(1) Equation (10.11) fitted to the measured data at Z = 10.3 for each Run.

(2) Equation (10.11) fitted to the measured data so that the spectral equation peak corresponds as nearly as possible to the peak of the measured data spectral curves.

(3) A spectral equation obtained from Kaimal et al (1972), describing the lateral component spectra :

$$\frac{nS_{vv}(n)}{U_*^2} = \frac{17f}{(1 + 9.5f)^{\frac{5}{3}}} , \qquad (10.12)$$

where $f = \frac{nZ}{\bar{V}_Z}$, (10.13)

and it has been assumed that $\sigma_v = 1.875U_*$.

It is immediately apparent in Figs.10.5,10.6 and 10.7 that the curves obtained from the ESDU spectral equation overestimate the measured spectral density at high frequencies, and near the peak, but tend to underestimate

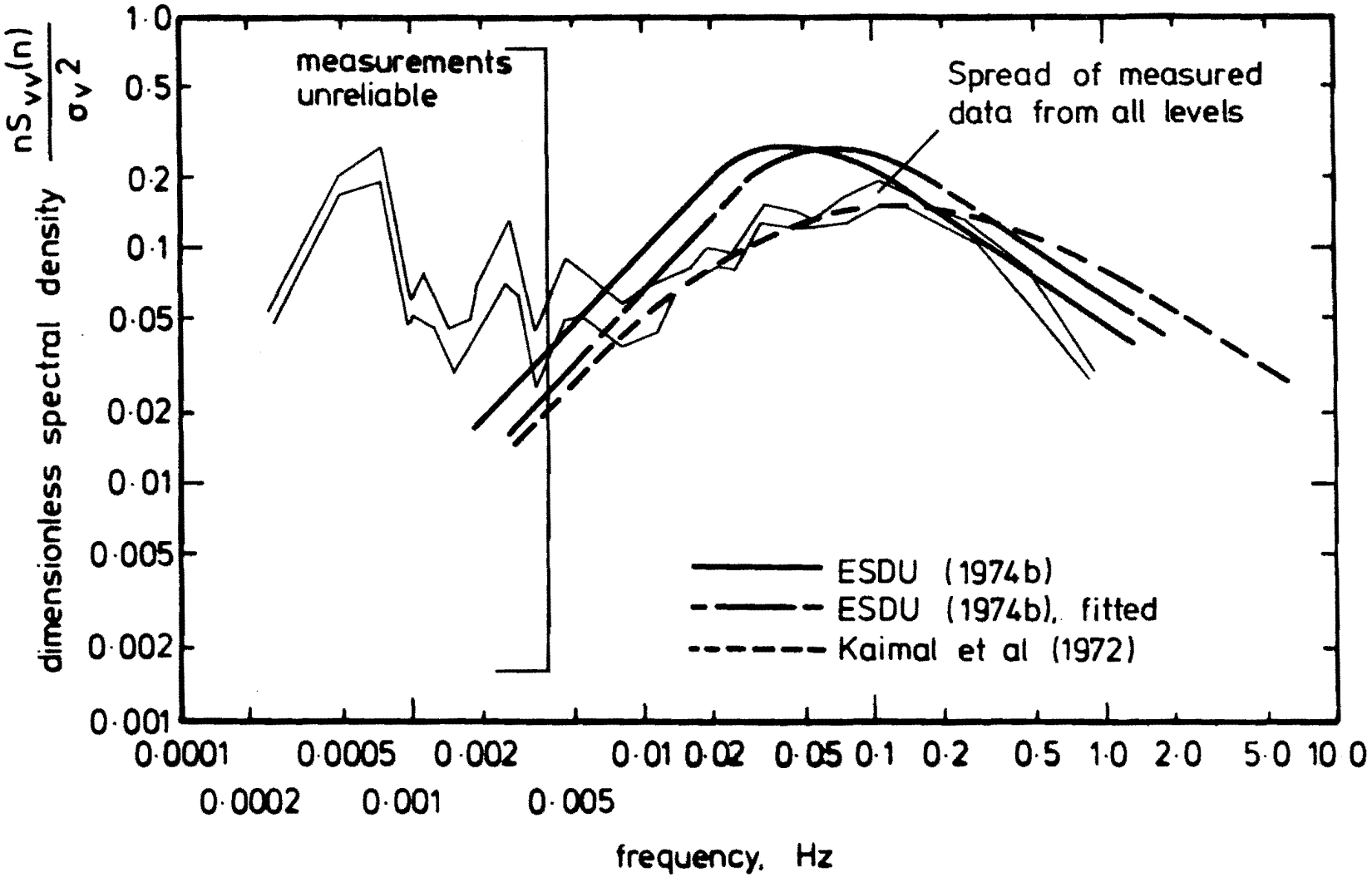

FIG 10·5 LATERAL COMPONENT v POWER SPECTRAL DENSITY FOR RUN 1.

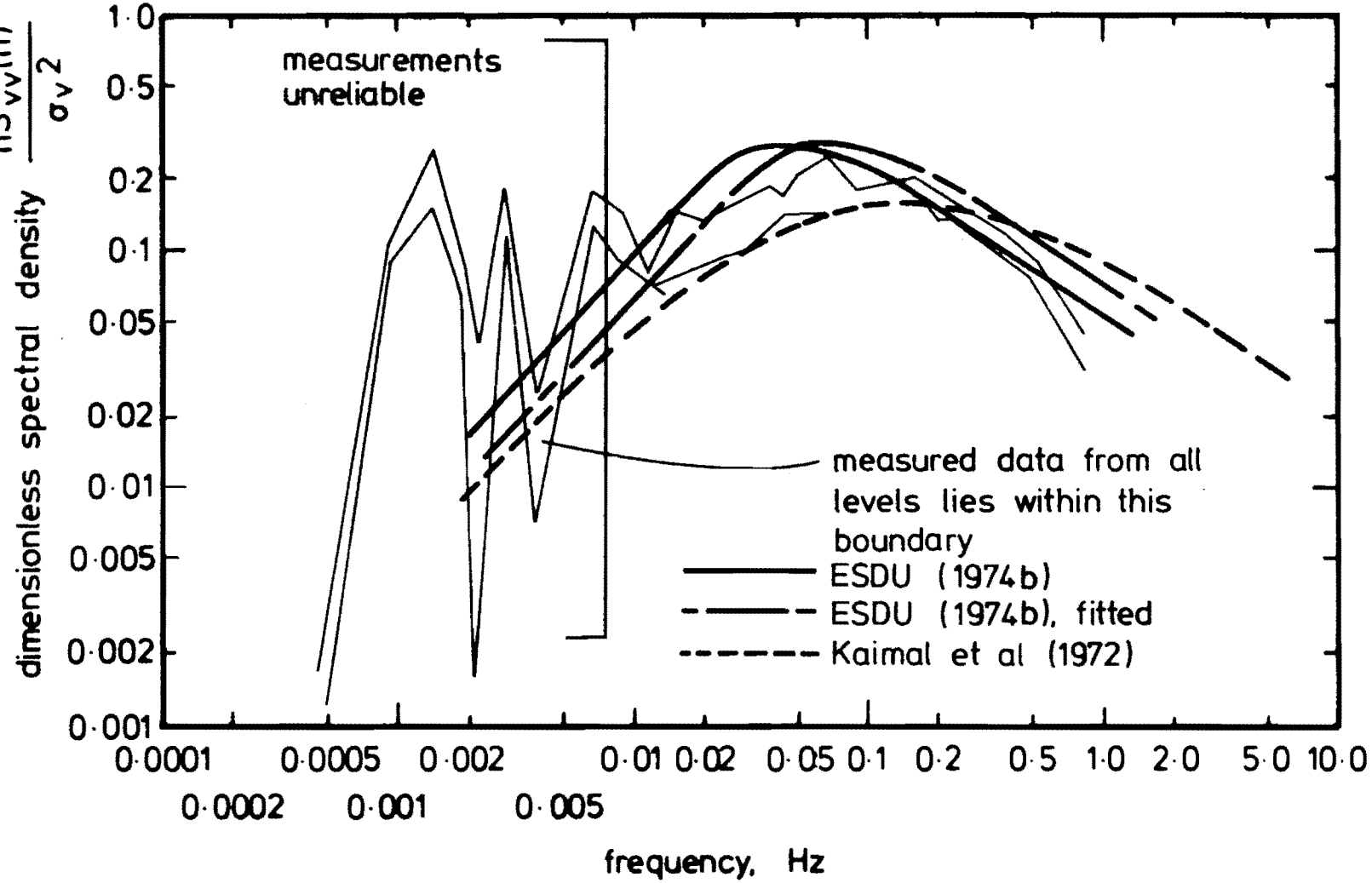

FIG 10·6 LATERAL COMPONENT v POWER SPECTRAL DENSITY FOR RUN 2.

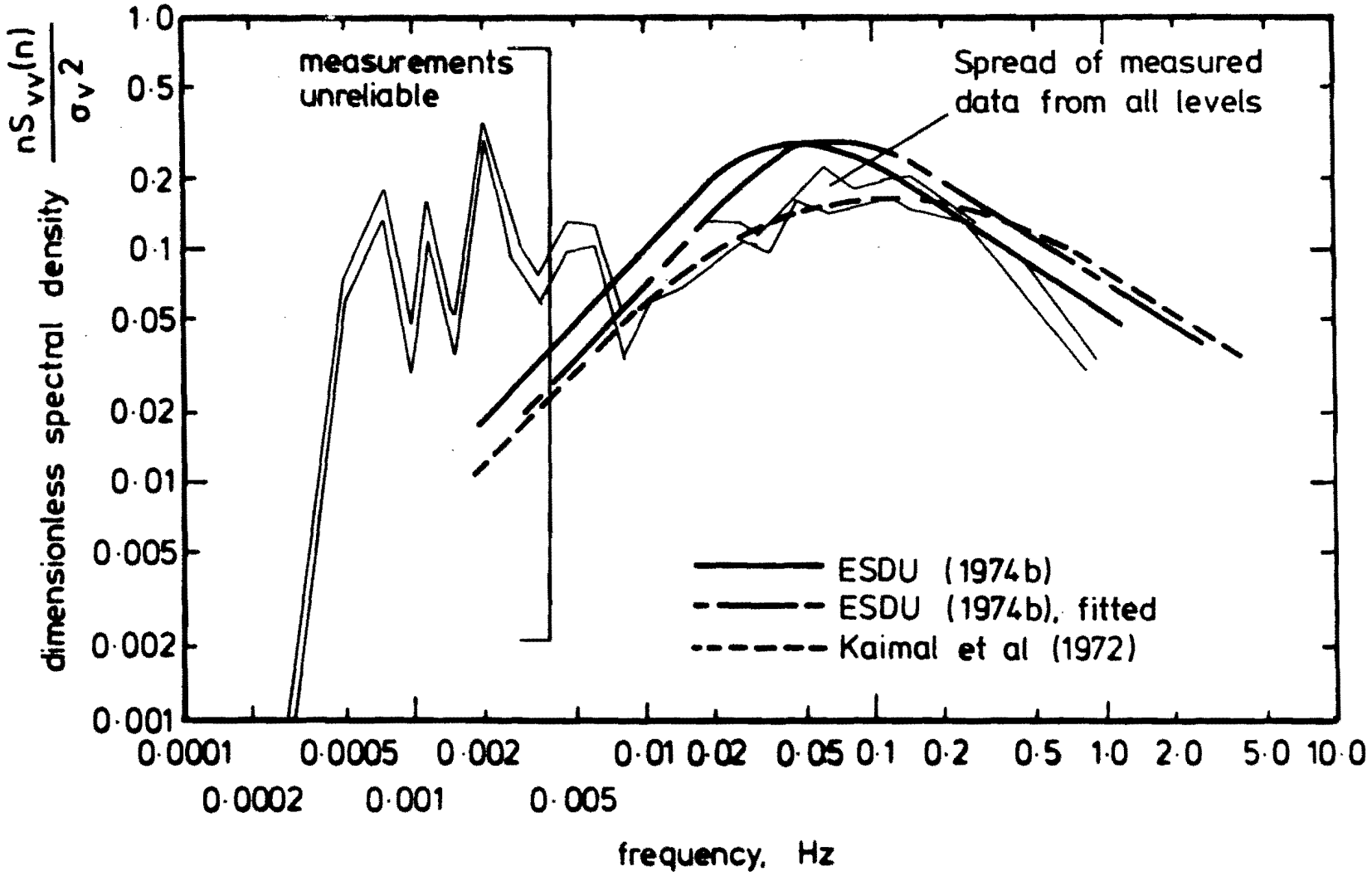

FIG 10·7 LATERAL COMPONENT v POWER SPECTRAL DENSITY FOR RUN 3.

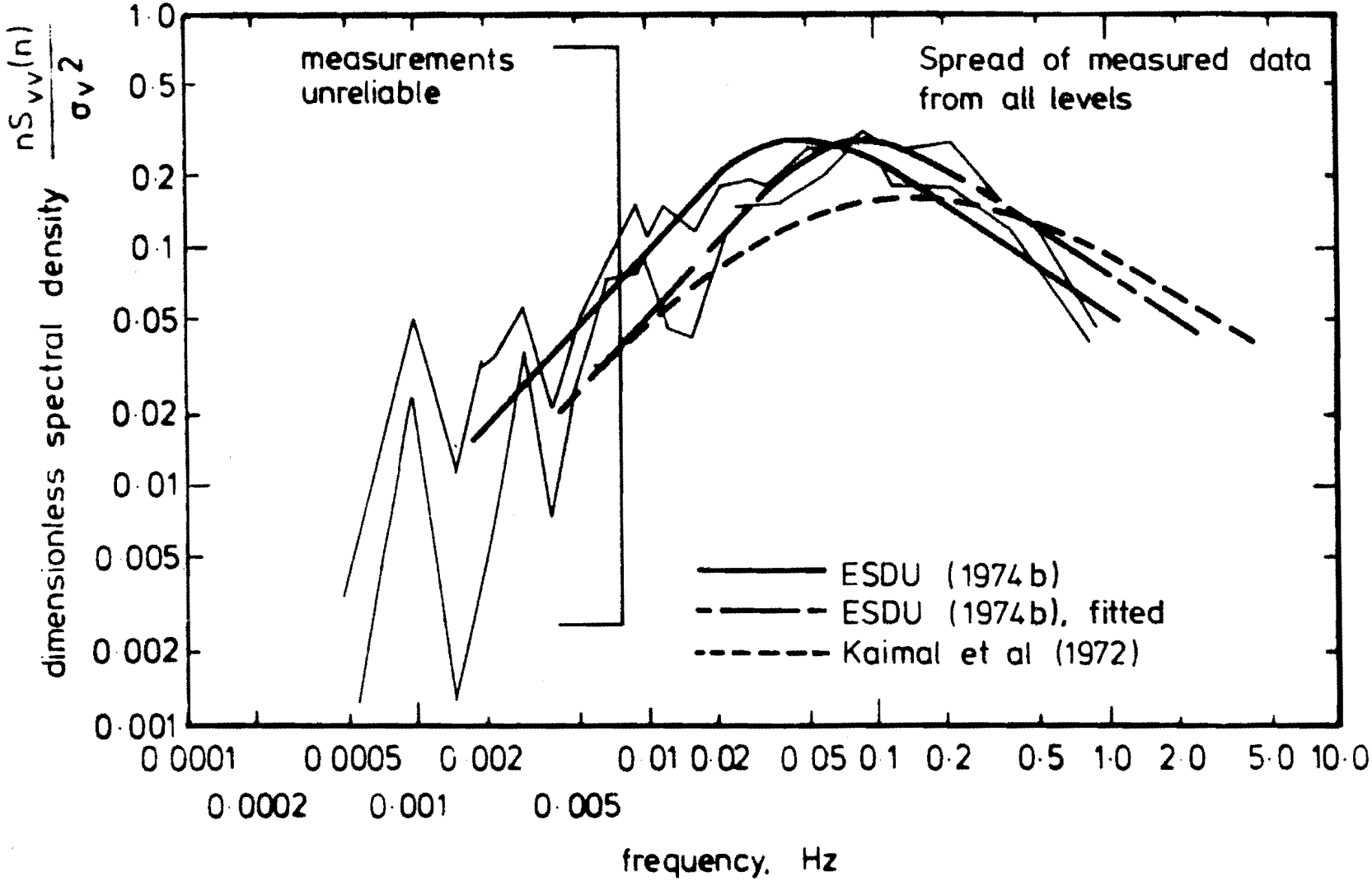

FIG 10·8 LATERAL COMPONENT v POWER SPECTRAL DENSITY FOR RUN 4.

it at low frequencies. The ESDU curve plotted using the velocity-height data at Z = 10.3 m is shifted towards lower frequencies compared with the actual data. When the ESDU curve is positioned with its peak at the same frequency as the estimated "peak" of the measured data, the ESDU spectral curve is shifted towards higher frequencies, compared with the theoretical position on the frequency axis.

The line corresponding to the spectral equation, Equation (10.12), from Kaimal et al (1972) has been positioned on the frequency axis by considering the measured data at the height Z = 10.3 m, where f has been obtained using Equation (10.13).

The curve corresponding to the spectral equation from Kaimal et al has been shown because there are very few empirical curves in the literature describing the lateral component spectral density. This equation has been obtained fairly recently from extensive measurements near the ground where it was derived by fitting a curve to the measured data in neutrally stable conditions.

It can be seen that in Figs.10.5,10.6 and 10.7 that it is a better fit to the measured data than the ESDU spectral equations between .01 and .1 Hz. Above .1 Hz it significantly overestimates the spectral components, and at frequencies less than .01 Hz it underestimates the spectral components. In Run 4 it underestimates all spectral components seriously except those above .3 Hz where it overestimates the components. For this Run, the spectral equation from ESDU fitted to the peak of the measured data describes the measured data quite well.

It should be noted that Runs 1,2, and 3 have large spectral components at very low frequencies whereas Run 4 does not. The measured spectral curves have been normalised by the component variance which makes the area under each curve equal to 1. Thus the large spectral components at low frequencies cause a lowering of the spectral components at high

frequencies when normalised in this manner.

The anemometer response characteristics cause the spectral estimates to be underestimated for frequencies greater than about .3 - .5 Hz. When this is considered it appears that generally the spectral equation from Kaimal et al (1972) describes the data from Runs 1,2, and 3 shown in Figs. 10.5,10.6 and 10.7 better than the ESDU (1974b) spectral equation, even when it is fitted to the peak of the data. However, the ESDU spectral equation fitted to the measured data in Run 4, shown in Fig.10.8, describes the measured data very well.

10.4 THE VERTICAL COMPONENT POWER SPECTRAL DENSITIES

The vertical component power spectrum has been measured relatively frequently, and measurements have often been reported in the literature.

The vertical component power spectral density contains energy at higher frequencies than both the longitudinal and lateral component spectrum, and is dependent on height above ground. The frequency at which the peak in the spectrum occurs decreases with increase in height from the ground. This implies that as the effect of ground proximity decreases, the vertical scale of the eddies can increase. Elderkin (1967) found that the peak value of the spectrum occurred when the reduced frequency, $f = \frac{nZ}{\bar{V}_Z}$ was equal to .40, compared with .03 for the longitudinal component spectrum. The peak in the vertical component spectrum was shown to occur at higher frequencies than that of the longitudinal component spectrum and to be proportional to $\bar{V}_Z$ and inversely proportion to Z.

Counihan (1975) stated that the empirical form of the vertical component spectrum most often used is that proposed by Busch and Panofsky (1968). The form of this equation is :

$$\frac{nS_{ww}(n)}{U_*^2} = \frac{1.075f/f_m}{1 + 1.5(f/f_m)^{\frac{5}{3}}} , \qquad (10.14)$$

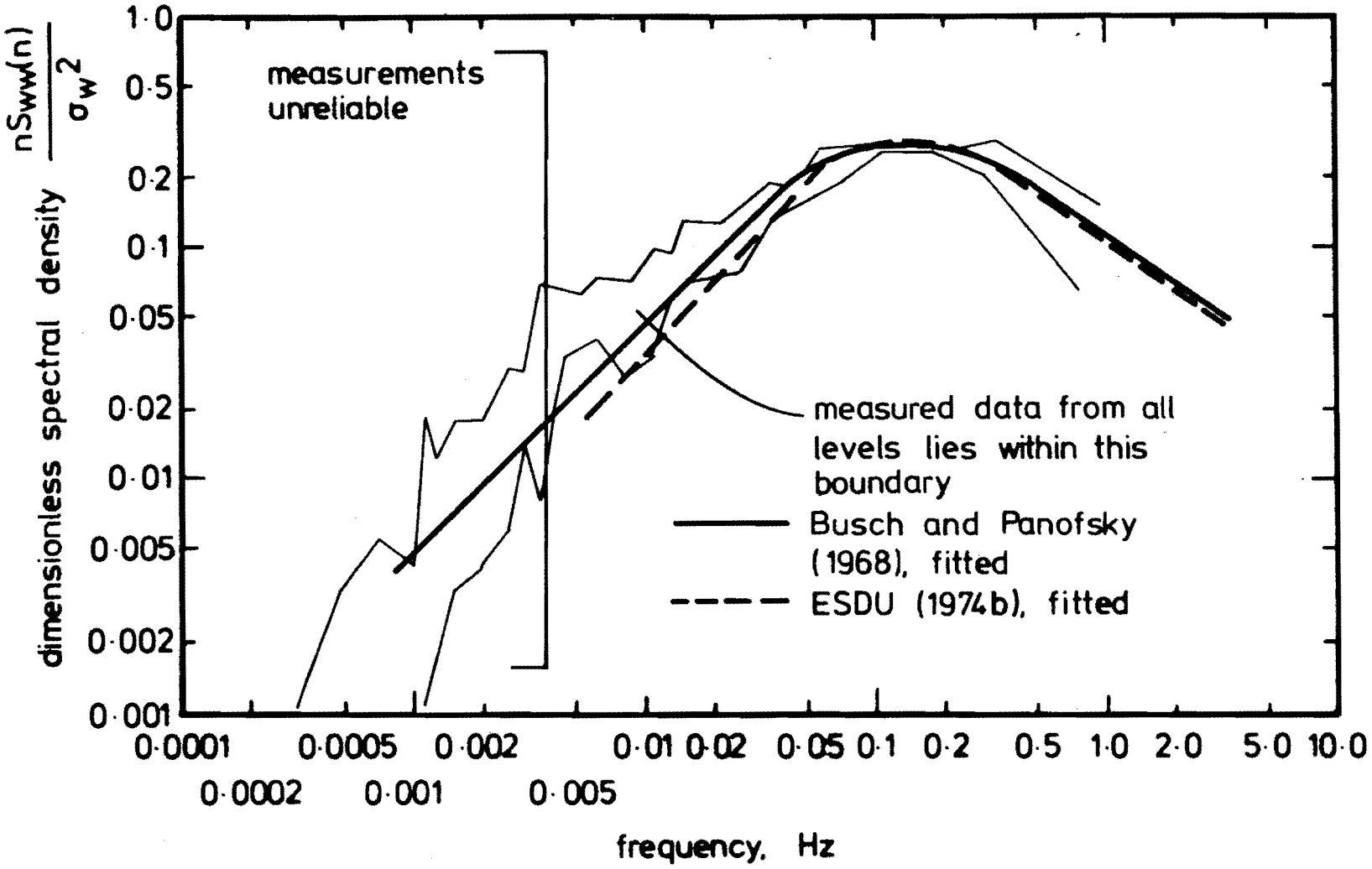

FIG 10·9 VERTICAL COMPONENT w POWER SPECTRAL DENSITY FOR RUN 1.

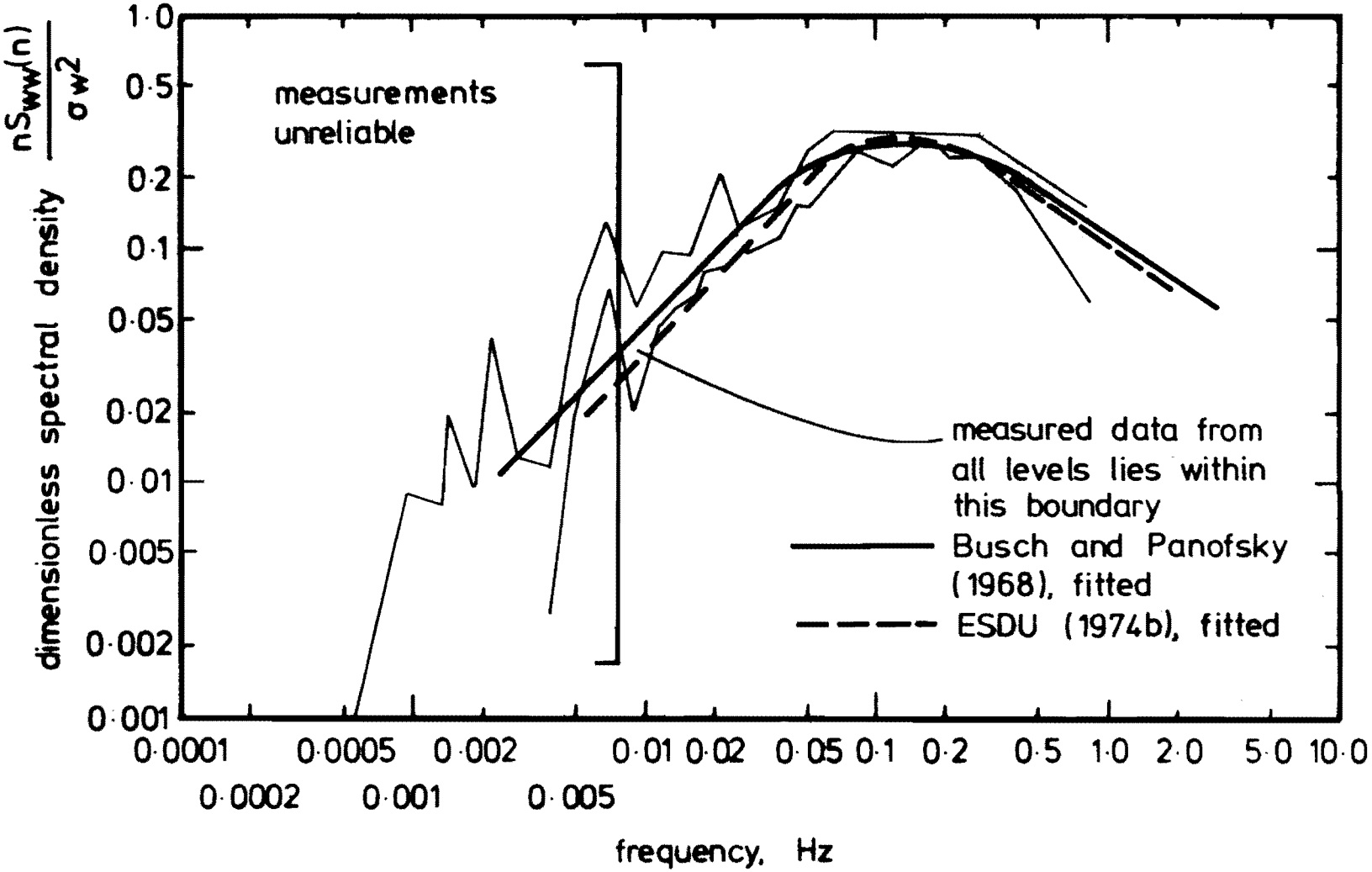

FIG. 10·10 VERTICAL COMPONENT w POWER SPECTRAL DENSITY FOR RUN 2

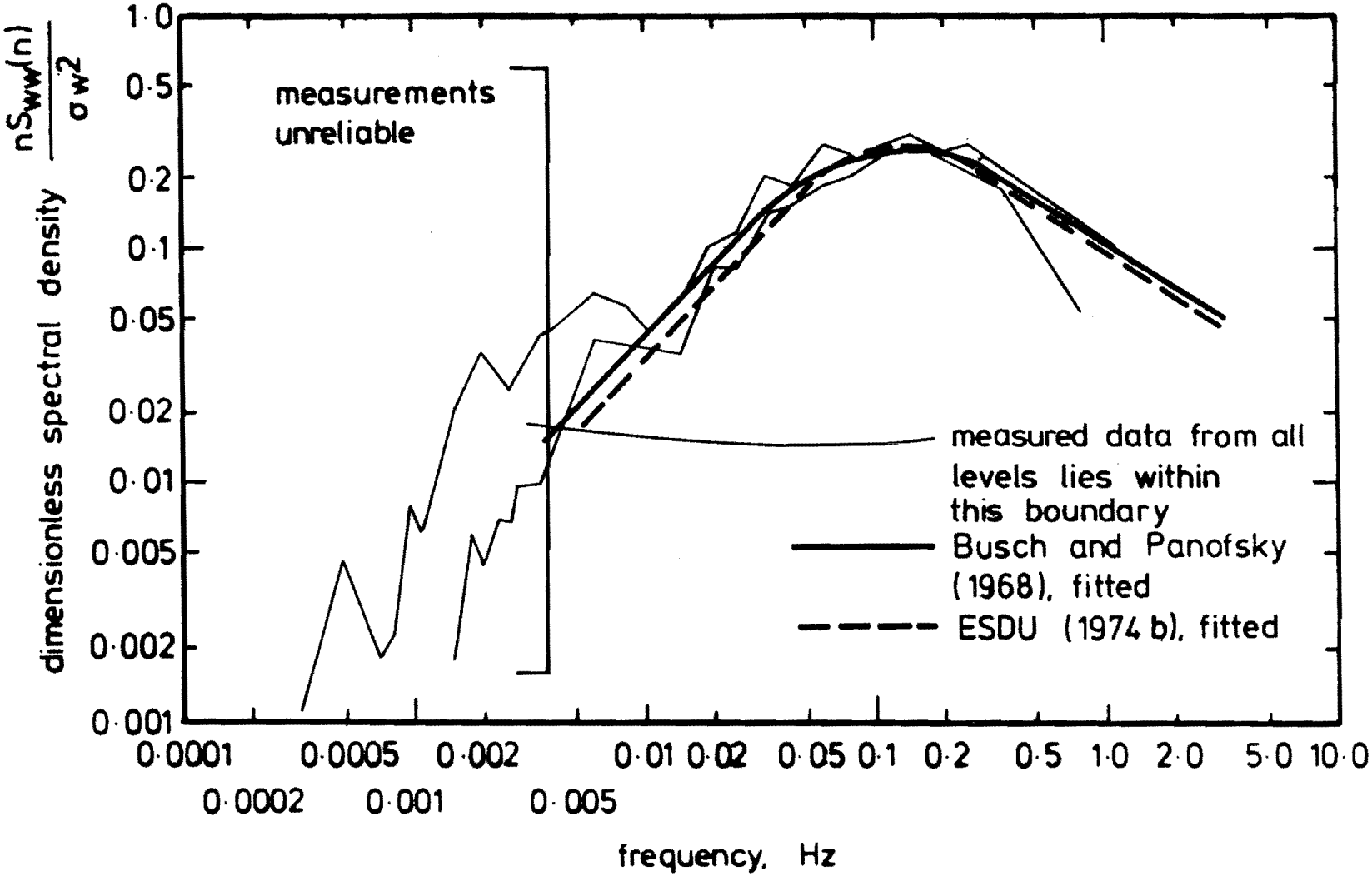

FIG. 10·11 VERTICAL COMPONENT w POWER SPECTRAL DENSITY FOR RUN 3.

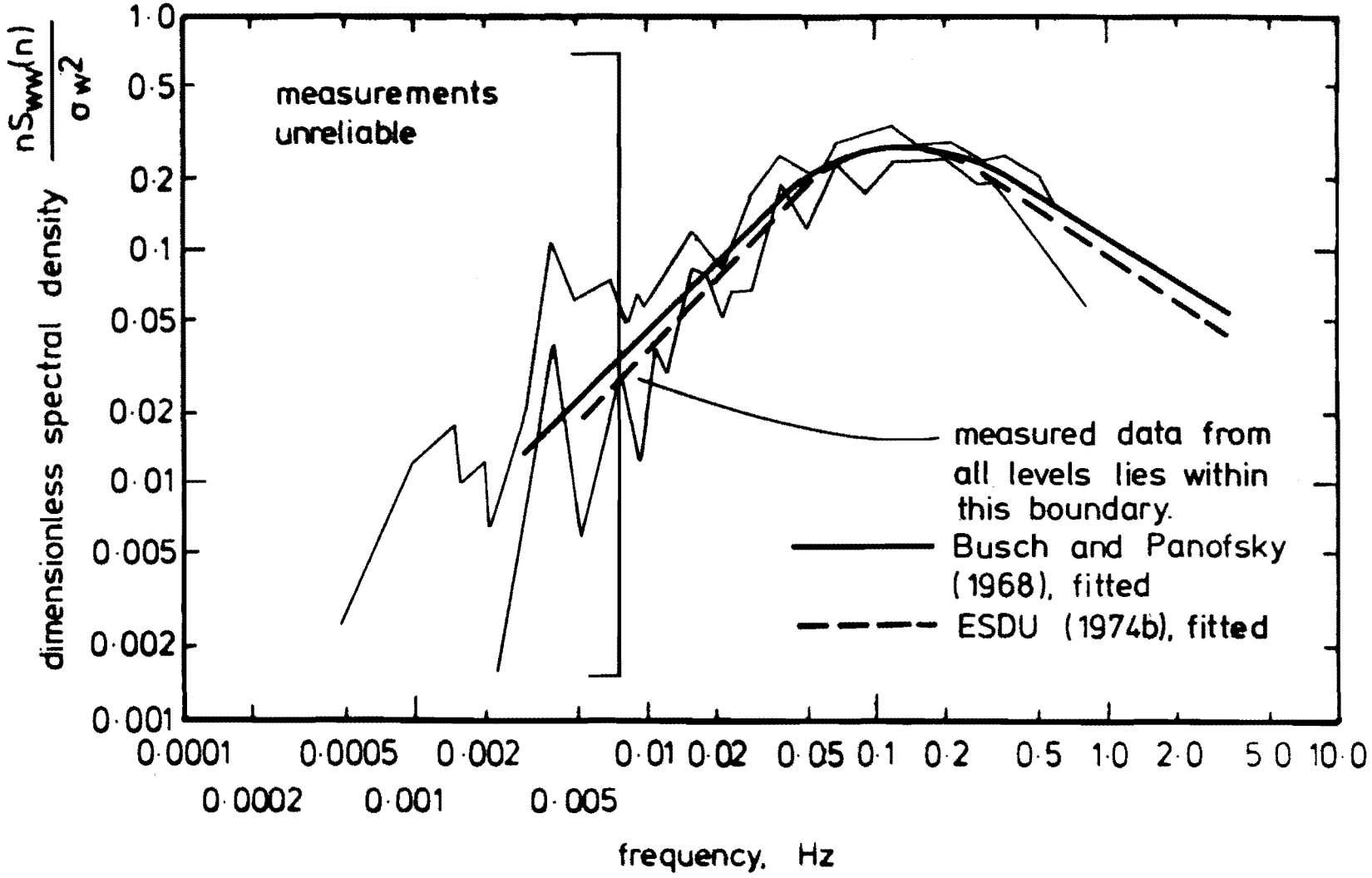

FIG. 10·12 VERTICAL COMPONENT w POWER SPECTRAL DENSITY FOR RUN 4

where $f = \frac{nZ}{\bar{V}_Z}$ and f_m is the frequency at which the spectrum obtains its peak. It has been assumed that $\sigma_w = 1.25\ U_*$ to transform the left hand side of Equation (10.14) into a similar format to that of the measured data. Both Busch and Panofsky (1968) and Counihan (1975) have suggested that $f_m = .32$ in Equation (10.14).

The equation given above has been plotted in Figs.10.9,10.10,10.11 and 10.12 with the measured vertical component spectra from Runs 1,2,3, and 4 respectively. The von Kármán form of the vertical component spectrum for isotropic turbulence, given by ESDU (1974b) is also plotted. This is :

$$\frac{S_{ww}(n)}{\sigma_w^2} = \frac{4\,\tilde{n}_w(1 + 755.2\,\tilde{n}_w^2)}{(1 + 288.2\,\tilde{n}_w^2)^{\frac{11}{6}}} \quad , \qquad (10.15)$$

where $\tilde{n}_w = \frac{x_{L_{w.n}}}{\bar{V}_Z}$, and is of the same form to the lateral component spectral equation.

The curves from both spectral equations have been fitted to the peak of the measured data. It can be seen that both curves describe the measured data reasonably well. The curve from Busch and Panofsky is slightly smoother than the one from ESDU, and the former describes the data slightly better than the latter although the difference is not great.

The measured data and the theoretical spectral curves peak to about the same value of the spectral density. The feature is also apparent that the presence of the ground reduces the contributions from eddies of low frequencies. The spectral density falls off much more quickly at frequencies less than the frequency at which the spectral peak occurs for the vertical component spectra compared with both the longitudinal and lateral component spectra.

The frequency at which the peak occurs is approximately the same for all levels of anemometers. However it has been observed, although it is not plotted, that the trend of the peak is towards higher frequencies with decrease in height from the ground. Also, the peak is relatively flat

so that it is difficult to determine the frequency of the peak very accurately.

For each Run, the peak of the Busch and Panofsky spectral equation fitted to the data was determined. Only one curve from the Busch and Panofsky spectral equations was fitted to the measured data from all levels of anemometers. From this value, the reduced frequency f was calculated for each level and compared with the value of $f_m = .32$. The values of f for each Run and anemometer level have been given in Table 10.1.

	Run 1		Run 2		Run 3		Run 4	
Z, m	n_p, Hz	$\frac{nZ}{\bar{V}_Z}$	n_p, Hz	$\frac{nZ}{\bar{V}_Z}$	n_p, Hz	$\frac{nZ}{\bar{V}_Z}$	n_p, Hz	$\frac{nZ}{\bar{V}_Z}$
3.2	.15	.07	.17	.07	.17	.08	.14	.06
5.3	.15	.11	.17	.10	.17	.11	.14	.09
7.9	.15	.15	.17	.15	.17	.16	.14	.13
10.3	.15	.19	.17	.18	.17	.19	.14	.16
12.8	.15	.23	.17	.23	.17	.23	.14	.20
15.3			.17	.25	.17	.26	.14	.22
19.2	.15	.31	.17	.32	.17	.31	.14	.26

n_p is the frequency at which the measured spectra peak.

TABLE 10.1 POSITIONS OF PEAK REDUCED FREQUENCY FOR VERTICAL COMPONENT MEASURED DATA

From Table 10.1, it is quite obvious that f_m calculated from the measured data, varies with height. In general, the values of f_m from this data are somewhat lower than the value of .32 quoted. However, this is not surprising when the response characteristics of the vertical component anemometer are considered. The vertical component anemometer is not particularly sensitive at its operating region for frequencies above approximately .3 Hz. This is very near the peak in the spectral density curve, and means that particularly when the anemometer is placed near the

ground, it would tend to move the frequency of the peak towards lower values. For heights above 10 m, the measured values of f_m are much closer to the value $f_m = .32$ as proposed by Counihan (1975) and Busch and Panofsky (1968). The difference in values is not particularly significant when the difficulty also of estimating the frequency of the peak is also considered.

10.5 CONCLUSIONS

The measured spectra from the four Runs and for each velocity component have been compared with common power spectral density equations from the current literature. The comparison has been made in the form of comparing plots of the power spectral densities, and these are given in Figs.10.1 to 10.12.

A host of spectral equations describing the longitudinal component spectrum are available from the literature. The equations used for comparison have been taken from ESDU (1974b), Kaimal et al (1972), and Harris (1971). In particular it would appear that for the longitudinal component spectrum, the forms proposed by Harris and ESDU overestimate the peak of the spectrum. They also underestimate the high frequency spectral components, although the ESDU spectrum is better than the Harris form. This is because the ESDU spectrum uses the length scale $^{x}L_u$ which varies with height above the ground. The Harris spectrum which is height invarient has a scaling factor $\mathcal{L}$, with the dimensions length, but this is a constant and is equal to 1800 m.

The spectral equation from Kaimal et al (1972) fitted the longitudinal component data the best of the three theoretical curves, except for Run 4, where the spectral equation from ESDU (1974b) fitted the best.

The longitudinal component spectra from the measured data vary significantly from Run to Run below frequencies of approximately .01 Hz. This variation could no doubt be reduced by ensemble averaging a large

number of spectra taken under the same sets of meteorological conditions, when all the sample records could be considered ergodic. However, insufficient numbers of Runs were taken to allow ensemble averaging. The low frequency variation could also have been reduced by increased averaging over frequency.

The relatively large contribution to the variance from the low frequencies in the longitudinal component spectrum, also observed in the lateral component spectrum, is probably due to nonstationarities in the flow. Observation of the velocity-time plots in Figs.7.2,7.3,7.4 and 7.5 show that at times there are relatively large variations from the mean longitudinal velocity, and sometimes what almost appear to be discontinuities. The removal of a parabolic trend line was likely not sufficient to remove all the trends. A higher order polynomial trend line is perhaps required to obtain trend free data. The low frequency spectral components could also have been removed by a digital high pass filter, however the problem then becomes one of determining the cut-off frequency.

High pass filtering of the data would remove the contribution to the variance of the low frequency spectral components and hence tend to increase the values of $\frac{nS_{ii}(n)}{\sigma_i^2}$, i = u,v,w at the higher frequencies. The shape of the spectrum at high frequencies would not be altered.

It was observed, although it hasn't been presented here, that generally the measured spectra, of the longitudinal component, were shifted very slightly towards higher frequencies as the height above ground decreased. This data does not scale as $\frac{nZ}{\bar{V}_Z}$ as prediced by Kaimal et al (1972), however nor does it scale as $\frac{n}{\bar{V}_{10}}$ as suggested by Davenport (1961b) and Harris (1971). It is closer to being height invariant than scaling as $\frac{nZ}{\bar{V}_Z}$ however.

The lateral component spectra of the measured data from the four Runs differ from empirical formulae more than either the longitudinal

or vertical measured components, from their corresponding formulae. For Runs 1,2, and 3, there is a large amount of low frequency energy in the lateral component spectra. The lateral component is very sensitive to the stability of the boundary layer. Unstable conditions greatly increase the low frequency portion of the spectrum, whilst leaving the high frequency part relatively unaffected. However, the data analysed here was recorded when the wind was blowing strongly, i.e. when $\bar{V}_{10} > \sim 10$ m/s, and in all Runs there was moderate cloud cover. For the low height range considered, it is reasonable to assume that the lapse rate was neutral and that the low frequency spectral components were not caused by an unstable boundary layer. It is more reasonable to assume that the data still contained trends, even after a parabolic trend line removal, as discussed similarly for the longitudinal component above.

The line corresponding to the spectral equation from Kaimal et al(1972)fitted the measured lateral component data the best for Runs 1,2, and 3, but the ESDU spectrum fitted the measured data from Run 4, in Fig.10.8, the best. This measured spectrum differs considerably from the other three measured lateral component spectra in that it has very little contribution from low frequency components.

Both spectral equations from ESDU (1974b) and Busch and Panofsky (1968) fitted the measured vertical component spectra shape well. The latter perhaps slightly better as it is a smoother curve. The presence of the ground is obvious as it damps out the fluctuations from low frequencies, and thus the data was easier to deal with because it was trend free.

Figs.10.9,10.10,10.11 and 10.12 show that the vertical component propeller anemometer produces spectra which have a similar shape to the expected result. However, the data in Table 10.1 indicates that especially near the ground, the high frequency spectral components are

underestimated. This tends to make the measured spectra peak at a lower frequency than the theoretical curves predict.

The results discussed in this Chapter have shown that adequate measurements can be made of power spectral densities using propeller anemometers, even of the vertical component spectrum, providing that the anemometers are not placed too close to the ground. However, spectral estimates at low frequencies are unreliable, and indicate that at least eight contiguous estimates should be averaged to obtain a smoother spectrum as suggested by Yuen and Fraser (1976). Thus probably the best method of averaging over frequency is to use linear averaging at low frequencies, and partial octave band averaging at higher frequencies. This is because when spectra are plotted against log (frequency), the high frequency estimates are compressed together.

The spectra also become unreliable above about .3 - .5 Hz when the inertial lag of the propeller tends to reduce the amplitude of the components. The spectra in the range .3 -1.0 Hz can be corrected approximately by the method suggested in Section 3.2.5.4 if this is required.

The following Chapter discusses the positions of the ESDU (1974b) spectra when fitted to the measured spectra in relation to determining integral length scales.

CHAPTER 11

AUTOCORRELATIONS

11.1 INTRODUCTION

11.1.1 Definitions

A covariance function is the mean product of fluctuating velocity components measured at one or more points in space either simultaneously or with a time lag between them. In particular, covariance functions may be formed from measurements at (i) a single point or (ii) at two points in space. In case (i) the function provides information on the extent of eddies or gusts in a time sense. When a signal is correlated with itself, the function is called an autocovariance function and is defined as

$$C_{ii}(\tau)=\overline{i(t).i(t+\tau)} = \lim_{T\to\infty} \frac{1}{T}\int_0^T i(t).i(t+\tau)\ dt \qquad (11.1)$$

$$i = u,v,w$$

When the time lag τ is 0 the autocovariance function reduces to the component variances, namely σ_u^2, σ_v^2 σ_w^2 as shown in Section 9.1.1.

Normally the autocovariance function is normalised by the appropriate standard deviation of the signal, giving the autocorrelation function :

$$\rho_{ii}(\tau) = C_{ii}(\tau)/\sigma_i^2 \ , \ i = u,v,w. \qquad (11.2)$$

To implement Equations (11.1) and (11.2) on a digital computer a discrete version is used. Also, since data recordings are of a finite length,autocorrelations with time lags greater than the data recording length are impossible. Practically, the autocorrelation is regarded as unreliable for time lags greater than 10% of the data recording length. Also only discrete values of the autocorrelation may be obtained for

time lags which are multiples of the time between consecutive samples.

The discrete version of Equations (11.1) and (11.2) used to obtain an autocorrelation function of a sample time history of N samples with Δt seconds between consecutive samples is :

$$\rho_{ii}(r\Delta t) = \frac{1}{N-r} \sum_{k=0}^{N-r-1} i(k).i(k+r)/\sigma_i^2 \qquad (11.3)$$

$$r = 0, 1, \ldots m ,$$

$$i = u,v,w$$

m is the maximum lag number and is limited to less than $N/10$.

11.1.2 Analysis Procedure

Equation (11.3) was not evaluated through an accumulation of lagged products as the form of the equation suggests. It was evaluated by the past Fourier transform techniques explained in Section 5.6.3, using program PSAUTCORS.

In all cases except when a cosine taper was applied to the data before obtaining a power spectrum,the autocorrelation function was obtained simply by taking an inverse Fourier transform of the power spectral density. This was then multiplied by the appropriate scaling factors. When a cosine taper was used to obtain power spectra and an autocorrelation was required, the velocity data was changed back to its untapered form before the forward transform was taken of the data. The method of obtaining power spectra is detailed in Section 10.1.2, and also in Section 5.6.

Thus the autocorrelation function could be evaluated after the power density of the appropriate data stream had been obtained with very little increase in computing time.

11.1.3 Theoretical Autocorrelation Formulae

The autocorrelation functions have been reported in the results of full scale field measurements less frequently than their corresponding

power spectral densities. The autocorrelation function provides no additional information over a power spectral density function, but presents the information in a different manner, i.e. in the time domain rather than the frequency domain.

The autocorrelation function shows the correlation of a data stream with itself a short time later (or sooner). Thus when the autocorrelation function is obtained from velocity data from the atmospheric surface layer, it gives an indication of the extent in time of the average sized eddies.

Ideally,the integral time scale is defined as the area under the autocorrelation function, i.e.

$$T_i = \int_0^\infty \rho_{ii}(\tau)\, d\tau \ , \quad i = u,v,w \tag{11.4}$$

In practice, usually the integration is taken until the correlation first falls to zero, or falls to 5%. In this work, the integration was taken until the autocorrelation function fell to 5%.

Taylor's Hypothesis is useful because it can be used to transform a time delay to an equivalent spatial separation. Taylor's Hypothesis states that provided $\bar{V}_Z$ is much greater than u(t), the turbulence field can be considered to be frozen in space and convected past a point with velocity $\bar{V}_Z$. Thus the variation of u(t) with time when the turbulence field is viewed from a stationary point is the same as the variation observed from the point moving with velocity $\bar{V}_Z$ across the "frozen" field of turbulence in the x direction. Thus Taylor's Hypothesis can be used to convert the integral time scales T_i, i = u,v,w, calculated from the autocorrelation functions to equivalent integral length scales thus :

$$^{x}L_i = \bar{V}_Z \int_0^\infty \rho_{ii}(\tau)\, d\tau \ , \quad i = u,v,w \tag{11.5}$$

The integral length scale is commonly calculated via two other methods. The first method is from the power spectral density function.

For example, a von Kármán spectral equation as obtained from ESDU (1974b) can be fitted to the measured power spectral density function. The position of the peak of the spectral equation on the frequency axis can then be used to find the integral length scale. For the ESDU (1974b) spectra in particular, the equations relating peak frequency and integral length scale are :

$$x_{L_u} = \frac{.146\ \bar{V}_Z}{n_p} \tag{11.6}$$

$$x_{L_v} = \frac{.106\ \bar{V}_Z}{n_p} \tag{11.7}$$

$$x_{L_w} = \frac{.106\ \bar{V}_Z}{n_p} \tag{11.8}$$

where n_p, Hz is the frequency at which the peak occurs.

However this method suffers from the disadvantage that often the measured spectral curves of the u and v components in particular are fairly flat near the position of the peak. This makes it difficult to fit the theoretical spectral equation accurately to the measured data, and errors of 100% are easily possible.

The second method of determining the integral length scale is to assume that the autocorrelation function falls in a negative exponential manner with time lag. The time, T_E is then taken for the curve to drop to a correlation of $\frac{1}{e}$ or .368. This gives an integral time scale, which when multiplied by $\bar{V}_Z$ gives the appropriate integral length scale for the component. This method is often useful when the autocorrelation function falls towards zero slowly due to the existence of trends in the data.

To compare the measured data with the theoretical autocorrelation functions, Figs.11.1,11.2,11.3 and 11.4 contain the measured autocorrelation functions for the longitudinal components from Runs 1,2,3, and 4 respectively, and theoretical autocorrelation functions from both

Harris (1971) and ESDU (1974b). Figs.11.5 to 11.8 and 11.9 to 11.12, which contain the lateral and vertical component autocorrelation functions respectively from Runs 1,2,3, and 4, also have plotted the corresponding theoretical autocorrelation functions from ESDU (1974b).

Both the ESDU (1974b) and Harris (1971) theoretical autocorrelation functions have been obtained from a Fourier transform of their respective theoretical power spectral density functions. The formula for the Harris (1971) longitudinal component autocorrelation function is :

$$\rho_{uu}(\tau) = \frac{2}{\Gamma(\frac{1}{3})}\left[\frac{2\sqrt{2}\ \pi\ \bar{V}_{10}\ \tau}{\mathcal{L}\ 2}\right]^{\frac{1}{3}}\ K_{\frac{1}{3}}\left[\frac{2\sqrt{2}\ \pi\ \bar{V}_{10}\ \tau}{\mathcal{L}}\right] \tag{11.9}$$

where $\Gamma(\frac{1}{3})$ is a Gamma function, $K_{\frac{1}{3}}\left[\frac{2\sqrt{2}\ \pi\ \bar{V}_{10}\ \tau}{\mathcal{L}}\right]$ is a modified Bessel function of the second kind of order $\frac{1}{3}$ and $\mathcal{L}$ = 1800 m. Harris (1968) has tabulated the Gamma and Bessel functions required in Equation (11.9). In Equation (11.9) it can be seen that all the quantities are fixed except $\bar{V}_{10}$ and τ , hence $\rho_{uu}(\tau)$ is a function of $\bar{V}_{10}$ and τ only, i.e. the formula is height invariant.

The theoretical autocorrelation functions from ESDU (1974b) are :

$$\rho_{uu}(\tau) = .5925\ (\tilde{\tau}_u)^{\frac{1}{3}}\ K_{\frac{1}{3}}\ (\tilde{\tau}_u) \tag{11.10}$$

$$\rho_{vv}(\tau) = .5925\left[(\tilde{\tau}_v)^{\frac{1}{3}}\ K_{\frac{1}{3}}\ (\tilde{\tau}_v) - \frac{1}{2}\ (\tilde{\tau}_v)^{\frac{4}{3}}\ K_{\frac{2}{3}}\ (\tilde{\tau}_v)\right] \tag{11.11}$$

$$\rho_{ww}(\tau) = .5925\left[(\tilde{\tau}_w)^{\frac{1}{3}}\ K_{\frac{1}{3}}\ (\tilde{\tau}_w) - \frac{1}{2}\ (\tilde{\tau}_w)^{\frac{4}{3}}\ K_{\frac{2}{3}}\ (\tilde{\tau}_w)\right] \tag{11.12}$$

where

$$\tilde{\tau}_u = .747\ \tau\ \bar{V}_Z/^{x}L_u \tag{11.13}$$

$$\tilde{\tau}_v = .3735\ \tau\ \bar{V}_Z/^{x}L_v \tag{11.14}$$

$$\tilde{\tau}_w = .3735\ \tau\ \bar{V}_Z/^{x}L_w \tag{11.15}$$

and $K_{\frac{1}{3}}$ and $K_{\frac{2}{3}}\ (\tilde{\tau}_i)$ are modified Bessel functions of the second kind, of

order $\frac{1}{3}$ and $\frac{2}{3}$ respectively.

Equations (11.10),(11.11) and (11.12) are functions of the variables $\bar{V}_z$, ${}^{x}L_i$, i = u,v,w and τ, and therefore are functions of height.

In Figs.11.1 to 11.12, the areas corresponding to the ESDU formulae have been indicated with edge lines, the lines being values predicted from the lowest and highest levels of anemometers on the tower. In Figs.11.1, 11.2,11.3 and 11.4, the longitudinal autocorrelation function proposed by Harris (1971) has been given as a full line.

11.2 THE LONGITUDINAL COMPONENT AUTOCORRELATION FUNCTIONS

The longitudinal component autocorrelation functions are shown plotted in Figs.11.1,11.2,11.3 and 11.4 from Runs 1,2,3, and 4 respectively. In Fig.11.1 each line has been obtained from one orthogonal array of anemometers. It is immediately apparent that the integral time scale T_u increases with increase in height. This means that not only are the eddies convected along at higher speeds at greater heights but they take longer to be convected past a point. Counihan (1975) has noted that the integral length scale ${}^{x}L_u$ decreases rapidly for decreasing heights above ground, particularly below about 5-10 m. This trend has also been noted in Runs 2,3, and 4 shown in Figs. 11.2,11.3 and 11.4, but in these figures the measured data has been defined by two edge lines. This is because it was difficult to distinguish between the seven curves obtained from the orthogonal arrays in each Run.

In Fig.11.1 it is apparent that the measured data has a much larger correlation than predicted by ESDU (1974b). It is closer to the theoretical curve predicted by Harris (1971), but even this does not describe the data well. The measured data has a correlation which falls rapidly for time lags up to about 10 seconds which corresponds to a correlation of approximately .4, after which it approaches a correlation of zero much

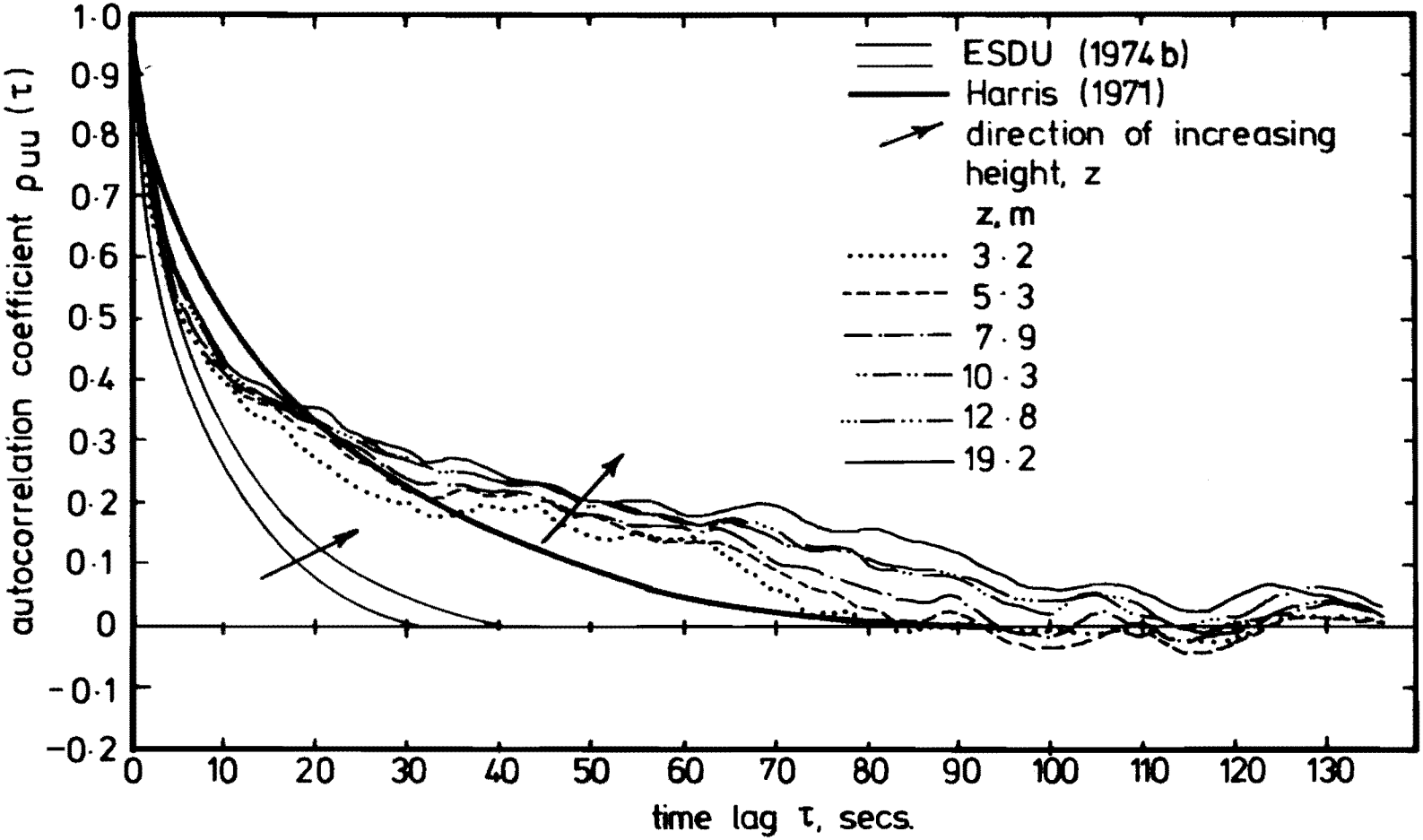

FIG. 11·1 LONGITUDINAL COMPONENT u AUTOCORRELATION FUNCTION FOR RUN 1.

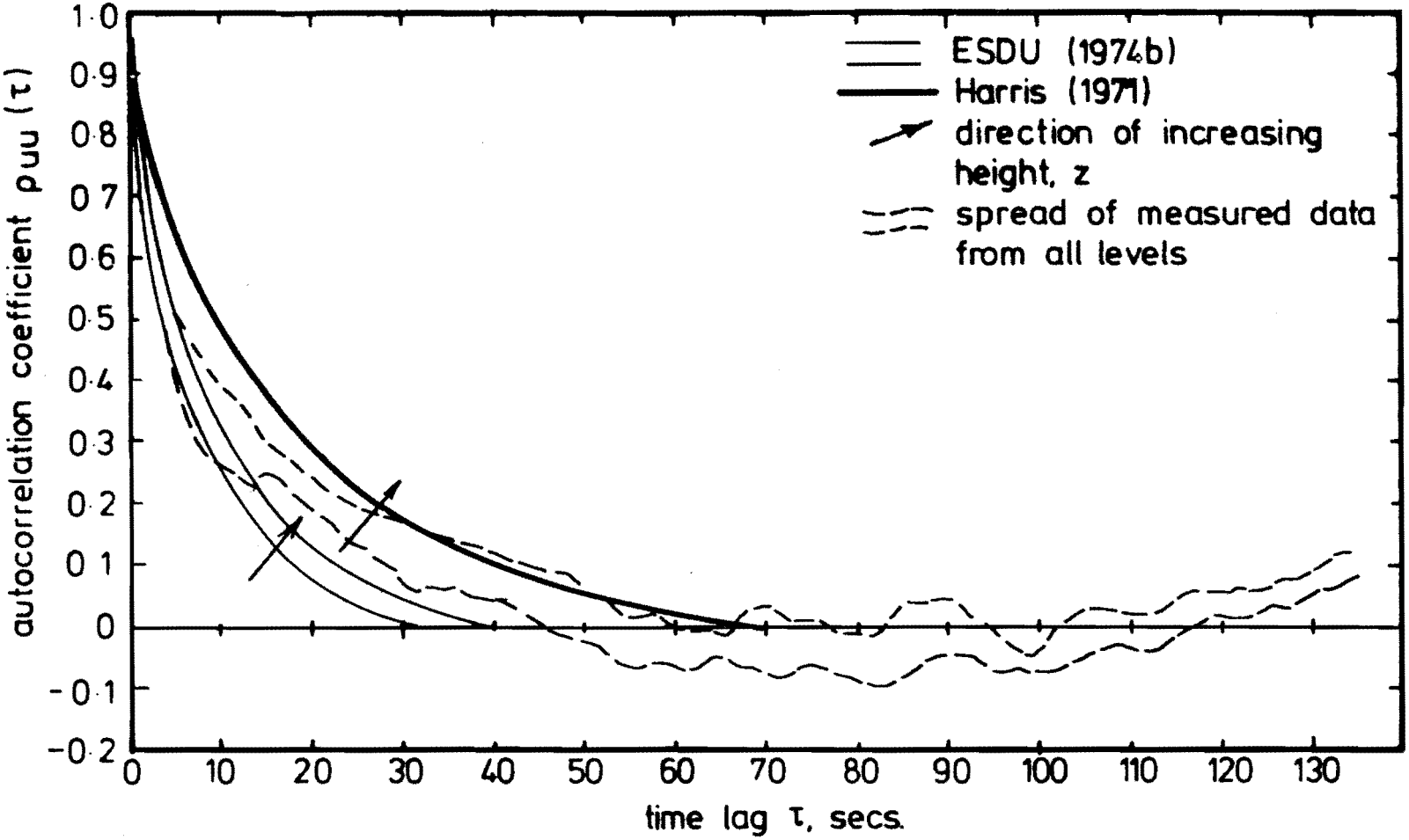

FIG. 11·2 LONGITUDINAL COMPONENT u AUTOCORRELATION FUNCTION FOR RUN 2.

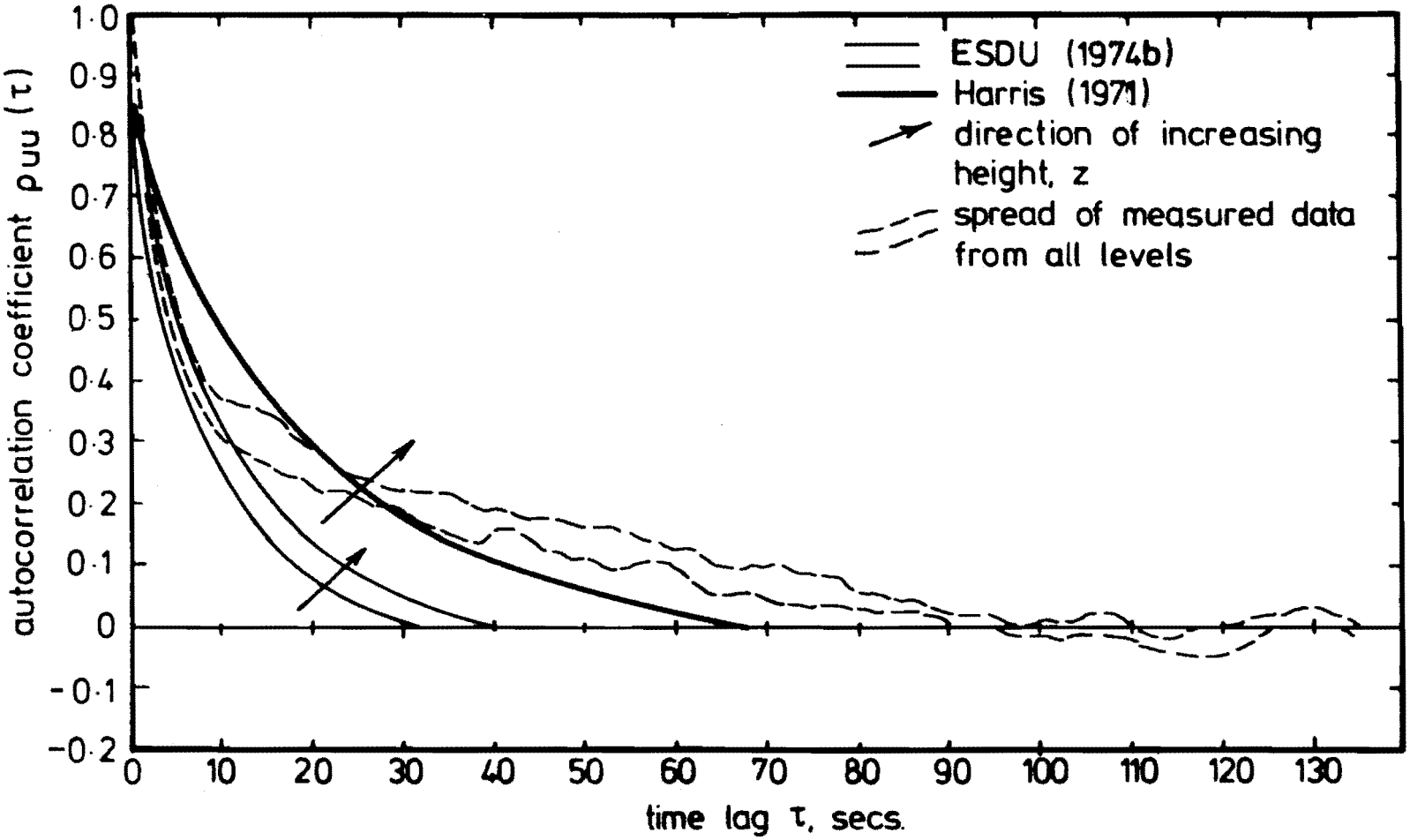

FIG. 11·3 LONGITUDINAL COMPONENT u AUTOCORRELATION FUNCTION FOR RUN 3

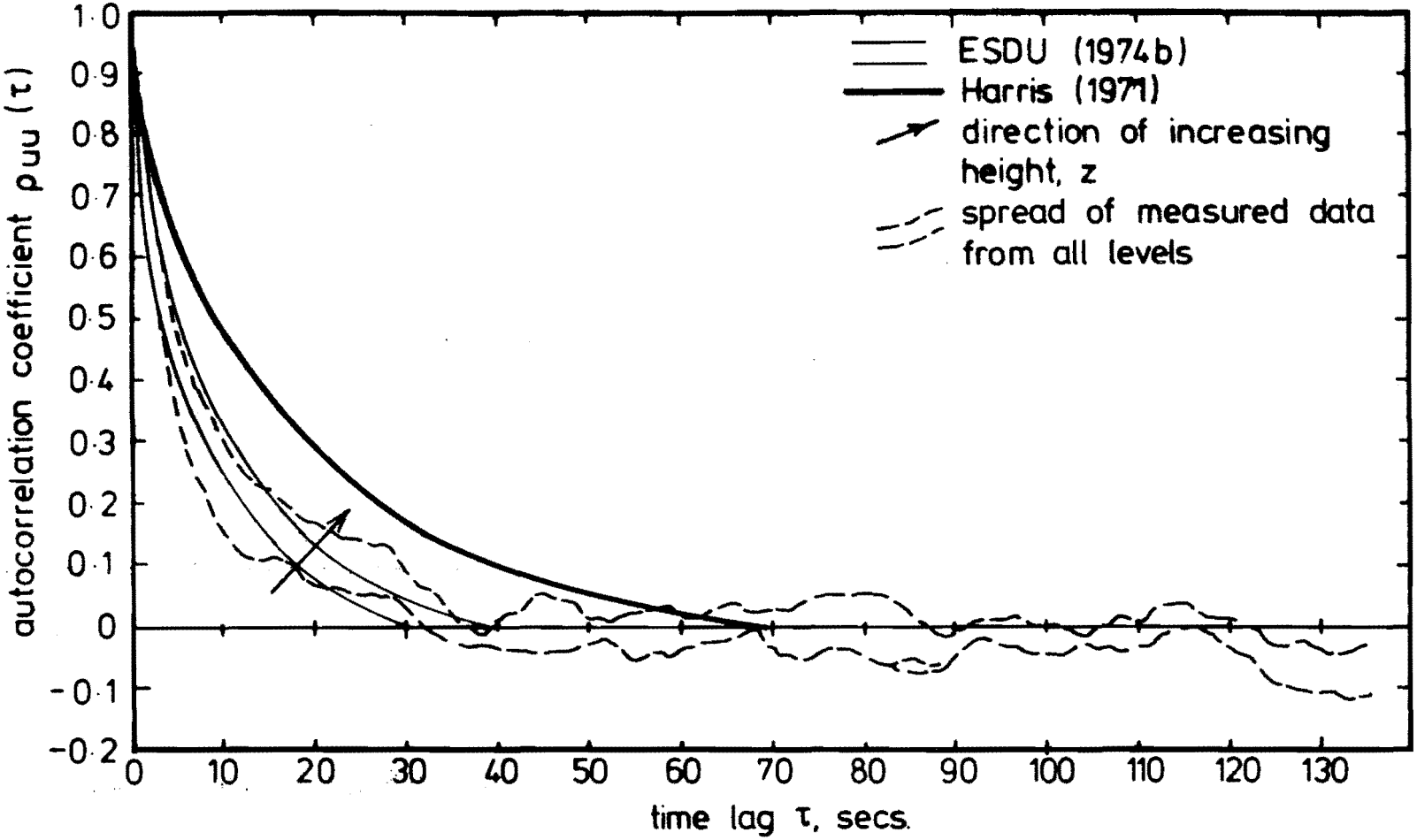

FIG. 11·4 LONGITUDINAL COMPONENT u AUTOCORRELATION FUNCTION FOR RUN 4.

more slowly. Fig.10.1 shows that the longitudinal component spectra from Run 1 have a relatively large contribution to the variance, or energy, at low frequencies. These low frequency spectral components cause the autocorrelation function in Fig.11.1 to fall slowly towards zero for large time lags.

Fig.11.2 shows the autocorrelation function for the longitudinal component of Run 2. The ESDU (1974b) curve fits this data well for correlations down to approximately .35, after which the measured data correlation falls towards zero more slowly than predicted by ESDU. The Harris formula overestimates the correlation for almost all time lags up to 60 seconds. The Run 2 measured autocorrelation function falls towards zero more slowly than the Run 1 data. It can also be noted by comparing Figs.10.1 and 10.2 that the Run 1 longitudinal component data has significantly more low frequency energy than the Run 2 data.

The autocorrelation functions for the longitudinal component of the Run 3 data are plotted in Fig.11.3. Like Run 2, the ESDU prediction compares well with the data down to a correlation of about .4, after which the autocorrelation curve tends to zero more slowly than predicted by ESDU. The Harris curve overestimates the correlations for short time lags, and underestimates it for long time lags.

The autocorrelation functions for the longitudinal component of the Run 4 data are plotted in Fig.11.4. The figure shows very good agreement between the measured data and ESDU, but poor agreement with the Harris curve. Fig.10.4 shows that the corresponding power spectral density function has the smallest contribution to the variance at low frequencies of all four Runs. The lack of large eddies has thus allowed the measured autocorrelation functions to fall to zero more quickly in Run 4 than in the three other Runs.

11.3 THE LATERAL COMPONENT AUTOCORRELATION FUNCTIONS

The lateral component autocorrelation functions for Runs 1,2,3, and 4 are given in Figs.11.5,11.6,11.7 and 11.8 respectively. Also plotted in each of the four figures are autocorrelation functions predicted by ESDU (1974b) for the height and wind speed range considered in the measured data.

The four curves from the measured data all fall rapidly to a correlation of approximately .4 which occurs after a time delay of approximately four seconds. For time lags greater than about four seconds, the correlation curves differ significantly from the variation predicted by ESDU for Runs 1,2 and 3. Run 4 compares well with the ESDU prediction.

Figs.10.5,10.6 and 10.7 show the large contribution from the low frequency spectral components to the lateral component power spectra of Runs 1,2, and 3 respectively. The energy at these low frequencies for the three Runs is significantly greater than for Run 4, which compares more favourably with the ESDU (1974b) power spectral density function.

In Chapter 10, the large contribution of the low frequency spectral components to the lateral component power spectral density function was discussed. It was concluded that the large amount of spectral energy at low frequencies was not caused by an unstable boundary layer, because of the relatively high wind speed and cloud cover existing at the times the data was recorded.

The low frequency spectral components must therefore be the result of trends in the data, which prevent the autocorrelation functions approaching zero even for large time delays.

It is obvious that estimation of integral time scales from such autocorrelation functions, and subsequently, integral length scales, by integrating the area under the curve until the correlation drops to say

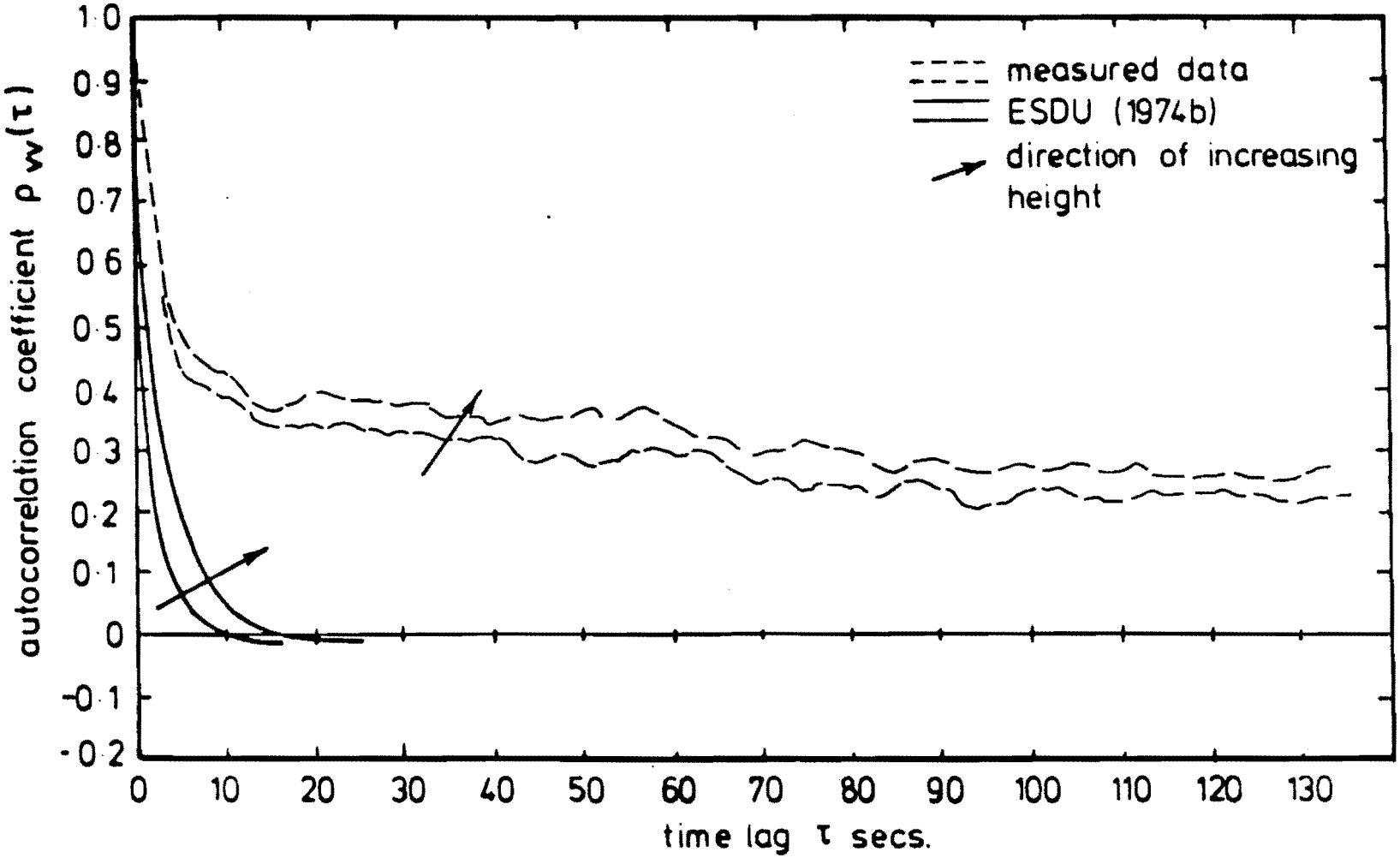

FIG. 11·5 LATERAL COMPONENT v AUTOCORRELATION FUNCTION FOR RUN 1.

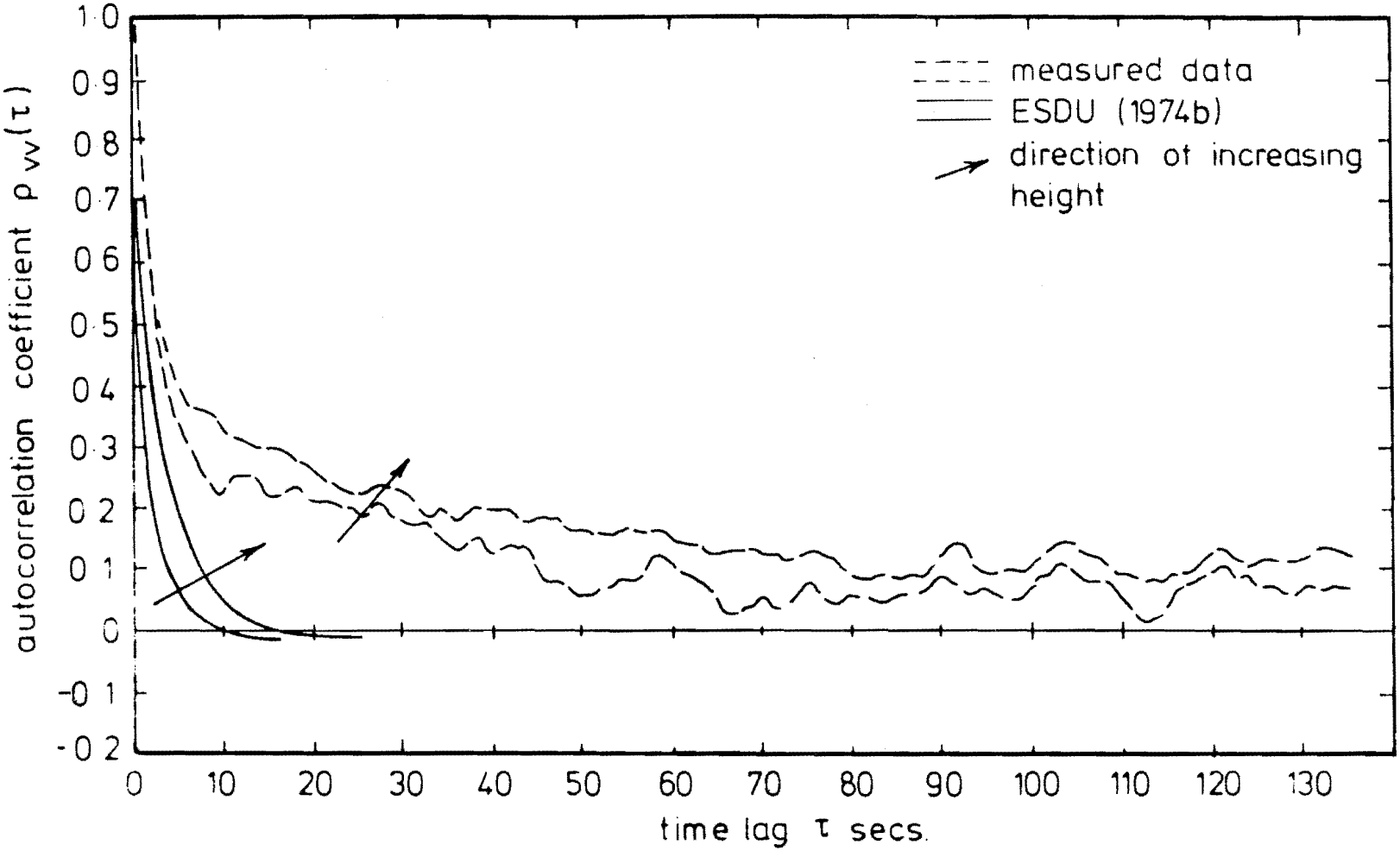

FIG. 11·6 LATERAL COMPONENT v AUTOCORRELATION FUNCTION FOR RUN 2.

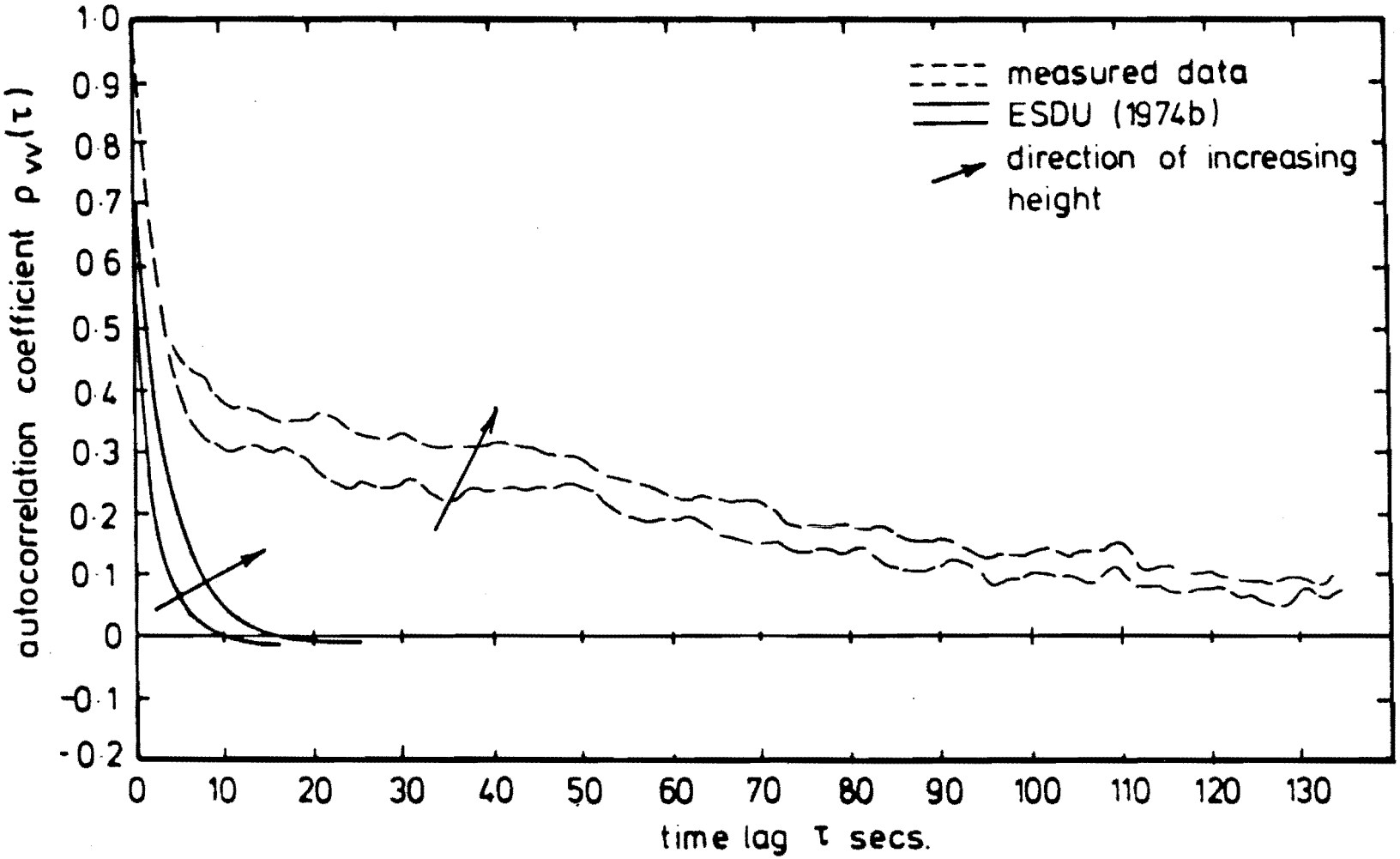

FIG. 11.7 LATERAL COMPONENT v AUTOCORRELATION FUNCTION FOR RUN 3

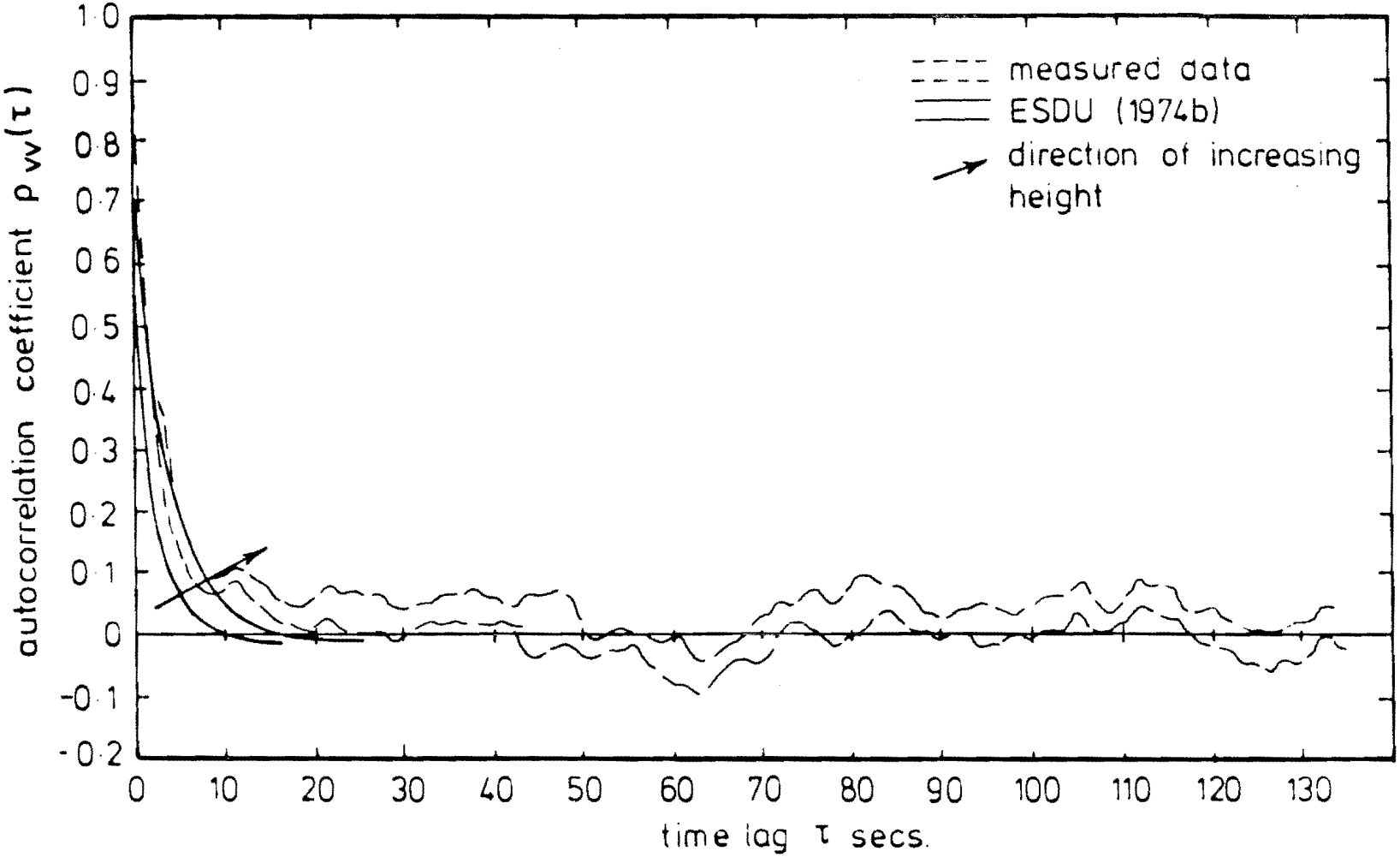

FIG 11 8 LATERAL COMPONENT v AUTOCORRELATION FUNCTION FOR RUN 4

5%, is very inaccurate. A better method to use in such cases is to assume that the autocorrelation function decreases exponentially with time. For such a function, the integral time scale computed by integration is numerically the same value as the time lag at which it drops to a correlation of $\frac{1}{e}$ or .368.

However, it can be observed in Fig.11.8 that the correlation is smaller for Run 4 even for very small time delays as well as for large time delays, compared with Run 1,2, and 3 data, in Figs.11.5,11.6 and 11.7 respectively. Consequently, estimates of T_v by assuming an exponential correlation curve may be unreliable for Runs 1,2, and 3, even when this is a better method than integrating the area under the appropriate autocorrelation function.

It can be seen from these lateral component autocorrelation functions that removing a parabolic trend line from the data streams did not make the data behave as if it was trend free. The data appeared to be stationary as determined by the *Run Test* on the longitudinal component data, explained in Section 8.2, but it would appear that this test is not severe enough. Alternatively, perhaps the test for stationarity should also be applied to the lateral component data as well.

As mentioned in Section 10.5, digitally high pass filtering the data could remove the contribution from the low frequency spectral components. The cut-off frequency would have to be selected carefully to remove the "trends in the mean" but leave the low frequency spectral component of interest. Alternatively, the removal of a higher order polynomial trend line could be investigated.

11.4 THE VERTICAL COMPONENT AUTOCORRELATION FUNCTIONS

The vertical component autocorrelation functions for Runs 1,2,3, and 4 are plotted in Figs.11.9,11.10, 11.11, and 11.12 respectively. The

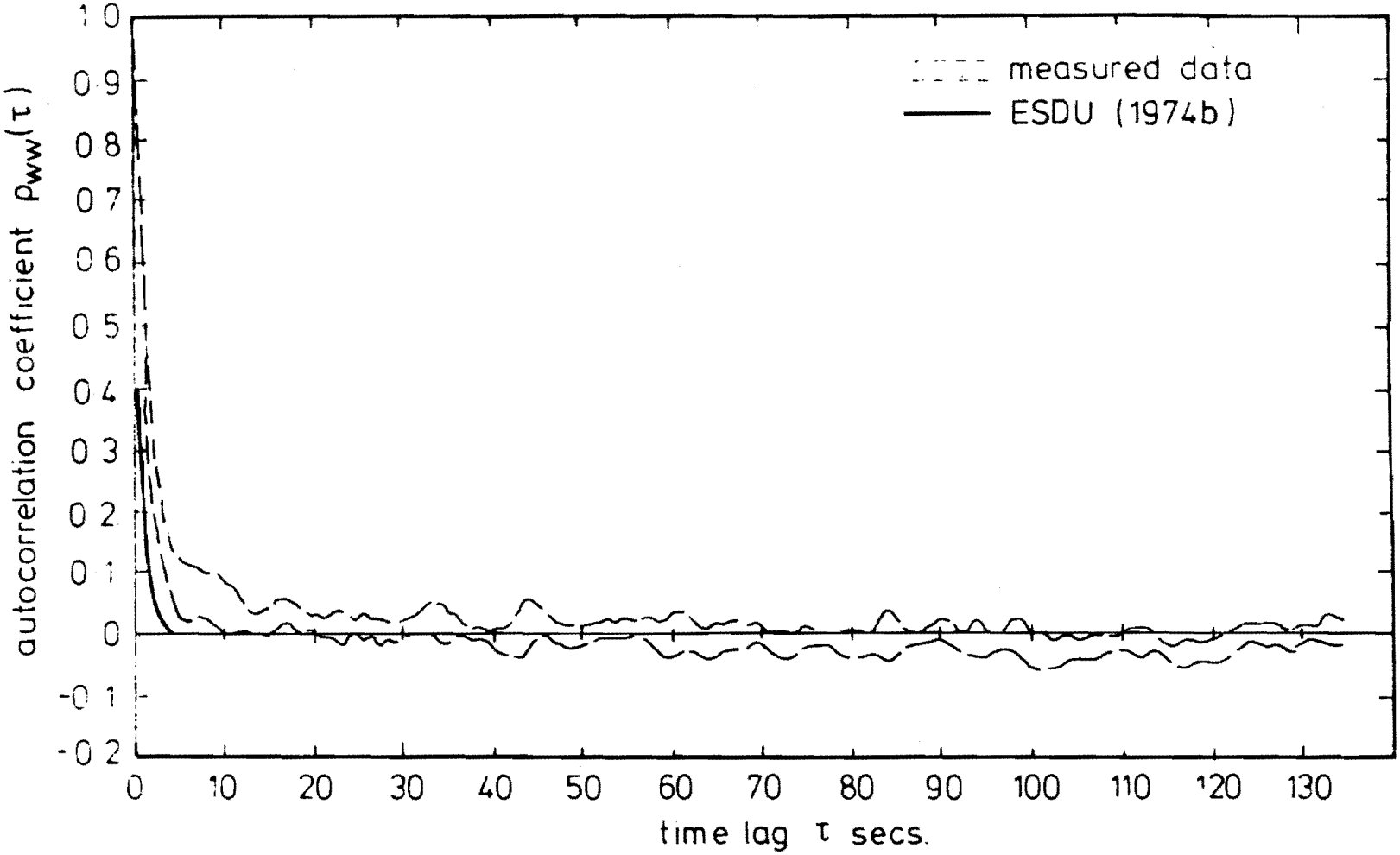

FIG 11·9 VERTICAL COMPONENT w AUTOCORRELATION FUNCTION FOR RUN 1

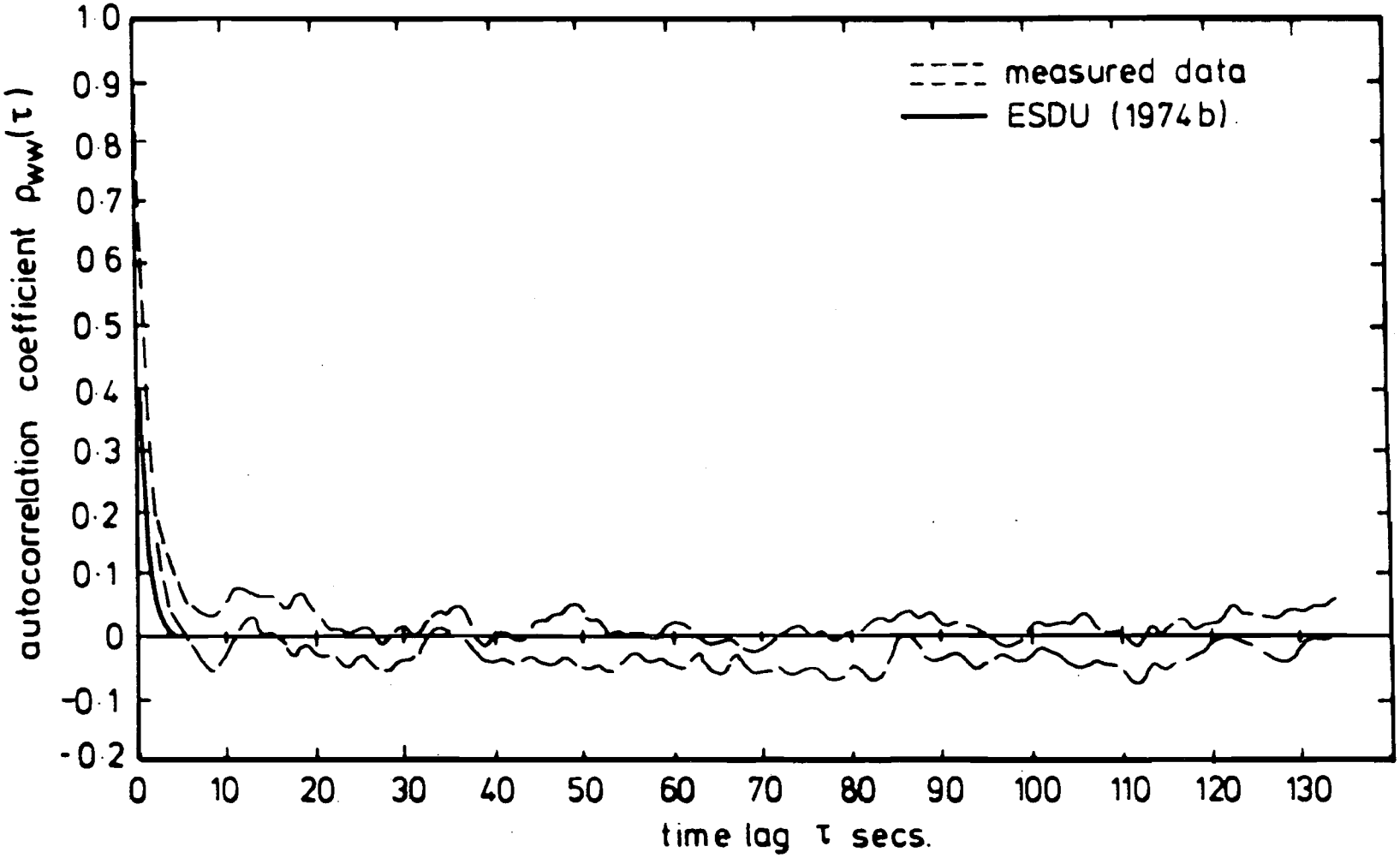

FIG 11·10 VERTICAL COMPONENT w AUTOCORRELATION FUNCTION FOR RUN 2

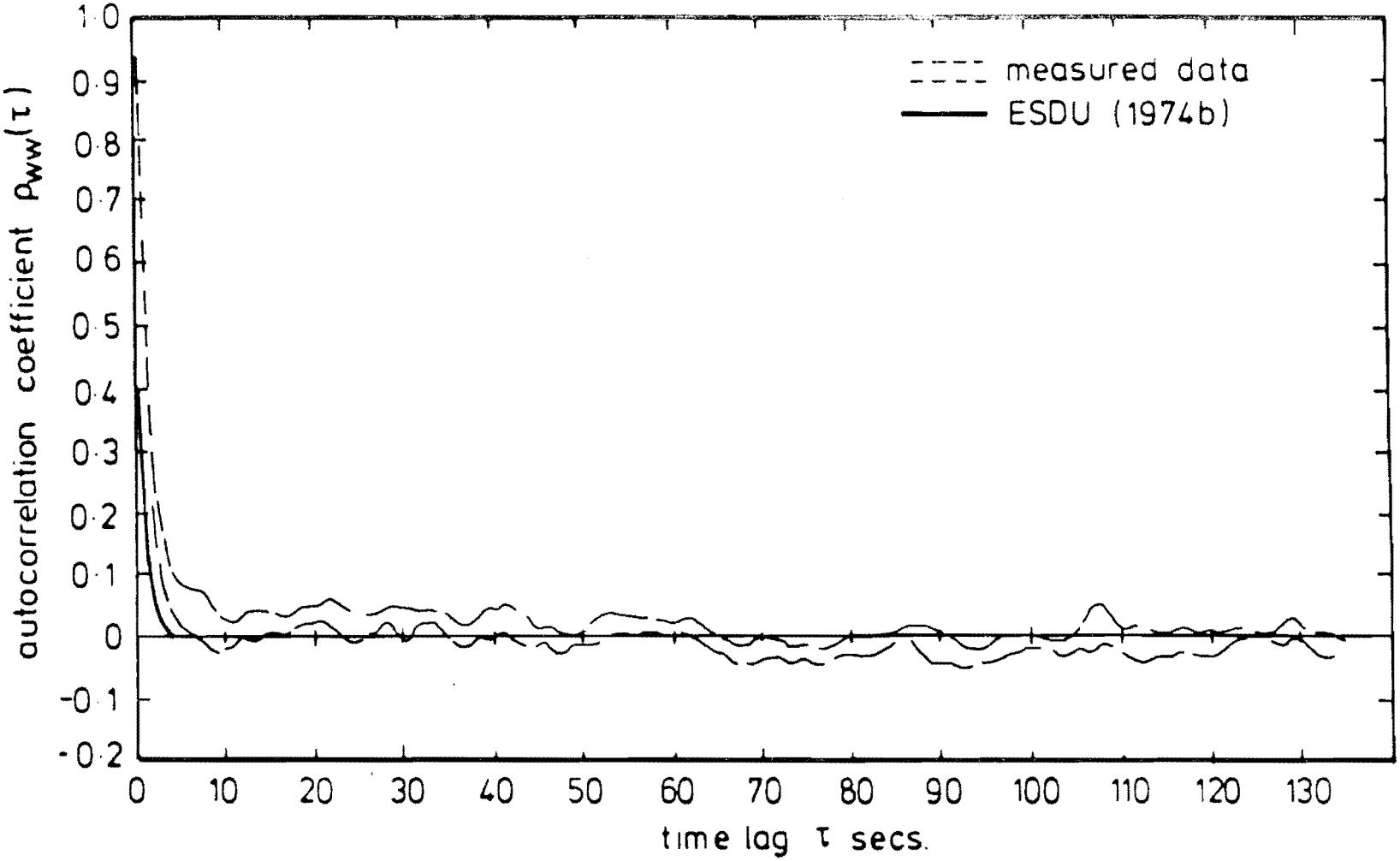

FIG 11·11 VERTICAL COMPONENT w AUTOCORRELATION FUNCTION FOR RUN 3

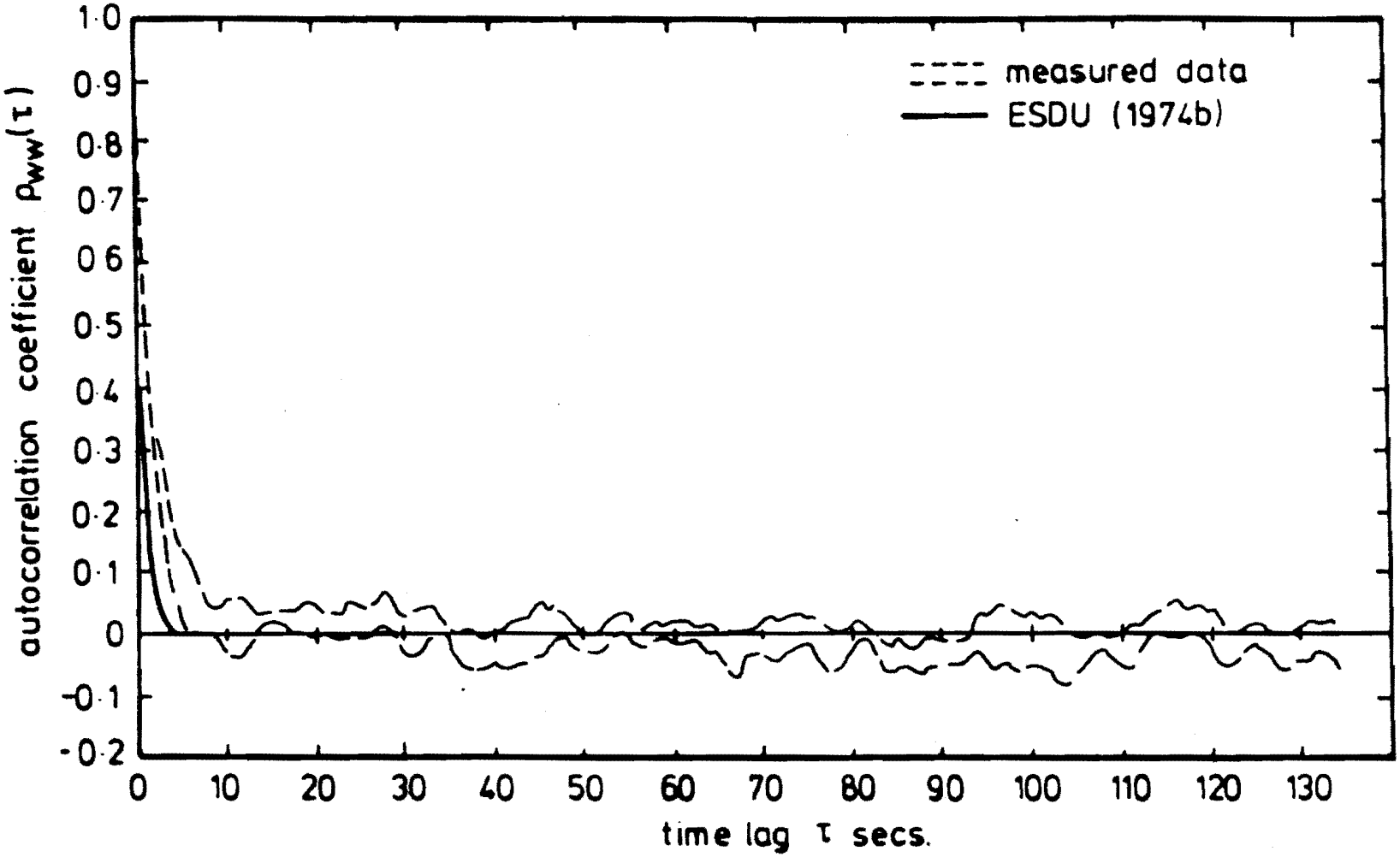

FIG 11·12 VERTICAL COMPONENT w AUTOCORRELATION FUNCTION FOR RUN 4

curves obtained from all Runs are virtually identical. The correlations fall very rapidly to zero and for Runs 2,3, and 4 the correlation is zero after seven seconds, but for Run 1 the correlation approaches zero after approximately twelve seconds. The correlation for all four Runs falls to .1 after approximately three to four seconds.

The presence of the ground restricts the formation of large eddies which means that the low frequency component in the power spectrum is therefore small and that the correlation falls to zero quickly.

Also plotted with the vertical component autocorrelation functions from the measured data is the autocorrelation curve predicted by ESDU (1974b) for the particular height and wind velocity range considered. This is given as a full line in the respective figures.

In all four Runs the ESDU curve underestimates the measured data. The vertical component propeller anemometer is rather insensitive to small vertical velocity fluctuations. This is because, as had been explained previously, the wind direction is usually very close to horixontal and often lies within the propeller's stalled region, or region where the length constant is rather large. This feature is also evident in the probability density functions of the vertical component data, given in Figs.8.10,8.11,8.12 and 8.13. The anemometer spends a relatively large proportion of time near its mean value, which presumably is the stopped position. It appears that a certain threshold vertical velocity is required to start the anemometer rotating.

It is the high frequency components of the vertical velocity fluctuations which contribute to the short time lags in the autocorrelation function. The lack of these high frequency components thus tends to increase the autocorrelation function for the vertical component velocities.

Although not shown in the figures, because of the difficulty of distinguishing different curves, it was apparent that there was a

small increase in correlation for a given time delay, say three seconds, with increase in anemometer height. This meant that the integral time scales in general increased with height and this feature is discussed further in the following Section.

11.5 THE INTEGRAL LENGTH SCALES OF TURBULENCE

The integral length scales from Runs 1,2,3, and 4 are shown plotted in Figs.11.13,11.14,11.15 and 11.16 respectively.

The integral length scales for the longitudinal component have been calculated and plotted for each level of anemometers using three methods :

(1) Integrating the autocorrelation function until the correlation dropped to .05, and then using Taylor's Hypothesis to convert the integral time scale to the integral length scale.

(2) Taking the time T_E, at which the autocorrelation dropped to a correlation of $\frac{1}{e}$ and again using Taylor's Hypothesis to convert the integral time scale to the integral length scale.

(3) Estimating the frequency of the peak of the ESDU (1974b) spectrum fitted to the measured data, and then calculating the integral length scale using Equation 11.6. (Note that the fitted ESDU spectrum is not shown in Figs.10.1,10.2, 10.3 and 10.4 which show the longitudinal component spectra.)

For Runs 1,2, and 3, in Figs.11.13,11.14 and 11.15 it can be observed that the length scale obtained by method (1) is larger than the value obtained by method (2) which is itself larger than the value obtained by method (3).

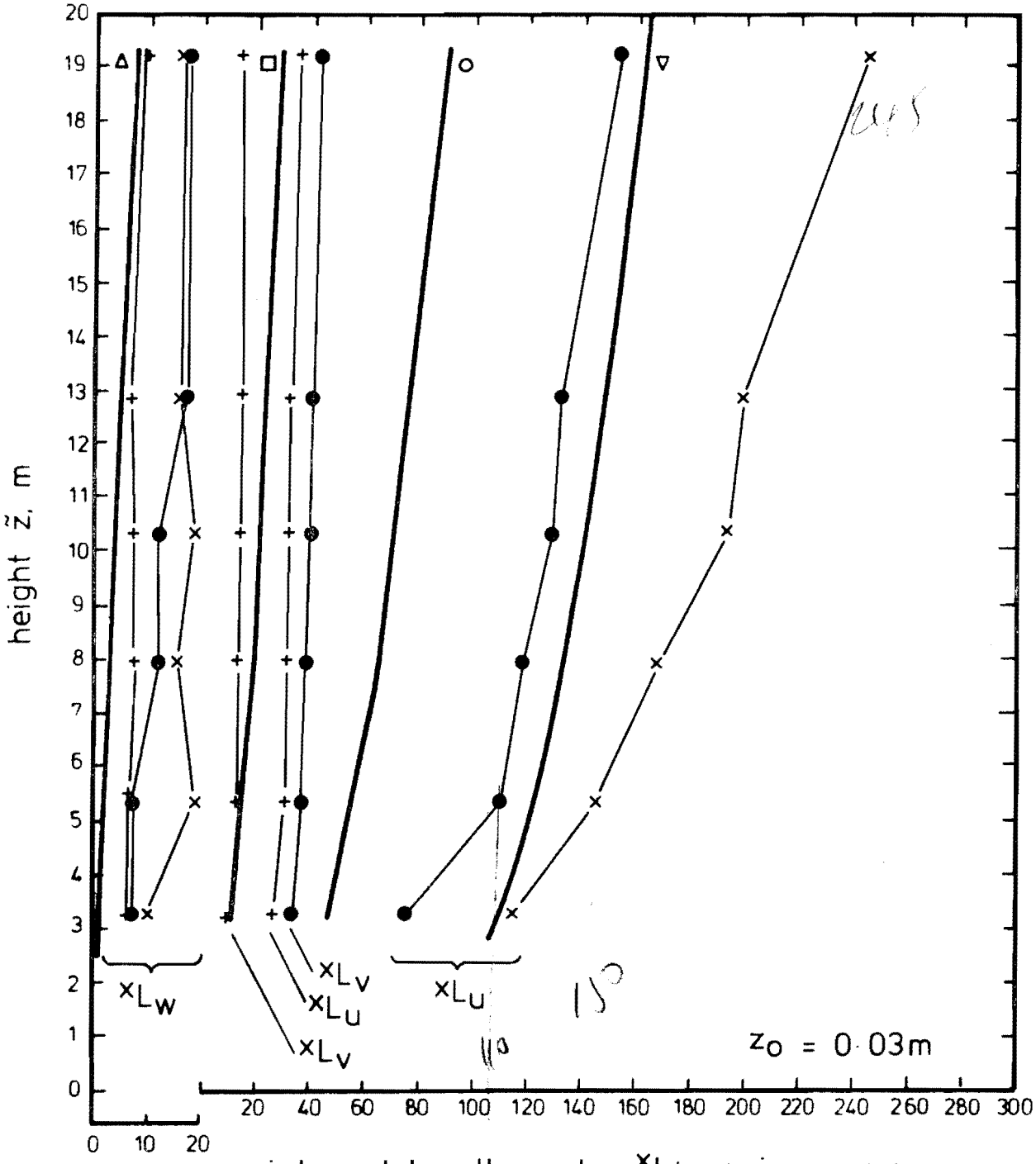

× $^{x}L_i = \bar{V}_{\tilde{z}} \int_0^{\rho_{ii}(\tau)\,=\,0.05} \rho_{ii}(\tau)\,d\tau$ i = u, v, w

● $^{x}L_i = \bar{V}_{\tilde{z}} \times T_E$ (at $\rho_{ii}(\tau) = \frac{1}{e}$) i = u, v, w

\+ $^{x}L_u = \frac{0.146\ \bar{V}_{\tilde{z}}}{n_p}$

$^{x}L_i = \frac{0.106\ \bar{V}_{\tilde{z}}}{n_p}$ i = v, w

Δ Teunissen (1970), ESDU (1974b) Counihan (1975), $^{x}L_w$

□ ESDU (1974b), $^{x}L_v$

o ESDU (1974b), $^{x}L_u$

▽ Counihan (1975), $^{x}L_u = 85(\tilde{z})^{0.22}$

FIG. 11·13 INTEGRAL LENGTH SCALE VARIATION WITH HEIGHT FOR RUN 1.

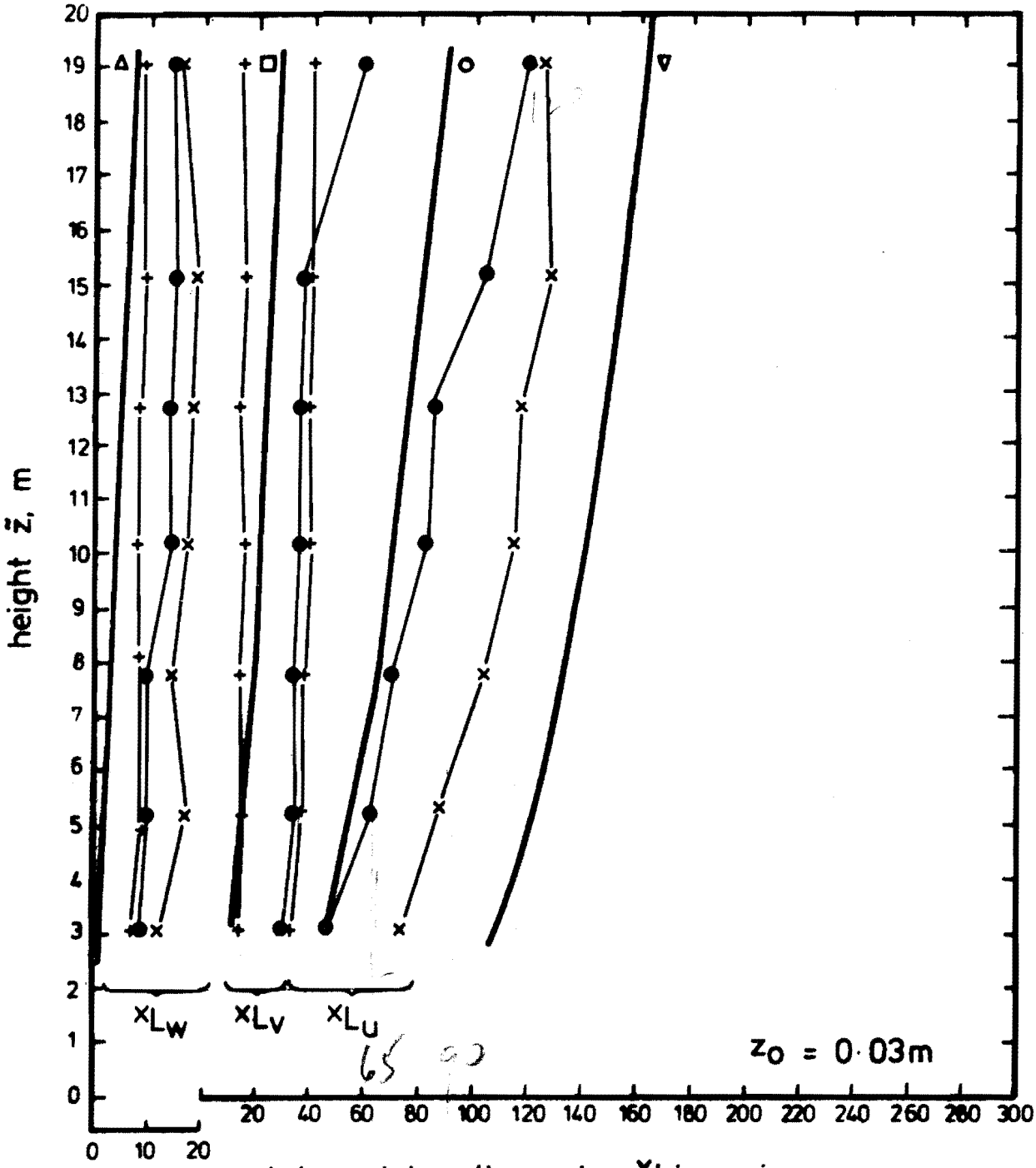

× $^{x}L_i = \bar{V}_{\tilde{z}} \int_0^{\rho_{ii}(\tau)=0.05} \rho_{ii}(\tau)\,d\tau$ i = u, v, w

● $^{x}L_i = \bar{V}_{\tilde{z}} \times T_E$ (at $\rho_{ii}(\tau) = \frac{1}{e}$) i = u, v, w

\+ $^{x}L_u = \dfrac{0.146\ \bar{V}_{\tilde{z}}}{n_p}$

$^{x}L_i = \dfrac{0.106\ \bar{V}_{\tilde{z}}}{n_p}$ i = v, w

▲ Teunissen (1970), ESDU (1974b) Counihan (1975), $^{x}L_w$

□ ESDU (1974b), $^{x}L_v$

○ ESDU (1974b), $^{x}L_u$

▽ Counihan (1975), $^{x}L_u = 85(\tilde{z})^{0.22}$

FIG. 11·14 INTEGRAL LENGTH SCALE VARIATION WITH HEIGHT FOR RUN 2.

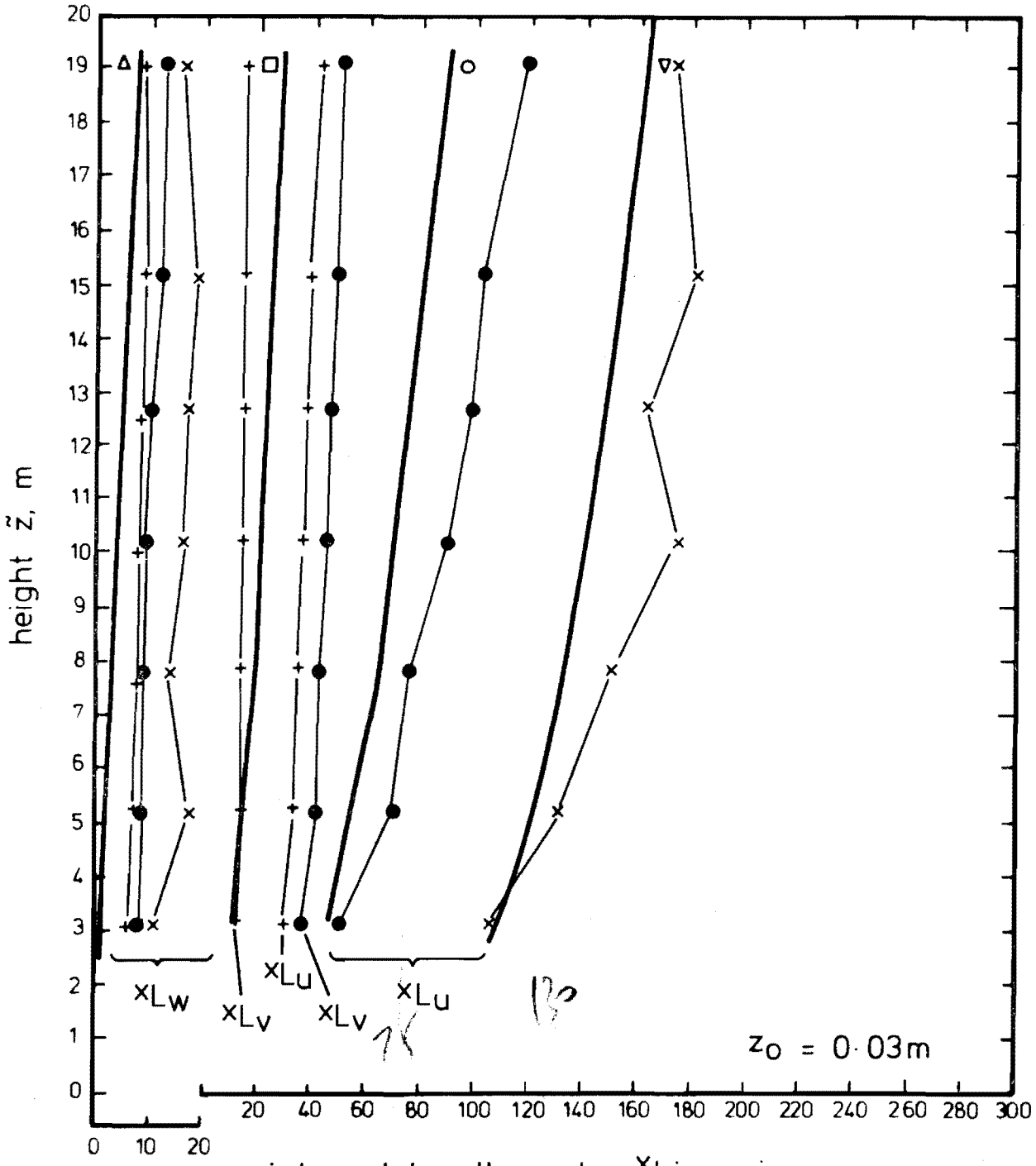

× $^{x}L_i = \bar{V}_{\tilde{z}} \int_0^{\rho_{ii}(\tau)=0.05} \rho_{ii}(\tau)\,d\tau$ i = u, v, w

● $^{x}L_i = \bar{V}_{\tilde{z}} \times T_E$ (at $\rho_{ii}(\tau) = \frac{1}{e}$) i = u, v, w

\+ $^{x}L_u = \frac{0.146\ \bar{V}_{\tilde{z}}}{n_p}$

$^{x}L_i = \frac{0.106\ \bar{V}_{\tilde{z}}}{n_p}$ i = v, w

△ Teunissen (1970), ESDU (1974b) Counihan (1975), $^{x}L_w$

□ ESDU (1974b), $^{x}L_v$

○ ESDU (1974b), $^{x}L_u$

▽ Counihan (1975), $^{x}L_u = 85(\tilde{z})^{0.22}$

FIG. 11·15 INTEGRAL LENGTH SCALE VARIATION WITH HEIGHT FOR RUN 3.

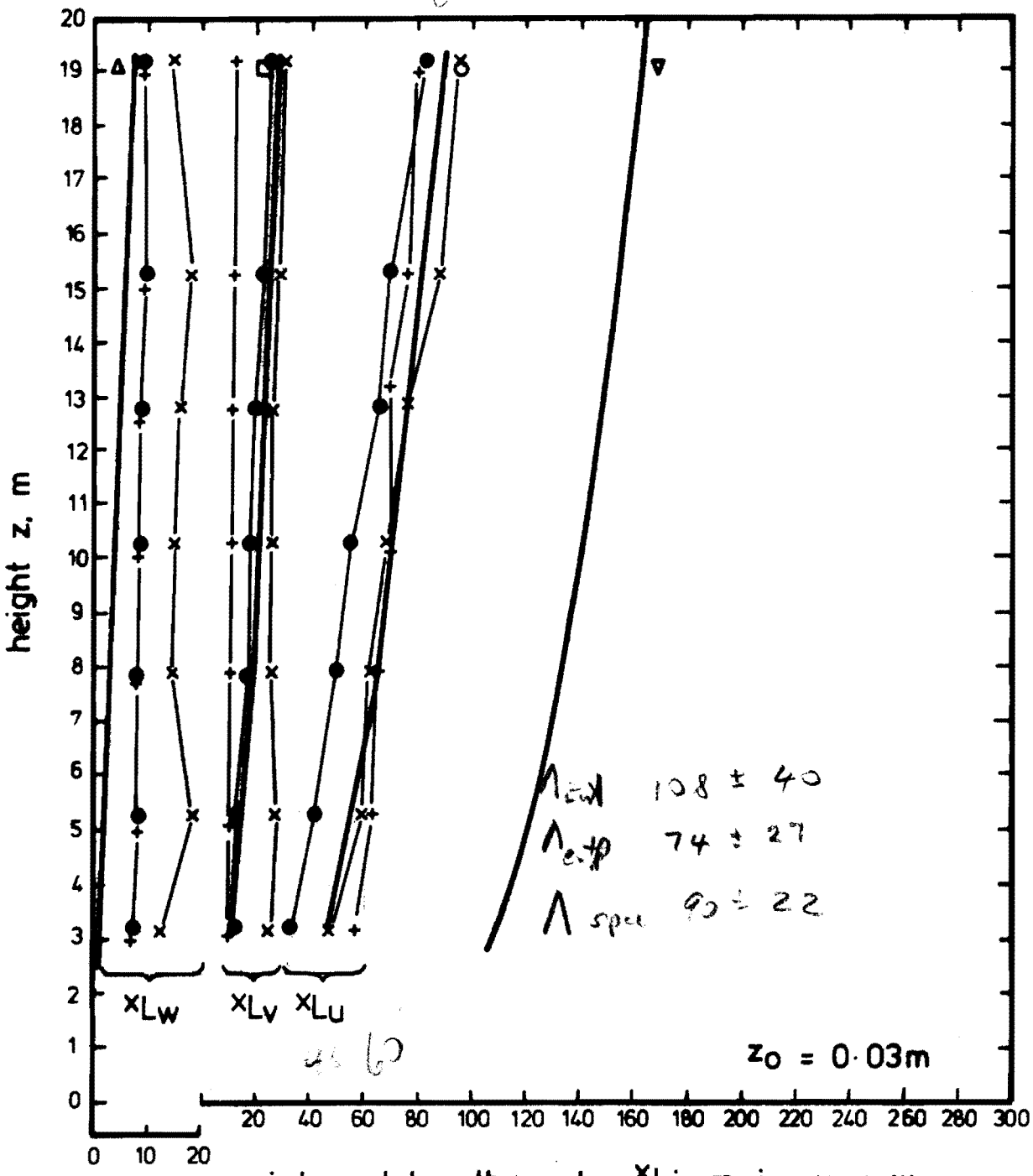

× $^{x}L_i = \bar{V}_{\tilde{z}} \int_0^{\rho_{ii}(\tau)=0.05} \rho_{ii}(\tau)\,d\tau$ i = u, v, w

● $^{x}L_i = \bar{V}_{\tilde{z}} \times T_E$ (at $\rho_{ii}(\tau) = \frac{1}{e}$) i = u, v, w

\+ $^{x}L_u = \frac{0.146\ \bar{V}_{\tilde{z}}}{n_p}$

$^{x}L_i = \frac{0.106\ \bar{V}_{\tilde{z}}}{n_p}$ i = v, w

▲ Teunissen (1970), ESDU (1974b) Counihan (1975), $^{x}L_w$

□ ESDU (1974b), $^{x}L_v$

○ ESDU (1974b), $^{x}L_u$

▽ Counihan (1975), $^{x}L_u = 85(\tilde{z})^{0.22}$

FIG. 11·16 INTEGRAL LENGTH SCALE VARIATION WITH HEIGHT FOR RUN 4.

Also plotted with the measured data, in the same figures are lines from empirical formulae suggested for the length scales from the results of previous research. Counihan (1975) recommends the formula

$$^{x}L_{u} = 85\ (Z)^{.22}$$

which is obtained when $Z_o = .03$ m. Values of $^{x}L_{u}$, $^{x}L_{v}$ and $^{x}L_{w}$ obtained off graphs from ESDU (1974b) are also plotted. The variation of $^{x}L_{w}$ recommended by ESDU (1974b) is virtually coincident with the variation suggested by Teunissen (1970) which is $^{x}L_{w} = .4Z$, and is also recommended by Counihan (1975).

For the longitudinal component, the integral length scale suggested by Counihan is much larger than that suggested by ESDU, in fact it is approximately twice as large. It is thus obvious that there is considerable variation in the values obtained from different literature. It is also apparent from the experimental results, that a considerable variation in values is obtained by computing the value by different methods.

The longitudinal component for Runs 1,2, and 3 shows that method (2) gives a more consistent result than method (i). Method (1) as stated previously is seriously affected by non-stationarities in the flow regime. Method (3) appears to underestimate the length scale compared with both the ESDU and Counihan predictions. Also, method (3) suffers from the problem that it is very difficult in practice to fit a spectral density curve, such as can be obtained from ESDU (1974b) to experimental data. This applies particularly at heights near the ground because the spectrum is fairly flat near the peak.

The data from Run 4 compares well with the values predicted by ESDU (1974b) for all heights. However it is considerably less than Counihan's prediction. It has already been noted that this data has less low frequency energy than the other Runs. The autocorrelation

curve fell towards zero more quickly than the others and consequently had a smaller length scale.

The lateral component integral length scales have been plotted on the same figures for each of the Runs. The experimental points for Runs 1,2, and 3 have been obtained by methods (2) and (3), (using Equation (11.7) instead of Equation (11.6) only, as it was obvious that method (1) would produce erroneous results because the autocorrelation curves approached towards zero slowly. The data from Run 4 has however been plotted by method (1) also.

For all four Runs the lateral component measured data is in good agreement with the variation in length scales predicted by ESDU. In all cases the length scale predicted by the peak of the power spectrum underestimates the ESDU values. The experimental values obtained by method (2) overestimate the ESDU prediction except for Run 4. In Run 4 all three methods obtain similar values.

The vertical component integral length scales are also plotted in the same figures but note the change of scale. Generally it is shown that ${}^{x}L_{w}$ computed via method (1) is greater than ${}^{x}L_{w}$ via method (2) which is greater than ${}^{x}L_{w}$ via method (3) (using Equation (11.8)). All three methods overestimate the integral length scale predicted by ESDU (1974b), Teunissen (1970) and Counihan (1975).

Physically it is possible for the vertical component anemometer to overestimate the autocorrelation function because it is insensitive to small scale vertical velocity fluctuations. This has been discussed more fully in the previous Section. The effect of non-stationarities on this component are negligible however, as the presence of the ground prevents the formation of eddies with a large vertical dimension, and low frequencies.

11.6 CONCLUSIONS

This Chapter discussed autocorrelation functions and integral length scales obtained from the four data Runs for each orthogonal velocity component.

It is immediately apparent from the longitudinal and lateral component autocorrelation functions, that non-stationarities in the flow prevented the autocorrelation curves approaching zero as rapidly as they should have done for trend free data, and thus made it difficult to obtain integral length scales from integral time scales. It is possible that a higher order trend line removed from the data would produce a more reliable result. Also high pass filtering the data to remove the very low frequency spectral components might help. Since the effect of non-stationarities in the flow did not appear to affect the correlation very much for correlations less than .3 to .4, it was possible to obtain length scales by assuming that the function behaved negative exponentially, and thus the time required for it to fall to a correlation of $\frac{1}{e}$ was taken.

Integral scales obtained from fitting spectral curves to experimental data are also subject to a large amount of error because of the difficulty of locating the peak frequency. The measured data showed that generally, fitting an ESDU spectrum to it gave relatively small values of the integral length scales, compared with the two other methods.

It has been mentioned many times in the literature that auto-correlation functions often do not fall to zero as quickly as they should, e.g. Blackman and Tukey (1958), Teunissen (1970), Harris (1971), Brook (1974) etc. It is a manifestation of the fact that at times appreciable amounts of energy lie in the range with periods between five minutes and two hours. It means that care has to be exercised when measurements of the atmospheric surface layer are taken.

The weather pattern must be stable.

The measured data showed that all components but particularly the longitudinal component integral time scale as well as the integral length scale increased with increase of height from the ground. This implies that not only are the eddies convected along faster at greater heights, but also their effect is apparent for longer periods of time because the integral time scale increases.

The values of the integral length scales obtained suggest that the eddies have a longitudinal dimension which is much larger than the lateral and vertical dimensions, and a lateral dimension which is longer than the vertical dimension.

It is interesting to note that ESDU (1974b) has the following comments regarding the measurements of autocorrelation functions. The comparisons discussed are with the ESDU (1974b) theoretical autocorrelation function formulae.

"Because the autocorrelation functions and power spectral densities are related by Fourier transforms, the uncertainties in estimating one function are reflected in the uncertainties in the other. No precise information on accuracy can be given but, in practice, providing non-stationarity effects are not present or are removed from measured data, then good agreement with the values of $\rho_{uu}(\tau)$ and $\rho_{vv}(\tau)$ *are obtained for heights above about 70 m. However, nearer the ground good agreement is still obtained for values of* τ *in the range corresponding to* $1.0 > \rho_{ii}(\tau) > \tilde{\sim} \cdot 3$ *but for larger time lags measured values of* $\rho_{ii}(\tau)$ *are erratic tending to be larger than those given by Equations (11.10 and (11.11)."*

"...The above comments relating to the u *and* v *components apply* [to the w component] *except that greater uncertainty can be expected for heights below about 100 m."*

CHAPTER 12

CROSS-CORRELATIONS WITH A VERTICAL SEPARATION

12.1 INTRODUCTION

12.1.1 Definitions

The definition of the cross-correlation function follows from the definition given for the autocorrelation function in Section 11.1.1. The cross-covariance function is defined as

$$C_{ij}(\underline{r},\underline{r}',\tau) = \overline{i(x,y,z,t).j(x',y',z',\ t+\tau)} \qquad (12.1)$$

$$\text{for } i,j = u,v \text{ or } w$$

where $\underline{r}$ and $\underline{r}'$ denote the position vectors of the two points.

$$= \lim_{T \to \infty} \frac{1}{T} \int_0^{\infty} i\ (\underline{r}\ ,\ t).j\ (\underline{r}'\ ,\ t+\tau)\ dt. \qquad (12.2)$$

$$i,j = u,v, \text{ or } w.$$

Usually the cross-covariance functions are normalised by dividing by the standard deviations of the constituent components to form cross-correlation functions, i.e.

$$\rho_{ij}\ (\underline{r}\ ,\ r',\ \tau) = \frac{C_{ij}(\underline{r}\ ,\ \underline{r}',\ \tau)}{\sigma_i\ \sigma_j} \qquad (12.3)$$

The discrete form of Equation (12.3) for sample time histories of N samples, Δt seconds between consecutive samples and a lag number of ℓ is

$$\rho_{ij}(\underline{r}\ ,\ \underline{r}',\ \ell\Delta t) = \frac{1}{N} \sum_{k=0}^{N-1} i(\underline{r}\ ,\ k).j(\underline{r}'\ ,\ k+\ell) \qquad (12.4)$$

$$i,j = u,v, \text{ or } w.$$

For an unbiased estimate, the Equation (12.4) becomes

$$\rho_{ij}(\underline{r}\ ,\ \underline{r}',\ \ell\Delta t) = \frac{1}{N-\ell} \sum_{k=0}^{N-\ell-1} i(\underline{r}\ k).j(\underline{r}'\ ,\ k+\ell) \qquad (12.5)$$

$$i,j = u,v, \text{ or } w\ ,\ \ell = 0,1,\ \ldots m\ .$$

and m is normally limited to less than $^{N}/10$.

For homogenous, isotropic turbulence, the cross-correlation should be a function only of the separation distance between the points considered.

It is often reasonable to assume horizontal homogenuity in the atmospheric surface layer if the terrain is of uniform roughness over a large area, and is reasonably flat. The atmospheric surface layer is not homogenous in a vertical direction however. Hence it is expected that cross-correlations obtained at different heights would vary with height and with the separation distance between the velocity components.

12.1.2 Analysis Procedure

Although Equations (12.4) and (12.5) could easily be calculated by a product summation technique, in a similar manner to calculating Reynolds stresses, the equation was not evaluated using that method. Instead the two data streams were calculated with the method involving Fourier transforms. The program used was PSAUTCORS, and the method of the analysis has been detailed in Section 5.6.2.3. The program calculated Equation (12.4), a biased estimate of $\rho_{ij}(\underline{r}, r', \ell\Delta t)$, but this was assumed to be a very good approximation to Equation (12.5) because m was only 1% - 5% of N.

The overall cross-correlation evaluation method is given briefly below.

Assume that there are two data streams which have been cosine corrected, trends removed, mean removed and normalised by dividing the appropriate standard deviations.

(1) Take the forward Fourier transform of both data streams.

(2) Turn one set of frequency data into its complex conjugate.

(3) Multiply the two frequency data streams together.

(4) Take the inverse Fourier transform of the resultant data stream of (3).

The cross-correlation data is now contained in the output data from (4). For short time lags compared with the number of data samples, the required data lies at the ends of the output arrays from (4).

12.1.3 The Significance of Cross-correlations

In determing the loading on tall structures, e.g. towers, chimneys, tall buildings etc., it is often desirable to know of the approximate physical dimensions of a gust likely to impinge on the structure at a given time. A cross-correlation function with a vertical separation, which can be obtained by simultaneous wind velocity measurements from a single vertical tower can help provide this information.

The correlation of velocities at points separated in the vertical direction gives an appreciation of how much a velocity measurement at one point can predict the velocity at another point. When the points are close, the velocity measurements are highly correlated, but for a large separation, providing that there are no trends, or periodicities in the flow, the correlation is small.

The most important correlation that can be measured by a single tower is $\rho_{uu}(\Delta z,0)$. This is the zero time delay cross-correlation between the longitudinal component velocity fluctuations separated by a vertical distance Δz. Since atmospheric turbulence is often horizontally homogeneous, but only vertically homogeneous at heights well above the surface layer, the correlation $\rho_{uu}(\Delta z,0)$ is a function of the actual positions of the two measurements, not just of the separation distance Δz.

Two other correlations which have been calculated and are presented here are $\rho_{vv}(\Delta Z,\tau)$ and $\rho_{ww}(\Delta Z,\tau)$. They are respectively the correlations between the lateral component wind velocities, and the vertical component wind velocities, both separated by a distance ΔZ, and with one signal delayed in time with respect to the other by τ seconds. These two cross-correlations are of lesser importance than $\rho_{uu}(\Delta Z,\tau)$.

Cross-correlation measurements of wind velocities obtained from anemometers are not particularly prevalent in the literature. However there are many more measurements of cross-correlations with ΔZ separation, than measurements with a ΔX and/or ΔY separation. This is because measurements have often been obtained from several anemometers up a single tower, but rarely have they been obtained from anemometers mounted on rows of towers, separated either in the predominantly streamwise, or across streamwise direction.

This work presents cross-correlation functions in the time domain. Often the cross-correlation function has been presented in the frequency domain where the function obtained is the coherence function defined as :

$$\gamma_{ii}^{2}(\Delta r,\, n) = \frac{\left|S_{ii}(\Delta r,\, n)\right|^{2}}{S_{ii}(n).S_{ii}'(n)} = \frac{P_{ii}^{2}(\Delta r,\, n) + Q_{ii}^{2}(\Delta r,\, n)}{S_{ii}(n).S_{ii}'(n)} \qquad (12.6)$$

$P_{ii}(\Delta r,\, n)$ and $Q_{ii}(\Delta r,\, n)$ are called the co-spectral density and quad-spectral density functions respectively, and are related to the phase-lag angle by

$$\theta_{ii}(\Delta r,\, n) = \tan^{-1}\frac{Q_{ii}(\Delta r,\, n)}{P_{ii}(\Delta r,\, n)} \qquad (12.7)$$

$S_{ii}(n)$ and $S'_{ii}(n)$ are the single point power spectral density functions at the two points $\underline{r}$ and $\underline{r}'$. Essentially the co-spectrum measures the contributions of different frequency intervals to the covariance between the variables, and the quad-spectrum measures such contributions when the spectral estimates of one series are shifted by 90° with respect to the

other series. ESDU (1974a) states that physically the coherence at frequency n can be thought of as being derived from the cross-correlation (or mean product) with zero time lag of the identically filtered signals $i(t;n,\delta n)$ and $j(t;n,\delta n)$. It thus gives a measure of the spatial scale of turbulence associated with that frequency.

The coherence has often been assumed to be a function with the form :

$$\gamma_{ii}(\Delta r, n) = \exp(- a.n.\Delta r/\bar{V}_z) \qquad (12.8)$$

where a is a constant depending upon the separation direction, stability and slightly on z_o, n is frequency, Δr separation distance, and $\bar{V}_z$ a representative velocity for the height or height range under consideration.

12.2 CROSS-CORRELATION VARIATION WITH TIME LAG τ

A typical cross-correlation curve for $\rho_{uu}(\Delta z, \tau)$ is given in Fig.12.1. It can be seen that the correlation has a maximum value near $\tau = 0$, but not exactly at $\tau = 0$. The correlation falls most rapidly for time lags near where the peak occurs and falls most rapidly for curves with large correlation values, so that they are much more "peaky" than curves with a low correlation. After time delays of $\sim \pm$ 15 seconds the curves for all separation distances tend to merge together, so that for time lags of $|\tau| > 15$ seconds, the actual distance between the anemometers is not important, and all correlations merge towards the same values.

It also can be observed in Fig.12.1 that as Δz increases, the time lag τ for maximum correlation occurs at more negative values. The graphs have been drawn such that when a maximum correlation occurs at negative values, it means that the data stream from the top anemometer array has been delayed in time with respect to the data stream from the bottom anemometer array. Physically this means that because of the wind

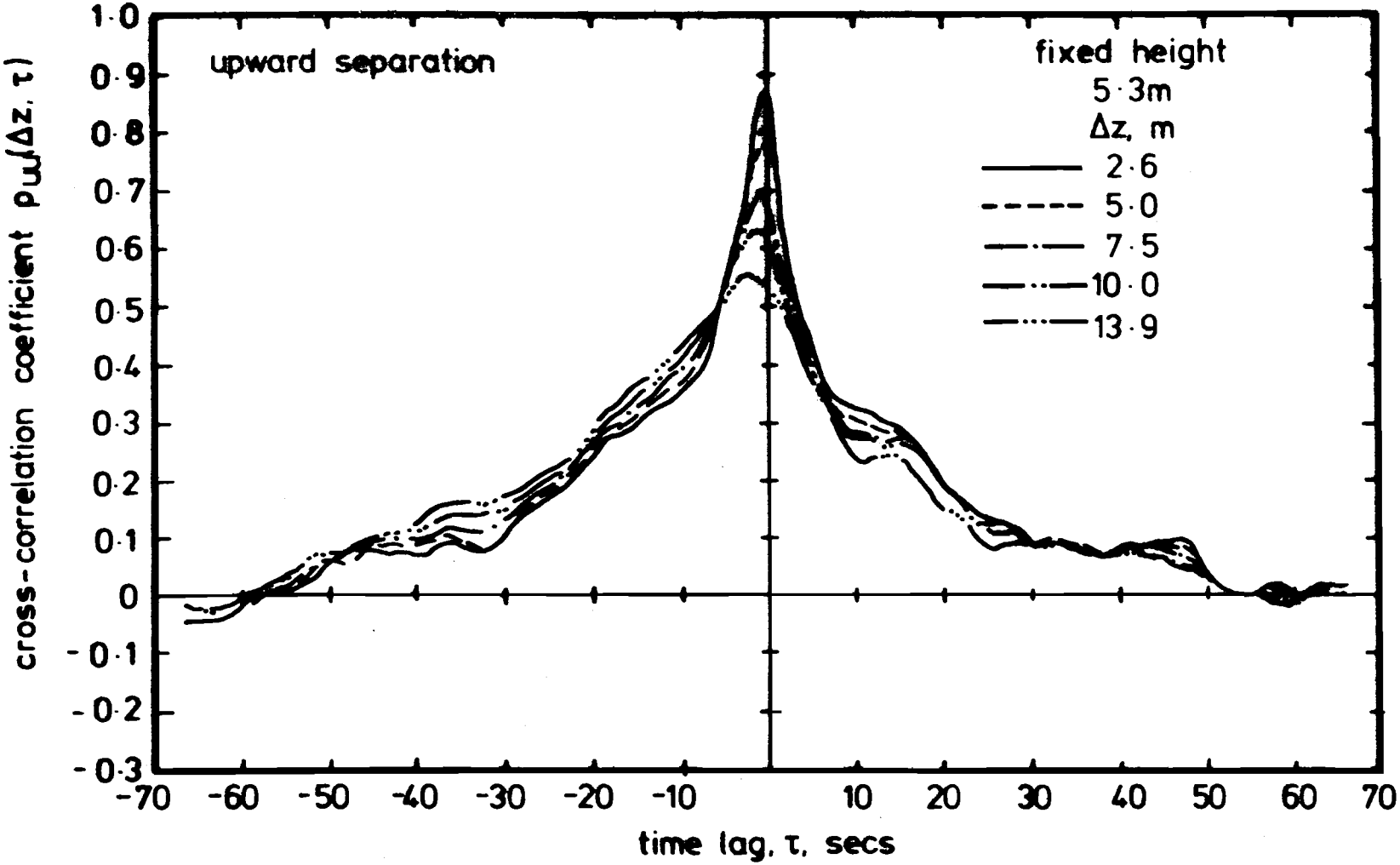

FIG. 12·1 LATERAL CROSS-CORRELATION $\rho_{uu}(\Delta z, \tau)$ FOR RUN 2.

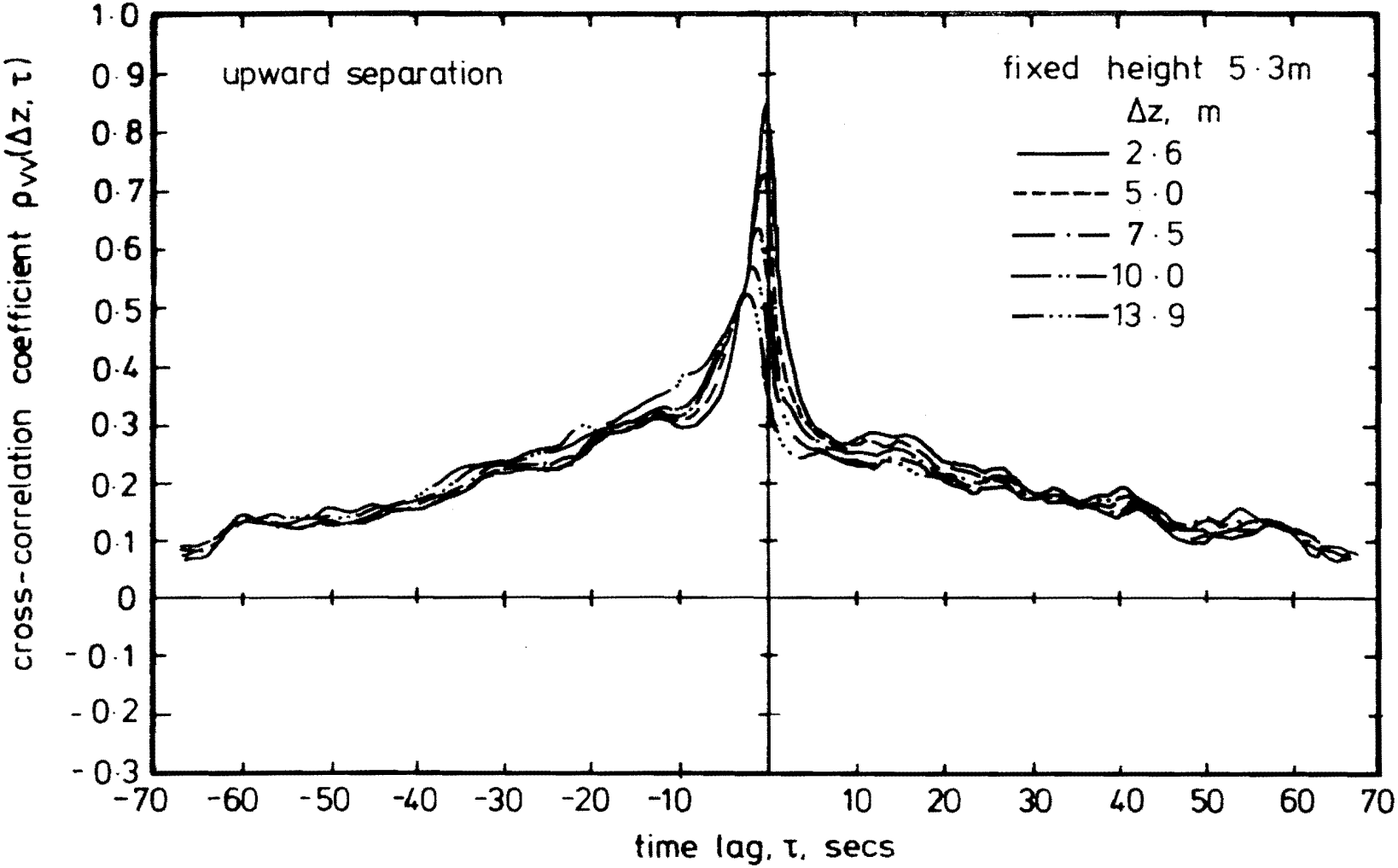

FIG. 12·2 LATERAL CROSS-CORRELATION $\rho_{vv}(\Delta z, \tau)$ FOR RUN 2.

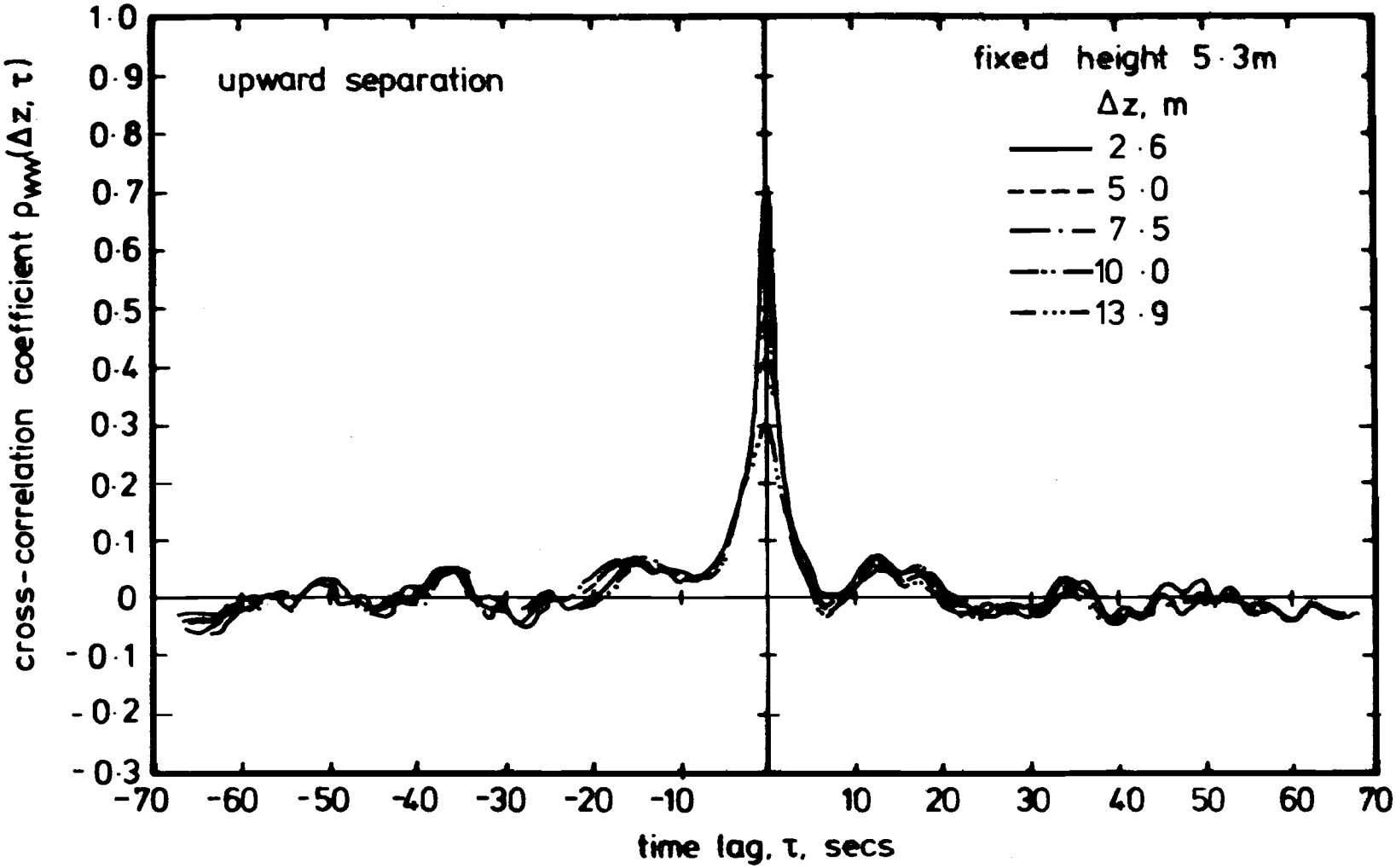

FIG. 12·3 LONGITUDINAL CROSS-CORRELATION $\rho_{ww}(\Delta z, \tau)$ FOR RUN 2.

shear, gusts occur at the top anemometer before reaching the bottom one. Fig.12.2 shows a series of cross-correlation curves for various vertical separation distances from Run 2 for the v component velocity. It can be seen that the same feature of the time for the maximum correlation is apparent as was observed for the longitudinal velocity component. This means that with both the longitudinal and the lateral velocity components, changes in wind velocity at a higher level are followed by "similar" changes in velocity at a lower level.

A typical vertical component $\rho_{ww}(\Delta Z, \tau)$ cross-correlation curve has been plotted in Fig.12.3. It can be seen that for the correlations shown the maximum correlation occurs at $\tau = 0$, i.e. changes in the vertical velocity component on average occur simultaneously at all levels. This means that the number of times changes at a higher level occur before changes at a lower level is approximately equal to the number of times changes at a lower level precede changes at a higher level.

It can also be observed from the figure that the correlation drops off very rapidly for $0 < |\tau| < 5$. For time lags greater than $\pm$ 5 seconds, the velocity components are virtually uncorrelated. Also a similar feature is observed in Fig.12.3 as shown in Figs.12.1 and 12.2. For time lags greater than $\pm$ 5 seconds all the correlation curves tend to merge together and are not functions of the separation distance between anemometers.

12.3 THE STREAMWISE CORRELATION FUNCTION $\rho_{uu}(\Delta Z, \tau)$

The correlation between the streamwise u components, with separation distance ΔZ is shown plotted in Fig.12.4. The correlation curves are a series of lines, with each curve having one fixed anemometer as a reference anemometer.

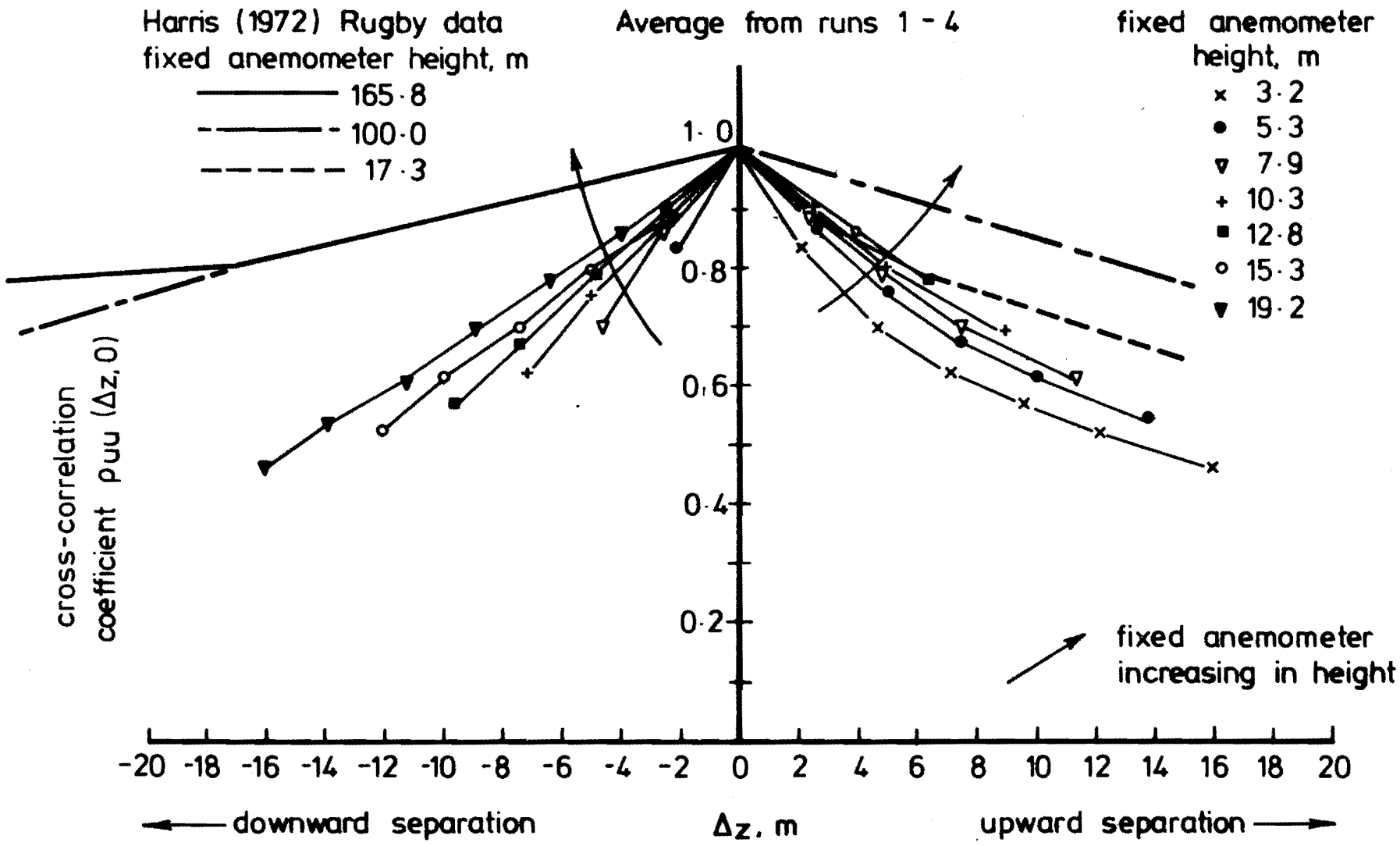

FIG 12·4 LATERAL CROSS-CORRELATION $\rho_{uu}(\Delta z, 0)$

It can be seen that the correlation curves are not only a function of Δz, but also of the height of the fixed anemometer which is used as a reference. It can be seen that the zero time lag correlations obtained for separations upward from a reference anemometer are larger than correlations taken with a downward separation for any given Δz. Also the correlation values increase as the reference height increases. This means that the size of the eddies increases with increase in distances from the ground.

It can be seen that even for the largest separation possible for this combination of anemometer heights, the correlation is still quite large, being about .45. Consequently estimation of the length scale $^{z}L_{u}$ would give a very unreliable value, and hence is not estimated. Also plotted on the same graph are correlation curves obtained by Harris (1972) on the 166 m tower at Rugby. The tower used in the work of Harris (1972) was much higher than the one used in this work. Harris measured zero lag cross-correlation values that are significantly larger than those measured here. However it can be observed that his reference anemometer heights are much greater than those in this work. The values of Harris observe the general trend that the correlation increases with increase in reference anemometer height above the ground.

In Fig.12.5, the zero time lag cross-correlation values and the maximum cross-correlation values obtained are plotted for fixed anemometer heights of 3.2, 10.3 and 19.2 m. It can be seen that the maximum cross-correlation value is only slightly larger than the zero lag cross-correlation value. This means that even though changes in wind velocity at a lower level follow changes in velocity at a higher level, adequate measurements of the maximum value of $\rho_{uu}(\Delta z, \tau)$ can be obtained simply with a zero time lag correlation. The integral length scale $^{z}L_{u}$ obtained would not be much different from a value obtained from integrating $\rho_{uu}(\Delta z, \tau_{m})$ where τ_{m} is the time lag when the maximum correlation occurs.

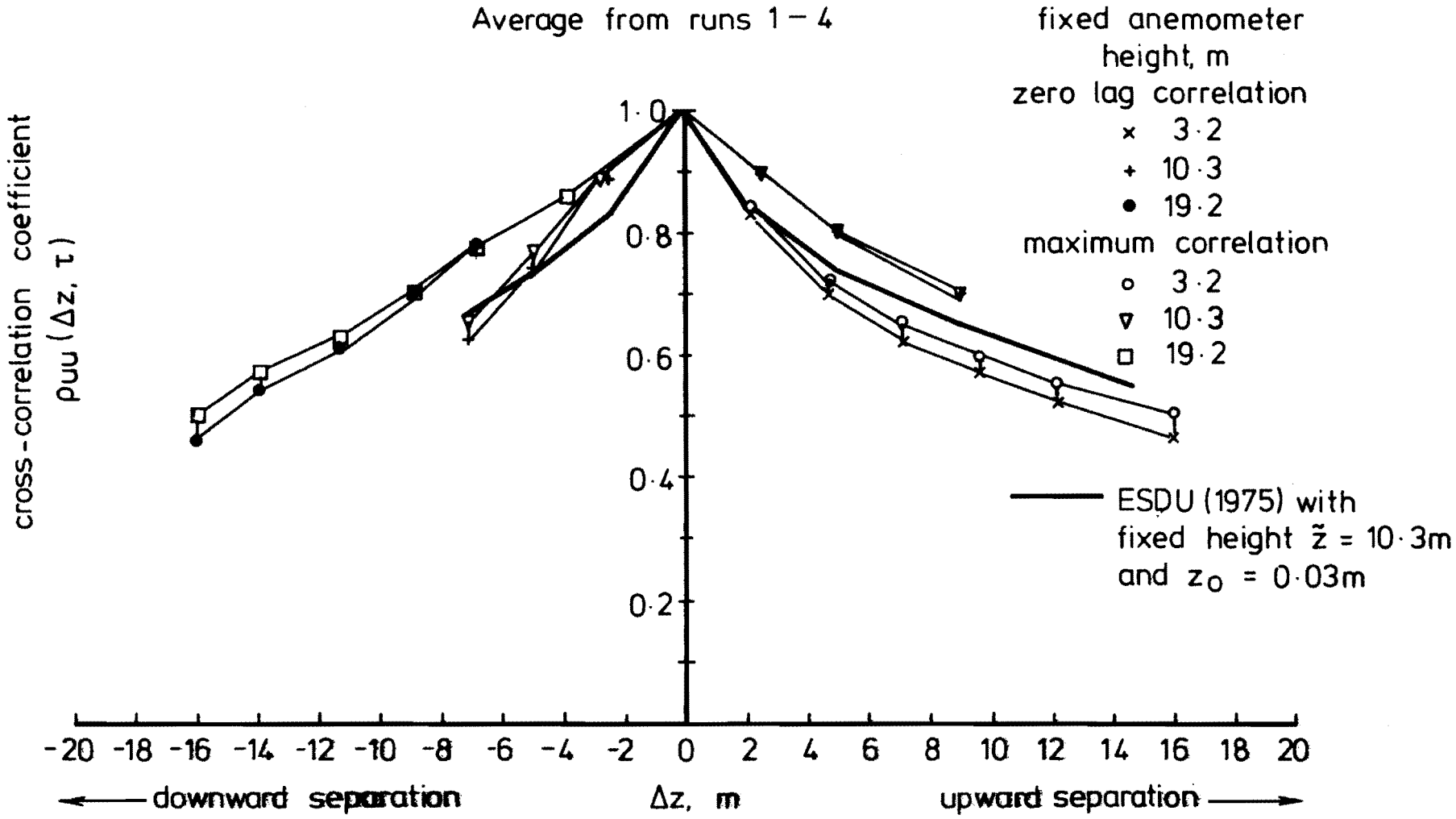

FIG 12·5. LATERAL CROSS-CORRELATION $\rho_{uu}(\Delta z, \tau)$ COMPARISON BETWEEN ZERO LAG CORRELATION, MAXIMUM CORRELATION AND ESDU (1975)

Also plotted in the same figure is a curve from ESDU (1975). It is a curve obtained for a fixed reference anemometer height of 10.3 m, for zero time lag and for the symmetrical or even part of the cross-correlation function. The symmetrical part of the cross-correlation has been estimated from the von Kármán equations for isotropic turbulence with appropriate values of the integral length scale to allow for the distortion of turbulence at heights close to the ground.

It can be seen that the estimate from ESDU (1975) is close to the measured values although it does underestimate slightly the measured values for the fixed anemometer height of Z = 10.3 m.

It was also decided to see how the position of maximum correlation, i.e. how the value of τ_m varied with ΔZ and the two heights Z_1 and Z_2 ($\Delta Z = Z_2 - Z_1$).

Consequently for each correlation curve for all combinations of levels and all Runs, τ_m was measured for the longitudinal and lateral velocity components. The average value of τ_m for each pair of levels over the four Runs was calculated. This value was then multiplied by the average value of $\frac{1}{2}(\bar{V}_{Z_2} + \bar{V}_{Z_1})$ over the four Runs, i.e. the average velocity for the pair of heights considered. This obtained an equivalent distance by which the upper anemometer signal preceded the lower one of the pair. This "delay distance" has been plotted in Fig.12.6 versus the separation distance ΔZ between anemometers. Curves have been drawn for both the longitudinal u, and lateral v velocity components.

Separate curves have been drawn depending on the height of the lower level anemometer of the pair considered. These curves could not be obtained very accurately because τ_m could only be estimated to approximately $\frac{1}{2}$ second, however the general trends can be observed.

For a given vertical separation ΔZ between anemometers the delay distance is longer the closer the anemometers are to the ground. The

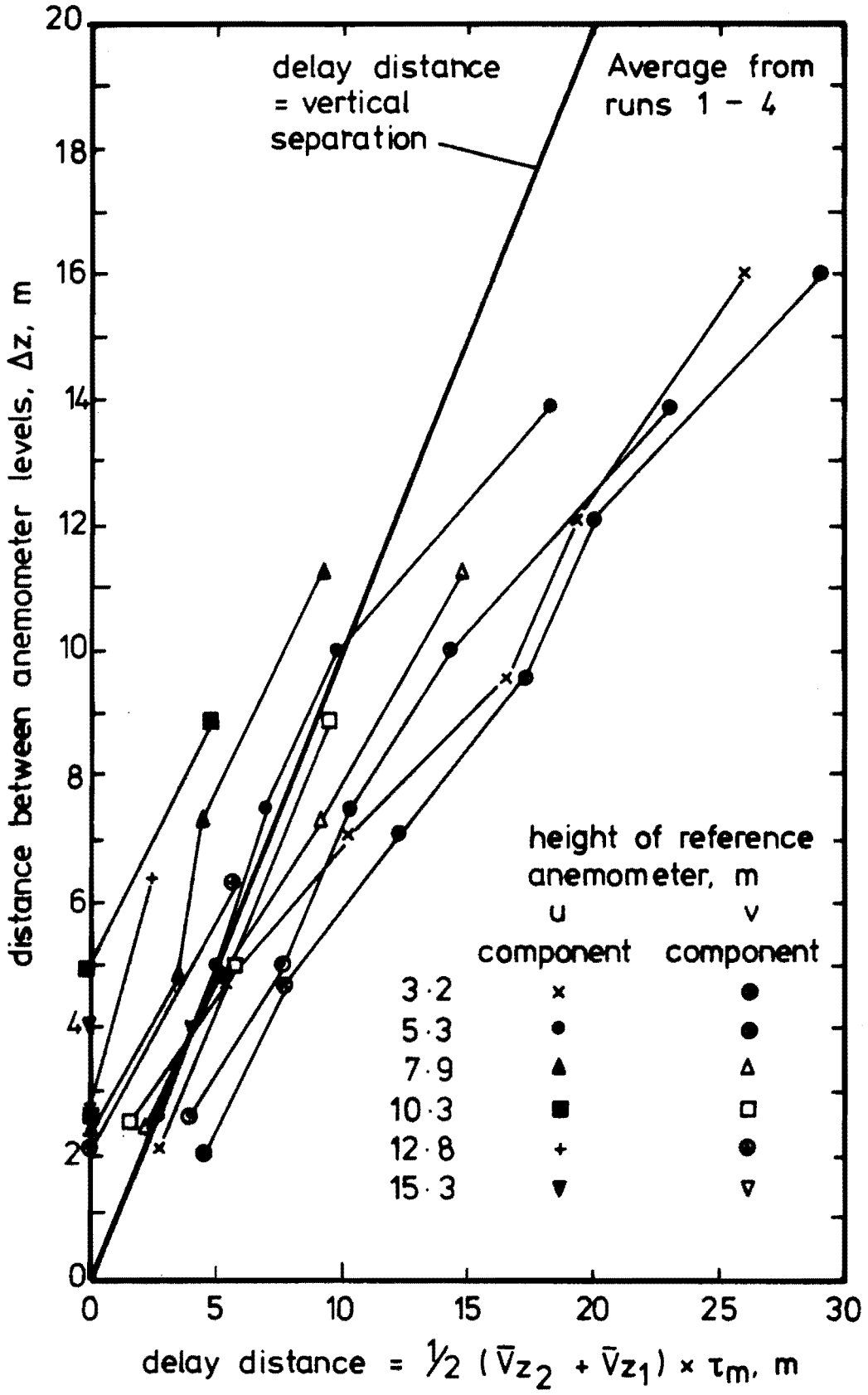

FIG. 12·6. VARIATION OF DELAY DISTANCE FOR MAXIMUM CORRELATION, WITH VERTICAL DISTANCE BETWEEN ANEMOMETERS, AND HEIGHT OF BOTTOM ANEMOMETER.

delay distance is approximately proportional to the separation distance ΔZ, although it appears to increase more the closer the anemometer pairs are to the ground. In all cases the delay distance for the lateral component is greater than the delay distance for the longitudinal component. Davenport (1961b) states that the maximum correlation occurs for the longitudinal component when the upper level station leads by an amount approximately equal to the vertical distance between stations. Davenport considered the longitudinal component only and this work would tend to support his earlier observation. Similar features regarding the variation of τ_m with height have also been observed by Shiotani and Iwatani (1971). It was also observed by Shiotani and Iwatani that for a given ΔZ the correlation increased with increase in height above the ground as has also been observed here. Harris (1968a) and Harris (1972) has observed similar features, although since the height range in the Harris data was much larger than the height range considered here, the correlations from Harris are larger as is shown in Fig.12.5.

Panofsky (1973) also states that the ratio of the horizontal delay distance to vertical separation between anemometers is of order unity and is twice as large for the v component than for the u component of velocity. This agrees with the observations made in this work.

12.4 THE CROSS STREAMWISE CORRELATION FUNCTION $\rho_{vv}(\Delta Z, \tau)$

Estimates of the cross-correlation values for $\rho_{vv}(\Delta Z, \tau)$ were more difficult to obtain because in Runs 1, 2 and 3 the correlation values did not drop to zero after about ± 10 seconds as expected. This is shown in Fig.12.2. Instead they tended to almost constant values for time lags greater than ± 20 seconds. This feature has been observed by others e.g. Panofsky (1961), who found that at night-time the correlation extended only to a plateau which may have been as high as a correlation of .80. Lumley and Panofsky (1964) state that this occurs in stable

air under low windspeed conditions when the wind direction changes slowly or meanders. Such eddies have periods of the order of 20 minutes or longer and perhaps have horixontal dimensions of the order of 100 m to several km.

Of course, the wind data recorded here was not recorded under stable conditions, however the variations in velocity and direction must have caused the correlation not to fall to zero. Since a parabolic trend line was removed from the data, the results tend to show that this was not sufficient and that higher order trends must have existed in the data.

However, Panofsky (1961) contains a formula which he ascribes to Webb (1955), which can be used to correct the correlation values when they do not approach towards zero for long time delays. Panofsky (1961) states that if a slowly varying function is superimposed on a rapidly varying record, the measured correlation function is given by

$$r_m = (1 - r_\infty)\, r_t + r_\infty \qquad (12.9)$$

r_t is the correlation function due to the rapid fluctuations only, r_∞ is the height of the plateau, or the correlation approached at large lags and r_m is the measured correlation.

For Runs 1,2 and 3, the lateral component correlation function and zero time lag and at τ_m was calculated using Equation (12.9). It was pleasing to observe that the values of r_t so calculated were very close to the values of the correlation coefficient for Run 4,which did not display the trend like behaviour.

The values of the correlations for all combinations of levels were averaged over the four Runs. The cross-correlation function $\rho_{vv}(\Delta Z, 0)$ has been plotted in Fig.12.7. Similar trends are observed in the figure to the longitudinal component, except that the correlation of

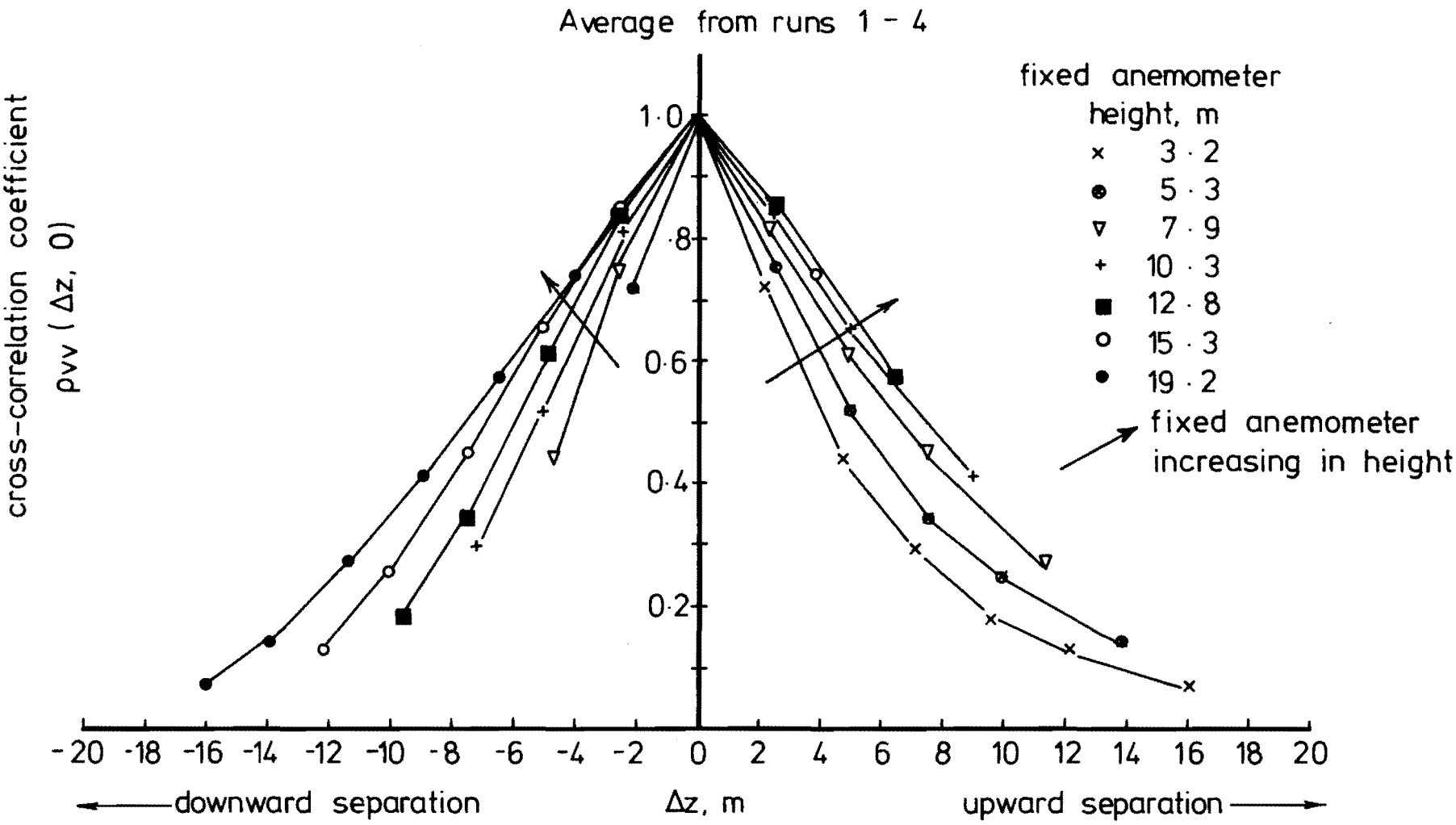

FIG 12·7 LATERAL CROSS-CORRELATION $\rho_{vv}(\Delta z, 0)$

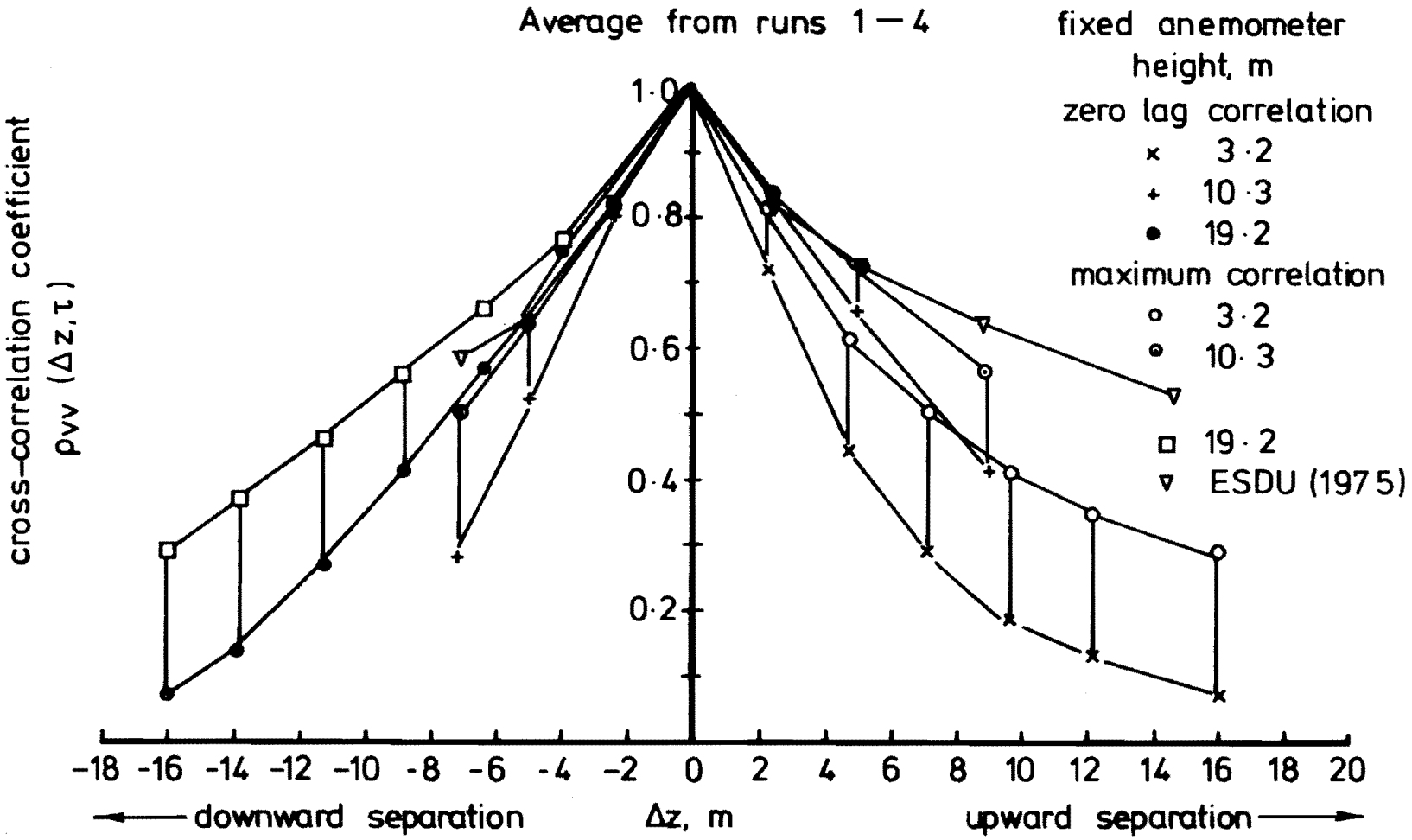

FIG 12·8 LATERAL CROSS-CORRELATION $\rho_{vv}(\Delta z, \tau)$ COMPARISON BETWEEN ZERO TIME LAG CORRELATION, MAXIMUM CORRELATION, AND ESDU (1975)

the lateral component decreases much more rapidly with increase in Δz. For a given Δz, the correlation increases with increasing height and for a given fixed anemometer level, the correlation with an anemometer above the fixed anemometer level is higher than the value of the correlation with an anemometer below the fixed anemometer level.

The zero time lag correlation and maximum correlation values of the lateral velocity components have been plotted in Fig.12.8 for three fixed anemometer levels. It is immediately obvious that the maximum correlation values are significantly greater than the zero time delay values. This means that a value of ${}^{z}L_{v}$ calculated from zero time delay cross-correlations is significantly smaller than ${}^{z}L_{v}$ calculated from cross-correlations at τ_m. However, the latter integral length scale is probably of little importance because for structural loading purposes the gust which envelopes the structure at one instant of time is of more physical significance. Also ${}^{z}L_{v}$ is significantly smaller than ${}^{z}L_{u}$.

The delay distance required between anemometers at different levels for the maximum correlation to occur is given in Fig.12.6. As stated in Section 12.3, the trends are the same for both the lateral and longitudinal components but the delay distance is greater for the lateral component than for the longitudinal component.

Since the correlation $\rho_{vv}(\Delta z, 0)$ falls nearly to zero in the height range considered, the length scale ${}^{z}L_{v}$ can be estimated approximately by integrating the area in Fig.12.7. This gives, ${}^{z}L_{v} = 6 - 8$ m. whereas ESDU (1975) for $z_o = .03$ m and $z = 10$ m gives ${}^{z}L_{v} = 16$ m.

12.5 THE VERTICAL COMPONENT CORRELATION FUNCTION $\rho_{ww}(\Delta z, \tau)$

Since the vertical component spectrum contains very little low frequency energy it does not show the trend like behaviour which is sometimes observed for the longitudinal and lateral components. Consequently the correlation curves for $\rho_{ww}(\Delta z, \tau)$ drop to zero quickly as can be

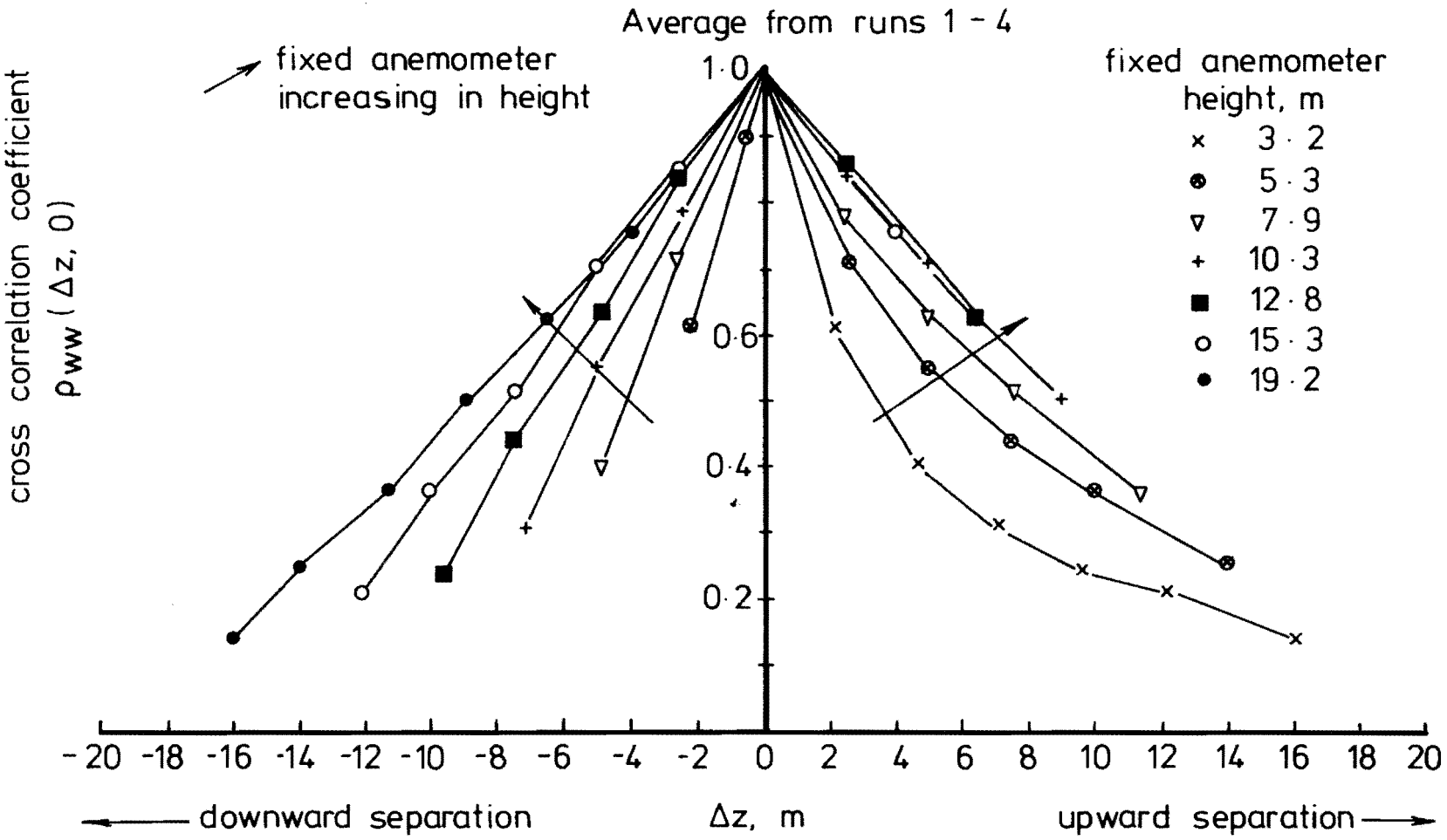

FIG 12·9 LONGITUDINAL CROSS-CORRELATION $\rho_{ww}(\Delta z, 0)$

observed in Fig.12.3. For each pair of anemometers, the correlation was simply read off the correlation-time lag graph at $\tau = 0$. This was because the maximum correlation occurred for this component when $\tau = 0$.

The value of $\rho_{ww}(\Delta Z, 0)$ for each pair of anemometer levels, averaged over the four Runs is given in Fig.12.9. It shows similar characteristics to both the longitudinal and lateral components, however for a given ΔZ the increase in $\rho_{ww}(\Delta Z, 0)$ with increase in height of the fixed anemometer is rather more striking. For a given fixed anemometer height and ΔZ, the upward correlation is again larger than the downward correlation. Comparing Fig.12.9 with Fig.12.7, it can be seen that ${}^{z}L_{w} \approx {}^{z}L_{v}$. This shows that like ${}^{z}L_{v}$, ${}^{z}L_{w} \approx 6 - 8$ m also, but is more strongly dependent on the height range above the ground.

$\rho_{ww}(\Delta Z, \tau)$ and ${}^{z}L_{w}$ are of little apparent importance physically, but have been presented here for completeness.

12.6 CONCLUSIONS

Cross-correlations of the three velocity components, separated in the vertical direction have been measured for four data Runs. The cross-correlation functions have been averaged over the four Runs for each vertical separation distance and compared with results from Harris (1968a,1972) and ESDU (1975).

For all three correlations calculated and for a given ΔZ, the correlations increased with height above the ground. Also for a given fixed anemometer height the correlation was larger when measured above that anemometer than when measured below the anemometer.

The zero time delay correlation $\rho_{uu}(\Delta Z, 0)$ was almost equal to $\rho_{uu}(\Delta Z, \tau_m)$ the maximum correlation, but $\rho_{vv}(\Delta Z, 0)$ was significantly smaller than $\rho_{vv}(\Delta Z, \tau_m)$. The vertical velocity component cross-correlation $\rho_{ww}(\Delta Z, \tau)$ had a maximum value when $\tau = 0$.

For both the longitudinal and lateral velocity components, fluctuations in velocity at upper levels were followed by "similar" fluctuations at a lower level, i.e. the maximum correlation was obtained when the upper anemometer data stream was delayed in time compared with the lower level. The upper lateral component data stream had to have a longer delay than the corresponding upper longitudinal component data stream to obtain the maximum correlation which agrees with Panofsky (1973). The observation made by Davenport (1961) and Shiotani and Iwatani (1971) that the "delay distance" for maximum correlation to occur is approximately the vertical separation has also been confirmed by this data. Also for a given ΔZ, the delay distance is greater for heights closer to the ground as observed by Shiotani and Iwatani (1971) and shown in Fig.12.6.

The correlation $\rho_{uu}(\Delta Z, 0)$ is much larger than either $\rho_{vv}(\Delta Z, 0)$ or $\rho_{ww}(\Delta Z, 0)$ for a given separation ΔZ, the latter two which were observed to be approximately equal.

The lateral component correlations which did not tend to zero for time lags greater than about $\pm$ 20 seconds were observed to agree well with the lateral component correlations from Run 4 which did tend to zero, when the former data streams were corrected with Equation (12.9).

The results of this chapter have shown that in order to make reliable measurements of cross-correlations with orthogonal arrays of propeller anemometers care must be taken in installing the anemometers, processing the data, and interpreting the results.

CHAPTER 13

SINGLE POINT TURBULENCE PARAMETER HORIZONTAL VARIATION

13.1 INTRODUCTION

13.1.1 The Data Analysed

To obtain data on the horizontal spatial characteristics of the wind structure at a height of 10 m in a rural boundary layer, a line of tower mounted anemometers was erected. The tower line was positioned perpendicular to the wind direction of 325 degrees which had been chosen to study. The reasons for the choice of this direction are given in Section 1.3, and details of the site and anemometer positions are given in Chapter 4.

The tower mounted anemometers were erected and aligned, cables joined and all equipment was operational by 9/11/77.

Data was recorded on 16/11/77, 17/11/77, 21/11/77, 22/11/77, 23/11/77, 24/11/77 and 19/12/77. However, for a variety of reasons many of the data files were not considered reliable enough to be processed. The data file collected on 16/11/77 was only 16 minutes long because the tape recorder failed, and was therefore considered not long enough to be processed. The wind direction was not perpendicular to the line of towers but from a westerly direction for the data collected on the 17/11/77. This meant that the wind had to flow over the shelter belt at the south-west end of the line of towers (see Fig.4.1) before it reached the line of towers. The wind flow could not then be considered horizontally homogeneous because of the different distances between each anemometer and the shelter belt. The x_1 anemometer also oscillated about zero indicating that it was somewhat sheltered by the anemometer aligned in the y_1 direction. It was therefore decided not to analyse this data file in detail.

The data collected on the 22/11/77 consisted of many very short files, often only a few minutes long because the tape recorder malfunctioned throughout the data recording. This data was consequently not analysed.

On the 23/11/77 a good data file was collected. The wind velocity was high and the direction was from the north-west. A field data tape with 81 minutes of data was obtained.

The data collected on 24/11/77 was only a short file, approximately 15 minutes because again the tape recorder malfuntioned, also the wind was from the westerly direction, therefore over the shelter belt, so it was decided not to analyse this data file as well.

The data recorded on the 19/12/77 was from a strong nor'westerly wind perpendicular to the tower line. The data file was however only 26 minutes long, which meant that the length of data corresponding to a number of samples which was a power of 2, was 18 minutes.

Considering the data collected, the time available for processing the data and a further restriction in that the equipment was required for other research so that more data files could not be recorded, it was decided to analyse in detail the data collected on the 23/11/77 and 19/12/77. Subsequently these data files will be referred to as Run 5 and Run 6 and the pertinent parameters relating to the two files are given in Table 13.1.

Run number	Date data recorded	Start time	File length, minutes	Sampling frequency, Hz	Number of Triplets	Weather Conditions
5	23/11/77	7.28 pm	81	15	12	Cloudy
6	19/12/77	†	26	15	12	†

† Data recorded by another person during author's absence whilst overseas attending a conference. Insolation and start time were not noted.

TABLE 13.1 MULTI 10 m TOWER DATA RECORDINGS

13.1.2 Scope of This Chapter

This chapter deals with the wind structure as it varies in space along a horixontal line at 10 m above the ground. The data was recorded when the average wind vector was approximately perpendicular to the line of towers, so the variation in the wind structure at any instant of time is that along a "gust front".

The chapter is arranged in sections, each section dealing with a specific wind structure parameter, evaluated at single points. Since the definitions of these turbulence parameters have been given previously in Chapters 7 to 12, they are not repeated here.

It should be noted that all the data from Runs 5 and 6 was corrected for non-cosine response. A parabolic trend line was also removed from all data streams before the data was used to calculate the detailed parameters given in this and the following chapter.

The measured data is compared with other single point wind structure measurements in the literature and with results already given in Chapters 6 to 12. The comparisons are made to check the reliability of the data because it is used in the following chapter to calculate cross-correlation functions.

13.2 VARIATION OF WIND VELOCITY AND DIRECTION ALONG TOWER LINE

It can be seen from Fig.13.1 that the average velocity along the row of towers is approximately constant. However in Run 5 the velocities at towers 7 and 8, and in Run 6 the velocity at tower 7 is somewhat lower than at the other towers. The velocity at tower 6 is perhaps also reduced slightly in both Runs. This is probably due to the sheltering effect of the shelter belt at the south-west end of the tower line. It can be seen in Fig.4.1 that a line drawn perpendicular to the tower line from tower 8 passes over the shelter belt. A line perpendicular to the tower line from towers 6 and 7 however does not

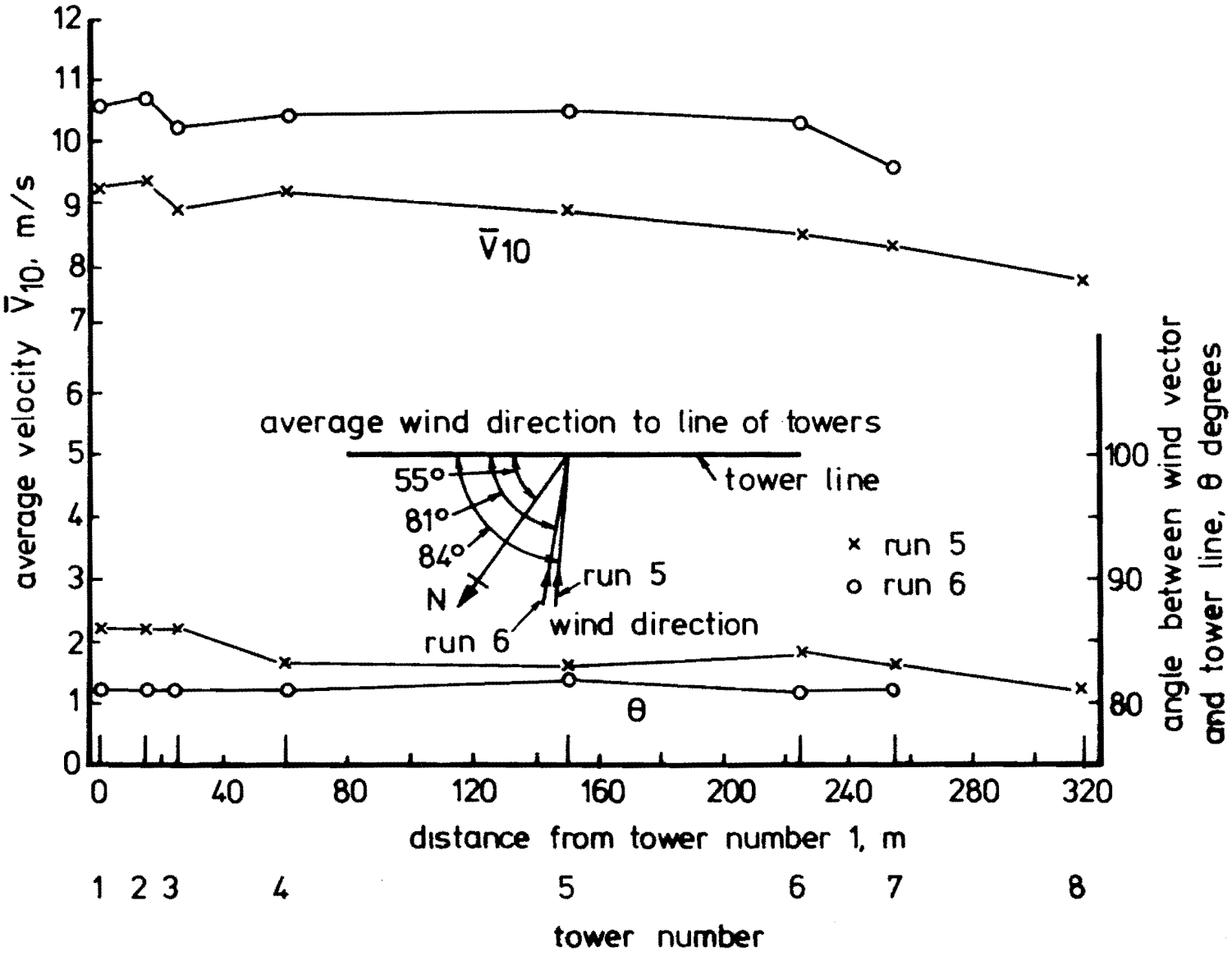

FIG. 13·1 VELOCITY VARIATION ALONG TOWER LINE

pass over the shelter belt. However the flow in the wake of the shelter belt could hardly be called horizontally homogeneous, the lateral motion of the eddies would cause mixing of the air and hence tend to accelerate the flow in the lee of the shelter belt and retard the flow which passed around the end of it.

The variations in the wind velocity at towers 1 to 5 is of a more random nature and is probably due to slight differences in response characteristics of individual anemometers. As stated earlier in Chapter 3, it was found from tests in an aeronautical wind tunnel that the calibration of different combinations of propellers and anemometer bodies varied slightly. During the experiment, propellers were sometimes broken during erection and subsequent maintenance of the equipment, and anemometers which failed electronically were replaced. Consequently the same calibration coefficient was used for all anemometer body - propeller combinations. This introduced a maximum error of ± 5% in the velocity which was assumed to be acceptable for this work.

It is therefore reasonable to assume that the wind velocity is constant at least over towers 1 to 5. Towers 6 to 8 are somewhat sheltered by the shelter belt at the south-west end of the tower line. Cross-correlation measurements involving towers 7 and 8 and perhaps 6 would therefore need to be interpreted with care.

Fig.13.1 also shows the angle between the average wind vector for both Runs, and the tower line. The two wind directions shown are the averages from all towers for each Run. It can be seen in the same figure that there is some variation in the angle θ measured between the wind vector and the x_1 anemometer between individual towers for each Run, but not an excessive variation. The method of obtaining the wind directions is subject to error as they were obtained by the method outlined below.

The anemometers were fixed to each tower and then the tower rotated until the horizontal component anemometers were all approximately

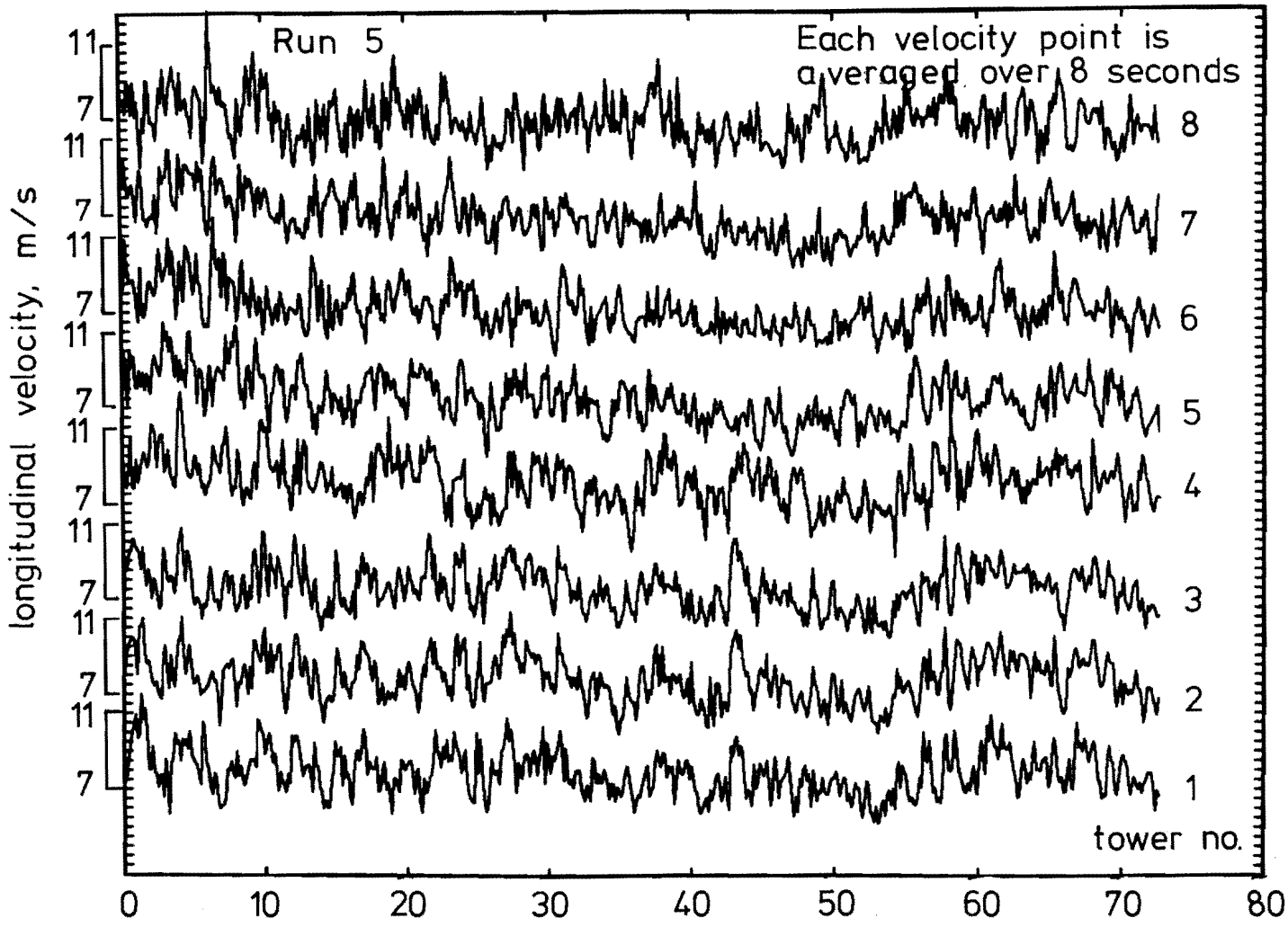

FIG 13·2 VELOCITY AS A FUNCTION OF TIME OVER MEASURED PERIOD FOR RUN 5

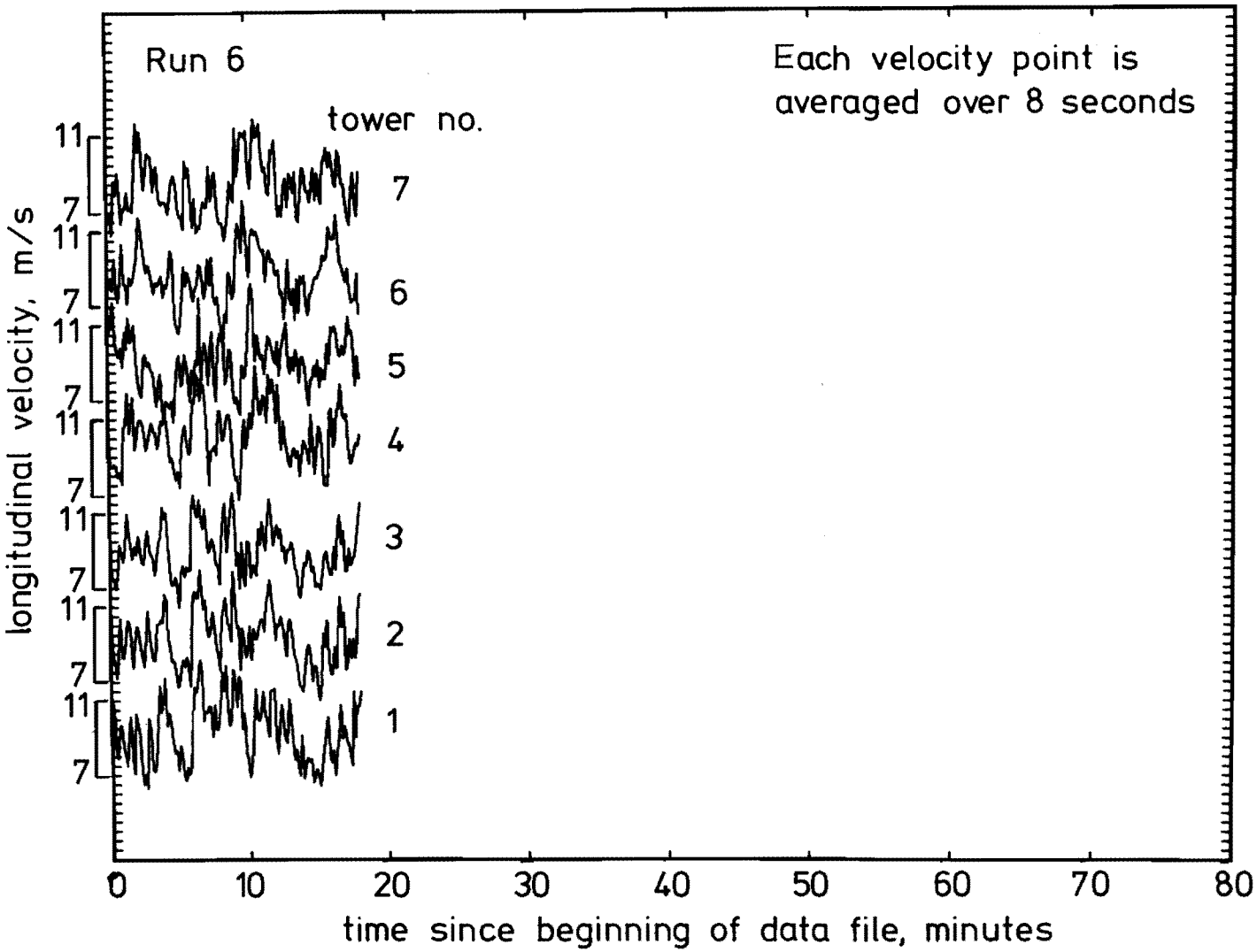

FIG. 13·3 VELOCITY AS A FUNCTION OF TIME OVER MEASURED PERIOD FOR RUN 6.

parallel to each other on all towers. The individual anemometer directions were then determined by using a compass which gave the angle between the x_1 anemometer and the tower line to approximately ± 3°. The angle between the wind vector and the x_1 anemometer was obtained during computer analysis of the data after correcting for the non-cosine response of the anemometers. This latter angle is also subject to a small random error due to the slightly different characteristics of individual anemometers. The angle between the wind vector and the tower line was obtained simply by adding the two angles together.

The velocity-time traces for the longitudinal velocity component from Runs 5 and 6 are given in Figs.13.2 and 13.3. It can be seen that Run 5 appears quite stationary. The velocities for towers 1,2 and 3 appear quite correlated, but correlation between data streams from other towers is not immediately obvious. The data stream comprising Run 6 is of 18 minutes duration and shows much greater velocity fluctuations than Run 5. The larger velocity fluctuations could be expected to result in higher σ_i, i = u,v,w values and higher turbulence intensities than Run 5,because Run 5 appears to be a steadier wind.

13.3 VARIATION OF TURBULENCE ALONG TOWER LINE

13.3.1 Standard Deviation of the Velocity Fluctuations

The standard deviations of the velocity fluctuations for both Runs 5 and 6 are plotted in Fig.13.4. It can be seen that as expected, from the velocity-time traces in Figs.13.2 and 13.3, σ_i, i = u,v,w is greater for Run 6 than for Run 5, especially for the longitudinal and lateral velocity components. For the vertical component there is only a slight increase from Run 5 to Run 6. No general trends are apparent in the standard deviations of the velocity fluctuations along the tower line except that for Run 5 there is an increase in σ_i, i = u,v,w between towers 7 and 8. This is not unexpected as the flow over the shelter

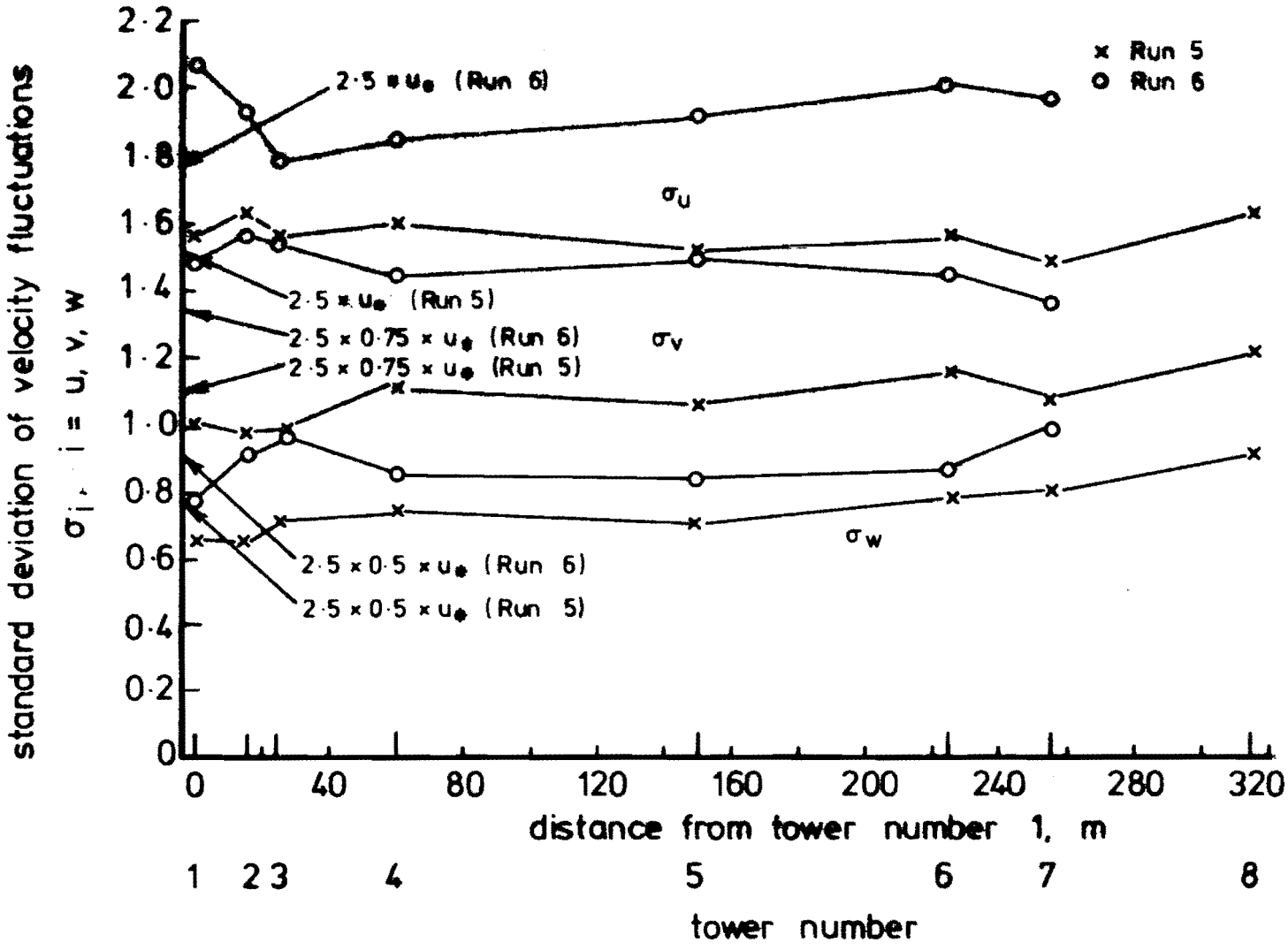

FIG. 13·4. VARIATION OF STANDARD DEVIATION OF VELOCITY FLUCTUATIONS ALONG TOWER LINE.

belt has made the flow more turbulent.

The variation in σ_i for the three components and for both Runs between towers 1 to 4 is surprising as these towers are quite close together and have the same terrain upstream. The difference must be due to slight differences in anemometer response characteristics.

As stated in Chapter 8, Counihan (1975) concluded after reviewing a large quantity of wind structure literature, that the component standard deviations and friction velocity should be in the ratio:

$$\sigma_u : \sigma_v : \sigma_w : U_* = 2.5 : 1.875 : 1.25 : 1 , \qquad (13.1)$$

which gives $\frac{\sigma_v}{\sigma_u} = .75$ and $\frac{\sigma_w}{\sigma_u} = .5$. Teunissen (1970) has also suggested similar ratios which are

$$\sigma_u : \sigma_v : \sigma_w : U_* = 2.5 : 2.0 : 1.3 : 1 , \qquad (13.2)$$

giving $\frac{\sigma_v}{\sigma_u} = .80$ and $\frac{\sigma_w}{\sigma_u} = .52$.

These ratios were also required for the data obtained off the row of towers. This meant that U_* needed to be evaluated.

To find U_* for each Run, the average velocity over all the towers was obtained. A log law velocity profile was then given the required average velocity at a height of 10 m using the value of Z_o obtained from Chapter 7. Thus in the equation :

$$\bar{V}_{10} = \frac{U_*}{k} \ln\left(\frac{10}{.03}\right) \qquad (13.3)$$

where $k = .4$, U_* was the only unknown and hence was evaluated for each Run.

For Run 5, the value of the friction velocity obtained was $U_* = .60$ m/s, and for Run 6 $U_* = .71$ m/s. Thus the ratios of the standard deviations and the friction velocity are :

$$\sigma_u : \sigma_v : \sigma_w : U_* = 2.6 : 1.8 : 1.2 : 1 ,$$

$$\text{and} \quad \frac{\sigma_v}{\sigma_u} = .69 , \frac{\sigma_w}{\sigma_u} = .47 \qquad (13.4)$$

for Run 5. For Run 6 the similar ratios are :

$$2.7 : 2.1 : 1.2 : 1 \ , \ \frac{\sigma_v}{\sigma_u} = .76 \ , \ \frac{\sigma_w}{\sigma_u} = .45 \ . \qquad (13.5)$$

The ratios from both Runs 5 and 6 compare favourably with both Counihan and Teunissen.

13.3.2 Turbulence Intensities

The turbulence intensities for both Runs have been given in Fig.13.5. Values from ESDU (1974b) with Z_o = .03 m have been plotted and values computed from

$$\frac{\sigma_u}{\bar{V}_Z} = \left(\ell n\left(\frac{Z}{Z_o}\right)\right)^{-1} \qquad (13.6)$$

from Counihan (1975. Theoretical values of $\frac{\sigma_v}{\bar{V}_Z}$ and $\frac{\sigma_w}{\bar{V}_Z}$ have been obtained by using Equation (13.6) and also Equation (13.1).

All components agree well with Counihan (1975) for both Runs. The lateral and vertical components agree well with ESDU (1974b) but again, as found in Chapter 8 the measured values of $\frac{\sigma_u}{\bar{V}_Z}$ are less than the ESDU prediction.

The turbulence intensities for Run 5 show an increase from tower 7 to tower 8. This is as expected because the average velocity at tower number 8 was lower than at tower number 7 and the former had larger standard deviations than the latter, both effects due to the shelter belt.

Apart from the increase from towers 7 to 8 in Run 5, the variation in turbulence intensity between towers show no apparent trends but some random variation. The turbulence intensity variation with position suggests that the flow is reasonably horizontally homogeneous between towers 1 to 7. In fact, the difference in σ_u for Run 6 between towers 1 and 3 is just as significant as the effect of the shelter belt, excluding tower number 8.

13.3.3 Probability Density Functions

The probability density functions for Run 5 for the three velocity components have been given in Fig.13.6. The longitudinal velocity components are seen to have a distribution near Gaussian although the data from

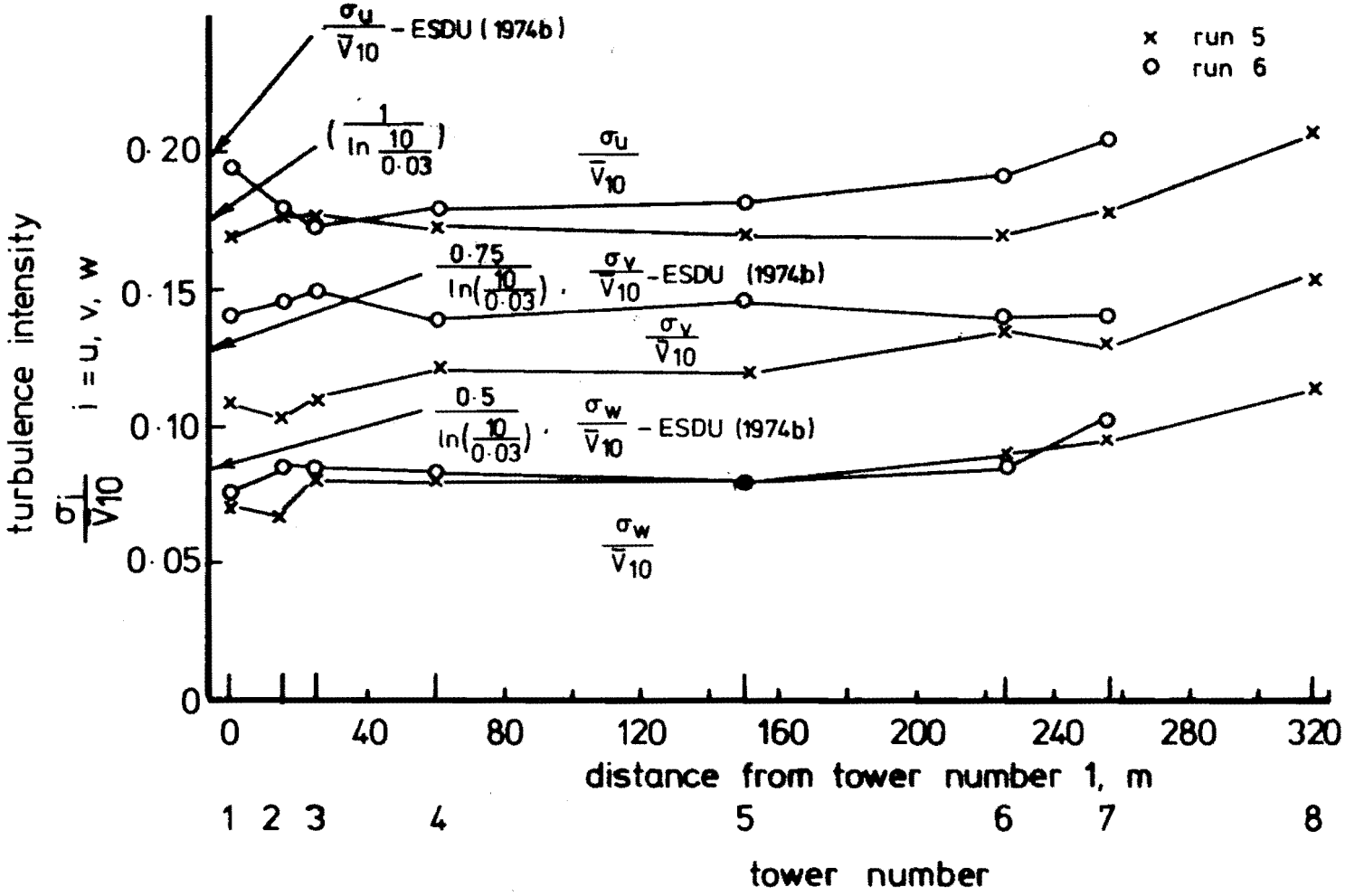

FIG. 13·5 VARIATION OF TURBULENCE INTENSITY ALONG TOWER LINE.

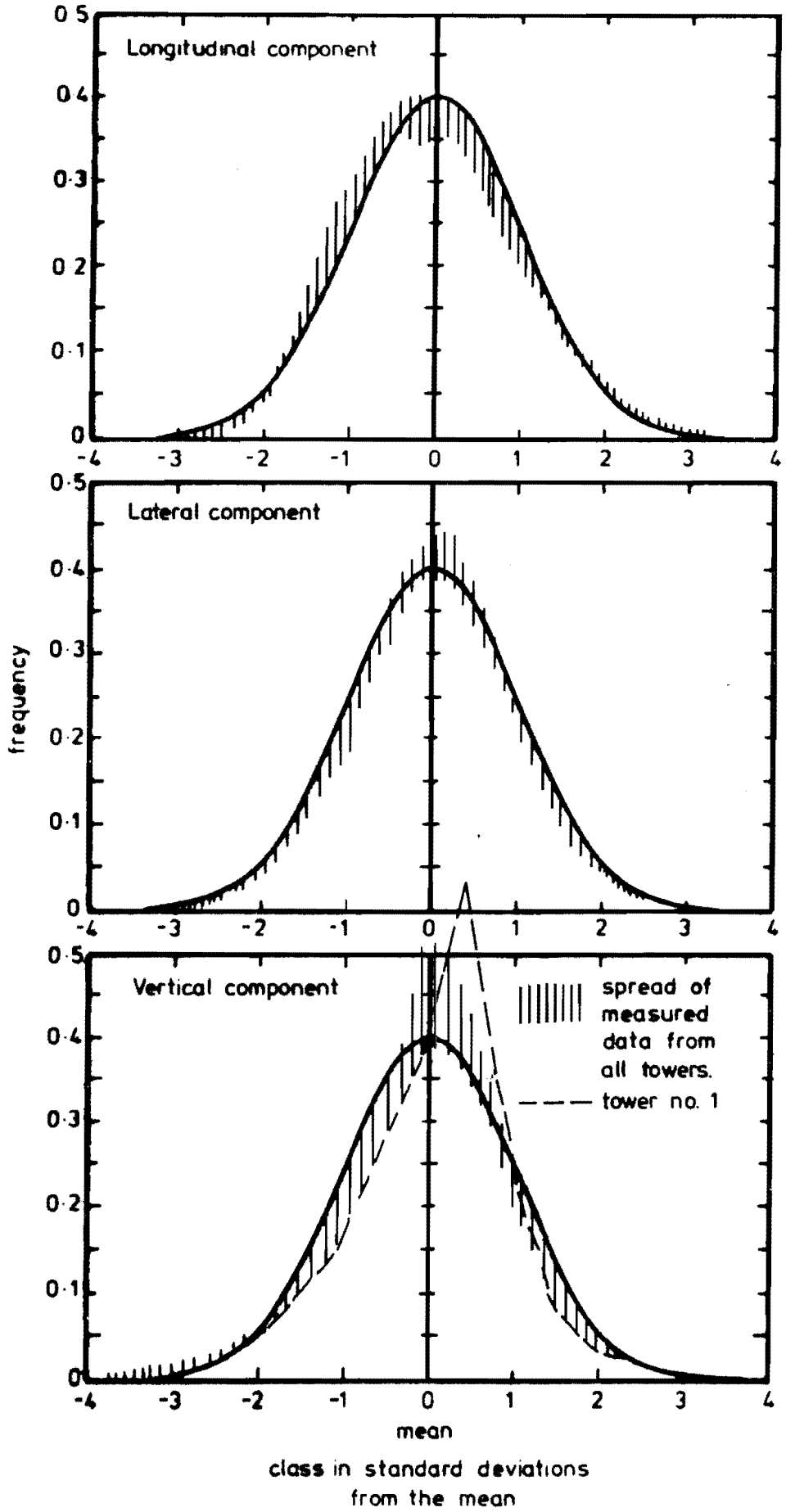

FIG. 13·6 WIND VELOCITY PROBABILITY DENSITY DISTRIBUTION FOR RUN 5.

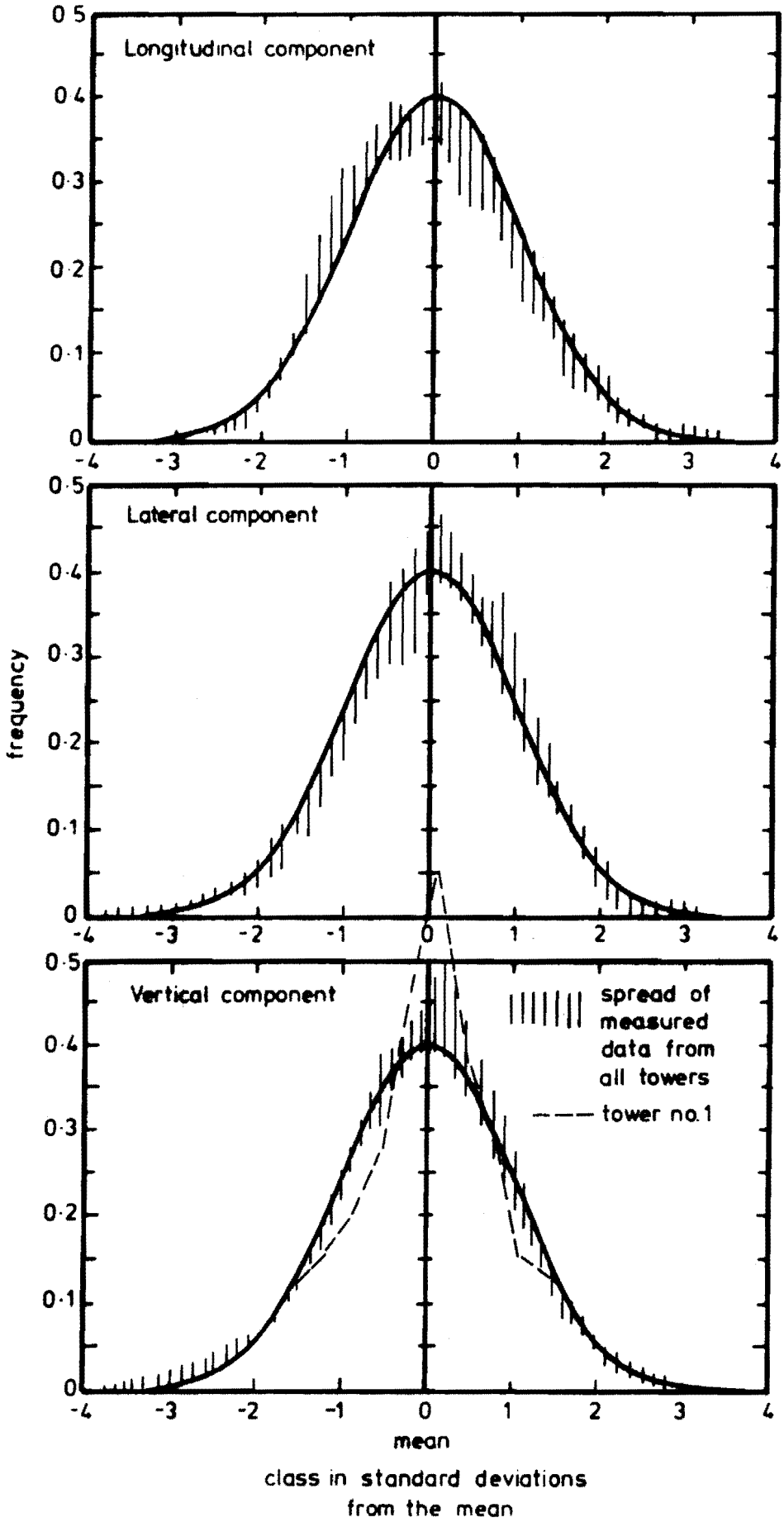

FIG. 13·7 WIND VELOCITY PROBABILITY DENSITY DISTRIBUTION FOR RUN 6.

some towers has a lower probability than Gaussian near the mean. Near the tails of the distribution the measured data varies from Gaussian somewhat. The lulls in velocity occur less often than predicted by the Gaussian distribution whereas the high velocities occur more often.

The lateral component probability density functions agree well with the Gaussian distribution although the measured data has velocities near zero more frequently than the Gaussian distribution predicts.

The vertical velocity components agree reasonably well with the Gaussian distribution. However for data from all but one tower, the probability at velocities near zero is significantly higher than predicted by the Gaussian distribution. Presumably if the vertical component anemometer was aligned exactly vertically, and for homogeneous terrain, the net velocity measured by the vertical component anemometer after a long period would be zero. As has been discussed in Chapter 8, it proved extremely difficult in practice to align the vertical component anemometer exactly vertical. Also wind tunnel tests have shown that the propeller has a region of stall where it doesn't rotate for approximately ± 3°. The region of measured high probability probably occurs for wind directions within this region. A somewhat lower than Gaussian probability can be observed either side of the region of high probability.

This is shown explicitly in Fig.13.6 for the vertical component data stream from tower number 1. It behaved least like a Gaussian distribution and shows very high probabilities near the mean, with reduced values either side. The same feature can be observed in Fig.13.7 for the data stream from the same tower for Run 6. This effect has also been discussed in Section 8.3. It suggests that the anemometer was faulty and may have had different bearing friction from the other anemometers.

For velocities greater than ± 1.5 standard deviations from the mean, the vertical component probability density distribution is much

closer to the Gaussian distribution except for the data stream from tower 1 as already stated.

The probability densities for the three velocity components for towers 1 to 7 from the Run 6 data are given in Fig.13.7. The same general features are apparent for these data streams as were described for the Run 5 data. The only difference is that since the data stream analysed in Run 6 was of a shorter duration, 18 minutes compared with 73 minutes, the width of the probability density distribution band from all towers is wider for Run 6 than for Run 5. The high probability near the mean of the vertical component probability density distribution is even more apparent for Run 6 than it was for Run 5.

13.4 VARIATION OF REYNOLDS STRESSES ALONG TOWER LINE

The Reynolds stress variation along the tower line for Runs 5 and 6 is plotted in Fig.13.8. The values of the three Reynolds stresses are similar for the two Runs and the variation along the tower line appears to be random.

Three values of $\rho_{uw}(0)$ from the literature are also shown. They are values from ESDU (1974b), Counihan (1975) and Teunissen (1970). The value from ESDU (1974b) for Z = 10 m and Z_o = .03 m underestimates the measured data whereas the value from Counihan agrees well with it. Teunissen's value lies between the ESDU and Counihan values.

The average value of $\rho_{uw}(0)$ for both Runs 5 and 6 was - .34. ESDU predicts - .27, Counihan predicts - .36 as detailed in Chapter 9 and Teunissen predicts - .31.

The measured values were obtained by the eddy correlation technique discussed in Chapter 9 and the program used was SEQVELTURBREY.

It has been shown in Chapter 7 that a log law velocity profile fitted the data from Runs 1,2,3, and 4 well. From the log profile and

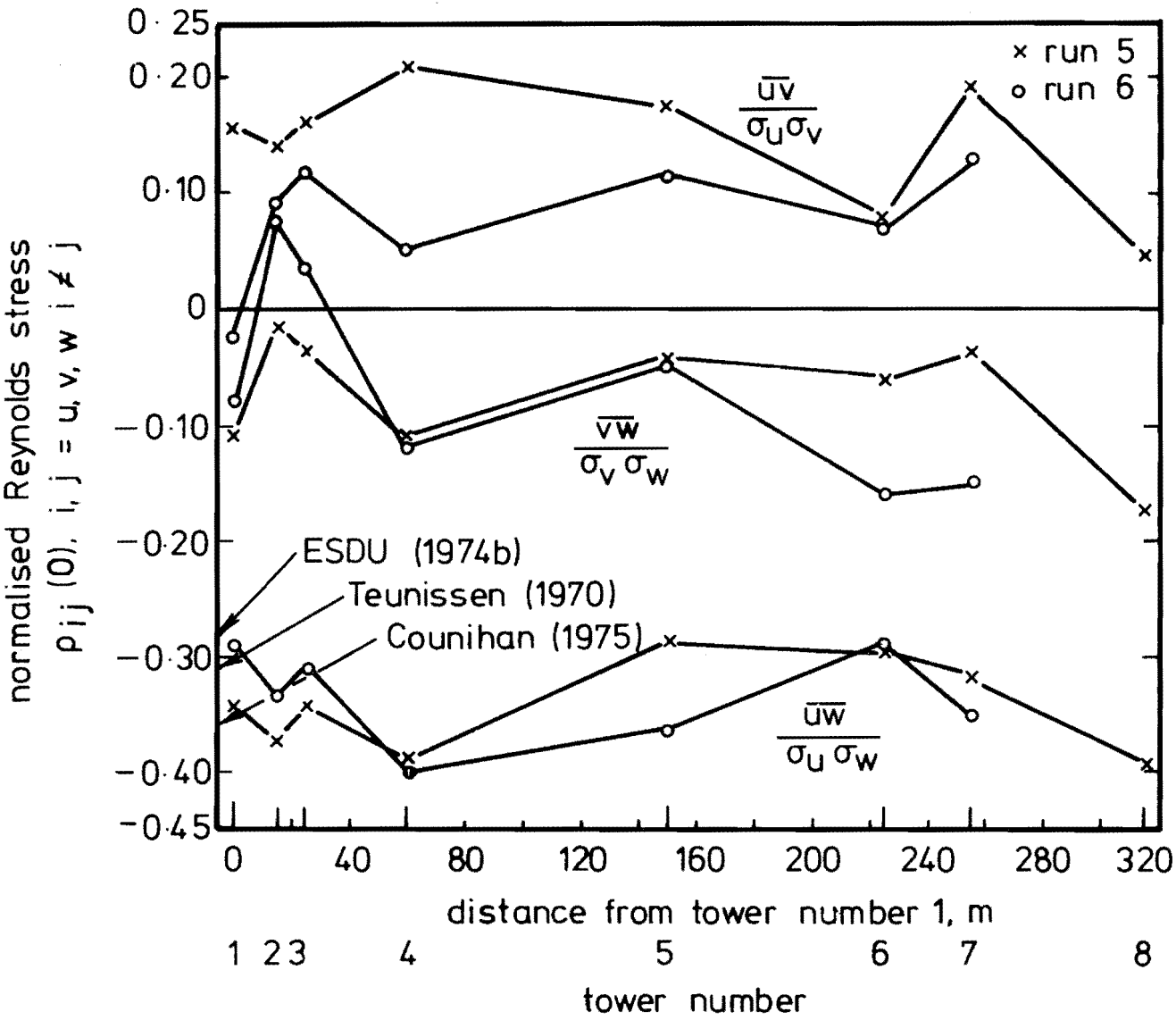

FIG. 13·8 NORMALISED REYNOLDS STRESS VARIATION ALONG TOWER LINE.

average value of $\rho_{uw}(0)$, the roughness length Z_o was calculated to be .03 m.

A log law velocity profile was fitted to the data from Runs 5 and 6 as explained in detail in Section 13.3.1 using Z_o = .03. This gave values of U_* of .60 and .71 m/s for Runs 5 and 6 respectively. Using the relationship $\overline{uw} = -U_*^2$ and measured values of σ_u and σ_w gave $\rho_{uw}(0)$ = -.31 and -.30 for Runs 5 and 6 respectively. Thus they are slightly smaller in magnitude than the values obtained by the eddy correlation technique. All the values are given in Table 13.2 and compared with average values from Runs 1,2,3, and 4.

	$\rho_{uw}(0)$ Reynolds Stress	
	eddy correlation	velocity profile Z_o = -0.03 m
Run 5	- .34	- .31
Run 6	- .34	-.30
Average over Runs 1 to 4 from Chapter 9	- .36	
ESDU (1974b) Z = 10 m Z_o = .03 m	- .27	
Teunissen (1970	- .31	
Counihan (1975) Z_o = .03 m	- .36	

TABLE 13.2 $\rho_{uw}(0)$ REYNOLDS STRESS VALUES

The two other Reynolds stresses are smaller in magnitude than $\rho_{uw}(0)$ and the average over all the towers for the two Runs are given in Table 13.3.

	$\rho_{uv}(0)$	$\rho_{vw}(0)$
Run 5	.143	- .073
Run 6	.079	- .072
Average over Runs 1 to 4 from Chapter 9	- .013	- .009

TABLE 13.3 $\rho_{uv}(0)$ AND $\rho_{vw}(0)$ REYNOLDS STRESS VALUES

This data is also in agreement with ESDU (1974b) which states that $\rho_{uw}(0) >> \rho_{uv}(0) >> \rho_{vw}(0)$.

Again similar results have been observed here as in Chapter 9. Propeller anemometers appear to make reliable measurements of the $\rho_{uw}(0)$ Reynolds stress. However for improved results of $\rho_{uv}(0)$ and $\rho_{vw}(0)$, averages over several Runs or several anemometer triplets are required. Similar features for the variation of $\rho_{uw}(\tau)$, $\rho_{uv}(\tau)$ and $\rho_{vw}(\tau)$ with time lag were observed from these two Runs as for the data discussed in Chapter 9. Although not shown here it was observed that $\rho_{vw}(\tau)$ oscillated either side of zero, $\rho_{uv}(\tau)$ was virtually constant for all time delays and $\rho_{uw}(\tau)$ had a maximum negative value at $\tau = 0$. $\rho_{uw}(\tau)$ reduced in magnitude quickly for $0 < |\tau| < 5$ seconds after which it gradually diminished in magnitude towards zero. It is interesting to note that Teunissen (1977b) observed that the peak of the measured $\rho_{uw}(\tau)$ Reynolds stress appeared at non-zero values of τ. Teunissen attributed this behaviour to the change in roughness upstream of the tower on which the instruments were mounted. The same feature is not observed here where there was no change in roughness upstream. In this work the peak $\rho_{uw}(\tau)$ Reynolds stress always occurred at $\tau = 0$.

13.5 VARIATION OF POWER SPECTRAL DENSITIES ALONG TOWER LINE

The power spectral densities for the three velocity components for Runs 5 and 6 were calculated in exactly the same manner as outlined in Chapter 10 and used for Runs 1,2,3, and 4. Run 5 which was 73 minutes long consisted of 8192 data samples per channel and Run 6 which was 18 minutes long consisted of 2048 data samples. This meant that the Run 6 spectral densities were subject to more random error than the Run 5 spectral densities.

The longitudinal, lateral and vertical power spectral densities for Run 5 have been plotted in Figs.13.9,13.10 and 13.11 respectively. Plotted in each figure is a line corresponding to the von Kármán spectral equation obtained from ESDU (1974b).

In the three figures it can be seen that the measured data from all the towers falls in a narrow band above a frequency of ν.004 Hz. This frequency corresponds to 16 times the fundamental frequency. At frequencies below this value, the spectra shows a lot more random variation.

The ESDU (1974b) spectrum fitted to the peak of the longitudinal component spectra describes it rather well. However, the measured data as usual has a peak which is less well resolved than the one of ESDU (1974b), which also peaks to a slightly higher value.

The ESDU spectrum fitted to the peak of the lateral component measured spectrum describes it rather well near the peak but underestimates the spectral components at lower frequencies. At very low frequencies the measured data shows a minor peak which is probably due to a non-stationarity effect.

The ESDU spectrum fitted to the measured data spectral peak also describes the vertical component spectrum rather well. Both the ESDU spectrum and the measured data peak to the same magnitude. At frequencies

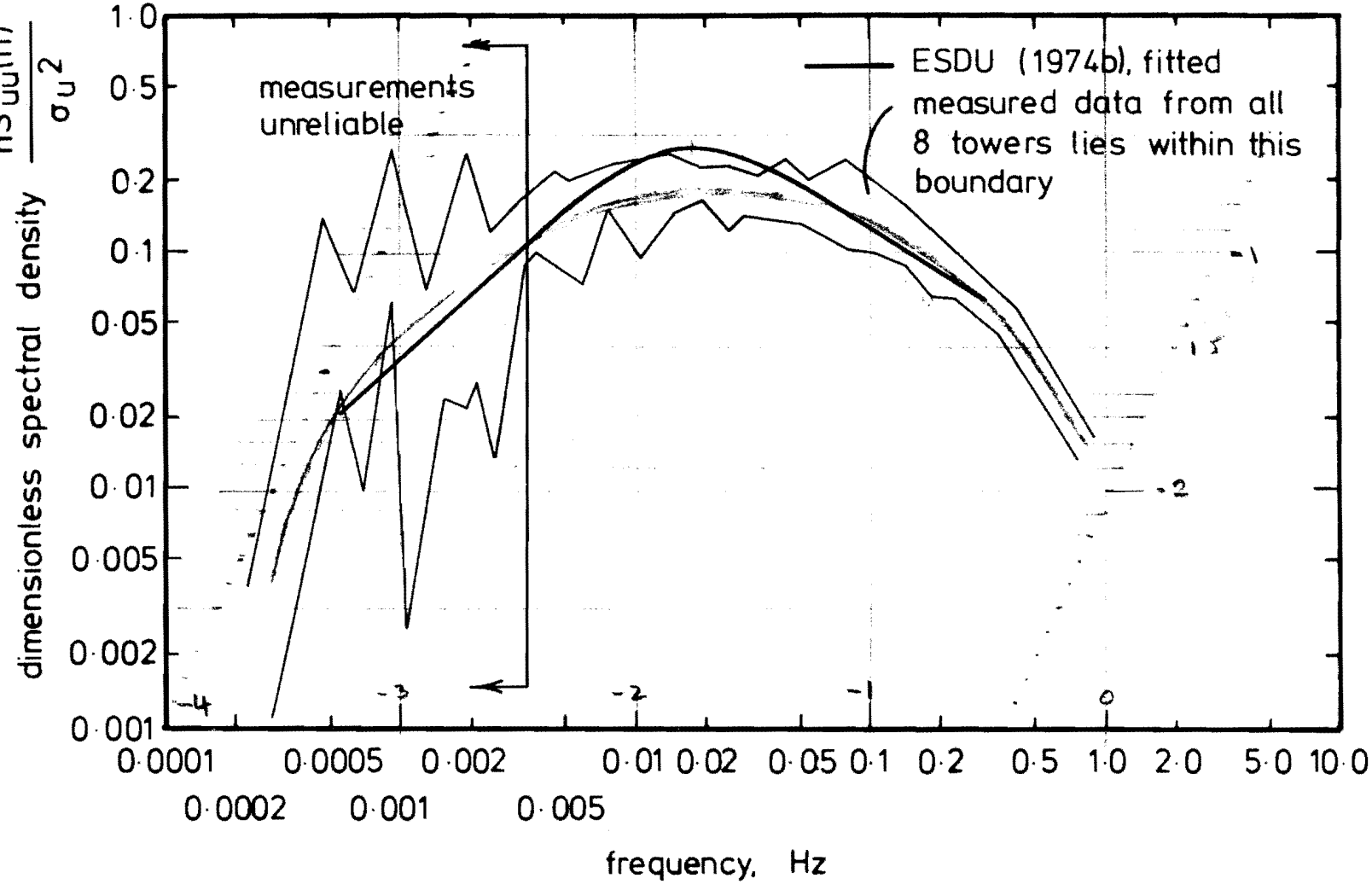

FIG. 13·9 LONGITUDINAL COMPONENT u, POWER SPECTRAL DENSITY FOR RUN 5.

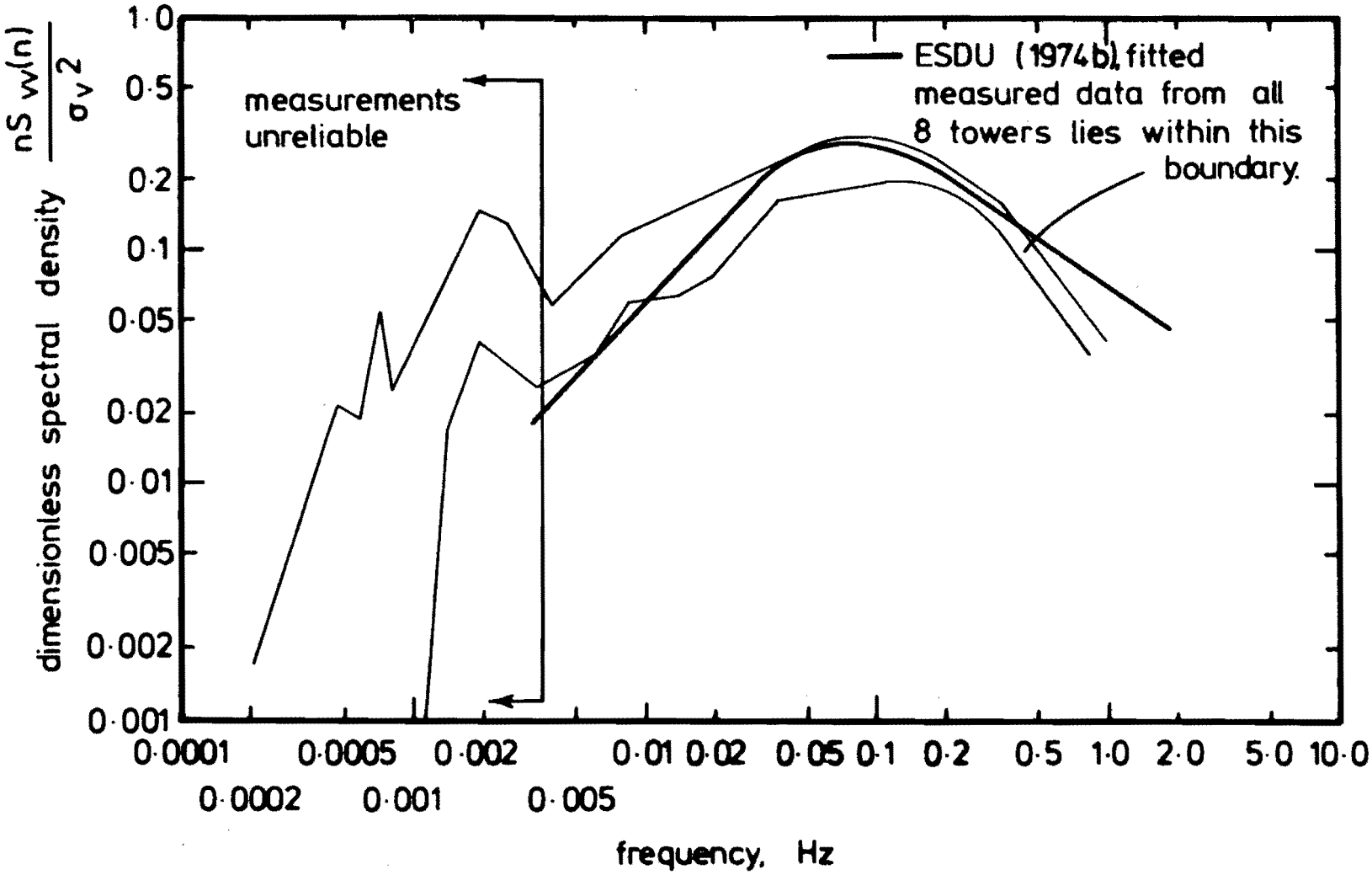

FIG. 13·10 LATERAL COMPONENT v POWER SPECTRAL DENSITY FOR RUN 5.

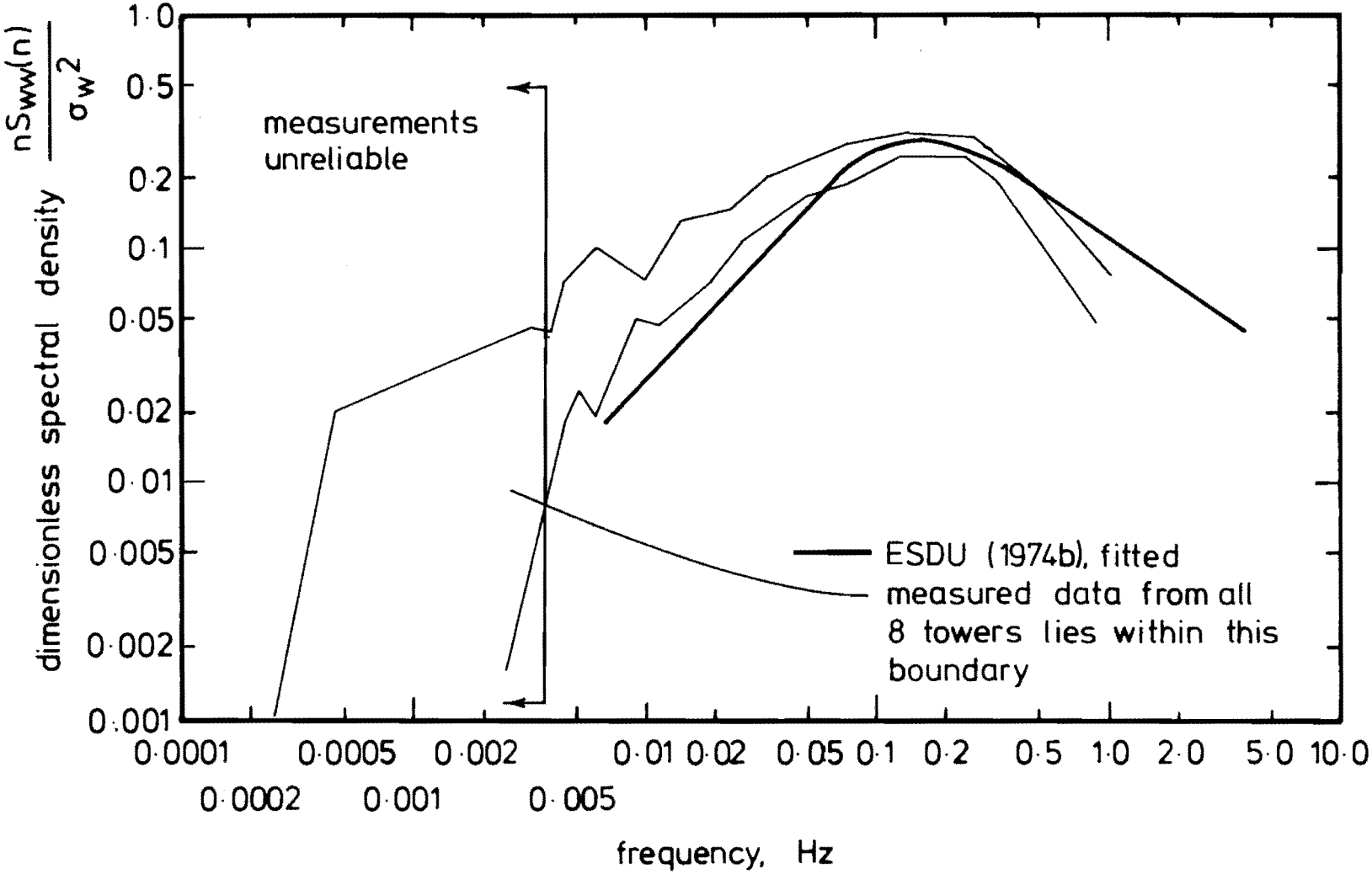

FIG 13·11 VERTICAL COMPONENT w POWER SPECTRAL DENSITY FOR RUN 5.

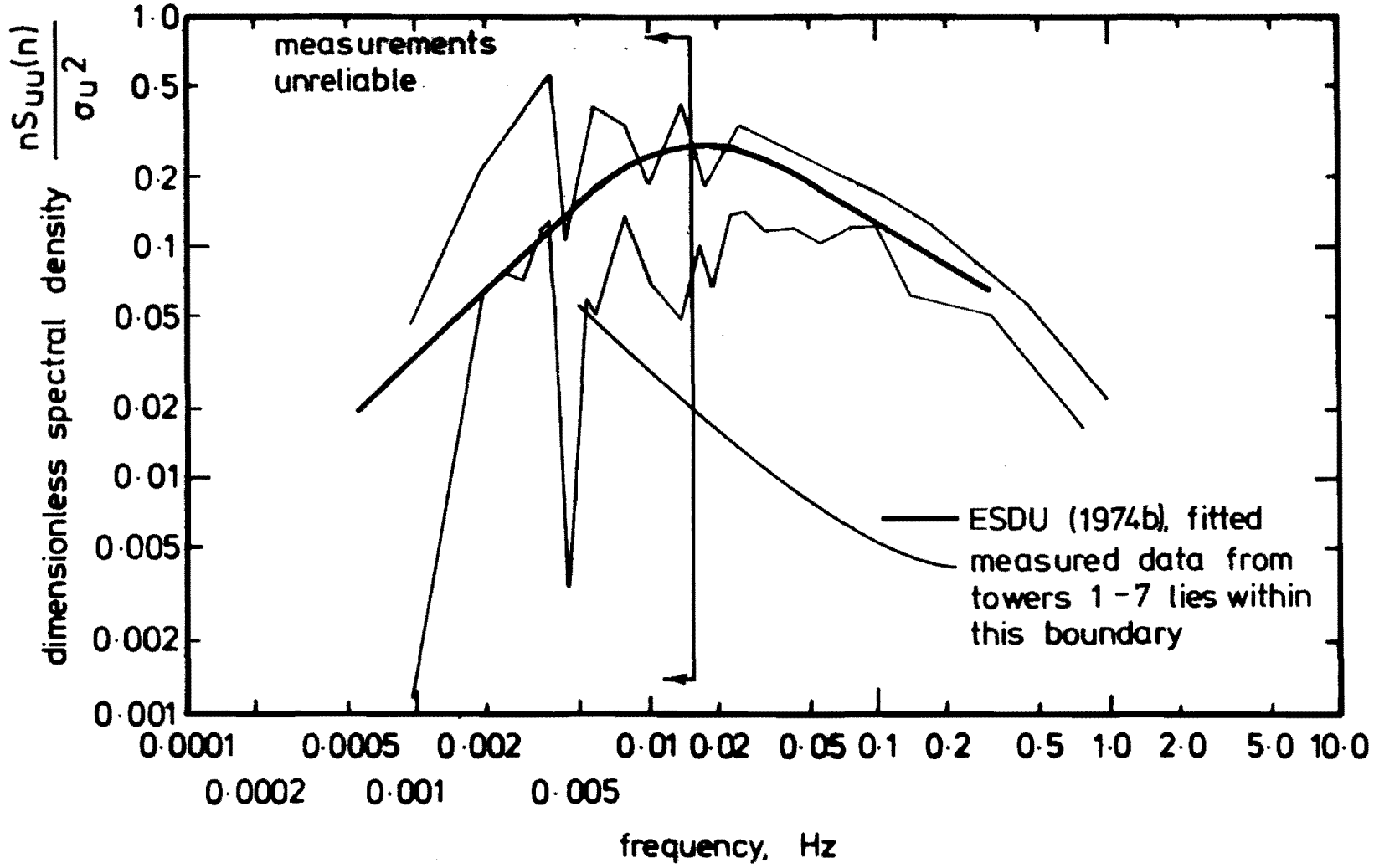

FIG. 13·12 LONGITUDINAL COMPONENT u POWER SPECTRAL DENSITY FOR RUN 6.

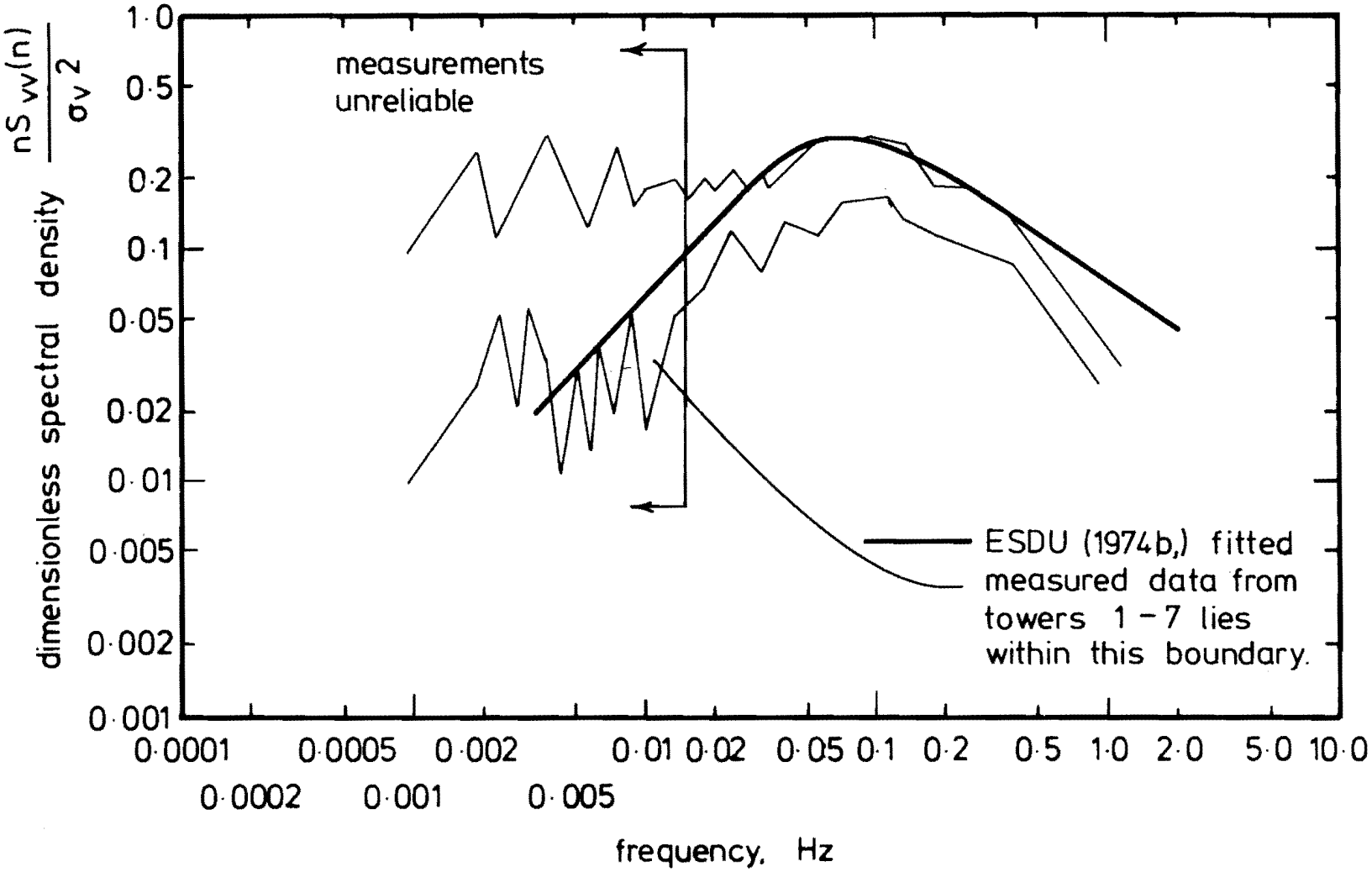

FIG 13·13 LATERAL COMPONENT v POWER SPECTRAL DENSITY FOR RUN 6.

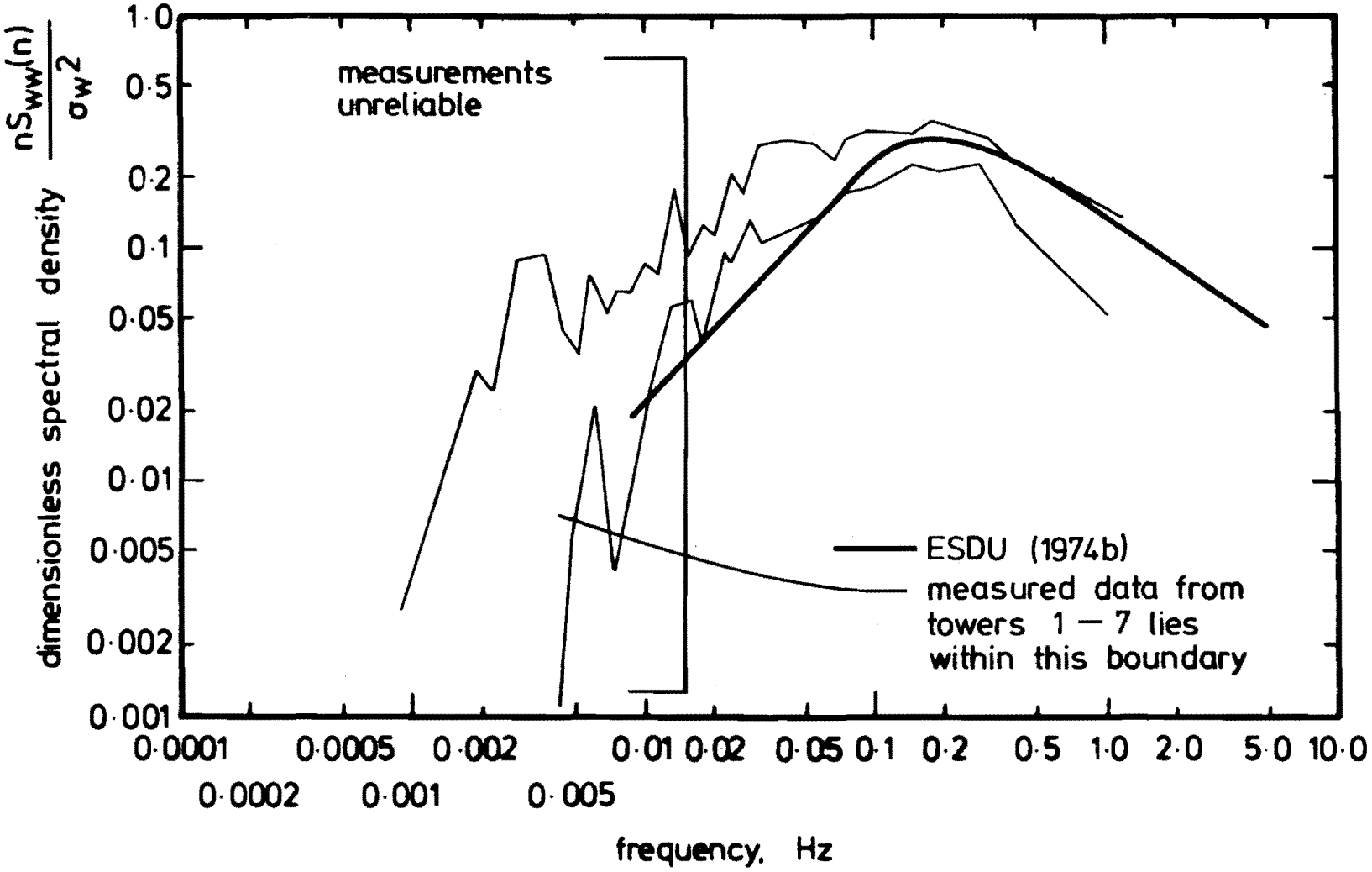

FIG 13·14 VERTICAL COMPONENT w POWER SPECTRAL DENSITY FOR RUN 6.

lower than the frequency at which the peak occurs, the measured data falls at a slower rate than predicted by ESDU. At higher frequencies the measured data falls more quickly than the ESDU spectrum due to the low pass filtering effect of the vertical component anemometers.

The power spectral densities for Run 6 are plotted in Figs.13.12, 13.13 and 13.14. The major features of the longitudinal component spectrum are the same as for Run 5 but as expected because of the shorter length of the data recording, the random error is increased. The peak is ill-defined but the high frequency variation is similar. The lateral component spectrum for Run 6 shows much more scatter than for Run 5. It also shows more energy at low frequencies which is probably because the data is not as trend free as the Run 5 data. The peak is also diminished somewhat so that the ESDU spectrum fitted to the measured data overestimates the peak.

The vertical component spectra from both Runs 5 and 6 exhibited similar characteristics even when Run 6 has been obtained from only a quarter as much data as Run 5. The similar characteristics result from the fact that the vertical component velocity is restricted by the presence of the ground. This prevents the formation of large low frequency eddies or trends which mean that the vertical component spectrum is less sensitive to the amount of data processed.

13.6 VARIATION OF AUTOCORRELATION FUNCTIONS ALONG TOWER LINE

13.6.1 The Longitudinal Component Autocorrelation Function

The autocorrelation functions have been calculated for Runs 5 and 6 in an analogous manner to the method used in Chapter 11 for the Run 1,2,3, and 4 data. Plots of the longitudinal, lateral and vertical autocorrelation functions have been given in Figs.13.15 to 13.20 for both Runs 5 and 6.

For the longitudinal and lateral components, the spread of the

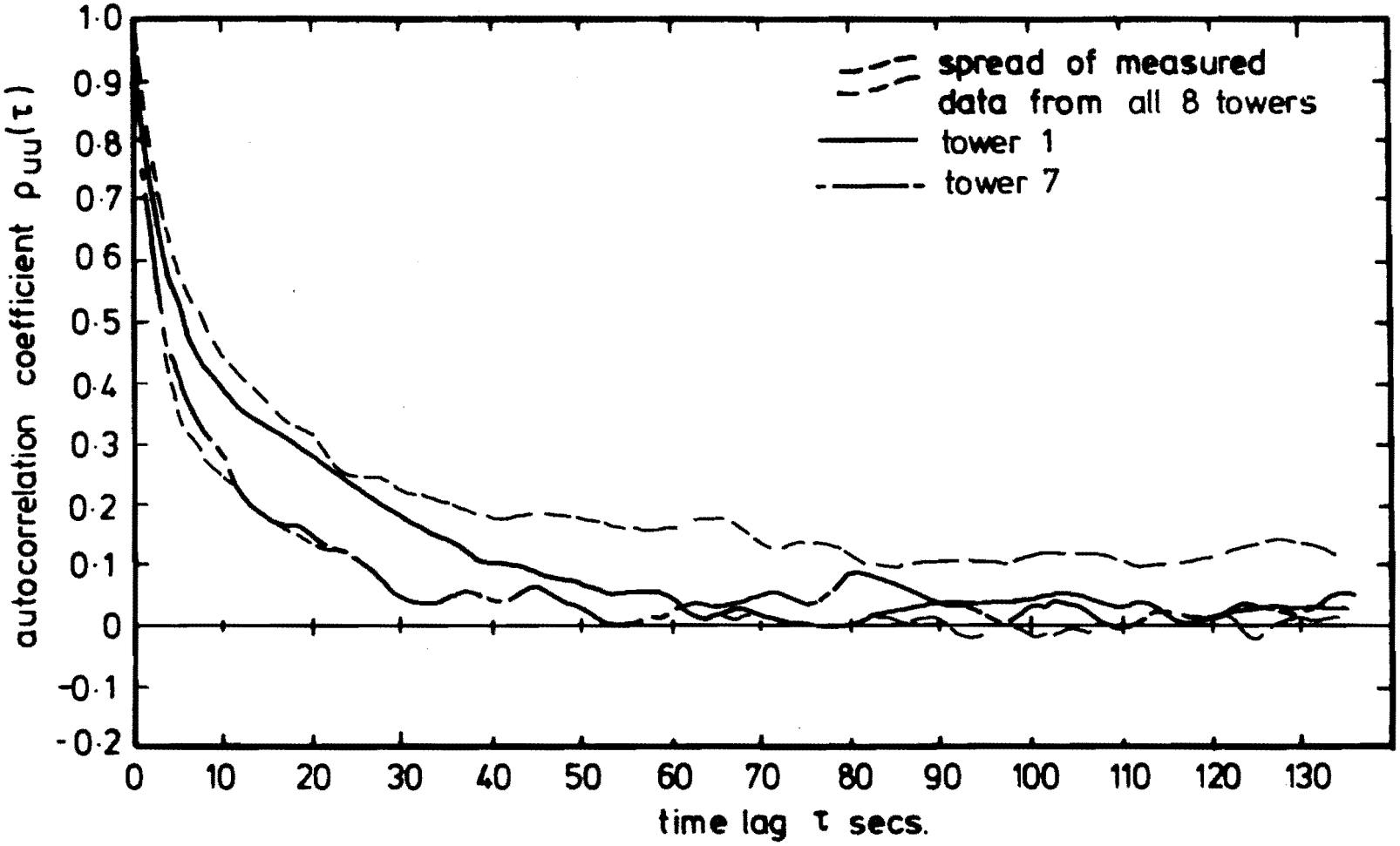

FIG 13·15 LONGITUDINAL COMPONENT u AUTOCORRELATION FUNCTION FOR RUN 5.

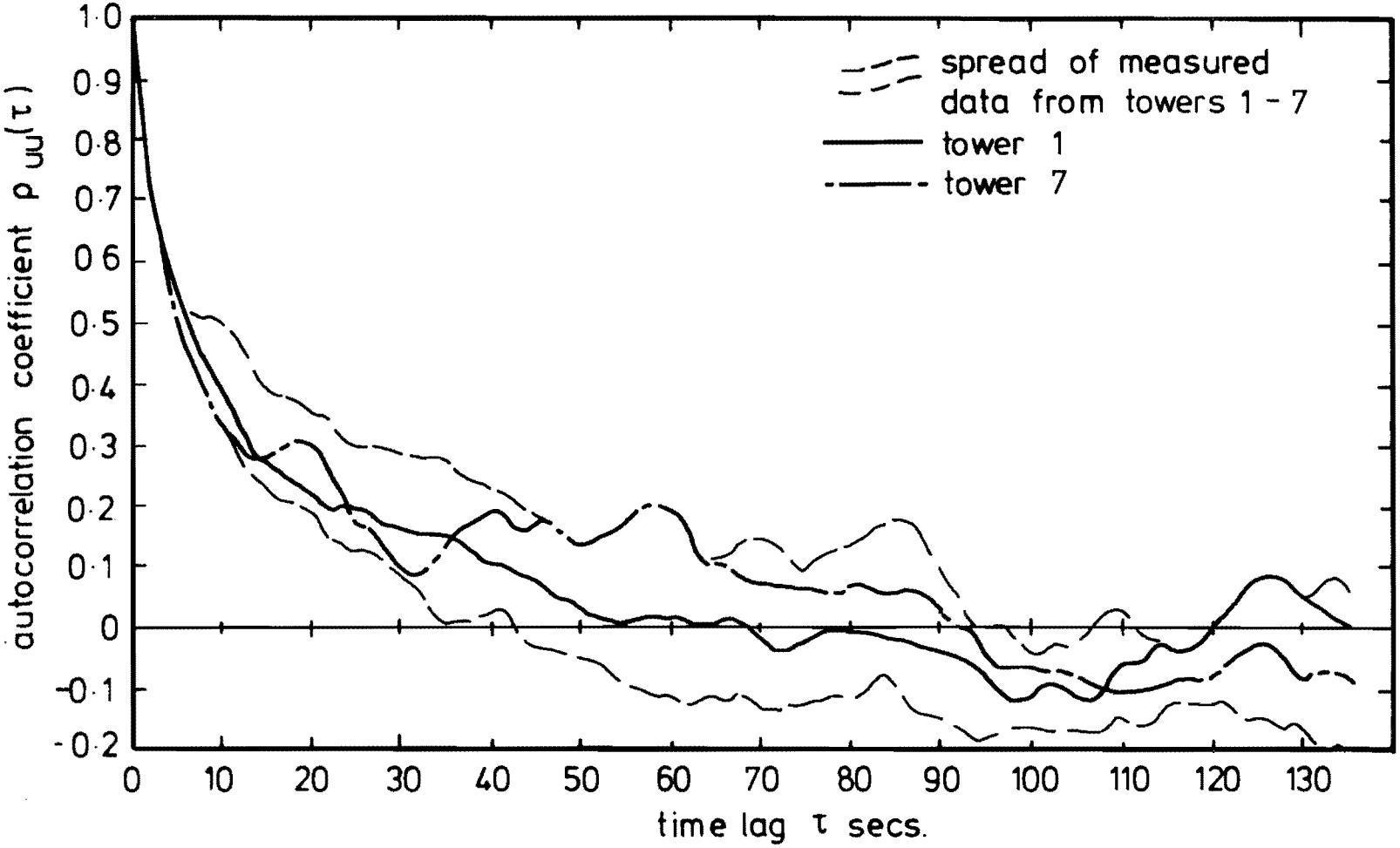

FIG. 13·16 LONGITUDINAL COMPONENT u AUTOCORRELATION FUNCTION FOR RUN 6.

autocorrelation functions has been indicated with two edge lines. Also shown are the measured autocorrrelation function curves from towers 1 and 7 only. This is because tower 1 was completely unaffected by the shelter belt and tower 7 was somewhat in the lee of it. Hence they are typical for each end of the tower line. More curves on the one graph made it very hard to distinguish between individual curves. For the vertical component, the behaviour of all curves was similar so only the two edge lines to the measured data have been shown.

The longitudinal component autocorrelation functions from Run 6 in Fig.13.16 show more variation with time lag τ than do the same functions from Run 5 shown in Fig.13.15. This is due to the increased length of the Run 5 data stream over Run 6. The longitudinal component autocorrelation functions from Run 5 indicate that the autocorrelation from towers 6,7, and 8 approach zero more rapidly than the curves from towers 1 to 5. This could reasonably be expected to be caused by the shelter belt at the south-west end of the tower line. The shelter belt has increased Z_o which consequently has reduced the integral length scales.

However, a similar feature was not evident in the autocorrelation functions from the Run 6 data for the longitudinal component. In fact the autocorrelation functions for towers 6 and 7 were rather higher than curves from towers 1 to 5. This figure also highlights the more random type of behaviour of the autocorrelation from tower 7, presumably because of the shelter belt.

Very little can therefore be concluded from the results on the effect of the shelter belt on the longitudinal component autocorrelation functions.

13.6.2 The Lateral Component Autocorrelation Function

Figs.13.17 and 13.18 show the lateral component autocorrelation functions for Runs 5 and 6 respectively. For Run 5 these behave typically

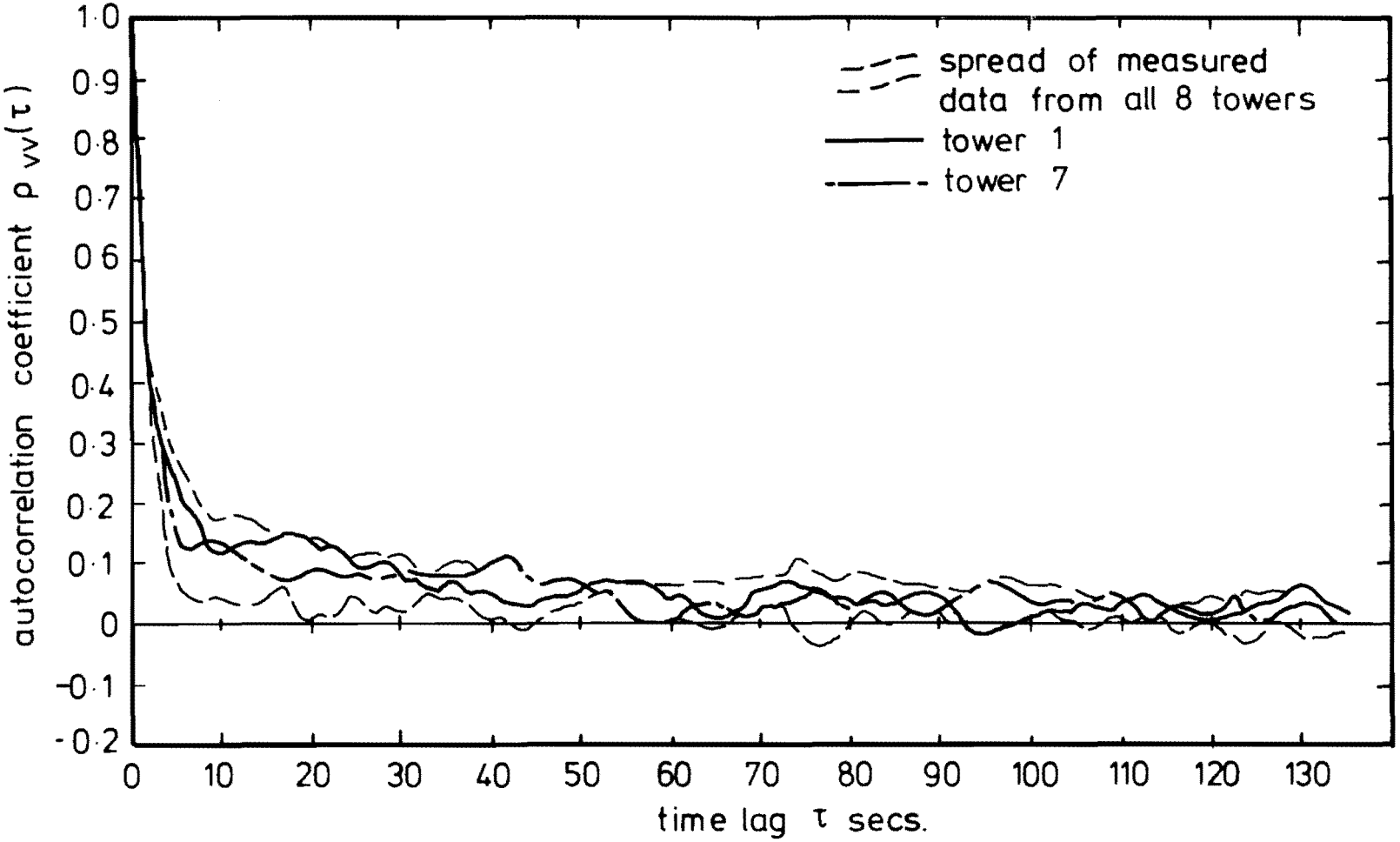

FIG. 13·17 LATERAL COMPONENT v AUTOCORRELATION FUNCTION FOR RUN 5

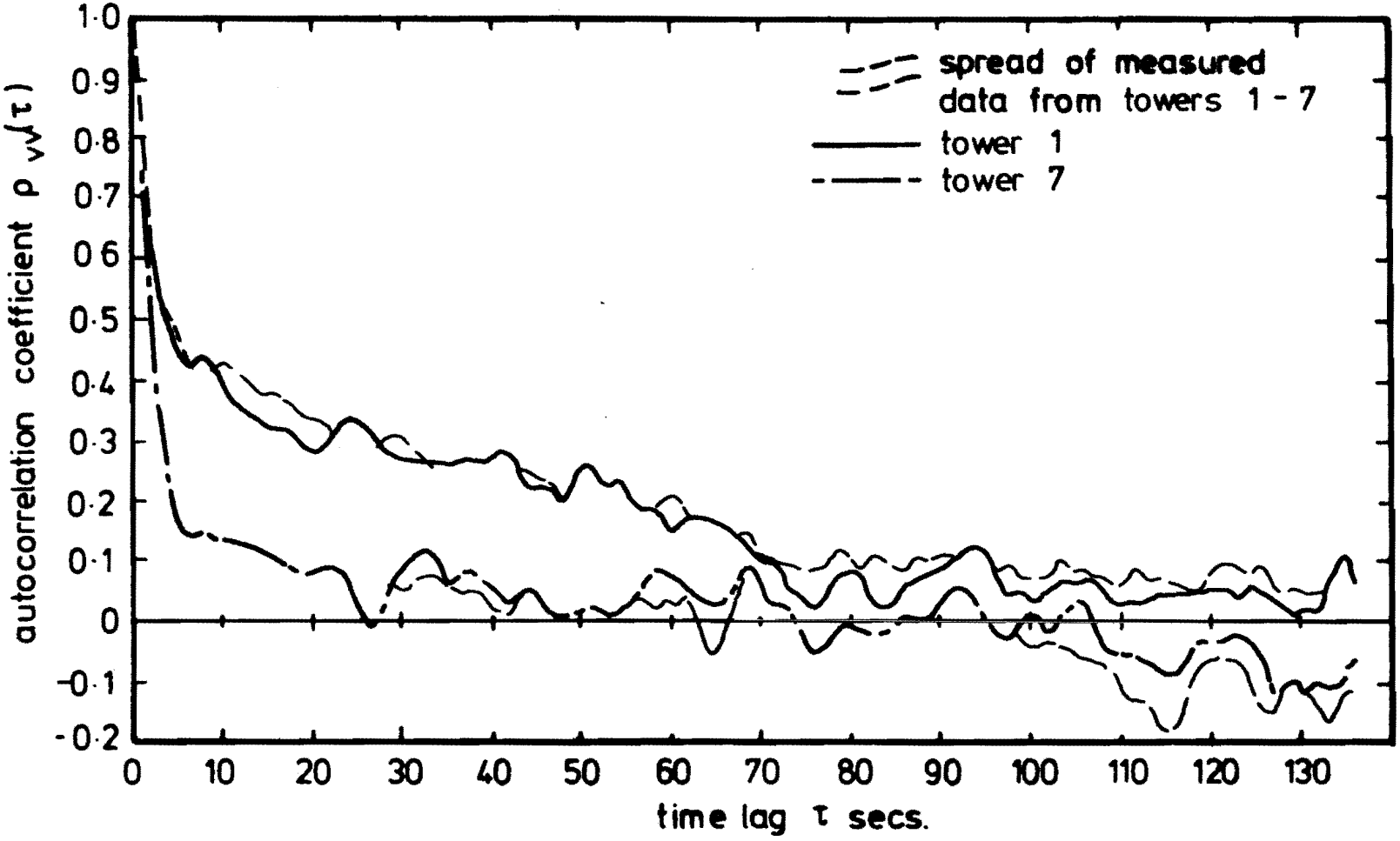

FIG 13·18 LATERAL COMPONENT v AUTOCORRELATION FUNCTION FOR RUN 6.

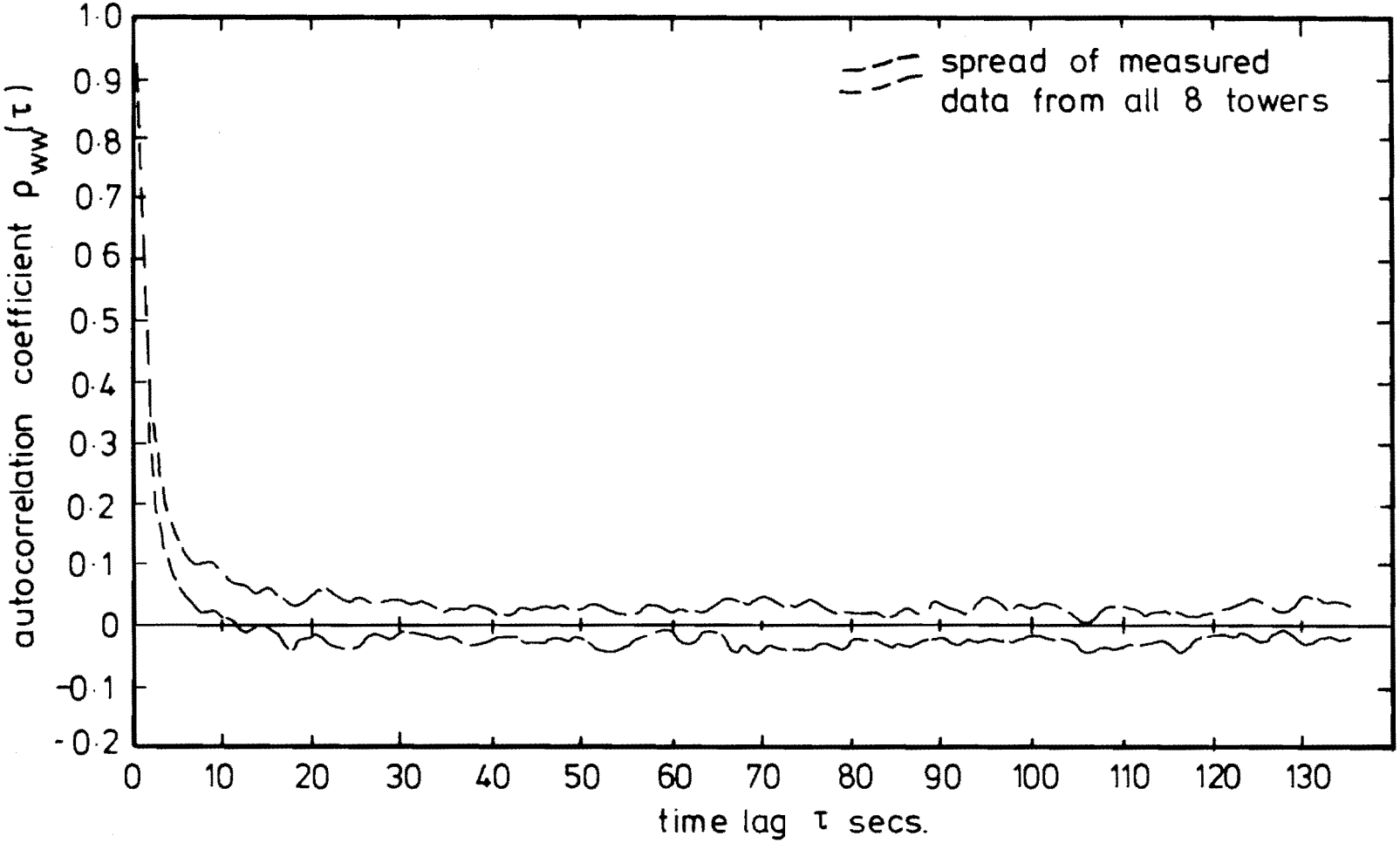

FIG. 13·19 VERTICAL COMPONENT w AUTOCORRELATION FUNCTION FOR RUN 5.

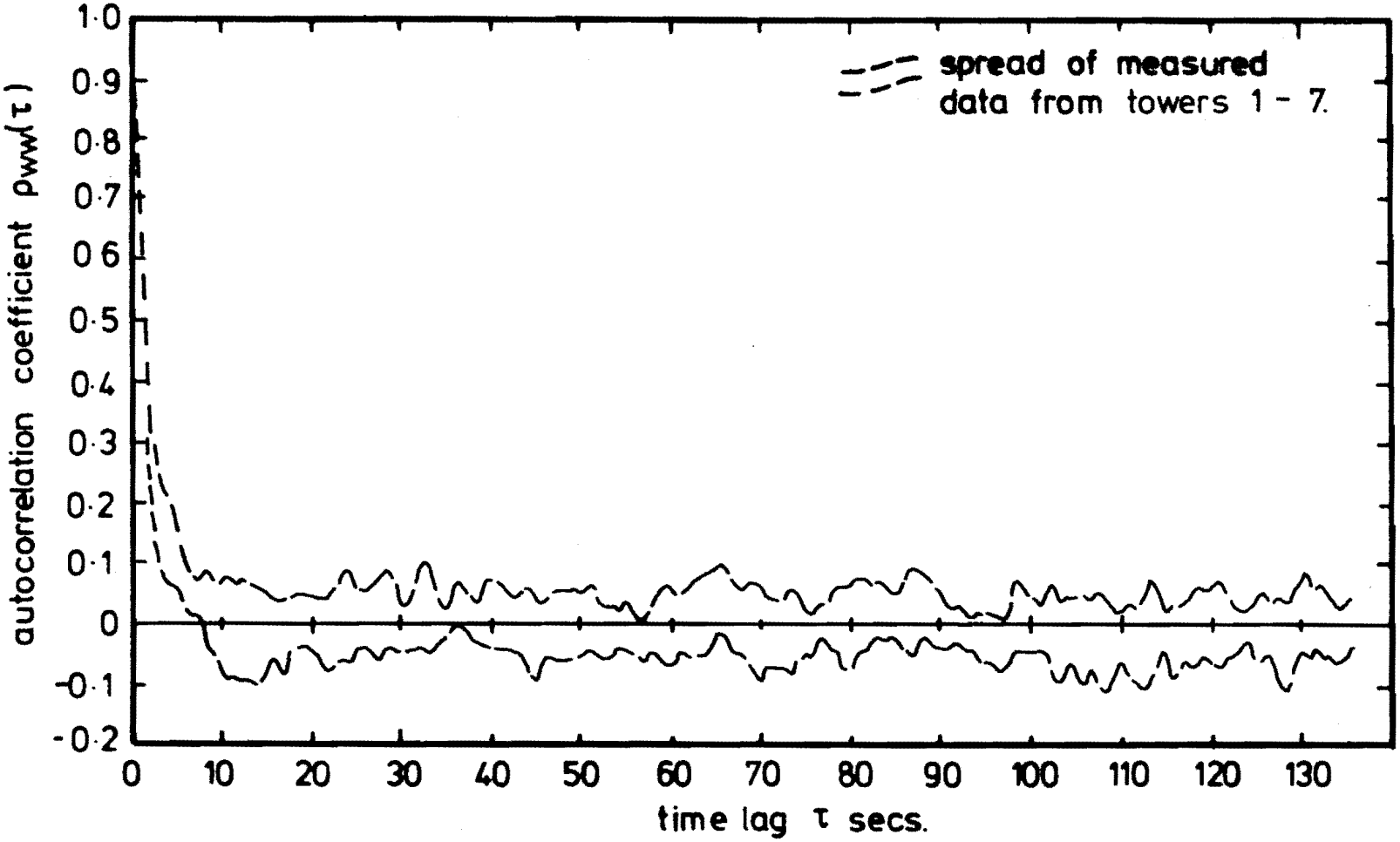

FIG 13.20 VERTICAL COMPONENT w AUTOCORRELATION FUNCTION FOR RUN 6

with all correlations dropping to .2 by τ = 10 seconds. The autocorrelation functions for Run 6 behave differently. The curves from towers 1 to 4 approach zero much more showly than do the curves from towers 5 to 7. The data from towers 1 to 4 behaves as if it contains a trend whereas the data from towers 5 to 7 does not exhibit this behaviour nearly so strongly. Again the presence of the shelter belt probably influences this behaviour.

13.6.3 The Vertical Component Autocorrelation Function

The vertical component autocorrelation functions for both Runs 5 and 6 exhibit similar behaviour. These are shown in Figs.13.19 and 13.20 for Runs 5 and 6 respectively and show that the correlation drops to about .1 after 5 seconds.

13.6.4 Integral Length Scales

The average integral length scales over the towers for each Run have been tabulated in Table 13.4. The length scales for each Run have been calculated via three methods. These are :

(1) From the peak of the ESDU (1974b) spectrum fitted to the measured power spectral density functions and using $\bar{V}_{10}$ averaged over all towers for each Run.

(2) By measuring the time T_E, required for the autocorrelation to drop to a correlation of $\frac{1}{e}$ and then by multiplying this time by $\bar{V}_{10}$ at each tower and then averaging the final result.

(3) By integrating the area under each autocorrelation function until the correlation dropped to 5%, and then multiplying this integral time scale by $\bar{V}_{10}$ from each tower for each Run. These values were then averaged over all towers.

	ESDU (1974b)	Counihan (1975)	Run 5			Run 6		
			$\bar{V}_Z.T_E$	$\bar{V}_Z.T_i$	From Spectrum peak	$\bar{V}_Z.T_E$	$\bar{V}_Z.T_i$	From Spectrum peak
^xL_u	70	144	88	144	71	106	144	94
^xL_v	21		22	54	13	79	137	16
^xL_w	3-5	4	18	19	7	21	19	6

TABLE 13.4 INTEGRAL LENGTH SCALES DERIVED FROM RUNS 5 AND 6

It is apparent from Table 13.4 from the values for ^xL_v that the method of obtaining the integral length scale by integrating the area under the autocorrelation function is unsatisfactory. It produces an estimate which is very dependent on the stationarity of the data. Estimates of $^xL_i, i = u,v,w$ from the time T_E, for the correlation to drop to $\frac{1}{e}$ are more satisfactory but both methods produce larger values than the length scale obtained from fitting the ESDU spectrum to the spectral peak of the measured data.

The values of ^xL_u obtained from the spectrum peak and from the time required for the autocorrelation to drop to $\frac{1}{e}$ agree reasonably well. However, the former method is also unreliable because the measured data spectral peak is often ill-resolved.

All three methods overestimate the value of ^xL_w quoted by ESDU (1974b) and Counihan (1975), as was found in Chapter 11. This is probably the result of the anemometer response characteristics and has been discussed in some detail in Chapter 11.

13.7 CONCLUSIONS

Although several data files were recorded with the wind blowing approximately perpendicular to the row of towers, due to instrumentation faults and other reasons, only two data files have been analysed in detail. Of the two analysed, one was of 73 minutes duration and the other was 18 minutes duration. The latter file had velocity measurements only from towers 1 to 7 and was a stronger wind than the former.

Comparison of the average velocities over the tower line showed that the shelter belt at the south-west end reduced the velocity on tower 8 and perhaps at tower to and 7 slightly also.

The standard deviations of the three components were compared on all towers. The only trend-like behaviour present was an increase in σ_i, i = u,v,w from tower 7 to 8 in Run 5. Consequently the turbulence intensities measured at tower 8 were larger than at the other positions.

Reynolds stress measurements showed variation between towers which appeared to be random. The average values of $\rho_{uw}(0)$ for both Runs 5 and 6 agreed well with the literature and with the measured values from Runs 1 to 4 given in Chapter 9.

Power spectral density measurements, autocorrelation functions and probability density functions showed some variation between different towers and Runs but were reasonably typical of atmospheric turbulence. Because Run 6 was shorter than Run 5 the results computed from it showed more variation than those of Run 5, but in general compared reasonably well.

The results in this chapter have been given to show that the data appears to be of a reasonable standard and thus can be used to make reliable and useful measurements of cross-correlation functions with a horizontal separation. The results agree reasonably well with values in the literature and with results from previous chapters. Discrepancies generally can be explained from physical arguments, e.g. the response

characteristics of the anemometer and the shelter belt at the south-west end of the tower line.

This chapter therefore justifies the use of the data from Runs 5 and 6 in the following chapter which discusses in detail the cross-correlation functions between different towers and the integral length scales of turbulence derived from these cross-correlation measurements.

CHAPTER 14

HORIZONTAL SPATIAL CROSS-CORRELATIONS

14.1 INTRODUCTION

The previous chapter has been used to show that the data obtained in Runs 5 and 6 exhibits characteristics which are acceptable for the terrain and the high wind speed conditions existing at the time the data was recorded. Thus the following results relating to cross-correlation measurements between velocities measured on different towers at the same height can be regarded as being representative of this type of terrain for a neutrally stable atmospheric boundary layer. However, from the results of the previous chapter it is apparent that care needs to be taken in interpreting results involving towers 6 to 8, as the wind structure appears to be somewhat influenced by the presence of the shelter belt.

Very few measurements of the spatial structure of the wind have been made with several tower mounted anemometers in a line, or some other combination of towers. Panofsky (1961) determined integral length scales from measurements taken during Project Prairie Grass. The anemometers were mounted at a height of 2 m. Panofsky found that the integral length scales were very strongly dependent on atmospheric stability. At night time when the air was stable, the horizontal spatial correlations and the autocorrelations fell much more quickly than in the daytime when the air was neutrally stable or unstable. Panofsky also observed a gradual slow change in wind velocity under stable and low wind speed conditions at night. This caused the autocorrelation function not to fall to zero but to fall to a plateau where the correlation remained constant for increased time delays.

It was also found that $^{x}L_{u} \approx {}^{x}L_{v}$ in unstable air but $^{x}L_{v} < {}^{x}L_{u}$ and

$^{x}L_u \approx 8.^{y}L_u$ in neutral and stable air. Panofsky also quoted some unpublished results of Davenport. Davenport had found that $^{x}L_u >> {}^{y}L_u$, from measurements on the Severn River Bridge, near Sharpness, during a storm when the wind was blowing perpendicular to the bridge.

Panofsky also found that when the wind was blowing along the row of anemometers, the maximum correlation occurred at time delays indicating that the gusts were convected along at a slightly higher velocity than the average wind speed at that height.

Piekle and Panofsky (1970) also discuss the turbulence characteristics measured from several towers. It was found that an exponential function fitted measured coherence functions obtained with a vertical separation. For horizontal separations it was assumed that the same type of function would fit the data although in the paper it was stated that there was a conspicuous lack of published correlation data with horizontal separations.

Shiotani has reported many results from measurements of wind structure made on the N.E. coast of Shikoku Island of Japan. These measurements were made from five towers, 40 m high positioned in a straight line on a sea wall. They thus had good exposure for all winds off the sea and also good exposure for most wind directions off the land.

Early results were obtained with Aerovane anemometers but more recent results have been obtained from three-component sonic anemometers and arrays of two Gill propeller anemometers, are mounted vertically and one mounted horizontally, perpendicular to the coastline.

The results from these measurements have been reported by Shiotani and Arai (1967), Shiotani and Iwatani (1971), Shiotani (1975), Shiotani and Iwatani (1976) and Shiotani et al (1978). However, the results from Shikoku Island do not compare directly with the results in this work because the anemometers used at Shikoku Island were 40 m high, compared with 10 m in this work. Also, many of their results were recorded when

the wind came off the sea in monsoon or typhoon wind conditions when the wind might well have a different structure.

Powell and Elderkin (1974) describe an experiment which was performed to investigate Taylor's Hypothesis. In this experiment for wind directions virtually parallel with their line of towers, they compared horizontal space correlations with autocorrelation functions in the three orthogonal directions. It was found that Taylor's Hypothesis was obeyed well, under less restrictive conditions than had been earlier thought necessary. It was also found that the eddies were convected along at a speed slightly higher than the average wind speed. This disagrees with the results of Shiotani and Iwatani (1976) but Shiotani and Iwatani state that their results were subject to considerable experiment error. However, Powell and Elderkin gave no results with the mean wind vector at approximately 90 degrees to the line of towers.

Ropelewski et al (1973) studied the coherence for streamwise and cross-stream wind components at four meteorological sites and compared it with a representative wind tunnel experiment. The object of the study was to find a_j^i, the decay parameter in :

$$\gamma_{ij}(n) = \exp(-a_j^i \cdot \Delta f_j) \ , \ \Delta f_j = n \cdot \Delta x_j / \bar{U} \qquad i,j = 1,2 \text{ or } 3$$

where i is an index that refers to the streamwise, cross-stream and vertical wind components respectively, and j is an index that refers to longitudinal, lateral and vertical instrument separations with respect to the mean wind $\bar{U}$. n is frequency in Hz, Δx_j, the separation distance and Δf_j is reduced frequency. a_j^i was required for various atmospheric stabilities, roughness lengths etc. The cross-spectral density function is the Fourier transform of the cross-correlation function, but Ropelewski et al (1973) did not discuss cross-correlation measurements with horizontal separations in detail.

With so few reported results of cross-correlation measurements with a horizontal separation approximately perpendicular to the average

wind direction, it was decided that further measurements of this turbulence parameter were justified.

14.2 LONGITUDINAL VELOCITY COMPONENT CROSS-CORRELATION VARIATION WITH τ AND ΔY, $\rho_{uu}(\Delta Y, \tau)$

It may be observed in Fig.13.1 that the average wind vector for both Runs 5 and 6 is almost perpendicular to the line of towers. Thus the maximum correlation between the two data streams from different towers should presumably occur near $\tau = 0$, but if τ was some small finite value, it would be a value such that the data stream from a tower to the north-east would be delayed in time with respect to the south-west side. This is because an eddy with a front perpendicular to the average wind direction would tend to strike a north-east anemometer before a south-west one.

To obtain information off a series of towers such as used in this experiment, a large number of correlation pairs and consequently graphical output has to be analysed. The total number of combinations of cross-correlations with even only eight towers is formidable. Consequently only representative cross-correlation versus time delay graphs with various values of ΔY have been given.

Figs.14.1 and 14.2 show cross-correlations of $\rho_{uu}(\Delta Y, \tau)$ for various combinations of towers for Runs 5 and 6 respectively. Note that all the correlations are near zero and show a random type of behaviour for separations of 60 and 150 m. The three curves with separations of 7.5, 15 and 22.5 m are shown to reach a maximum value near $\tau = 0$ and to fall for $|\tau| > 0$ seconds. The correlation reduction is not nearly so sudden with increase of $|\tau|$ as it was for $\rho_{uu}(\Delta Z, \tau)$ discussed in Chapter 12. For $|\tau| > 20$ seconds the three cross-correlation functions with separation distances of 7.5,15 and 22.5 m tend to merge together showing that the correlations for timelags of this duration are not very

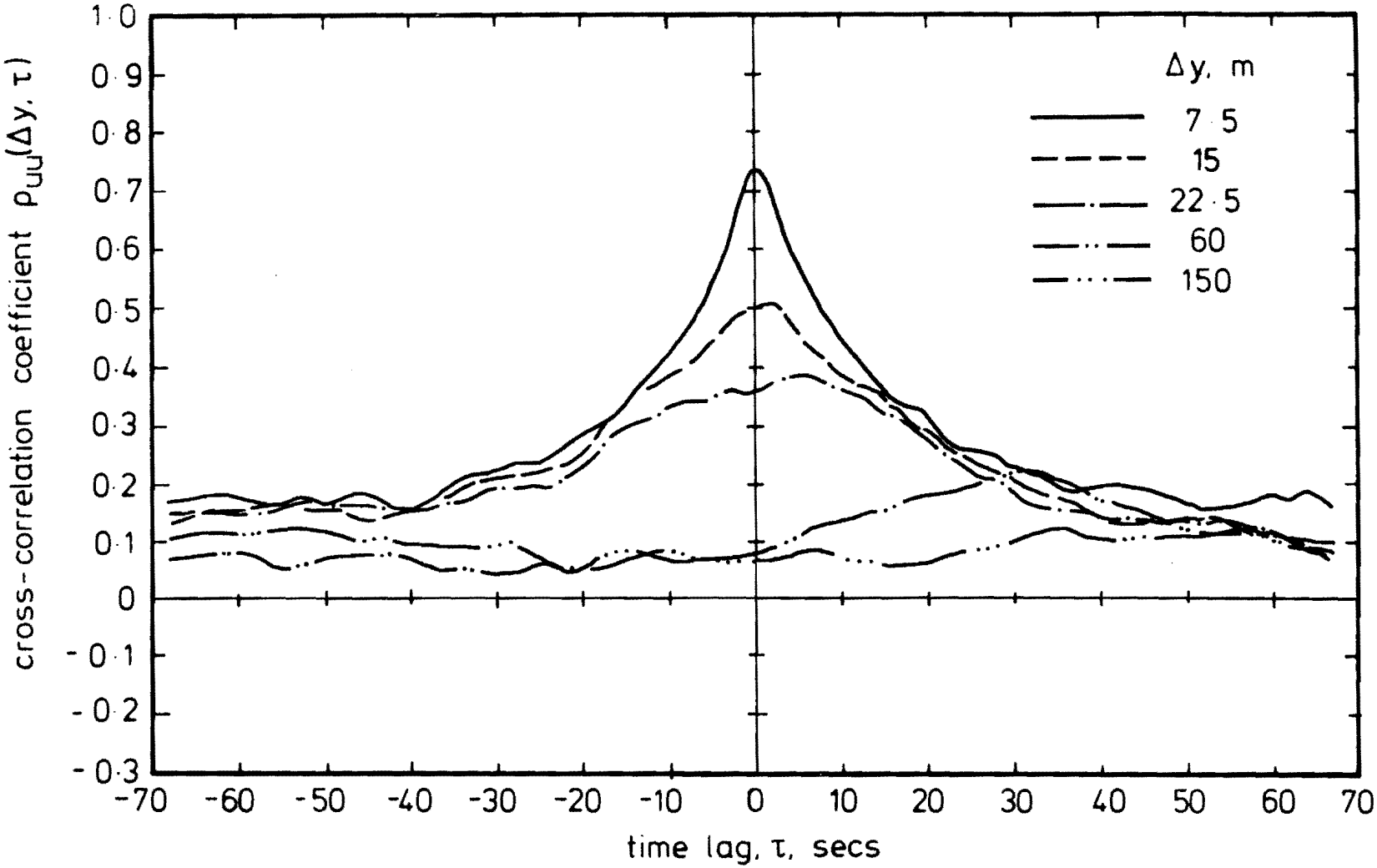

FIG. 14·1 LATERAL CROSS-CORRELATION $\rho_{uu}(\Delta y, \tau)$ FOR RUN 5.

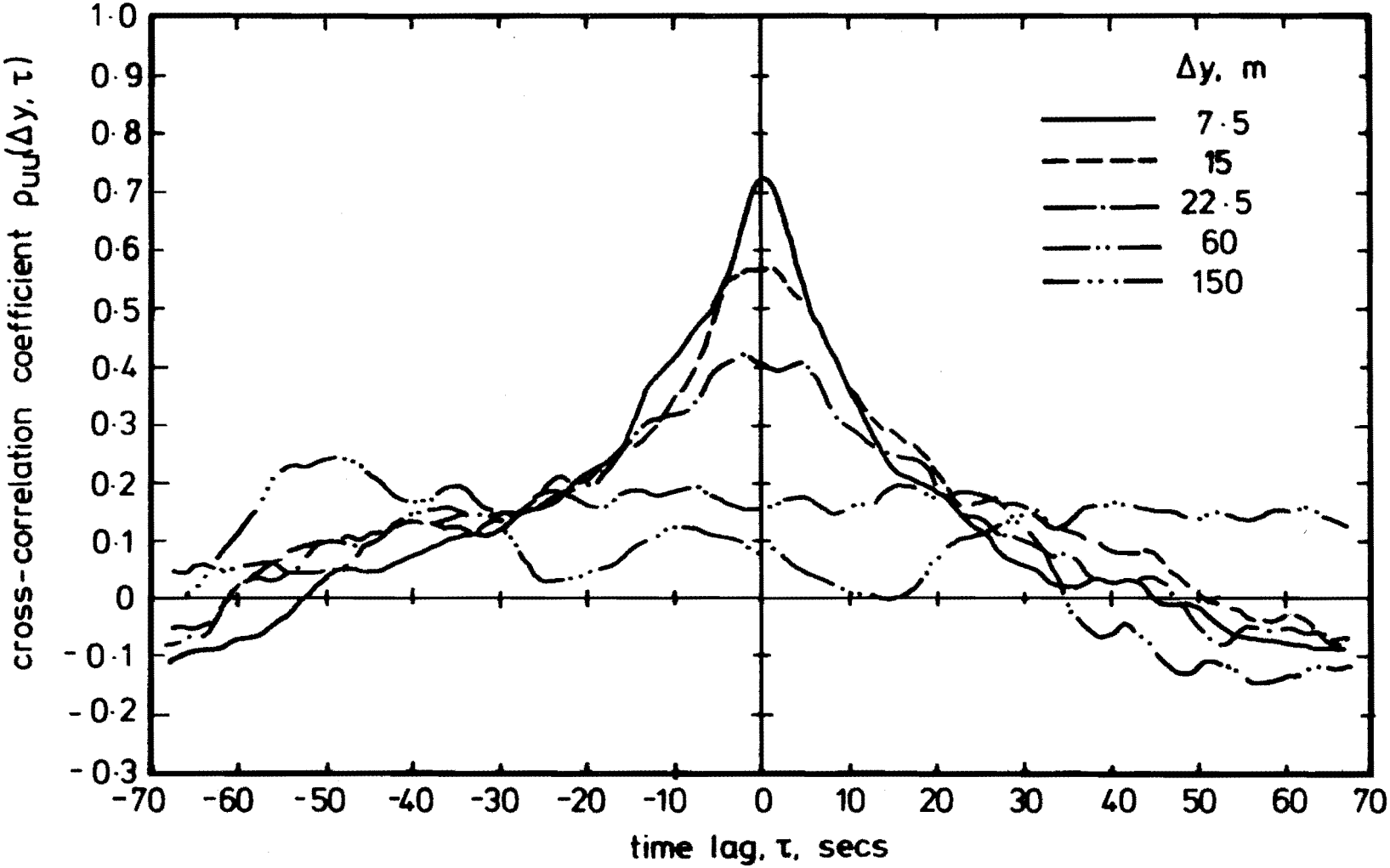

FIG. 14·2 LATERAL CROSS-CORRELATION $\rho_{uu}(\Delta y, \tau)$ FOR RUN 6.

dependent on the separation distance ΔY between the anemometers. The same features are apparent for both the Run 5 and 6 data but the Run 6 result shows more fluctuation than the Run 5 result.

From a series of similar curves to those shown in Figs.14.1 and 14.2 the integral length scale ${}^{y}L_{u}$ was obtained from the values of $\rho_{uu}(\Delta Y, 0)$ for different values of ΔY. It was observed that the maximum correlation for $\rho_{uu}(\Delta Y, \tau)$ occurred at τ very close to zero so the values of $\rho_{uu}(\Delta Y, 0)$ were a good indication of the maximum correlation.

14.3 LATERAL VELOCITY COMPONENT CROSS-CORRELATION VARIATION WITH τ AND ΔY, $\rho_{vv}(\Delta Y, \tau)$

This cross-correlation is called a longitudinal cross-correlation because the velocity components considered at the points are parallel to the line separating them. It is probably of little importance physically because it considers velocity fluctuations which are parallel to the face of a structure when the structure is perpendicular to the wind direction.

The cross-correlations $\rho_{vv}(\Delta Y, \tau)$ are plotted in Figs.14.3 and 14.4 for Runs 5 and 6 for the same separation distances ΔY which were used for the plots of $\rho_{uu}(\Delta Y, \tau)$ in Figs.14.1 and 14.2. The lateral velocity component cross-correlations exhibit similar characteristics to the longitudinal velocity component cross-correlations given in Figs.14.1 and 14.2. It is however clearly apparent that the lateral component correlations decrease far more rapidly for $|\tau| > 0$ than do the longitudinal component correlations.

The lateral velocity component cross-correlation from Run 6 shows the existence of a trend in the data. It can be seen that the correlation does not fall particularly close to zero, even for $|\tau| = 67$ seconds. Because the correlation is not zero for large τ, the correlation at $\tau = 0$ is also overestimated slightly.

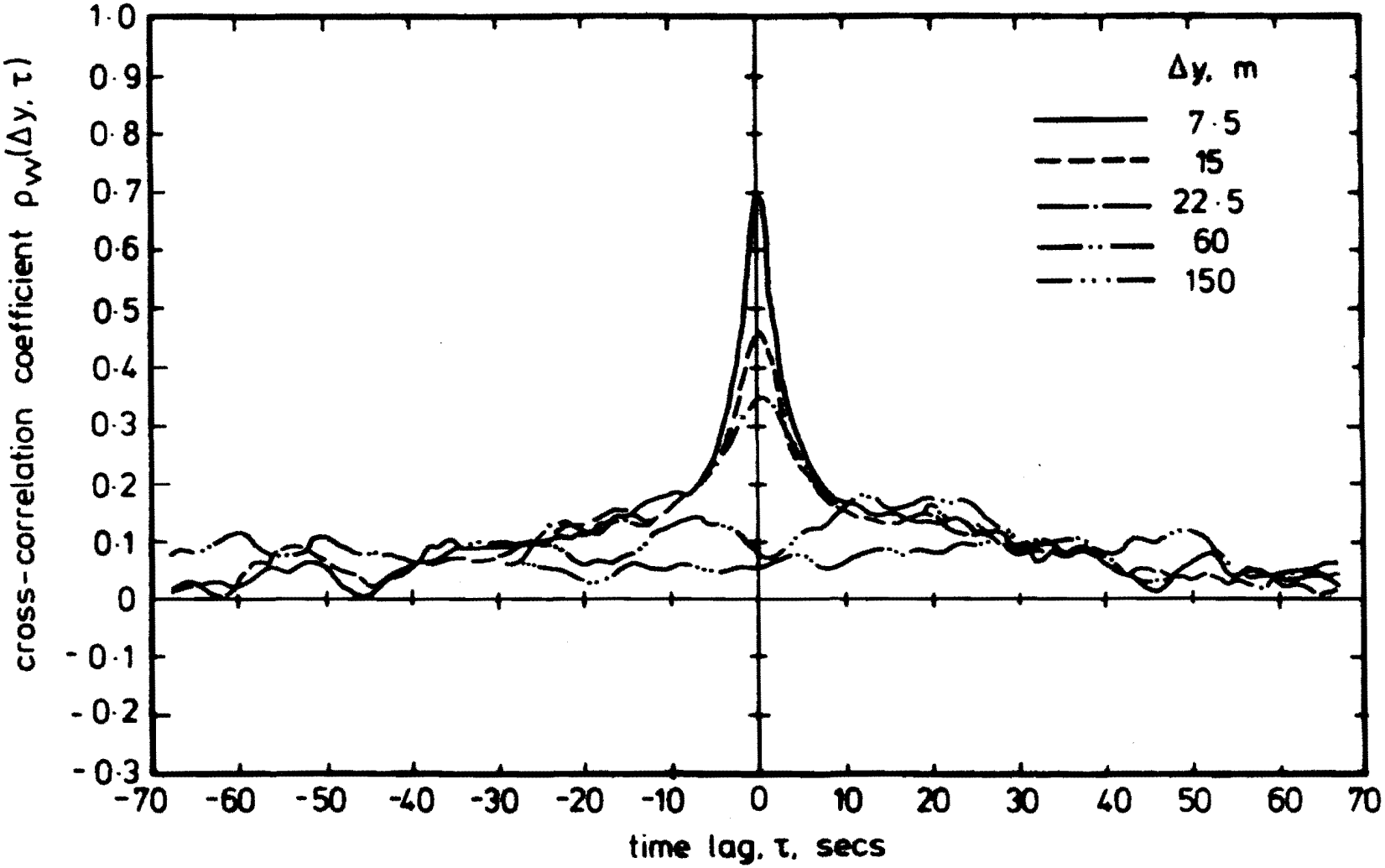

FIG. 14·3 LONGITUDINAL CROSS-CORRELATION $\rho_{vv}(\Delta y, \tau)$ FOR RUN 5.

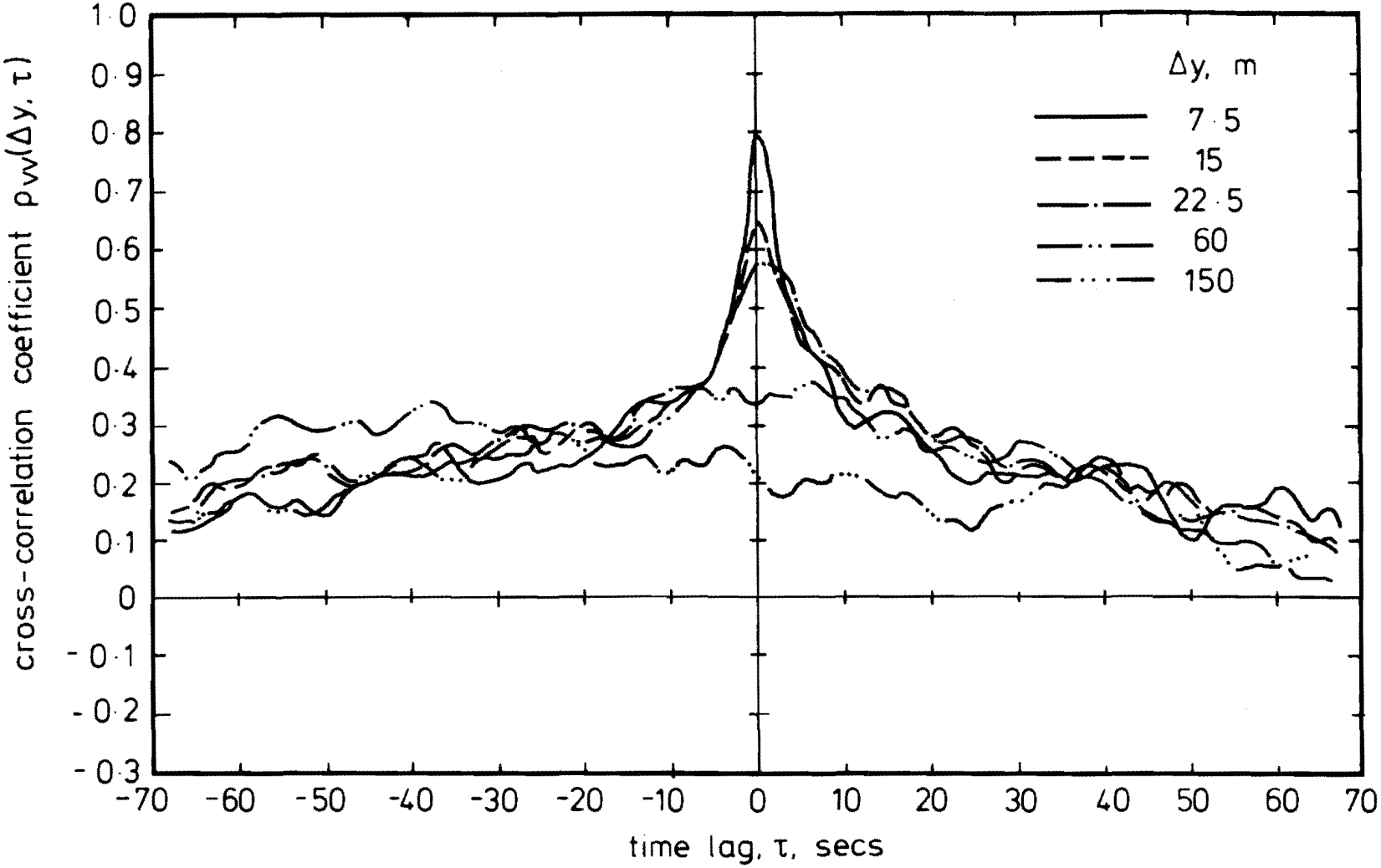

FIG. 14·4 LONGITUDINAL CROSS-CORRELATION $\rho_{vv}(\Delta y, \tau)$ FOR RUN 6.

Figs.14.3 and 14.4 show that the maximum correlation occurs at $\tau = 0$, which is consistent with the wind direction. Hence a "corrected" correlation for the Run 6 data can be found by using the formula from Panofsky (1961) and also used in Chapters 12 and 13, i.e.

$$r_m = (1 - r_\infty)\, r_t + r_\infty,$$

with the usual meaning of the terms.

The zero time delay correlations for the separations ΔY used in Fig.14.4, are given in Table 14.1, both corrected and uncorrected for the trends in the data.

ΔY	$\rho_{vv}(\Delta Y, \tau)$	
	uncorrected	corrected
7.5	.81	.78
15	.66	.59
22.5	.58	.48
60	.33	.16
150	.20	.06

TABLE 14.1 $\rho_{vv}(\Delta Y, \tau)$ CORRECTED AND UNCORRECTED FOR TRENDS IN THE DATA

Table 14.1 shows that there is a substantial reduction in the cross-correlation values particularly for large values of ΔY. For small values of ΔY (high correlations) the values are only slightly affected by the correction.

14.4 VERTICAL VELOCITY COMPONENT CROSS-CORRELATION VARIATION WITH τ AND ΔY, $\rho_{ww}(\Delta Y, \tau)$

From the curves shown in Figs.14.5 and 14.6, it is immediately apparent that vertical velocity component correlations extend for a much smaller lateral distance than either the longitudinal or lateral velocity component correlations. In fact the correlations between pairs of vertical velocity data streams are very close to zero for a separation

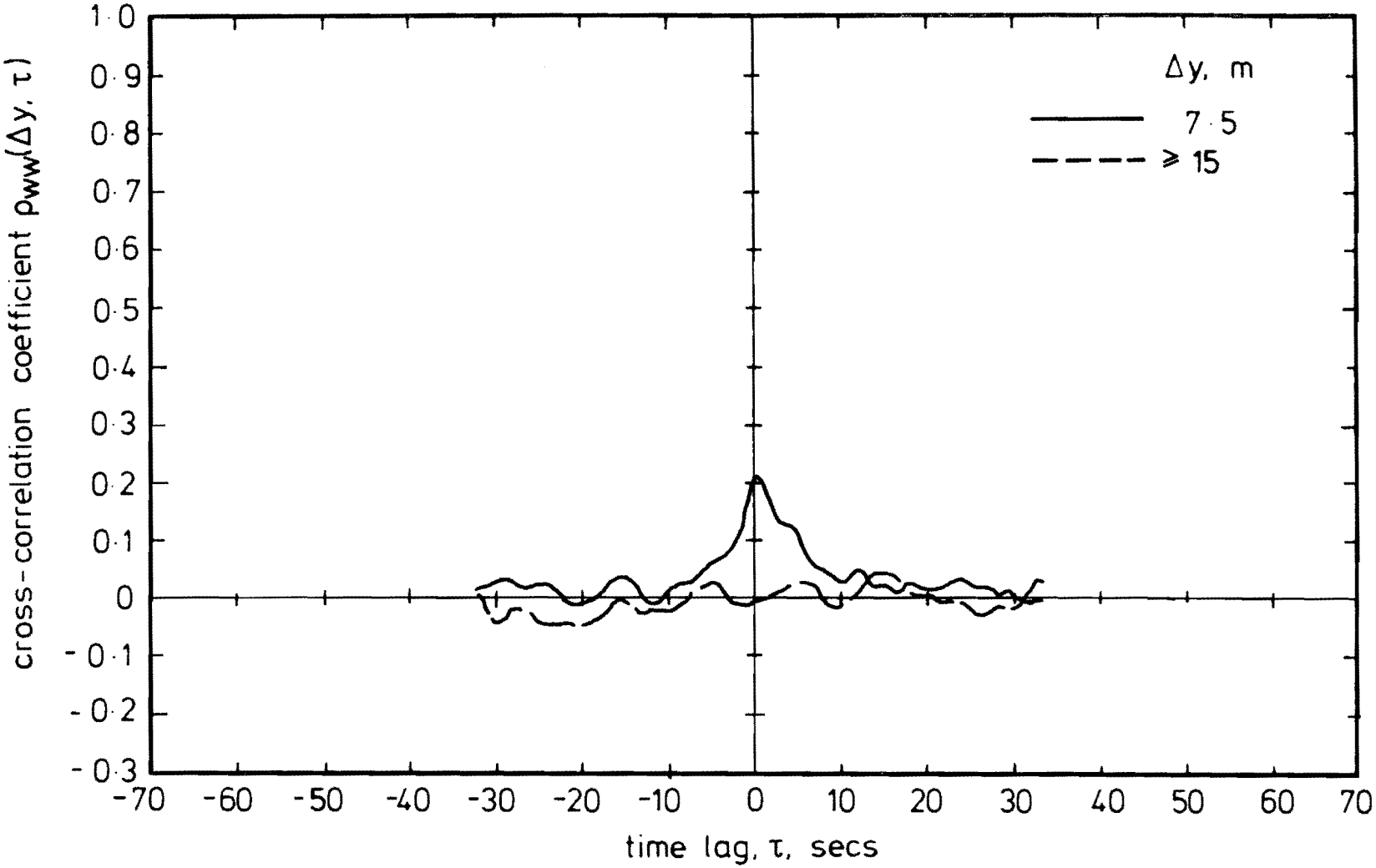

FIG. 14·5 LATERAL CROSS-CORRELATION $\rho_{ww}(\Delta y, \tau)$ FOR RUN 5.

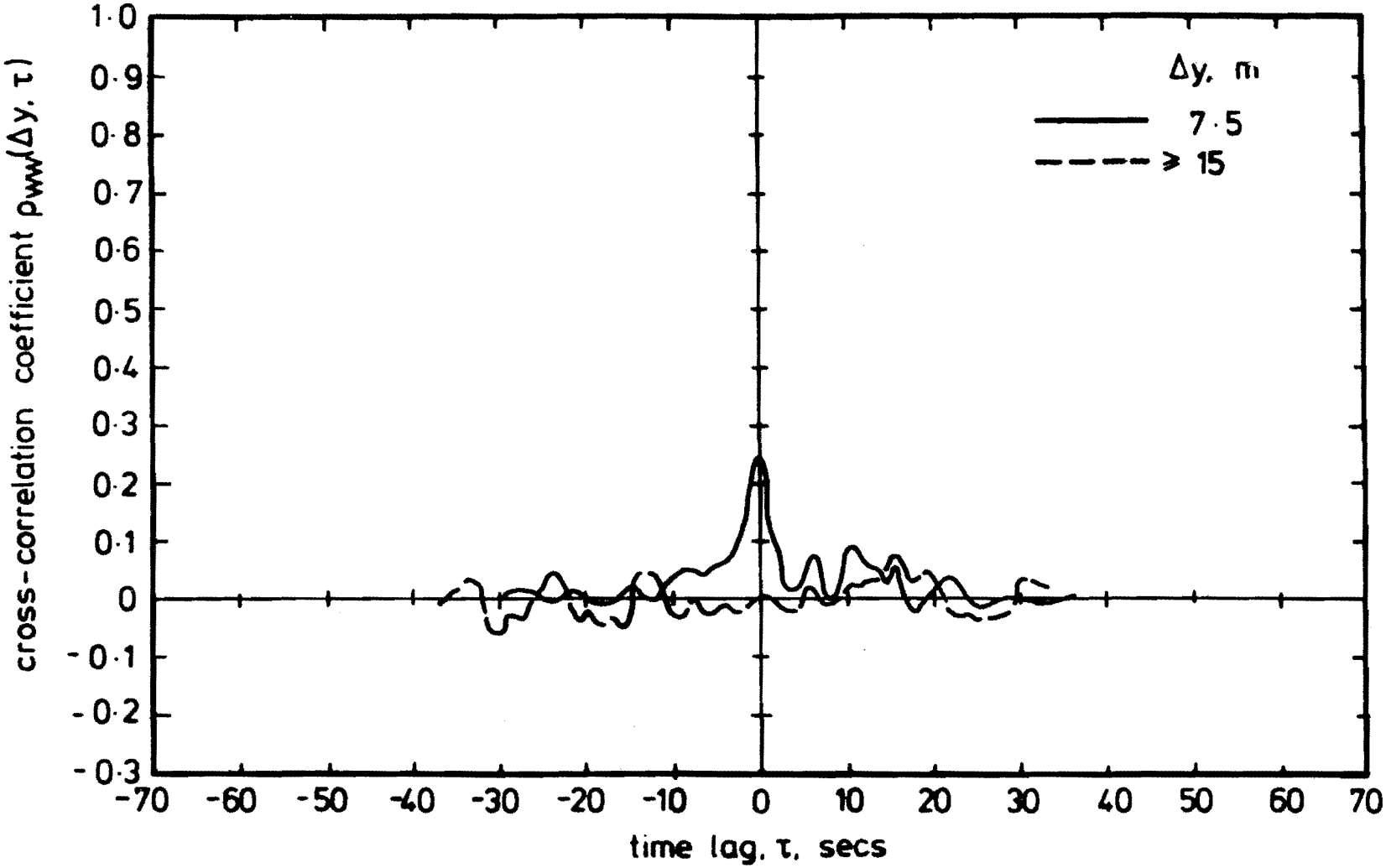

FIG. 14·6 LATERAL CROSS-CORRELATION $\rho_{ww}(\Delta y, \tau)$ FOR RUN 6.

distance of $\Delta Y = 15$ m. For the separation $\Delta Y = 7.5$ m, the maximum correlation is significant and occurs at $\tau = 0$. For $|\tau| > 0$ the correlation quickly drops towards zero. For all combinations of separations greater than 7.5 m and all values of $|\tau| < 68$ seconds, the correlation lies within + .05 and - .05 for the Run 5 data.

The data from both Runs 5 and 6 exhibits similar characteristics although the Run 6 result again shows slightly more variation so that for $\Delta Y > 7.5$ m and $|\tau| < 68$ seconds, the correlations lie within the band bounded by correlations of $\pm .1$.

This correlation is closely related to the correlation of the angle of inclination of the wind vector to the horizontal. This follows because the angle of inclination $\xi = \tan^{-1} \frac{w}{\bar{V}_Z + u}$ at each time instant.

Thus if $u << \bar{V}_Z$, and for small ξ, $\tan \xi = \xi$

$$\Rightarrow \xi = \frac{w}{\bar{V}_Z} = \text{constant x } w.$$

The knowledge of this correlation is useful for determining the vertical component of forces on long slender structures, as it determines the width of the gust which has well correlated vertical velocity components.

These results show that the vertical component velocities are well correlated only for small lateral separation distances ΔY. Therefore most structures which would require the determination of wind loading would be significantly longer than the distance ΔY required for $\rho_{ww}(\Delta Y, 0)$ to fall to zero.

14.5 THE INTEGRAL LENGTH SCALE $^{y}L_u$

The values of $\rho_{uu}(\Delta Y, 0)$ obtained from various separation distances ΔY from different combinations of pairs of towers enabled the integral length scale $^{y}L_u$ to be evaluated. Values of $\rho_{uu}(\Delta Y, 0)$ were obtained from

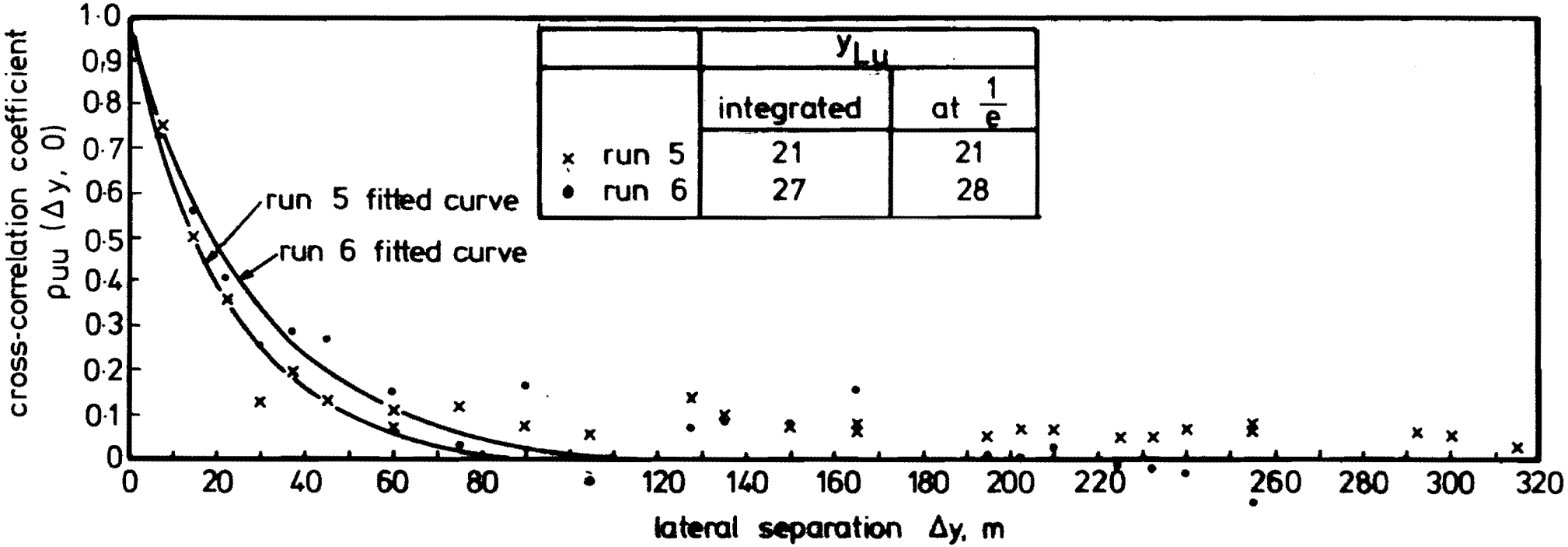

FIG. 14·7 VARIATION OF CROSS-CORRELATION ρ_{uu} (Δy, 0) WITH HORIZONTAL SEPARATION Δy.

similar graphs to the two described in Section 14.2 and given in Figs. 14.1 and 14.2. This enabled the data to be presented in the format shown in Fig.14.7 with the correlation plotted against the lateral separation distance ΔY.

The two curves which have been fitted to the measured data from both Runs 5 and 6 are similar in shape. Both could be well approximated by negative exponential curves.

Integrating the area under the two curves until the correlation reaches zero gives

$$^{y}L_{u} = 21 \text{ m for Run 5} \quad \text{and}$$

$$^{y}L_{u} = 27 \text{ m for Run 6.}$$

These values are compared with other published values in Table 14.2.

	Run 5	Run 6	ESDU (1975)	SHIOTANI (1976)	COUNIHAN (1975) $.35x\ ^{x}L_{u}$	TEUNISSEN (1977c)
height, Z, m	10	10	10	40	10	10
$^{y}L_{u}$, m	21	27	30	60	50	12-26

TABLE 14.2 THE INTEGRAL LENGTH SCALE $^{y}L_{u}$.

The measured values are shown,in Table 14.2,to compare reasonably with ESDU (1975) but not so well with Counihan (1975). It is not unexpected that the value of $^{y}L_{u}$ given by Shiotani (1976) is significantly higher than the measured results presented here since Shiotani's measurements were taken on a much taller tower.

The curves in Fig.14.7 show that the correlation falls rapidly to very low values for separations of up to approximately 40 m. At a lateral separation of 80 m the longitudinal velocity components are virtually uncorrelated. However it is also apparent that there appears

to be a slight correlation existing even for much larger separations than 80 m for both Runs. This is no doubt due to trends in the longitudinal component measured data streams.

Fig.14.7 shows all the zero time delay cross-correlations evaluated for all combinations of towers. It is interesting to note that the correlations fell to zero well within the 315 m span of the towers. The results from correlations involving towers 6,7, and 8 have been used as the values obtained did not appear to be significantly different from similar separation distances involving the other five towers. However, had it been necessary, the results involving towers 6,7, and 8 could have been disregarded, and the results obtained from the 5 towers left would have been quite sufficient to define the correlation and the same curves shown in Fig.14.7 would have been obtained.

The integral length scale $^{y}L_{u}$ is of the most importance physically of the three length scales obtained from the row of tower mounted anemometers. It determines the apparent "width" of a gust, or the horizontal distance over which the longitudinal velocity components are significantly correlated. Thus these results indicate that the longitudinal velocity components are well correlated for separations (at 10 m) up to 20 to 40 m. Above 80 m, no correlation, due to the turbulence superimposed on the mean flow, exists.

14.6 THE INTEGRAL LENGTH SCALE $^{y}L_{v}$

In a similar manner as discussed in Section 14.3, the length scale $^{y}L_{v}$ was obtained from the zero time delay cross-correlation $\rho_{vv}(\Delta Y, 0)$, for various values of ΔY from different tower pairs. The data corresponding to the zero time delay cross-correlations for various distances is plotted in Fig.14.8 for both Runs 5 and 6.

Three curves are shown, one from the Run 5 data, and two from the Run 6 data. Two curves from the Run 6 data have been obtained, one from

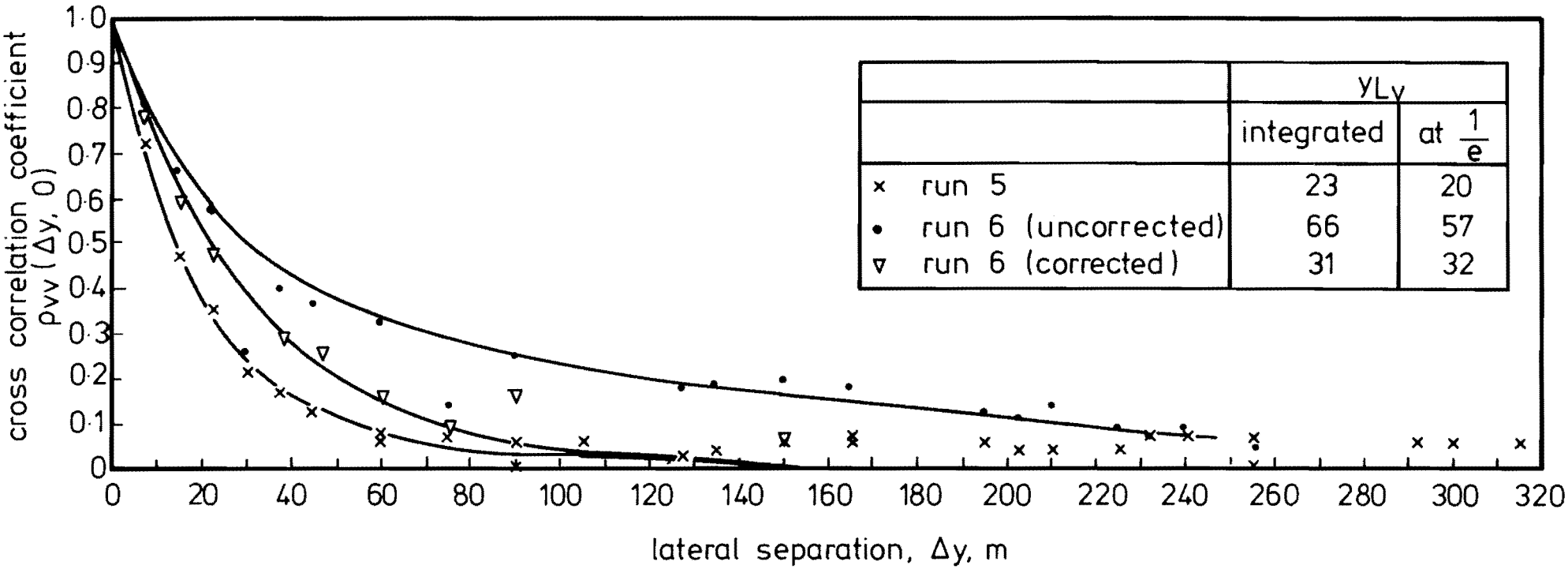

FIG. 14·8 VARIATION OF CROSS-CORRELATION $\rho_{vv}(\Delta y, 0)$ WITH HORIZONTAL SEPARATION Δy.

results uncorrected for the presence of trends in the data, and one corrected for the trends. The correction for the trends has been described in Section 14.3, and typical changes in the correlation through the correction have been given in Table 14.1 for various values of ΔY,

It can be seen in Fig.14.8 that the curve fitted to the uncorrected data from Run 6 approaches a zero correlation much more slowly than does the curve fitted to the Run 5 data. If was also noticed in some of the lateral velocity component autocorrelation functions for Run 6 in Section 13.6.2 that they approached a zero correlation rather more slowly than the corresponding autocorrelation functions from Run 5.

Fig.14.4 shows the lateral velocity component cross-correlation functions for Run 6. In the figure it can be observed that even for $\tau = \pm$ 67 seconds, the correlations are still near .1 to .2, and show a lot of random fluctuation because of the short duration of the data file. Since it is apparent that this effect is caused by non-stationarities in the flow, they have been corrected as stated in Section 14.3

The curve fitted to the corrected correlation data from Run 6 does approach towards zero for large separation distances and is much closer to the curve fitted to the Run 5 data.

The integral length scales $^{y}L_{v}$ have been obtained from the curves. The values for Run 5 and Run 6 (corrected) were obtained by integrating the corresponding curves until the correlation dropped to zero. The curve for the Run 6 (uncorrected) result was integrated until it fell to a correlation of 5% to obtain the integral length scale. These values have been tabulated in Table 14.3 with an unpublished result from Teunissen (1977c), and also with the integral length scale evaluated by taking the distance for the correlation to fall to $\frac{1}{e}$.

	$^{y}L_{v}$	
	integrated, m	distance for correlation to drop to $\frac{1}{e}$, m
Run 5	23	20
Run 6 (uncorrected)	66	57
Run 6 (corrected)	31	32
Teunissen (1977c)	17-30	

TABLE 14.3 THE INTEGRAL LENGTH SCALE $^{y}L_{v}$

There is good agreement between the results obtained by integrating the curves and also by estimating the distance required for them to fall to a correlation of $\frac{1}{e}$. This suggests that the correlation functions could be reasonably represented by negative exponential curves.

Values of $^{y}L_{v}$ are not very prominent in the literature. The only result the author has found is that from Teunissen (1977c). No estimates are given by ESDU (1975), Counihan (1975) or Shiotani. Consequently it is difficult to compare with others. A probable reason for the paucity of data relating to it is its apparent little physical significance.

14.7 THE INTEGRAL LENGTH SCALE $^{y}L_{w}$

This length scale was obtained from the zero time delay cross-correlation function $\rho_{ww}(\Delta Y, 0)$ for various separation distances ΔY, in a similar manner to the way in which $^{y}L_{u}$ and $^{y}L_{v}$ were evaluated. The correlation between the vertical velocity components as a function of the lateral separation distance ΔY is shown in Fig.14.9 for both

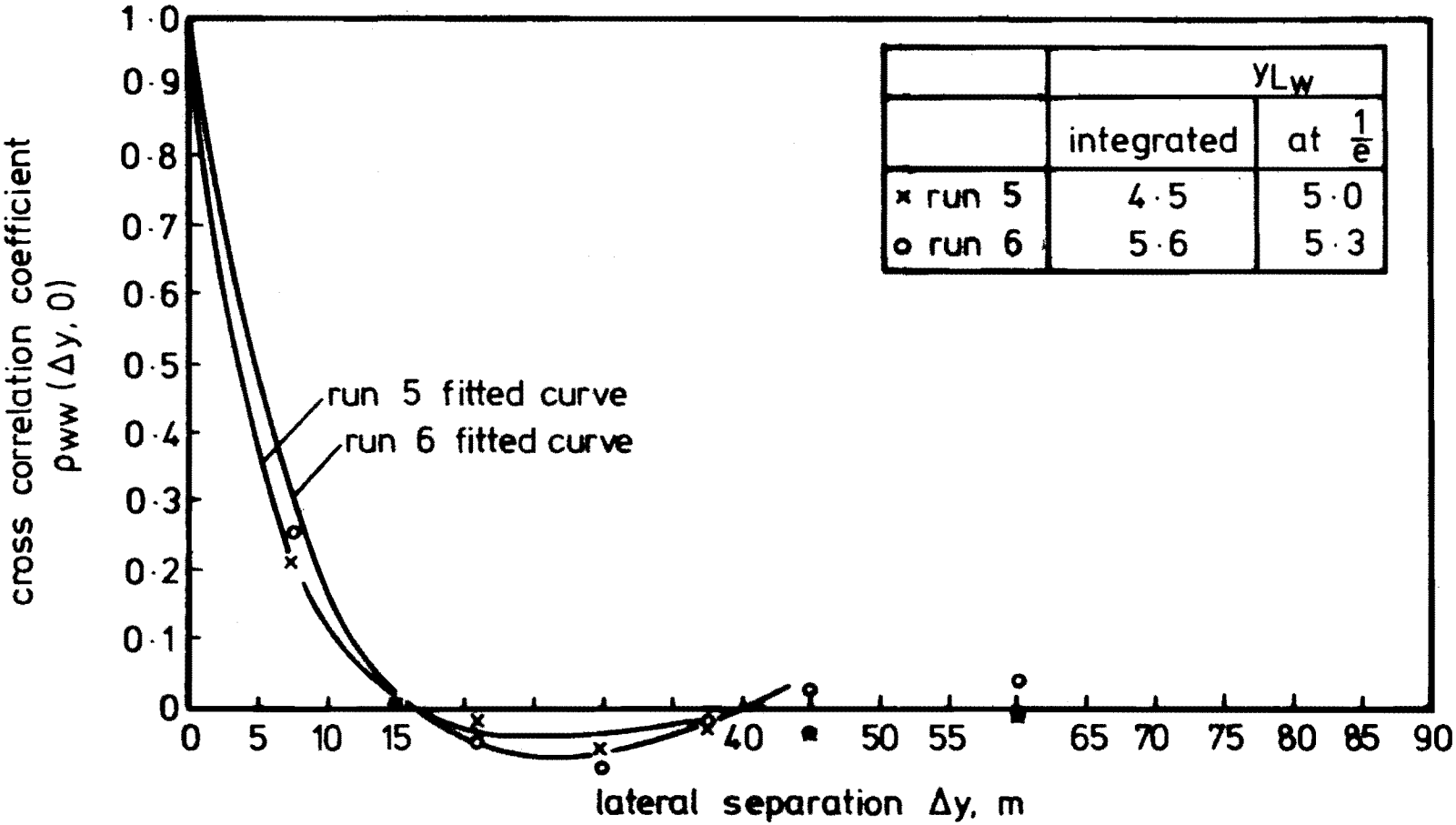

FIG. 14·9 VARIATION OF CROSS-CORRELATION $\rho_{ww}(\Delta y, 0)$ WITH HORIZONTAL SEPARATION Δy.

Runs 5 and 6. Note the change in scale compared with Figs.14.7 and 14.8, relating to $^{y}L_{u}$ and $^{y}L_{v}$ respectively.

$^{y}L_{w}$ is significantly smaller than both $^{y}L_{u}$ and $^{y}L_{v}$. Integrating the two curves to the first zero crossing in Fig.14.9 gives values of :

$$^{y}L_{w} = 4.5 \text{ m} \quad \text{for Run 5 and}$$

$$^{y}L_{w} = 5.6 \text{ m} \quad \text{for Run 6.}$$

These values are compared with other values from the literature in Table 14.4.

	Run 5	Run 6	ESDU (1975)	SHIOTANI (1978)	TEUNISSEN (1977c)
height Z, m	10	10	10	40	10
$^{y}L_{w}$, m	4.5	5.6	3.5	13	2-4.5

TABLE 14.4 THE INTEGRAL LENGTH SCALE $^{y}L_{w}$

The measured values are seen to agree well with Teunissen (1977c) and ESDU (1975) but poorly with Shiotani et al (1978). However the result of Shiotani was obtained at a height of 40 m, whereas the other measurements from the literature were made at a height of 10 m.

The small value of $^{y}L_{w}$ measured is physically desirable as stated in Section 14.4 because it is this component which causes the vertical buffeting of horizontal structures.

14.8 CONCLUSIONS

The wind direction was almost perpendicular to the line of towers for both Runs so that it was expected that the maximum correlation between different towers for all components would occur near $\tau = 0$. This feature

was observed in the results of the data. It was however noted that although $\rho_{uu}(7.5,0)$ was not much larger than $\rho_{vv}(7.5,0)$, the latter correlation dropped far more quickly towards zero for $|\tau| > 0$. This is a similar feature to the observed behaviour of $\rho_{uu}(\Delta Z, \tau)$ and $\rho_{vv}(\Delta Z, \tau)$, as the latter correlation also approached zero more quickly than $\rho_{uu}(\Delta Z, \tau)$ for a given ΔZ, when the data was trend free.

The correlation $\rho_{ww}(\Delta Y, 0)$ was much smaller than the two other measured horizontal cross-correlations and dropped completely to zero for $\Delta Y = 15$ m. It also appeared to be slightly negatively correlated for separation distances ΔY between 15 and 35 m, but this might have been a feature of the data analysed.

From the three cross-correlations, the integral length scales ${}^{y}L_{u}$, ${}^{y}L_{v}$ and ${}^{y}L_{w}$ were evaluated. These are tabulated in Table 14.5 and compared with the average values of ${}^{x}L_{u}$, ${}^{x}L_{v}$ and ${}^{x}L_{w}$ from Runs 1 to 4 obtained at Z = 10 m, discussed in Chapter 11. Also shown in the same figure are the values of ${}^{z}L_{v}$ and ${}^{z}L_{w}$ evaluated in Chapter 12, and finally values of ${}^{x}L_{u}$, ${}^{x}L_{v}$ and ${}^{x}L_{w}$ obtained from Runs 5 and 6 in Chapter 13.

The length scales given from Chapter 11 have been evaluated from the time required for the correlation to fall to a correlation of $\frac{1}{e}$ and then by multiplying this integral time scale by the average velocity for that particular height and Run. The values of ${}^{x}L_{i}$, i = u,v,w from Runs 5 and 6 have been obtained in the same way. ${}^{z}L_{i}$ and ${}^{y}L_{i}$, i = u,v,w were obtained by integrating the correlations until they reached zero. Note that the value of ${}^{y}L_{v}$ for Run 6 given is the value corrected for the trends in the data.

It was found by Shiotani (1976) that

$$ {}^{x}L_{u} \approx (2.5 \text{ to } 4).\ {}^{y}L_{u} $$

and this agrees well with the range recommended by Counihan (1975) which is :

$$ {}^{x}L_{..} \approx (2.5 \text{ to } 3.5).\ {}^{y}L_{..} $$

	Run 5	Run 6	average of Runs 1 to 4
x_{L_u}	88	106	90
x_{L_v}	22	79	38
x_{L_w}	18	21	11
y_{L_u}	21	27	
y_{L_v}	23	31	
y_{L_w}	4.5	5.6	
z_{L_v}			6-8
z_{L_w}			6-8

TABLE 14.5 INTEGRAL LENGTH SCALE COMPARISON

Using values of x_{L_u} and y_{L_u} from Run 5 gives

$$x_{L_u} = 4. y_{L_u} \text{ for the measured data.}$$

The same value is also obtained using the Run 6 data. Thus the measured data is in agreement with Shiotani and is close to the range recommended by Counihan.

Shiotani et al (1978) has also reported that it was found that

$$y_{L_w} \approx \frac{1}{4} . y_{L_u} \text{ and } x_{L_w} \approx \frac{1}{6} . x_{L_u} .$$

Using the measured data from Run 5 gives

$$y_{L_w} = \frac{1}{4.7} . y_{L_u} \text{ , and using the measured data from Run 6}$$

gives

$$^{y}L_{w} = \frac{1}{4.8} \cdot {}^{y}L_{u} \cdot$$

The measured data gives

$$^{x}L_{w} = \frac{1}{5} \cdot {}^{x}L_{u} \text{ for both Runs 5 and 6.}$$

Again, the measured data is in fair agreement with the results found by Shiotani.

The measured data did not allow $^{z}L_{u}$ to be evaluated as the correlation was still high even when the largest separation distance ΔZ possible on the 20 m tower was used. However Counihan suggests that it should be

$^{z}L_{u} = (.5 \text{ to } .6)\ {}^{x}L_{u}$, which with the measured values of $^{x}L_{u}$ would make it between 50 and 60 m.

The main features of the cross-correlation functions and resultant integral length scales can be summarised as follows.

The measured values of $^{y}L_{u}$ agree well with ESDU (1975) and Teunissen (1977c) but Counihan's values for $^{y}L_{u}$ are larger than the values measured here. Shiotani's data suggests that $^{y}L_{u}$ increases with height.

Of the longitudinal cross-correlation function $^{y}L_{v}$ very little is known. The only values the author has found are from Teunissen (1977c) which are in good agreement with the results measured in this work.

For $^{y}L_{w}$, it has been shown that these results agree well with ESDU (1975), and Teunissen (1977c). The data of Shiotani et al (1978) gives larger values indicating an increase with height, but might also be affected by the monsoon and typhoon winds analysed from off the sea.

In retrospect it can be seen that the overall span of the towers of 315 m was not required for this particular experiment. A span of

150 m or at the very most 200 m would have allowed the correlations $\rho_{uu}(\Delta Y, 0)$ and $\rho_{vv}(\Delta Y, 0)$ ample distance to drop to zero, providing of course that there were no periodicities in the data. The towers then could have been better utilised by reducing the separation distance between individual towers. This applies particularly to the measurement of $\rho_{ww}(\Delta Y, 0)$ as the arrangement used allowed only one separation distance of $\Delta Y = 7.5$ m which yielded a reasonably high correlation.

The geometry of the layout used here was good, i.e. it allowed many combinations of towers giving different horizontal separation distances, ΔY. Reducing each separation to half of the distance used in this work would be a useful change for further measurements.

However, measurements of ${}^{x}L_{u}$ from spatial correlations as comparisons with ${}^{x}L_{u}$ evaluated using Taylor's Hypothesis and autocorrelation functions, would require the present maximum separation distance or more to allow the correlation $\rho_{uu}(\Delta X, \tau)$ the separation distance required to fall completely to zero.

CHAPTER 15

SUMMARY OF CONCLUSIONS

The objectives of this work were to :

(1) Develop instrumentation capable of making full scale field measurements of wind structure at low levels.

(2) Write software to calculate wind structure parameters from velocity data recorded onto magnetic tape.

(3) Perform field experiments, using the instrumentation developed, the results of which could be used to establish the total system reliability, by comparing the measured results with reported results which were considered to be reliable.

(4) Perform field experiments for which little or no data was available in the relevant literature, to make a contribution to that area of research.

15.1. CONCLUSIONS TO CHAPTERS 3 to 6

The propeller anemometer was found to be reasonably reliable from the time in which it was purged with Nitrogen and generally it is a reasonable compromise between sensitivity, reliability and expense. It is not as sensitive to high frequency velocity fluctuations as perhaps is desirable, particularly for measurements of the vertical velocity components at heights less than 10 m above the ground. The calibration coefficient was found to vary between different anemometer body-propeller combinations. This variation was primarily a function of the individual propeller shape, not of the anemometer bearing stiffness. For future measurements therefore the calibration coefficient variation could be virtually eliminated by more careful manufacture of

the next batch of propellers. Bearing friction did have an effect which was more apparent for the vertical component anemometer and this has been discussed in Chapter 13.

The size of the counters which the anemometers service is perhaps a little small. The horizontal component anemometer propellers rotate at a speed of about 10 times the vertical component anemometer propeller's rotational speed. This means that when a scan rate is selected which is consistent with the number of counts from the horizontal component anemometers, the counter served by the vertical component anemometer counts only up to small values which can lead to a quantisation error if the scan rate selected is much above the minimum required. The system whereby a square wave proportional to the rotational speed drives a counter is good because it helps to eliminate aliasing.

A significant problem with orthogonal arrays of three propeller anemometers is the one of alignment. Not only should the vertical component anemometer be mounted vertically to enable reliable Reynolds stress measurements to be made, but the horizontal component anemometers need to be mounted so that they are not sheltered by each other or by the tower on which they are mounted. With most towers this means that data can only be recorded for the relatively small range of wind directions when the wind vector lies between the two horizontal component anemometers. If data is recorded where sheltering of the anemometers does occur, extensive wind tunnel tests of the instruments are necessary to see in what way the data is compromised.

The site where the wind velocity data was recorded would have ideally been horizontally homogeneous. There was good exposure of the 20 m tower for nor'westerly winds, used to measure the vertical variation of the wind structure. However, the exposure for towers 7 and 8, and perhaps even tower 6 in the line of 10 m towers was somewhat affected by the shelter belt at the south-west end of the tower line, for wind

directions, perpendicular to the tower line. The span of the towers was rather longer than necessary, hence analysis could have been restricted to data streams from the towers with good exposure had this been necessary.

The amount of data generated during field measurements of wind structure is considerable, however part of the work in this thesis has been to investigate the amount of data needed for reliable results. It was found that the analysis of the data can be done on a medium sized computer for a reasonable cost.

The series of computer programs written and presented here enable the data to be processed a step at a time. If at any step the data is found to be unsatisfactory it can be rejected, otherwise analysis can proceed at the next step.

The programs enable all the turbulence parameters of interest to be calculated, the notable exception being the coherence. It is recommended that this be included into the program PSAUTCORS at a later date. This work concerned itself with wind structure parameters of direct interest to engineers, which meant that cross-correlation functions were evaluated, i.e. the Fourier transform of the cross-spectral density function.

Data analysis involved the extensive use of fast Fourier transform techniques which has now become fairly traditional for spectral and correlation analysis.

A large section of the work involved looking at the effects of different processing methods and data file constraints on the turbulence parameters being calculated. The results of this analysis have shown that :

(1) Correcting for the non-cosine response of the anemometers is important.

(2) To get reliable values of power spectral densities in particular, the data file should be as long as possible. Lengths of 30 to 60 minutes are recommended.

(3) Trend removal is an important part of the analysis process to get reliable correlation estimates. A parabolic trend line removal is the lowest order trend line removal recommended. Higher order polynomial trend lines should be used if the data does not appear to be particularly trend free after a parabolic trend removal.

(4) The minimum sampling frequency which gives uncompromised estimates of the parameters is 1.875 Hz.

(5) The advantages of applying a cosine taper to the velocity data to get better spectral estimates are not particularly obvious.

Although a high pass digital filter was not used in this work, it may be useful to investigate its effect in future measurements, especially with regard to its effect on the calculation of autocorrelations and cross-correlations.

15.2 CONCLUSIONS TO CHAPTERS 7 TO 12

It was found that the variation with height, of the velocity data collected on the four different days from the 20 m profile tower, was well described by a log law velocity profile. The values of U_* obtained agreed with values of $-\sqrt{\overline{uw}}$, discussed later, and the roughness length was estimated to be .03 m from the velocity profile. The measured value of Z_o was in the range expected for the type of terrain.

Turbulence intensity values of all three velocity components generally agreed well with accepted values from the literature although the longitudinal velocity component turbulence intensity was less than

suggested by ESDU (1974b). The probability density distributions of the measured longitudinal and lateral component velocity fluctuations agreed well with a Gaussian distribution. The vertical component velocity fluctuations agreed with the Gaussian distribution well near the tails of the distribution, but not so well for small velocity excursions from the mean where the anemometer response was poor.

The measurements of $\rho_{uw}(0)$ agreed well with other published data and also with U_* obtained from the velocity-height data. Arrays of propeller anemometers obviously can make reliable measurements of the $\frac{\overline{uw}}{\sigma_u \sigma_w}$ Reynolds stress in particular, even though the response of the vertical component anemometer is somewhat less than ideal. However, the small eddies are more isotropic than the large ones and therefore do not contribute much to $\overline{uw}$. Measurements of $\rho_{uv}(0)$ showed a lot of variation between Runs and the correction for the non-cosine response introduced a large change in its value. Measurements of $\rho_{uv}(0)$ are therefore not regarded as very reliable. $\rho_{vw}(0)$ was very small in all cases.

Measurements of the three orthogonal power spectral densities and corresponding autocorrelation functions showed that these quantities are difficult to measure accurately. The large magnitude of the fluctuations of the low frequency components in the power spectral densities indicated that better estimates with less random error could have been made by increasing the bandwidth that the low frequency estimates were averaged over.

The spectra did however show some interesting features.

The peak of the longitudinal component was flatter than predicted by spectral equations developed for isotropic turbulence. The high frequency part of the spectrum, above about .5 Hz, fell at a rate greater than $-\frac{2}{3}$ with increase of frequency, because of anemometer response. The frequencies at which the peak occurred for the lateral and vertical

component spectra were much higher than the frequency of the peak for the longitudinal component.

The autocorrelations sometimes showed a tendency to approach zero very slowly with increase in the delay times. This is a difficulty which has often been experienced by others analysing wind velocity measurements and it was repeated here. The same feature was also observed for cross-correlation functions, with a vertical separation particularly for the lateral velocity components. The difficulty of estimating the maximum correlation and correlation at $\tau = 0$ was overcome by using a formula from Panofsky (1961), and discussed in Section 12.4.

The zero time delay vertical separation cross-correlation functions showed that there was an increase in the length scales with height. When one anemometer was used as a reference, the correlation measured upwards from it was greater than the correlation measured downwards.

15.3 CONCLUSIONS TO CHAPTERS 13 and 14

It was disappointing that only two suitable Runs of data were available to be analysed because of hardware and time limitations. However, even from this limited amount of data, useful results have been obtained.

Chapter 13 discussed single point turbulence parameters and made comparisons with results from Chapters 7 to 12 and with other literature. It suggested that the data recorded was representative of atmospheric turbulence for the type of terrain over which the wind flowed and the strong wind conditions. Hence conclusions regarding the cross-correlations between anemometers on different towers discussed in Chapter 14 could be regarded as being accurate.

The wind blew from a direction which was very close to perpendicular to the line of towers. Not surprisingly then, the maximum

correlation occurred when τ was equal to zero. It was found in Run 6 that the cross-correlations of the lateral velocity components did not tend to zero even for large values of τ. Hence the method of Panofsky (1961) was used to correct for the existence of trends in the data and to calculate the correlations for $\tau = 0$.

Using the corrected data from Run 6, and the data from Run 5, it appears that for Z = 10 m and Z_o = .03 m, $^{y}L_u \approx {}^{y}L_v \approx$ 20 to 30 m. This was obtained from cross-correlation functions which showed that the u and v velocity components were virtually uncorrelated for a lateral separation distance ΔY greater than about 60 to 80 m. The length scale $^{y}L_w$ was observed to be much smaller, and again for Z = 10 m, Z_o = .03 m, $^{y}L_w$ appears to lie in the range 4 to 6 m from these results. The correlation curves from which this range was derived indicated that the $\rho_{ww}(\Delta Y, 0)$ was zero for ΔY = 15 m. For ΔY in the range 15 - 35 m, there appeared to be a small negative correlation, although this may have just been a sampling error.

15.4 GENERAL CONCLUSIONS

The stated objectives of this research have been achieved. The Department of Mechanical Engineering of the University of Canterbury now has a facility which can be used to measure full scale wind velocity data. The data collection system is portable so that measurements may be taken at any particular site. Later analysis of the results can be done on the University's Burroughs 6712 Computer.

The limitations of all facets of the analysis facility have been discussed so that compromises in the derived turbulence parameter resulting from sensor response and processing techniques are understood.

In the future use of this facility, results of field experiments will be obtained far more quickly than the time which was required to

obtain the results presented in this thesis. The computer programs, in their fully developed, final form, are simple to use and the instrumentation now has improved reliability since the anemometers were purged with Nitrogen.

The facility may now be used as required for a variety of field measurements such as investigating the flow around buildings, wind tubines, over escarpments, cliffs, hills and behind wind breaks.

REFERENCES

AKINS, R.E. and PETERKA, J.A. (1975) Computation of power spectral densities and correlations using digital FFT techniques. CER-76REA-JAP13, Dept.Civil Eng., Colorado State Univ. Fort Collins, Colorado, 84p, Dec.

BENDAT, J.S. and PIERSOL, A.G. (1971) Random Data: Analysis and measurement Procedures. John Wiley and Sons, New York, U.S.A. 407p.

BERGLAND, G.D. (1969) A guided tour of the fast Fourier transform. IEEE Spectrum, 41-52, July.

BEST, A.C. (1935) Transfer of heat and momentum in the lowest layers of the atmosphere. Geophys.Mem.Meteor.Office. No.65.

BLACKADAR, A.K. (1960) A survey of wind characteristics below 1500 ft. Paper 1, Meteor.Monogr. Topics in Engineering Meteorology, 4,22,3-11 May.

BLACKMAN, R.B. and TUKEY, J.W. (1958) The measurement of power spectra. Dover Publications, N.Y. 190p.

BOWEN, A.J. and LINDLEY, D. (1974) Measurement of the mean wind flow over various escarpment shapes. Proc.Fifth Australasian Conf. on Hydraulics and Fluid Mechanics, Christchurch, New Zealand, 1, 221-219, December.

BOWEN, A.J. and LINDLEY, D. (1977) A wind tunnel investigation of the wind speed and turbulence characteristics close to the ground over various escarpment shapes. Boundary-Layer Meteorology, 12, 259-271

BRADLEY, E.F., (1968) A shearing stress meter for micro-meteorological studies, Quart.J.Roy.Met.Soc., 94, 380-387.

BRIGHAM, E.O. (1974) The fast Fourier transform. Prentice-Hall, Inc. N.J. U.S.A. 252p.

BROOK, R.R. (1974) A study of wind structure in an urban environment. Meteor.Study No. 27, Melbourne, Univ. of Melbourne, 232p. (Thesis: Ph.D).

BROOK, R.R. (1977) Effective dynamic response of paired Gill anemometers. Boundary-Layer Meteor., 11, 33-37.

BUSCH, N.E. and PANOFSKY, H.A. (1968) Recent spectra of atmospheric turbulence. Quart.J.Roy.Meteor.Soc., 94, 132-148.

CALDER, K.L. (1966) Concerning the similarity theory of A.S. Monin and A.M. Obukhov for the turbulent structure of the thermally stratified surface layer of the atmosphere. Quart. J.Roy.Meteor.Soc., 92, 141-146.

CAMP, D.W. et al (1970) Response tests of cup, vane and propeller wind sensors. J.Geophys. Res., 75, 5265-5270.

CERMAK, J.E. and ARYA, S.P.S. (1970) Problems of atmospheric shear flows and their laboratory simulation. Boundary-Layer Meteor., 1, 40-60.

CHERRY, N.J. (1977) Private communication.

COUNIHAN, J. (1975) Adiabatic atmospheric boundary layers: A review and analysis of data from the period 1880-1972. Atmospheric Environment, 9, 1-35.

CRAMER, H.E. (1959) Measurements of turbulence structure near the ground within the frequency range from 0.5 to .1 cycles sec^{-1}. Advances in Geophysics, 6, 75-96.

CRAMER, H.E. (1960) Use of power spectra and scales of turbulence in estimating wind loads, Paper 2, Met.Monographs: Topics in Engineering Meteorology, 4, 22, 12-18, May.

DAVENPORT, A.G. (1960) Rationale for determining design wind velocities. J.Struc.Div.Proc. ASCE, 86,39.

DAVENPORT, A.G. (1961a) Application of statistical concepts to the windloading of structures. Proc.Inst.Civ.Engrs. 19, 449-472.

DAVENPORT, A.G. (1961b) The spectrum of horizontal gustiness near the ground in high winds. Quart.J.Roy.Meteor.Soc., 87, 194-211.

DAVENPORT, A.G. (1963) The relationship of wind structure to wind loading. Paper 2, N.P.L.Symp. on Wind Effects on Buildings and Structures. H.M.S.O.

DAVENPORT, A.G. (1964) The buffeting of large superficial structures by atmospheric turbulence. Annals New York Acad.Sci., 116, 135-159.

DAVENPORT, A.G. (1967) The dependence of wind loads on meteorological parameters. Paper 2. Conf. on Wind Loads on Buildings, Univ.Toronto Press, Toronto.

DEACON, E.L. (1949) Vertical diffusion in the lowest layers of the atmosphere. Quart.J.Roy.Met.Soc., 75, 89-103.

DEAVES, D.M. and HARRIS, R.I. (1976) A mathematical model of the structure of strong winds. ESRU Report No. 24, December, 86 p.

DRINKROW, R. (1972) A solution to the paired Gill - Anemometer response function. J.Appl.Meteor., 11, 76-80.

DUCHÊNE - MARULLAZ, P. (1974) Structure fine du vent: Premiers resultats. C.S.T.B. Report.

DUCHÊNE - MARULLAZ, P. (1975) Turbulence atmospherique au voisinage d'une ville. C.S.T.B. Report.

DUCHÊNE - MARULLAZ, P. (1976) Structure du vent en zone suburbaine rugosite et correlation laterale. C.S.T.B. Report.

DUCHÊNE - MARULLAZ, P. (1977) Full-scale measurements of atmospheric turbulence in a suburban area. Proc. of the 4th.Int.Conf. on Wind Effects on Buildings and Structures, Cambridge Univ.Press.

ELDERKIN, C.E. (1966) Experimental investigation of the turbulent structure in the lower atmosphere. Battelle-Northwest Report 329, Pacific Northwest Laboratory, Richland, Washington, U.S.A.

ESDU (1972) Characteristics of the wind speed in the lower layers of the atmosphere near the ground : Strong winds (neutral atmosphere). Engineering Sciences Data Item No. 72026, November, 35p.

ESDU (1974a) Characteristics of atmospheric turbulence near the ground. Part I: Definitions and general information. Engineering Sciences Data Item No. 74030, October, 14p.

ESDU (1974b) Characteristics of atmosphere turbulence near the ground. Part II: Single point data for strong winds (neutral atmosphere). Engineering Sciences Data Item No. 74031, October 23p.

ESDU (1975) Characteristics of atmospheric turbulence near the ground. Part III: Variation in space and time for strong winds (neutral atmosphere). Engineering Sciences Data Item No. 75001, July, 27p.

FICHTL, G.H. (1968) Characteristics of turbulence observed at the NASA 150 m meteorological tower. J.App.Meteor. 7, 838-850.

FICHTL, G.H. and McVEHIL, G.E. (1969) Longitudinal and lateral spectra of turbulence in the atmospheric boundary-layer at the Kennedy Space Center. J.App.Meteor., 9, 51-63.

GARRATT, J.R. (1975) Limitations of the eddy-correlation technique for the determination of turbulent fluxes near the surface. Boundary-Layer Meteor., 8, 255-259.

GILL, G.C. (1966) Temperature and wind measuring systems - Basic principles and dynamic response. Seminar Series at White Sands Missile Range, Oct. 24-28.

GILL, G.C.,(1967) On the dynamic response of meteorological sensors and recorders. Proc. 1st. Canadian Conf. on Micrometeorology, Part I. Meteor. Service of Canada,Toronto, 1-27.

GILL, G.C. (1975) Development and use of the Gill UVW anemometer. Boundary-Layer Meteor., 8, 475-495.

GILL, G.C. et al (1967) Accuracy of wind measurements on towers or stacks. Bull.Am.Meteor.Soc., 48, 9, 665-674, Sept.

HARRIS, R.I. (1963) The response of structures to gusts. Paper 18, Proc. of the Conf.held at N.P.L. on Wind Effects on Buildings and Structures, 26-28, June.

HARRIS, R.I. (1968a) Measurement of wind structure at heights up to 598 ft. above ground level. Symp. on Wind Effects on Buildings and Structures at Loughborough Univ. of Technology, N.P.L. 2-4 April.

HARRIS, R.I. (1968b) On the spectrum and autocorrelation function of gustiness in high winds. E.R.A. Report No. 5273, Surrey.

HARRIS, R.I. (1971) The nature of the wind. Paper 3 from the Modern Design of Wind Sensitive Structures, Proc. of a Seminar on June 18 1970, at Institute of Civil Engrs., London. Publ. by Construction Industry Research and Information Ass., 29-55.

HARRIS, R.I. (1972) Measurements of wind structure. Symp. External Flows, Bristol Univ. July.

HAUGEN, D.A. et al (1971) An experimental study of Reynolds stress and heat flux in the atmospheric surface layer. Quart.J.Roy.Meteor. Soc., 97, 168-180.

HICKS, B.B. (1972) Propeller anemometers as sensors of atmospheric turbulence. Boundary-Layer Meteorology, 3, 214-228.

HOLMES, R.M., et al (1964) A propeller-type vertical anemometer. J.Appl.Meteor., 3, 802-804.

HORST, T.W. (1973a) Corrections for response errors in a three-component propeller anemometer. J.Appl.Meteor. 12, 716-725.

HORST, T.W. (1973b) A computer algorithm for correcting non-cosine response in the Gill anemometer. Battelle Northwest Laboratories, Report BNWL-1651 PT 1, Richland, Wash.

HYSON, P. et al (1977) Algebraic and electronic corrections of measured uw covariance in the lower atmosphere. J.Appl.Meteor., 16, 1, 43-47, Jan.

IWATANI, Y. (1977) Some features of the spatial structures of the surface layer turbulence in high wind conditions. J.Meteor.Soc. Japan, II, 55, 1, 130-138, Feb.

KAIMAL, J.C. et al (1972) Spectral characteristics of surface-layer turbulence. Quart.J.Roy.Meteor.Soc., 98, 563-589.

LINDLEY, D. (1975) The design and performance of a 6 cup anemometer. J.Appl.Meteor., 14, 6, 1135-1145.

LINDLEY, D. and BOWEN, A.J. (1974) The response of cup and propeller anemometers to fluctuating wind speeds. Fifth Australasian Conf. on Hydraulics and Fluid Mechanics, Univ. of Canterbury, New Zealand, Dec. 9-13, 269-277.

LINDLEY, D. et al (1974) A propeller anemometer for a digital wind data acquisition system. Fifth Australasian Conf. on Hydraulics and Fluid Mechanics, Univ. of Canterbury, New Zealand, Dec.9-13, 258-268.

LUMLEY, J.L. and PANOFSKY, H.A. (1964) The structure of atmospheric turbulence. John Wiley and Sons, N.Y. 239p.

MACCREADY, P.B., Jr. and JEX, H.R. (1964) Response characteristics and meteorological utilisation of propeller and vane wind sensors. J. Appl.Meteor., 3, 182-193.

MACCREADY, P.B. (1965) Dynamic response characteristics of meteorological sensors. Bulletin Amer.Meteor.Soc. 46, 9, 533-588, Sept.

MACCREADY, P.B. (1966) Mean wind speed measurements in turbulence. J.Appl.Meteor., 5, 219-275.

MACCREADY, P.B. (1970) Theoretical considerations in instrument design. Meteor.Monogr. 11, 33, 202-210.

MERONEY, R.N. et al (1978) Wind characteristics over complex terrain: Laboratory simulation and field measurements at Rakaia Gorge, New Zealand.Draft Report No. TH/FL 102/78. Dept.of Mech.Eng., University of Canterbury, 218p.

NG, A. (1973) The performance of cup and propeller anemometers in steady and fluctuating wind streams. Dept.Mech.Eng., Univ. of Canterbury, 160p. (Thesis: M.E. Engineering).

OMAR, H.B. and OW, C.S. (1972) Fast response propeller anemometer and gust generator design. Project Report No. 4/72, Dept.Mech.Eng. Univ. of Canterbury, 169p.

ONG, C.T. and DIEN, T.H. (1974) Response characteristics of propeller anemometers. Project Report No. FL/2/74. Dept.Mech.Eng., Univ. of Canterbury, 116p.

PANOFSKY, H.A. (1961) Scale analysis of atmospheric turbulence at 2 m. Quart.J.Roy.Met.Soc., 88, 57-69.

PANOFSKY, H.A. (1973) Tower micrometeorology. Workshop on Micrometeorology, Amer.Meteor.Soc. Ed. by D.A. Haugen, 151-176.

PANOFSKY, H.A. (1977) Wind structure in strong winds below 150 m, Wind Engineering 1, 2, 91-103.

PANOFSKY, H.A. and DELAND, R.J. (1959) One-dimensional spectra of atmospheric turbulence in the lowest 100 metres. Advances in Geophysics, 6, 41-64.

PASQUILL, F. (1971) Wind structure in the atmospheric boundary-layer. Discus.on Archit.Aero., Phil.Trans.Royal Soc., A269, 439-456.

PIEKLE, R.A. and PANOFSKY, H.A. (1970) Turbulence characteristics along several towers. Boundary-Layer Met., 1, 115-130.

POWELL, D.C. and ELDERKIN, C.E. (1974) An investigation of the application of Taylor's Hypothesis to atmospheric boundary-layer turbulence. J.of the Atmos.Sciences, 31, 990-1002.

PRITCHARD, F.E. (1966) The turbulence and terrain environments affecting low altitude high speed flight. Cornell Aero.Lab. Ref. FEM 393.

RAINE, J.K. (1974) Modelling the natural wind: Wind protection by fences. Christchurch, University of Canterbury, 559p. (Thesis: Ph.D: Engineering).

ROPELEWSKI, C.F. et al (1973) Horizontal coherence of wind fluctuations. Boundary-Layer Meteor., 5, 353-363, July.

SCHLICTING, H. (1960) Boundary-layer theory. McGraw-Hill, U.S.A. 647p.

SCRASE, F.J. (1930) Some characteristics of eddy motion in the atmosphere. Geophys.Mem. No. 52.

SHIOTANI, M. (1975) Turbulence measurements at the sea coast during high winds. J. Meteor Soc., Japan, 53, 340-354.

SHIOTANI, M. and ARAI, H. (1967) Lateral structures of gusts in high winds. Paper 20, Proc.of Conf. on Wind Effects on Buildings and Structures, at NRC, Ottawa, Sept. Univ. of Toronto Press, 1968.

SHIOTANI, M. and IWATANI, Y. (1971) Correlations of wind velocities in relation to the gust loadings. Proc. of the 3rd. Int.Conf. on Wind Effects on Buildings and Structures, Tokyo, Sept. 57-68.

SHIOTANI, M. and IWATANI, Y. (1976) Horizontal space correlations of velocity fluctuations during strong winds. J.Met.Soc.Japan, II, 54, 1, 5 9-67, Feb.

SHIOTANI, M. et al (1978) Magnitudes and horizontal correlations of vertical velocities in high winds. J.Met.Soc.Japan, II, 56, 1, 35-42, Feb.

STEVENSON, D.C. (1968) The University of Canterbury wind tunnel. New Zealand Engineering, 403-407. 15 Oct.

SUTTON, O.G. (1953) Micrometeorology. McGraw-Hill, U.S.A. 333p

SUTTON, O.G. (1955) Atmospheric turbulence. 2nd edition. John Wiley and Sons, U.S.A., 111p.

SWANSON, R.N. and CRAMER, H.E. (1965) A study of lateral and longitudinal intensities of turbulence. J.Appl.Meteor., 4, 409-417.

TENNEKES, H. (1973) The logrithmic wind profile. J. of the Atmos. Sciences, 30, 234-238.

TEUNISSEN, H.W. (1970) Characteristics of the mean wind and turbulence in the planetary boundary-layer. UIIAS Review No. 32, October.

TEUNISSEN, H.W. (1977a) A measurement and analysis facility for full-scale atmospheric wind and turbulence data. Internal Report No. MSRB-77-2, Atmos.Environment Service, Toronto, 78p, July.

TEUNISSEN, H.W. (1977b) Measurements of planetary boundary-layer wind and turbulence characteristics over a small suburban airport. Internal Report No. MSRB-77-4. Atmos.Environment Service, Toronto, 46p, July.

TEUNISSEN, H.W. (1977c) Private communication.

WEBB, E.K. (1955) C.S.I.R.O. Div.Met.Phys.Tech. Pap. 5. Victoria, Australia.

YUEN, C.K. and FRASER, D. (1976) Digital spectral analysis. Hobart, Univ.of Tasmania. 192p.

APPENDIX A

PROPELLER ANEMOMETER NON-COSINE RESPONSE CORRECTION FACTORS

The correction factors given below were obtained from windtunnel tests on batches of four bladed 190.5 mm diameter propeller anemometers. The correction factors were derived from two windtunnel tests, one in March, 1977 and one in February, 1978. The Mechanical Engineering Departmental Aeronautical Windtunnel described by Stevenson (1968) was used for both tests.

The correction factors are for use in an interative non-cosine response correction procedure, modified from Horst (1973b), to run in Algol on a Burroughs 6712 computer. This procedure is used in the two programs SEQVELTURBREY and PSAUTCORS.

The correction factors are defined such that when the true angle between the propeller anemometer axis and the mean wind vector is θ ,

$$\text{correction factor} = \frac{\text{ideal response}}{\text{actual response}} = \frac{\bar{U}\cos\theta}{\text{actual response}}$$

and when $\theta = 0$, the correction factor is equal to 1.0.

The correction factors given below have been multiplied by 100, and the values given for any θ are the average correction factors obtained from the measured response at $+\theta$ and $-\theta$.

1

cos θ	correction factor
-1.0	111
- .98	106
- .96	105
- .94	106
- .92	108
- .90	108
- .88	110
- .86	110
- .84	112
- .82	112
- .80	113
- .78	115
- .76	116
- .74	117
- .72	119
- .70	118
- .68	120
- .66	120
- .64	124
- .62	125
- .60	128
- .58	125
- .56	127
- .54	126
- .52	127
- .50	126
- .48	130
- .46	129
- .44	128
- .42	126
- .40	128
- .38	125
- .36	125
- .34	124

2

cos θ	correction factor
- .32	125
- .30	123
- .28	122
- .26	121
- .24	122
- .22	125
- .20	133
- .18	133
- .16	137
- .14	145
- .12	150
- .10	155
- .08	160
- .06	180
- .04	200
- .02	270
+ 0	270
+ .02	270
+ .04	260
+ .06	230
+ .08	205
+ .10	185
+ .12	171
+ .14	160
+ .16	152
+ .18	150
+ .20	148
+ .22	147
+ .24	144
+ .26	139
+ .28	135
+ .30	133
+ .32	133
+ .34	131

3

cos θ	correction factor
+ .36	131
+ .38	129
+ .40	127
+ .42	125
+ .44	127
+ .46	126
+ .48	126
+ .50	127
+ .52	127
+ .54	128
+ .56	129
+ .58	128
+ .60	128
+ .62	129
+ .64	127
+ .66	126
+ .68	124
+ .70	122
+ .72	121
+ .74	119
+ .76	118
+ .78	116
+ .80	113
+ .82	112
+ .84	110
+ .86	108
+ .88	107
+ .90	106
+ .92	105
+ .94	104
+ .96	103
+ .98	101
+1.00	100

APPENDIX B

PROGRAM 'CHECKDATA'

B.1. Typical Work flow Language (WFL) for using this Program

B.1.1 Simple File Check

Assume that some wind velocity data has been recorded onto a 7 track unlabelled tape called WIND1. There have been six files recorded onto the tape, and it is desired to "check" these files for errors. The source file corresponding to the program CHECKDATA is assumed to be stored on Computer Centre library tape A999.

A typical JOB to check the files is given below

```
7
5  JOB CHECK WIND1;  DESTNAME=SITE.; PROCESSTIME=600.
   USER MECH021/PASSWORD; CLASS=10; BEGIN
7
5  DISPLAY "WIND1 IS A UL 7 TRACK TAPE";
   DISPLAY "RENTED BY MECH021";
   COPY CHECKDATA FROM A999;
   COMPILE CHECKIT ALGOL LIBRARY;
   COMPILER FILE TAPE=CHECKDATA;
   DATA
$  SET MERGE
$  RESET LIST
7
5  IF FILE CHECKIT IS PRESENT THEN RUN CHECKIT;
   FILE DATA=WIND1;†
   DATA INFO;
   0,0
   6,
   9,
   0,
7
5  END JOB
```

Note the first data card indicates that there are no files to skip and no records in the first file to be processed, to skip.

The next card indicates that there are six files to be processed on the tape. The next card indicates that the maximum difference between consecutive samples in the same channel before it constitutes an error is 9. The last card indicates that reformatted data is not to be written to a disk file

† This statement equates the program internal file name DATA with the physical file WIND1.

B.1.2 File Copy to Library Tape

Assume the same data files on tape WIND1 as in B.1.1, but part of the 5th. file is to be written to the library tape B123. The first 1000 records in the 5th. file are to be ignored. The scan rate, of the data written to the library tape, required is 2.

The WFL cards are the same as for B.1.1 up to DATA INFO; but the cards following DATA INFO; are different and are given below.

```
  4,1000,
  1,
  9,
  1,2,
7
5 COPY OUTPUTFILE AS WINDY251278 TO B123;
7
5 END JOB
```

B.2 Listing of Program CHECKDATA

```
 CCC  H   H EEEE   CCC  K   K DDDD   AAA  TTTTT  AAA
C   C H   H E     C   C K  K  D   D A   A   T   A   A
C     H   H E     C     K K   D   D A   A   T   A   A
C     HHHHH EEE   C     KK    D   D AAAAA   T   AAAAA
C     H   H E     C     K K   D   D A   A   T   A   A
C   C H   H E     C   C K  K  D   D A   A   T   A   A
 CCC  H   H EEEEE  CCC  K   K DDDD  A   A   T   A   A


604 RECORDS. CREATED 23/11/78

     100 $ SET $
     200 $ SET LINEINFO
     300 BEGIN
     400   DIRECT FILE DATA(KIND=TAPE7,MAXRECSIZE=64,BLOCKSIZE=64,UNITS=WORDS);
     500   DIRECT ARRAY ND[0:63];
     600   BOOLEAN BR;
     700   FILE FOO(KIND=PRINTER);
     800   FILE INFO(KIND=READER);

     900   PROCEDURE SPACEFILE(N);VALUE N;REAL N;
    1000   %    THIS IS A PROCEDURE TO SPACE OVER 7 TRACK RECORDS OF INPUT TAPE.
    1100   %    INPUT TO IT IS THE NUMBER OF RECORDS TO BE SPACED OVER
    1200   %
    1300   BEGIN
    1400     THRU N DO
    1500     BEGIN
    1600       WAIT(ND);
    1700       READ(DATA,64,ND);
    1800     END;
    1900   END  E N D   O F   S P A C E F I L E ;

    2000   REAL PROCEDURE NEXTVAL(PA,SHIFT);
    2100   %    BIT CONCACTENATION USED AFTER A SIX BIT SLIP
    2200   VALUE SHIFT;
    2300   INTEGER SHIFT;
    2400   POINTER PA;
    2500   BEGIN
    2600     CASE SHIFT OF
    2700     BEGIN
    2800       0: NEXTVAL:=REAL(PA,1);
    2900       6: NEXTVAL:=0&REAL(PA,1)[1:7:2]&REAL(PA-1,1)[7:5:6];
    3000       12: NEXTVAL:=0&REAL(PA,1)[3:7:4]&REAL(PA-1,1)[7:3:4];
    3100       18: NEXTVAL:=0&REAL(PA,1)[5:7:6]&REAL(PA-1,1)[7:1:2];
    3200     END;
    3300     PA:=PA+1;
    3400   END OF NEXTVAL;
    3500   %
    3600   %
    3700   %

    3800   PROCEDURE CHECKCHAR(NOCHAR,PA,CASE,N);
    3900   %
    4000   %    READS IN DATA OFF 7 TRACK TAPE. USES DIRECT IO. QUICKER AND
    4100   %    CAN COPE WITH TRYING TO READ BLANK TAPE
    4200   %
    4300   INTEGER NOCHAR,CASE;
    4400   POINTER PA;
    4500   INTEGER ARRAY N[*];
    4600   BEGIN
    4700     LABEL PP1,BL1;
    4800     LABEL PP2;
    4900     LABEL PP3;
    5000     LABEL AAA;
    5100     LABEL DTAERR;
    5200     LABEL LAB;
    5300     INTEGER PARCOUNT;
    5400     BEGIN
    5500       IF NOCHAR<=384 THEN GO TO BL1
    5600       ELSE
    5700       BEGIN
    5800         NOCHAR:=1;
    5900         PA:=PA-1;
    6000         N[0]:=REAL(PA,1);
    6100         %    SAVES LAST DATA SAMPLE OF PREVIOUS READ STATEMENT IN N[0]
    6200         %
    6300         AAA:
    6400         IF BR:=WAIT(ND) THEN BEGIN
    6500           IF BR.[15:1] THEN GO TO  LAB;  %  TAPE BLANK
    6600           IF ND.IOERRORTYPE=2 THEN GO TO PP3;%   PARITY ERROR
    6700           IF ND.IOERRORTYPE>4 THEN GO TO PP2; % EOF
    6800           GO TO DTAERR;
    6900         END;
    7000         REPLACE N[1] BY POINTER(ND) FOR 64 WORDS;
    7100         READ(DATA,64,ND);
    7200         GO TO PP1;
    7300       END;
    7400       LAB:
    7500       WRITE(FOO,<"BLANK TAPE HENCE FINISH">);
    7600       GO TO PP2;
    7700       PP3:
    7800       WRITE(FOO,<X10,"PARITY ERROR-REREAD">);
    7900       PARCOUNT:=*+1;
```

```
 8000        IF PARCOUNT>2  THEN BEGIN
 8100          WRITE(FOO,<"TAPE DRIVE READING RUBBISH",/,"PROBABLY A READ STATEMEN
 8200          T HAS  JUMPED OVER THE END OF THE DATA",/,"PUT CASE=255 FOR SOME OUTPUT"
 8300          >);
 8400        GO TO PP2;
 8500        END;
 8600        GO TO AAA;
 8700        DTAERR:
 8800        WRITE(FOO,<"CONFLICT BETWEEN FORMAT AND THE DATA",/,"PUT CASE=255 A
 8900        NYWAY SO AS TO OUTPUT RESULTS",/,"THIS MAY BE THE END OF A TAPE">);
 9000        PP2:CASE:=255;
 9100        PP1:
 9200        PA:=POINTER(N[1],8);
 9300        BL1:
 9400        NOCHAR:=NOCHAR+1;
 9500      END;
 9600    END OF CHECKCHAR;
 9700    %
 9800    %
 9900    %
10000    %
10100    %
10200    %
10300    %
10400    %
10500    %
10600    %
10700    %

10800    PROCEDURE SPECIAL(CHECKN,IKK);VALUE CHECKN,IKK;
10900    %
11000    %   CHECKS WHICH SPECICAL CHANNELS ARE ON , WHEN THEY WERE TURNED ON
11100    %   AND IF THEY HAVE BEEN CHANGED AT ALL DURING DATA RECORDING
11200    %
11300    INTEGER CHECKN;
11400    INTEGER IKK;
11500    BEGIN
11600      OWN INTEGER CHECKO,BO;
11700      LABEL EXIT;
11800      IF BO=0 AND CHECKN=0 THEN GO TO EXIT;
11900      IF BO=1 AND CHECKN=CHECKO THEN GO TO EXIT;
12000      IF BO=1 AND CHECKN NEQ CHECKO THEN
12100      BEGIN
12200        BO:=0;
12300        CASE CHECKO OF
12400        BEGIN
12500          1:WRITE(FOO,<X5,"SPECIAL CHANNEL 1 TURNED OFF AFTER",I10,"  SCANS">,IKK-
12600          1);
12700          2:WRITE(FOO,<X5,"SPECIAL CHANNEL 2 TURNED OFF AFTER",I10,"  SCANS">,IKK-
12800          1);
12900          3:WRITE(FOO,<X5,"SPECIAL CHANNELS 1 AND 2 TURNED OFF AFTER",I10,"  SCANS
13000          ">,IKK-1);
13100          4:WRITE(FOO,<X5,"SPECIAL CHANNEL 3 TURNED OFF AFTER",I10,"  SCANS">,IKK-
13200          1);
13300          5:WRITE(FOO,<X5,"SPECIAL CHANNELS 1 AND 3 TURNED OFF AFTER",I10,"  SCANS
13400          ">,IKK-1);
13500          6:WRITE(FOO,<X5,"SPECIAL CHANNELS 2 AND 3 TURNED OFF AFTER",I10,"  SCANS
13600          ">,IKK-1);
13700          7:WRITE(FOO,<X5,"SPECIAL CHANNELS 1,2 AND 3 TURNED OFF AFTER",I10,"  SCA
13800          NS">,IKK-1);
13900        END;
14000      END;
14100      IF BO=0 AND CHECKN NEQ 0 THEN
14200      BEGIN
14300        BO:=1;CHECKO:=CHECKN;
14400        CASE CHECKN OF
14500        BEGIN
14600          1:WRITE(FOO,<X5,"SPECIAL CHANNEL 1 TURNED ON AT SCAN",I10>,IKK);
14700          2:WRITE(FOO,<X5,"SPECIAL CHANNEL 2 TURNED ON AT SCAN",I10>,IKK);
14800          3:WRITE(FOO,<X5,"SPECIAL CHANNEL 1 AND  2  TURNED ON AT SCAN",I10>,IKK);
14900          4:WRITE(FOO,<X5,"SPECIAL CHANNEL 3 TURNED ON AT SCAN",I10>,IKK);
15000          5:WRITE(FOO,<X5,"SPECIAL CHANNEL 1 AND  3  TURNED ON AT SCAN",I10>,IKK);
15100          6:WRITE(FOO,<X5,"SPECIAL CHANNEL 2 AND  3  TURNED ON AT SCAN",I10>,IKK);
15200          7:WRITE(FOO,<X5,"SPECIAL CHANNEL 1,2 AND 3 TURNED ON AT SCAN",I10>,IKK);
15300        END;
15400      END;
15500      EXIT:
15600    END;
15700    %
15800    %   DECLARE VARIABLES ETC FOR MAINLINE
15900    %
16000    INTEGER AA,BB,CC,DD; ARRAY CORRECTMEANS[1:36],SAVE,TSAVE[1:36,
16100    0:255];
16200    FILE OUTPUTFILE(KIND=DISK,FILETYPE=7,MAXRECSIZE=256,
16300    BLOCKSIZE=768,AREASIZE=60,FLEXIBLE=TRUE,PROTECTION=SAVE,
16400    UNITS=WORDS);
16500    INTEGER SF;
16600    REAL LENGTH;
16700    INTEGER PART;
16800    INTEGER ARRAY N[0:65];
16900    INTEGER ARRAY NS1,NS2,NS3[0:256];
17000    INTEGER ARRAY NAX[1:45,0:256];
17100    INTEGER RN,NR,TIME;
17200    REAL ARRAY MEAN[0:40];
17300    INTEGER NOCHAR,TOTCHAR,SHIFT,PASS,CASE,CH,IKK,IJK;
```

```
17400   INTEGER TOTE,NOOFFILES,NOCH,SCAN,SYNC;
17500   INTEGER ARRAY A[0:48];
17600   INTEGER SIZE,I;
17700   INTEGER SYNCOUNT;
17800   POINTER PA;
17900   INTEGER X;
18000   INTEGER NP;
18100   LABEL UU2;
18200   LABEL LB5B;
18300   LABEL LB16,LB14,LB8,LB5A,LB9,LB10,LB11,LB13,LB12;
18400   LABEL END1;
18500   FORMAT RELOST("SYNC LOST AFTER ",I7,"SCANS-RESTARTING");
18600   FORMAT FOUND(///X10,"SYNC FOUND", X10,"AMOUNT OF SLIP= ",I3,"BITS");
18700   FORMAT ENDLOST("SYNC LOST AND APPEARS AS", I4,"SO FILE ENDED");
18800   FORMAT SCANLOSS("SCANRATE CHANGED AND APPEARS AS",I6,"SO FILE ENDED");
18900   FORMAT CHANC("NO OF CHANNELS ALTERED TO",I6,"SO FILE ENDED");
19000   FORMAT GOOD(/"THIS DATA HAS BEEN RECORDED PROPERLY AND THE END OF A DATA
19100   FILE HAS BEEN REACHED");
19200   FORMAT FINISH(X5,"TOTAL NO OF SCANS=",I7,X10,"SCANRATE="I3,X10,"NO OF CH
19300   ANNELS=",I4);
19400   FORMAT START(//X30,"RESULTS FROM RECORD  ",I4,"  PART",  I4);
19500   FORMAT MEANS(3("CHANNEL",I3,"   MEAN VALUE=  ",F13,6,X5));
19600   FORMAT SCANCH("SCAN RATE CHANGED AFTER",I3,"SCANS-RESTARTING"/);
19700   FORMAT CHANL("NO  OF CHANNELS ALTERED AFTER",I3,"  SCANS-RESTARTING"/);
19800   FORMAT FINP(I4);
19900   FORMAT LNGTH("LENGTH OF THE RECORDING OF THIS PART="F8.2,"  MINUTES");
20000   FORMAT LOST(X10,"SYNC NEVER FOUND");
20100   FORMAT MANU("CHANNEL NO",I4," FAILED MANUALLY AT SCAN NO",I10);
20200   FORMAT OVERF("CHANNEL NO",I4,X2,"NEAR OVERFLOW AT SCAN ",I10," VALUE=",
20300   I6);
20400   FORMAT OK("DATA NOT NEAR OVERFLOW ANYMORE AT SCAN",I10);
20500   FORMAT PRIN("IT WOULD BE WISE TO WRITE OUT THE DATA AROUND THIS REGION,
20600   CHANNEL ",X2,I3,X1,"TO SEE IF OVERFLOW HAS OCURRED. SCAN",X2,I7);
20700   FORMAT FAIL("  ETC.....ETC....ETC.....ETC....IN CHANNEL..",I4);
20800   FORMAT UNFAIL("  CHANNEL",I4,"  UNFAILED AT SCAN",I10);
20900   LABEL UP3,UP2,UP1;
21000   LABEL LB1,LB2,LB3,LB4,LB5,LB6,LB7;
21100   REAL XXX;
21200   INTEGER XX;
21300   INTEGER K;
21400   REAL ARRAY MEAN1[1:36];
21500   REAL ME,Q;INTEGER P;ARRAY AR[1:256],NE[1:6,1:256];
21600   INTEGER H;
21700   REAL THETA;
21800   INTEGER ARRAY C[1:36];
21900   INTEGER DIFF;
22000   REAL MULT;
22100   INTEGER ARRAY LASTVALUE[0:45];
22200   INTEGER ARRAY B[0:48];
22300   INTEGER PARCOUNT;
22400   LABEL SKIPOVER;
22500   INTEGER NOFILESTOSKIP,NORECSTOSKIP,OUTPUTSCANRATE;BOOLEAN WRITEOUT;
22600   ARRAY MX,CMX,MN,CMN,MMX,CMMX,MMN,CMMN[1:50];
22700   %*************************************************************************
22800   %*************************************************************************
22900   %
23000   %               MAINLINE
23100   %
23200   %
23300   BEGIN
23400     ND.IOMASK:=1&1[15:1];
23500     READ(INFO,/,NOFILESTOSKIP,NORECSTOSKIP);
23600     WRITE(FOO,*/,NOFILESTOSKIP,NORECSTOSKIP);
23700     READ(INFO,/,NOOFFILES);
23800     WRITE(FOO,<"NUMBER OF FILES TO BE PROCESSED FROM THIS"
23900     " TAPE IS=",I4>,NOOFFILES);
24000     READ(INFO,/,DIFF);
24100     WRITE(FOO,<"DIFFERENCE TEST OF",X2,I2>,DIFF);
24200     READ(INFO,/,WRITEOUT,IF WRITEOUT THEN OUTPUTSCANRATE);
24300     IF WRITEOUT THEN WRITE(FOO,<"THE DATA WILL BE REFORMATTED"
24400     " AND WRITTEN IN RECORDS OF 256 DATA SAMPLES TO OUTPUT FILE"/
24500     "THE RECORDS WILL BE WRITTEN IN THE ORDER-CHANNEL 1,2,3...N"
24600     " WHERE N IS THE NUMBER OF ANEMOMETERS BEING RECORDED"/
24700     "THE OUTPUTSCANRATE=",I3," IT HAS TO BE A POWER OF 2"
24800     " AND LESS OR EQUAL TO THE ACTUAL PHYSICAL RECORDING SCANRATE">,
24900     OUTPUTSCANRATE) ELSE WRITE(FOO,<"THE DATA IS BEING"
25000     " CHECKED ONLY, NOT WRITTEN TO AN OUTPUT FILE">);
25100     H:=0;
25200     TIME:=0;
25300     PART:=1;
25400     LB16:
25500     FOR I:=1 STEP 1 UNTIL 36 DO BEGIN
25600       MX[I]:=MMX[I]:=-1000;MN[I]:=MMN[I]:=1000;END;
25700     PARCOUNT:=0;
25800     SYNC:=127;
25900     PASS:=0;
26000     CASE:=0;
26100     SHIFT:=0;
26200     NOCHAR:=0;
26300     PA:=POINTER(N[1],8);
26400     UP3:
26500     %
26600     READ(DATA,64,ND);
26700     IF NOFILESTOSKIP>0 THEN
26800     THRU NOFILESTOSKIP DO BEGIN SPACEFILE(1);CLOSE(DATA,*); END;
```

```
26900     IF NORECSTOSKIP>0 THEN BEGIN SPACEFILE(NORECSTOSKIP);WRITE(FOO,*/,
27000       NORECSTOSKIP);NORECSTOSKIP:=0;END;
27100     IF BR:=WAIT(ND) THEN IF ND.IOERRORTYPE=5 THEN GO TO UP2 ELSE GO TO UU2;
27200     REPLACE N[1] BY POINTER(ND) FOR 64 WORDS;
27300     READ(DATA,64,ND);
27400     GO TO LB5B;
27500     UU2:
27600     %   PARITY CONDITION ERROR MESSAGE
27700     WRITE(FOO,<X10,"PARITY ERROR">);
27800     PARCOUNT:=*+1;
27900     IF PARCOUNT>10 THEN BEGIN
28000       WRITE(FOO,<" APPEARS TO BE ONLY RUBBISH ON THE TAPE",/,"THEREFORE F
28100       INISH">);
28200       GO TO END1;
28300     END;
28400     GO TO UP3;
28500     UP2:
28600     %   END OF FILE ON FIRST READ OF THE FILE
28700     %   FILE IS CLOSED AND IF THERE IS ANOTHER ONE, IT
28800     %   IS STARTED
28900     %
29000     CLOSE(DATA,*);
29100     WRITE(FOO,<X10,"NEW RECORD READ ON FIRST READ">);
29200     TIME:=TIME+1;
29300     IF TIME<NOOFFILES THEN GO TO UP3 ELSE GO TO END1;
29400     GO TO UP3;
29500     LB5B:
29600     %   THE BEGINNING OF THE FILE HAS TO BE POSITIVELY IDENTIFIED
29700     %   THIS IS DONE BY FINDING 3 CONSECUTIVE SYNCHRONISM WORDS-EACH OF
29800     %   WHICH INDICATE THE BEGINNING OF A SCAN. IT IS EQUAL TO
29900     %   7 BITS ON OR 127. THEY OCCUR IN EVERY (3 PLUS
30000     %   NUMBER OF ANEMOMETER CHANNELS) POSITIONS DOWN THE FILE
30100     %   THE EXTRA 3 LOTS OF 8 BITS ARE 1. THE SYNCHRONISM WORD
30200     %   01111111,2. THE SPECIAL CHANNELS AND SCANRATE
30300     %   0XXX0XXX,BIT 4 ON MEANS SPECIAL CHANNEL 3 ON, BIT 5 ON
30400     %   SPECIAL CHANNEL 2 ON, BIT 6 ON SPECIAL CHANNEL 3 ON
30500     %   BITS 0,1,2 INDICATE THE SCANRATE.SIMPLE BINARY
30600     %   NUMBERS 1,2,3,4,5 INDICATE SCANRATES OF 8,16,32,64,128  RESPECTIVELY
30700     %   3. THE NUMBER OF CHANNELS USES BITS 0 THROUGH 5. IT
30800     %   IS A SIMPLE BINARY NUMBER BUT A MULTIPLE OF 3-THIS
30900     %   IS BECAUSE THE NUMBER OF CHANNELS IS SWITCH SELECTABLE
31000     %   IN 3'S.
31100     FOR I:=0 STEP 1 UNTIL 48 DO
31200     MEAN[I]:=0;
31300     REPLACE POINTER(CORRECTMEANS) BY 0 FOR NOCH WORDS;
31400     LB5A:
31500     SYNCOUNT:=0;
31600     UP1:
31700     NOCHAR:=NOCHAR+1;
31800     IF NOCHAR>=383 THEN GO TO LB1;
31900     LB5:  NS1[0]:=NEXTVAL(PA,SHIFT);
32000     LB2:
32100     IF NS1[0]=SYNC THEN SYNCOUNT:=SYNCOUNT+1 ELSE GO TO LB5A;
32200     IF SYNCOUNT=3 THEN GO TO LB4;
32300     NOCHAR:=NOCHAR+1;
32400     IF NOCHAR>=383 THEN GO TO LB1;
32500     NS2[0]:=NEXTVAL(PA,SHIFT);
32600     SCAN:=NS2[0].[2:3];
32700     IF SCAN>5 THEN GO TO LB5A;
32800     NOCHAR:=NOCHAR+1;
32900     IF NOCHAR>=383 THEN GO TO LB1;
33000     NS3[0]:=NEXTVAL(PA,SHIFT);
33100     NOCHAR:=NOCHAR+NS3[0]+1;
33200     IF NOCHAR>=383 THEN GO TO LB1;
33300     PA:=*+NS3[0];
33400     GO TO LB5;
33500     LB1:
33600     PASS:=PASS+1;
33700     IF PASS=4 THEN GO TO LB6;
33800     SHIFT:=PASS*6;
33900     PA:=POINTER(N[1],8)+PASS;
34000     NOCHAR:=PASS;
34100     GO TO UP1;
34200     LB4:
34300     WRITE(FOO,FOUND,SHIFT);
34400     GO TO LB7;
34500     LB6:
34600     WRITE (FOO,LOST);
34700     WRITE(FOO,<"NEXT RECORD IN THE FILE WILL BE READ">);
34800     GO TO LB16;
34900     LB7:
35000     %   THE BEGINNING OF THE FILE HAS BEEN POSITIVELY IDENTIFIED
35100     %   CALC SCANRATE-INTEGER VALUE-ACTUAL SAMPLING FREQUENCY
35200     %   =SCANRATE(RN)*15/16
35300     RN:=2**(SCAN+2);
35400     NOCH:=NS3[0];
35500     NOCHAR:=NOCHAR-2*NOCH-5;
35600     TOTCHAR:=384;
35700     XX:=2*(NOCH)+7;
35800     PA:=PA-XX;
35900     IJK:=0;
36000     SIZE:=256;
36100     IKK:=1;
36200     LB14:
36300     %   SHIFT=0 WHEN THERE IS NO SIX BIT SLIP
```

```
36400     IF SHIFT=0 THEN BEGIN NS1[IJK]:=REAL(PA,1); PA:=*+1; END ELSE
36500     NS1[IJK]:=NEXTVAL(PA,SHIFT);
36600     %
36700     IF NOCHAR<=384 THEN NOCHAR:=*+1  ELSE
36800     BEGIN
36900       CHECKCHAR(NOCHAR,PA,CASE,N);
37000       %   CHECKCHAR IS USED TO READ IN THE NEXT 7 TRACK TAPE RECORD
37100       %   INTO ARRAY N
37200       %
37300       IF CASE=255 THEN GO TO LB12;
37400       %   CASE=255 ON END OF FILE CONDITION
37500     END;
37600     IF NS1[IJK]=SYNC THEN GO TO LB8 ELSE
37700     BEGIN
37800       IF IKK<6 THEN
37900       BEGIN
38000         %   LESS THAN 6 SCANS -START AGAIN
38100         WRITE(FOO,RELOST,IKK);
38200         GO TO LB5B;
38300       END
38400       ELSE
38500       BEGIN
38600         %   WRITE ERROR STATEMENT,OUTPUT VARIABLES ALREADY CALCULATED
38700         %   TRY TO FIND THE BEGINNING OF THE DATA AGAIN
38800         WRITE(FOO,ENDLOST,NS1[IJK]);
38900         GO TO LB9;
39000       END
39100     END;
39200     LB8:
39300     %
39400     IF SHIFT=0 THEN BEGIN NS2[IJK]:=REAL(PA,1); PA:=*+1; END ELSE
39500     NS2[IJK]:=NEXTVAL(PA,SHIFT);
39600     %
39700     IF NOCHAR<=384 THEN NOCHAR:=*+1  ELSE
39800     BEGIN
39900       CHECKCHAR(NOCHAR,PA,CASE,N);
40000       IF CASE=255 THEN GO TO LB12;
40100     END;
40200     IF NS2[IJK].[2:3]=SCAN THEN BEGIN
40300       %   CHECK TO SEE IF SPECIAL CHANNELS ARE OPERATING
40400       SPECIAL (0&NS2[IJK][2:6:3],IKK);
40500       GO TO LB10; END ELSE
40600     BEGIN
40700       IF IKK<6 THEN
40800       BEGIN
40900         %   SCANRATE CHANGED-START AGAIN
41000         WRITE(FOO,SCANCH,IKK);
41100         GO TO LB5B;
41200       END
41300       ELSE
41400       BEGIN
41500         %   SCANRATE CHANGED-WRITE OUT ERROR MESSAGE,VARIABLES
41600         %   START AGAIN
41700         WRITE (FOO,SCANLOSS,NS2[IJK].[2:3]);
41800         GO TO LB9;
41900       END
42000     END;
42100     LB10:
42200     IF SHIFT=0 THEN BEGIN NS3[IJK]:=REAL(PA,1); PA:=*+1; END ELSE
42300     NS3[IJK]:=NEXTVAL(PA,SHIFT);
42400     IF NOCHAR<=384 THEN NOCHAR:=*+1  ELSE
42500     BEGIN
42600       CHECKCHAR(NOCHAR,PA,CASE,N);
42700       IF CASE=255 THEN GO TO LB12;
42800     END;
42900     IF NS3[IJK]=NOCH THEN GO TO LB11 ELSE
43000     BEGIN
43100       IF IKK<6 THEN
43200       BEGIN
43300         %   NUMBER OF CHANNELS CHANGED-START AGAIN
43400         WRITE(FOO,CHANL,IKK);
43500         GO TO LB5B;
43600       END
43700       ELSE
43800       BEGIN
43900         %   NUMBER OF CHANNELS IS CHANGED-WRITE OUT ERROR
44000         %   MESSAGE,VARIABLES-START AGAIN
44100         WRITE(FOO,CHANC,NS3[IJK]);
44200         GO TO LB9;
44300       END
44400     END;
44500     LB11:
44600     %   CHANNELS CH=1,2,...NOCH CONTAIN THE ANEMOMETER
44700     %   DATA
44800     MULT:=(IKK-1)/IKK;
44900     FOR CH:=1 STEP 1 UNTIL NOCH DO
45000     BEGIN
45100       %
45200       %
45300       IF SHIFT=0 THEN BEGIN NP:=REAL(PA,1);PA:=*+1; END ELSE
45400       NP:=NEXTVAL(PA,SHIFT);
45500       %
45600       %  NEW STYLE CHECKFAIL
45700       %
45800       BEGIN
```

```
45900         IF NP>124 AND NP<132 AND NP NEQ 128 THEN
46000         BEGIN
46100           %   DATA IN THIS RANGE ARE NEAR THE MAXIMUM VALUES
46200           %   FOR THE COUNTERS-OVERFLOW COULD OCCUR,I,E,
46300           %   POSITIVE ROTATIONAL VELOCITIES COULD APPEAR AS NEGATIVE
46400           %   AND VICE VERSA
46500           A[CH]:=*+1;
46600           IF A[CH]=10 THEN WRITE(FOO,PRIN,CH,IKK);
46700           IF A[CH]<10 THEN WRITE(FOO,OVERF,CH,IKK,NP);
46800         END ELSE
46900         IF A[CH]>10 AND (NP<105 OR NP>141) THEN BEGIN WRITE(FOO,OK,IKK);A[CH]:=0
47000           %   VELOCITIES HAVE DROPPED AWAY FROM THE DANGEROUS REGION
47100           ;
47200         END;
47300       END;
47400       %
47500       IF NOCHAR<=384 THEN NOCHAR:=*+1 ELSE
47600       CHECKCHAR(NOCHAR,PA,CASE,N);
47700       IF CASE =255 THEN GO TO LB12;
47800       %
47900       %  NEW STYLE MEANANS
48000       %
48100       %   CALCULATE RUNNING MEAN FROM EACH ANEMOMETER. THESE ARE
48200       %   THE MEANS OF THE ACTUAL NUMBERS ON THE TAPE WITHOUT BEGIN
48300       %   MODIFIED IN ANY WAY
48400       MEAN[CH]:=*+MULT+NP/IKK;
48500       IF NP>MX[CH] THEN BEGIN MX[CH]:=NP;CMX[CH]:=IKK;END ELSE
48600       IF NP<MN[CH] THEN BEGIN MN[CH]:=NP;CMN[CH]:=IKK;END;
48700       %
48800       %    NEW STYLE FIRSTDIFF
48900       %   COMPARES CONSECUTIVE DATA FROM EACH ANEMOMETER
49000       %   IF THE DIFFERENCE IS TOO LARGE AN ERROR MESSAGE IS
49100       %   WRITTEN
49200       IF NP>128 THEN NP:=NP-256;
49300       IF(ABS(LASTVALUE[CH]-NP)>DIFF) THEN BEGIN
49400         IF IKK=1 THEN GO TO SKIPOVER;
49500         C[CH]:=*+1;
49600         IF C[CH]<11 THEN WRITE(FOO,<"DIFFERENCE TOO LARGE CHANNEL"I6,X2,
49700         "VALUES ARE",I6,X2,I6,X2,"SCAN NUMBERS ARE",I6,X2,I6,>,CH,LASTVALUE[CH],
49800         NP,IKK-1,IKK);
49900       END;
50000       SKIPOVER:
50100       LASTVALUE[CH]:=NP;
50200       %   CALCULATE MEANS CORRECTING FOR ANY SIGN CHANGES
50300       CORRECTMEANS[CH]:=*+MULT+NP/IKK;
50400       IF NP>MMX[CH] THEN BEGIN MMX[CH]:=NP;CMMX[CH]:=IKK;END ELSE
50500       IF NP<MMN[CH] THEN BEGIN MMN[CH]:=NP;CMMN[CH]:=IKK;END;
50600       IF WRITEOUT THEN SAVE[CH,IJK]:=NP;
50700       %
50800     END;
50900     LB13:
51000     IJK:=IJK+1;
51100     IKK:=IKK+1;
51200     IF IJK=256 THEN BEGIN
51300       IJK:=0;
51400       IF WRITEOUT THEN BEGIN
51500         AA:=(IKK-257)/256;% NUMBER OF PREVIOUS TIMES BLOCK ENTERED
51600         BB:=RN/OUTPUTSCANRATE;%NUMBER OF SAMPLES TO BE ADDED TOGETHER
51700         %   256/BB IS THE NUMBER OF DATA STORED IN TSAVE[CH,*]
51800         %   PER ENTRY TO THE BLOCK
51900         CC:=AA MOD BB; % NUMBER OF TIMES DATA HAS BEEN
52000         %   WRITTEN INTO TSAVE SINCE THE LAST WRITE STATEMENT
52100         DD:=CC*256/BB;% NUMBER OF DATA ALREADY WRITTEN INTO
52200         %   TSAVE[CH,*]
52300         FOR CH:=1 STEP 1 UNTIL NOCH DO
52400         FOR I:=0 STEP 1 UNTIL 255 DO
52500         TSAVE[CH,DD+(I DIV BB)]:=*+SAVE[CH,I];
52600         IF CC=(BB-1) THEN
52700         FOR CH:=1 STEP 1 UNTIL NOCH DO BEGIN
52800           WRITE(OUTPUTFILE,256,TSAVE[CH,*]);
52900           REPLACE POINTER(TSAVE[CH,*]) BY 0 FOR 256 WORDS;
53000         END;
53100       END OF WRITEOUT BLOCK;
53200     END OF IJK EQ 256 BLOCK;
53300     GO TO LB14;
53400     LB12:
53500     %   END OF FILE FOUND. THIS USUALLY INDICATES THAT THE
53600     %   DATA HAS BEEN RECORDED PROPERLY WITH AN END OF FILE
53700     %   MARK AT THE END OF THE FILE.
53800     CLOSE(DATA,*);
53900     WRITE(FOO,GOOD);
54000     WRITE(FOO,START,TIME+1,PART);
54100     TIME:=TIME+1;
54200     PART:=0;
54300     GO TO LB3;
54400     LB9:
54500     WRITE(FOO,START,TIME+1,PART);
54600     LB3:
54700     PART:=PART+1;
54800     WRITE(FOO,FINISH,IKK,RN,NOCH);
54900     IF RN NEQ 0 THEN
55000     LENGTH:=IKK*16/(RN*15*60)
55100     ELSE LENGTH:=0.;
55200     WRITE(FOO,LNGTH,LENGTH);
55300     WRITE(FOO,</"RAW MEANS WITHOUT CONSIDERING THE SIGN OF THE"
```

```
55400      " DATA"/>);
55500      FOR I:=1 STEP 3 UNTIL NOCH DO
55600      BEGIN
55700        WRITE(FOO,MEANS,I,MEAN[I],I+1,MEAN[I+1],I+2,MEAN[I+2]);
55800      END;
55900      FOR I:=1 STEP 1 UNTIL NOCH DO
56000      IF MEAN[I]>128 THEN MEAN[I]:=256-MEAN[I];
56100      FOR I:=1 STEP 3 UNTIL NOCH DO
56200      BEGIN
56300        XXX:=ARCTAN2(MEAN[I+1],MEAN[I]);
56400        WRITE(FOO,<"AVERAGE ANGLE OF ATTACK --TAN-1(V/U) ARRAY",X1,I3,
56500        "IS",F13.7>,(I+2)/3,XXX*180/3.1415926);
56600      END;
56700      WRITE(FOO,</"MEANS WITH EACH DATA SAMPLE CORRECTED FOR ANY"
56800      " SIGN CHANGE">);
56900      FOR I:=1 STEP 3 UNTIL NOCH DO
57000      WRITE(FOO,<"CHANNEL",I4,"  MEAN VALUE=",F10.4,"  CHANNEL",I4,
57100      "  MEAN VALUE=",F10.4,"  CHANNEL",I4,"  MEAN VALUE=",F10.4>,
57200      I,CORRECTMEANS[I],I+1,CORRECTMEANS[I+1],I+2,CORRECTMEANS[I+2]);
57300      WRITE(FOO,</"CORRECTED DATA AVERAGE ANGLES">);
57400      FOR I:=1 STEP 3 UNTIL NOCH DO
57500      WRITE(FOO,<"AVERAGE ANGLE FROM X ANEMOMETER ARRAY",
57600      I3," IS",F13.7," DEGREES">,(I+2)/3,180/3.14159*
57700      ARCTAN2(CORRECTMEANS[I+1],CORRECTMEANS[I]));
57800      FOR CH:=1 STEP 1 UNTIL NOCH DO BEGIN
57900        IF C[CH]>11 THEN WRITE(FOO,<"CHANNEL",I5,X2,"HAS",I6,X2,"FIRST DIFF
58000        ERENCES LARGER THAN",I6>,CH,C[CH],DIFF);
58100        C[CH]:=0;
58200      END;
58300      FOR I:=0 STEP 1 UNTIL 48 DO
58400      BEGIN
58500        A[I]:=0;
58600        B[I]:=0;
58700      END;
58800      WRITE(FOO,</"UNCORRECTED MAX AND MINS FROM EACH CHANNEL">);
58900      FOR I:=1 STEP 1 UNTIL NOCH DO
59000      WRITE(FOO,<"CHANNEL",I3," MAX=",F10.2," AT SCAN",I7,
59100      "     MIN=",F10.2," AT SCAN",I7>,I,MX[I],CMX[I],MN[I],CMN[I]);
59200      WRITE(FOO,</"CORRECTED MAX AND MINS FROM EACH CHANNEL">);
59300      FOR I:=1 STEP 1 UNTIL NOCH DO
59400      WRITE(FOO,<"CHANNEL",I3,"MAX=",F10.2," AT SCAN "I7,
59500      "    MIN=",F10.2,"  AT SCAN NO",I7>,I,MMX[I],CMMX[I],
59600      MMN[I],CMMN[I]);
59700      IF TIME<NOOFFILES THEN
59800      BEGIN
59900        %
60000        GO TO LB16;
60100      END;
60200    END;
60300    END1:
60400  END.

INPUT STRING WAS
"CHECKDATA STEP 2"
```

APPENDIX C

PROGRAM 'COPYDATA'

C.1 Typical WFL For Using This Program

C.1.1 Simple File Copy

Assume that the 7 track tape WIND2 has two files both with a scan rate of 16. It is desired to copy the second file consisting of 65536 scans, and with 12 orthogonal arrays, i.e. 36 channels, to the library tape C456 at a scan rate of 4. However only the data from the first six and last three channels is required for storage on the library tape. Assume that the source file corresponding to program COPYDATA is on library tape A999. The JOB required to achieve the above is given below

```
7
5 JOB COPYDATA/WIND2  TO  A999; PROCESSTIME=600;
  IOTIME=600; DESTNAME=SITE;
  USER MECH021/PASSWORD; CLASS=10; BEGIN
7
5 DISPLAY "WIND2 IS AN UNLABELLED TAPE RENTED BY";
  DISPLAY "MECH021";
  COPY COPYDATA FROM A999;
  COMPILE COPYIT ALGOL LIBRARY;
  COMPILER FILE TAPE=COPYDATA;
  DATA
$ SET MERGE
$ RESET LIST
7
5 IF FILE COPYIT ISNT PRESENT THEN GO ENDIT;
  RUN COPYIT;
  FILE FIELD7TAPE=WIND2; FILE OUTPUTFILE=F;
  DATA KR;
  1,
  1,
```

```
  12, 65536, 16, 4,
  0,
  0,0,
  9,
  1,2,3,                                /
  4,5,6,34,35,36,
7
5 COPY F AS WIND2/D071277 TO C456;
7
5 ENDIT:
7
5 END JOB
```

C.1.2 How to Join Files from Several Tapes

Assume that the 7 track tape WIND3 has three files all with 10 triplets (orthogonal arrays), and all with a scan rate of 32. The 7 track tape WIND4 contains two files with 10 triplets and a scan rate of 16. It is desired to join the last two files on WIND3 and the first file on WIND4 together, also to reduce the scan rate to 2 and to only copy the data from the last 9 triplets of the input files to the library tape D203. It is also necessary to ignore the data (for some reason) from the first 500 records of the second file on WIND3. Channel B in the first file on WIND4 was also observed to overflow.

The JOB to do this is given below. It is similar to the JOB given in Section C.1.1 up to "RUN COPYIT".

```
7
5 FILE FIELD7TAPE=WIND3;
  DATA KR;
  1,
  2,
  10, 6000, 32, 2,
  500,
  0, 0,
  27,
```

```
  4,5,6,7,8,9,10,11,12,13,14,15,16,17,18,19,20,21,    /
  22,23,24,25,26,27,28,29,30,
  10, 65000, 32, 2
  0,
  0, 0,
  27,
  4,5,6,7,8,9,10,11,12,13,14,15,16,17,18,19,    /
  20,21,22,23,24,25,26,27,28,29,30,
7
5 DISPLAY "WIND4 IS AN UNLABELLED 7 TRACK TAPE";
  RUN COPYIT;
  FILE FIELD7TAPE=WIND4;
  DATA KR;
  0,
  1,
  10, 30000, 16, 2,
  0,
  0, 1,
  27,
  4,5,6,7,8,9,10,11,12,13,14,15,16,17,18,19,20,21,22,23,24,  /
  25,26,27,28,29,30,
7
5 COPY OUTPUTFILE AS WDLINCOLN TO D203;
7
5 END JOB
```

C.2. Listing of Program COPYDATA

```
 CCC   OOO  PPPP  Y   Y DDDD   AAA  TTTTT  AAA
C   C O   O P   P  Y Y  D   D A   A   T   A   A
C     O   O P   P   Y   D   D A   A   T   A   A
C     O   O PPPP    Y   D   D AAAAA   T   AAAAA
C     O   O P       Y   D   D A   A   T   A   A
C   C O   O P       Y   D   D A   A   T   A   A
 CCC   OOO  P       Y   DDDD  A   A   T   A   A


251 RECORDS, CREATED 23/11/78

    1000 BEGIN
    2000   %               DECLARE FILES,INTEGERS,REALS,LABELS
    3000   FILE FIELD7TAPE(KIND=TAPE7,FILETYPE=7,MAXRECSIZE=64,BLOCKSIZE=64,LABELTY
    4000   PE=STANDARD,UNITS=WORDS);
    5000   FILE OUTPUTFILE(KIND=DISK,FILETYPE=7,MAXRECSIZE=256,BLOCKSIZE=768,
    6000   AREASIZE=60,FLEXIBLE=TRUE,PROTECTION=SAVE,UNITS=WORDS);
    7000   FILE KR(KIND=READER);
    8000   FILE LP(KIND=PRINTER);
    9000   INTEGER NOOFFILES,FILECOUNTER;
   10000   INTEGER I,J,RECORDNO,NOOFARRAYS,COUNT;
   11000   INTEGER NOOFSCANS;
   12000   INTEGER ACTUALSR;
   13000   INTEGER NEWSR,TE,P,PSA;
   14000   INTEGER II,NOOFOUTPUTCHANNELS,NORECSTOSKIP;
   15000   INTEGER SAVESR;
   16000   LABEL LOOPBACK;
   17000   LABEL ENDLBL;
   18000   INTEGER NOOFFILESTOSKIP;
   19000   BOOLEAN AOVERFLOW,BOVERFLOW;
   20000   %
   21000   %                     MAINLINE
   22000   %
   23000   %     SET FILECOUNTER TO ZERO
   24000   READ(KR,/,NOOFFILESTOSKIP);WRITE(LP,*/,NOOFFILESTOSKIP);
   25000   IF NOOFFILESTOSKIP>0 THEN
   26000   THRU NOOFFILESTOSKIP DO BEGIN
   27000     SPACE(FIELD7TAPE,1);CLOSE(FIELD7TAPE,*);END;
   28000   FILECOUNTER:=0;
   29000   READ(KR,/,NOOFFILES);
   30000   %     NUMBER OF FILES ON 7 TRACK FIELD DATA TAPE TO BE PROCESSED
   31000   LOOPBACK:
   32000   %     LABEL USED WHEN MORE THAN 1 FILE ON A 7 TRACK FIELD DATA
   33000   %     TAPE IS TO BE PROCESSED
   34000   READ(KR,/,NOOFARRAYS,NOOFSCANS,ACTUALSR,NEWSR);
   35000   WRITE(LP,<"NUMBER OF ORTHOGONAL ARRAYS=",I4>,NOOFARRAYS);
   36000   WRITE(LP,<"  NUMBER OF SCANS, IE THE NUMBER OF DATA PER CHANNEL=",
   37000   I6>,NOOFSCANS);
   38000   WRITE(LP,<"LENGTH OF THIS DATA FILE=",F7.2,X2,"MINUTES">,
   39000   NOOFSCANS*16/(ACTUALSR*15*60));
   40000   WRITE(LP,<"DATA COLLECTED AT A SCANRATE OF ",I4," HERTZ">,ACTUALSR);
   41000   WRITE(LP,<"DATA IS TO BE WRITTEN TO THE LIBRARY TAPE AT A SCAN RATE OF",
   42000   I4>,NEWSR);
   43000   WRITE(LP,<"  NUMBER OF 7 TRACK RECORDS FOR THIS AMOUNT OF DATA IS=",
   44000   I4>,(NOOFSCANS*3*(NOOFARRAYS+1))/384);
   45000   WRITE(LP,<"NUMBER OF LIBRARY TAPE RECORDS FOR THIS AMOUNT OF DATA IS=",
   46000   I4>,3*NOOFARRAYS*NOOFSCANS/256*NEWSR/ACTUALSR);
   47000   SAVESR:=LOG(ACTUALSR)/LOG(2)-2;
   48000   READ(KR,/,NORECSTOSKIP); % RECORDS MAY NEED SKIPPING BECAUSE OF A
   49000   %     PARITY ERROR OR BAD DATA,OR TO SYNCHRONISE THE DATA IE,
   50000   %     MAKE THE BEGINNING OF A SCAN OCCUR AT THE BEGINNING OF A RECORD
   51000   WRITE(LP,*/,NORECSTOSKIP);
   52000   IF NORECSTOSKIP>0 THEN
   53000   WRITE(LP,<///"THE FIRST",I4," RECORDS,=",F10.4," SCANS"/
   54000   "ARE BEING SKIPPED, IE THE DATA THEY CONTAIN IGNORED">,
   55000   NORECSTOSKIP,NORECSTOSKIP*384/(3*NOOFARRAYS+3));
   56000   READ(KR,/,AOVERFLOW,BOVERFLOW);
   57000   IF AOVERFLOW THEN WRITE(LP,<"THE DATA AS RECORDED HAS OVERFLOWED I"
   58000   "N CHANNEL A"/"WHICH WAS OBSERVED TO ROTATE IN A POSITIVE DIRECT"
   59000   "ION AT ALL TIMES"/>);
   60000   IF BOVERFLOW THEN WRITE(LP,<"THE DATA AS RECORDED HAS OVERFLOWED"
   61000   " IN CHANNEL B"/"WHICH WAS OBSERVED TO ROTATE IN A POSITIVE"
   62000   " DIRECTION AT ALL TIMES"/>);
   63000   READ(KR,/,NOOFOUTPUTCHANNELS);% THE NUMBER OF DATA CHANNELS IN THE
   64000   %     OUTPUT FILE MAY BE DIFFERENT FROM THE ORIGINAL NUMBER OF THE 7
   65000   %     TRACK FILLD TAPE. THIS COULD BE DUE TO BAD DATA IN SOME
   66000   %     CHANNELS OR UNUSUAL CABLE CONNECTIONS IN THE FIELD ETC.
   67000   %     THE NUMBER OF OUTPUT CHANNELS SHOULD BE A MULTIPLE OF 3, IN
   68000   %     TRIPLETS OF ANEMOMETERS, EACH TRIPLET BEING IN THE ORDER
   69000   %     U, V, W.
   70000   IF(NOOFOUTPUTCHANNELS MOD 3) NEQ 0 THEN BEGIN
   71000     WRITE(LP,<"THE NUMBER OF OUTPUT CHANNELS SHOULD BE A MULTIPLE OF"
   72000     " 3">); GO TO ENDLBL; END;
   73000   %     TE IS THE NUMBER OF CONSECUTIVE DATA IN EACH CHANNEL TO BE
   74000   %     ADDED TOGETHER
   75000   TE:=ACTUALSR/NEWSR;
   76000   %     THIS POSITIONS THE WRITE POINTER TO THE LAST RECORD OF THE
   77000   %     FILE, IF IT EXISTS FROM A PREVIOUS RUN OF THE PROGRAMME
   78000   %     SUBSEQUENT WRITES TO THE FILE THEN CARRY ON WITH NO GAPS
   79000   %     OR DATA BEING WRITTEN OVER EXISTING DATA
   80000   IF OUTPUTFILE.PRESENT THEN
   81000   IF  (COUNT:=OUTPUTFILE.LASTRECORD) GEQ 0 THEN
   82000   READ(OUTPUTFILE[COUNT],<A1>,COUNT);
```

```
BEGIN
  %
  %          DECLARE POINTERS,LABELS,DYNAMICALLY DIMENSION ARRAYS
  %
  ARRAY MAXM,COUNTMAX,MINM,COUNTMIN[3:3*NOOFARRAYS+2];
  POINTER PA;
  LABEL L1,L2;
  LABEL L3;
  LABEL PRINTIT;
  LABEL READAGAIN,PAR;
  LABEL JUMP;
  ARRAY N[0:63],M[0:768*NOOFARRAYS+767],D[3:3*NOOFARRAYS+2,0:255];
  ARRAY ST[3:3*NOOFARRAYS+2,0:255];
  ARRAY OUTPUT[0:NOOFOUTPUTCHANNELS-1];
  LABEL LAB2,LAB3;
  REPLACE POINTER(MAXM[3]) BY -1000 FOR 3*NOOFARRAYS+3 WORDS;
  REPLACE POINTER(MINM[3]) BY +1000 FOR 3*NOOFARRAYS+3 WORDS;
  READ(KR,/,FOR I:=0 STEP 1 UNTIL NOOFOUTPUTCHANNELS-1 DO
  OUTPUT[I]);
  WRITE(LP,<"CHANNELS SELECTED FROM FIELD DATA TAPE FOR COPYING TO"
  " A LIBRARY TAPE ARE">);
  WRITE(LP,<1217>,FOR I:=0 STEP 1 UNTIL NOOFOUTPUTCHANNELS-1
  DO OUTPUT[I]);
  IF NORECSTOSKIP>0 THEN BEGIN
    I:=0;
    DO BEGIN
      READ(FIELD7TAPE,64,N)[:LAB2];
      GO TO LAB3;
      LAB2:
      WRITE(LP,<"PARITY ERROR ON THE",I4," TH READ - THE ",I4," RECORD">,
      I+1,I+1);
      LAB3:
    END UNTIL I:=*+1=NORECSTOSKIP; END;
  %
  %     THIS IS THE BEGINNING OF THE DECODING AND REFORMATTING PART
  %
  FOR COUNT:=1 STEP 1 UNTIL NOOFSCANS/256 DO
  %     FOR EACH VALUE OF COUNT,256 DATA FROM EACH CHANNEL ARE READ
  %     IN FROM THE 7 TRACK FIELD DATA TAPE
  BEGIN
    %                                                    LOOP 1
    FOR I:=1 STEP 1 UNTIL 2*NOOFARRAYS+2 DO
    %     2*NOOFARRAYS+2 IS THE NUMBER OF 7 TRACK TAPE RECORDS TO GIVE 256
    %     DATA FROM EACH CHANNEL
    BEGIN
      %                                                    LOOP 2
      PA:=POINTER(N[0],8);
      READAGAIN:
      %         READ 64 WORDS, WHICH IS EQUAL TO ONE 7 TRACK FIELD
      %         DATA TAPE RECORD INTO ARRAY N
      READ(FIELD7TAPE,64,N[*])[L1:PAR];
      GO TO L3;
      %     L1 IS A LABEL USED WHEN THE END OF THE INPUT FIELD DATA
      %     TAPE FILE IS REACHED
      L1:
      WRITE(LP,<X10,"END OF 7 TRACK TAPE FILE BEFORE EXPECTED">);
      WRITE(LP,<X10,"COUNT=",I4,"   I=",I8>,COUNT,I);
      GO TO L2;
      %     PAR IS A LABEL USED WHEN A PARITY ERROR IS FOUND ON THE
      %     7 TRACK FIELD DATA TAPE
      PAR:
      WRITE(LP,<X5,"PARITY ERROR,READ NEXT RECORD, WRITE OUT"/
      "VARIABLES TO SEE WHEN ERROR OCCURRED">);
      WRITE(LP,<"COUNT=",I6," I=",I6,/"THE PARITY ERROR OCCURRED IN"
      " THE(COUNT-1)*(2*NOOFARRAYS+2)+I RECORD=",I6," RECORD">,COUNT,I,
      (COUNT-1)*(2*NOOFARRAYS+2)+I);
      GO TO READAGAIN;
      L3:
      FOR J:=0 STEP 1 UNTIL 383 DO
      BEGIN
        %                                                  LOOP 3
        %
        %     PUT ONE CHARACTER OF 8 BITS, EXTRACTED WITH THE POINTER PA
        %     FROM ARRAY N INTO ONE WORD, OF 48 BITS, IN THE ONE
        %     DIMENSIONAL ARRAY M
        %     PA IS AN 8 BIT POINTER, POINTING AT ARRAY N, AND
        %     UPDATED ALONG IT IN MULTIPLES OF 8 BITS. IT CAN THUS
        %     EXTRACT 6 8 BIT CHARACTERS FROM ONE 48 BIT WORD OF
        %     ARRAY N
        %     EACH 7 TRACK TAPE RECORD CONTAINS 384  8 BIT
        %     CHARACTERS (64X48 BIT WORDS, 512X6 BIT CHARACTERS)
        M[384*(I-1)+J]:=REAL(PA,1);
        PA:=PA+1;
      END;
      %                                                  END OF LOOP 3;
    END;
    %                                                  END OF LOOP 2
    %     CHECK THAT THE DATA IS STILL IN THE RIGHT SEQUENCE
    IF M[0] NEQ 127 THEN BEGIN
      WRITE(LP,<"THE FIRST VALUE OF THE M ARRAY IS NOT EQUAL TO 127. SOME
      VALUES ARE PRINTED OUT TO SEE WHEN THE ERROR OCCURRED">);
      GO TO PRINTIT; END;
    IF M[1] NEQ SAVESP THEN BEGIN WRITE(LP,<"THE CONTROL"
      " PARAMETER SCANRATE DOES NOT AGREE WITH THE VALUE READ"/
      "OFF THE FIELD DATA TAPE">); GO TO PRINTIT; END;
```

```
178000       IF M[2] NEQ 3*NOOFARRAYS THEN BEGIN WRITE(LP,<"THE NUMBER OF"
179000         " ARRAYS AS AN INPUT PARAMETER DOES NOT AGREE WITH"
180000         /"THE VALUE ON THE FIELD DATA TAPE">); GO TO PRINTIT;
181000       END;
182000       II:=0;
183000       DO
184000       BEGIN
185000         %                                                    LOOP 2
186000         I:=OUTPUT(II)+2;
187000         FOR J:=0 STEP 1 UNTIL 255 DO
188000         BEGIN
189000           %                                                   LOOP 3
190000           D[I,J]:=M[(NOOFARRAYS+1)*3*J+I];
191000           IF AOVERFLOW THEN IF (I MOD 3)=0 THEN GO TO JUMP;
192000           IF BOVERFLOW THEN IF ((I-1) MOD 3)=0 THEN GO TO JUMP;
193000           IF D[I,J]>128 THEN D[I,J]:=D[I,J]-256;
194000           JUMP:
195000           IF (D[I,J])>(MAXM[I]) THEN BEGIN MAXM[I]:=D[I,J];COUNTMAX[I]
196000             :=256*(COUNT-1)+1+J;    END ELSE
197000           IF D[I,J]<MINM[I] THEN BEGIN
198000             MINM[I]:=D[I,J];COUNTMIN[I]:=256*(COUNT-1)+1+J;END;
199000         END;
200000         %                                                   END OF LOOP 3
201000         PSA:=((COUNT-1) MOD TE)*256/TE;
202000         FOR P:=0 STEP 1 UNTIL 255 DO
203000         ST[I,PSA+(P DIV TE)]:=*+D[I,P];
204000         IF (COUNT MOD TE) =0 THEN
205000         BEGIN
206000           %                                                   LOOP 3
207000           WRITE(OUTPUTFILE,256,ST[I,*]);
208000           REPLACE POINTER(ST[I,0]) BY 0 FOR 256 WORDS;
209000         END;
210000         %                                                   END OF LOOP 2
211000       END UNTIL (II:=*+1)=NOOFOUTPUTCHANNELS;
212000       %                                                   END OF LOOP 2
213000     END;
214000     %                                                     END OF LOOP 1
215000     GO TO L2;
216000     PRINTIT:
217000     %     USED ONLY ON ERROR CONDITION
218000     WRITE(LP,<"COUNT=",I6," NUMBER OF SCANS READ FROM INPUT TAPE FILE IS"
219000     " (COUNT-1)*256=",I6>,(COUNT-1)*256);
220000     WRITE(LP,<"NUMBER OF DATA CHANNELS ON FIELD DATA INPUT TAPE=",
221000     I5,/"THEREFORE NUMBER OF 7 TRACK DATA INPUT TAPE RECORDS"
222000     " READ SUCCESSFULLY IS AT LEAST (COUNT-1)*(2*NOOFARRAYS+2)="
223000     ,I6>,3*NOOFARRAYS,
224000     (COUNT-1)*(2*NOOFARRAYS+2));
225000     WRITE(LP,<"NUMBER OF LIBRARY TAPE RECORDS WRITTEN"
226000     " IS (COUNT-1)*NOOFOUTPUTCHANNELS"
227000     " =",I6>,(COUNT-1)*NOOFOUTPUTCHANNELS);
228000     L2:
229000     %     OUTPUT SOME PARAMETERS FOR CHECKING PURPOSES
230000     WRITE(LP,<X5,"DATA IN M ARRAY PRINTED OUT TO ENSURE NO ERRORS"/X5,
231000     "CORRECT DATA SHOULD HAVE",/X5,"M[0]=127,2**(M[1]+2)=ACTUALSR,"
232000     " M[2]=NUMBER OF CHANNELS">);
233000     WRITE(LP,<"M ARRAY">);
234000     WRITE(LP,<X5,12I7>,FOR I:=0 STEP 1 UNTIL (1+NOOFARRAYS)*3 DO M[I]);
235000     WRITE(LP,<"MAXIMUMS AND MINIMUMS FROM EACH CHANNEL">);
236000     FOR I:=3 STEP 1 UNTIL 3*NOOFARRAYS+2 DO
237000     WRITE(LP,<"CHANNEL",I3," MAXM ",F9.2,"  AT SCAN NO",I7,
238000     "   MIN=",F9.2," AT SCAN NO",I7>,I-2,MAXM[I],COUNTMAX[I],
239000     MINM[I],COUNTMIN[I]);
240000   END;
241000   FILECOUNTER:=*+1;
242000   IF FILECOUNTER<NOOFFILES THEN
243000   BEGIN
244000     %     THE READ 7 TRACK FIELD DATA TAPE FILE POINTER
245000     %     IS POSITIONED AT THE BEGINNING OF THE NEXT FILE
246000     CLOSE(FIELD7TAPE,*); GO TO LOOPBACK;
247000   END;
248000   %     END OF PROGRAMME.
249000   ENDLBL:
250000   WRITE(LP,<X10,/"END OF PROGRAMME">);
251000 END.


INPUT STRING WAS
"COPYDATA STEP 2"
```

APPENDIX D

PROGRAM 'VTPDMS'

D.1 Typical WFL For Using This Program

Assume that the library tape A987 contains a file called TA987/FILE12, which contains data collected by the propeller anemometers. The file contains 8192 samples per channel from seven orthogonal arrays, i.e. 21 anemometers. The scan rate of the data on the tape is 8. It is desired to run the program VTPDMS using a scan rate within the program equal to 2. The results are required to be obtained for no, linear and parabolic trend removal. The data has been obtained from anemometer arrays all at the same height so that their average velocity is about the same, 22 classes are required in the probability density distribution plots and all orthogonal arrays are to be processed.

A JOB to output the results in the desired format is given below. The source file VTPDMS is assumed to be on tape A999.

```
7
5 JOB VTPDMS/VISUALCHECK ON TA987/FILE12;
  DESTNAME=SITE; PROCESSTIME=300;IOTIME=300;
  USER MECH021/PASSWORD;CLASS=6,BEGIN
7
5 COPY VTPDMS FROM A999;
  COMPILE LOOKATIT ALGOL LIBRARY;
  COMPILER FILE TAPE=VTPDMS;
  DATA
$ SET MERGE
$ RESET LIST
7
5 IF FILE LOOKATIT ISNT PRESENT THEN GO HOME;
  COPY TA987/FILE12 FROM A987;
  RUN LOOKATIT;
```

```
  FILE INFYLE=TA987/FILE12;
  DATA KR;
  8192, 7, 8, 22, 1,
  2,
  1,
  0,
7
5 REMOVE TA987/FILE12;
  HOME:
7
5 END JOB
```

To analyse the data from only one orthogonal array, number 5 in the above file TA987/FILE12, and using no trend removal only, the following data cards are required. The work flow language is the same as for the JOB above.

```
8192, 7, 8, 22, 0,
2,
1,
1,5,
```

D.2 Listing of Program VTPDMS

```
V    V TTTTT PPPP  DDDD  M    M  SSS
V    V   T   P   P D   D MM  MM S   S
V    V   T   P   P D   D M M M M S
 V  V    T   PPPP  D   D M M M M  SSS
 V  V    T   P     D   D M   M      S
  V      T   P     D   D M   M S    S
  V      T   P     DDDD  M   M  SSS

513 RECORDS, CREATED 22/11/78

    1000 $ SET AUTOBIND
    2000 $BINDER RESET LIST
    3000 $ SET LINEINFO
    4000 %     BIND PLOT PROCEDURES,RESIDENT ON DISK,INTO THIS PROGRAMME
    5000 $ BIND = FROM PLOTA/=
    6000 BEGIN
    7000   %     DECLARE VARIABLES GLOBAL TO ALL PROCEDURES
    8000   BOOLEAN SAMEHEIGHTS;
    9000   $ INCLUDE  "PLOTA/EXTLDECLS"
   10000   BOOLEAN ONEARRAY;INTEGER ARRAYNO;
   11000   %     PLOT VELOCITIES(AVERAGED OVER 8 SECONDS)AS FUNCTIONS
   12000   %     OF TIME

   13000   PROCEDURE PLOTVELTIME(V,SR,NA,JD);VALUE SR,NA,JD;
   14000   ARRAY V[*,*];INTEGER SR,NA,JD;
   15000   BEGIN
   16000     ARRAY L1[0:2],L2[0:4],L3[0:7],L4[0:9],CHAR[0:12],X[0:JD/150];
   17000     REAL TEMP; INTEGER I,HT;
   18000     % THIS PROCEDURE PLOTS VELOCITY RUNS FROM
   19000     % ARRAYS OF ANEMOMETERS
   20000     REPLACE POINTER(L1) BY "TIME IN MINUTES";
   21000     REPLACE POINTER(L2) BY "LONGITUDINAL VELOCITY IN M/S";
   22000     REPLACE POINTER(L3) BY "VELOCITY POINTS ARE AVERAGED OVER 8 SECONDS";
   23000     REPLACE POINTER(L4) BY "WHICH IS PLOTTED IN INCREMENTS OF TWO HUNDREDTHS
   24000     OF AN INCH";
   25000
   26000     % SCALING COUNTS TO M/S HAS BEEN DONE ON THE READ IN STATEMENT
   27000     %CALL PLOT SUBROUTINES
   28000     AINIT(1400);
   29000     ASPEED(4);
   30000     AORIG(100,80);
   31000     ABOX(0,0,8,90,150,10,2);
   32000     ASCA(-40,-12,150,0,0,10,9,1,2);
   33000     ALAB( 500,-30,L1,15,1,2);
   34000     ALAB(-50,350,L2,28,1,4);
   35000     ALAB(250,950,L3,43,1,2);
   36000     ALAB(250,910,L4,59,1,2);
   37000     TEMP:=5  ;
   38000     IF ONEARRAY THEN BEGIN HT:=ARRAYNO-1;
   39000       ALINEX(0,2,V[HT,*],JD,-5,2);
   40000       ASCA(-60,0,0,100,-5,2,11,1,2);END ELSE
   41000     FOR HT:=0 STEP 1 UNTIL NA-1 DO
   42000     ALINEX(0,2,V[HT,*],JD,+2.5-5.0*HT,TEMP);
   43000     AEND;
   44000     %
   45000   END   E N D   O F   P R O C E D U R E   P L O T V E L T I M E ;
   46000   %
   47000   %     PLOT PROBABILITY DENSITY FUNCTION TO COMPARE WITH A
   48000   %     GAUSSIAN DISTRIBUTION

   49000   PROCEDURE PLOTPROBDIST(FREQ,MDPT,SDV,VM,NA,NCL,SR,TRENDTYPE);
   50000   VALUE NA,NCL,SR,TRENDTYPE;INTEGER NA,NCL,SR,TRENDTYPE;
   51000   ARRAY FREQ[*,*,*],MDPT[*,*,*],SDV[*],VM[*];
   52000   BEGIN
   53000     INTEGER HT,J,I;ARRAY L1[0:0],L2[0:4],L3[0:1],L4[0:5],
   54000     L5[0:3],L6[0:7],FMT[0:0];
   55000     ARRAY B1[0:NA-1,0:9],B2[0:NA-1,0:11],B3[0:3];
   56000     LABEL BACK;
   57000     LABEL LAB;
   58000     REAL RE;
   59000     ARRAY Y[0:80];
   60000     %THE OBJECT OF THIS PROCEDURE IS TO PLOT OUT WIND VELOCITY FLUCTUATIONS
   61000     %IN A PROBABILITY DENSITY FORMAT SO THAT THEY MAY BE COMPARED WITH
   62000     %THE GAUSSIAN DISTRIBUTION WHICH IS AN OFTEN USED MODEL
   63000     %
   64000     %          LABELS
   65000     REPLACE POINTER(L1) BY "MEAN";
   66000     REPLACE POINTER(L2) BY "CLASS IN STANDARD DEVIATIONS";
   67000     REPLACE POINTER(L3) BY "FREQUENCY";
   68000     REPLACE POINTER(L4) BY "STANDARDISED NORMAL DENSITY FUNCTION";
   69000     REPLACE POINTER(L6) BY "DATA COLLECTED AT A SCANRATE OF",SR*15/16 FOR 5
   70000     NUMERIC," HZ    ";
   71000     REPLACE POINTER(FMT) BY "F4.2";
   72000     IF TRENDTYPE=0 THEN REPLACE POINTER(B3) BY "NO TREND REMOVAL"
   73000     "       ";
   74000     IF TRENDTYPE=1 THEN REPLACE POINTER(B3) BY "LINEAR TREND REMOVAL"
   75000     "   ";
   76000     IF TRENDTYPE=2 THEN REPLACE POINTER(B3) BY "PARABOLIC TREND REMOVAL";
   77000     %     GENERATE GAUSSIAN CURVE
   78000     RE:=1/(SQRT(2*3.1415926));
   79000     FOR I:=0 STEP 1 UNTIL 80 DO
   80000     Y[I]:=RE*EXP(-((I/10-4)**2)/2);
```

```
81000     J:=0;
82000     BACK:
83000     IF J=1 THEN AORIG(50,578) ELSE BEGIN AINIT(890);ASPEED(4);
84000       AORIG(50,38);END;
85000     GO TO LAB;
86000     FOR I:=0 STEP 1 UNTIL NA-1 DO
87000     BEGIN
88000       REPLACE POINTER(B1[I,*])BY "MEAN WIND VELOCITY ARRAY",I+1 FOR 2
89000       NUMERIC," =",VM[I*3+J] FOR 7 NUMERIC," METRES PER SECOND";
90000       REPLACE POINTER(B2[I,*])BY "STANDARD DEVIATION OF WIND FLUCTUATIONS="
91000       ,
92000       SDV[I*3+J] FOR 7 NUMERIC," METRES PER SECOND";
93000       ALAB(0,750-40*I,B1[I,*],53,1,2);
94000       ALAB(0,730-40*I,B2[I,*],65,1,2);
95000     END;
96000     LAB:
97000     IF J=0 THEN REPLACE POINTER(L5) BY "LONGITUDINAL DIRECTION";
98000     IF J=1 THEN REPLACE POINTER(L5) BY "LATERAL DIRECTION     ";
99000     IF J=2 THEN REPLACE POINTER(L5) BY "VERTICAL DIRECTION    ";
100000    ABOX(0,0,4,10,100, 50,2); ABOX(400,0,4,10,100, 50,2);
101000    ASCA(-40,-12,100,0,-4,1,9,1,2);
102000    ASCALE(-40,0,0, 50,0,.05,11,1,2,FMT,4);
103000    ALAB(380,-25,L1,4,1,2);
104000    ALAB(260,-37,L2,28,1,2);
105000    ALAB(390,200,L3,9,1,4);
106000    ALAB(12,470,L4,36,1,2);
107000    ALAB(12,430,L5,22,1,2);
108000    ALAB(12,450,L6,42,1,2);
109000    ALAB(12,410,B3,23,1,2);
110000    ALINEX(0,10,Y,81,0,.1);
111000    FOR HT:=0 STEP 1 UNTIL NA-1 DO
112000    BEGIN IF ONEARRAY THEN HT:=ARRAYNO-1;
113000      ALINED(MDPT[HT,J,*],FREQ[HT,J,*],NCL,-4,0,1,.1,2+HT*3,2+HT*3);
114000      IF ONEARRAY THEN HT:=NA-1;END;
115000    IF J NEQ 0 THEN AEND;
116000    IF (J:=J+1)<3 THEN GO TO BACK;
117000    %PLOTS OF PROBABILITY DISTRIBUTION NOW FINISHED
118000  END   E N D   O F   P R O C E D U R E   P L O T P R O B D I S T ;
119000  %
120000  %     PLOT MEAN SQUARES AVERAGED OVER 2.27 MINUTES TO SEE
121000  %     HOW STATIONARY THE DATA IS

122000  PROCEDURE PLOTSTATIONARITY(MSX,NA,JD,TRENDTYPE,SR);
123000  VALUE NA,SR,JD,TRENDTYPE;INTEGER NA,JD,SR,TRENDTYPE;
124000  ARRAY MSX[*,*];
125000  BEGIN
126000    ARRAY L1[0:2],L2[0:2],L3[0:3],L4[0:6],L5[0:3],L6[0:6],L7[0:7],CHAR[0:NA-
127000    1],X[0:JD/2]; INTEGER HT,I;
128000    ARRAY L8[0:3),L9[0:9],L10[0:9];
129000    %     LABELS FOR GRAPH
130000    REPLACE POINTER(L1) BY "TIME IN MINUTES";
131000    IF TRENDTYPE=0 THEN REPLACE POINTER(L2) BY "MEAN SQUARES"
132000    ELSE REPLACE POINTER(L2) BY "MEAN SQUARES *40";
133000    REPLACE POINTER(L3) BY "CHECK FOR STATIONARITY";
134000    REPLACE POINTER(L4) BY "AVERAGES CALCULATED OVER 2.2756 MINUTES";
135000    REPLACE POINTER(L5) BY "LONGITUDINAL DIRECTION";
136000    REPLACE POINTER(L6) BY "MEAN SQUARES FROM ALL ARRAYS ARE PLOTTED";
137000    REPLACE POINTER(L7) BY "DATA COLLECTED AT A SCANRATE OF",SR*15/16 FOR 5
138000    NUMERIC," HERTZ";
139000    AINIT(1400);ASPEED(4);AORIG(100,80);
140000    ABOX(0,0,8,12,150,50,2);
141000    ASCA(-40,-12,150,0,0,10,9,1,2);
142000    IF TRENDTYPE=0 THEN
143000    ASCA(-55,-5,0,50,0,10,13,1,2);
144000    IF TRENDTYPE=0 THEN REPLACE POINTER(L8) BY "NO TREND REMOVAL";
145000    IF TRENDTYPE=1 THEN REPLACE POINTER(L8) BY "LINEAR TREND"
146000    " REMOVAL";
147000    IF TRENDTYPE=2 THEN REPLACE POINTER(L8) BY "PARABOLIC"
148000    " TREND REMOVAL";
149000    ALAB(500,-30,L1,15,1,2);
150000    ALAB(-40,440,L2,16,1,4);
151000    ALAB(100,950,L3,22,1,2);
152000    ALAB(100,930,L4,39,1,2);
153000    ALAB(100,910,L5,22,1,2);
154000    ALAB(100,890,L6,40,1,2);
155000    ALAB(100,870,L7,42,1,2);
156000    ALAB(100,850,L8,23,1,2);
157000    %     DIFFERENT SCALES DEPENDING ON THE TYPE OF DATA I.E.
158000    %     HAS IT HAD ANY TRENDS REMOVED,IN WHICH CASE THE
159000    %     MEANS SQUARES ARE ALL QUITE SMALL
160000    %     ARE THE ANEMOMETER ARRAYS AT THE SAME HEIGHT, IN
161000    %     WHICH CASE THE MEANS SQUARES WOULD ALL BE ABOUT THE SAME
162000    %     SIZE
163000    IF TRENDTYPE NEQ 0 THEN BEGIN
164000      REPLACE POINTER(L9) BY "SCALE 1 UNIT PER INCH Y DIRN, HALF"
165000      " INCH BETWEEN LINES";
166000      REPLACE POINTER(L10) BY "Y ZERO IE X AXIS IS PLUS HALF A UNIT";
167000      ALAB(100,830,L9,56,1,2);ALAB(100,810,L10,36,1,2);
168000    END;
169000    IF SAMEHEIGHTS AND TRENDTYPE=0 THEN BEGIN
170000      REPLACE POINTER(L9) BY "SCALE 40 UNITS PER INCH Y DIRN, HALF"
171000      " INCH BETWEEN LINES";
172000      REPLACE POINTER(L10) BY "Y ZERO IE X AXIS = 20 M/S**2 FOR FIRST"
173000      " LINE, 0 FOR NEXT ETC";
174000      ALAB(100,830,L9,56,1,2);ALAB(100,810,L10,60,1,2);END;
```

```
175000      IF SAMEHEIGHTS AND TRENDTYPE=0 THEN BEGIN
176000        FOR HT:=0 STEP 1 UNTIL NA-1 DO
177000        BEGIN IF ONEARRAY THEN HT:=ARRAYNO-1;
178000          ALINEX(17,34,MSX[HT,*],JD,20-20*HT,40);
179000          IF ONEARRAY THEN HT:=NA-1;END;
180000      END ELSE
181000      FOR HT:=0 STEP 1 UNTIL NA-1 DO
182000      BEGIN IF ONEARRAY THEN HT:=ARRAYNO-1;
183000        IF TRENDTYPE=0 THEN
184000        ALINEX(17,34,MSX[HT,*],JD,0,20) ELSE ALINEX(17,34,MSX[HT,*],JD,
185000        +.5-.5*HT,1);
186000        IF ONEARRAY THEN HT:=NA-1; END;
187000      AEND;
188000      %
189000    END   E N D   O F   P R O C E D U R E   P L O T S T A T I O N A R I T Y
190000    ;
191000    %
192000    %     **********     MAINLINE     **********
193000    %
194000    %     DECLARE FILES,ARRAYS,INTEGERS,REALS,LABELS
195000    REAL TIME1,TIME2;
196000    REAL TIME3;
197000    FILE KR(KIND=READER),LP(KIND=PRINTER),INFYLE(KIND=DISK,FILETYPE=7,
198000    UNITS=WORDS);
199000    FILE FILE6(KIND=PRINTER);
200000    INTEGER N,NA,SR,NCL,T,S,P,R,N1,HT,I,J,        IA,TRENDTYPE;
201000    ARRAY ISM,ILA[0:2];
202000    REAL CNVRTORPS,ARG,SI,CO,VEL,MSY,MSZ,Q,AVU,AVV,AVW;
203000    ARRAY CUM[0:2];
204000    INTEGER PROGSTARTSR,AA,BB,CC,NIT;
205000    BOOLEAN FIRSTTIME,TREMOVAL;
206000    INTEGER TRENDTYPE;
207000    ARRAY TYPLAB[0:10];
208000    %
209000    TRENDTYPE:=0;
210000    %     READ CONTROL PARAMETERS
211000    WRITE(FILE6,<"INPUT NPTS,NARRAYS,SCANRATE,NCLASSES,TREMOVAL">);
212000    READ(KR,/,N,NA,SR,NCL,TREMOVAL); % N NO OF SAMPLES,NA NO OF ARRA
213000    % SCANRATE(INTEGER),NCL NO OF CLASSES IN PROB DIST GRAPH
214000    %TREMOVAL, TRUE(=1) FOR TREND REMOVALS, ELSE FALSE (=0) ;
215000    WRITE(LP,*/,N,NA,SR,NCL,TREMOVAL);
216000    WRITE(FILE6,*/,N,NA,SR,NCL,TREMOVAL);
217000    N:=(N DIV 256)*256;WRITE(LP,<"N MULTIPLE OF 256=",I6>,N);
218000    WRITE(FILE6,<"INPUT PROGSTARTSR- 2,4,8 ETC BUT <=SR">);
219000    READ(KR,*/,PROGSTARTSR);
220000    WRITE(LP,*/,PROGSTARTSR); WRITE(FILE6,*/,PROGSTARTSR);
221000    WRITE(FILE6,<"INPUT SAMEHEIGHTS T OR F">);
222000    READ(KR,/,SAMEHEIGHTS);WRITE(LP,*/,SAMEHEIGHTS);
223000    AA:=SR/PROGSTARTSR;
224000    IF AA>1 THEN BEGIN
225000      %     THIS BLOCK IS ENTERED WHEN THE ACTUAL SCAN RATE OF THE DATA IS
226000      %     TO BE REDUCED BEFORE MAIN ANALYSIS IS STARTED
227000      SR:=PROGSTARTSR;N:=(N DIV (256*AA))*256;
228000      IF N<256*AA-1 THEN NIT:=256*AA-1 ELSE BEGIN NIT:=N-1;
229000        WRITE(FILE6,<"THE NEW SR IS=",I5,/"THE NEW NO OF POINTS FOR ACTUAL"
230000        " PROCESSING =",I6,/,"THE LENGTH "
231000        "OF IN[  ] ARRAY (NIT)=",I6>,PROGSTARTSR,N,NIT);
232000      END OF IF N BLOCK;
233000    END ELSE
234000    BEGIN
235000      WRITE(FILE6,<"REDUCING SR PART OF PROGRAME WILL NOT BE USED"/
236000      "AS SR/PROGSTARTSR IS NOT > 1">);
237000      NIT:=N;
238000    END;
239000    WRITE(FILE6,<"INPUT ONEARRAY (BOOLEAN) & THE HEIGHT NO">);
240000    READ(KR,/,ONEARRAY,IF ONEARRAY THEN ARRAYNO);
241000    WRITE(FILE6,*/,ONEARRAY,ARRAYNO);WRITE(LP,*/,ONEARRAY,ARRAYNO);
242000    T:=SR*15/2;% NO OF DATA TO MAKE 8 SECONDS
243000    S:=N DIV T; % NO OF BLOCKS OF 8 SECONDS
244000    P:=128*SR; % NO OF DATA TO MAKE 2.2756 MINUTES
245000    R:=N DIV P; % NO OF BLOCKS OF 2.2756 MINUTES
246000    N1:=N-1;
247000    BEGIN
248000      ARRAY LA,SM[0:2],SDV[0:NA*3-1],VM[0:NA*3-1],STDDEV[0:2],
249000      MSTOT[0:NA-1],T1,T2[0:2],MDPT,FREQ[0:NA-1,0:2,0:NCL+1],
250000      IN[0:2,0:NIT],V[0:NA,0:S],MSX[0:NA-1,0:R],CORFCTR[1:NA*3],
251000      AV[0:2];
252000      LABEL START,ENOF,L1,LOOPOUT;
253000      ARRAY SV,ST2,STV,ST3,ST4,ST2V,A0,A1,B0,B1,B2,C1,C2,C3,C4[0:NA*3+2]
254000      ;
255000      REAL ST;INTEGER A;
256000      INTEGER INT1,INT2,INT3,AA1,NA3,NA1;
257000      LABEL HOP;
258000      TIME3:=*-TIME(12);
259000      %
260000      IF AA>1 THEN BEGIN
261000        %     REDUCE SCAN RATE BY ADDING CONSECUTIVE SAMPLES TOGETHER
262000        %     FROM EACH CHANNEL
263000        AA1:=AA-1;NA3:=3*NA;NA1:=NA-1;
264000        FOR BB:=0 STEP 1 UNTIL N/256-1 DO BEGIN INT3:=BB*3*NA;INT1:=INT3*
265000          AA;
266000          FOR HT:=0 STEP 1 UNTIL NA1 DO BEGIN INT2:=3*HT;
267000            IF ONEARRAY THEN BEGIN HT:=ARRAYNO-1;INT2:=3*HT;END;
268000            FOR J:=0,1,2 DO
269000            BEGIN
```

```
270000            FOR I:=0 STEP 1 UNTIL AA1 DO
271000            READ(INFYLE[J+INT2+I*NA3+INT1),256,IN[J,I*256]);
272000            FOR I:=1 STEP 1 UNTIL AA1 DO
273000            IN[J,0]:=*+IN[J,I];
274000            FOR I:=1 STEP 1 UNTIL 255 DO BEGIN IN[J,I]:=0;
275000              FOR CC:=0 STEP 1 UNTIL AA1 DO
276000              IN[J,I]:=*+IN[J,I*AA+CC];
277000            END;
278000            WRITE(INFYLE[J+INT2+INT3],256,IN[J,0]);
279000          END;
280000          IF ONEARRAY THEN HT:=NA1;
281000        END;
282000      END;
283000    END OF IF AA GTR 1 BLOCK;
284000    TIME3:=*+TIME(12);WRITE(LP,*/,TIME3*2.4@-6);
285000    CNVRTORPS:=SR/32;
286000    HT:=0;
287000    REPLACE POINTER(CORFCTR[1]) BY .2744 FOR NA*3 WORDS;
288000    FIRSTTIME:=TRUE;
289000    REPLACE POINTER(TYPLAB) BY "IF BIRO WORKING OK THEN USE IT ELSE"
290000    " WET INK .2MM NIB PLEASE";
291000    AINIT(1);ATYPE(TYPLAB,55);AEND;
292000    START:% PROGRAMME LOOPS BACK TO HERE FOR NEXT TRIPLET
293000    IF ONEARRAY THEN HT:=ARRAYNO-1;
294000    FOR J:=0,1,2 DO AV[J]:=0;
295000    MSTOT[HT]:=0;
296000    %
297000    % READ IN DATA. INITIALISE VARIABLES
298000    %     ONE TRIPLET (ORTHOGONAL ARRAY) IS PROCESSED AT A TIME
299000    FOR I:=0 STEP 1 UNTIL N/256 -1 DO
300000    FOR J:=0,1,2 DO
301000    BEGIN
302000      READ(INFYLE[I*3*NA+J+3*HT],256,IN[J,I*256])[ENOF];
303000      DO VECTORMODE(IN[J,I*256],PX=AV[J],CORFCTR[HT*3+J+1],FOR
304000      256) BEGIN IN:=IN*CORFCTR*CNVRTORPS;PX:=*+IN;
305000        INCREMENT IN; END;
306000    END OF I AND J LOOPS;
307000    GO TO L1;
308000    ENOF:
309000    WRITE(LP,<"END OF FILE ON READ STATEMENT",/,"HT=",I4,X2,
310000    "I=",I4,X2,"J=",I4>,HT,I,J);
311000    CLOSE(INFYLE,*);
312000    GO TO LOOPOUT;
313000    L1:
314000    % CALCULATE AVERAGE ANGLE OF ATTACK,SIN,COS,SUMMATIONS
315000    ARG:=ARCTAN2(AV[1],AV[0]);SI:=SIN(ARG);CO:=COS(ARG);
316000    FOR I:=0,1,2 DO AV[I]:=*/N;
317000    VEL:=AV[0]*CO+AV[1]*SI;
318000    IF HT=0 THEN BEGIN
319000      IF TRENDTYPE=0 THEN WRITE(LP,</40("*"),"     RESULTS WITH NO TREND"
320000      " REMOVAL     ",40("*")/>);
321000      IF TRENDTYPE=1 THEN WRITE(LP,</40("*"),"   RESULTS WITH LINEAR TRE"
322000      "ND REMOVAL   ",40("*")/>);
323000      IF TRENDTYPE=2 THEN WRITE(LP,</40("*"),"   RESULTS WITH PARABOLIC"
324000      " TREND REMOVAL   ",40("*")/>);
325000    END;
326000    WRITE(LP,</50("*"),"  ARRAY NO ",I3,X2,50("*")/>,HT+1);
327000    WRITE(LP,<"AVERAGE LONGITUDINAL VELOCITY,ARRAY NO",I4,X2,
328000    "IS",F10.5,X2,"METRES PER SECOND",/,"AT AN ANGLE OF",F10.5,
329000    X2,"DEGREES FROM THE U ANEMOMETER">,HT+1,VEL,ARG*
330000    180/3.14159);
331000    % RESOLVE INTO LONGITUDINAL AND LATERAL COMPONENTS
332000    % INITIALISE VARIABLES TO ZERO
333000    TIME1:=*+TIME(12);TIME2:=*-TIME(12);
334000    MSY:=MSZ:=AVU:=AVV:=AVW:=0;
335000    REPLACE POINTER(V[HT,0]) BY 0 FOR S WORDS;
336000    FOR I:=0 STEP 1 UNTIL R DO MSX[HT,I]:=0;
337000    FOR J:=0,1,2 DO BEGIN LA[J]:=-1000;SM[J]:=1000;END;
338000    INT1:=HT*3;INT2:=INT1+1;INT3:=INT2+1;
339000    FOR I:=0 STEP 1 UNTIL N1 DO
340000    BEGIN
341000      %     THIS BLOCK CALCULATES SUMMATIONS,REMOVES TRENDS,FINDS
342000      %     MAXIMUMS AND MINIMUMS FROM EACH CHANNEL
343000      Q:=IN[0,I];
344000      IF TRENDTYPE=0 THEN BEGIN
345000        AVU:=*+(IN[0,I]:=**CO+IN[1,I]*SI) ;
346000        AVW:=*+IN[2,I];
347000        AVV:=*+(IN[1,I]:=**CO*(-1)+Q*SI); END;
348000      IF TRENDTYPE=1 THEN BEGIN
349000        AVU:=*+(IN[0,I]:=**CO+IN[1,I]*SI-A0[INT1]-A1[INT1]*I);
350000        AVW:=*+(IN[2,I]:=*-A0[INT3]-A1[INT3]*I);
351000        AVV:=*+(IN[1,I]:=**CO*(-1)+Q*SI-A0[INT2]-A1[INT2]*I);
352000      END;
353000      IF TRENDTYPE=2 THEN BEGIN
354000        AVU:=*+(IN[0,I]:=**CO+IN[1,I]*SI-B0[INT1]-B1[INT1]*I
355000        -B2[INT1]*I**2);
356000        AVW:=*+(IN[2,I]:=*-B0[INT3]-B1[INT3]*I-B2[INT3]*I**2);
357000        AVV:=*+(IN[1,I]:=**CO*(-1)+Q*SI-B0[INT2]-B1[INT2]*I
358000        -B2[INT2]*I**2);  END;
359000      V[HT,I DIV T]:=*+IN[0,I];
360000      MSX[HT,I DIV P]:=*+ IN[0,I]*IN[0,I];
361000      MSY:=*+IN[1,I]*IN[1,I];
362000      MSZ:=*+IN[2,I]*IN[2,I];
363000      FOR J:=0,1,2 DO BEGIN
364000        IF IN[J,I]<SM[J] THEN BEGIN SM[J]:=IN[J,I];ISM[J]:=I;
```

```
365000          END ELSE
366000          IF IN[J,I]>LA[J] THEN BEGIN LA[J]:=IN[J,I];ILA[J]:=I;
367000          END;
368000        END OF J LOOP;
369000      END OF RESOLVE AV LONG RMS LARGEST AND SMALLEST LOOP;
370000      TIME2:=*+TIME(12);
371000      IF (HT+1)=NA THEN WRITE(LP,*/,TIME2*2.40-6);
372000      %
373000      % IF TREND REMOVAL BEING USED CALCULATE PARAMETERS AND WRITE OUT
374000      %
375000      IF TRENDTYPE=0 AND TREMOVAL THEN BEGIN
376000        SV[HT*3]:=AVU;  SV[HT*3+1]:=AVV; ST:=N1*N/2;SV[3*HT+2]:=AVW;
377000        FOR J:=0,1,2 DO BEGIN A:=HT*3+J;FOR I:=0 STEP 1 UNTIL N1 DO BEGIN
378000            ST2[A]:=*+I*I; STV[A]:=*+I*IN[J,I];
379000            ST3[A]:=*+I**3; ST4[A]:=*+I**4;
380000            ST2V[A]:=*+I*I*IN[J,I];
381000        END;% E N D   O F  I  L O O P ;
382000        END;%E N D   O F  J   L O O P ;
383000        FOR J:=0,1,2 DO BEGIN A:=HT*3+J;
384000          A0[A]:=(STV[A]*ST-ST2[A]*SV[A])/(ST*ST-N*ST2[A]);
385000          A1[A]:=(SV[A]/N-STV[A]/ST)/(ST/N-ST2[A]/ST);
386000          C1[A]:=(SV[A]*ST3[A]-STV[A]*ST2[A])/(ST*ST3[A]-ST2[A]**2);
387000          C2[A]:=(STV[A]*ST4[A]-ST2V[A]*ST3[A])/(ST2[A]*ST4[A]-ST3[A]**2);
388000          C3[A]:=(N*ST3[A]-ST*ST2[A])/(ST*ST3[A]-ST2[A]**2);
389000          C4[A]:=(ST*ST4[A]-ST2[A]*ST3[A])/(ST2[A]*ST4[A]-ST3[A]**2);
390000          B0[A]:=(C1[A]-C2[A])/(C3[A]-C4[A]);
391000          B1[A]:=C1[A]-B0[A]*C3[A];
392000          B2[A]:=(SV[A]-B1[A]*ST-B0[A]*N)/ST2[A];
393000        END; %  E N D  O F  J  L O O P ;
394000        %
395000        %  WRITE OUT
396000        %
397000        WRITE(FILE6,</"ARRAY NO",I4,"RESULTS FOR TREND REMOVAL PARAMETERS">
398000        ,HT+1);
399000        WRITE(FILE6,<"LONGITUDINAL DIRECTION">);
400000        A:=3*HT;
401000        WRITE(FILE6,<"LONG AV AS CALCULATED=",F10.4>,AVU/N);
402000        WRITE(FILE6 ,*/,A0[A],A1[A],B0[A],B1[A],B2[A]);
403000        WRITE(FILE6,*/,A0[A]+A1[A]*N1,B0[A]+B1[A]*N1+B2[A]*N1**2,
404000        -B1[A]/(2*B2[A]),B0[A]-B1[A]**2/(4*B2[A]));
405000        WRITE(FILE6,<"WHICH IN LONG DIRN GIVES AN AVERAGE OF",/,
406000        "E OF A0+A1*N/2=",F12.6>,A0[A]+A1[A]*N/2);
407000        WRITE(FILE6,<"LATERAL DIRECTION">);
408000        WRITE(FILE6,<"LAT AV AS CALCULATED=",F10.4>,AVV/N);
409000        A:=*+1; WRITE(FILE6,*/,A0[A],A1[A],B0[A],B1[A],B2[A]);
410000        WRITE(FILE6,<"WHICH GIVES AVERAGE IN LAT DIRN OF="
411000        ,F12.6>,A0[A]+A1[A]*N/2);
412000        WRITE(FILE6,*/,A0[A]+A1[A]*N1,B0[A]+B1[A]*N1+B2[A]*N1**2,
413000        -B1[A]/(2*B2[A]),B0[A]-B1[A]**2/(4*B2[A]));
414000        WRITE(FILE6,<"VERTICAL DIRN"/"VERT AVRG AVW/N=",F13.6>,AVW/N);
415000        A:=*+1; WRITE(FILE6,*/,A0[A],A1[A],B0[A],B1[A],B2[A]);
416000        WRITE(FILE6,<"WHICH GIVES AV IN VER DIRN A0+A1*N/2 OF="
417000        ,F12.6>,A0[A]+A1[A]*N/2);
418000        WRITE(FILE6,*/,A0[A]+A1[A]*N1,B0[A]+B1[A]*N1+B2[A]*N1**2,
419000        -B1[A]/(2*B2[A]),B0[A]-B1[A]**2/(4*B2[A]));
420000        %
421000        %
422000      END; %END OF TREND REMOVAL CALCULATIONS
423000      %     CONVERT TO M/S ETC WRITE OUT RESULTS
424000      FOR I:=0 STEP 1 UNTIL N1 DIV T DO
425000      V[HT,I]:=*/T;
426000      AVU:=*/N;AVV:=*/N;AVW:=*/N;
427000      VM[HT*3]:=AVU;VM[HT*3+1]:=AVV;VM[HT*3+2]:=AVW;
428000      FOR I:=0 STEP 1 UNTIL N1 DIV P DO
429000      MSTOT[HT]:=*+(MSX[HT,I]:=*/P)/R;
430000      MSY:=*/N;MSZ:=*/N;
431000      STDDEV[0]:=SQRT(ABS(MSTOT[HT]-AVU**2));
432000      STDDEV[1]:=SQRT(ABS(MSY-AVV**2));
433000      STDDEV[2]:=SQRT(ABS(MSZ-AVW**2));
434000      FOR J:=0,1,2 DO SDV[HT*3+J]:=STDDEV[J];
435000      WRITE(LP,<"AV IN LONG DIRN=",F12.5," M/S">,AVU);
436000      WRITE(LP,<"AV IN LAT DIRN=",F10.2,X2,"AV IN VER DIRN=",F10.2,"METRES"
437000      " PER SECOND">,AVV,AVW);
438000      WRITE(LP,<"MEAN SQUARE IN X DIRN=",F12.4,X2,"MEAN SQUARE IN Y DIRN=",
439000      F12.4,X2,"MEAN SQUARE IN Z DIRN=",F12.4>,MSTOT[HT],
440000      MSY,MSZ);
441000      WRITE(LP,<"VARIANCE IN X DIRN=",F12.4,X2,"STANDARD DEVIATION IN",
442000      " X DIRN=",F12.4>,MSTOT[HT]-AVU**2,SQRT(ABS(MSTOT[HT]-AVU**2)));
443000      FOR J:=0,1,2 DO
444000      WRITE(LP,<"CHANNEL",I3,X2,"LARGEST VALUE",F12.4,X2,"AT SCAN NO"
445000      ,I7,X2,"SMALLEST VALUE",F12.4,X2,"AT SCAN",I7>,HT*3+J+1,
446000      LA[J],ILA[J],SM[J],ISM[J]);
447000      WRITE(LP,</,"MEAN SQUARE VALUES IN LONGITUDINAL DIRECTION AS",
448000      " CALCULATED EVERY 2.2756 MINUTES AT ARRAY NUMBER",I4,/,(10F13.4)>,
449000      HT+1,FOR I:=0 STEP 1 UNTIL N1 DIV P DO MSX[HT,I]);
450000      WRITE(LP,</"MEDIAN MEAN SQUARE VALUE=",F13.4>,IF((N1 DIV P)
451000      +1) MOD 2=0 THEN (MSX[HT,((N1 DIV P)-1)/2]+MSX[HT,((N1 DIV P)
452000      +1)/2])/2 ELSE MSX[HT,(N1 DIV P)/2]);
453000      % NOW CALCULATE THE CLASS MID POINTS FOR PROBABILITY DIST
454000      FOR J:=0,1,2 DO  BEGIN
455000        T1[J]:=SM[J]+(LA[J]-SM[J])/(2*NCL); T2[J]:=(LA[J]-SM[J])/NCL; END;
456000      % NOW THAT MID POINTS ARE KNOWN CALCULATE FREQUENCIES
457000      FOR J:=0,1,2 DO BEGIN CO:=SM[J];SI:=T2[J];
458000        REPLACE POINTER(FREQ[HT,J,0]) BY 0 FOR NCL+1 WORDS;
459000        %     COUNT THE DATA INTO THE RIGHT BINS.THIS IS DONE AFTER
```

```
460000        %     THE MAXIMUM AND MINIMUM VALUES HAVE BEEN FOUND
461000        FOR I:=0 STEP 1 UNTIL N1 DO
462000        BEGIN
463000          IA:=ENTIER((IN[J,I]-CO)/SI);
464000          FREQ[HT,J,IA]:=*+1;
465000        END 1;
466000        FREQ[HT,J,NCL-1]:=FREQ[HT,J,NCL-1]+FREQ[HT,J,NCL];
467000      END J;
468000      % OUTPUT FREQUENCY AND CUMULATIVE FREQUENCY FOR CHECKING
469000      FOR J:=0,1,2 DO CUM[J]:=0;
470000      WRITE(LP,<X6,3(X12,"CHANNEL",I3,X20)>,HT*3+1,HT*3+2,HT*3+3);
471000      WRITE(LP,<X6,3(X5,"MID",X3,"NUMBER",X3,"CUM",X4,"PROB",X4,"MDPT="
472000      "VM")>);
473000      WRITE(LP,<X6,3(X4,"VALUES",X1,"SAMPLES",X2,"FREQ",X2,"ABILITY",
474000      X2,"(SDEVS)")>);
475000      FOR I:=0 STEP 1 UNTIL NCL-1 DO
476000      BEGIN
477000        FOR J:=0,1,2 DO
478000        CUM[J]:=*+FREQ[HT,J,I]/N;
479000        WRITE(LP,<"BIN",I3,3(X3,F7.3,X1,I6,X1,F7.5,X1,F7.5,X1,F8.5)>,
480000        I,T1[0]+T2[0]*I,FREQ[HT,0,I],CUM[0],FREQ[HT,0,I]:=**STDDEV[0]
481000        /(N*T2[0]),MDPT[HT,0,I]:=(T1[0]+T2[0]*I-VM[HT*3])/STDDEV[0],
482000        T1[1]+T2[1]*I,FREQ[HT,1,I],CUM[1],FREQ[HT,1,I]:=**STDDEV[1]/
483000        (N*T2[1]),MDPT[HT,1,I]:=(T1[1] +T2[1]*I-VM[HT*3+1])/STDDEV[1],
484000        T1[2]+T2[2]*I,FREQ[HT,2,I],CUM[2],FREQ[HT,2,I]:=**STDDEV[2]/
485000        (N*T2[2]),MDPT[HT,2,I]:=(T1[2]+T2[2]*I-VM[HT*3+2])/STDDEV[2]);
486000      END OF I LOOP;%E N D  O F I   L O O P
487000      FOR J:=0,1,2 DO FOR I:=0 STEP 1 UNTIL NCL-1 DO
488000      IF MDPT[HT,J,I]>4 THEN MDPT[HT,J,I]:=4 ELSE
489000      IF MDPT[HT,J,I]<-4 THEN MDPT[HT,J,I]:=-4;
490000      % NOW EVERYTHING HAS BEEN CALCULATED FOR THAT PARTICULAR
491000      % HEIGHT
492000      WRITE(LP,*/,TIME(2)/60,TRENDTYPE,HT);
493000      IF ONEARRAY THEN GO TO HOP;
494000      HT:=*+1;
495000      IF HT<NA THEN GO TO START;
496000      HOP:
497000      % PLOT RESULTS. TEST FOR TREND REMOVAL AND THEN FINISH
498000      IF TRENDTYPE=0 THEN
499000      PLOTVELTIME(V[*,*],SR,NA,N1 DIV T);
500000      PLOTPROBDIST(FREQ[*,*,*],MDPT[*,*,*],SDV[*],VM[*],NA,NCL,
501000      SR,TRENDTYPE);
502000      PLOTSTATIONARITY(MSX[*,*],NA,N DIV P,TRENDTYPE,SR);
503000      % INCREMENT HEIGHT COUNTER AND LOOP BACK.REPEAT AND THEN FINISH
504000      IF TREMOVAL THEN BEGIN TRENDTYPE:=*+1;  HT:=0;
505000        IF TRENDTYPE>2 THEN GO TO LOOPOUT ELSE GO TO START; END;
506000      LOOPOUT:% LABEL FOR USE ON END OF FILE CONDITION ON INPUT
507000      % DATA
508000      REPLACE POINTER(TYPLAB) BY "END OF MECH021 PLOTS";
509000      AINIT(1);ATYPE(TYPLAB,20);AEND;
510000      WRITE(LP,*/,TIME1*2.40-6,TIME2*2.40-6);
511000      WRITE (LP,<"END OF PROGRAMME">);
512000    END;
513000  END.


INPUT STRING WAS
"VTPDMS STEP 2"
```

APPENDIX E

PROGRAM 'SEQVELTURBREY'

E.1 Determination of Wind Structure Parameter for Program SEQVELTURBREY

E.1.1 Introduction

Consider the co-ordinate system:

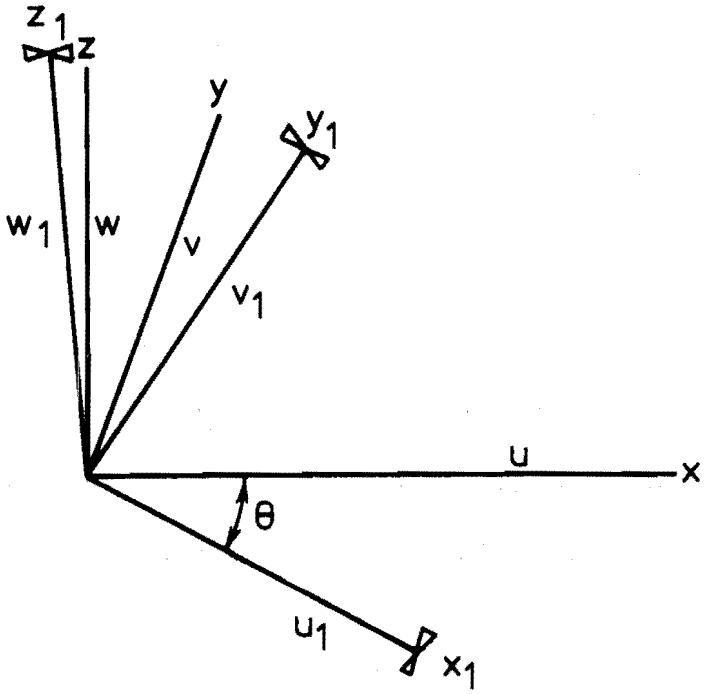

The anemometers lie along the axes x_1, y_1 and z_1. At each sample they measure the wind velocities u_1, v_1 and w_1 respectively.

The x,y and z co-ordinate system lies with its three axes along the average wind direction, perpendicular to it and vertically respectively. The wind velocities measured at each instant on these axes are u,v, and w respectively. θ is defined as the angle between wind vector for the averaging period chosen and the anemometer aligned along the x_1 axis.

In the anslysis which follows it is assumed that n discrete samples of the velocity components u_1,v_1 and w_1 have been measured. For ease of writing, subscripts denoting individual samples have not been used.

The analysis which follows is exactly similar for data which has and hasn't been corrected for non-cosine response. In the former case the data is corrected for non-cosine response by some kind of iterative procedure before any totals of the type described below are calculated.

The following equations are common to all of the turbulence parameter calculations.

(1) The letter $\sum$ is assumed to be the summation over n, i.e. $\sum_{1}^{n}$.

(2) The angle θ between the wind vector and the x_1 anemometer is defined as

$$\theta = \tan^{-1}\left[\frac{\sum v_1}{\sum u_1}\right]$$

for the averaging period chosen.

(3) For each sample, the longitudinal, lateral and vertical components are defined by the following equations :

$$u = u_1\cos\theta + v_1\sin\theta$$

$$v = v_1\cos\theta - u_1\sin\theta$$

$$w = w_1$$

(4) In the x, y, z co-ordinate system

$$\bar{u} = \frac{1}{n}\sum u \ ,$$

$$\bar{v} = 0 \ ,$$

$$\bar{w} = \frac{1}{n}\sum w$$

which may not be zero if the anemometer is not aligned exactly vertically.

(5) Similarly for the x_1, y_1, z_1 co-ordinate system

$$\bar{u}_1 = \frac{1}{n} \sum u_1 ,$$

$$\bar{v}_1 = \frac{1}{n} \sum v_1 ,$$

$$\bar{w}_1 = \frac{1}{n} \sum w_1$$

(6) In both co-ordinate systems the velocity fluctuations about their mean values are defined by

$$u_1' = u_1 - \bar{u}_1 \qquad u' = u - \bar{u}$$

$$v_1' = v_1 - \bar{v}_1 \quad \text{and} \quad v' = v - \bar{v} = v$$

$$w_1' = w_1 - \bar{w}_1 \qquad w' = w - \bar{w}$$

E.1.2 LONGITUDINAL VARIANCE σ_u^2 CALCULATION

$$\sigma_u^2 = \overline{u'u'} = \frac{1}{n} \sum u'u'$$

$$\sum u'u' = \sum (u - \bar{u})^2$$

$$= \sum (u_1 \cos\theta + v_1 \sin\theta - \bar{u}_1 \cos\theta - \bar{v}_1 \sin\theta)^2$$

$$\Rightarrow \sigma_u^2 = \frac{1}{n} \Big[\cos^2\theta \left\{ \sum u_1^2 - n \bar{u}_1^2 \right\}$$

$$+ \sin^2\theta \left\{ \sum v_1^2 - n \bar{v}_1^2 \right\}$$

$$+ 2 \sin\theta \cos\theta \left\{ \sum u_1 v_1 - n \bar{u}_1 v_1 \right\} \Big]$$

E.1.3 LATERAL VARIANCE σ_v^2 CALCULATION

$$\sigma_v^2 = \overline{v'v'} = \frac{1}{n} \sum v'v' = \frac{1}{n} \sum (v - \bar{v})^2$$

but $\bar{v} = 0$

$$\Rightarrow \quad \sigma_v^2 = \frac{1}{n} \sum (v_1 \cos\theta - u_1 \sin\theta)^2$$

$$= \frac{1}{n} \left[\cos^2\theta \sum v_1^2 + \sin^2\theta \sum u_1^2 \right.$$

$$\left. + 2 \sin\theta \cos\theta \sum v_1 u_1 \right]$$

E.1.4 VERTICAL VARIANCE σ_w^2 CALCULATION

$$\sigma_w^2 = \overline{w'w'} = \frac{1}{n}\sum (w-\bar{w})^2$$

$$= \frac{1}{n}\sum (w_1-\bar{w}_1)^2$$

$$= \frac{1}{n}\left[\sum w_1^2 - n\bar{w}_1^2\right]$$

E.1.5 REYNOLDS STRESS $\rho_{uw}(0)$ CALCULATION

$$\rho_{uw}(0) = \frac{\overline{u'w'}}{\sigma_u \sigma_w}$$

σ_u, σ_w calculated as above

$$\overline{u'w'} = \frac{1}{n}\sum u'w' = \frac{1}{n}\sum (u-\bar{u})(w-\bar{w})$$

$$= \frac{1}{n}\sum \left[\left\{(u_1-\bar{u}_1)\cos\theta + (v_1-\bar{v}_1)\sin\theta\right\}(w_1-\bar{w}_1)\right]$$

$$= \frac{1}{n}\left[\cos\theta\left(\sum u_1w_1 - n\bar{u}_1\bar{w}_1\right) + \sin\theta\left(\sum v_1w_1 - n\bar{v}_1\bar{w}_1\right)\right]$$

Following Hyson et al (1977) a correction allowing for vertical component anemometer misalignment has been added. This is

$$-\sigma_u^2\,(\bar{w}_1/\bar{u}),$$

which gives the following formula:

$$\overline{u'w'} = \frac{1}{n}\left[\cos\theta\left(\sum u_1w_1 - n\bar{u}_1\bar{w}_1\right) + \sin\theta\left(\sum v_1w_1 - n\bar{v}_1\bar{w}_1\right) - \sigma_u^2\,\bar{w}_1/(\bar{u}_1\cos\theta + \bar{v}_1\sin\theta)\right]$$

E.1.6 REYNOLDS STRESS $\rho_{uv}(0)$ CALCULATION

$$\rho_{uv}(0) = \frac{\overline{u'v'}}{\sigma_u \sigma_v}$$

$\sigma_u \sigma_v$ calculated as above.

$$\overline{u'v'} = \frac{1}{n} \sum u'v' = \frac{1}{n} \sum (u-\bar{u})(v-\bar{v}) \quad , \quad \text{but } \bar{v} = 0$$

$$= \frac{1}{n} \sum \left[\left\{ (u_1-\bar{u}_1)\cos\theta + (v_1-\bar{v}_1)\sin\theta \right\} (v_1\cos\theta - u_1\sin\theta) \right]$$

$$= \frac{1}{n} \left[(\cos^2\theta - \sin^2\theta)(\sum u_1 v_1 - n\bar{u}_1 \bar{v}_1) \right.$$

$$\left. + \cos\theta \sin\theta (\sum v_1^2 - \sum u_1^2 - n\bar{v}_1^2 + n\bar{u}_1^2) \right]$$

E.1.7 REYNOLDS STRESS $\rho_{vw}(0)$ CALCULATION

$$\rho_{vw}(0) = \frac{\overline{v'w'}}{\sigma_v \sigma_w}$$

σ_v, σ_w calculated as above.

$$\overline{v'w'} = \frac{1}{n} \sum v'w' = \frac{1}{n} \sum (v-\bar{v})(w-\bar{w}), \text{ but } \bar{v} = 0$$

$$= \frac{1}{n} \sum (v_1\cos\theta - u_1\sin\theta)(w_1-\bar{w}_1)$$

$$= \frac{1}{n} \left[\cos\theta (\sum v_1 w_1 - n\bar{v}_1 \bar{w}_1) \right.$$

$$\left. - \sin\theta (\sum u_1 w_1 - n\bar{u}_1 \bar{w}_1) \right]$$

E.1.8 CONCLUSION

From the above calculations, it is found that all the means, standard deviations, and Reynolds stresses can be calculated with the following summations :

$$\sum u_1 \, , \sum v_1 \, , \sum w_1 \, , \sum u_1 w_1 \, , \sum u_1 v_1 \, , \sum v_1 w_1 \, ,$$

$$\sum u_1^2 \, , \sum v_1^2 \, , \sum w_1^2 \, .$$

Consequently, in order to determine the turbulence parameters for a variety of file lengths, the above totals can be accumulated and individual samples from orthogonal anemometer arrays do not need to be resolved into components parallel and perpendicular to the average wind direction for each file length.

By adding to these totals, the turbulence parameters can thus be calculated for increasing file lengths as the data is read sequentially from the file.

E.2 Typical WFL for using this Program

E.2.1 All parameters printed and plotted every 4.551 minutes, for a variety of scan rates

Assume that the tape N789 contains a file called WINDY which has 65536 scans of velocity data from eight orthogonal arrays of anemometers. The scan rate of the data is 16 and all the mean velocities and angles, turbulence intensities, and Reynolds stresses are required to be calculated, printed and plotted every 4.551 minutes. It is also required that they be calculated for scan rates of 16, 8,4,2,1,.5,.25 Hz. It is assumed that the source file SEQVELTURBREY is stored on tape A999.

A JOB to do this is given below.

```
7
5  JOB INVESTIGATE SCAN RATE AND FILE LENGTH;
   DESTNAME=SITE; PROCESSTIME=1000; IOTIME= 800;
   USER MECH031/PASSWORD; CLASS=10; BEGIN
7
5  COPY SEQVELTURBREY FROM A999;
   COMPILE SRFILELNGTH ALGOL LIBRARY
   COMPILER FILE TAPE=SEQVELTURBREY;
   DATA
```

```
$  SET MERGE
$  RESET LIST
7
5  IF FILE SRFILELNGTH ISNT PRESENT THEN GO OVER;
   COPY WINDY FROM N789;
   RUN SRFILELNGTH; FILE DISKDATA=WINDY
   DATA K;
   24,16,65536,
   1,
   7,
   16,
   0, 0,
```

[Four cards containing the non-cosine response correction factors in 26I3 format, given in Appendix A]

[36 anemometer calibration factors in the order: triplet 1 - x_1, y_1, z_1, triplet 2 - x_1, y_1, z_1 ... up to triplet 12, and in free format

e.g. .2, .2, .4, /

.8, .275, /

etc.]

```
1 bbbbb2bbbbb3 .... etc.  up  to  9
                                        [b = one blank space]
A bbbbbBbbbbbC .... etc.  up  to  I
7
5  OVER
7
5  END JOB
```

E.2.2 Results printed after all the data has been processed

Using the same file WINDY given in E.2.1, it is desired that the results be printed only, not plotted, after all the 65536 scans of data have been processed. It is also desired that the processing be done only at one scan rate of 2. The alteration in the data cards from those

given in E.2.1 are given below. The WFL is the same as in E.2.1.

```
7
5  DATA K;

   24,16,65536,

   1,

   1,

   2,

   1, 1,
```

The rest of the data cards are the same as for E.2.1

E.3. Listing of Program SEQVELTURBREY

```
 SSS  EEEE   QQQ  V   V EEEE  L     TTTTT U   U RRRR  BBB   RRRR  EEEE  Y   Y
S   S E     Q   Q V   V E     L       T   U   U R   R B  B  R   R E      Y Y
S     E     Q   Q V   V E     L       T   U   U R   R B  B  R   R E       Y
 SSS  EEE   Q   Q  V V  EEE   L       T   U   U RRRR  BBBB  RRRR  EEE     Y
    S E     Q Q Q  V V  E     L       T   U   U R R   B   B R R   E       Y
S   S E     Q  QQ   V   E     L       T   U   U R  R  B   B R  R  E       Y
 SSS  EEEEE  QQQQ   V   EEEEE LLLLL   T    UUUU R   R BBBB  R   R EEEEE   Y
```

788 RECORDS, CREATED 22/11/78

```
    1000 $ SET $
    2000 $ BINDER RESET LIST
    3000 $ SET LINEINFO
    4000 $ SET AUTOBIND
    5000 $ BIND=FROM PLOTA/=
    6000 BEGIN
    7000   %
    8000   %  THE PLOTTING PROCEDURES ARE ALREADY COMPILED AND RESIDENT ON
    9000   %  THE COMPUTER DISK.
   10000   %  THEY ARE BOUND INTO THIS PROGRAMME AT COMPILATION AND HAVE BEEN
   11000   %  DECLARED AS EXTERNAL PROCEDURES.PLOT PROCEDURES USED IN THIS
   12000   %  PROGRAMME ARE:AINIT,ASPEED,AORIG,ABOX,ASCA,ASCALE,ALAB,ALINEC
   13000   %  ATYPE,AEND
   14000   $ INCLUDE "PLOTA/EXTLDECLS"
   15000   COMMENT
   16000   THIS PROGRAMME CALCULATES AVERAGE VELOCITIES AND DIRECTIONS,
   17000   TURBULENCE INTENSITIES IN THE THREE ORTHOGONAL DIRECTIONS,AND
   18000   THE UV,UW,VW REYNOLDS STRESSES.THE ABOVE ARE CALCULATED
   19000   BY READING DATA FROM EACH CHANNEL SEQUENTIALLY ALONG THE DATA
   20000   FILE.
   21000   THE PARAMETERS CAN BE CALCULATED AND PLOTTED WITH:
   22000   (1)DATA CORRECTED FOR THE NON-COSINE RESPONSE OF THE PROPELLORS
   23000   (2)DATA NOT CORRECTED FOR THE NON-COSINE RESPONSE OF THE PROPELLORS
   24000   (3)DIFFERENT SCAN RATES(SAMPLING FREQUENCIES).THIS IS
   25000   DONE BY ADDING CONSECUTIVE DATA FROM EACH ANEMOMETER
   26000   (4)ANY LENGTH OF DATA RECURDING CONSIDERED,PROVIDING THAT THE
   27000   LENGTH IS A MULTIPLE OF 4.5511 MINUTES AND IT IS LESS THAN
   28000   THE LENGTH OF THE DATA FILE.                                  ;
   29000   %
   30000   %      DECLARE FILES,BOOLEANS AND INTEGERS SO THAT CONTROL
   31000   %      PARAMETRES CAN BE READ IN
   32000   %
   33000   FILE FILE6(KIND=PRINTER);
   34000   FILE L(KIND=PRINTER);
   35000   FILE K(KIND=READER);
   36000   FILE DISKDATA(KIND=DISK,FILETYPE=7,UNITS=WORDS);
   37000   %
   38000   BOOLEAN LASTVALUEONLY,NOPLOTS;LABEL FINISHIT;
   39000   INTEGER NFL,AA,PSR;
   40000   INTEGER NOCH,SR,IKK;
   41000   INTEGER IFTEST;
   42000   %
   43000   %      READ IN CONTROL PARAMETERS
   44000   %
   45000   WRITE(FILE6,<"INPUT NOCH    SR     IKK">);
   46000   READ(K,/,NOCH,SR,IKK);
   47000   WRITE(FILE6,<"INPUT IFTEST (=1 MEANS ALL OUTPUT PRINTED)">);
   48000   READ(K,/,IFTEST);
   49000   WRITE(L,*/,NOCH,SR,IKK,IFTEST);
   50000   WRITE(FILE6,<"INPUT NO OF SCANRATES FOR DATA TO BE PROCESSED AT">);
   51000   READ(K,/,NFL);
   52000   WRITE(L,*/,NFL);
   53000   WRITE(FILE6,<"INPUT HIGHEST SR FOR ACTUAL PROCESSING (=<SR BUT"
   54000   " >=2)">);
   55000   READ(K,/,PSR);WRITE(L,*/,PSR);
   56000   WRITE(FILE6,<"INPUT LASTVALUEONLY T OR F, NOPLOTS T OR F">);
   57000   READ(K,/,LASTVALUEONLY,NOPLOTS);
   58000   WRITE(L,*/,LASTVALUEONLY,NOPLOTS);
   59000   IF IFTEST=1 THEN
   60000   WRITE(L,<"RESULTS WILL BE PRINTED OUT SEQUENTIALLY"//>)
   61000   ELSE
   62000   WRITE(L,<"RESULTS WILL NOT BE PRINTED OUT"//>);
   63000   BEGIN
   64000     %          DECLARE VARIABLES GLOBAL TO ALL THE PROCEDURES
   65000     INTEGER COUNTER;
   66000     ARRAY HNO[0:6];
   67000     INTEGER CTR;
   68000     INTEGER Q,Z,A,B,C,LZ,KZ,I,CHU,CHV,CHW;
   69000     ARRAY HORCOR[1:101];
   70000     ARRAY CUS,CVS,UUS,UVS,CUVS,CUWS,CVWS,UUVS,UUWS,
   71000     UVWS,CU2S ,CV2S,CW2S,UU2S,UV2S,UW2S,CWS,UWS[1:NOCH];
   72000     REAL CTHETA,CSIN,CCOS,UTHETA,USIN,UCOS,CUAV,CVAV,
   73000     UUAV,UVAV,CMEAN,UMEAN,CUTHETA,CUSIN,CUCOS,CUMEAN,
   74000     CWAV,UWAV;
   75000
   76000     ARRAY CCD,UCCD[1:NOCH,0:255];
   77000     INTEGER ARRAY ISAVE[1:NOCH];
   78000     ARRAY CU,CV,UU,UV,CUV,CUW,UUV,UUW,CU2,CV2,CW2,
   79000     CVW,UVW,UW2,
   80000     UU2,UV2,CW,UW[1:NOCH];
   81000     BOOLEAN COMPACTVELANG;
   82000     ALPHA ARRAY COMPACTLBL[0:9];
```

```
ALPHA ARRAY TYPELBL[0:9];
ARRAY PCMEAN,PUMEAN,PCTHETA,PUTHETA[0:NOCH/3-1,0:NFL-1,0:IKK/(SR*256)-1]
;
%     WHEN COMPACTVELANG IS TRUE,THE NUMBER OF VELOCITY,ANGLE
%     VERSUS LENGTH OF RECORDING,GRAPHS IS REDUCED TO ONE.
%     THIS IS POSSIBLE BECAUSE THE AVERAGE VELOCITY IS NOT
%     AFFECTED BY ANY REDUCTION IN THE SCAN RATE
COMPACTVELANG:=TRUE;
%     SET UP SOME LABELS FOR SUBSEQUENT PLOTS
FILL COMPACTLBL[*] WITH "UNCORRECTED RESULT ON LEFT, COSINE CORRECTED ON
RIGHT";
FILL TYPELBL[*] WITH "PLEASE USE WET INK "
" .2 MM NIB          ";
%
BEGIN
  %     PROCEDURE AFTER HORST(1973)CONVERTED TO ALGOL AND
  %     MODIFIED SLIGHTLY.IT CORRECTS FOR THE NON-COSINE RESPONSE OF
  %     THE PROPELLOR ANEMOMETERS.

  PROCEDURE HORSTCORRECTION(C,TEST);
  VALUE C,TEST;INTEGER C,TEST;
  BEGIN
    INTEGER NN,I,J,K,II,JJ,KK,IA;
    LABEL L1,L2,L3,L4,L5,L6,L7,L8;
    REAL GU,GV,GW,U,V,W,S;
    I:=ISAVE[CHU:=C*3-2];J:=ISAVE[CHV:=CHU+1];K:=ISAVE[CHW:=CHV+1];
    FOR IA:=0 STEP 1 UNTIL TEST DO
    BEGIN
      % INITIALISE DIRECTION COSINES
      NN:=0;
      % NN KEEPS TRACK OF THE NUMBER OF ITERATIONS
      % CORRECT DATA FOR NON-COSINE RESPONSE
      % USE CURRENT DIRECTION COSINES
      GU:=UCCD[CHU,IA];
      GV:=UCCD[CHV,IA];
      GW:=UCCD[CHW,IA];
      L1:
      U:=GU*HORCOR[I];
      V:=GV*HORCOR[J];
      W:=GW*HORCOR[K];
      % CONVERT THESE MORE CORRECT VALUES TO SUBSCRIPTS
      % TO FIND BETTER CORRECTION FACTORS
      S:=SQRT(U*U+V*V+W*W)+.01;
      II:=U*50/S+51;
      JJ:=V*50/S+51;
      KK:=W*50/S+51;
      % COMPARE NEW COSINES WITH OLD ONES
      % ITERATE IF TOO DIFFERENT
      IF(ABS(II-I)-1) GTR 0 THEN GO TO L4;
      IF(ABS(JJ-J)-1) GTR 0 THEN GO TO L4;
      IF(ABS(KK-K)-1) LEQ 0 THEN GO TO L7;
      % CHECK NUMBER OF ITERATIONS
      % STOP IF TOO LARGE
      L4:
      IF (NN:=*+1) GEQ 6 THEN GO TO L2;
      % REITERATION WITH NEW DIRECTION COSINES
      L6:I:=II; J:=JJ;K:=KK;
      GO TO L1;
      L2:IF (CTR:=*+1) < 50 THEN
      %     WRITES OUT VARIABLES IF 6 ITERATIONS USED,USED TO CHECK THAT THE
      %     PROCEDURE CONVERGES QUICKLY
      WRITE(L,<"6 ITS IN HORST I=",I3," J=",I3," K=",I3," II=",I3," JJ=",I3,
      " KK=",I3," C=",I3," IA=",I3," GU=",F9.4," GV=",F9.4," GW=",F10.6,
      " A=",I2," Z=",I4>,I,J,K,II,JJ,KK,C,IA,GU,GV,GW,A,Z);
      W:=GW*HORCOR[(K+KK) DIV 2];
      % REPLACE RAW DATA WITH CORRECTED DATA
      L7:
      %     COUNTS UP THE NUMBER OF TIMES 0,1,2,3,4,5,6 ITERATIONS OCCUR
      HNO[NN]:=*+1;
      CCD[CHU,IA]:=U;CCD[CHV,IA]:=V;CCD[CHW,IA]:=W;
      % SAVE CURRENT COSINES TO INITIALISE
      % CORRECTION OF NEXT DATA SAMPLE
    END OF IA LOOP;
    ISAVE[CHU]:=I;ISAVE[CHV]:=J;ISAVE[CHW]:=K;

  END OF PROCEDURE HORSTCORRECTION;
  %
  %
  %     THIS PROCEDURE READS THE DATA OFF A DISK FILE AT ITS EXISTING
  %     SCAN RATE.IT ADDS CONSECUTIVE SAMPLES TOGETHER IN EACH CHANNEL TO
  %     REDUCE THE SCAN RATE,AND THEN WRITES THE DATA AT THE REDUCED
  %     SCAN RATE BACK TO THE DISK FILE.
  %     IT IS USED TO REDUCE COMPUTING TIME BY REDUCING THE AMOUNT
  %     OF DATA TO BE PROCESSED.

  PROCEDURE REDUCEDATA;
  BEGIN
    INTEGER AA1,INT3,INT1,BB,CC;
    ARRAY ARY[1:NOCH,0:AA*256-1];
    AA1:=AA-1;
    %     EACH RECORD IS 256 WORDS LONG.
    FOR BB:=0 STEP 1 UNTIL IKK/256-1 DO BEGIN
      INT3:=BB*NOCH;INT1:=INT3*AA;
      FOR B:=1 STEP 1 UNTIL NOCH DO
      BEGIN
```

```
175000            FOR I:=0 STEP 1 UNTIL AA1 DO
176000            READ(DISKDATA[B-1+I*NOCH+INT1],256,ARY[B,I*256]);
177000            FOR I:=1 STEP 1 UNTIL AA1 DO ARY[B,0]:=*+ARY[B,I];
178000            FOR I:=1 STEP 1 UNTIL 255 DO BEGIN
179000              ARY[B,I]:=0;
180000              FOR CC:=0 STEP 1 UNTIL AA1 DO
181000              ARY[B,I]:=*+ARY[B,I*AA+CC];
182000            END;
183000            WRITE(DISKDATA[B-1+INT3],256,ARY[B,0]);
184000          END;
185000        END;
186000        %     POSITION READ/WRITE POINTER BACK TO THE FIRST RECORD OF THE FILE
187000        REWIND(DISKDATA);

188000      END OF PROCEDURE R E D U C E D A T A ;
189000      %
190000      %
191000      %     THIS PROCEDURE CALCULATES SUMMATIONS AND PRODUCTS FROM 256
192000      %     DATA SAMPLES IN EACH CHANNEL.THESE NEW SUMMATIONS ARE THEN
193000      %     ADDED TO EXISTING VALUES OF OTHER PARAMETERS SO THAT THE
194000      %     TURBULENCE PARAMETERS FOR A LONGER DATA FILE MAY BE CALCULATED.

195000      PROCEDURE SUM(C);
196000      VALUE C;INTEGER C;
197000      BEGIN
198000        DO VECTORMODE (CCD[CHW,*],P=CW[C],FOR 256) BEGIN P:=*+CCD;INCREMENT CCD;
199000        END;
200000        DO VECTORMODE (CCD[CHU,*],P=CU[C],FOR 256) BEGIN P:=*+CCD;INCREMENT CCD;
201000        END;
202000        DO VECTORMODE (CCD[CHV,*],P=CV[C],FOR 256) BEGIN P:=*+CCD;INCREMENT CCD;
203000        END;
204000        DO VECTORMODE (UCCD[CHU,*],P=UU[C],FOR 256) BEGIN P:=*+UCCD;
205000          INCREMENT UCCD; END;
206000        DO VECTORMODE (UCCD[CHV,*],P=UV[C],FOR 256) BEGIN P:=*+UCCD;
207000          INCREMENT UCCD; END;
208000        DO VECTORMODE (UCCD[CHW,*],P=UW[C],FOR 256) BEGIN P:=*+UCCD;
209000          INCREMENT UCCD; END;
210000        DO VECTORMODE (CCD[CHU,*],P=CU2[C],FOR 256) BEGIN P:=*+CCD*CCD;
211000          INCREMENT CCD; END;
212000        DO VECTORMODE (CCD[CHV,*),P=CV2[C],FOR 256) BEGIN P:=*+CCD*CCD;
213000          INCREMENT CCD; END;
214000        DO VECTORMODE (CCD[CHW,*],P=CW2[C],FOR 256) BEGIN P:=*+CCD*CCD;
215000          INCREMENT CCD; END;
216000        DO VECTORMODE (UCCD[CHU,*],P=UU2[C],FOR 256) BEGIN P:=*+UCCD*UCCD;
217000          INCREMENT UCCD; END;
218000        DO VECTORMODE (UCCD[CHV,*],P=UV2[C],FOR 256) BEGIN P:=*+UCCD*UCCD;
219000          INCREMENT UCCD; END;
220000        DO VECTORMODE (UCCD[CHW,*],P=UW2[C],FOR 256) BEGIN P:=*+UCCD*UCCD;
221000          INCREMENT UCCD; END;
222000        DO VECTORMODE (CCD[CHU,*],R=CCD[CHV,*],P=CUV[C],FOR 256) BEGIN
223000          P:=*+CCD*R;INCREMENT CCD,R;END;
224000        DO VECTORMODE (CCD[CHU,*],R=CCD[CHW,*],P=CUW[C],FOR 256) BEGIN
225000          P:=*+CCD*R;INCREMENT CCD,R;END;
226000        DO VECTORMODE (CCD[CHV,*],R=CCD[CHW,*],P=CVW[C],FOR 256) BEGIN
227000          P:=*+CCD*R;INCREMENT CCD,R;END;
228000        DO VECTORMODE (UCCD[CHU,*],R=UCCD[CHV,*],P=UUV[C],FOR 256) BEGIN
229000          P:=*+UCCD*R;INCREMENT UCCD,R;END;
230000        DO VECTORMODE (UCCD[CHU,*],R=UCCD[CHW,*],P=UUW[C],FOR 256) BEGIN
231000          P:=*+UCCD*R;INCREMENT UCCD,R;END;
232000        DO VECTORMODE (UCCD[CHV,*],R=UCCD[CHW,*],P=UVW[C],FOR 256) BEGIN
233000          P:=*+UCCD*R;INCREMENT UCCD,R;END;

234000      END OF PROCEDURE SUM;
235000      %  THIS PROCEDURE USES A "RUNNING MEAN" TYPE OF TECHNIQUE TO ADD THE
236000      %     SUMMATIONS AND PRODUCTS,JUST CALCULATED FOR THE NEW BLOCK OF 4.551
237000      %    MINUTES,
238000      %     TO THE EXISTING VALUES FOR THE PREVIOUS BLOCKS OF 4.5511 MINUTES
239000      %     ALREADY CALCULATED.

240000      PROCEDURE NEWSUM(C);
241000      VALUE C; INTEGER C;
242000      BEGIN
243000        %
244000        REAL ZA;
245000        ZA:=(Z-1)/Z;
246000        CWS[C]:=**ZA+CW[C]/Z;
247000        UWS[C]:=**ZA+UW[C]/Z;
248000        CUS[C]:=**ZA+CU[C]/Z;
249000        CVS[C]:=**ZA+CV[C]/Z;
250000        UUS[C]:=**ZA+UU[C]/Z;
251000        UVS[C]:=**ZA+UV[C]/Z;
252000        CUVS[C]:=**ZA+CUV[C]/Z;
253000        CUWS[C]:=**ZA+CUW[C]/Z;
254000        CVWS[C]:=**ZA+CVW[C]/Z;
255000        UUVS[C]:=**ZA+UUV[C]/Z;
256000        UUWS[C]:=**ZA+UUW[C]/Z;
257000        UVWS[C]:=**ZA+UVW[C]/Z;
258000        CU2S[C]:=**ZA+CU2[C]/Z;
259000        CV2S[C]:=**ZA+CV2[C]/Z;
260000        CW2S[C]:=**ZA+CW2[C]/Z;
261000        UU2S[C]:=**ZA+UU2[C]/Z;
262000        UV2S[C]:=**ZA+UV2[C]/Z;
263000        UW2S[C]:=**ZA+UW2[C]/Z;
264000        CTHETA:=ARCTAN2(CVS[C],CUS[C]);
265000        CSIN:=SIN(CTHETA);
```

```
266000          CCOS:=COS(CTHETA);
267000          UTHETA:=ARCTAN2(UVS[C],UUS[C]);
268000          USIN:=SIN(UTHETA);
269000          UCOS:=COS(UTHETA);
270000          CUAV:=CUS[C]/Q;
271000          CVAV:=CVS[C]/Q;
272000          CWAV:=CWS[C]/Q;
273000          UUAV:=UUS[C]/Q;
274000          UVAV:=UVS[C]/Q;
275000          UWAV:=UWS[C]/Q;
276000          CMEAN:=CUAV*CCOS+CVAV*CSIN;
277000          UMEAN:=UUAV*UCOS+UVAV*USIN;
278000          % NOW A LITTLE BIT OF MANIPULATION IS DONE TO GET THE
279000          % COSINE CORRECTED MEANS OF RAW DATA
280000          UCCD[C*3-2,0]:=UUAV;
281000          UCCD[C*3-1,0]:=UVAV;
282000          UCCD[C*3,0]:=UWAV;
283000          HORSTCORRECTION(C,0);
284000          CUTHETA:=ARCTAN2(CCD[C*3-1,0],CCD[C*3-2,0]);
285000          CUSIN:=SIN(CUTHETA);
286000          CUCOS:=COS(CUTHETA);
287000          CUMEAN:=CCD[C*3-2,0]*CUCOS+CCD[C*3-1,0]*CUSIN;

288000        END OF PROCEDURE NEWSUM;
289000        %
290000        %
291000        %       THIS PROCEDURE CALCULATES TURBULENCE INTENSITIES,REYNOLDS STRESSES
292000        %       FOR A PARTICULAR SCAN RATE AND LENGTH OF DATA FILE CONSIDERED

293000        PROCEDURE TURBCALC(A,B,C,Q,D,E,F,G,H,I,J,K,M,XTI,YTI,ZTI,
294000        REXY,REXZ,REYZ);
295000        VALUE A,B,C,D,E,F,G,H,I,J,K,M,Q;
296000        REAL A,B,C,D,E,F,G,H,I,J,K,M;INTEGER Q;
297000        REAL REXY,REXZ,REYZ;
298000        REAL XTI,YTI,ZTI;
299000        BEGIN
300000          REAL TXY,TXZ,TYZ,TXX,TYY,TZZ,RMSX,RMSY,RMSZ,RMSTOT;
301000          REAL CM;
302000          LABEL LABH;
303000          %
304000          CM:=K**2;
305000          TXY:=(((A**2-B**2)*(C/Q-D*E))+A*B*(D**2-
306000          F/Q-E**2+G/Q))/CM;
307000          IF COUNTER=0 THEN WRITE(L,*/,A,B,C,Q,D,E,F,G,H,I,J,K,M);
308000          TYZ:=(A*(I/Q-E*M)-B*(H/Q-D*M))/CM;
309000          TXX:=((A**2)*(F/Q-D**2)+(B**2)*(G/Q-E**2)
310000          +2*A*B*(C/Q-D*E))/CM;
311000          TYY:=(A**2*G/Q-2*A*B*C/Q+B**2*F/Q)/CM;
312000          TZZ:=(J/Q-M*M)/CM;
313000          XTI:=SQRT(ABS(TXX));
314000          YTI:=SQRT(ABS(TYY));
315000          ZTI:=SQRT(ABS(TZZ));
316000          RMSX:=XTI*K;
317000          RMSY:=YTI*K;
318000          RMSZ:=ZTI*K;
319000          RMSTOT:=SQRT(ABS(TXX+TYY+TZZ)*CM);
320000          TXZ:=(A*(H/Q-D*M)+B*(I/Q-E*M)-RMSX**2*M/K)/CM;
321000          IF XTI=0 OR YTI=0 THEN REXY:=0 ELSE
322000          REXY:=TXY/(XTI*YTI);
323000          IF XTI=0 OR ZTI=0 THEN REXZ:=0 ELSE
324000          REXZ:=TXZ/(XTI*ZTI);
325000          IF YTI=0 OR ZTI=0 THEN REYZ:=0 ELSE
326000          REYZ:=TYZ/(YTI*ZTI);
327000          IF IFTEST=1 THEN
328000          BEGIN
329000            WRITE(L,<X20,"TXZ=",F9.6," WITHOUT CORRECTION TXZ=",F9.6," TXY=",
330000            F9.6," TYZ=",F9.6," XTI=",F6.4," YTI=",F6.4," ZTI=",F6.4>,TXZ,
331000            TXZ+RMSX**2*M/(K*CM),TXY,TYZ,XTI,YTI,ZTI);
332000            WRITE(L,<"RMSX=",F9.6," RMSY=",F9.6," RMSZ=",F9.6," REXY",F9.6,
333000            " REXZ=",F9.6," REYZ=",F9.6," TXX=",F8.5,
334000            " TYY=",F8.5," TZZ=",F8.5>,RMSX,RMSY,RMSZ,REXY,REXZ,REYZ,
335000            TXX,TYY,TZZ);
336000          END;
337000          GO TO LABH;
338000          LABH:

339000        END OF PROCEDURE TURBCALC;
340000        %  THIS PROCEDURE PLOTS AVERAGE LONGITUDINAL VELOCITIES AND DIRECTIONS
341000        %       FOR DIFFERENT LENGTHS OF THE DATA FILE CONSIDERED.

342000        PROCEDURE PLOTVELANG(LABELX,XNO,GRAPHNAME,NOCHAR,DATAVEL,DATAANG, NOOFDA
343000        TA,NOOFLINES,XDIST,CHAR,ARRAYNO);
344000        VALUE XNO,NOCHAR,NOOFDATA,NOOFLINES;
345000        INTEGER XNO,NOCHAR,NOOFDATA,NOOFLINES;
346000        ALPHA ARRAY LABELX,GRAPHNAME,CHAR,ARRAYNO[*];
347000        ARRAY DATAVEL,DATAANG[*,*],XDIST[*];
348000        BEGIN
349000          OWN INTEGER TEST;
350000          OWN ALPHA ARRAY VE1,VE2,PL1,PL2[0:24];
351000          INTEGER I;
352000          IF TEST=0 THEN BEGIN
353000            REPLACE POINTER(VE1) BY "AVERAGE WIND VELOCITY";
354000            REPLACE POINTER(VE2) BY "FOR PERIOD IN M/S";
355000            REPLACE POINTER(PL1) BY "ANGLE OF ATTACK OF WIND";
356000            REPLACE POINTER(PL2) BY "VECTOR TO U ANEMOMETER";
```

```
357000          TEST:=1;
358000        END;
359000        AINIT(950);
360000        ASPEED(3);
361000        ATYPE(TYPELBL,38);
362000        AORIG(70,60);
363000        ABOX(0,0,8,15,100,50,1);
364000        ASCA(-55,0,0,50,0,1,16,1,2);
365000        ASCA(-40,-20,100,0,0,10,9,1,2);
366000        ASCA(780,0,0,50,0,20,6,1,2);
367000        ALAB(-50,400,VE1,21,1,4);
368000        ALAB(-30,400,VE2,17,1,4);
369000        ALAB(300,-40,LABELX,XNO,1,2);
370000        ALAB(844,10,PL1,23,1,4);
371000        ALAB(862,10,PL2,22,1,4);
372000        % COMPACTVELANG WOULD NORMALLY BE TRUE BECAUSE WHEN TRUE THE VELOCITIES
373000        %   AND DIRECTIONS ARE ALL PLOTTED ON ONE GRAPH.THIS REDUCES THE NUMBER
374000        %  OF PLOTS REQUIRED,AND IS POSSIBLE BECAUSE THE AVERAGE WIND VELOCITY
375000        %AND DIRECTIONS CALCULATED ARE NOT AFFECTED BY CHANGES IN THE SCAN RATE
376000        IF COMPACTVELANG THEN
377000        BEGIN
378000          FILL GRAPHNAME[*] WITH "EACH NUMBER CORRESPONDS  TO THE NUMBER OF THE OR
379000          THOGONAL ARRAY OF ANEMOMETERS";
380000          ALAB(3,775,GRAPHNAME,76,1,2);
381000          ALAB(3,755,COMPACTLBL,54,1,2);
382000          FOR I:=0 STEP 1 UNTIL NOCH/3-1 DO
383000          BEGIN
384000            ALINEC(XDIST,PUMEAN[I,0,*],NOOFDATA,0,0,10,2,CHAR[I],-11,-5,1,2);
385000            ALINEC(XDIST,PCMEAN[I,0,*],NOOFDATA,0,0,10,2,CHAR[I],1,-5,1,2);
386000          END;
387000          FOR I:=0 STEP 1 UNTIL NOCH/3-1 DO
388000          BEGIN
389000            ALINEC(XDIST,PUTHETA[I,0,*],NOOFDATA,0,0,10,40,CHAR[I],-11,-5,1,2);
390000            ALINEC(XDIST,PCTHETA[I,0,*],NOOFDATA ,0,0,10,40,CHAR[I],1,-5,1,2);
391000          END;
392000        END
393000        ELSE
394000        %     PLOTS VELOCITIES,DIRECTIONS ON SEPARATE GRAPHS
395000        BEGIN
396000          ALAB(300,700,GRAPHNAME,NOCHAR,1,2);
397000          ALAB(250,750,ARRAYNO,25,1,2);
398000          FOR I:=0 STEP 1 UNTIL NOOFLINES DO
399000          ALINEC(XDIST,DATAVEL[I,*],NOOFDATA,0,0,10,5,CHAR[I],-5,-5,1,2);
400000          AORIG(120,560);
401000          FOR I:=0 STEP 1 UNTIL NOOFLINES DO
402000          ALINEC(XDIST,DATAANG[I,*],NOOFDATA,0,0,10,60,CHAR[I],-5,-5,1,2);
403000        END;
404000        AEND;

405000      END OF PROCEDURE PLOTVELANG;
406000      %
407000      %
408000      %     THIS PROCEDURE PLOTS TURBULENCE INTENSITIES IN THE 3 ORTHOGONAL
409000      %     DIRECTIONS AS FUNCTIONS OF CORRECTING FOR NON-COSINE RESPONSE,SCAN
410000      %     RATE,LENGTH OF DATA FILE.THE PROCEDURE IS CALLED ONCE PER
411000      %     ORTHOGONAL ARRAY OF ANEMOMETERS

412000      PROCEDURE PLOTTIXYZ(LABELX,XNO,GRAPHNAME,NOCHAR,CDATAX,CDATAY,CDATAZ,
413000      UDATAX,
414000      UDATAY,UDATAZ,NOOFDATA,NOOFLINES,XDIST,CHAR,CHARY,ARRAYNO);
415000      VALUE XNO,NOCHAR,NOOFDATA,NOOFLINES;
416000      INTEGER XNO,NOCHAR,NOOFDATA,NOOFLINES;
417000      ALPHA ARRAY LABELX,GRAPHNAME,CHAR,CHARY,ARRAYNO[*];
418000      ARRAY CDATAX,CDATAY,CDATAZ,UDATAX,UDATAY,UDATAZ[*,*],XDIST[*];
419000      BEGIN
420000        OWN INTEGER TEST;
421000        OWN ALPHA ARRAY TI1[0:24],TI2[0:4];
422000        INTEGER I;
423000        ARRAY FMT[0:0];
424000        REPLACE POINTER(FMT) BY "F4.2";
425000        %
426000        IF TEST=0 THEN BEGIN
427000          REPLACE POINTER(TI1) BY "TURBULENCE INTENSITY";
428000          REPLACE POINTER(TI2) BY "IN X,Y AND Z DIRECTIONS       ";
429000          TEST:=1;
430000        END;
431000        AINIT(940);
432000        ASPEED(3);
433000        AORIG(95,200);
434000        ABOX(0,0,8,12,100,50,1);
435000        ASCALE(-60,0,0,50,0,.05,13,1,2,FMT,4);
436000        ASCA(-40,-20,100,0,0,10,9,1,2);
437000        ALAB(-80,200,TI1,20,1,4);
438000        ALAB(-60,150,TI2,30,1,4);
439000        ALAB(300,-40,LABELX,XNO,1,2);
440000        ALAB(50,400,GRAPHNAME,NOCHAR,1,2);
441000        ALAB(50,450,ARRAYNO,25,1,2);
442000        FOR I:=0 STEP 1 UNTIL NOOFLINES DO
443000        BEGIN
444000          ALINEC(XDIST,UDATAX[I,*],NOOFDATA,0,0,10,.1,CHAR[I],-11,-5,1,2);
445000          ALINEC(XDIST,UDATAY[I,*],NOOFDATA,0,0,10,.1,CHARY[I],-11,-5,1,2);
446000          ALINEC(XDIST,UDATAZ[I,*],NOOFDATA,0,0,10,.1,CHAR[I],-11,-5,1,2);
447000          ALINEC(XDIST,CDATAX[I,*],NOOFDATA,0,0,10,.1,CHAR[I],  1,-5,1,2);
448000          ALINEC(XDIST,CDATAY[I,*],NOOFDATA,0,0,10,.1,CHARY[I],1,-5,1,2);
449000          ALINEC(XDIST,CDATAZ[I,*],NOOFDATA,0,0,10,.1,CHAR[I],  1,-5,1,2);
```

```
450000          END;
451000          AEND;

452000        END OF PROCEDURE PLOTTIXYZ;
453000        %
454000        %       THIS PROCEDURE PLOTS NORMALISED REYNOLDS STRESSES-UW,UV,VW
455000        %       AS FUNCTIONS OF CORRECTING FOR NON-COSINE RESPONSE,SCAN RATE,
456000        %       LENGTH OF DATA FILE.THE PROCEDURE IS CALLED ONCE PER ORTHOGONAL
457000        %       ARRAY OF ANEMOMETERS.

458000        PROCEDURE PLOTREYNOLDSSTRESS(LABELX,XNO,GRAPHNAME,NOCHAR,CDATAARRAY,UDAT
459000        AARRAY,NOOFDATA,NOOFLINES,XDIST,CHAR,WHICHREY,NOCHA,ARRAYNO,
460000        CDUV,UDUV,CDVW,UDVW,CHARY);
461000        VALUE XNO,NOCHAR,NOOFDATA,NOOFLINES,NOCHA;
462000        INTEGER XNO,NOCHAR,NOOFDATA,NOOFLINES,NOCHA;
463000        ALPHA ARRAY LABELX[*],GRAPHNAME[*],CHAR[*],WHICHREY[*];
464000        ALPHA ARRAY ARRAYNO[*];
465000        ARRAY CDATAARRAY,UDATAARRAY[*,*],XDIST[*];
466000        ARRAY CDUV,UDUV,CDVW,UDVW[*,*],CHARY[*];
467000        BEGIN
468000          OWN INTEGER TEST  ;
469000          OWN ALPHA ARRAY RE[0:40];
470000          INTEGER I;
471000          ARRAY FMT[0:0];
472000          REPLACE POINTER(FMT) BY "F5.2";
473000          %
474000          IF TEST=0 THEN
475000          BEGIN
476000            REPLACE POINTER(RE) BY "NORMALISED      REYNOLDS STRESS       ";
477000            TEST:=1;
478000          END;
479000          AINIT(900);
480000          ASPEED(3);
481000          AORIG(80,100);
482000          ABOX(0,0,8,10,100,50,1);
483000          ASCA(-40,-20,100,0,0,10,9,1,2);
484000          ASCALE(-60,0,0,50,.3,-.1,11,1,2,FMT,5);
485000          ALAB(300,-40,LABELX,XNO,1,2);
486000          ALAB(10,400,GRAPHNAME,NOCHAR,1,2);
487000          ALAB(-60,80,RE,38,1,4);
488000          ALAB(-60,210,WHICHREY,NOCHA,1,4);
489000          ALAB(10,370,ARRAYNO,25,1,2);
490000          FOR I:=0 STEP 1 UNTIL NOOFLINES DO
491000          BEGIN
492000            ALINEC(XDIST,UDATAARRAY[I,*],NOOFDATA,0,.3,10,-.2,CHAR[I],-11,-
493000            5,1,2);
494000            ALINEC(XDIST,CDATAARRAY[I,*],NOOFDATA,0,.3,10,-.2,CHAR[I],1,-5,
495000            1,2);
496000            ALINEC(XDIST,UDUV[I,*],NOOFDATA,0,.3,10,-.2,CHARY[I],-11,-
497000            5,1,2);
498000            ALINEC(XDIST,CDUV[I,*],NOOFDATA,0,.3,10,-.2,CHARY[I],1,-5,
499000            1,2);
500000            ALINEC(XDIST,UDVW[I,*],NOOFDATA,0,.3,10,-.2,CHAR[I],-11,-
501000            5,1,2);
502000            ALINEC(XDIST,CDVW[I,*],NOOFDATA,0,.3,10,-.2,CHAR[I],1,-5,
503000            1,2);
504000          END;
505000          AEND;

506000        END OF PROCEDURE PLOTREYNOLDSSTRESS;
507000        %
508000        %     READ IN CORRECTION FACTORS FOR NON-COSINE RESPONSE CORRECTION
509000        READ(K,<26I3>,FOR I:=1 STEP 1 UNTIL 101 DO
510000        HORCOR[I]);
511000
512000        WRITE(L,<"     HORCOR ARRAY",/>);
513000        WRITE(L,<25I5>,FOR I:=1 STEP 1 UNTIL 101 DO HORCOR[I]);
514000
515000
516000        FOR I:=1 STEP 1 UNTIL 101 DO
517000        HORCOR[I]:=*/100;
518000        BEGIN
519000          %
520000          %     TIME(12)IS A SYSTEM CLOCK GIVING THE ELAPSED PROCESSOR TIME
521000          %                     DECLARATIONS
522000          DEFINE T=TIME(12)*2.40-6#;
523000          REAL T1,T2,T3,T4,T5,T6,T7,T8;
524000          LABEL L1,L2,RESTART,FINISH;
525000          LABEL L3;
526000          LABEL REBEGIN,EXIT;
527000          INTEGER RP;
528000          REAL ARRAY CPXTI,CPYTI,CPZTI,UPXTI,UPYTI,UPZTI[
529000          0:NOCH/3-1,0:NFL-1,0:IKK/(SR*256)-1];
530000          ARRAY CPREXY,CPREXZ,CPREYZ,
531000          UPREXY,UPREYZ,UPREXZ[0:NOCH/3-1,0:NFL-1,0:IKK/(SR*256)-1];
532000          ALPHA ARRAY LABELX[0:30];
533000          ALPHA ARRAY CNAME,D1,D2,D3[0:24],UNAME[0:30],
534000          CHAR[0:8];
535000          ALPHA ARRAY XY,XZ,YZ[0:0];
536000          REAL ARRAY XDIST[0:20];
537000          INTEGER NFD;
538000          LABEL LAB;
539000          REAL AB;
540000          ALPHA ARRAY CHARY[0:8];
541000          ALPHA ARRAY ARRAYNO[0:11,0:4];
```

```
542000          REAL CNVRTTORPS;
543000          ARRAY CORFCTR[1:36];
544000          NFD:=ENTIER(IKK/(SR*256));
545000          IF NOT NOPLOTS THEN
546000          WRITE(L,<"NO OF LINES ON GRAPHS ARE",X2,I5,"NO OF POINTS ON TIME AXIS IS
547000          ",X2,I5>,NFL,NFD);
548000          COUNTER:=0;
549000          RP:=1;
550000
551000          READ(K,/,FOR I:=1 STEP 1 UNTIL 36 DO CORFCTR[I]);
552000          AA:=SR/PSR;IF AA>1 THEN BEGIN
553000            IKK:=*/AA;SR:=PSR;
554000            WRITE(L,<"HIGHEST SCANRATE FOR ACTUAL PROCESSING=",I6," ACTUAL"
555000            " NOS OF POINTS FOR PROCESSING=",I6>,SR,IKK);REDUCEDATA;END;
556000          CNVRTTORPS:=SR/32;
557000          RESTART:
558000          %     Q IS THE NUMBER OF SCANS TO MAKE 4.511 MINUTES
559000          Q:=SR*256;
560000          WRITE(L,<// "NUMBER OF CHANNELS=",I3," SCANRATE="I3," SCANS PER SECOND
561000          NUMBER OF SAMPLES=",I10>,NOCH,SR,IKK);
562000          REBEGIN:
563000          AB:=2**COUNTER;
564000          %     INITIALISE ISAVE FOR NON-COSINE RESPONSE CORRECTION PROCEDURE
565000          FOR I:=1 STEP 1 UNTIL NOCH/3 DO BEGIN ISAVE[I*3-2]:=
566000            ISAVE[I*3-1]:=75;ISAVE[I*3]:=50;END;
567000          %     FOR EACH VALUE OF Z,Z*4.5511 IS THE AMOUNT OF DATA IN
568000          %     MINUTES BEING PROCESSED.
569000          FOR Z:=1 STEP 1 UNTIL IKK/Q DO
570000          BEGIN
571000            % RESET SOME VARIABLES TO ZERO
572000            FOR I:=1 STEP 1 UNTIL NOCH DO
573000            BEGIN
574000              CW[I]:=UW[I]:=0;
575000              CU[I]:=CV[I]:=UU[I]:=UV[I]:=CUV[I]:=CUW[I]:=CVW[I]:=0;
576000              UUV[I]:=UUW[I]:=UVW[I]:=CU2[I]:=CV2[I]:=CW2[I]:=0;
577000              UU2[I]:=UV2[I]:=UW2[I]:=0;
578000            END;
579000            %     READ IN 4.5511 MINUTES OF DATA
580000            FOR A:=1 STEP 1 UNTIL SR DO
581000            BEGIN
582000              %     B IS THE CHANNEL NUMBER
583000              FOR B:=1 STEP 1 UNTIL NOCH DO
584000              BEGIN
585000                READ(DISKDATA,256,UCCD[B,*])[L1];
586000                %     CONVERT COUNTS INTO M/S
587000                FOR I:=0 STEP 1 UNTIL 255 DO UCCD[B,I]:=UCCD[B,I]*CNVRTTORPS*CORFCTR[B];
588000              END;
589000              GO TO L2;
590000              L1:
591000              WRITE(L,<X5/,"END OF FILE ON ",I4,"TIME THROUGH AFTER ONLY",
592000              I4,"ADDITIONS INSTEAD OF",I4>,Z,A,Q);
593000              GO TO L3;
594000              L2:
595000              FOR C:=1 STEP 1 UNTIL NOCH/3 DO
596000              BEGIN
597000                T1:=*-T;
598000                %     CORRECT THE DATA FOR NON-COSINE RESPONSE AND STORE IN ANOTHER
599000                %     ARRAY
600000                HORSTCORRECTION(C,255);
601000                T1:=*+T; T2:=*-T;
602000                %     CALCULATE SUMMATIONS AND PRODUCTS FOR THE 256 DATA IN EACH
603000                %     CHANNEL WHICH HAS JUST BEEN READ
604000                SUM(C);
605000                T2:=*+T;
606000              END;
607000            END;
608000            %
609000            FOR C:=1 STEP 1 UNTIL NOCH/3 DO
610000            BEGIN
611000              T3:=*-T;
612000              %     ADD THE SUMMATIONS AND PRODUCTS CALCULATED FROM THE NEW
613000              %     BLOCK TO VALUES CALCULATED FROM THE PREVIOUS BLOCKS
614000              NEWSUM(C);
615000              T3:=*+T;
616000              IF (LASTVALUEONLY AND Z=(IKK/Q)) OR NOT LASTVALUEONLY THEN BEGIN
617000                % THIS BLOCK CAN CALCULATE THE TURBULENCE PARAMETERS FOR EACH PARTICULAR
618000                %     SCAN RATE AND LENGTH OF FILE.IT IS ENTERED ONCE ONLY,AT THE END
619000                %     OF THE DATA STREAM IF LASTVALUEONLY IS TRUE,OTHERWISE IT
620000                %     IS ENTERED FOR ALL COMBINATIONS OF SCAN RATE,LENGTH OF RECORD AND
621000                %     FOR EACH ORTHOGONAL ARRAY OF ANEMOMETERS.
622000                IF IFTEST=1 THEN
623000                BEGIN
624000                  WRITE(L,</"ORTHOG ARY",I3," AFTER",F7.3," MIN  UNCOR AV U",F7.3,
625000                  " V",F7.3," W",F7.4,"  COR AV U",F7.3," V",F7.3," W",F7.4,"  COR"
626000                  " RAWAV U",F7.3," V",F7.3>,C,4.55111*Z,UUAV/AB,UVAV/AB,UWAV/AB,
627000                  CUAV/AB,CVAV/AB,CWAV/AB,CCD[C*3-2,0]/AB,CCD[C*3-1,0]/AB);
628000                  WRITE(L,<"VECTOR MEANS UNCOR",F8.3," M/S AT",F8.3," DEG COR",
629000                  F8.3," M/S AT",F8.3," DEG COR RAW AVS",F8.3," M/S AT",F8.3," DEG"
630000                  " CORRAWAV",F7.3>,UMEAN/AB,UTHETA*180/3.14159,CMEAN/AB,CTHETA*180
631000                  /3.14159,CUMEAN/AB,CUTHETA*180/3.14159,CCD[C*3,0]);
632000                END;
633000                IF IFTEST=1 THEN
634000                WRITE(L,<X3,"COSINE CORRECTED RESULTS WITH MEANS OF COSINE CORRECTED R"
635000                "ESULTS">);
636000                GO TO LAB;
```

```
637000              LAB:
638000              %
639000              %
640000              T4:=*-T;
641000              %  CALCULATE TURBULENCE PARAMETERS USING DATA CORRECTED FOR NON-COSINE
642000              %     RESPONSE
643000              TURBCALC(CCOS,CSIN,CUVS[C],Q,CUAV,CVAV,CU2S[C],CV2S[C],CUWS[C],
644000              CVWS[C],CW2S[C],
645000              CMEAN,CWAV,CPXTI[C-1,COUNTER,Z-1],CPYTI[C-1,
646000              COUNTER,Z-1],CPZTI[C-1,COUNTER,Z-1],CPREXY[C-1,COUNTER,
647000              Z-1],CPREXZ[C-1,COUNTER,Z-1],CPREYZ[C-1,COUNTER,Z-1]);
648000              IF IFTEST=1 THEN
649000              WRITE(L,<X3,"UNCORRECTED RESULTS WITH MEANS OF UNCORRECTED RESULTS">);
650000              %
651000              %
652000              %CALCULATE TURBULENCE PARAMETERS USING DATA NOT CORRECTED FOR NON-COSINE
653000              %     RESPONSE
654000              TURBCALC(UCOS,USIN,UUVS[C],Q,UUAV,UVAV,UU2S[C],UV2S[C],
655000              UUWS[C],UVWS[C],UW2S[C],
656000              UMEAN,UWAV,UPXTI[C-1,COUNTER,Z-1],UPYTI[C-1,
657000              COUNTER,Z-1],UPZTI[C-1,COUNTER,Z-1],UPREXY[C-1,COUNTER,
658000              Z-1],UPREXZ[C-1,COUNTER,Z-1],UPREYZ[C-1,COUNTER,Z-
659000              1]);
660000              T4:=*+T;
661000              %
662000              %     CALCULATE AVERAGE VELOCITIES,ANGLES
663000              PCMEAN[C-1,COUNTER,Z-1]:=CMEAN/AB;
664000              PUMEAN[C-1,COUNTER,Z-1]:=UMEAN/AB;
665000              PCTHETA[C-1,COUNTER,Z-1]:=CTHETA*180/3.1415926;
666000              PUTHETA[C-1,COUNTER,Z-1]:=UTHETA*180/3.1415926;
667000            END;
668000          END OF C LOOP;
669000          %     PROCESSOR TIMES FOR VARIOUS PARTS OF THE PROGRAMME
670000          WRITE(L,*/,Z,T1,T2,T3,T4);
671000        END OF Z LOOP;
672000        COMMENT: NOW EVERY TWO DATA SAMPLES ARE ADDED
673000        TOGETHER IN EACH CHANNEL AND THE WIND STRUCTURE
674000        PARAMETERS CALCULATED AGAIN;
675000        %
676000        WRITE(L,<"NO OF TIMES 6 ITS OCCURRED IN HORST (CTR)=",I7>,CTR);
677000        WRITE(L,<"NO OF TIMES 0 ITS OCCURRED",I7," 1 IT=",I7," 2 ITS=",I7,
678000        " 3 ITS=",I7," 4 ITS=",I7" 5 ITS=",I7," 6 ITS=",I7>,HNO[0],HNO[1],
679000        HNO[2],HNO[3],HNO[4],HNO[5],HNO[6]);
680000        L3:
681000        %          **********          REDUCE SCAN RATE BLOCK          ********
682000        COUNTER:=*+1;
683000        IF COUNTER=NFL THEN GO TO EXIT;
684000        IF SR=1 THEN GO TO FINISH;
685000        T5:=*-T;
686000        FOR LZ:=0 STEP 1 UNTIL IKK/512-1 DO
687000        BEGIN
688000          FOR B:=1 STEP 1 UNTIL NOCH DO
689000          READ(DISKDATA[2*LZ*NOCH+B-1],256,UCCD[B,*]);
690000          FOR B:=1 STEP 1 UNTIL NOCH DO
691000          READ(DISKDATA[(2*LZ+1)*NOCH+B-1],256,CCD[B,*]);
692000          FOR B:=1 STEP 1 UNTIL NOCH DO
693000          BEGIN
694000            FOR KZ:=0 STEP 1 UNTIL 127 DO
695000            UCCD[B,KZ]:=UCCD[B,KZ*2]+UCCD[B,KZ*2+1];
696000            FOR KZ:=0 STEP 1 UNTIL 127 DO
697000            UCCD[B,KZ+128]:=CCD[B,2*KZ]+CCD[B,2*KZ+1];
698000          END;
699000          FOR B:=1 STEP 1 UNTIL NOCH DO
700000          WRITE(DISKDATA[LZ*NOCH+B-1],256,UCCD[B,*]);
701000        END;
702000        SR:=SR/2;
703000        IKK:=(ENTIER(IKK/512))*256;
704000        REWIND(DISKDATA);
705000        T5:=*+T;WRITE(L,*/,SR,COUNTER,T5);
706000        GO TO RESTART;
707000        FINISH:
708000        T6:=*-T;
709000        FOR LZ:=0 STEP 1 UNTIL IKK/256*RP-1 DO
710000        BEGIN
711000          FOR B:=1 STEP 1 UNTIL NOCH DO
712000          BEGIN
713000            READ(DISKDATA[LZ*NOCH+B-1],256,UCCD[B,*]);
714000            FOR KZ:=0 STEP 1 UNTIL 127 DO
715000            UCCD[B,KZ]:=UCCD[B,KZ*2]+UCCD[B,2*KZ+1];
716000            IF RP=1 THEN
717000            BEGIN
718000              FOR KZ:=0 STEP 1 UNTIL 127 DO
719000              UCCD[B,KZ+128]:=0;
720000            END;
721000            WRITE(DISKDATA[LZ*NOCH+B-1],256,UCCD[B,*]);
722000          END;
723000        END;
724000        RP:=RP*2;
725000        Q:=Q/2;
726000        IKK:=IKK/2;
727000        WRITE(L,<///"NUMBER OF CHANNELS=",I3,"  AVERAGING PERIOD=",I3," SECONDS
728000        NUMBER OF SAMPLES=",I7>,NOCH,RP,IKK);
729000        REWIND(DISKDATA);
730000        T6:=*+T;WRITE(L,*/,RP,COUNTER,T6);
731000        %          **********     END OF REDUCE SCAN RATE BLOCK     **********
```

```
732000          GO TO REBEGIN;
733000          EXIT:
734000          IF NOPLOTS THEN GO TO FINISHIT;
735000          %     SET UP SOME ARRAYS AND MAKE LABELS FOR PLOTTING THE
736000          %     TURBULENCE PARAMETERS
737000          FOR I:=0 STEP 1 UNTIL 19 DO
738000          XDIST[I]:=4.5511*(I+1);
739000          REPLACE POINTER(LABELX) BY "RECORDING PERIOD IN MINUTES";
740000          REPLACE POINTER(CNAME) BY "COSINE CORRECTED RESULTS";
741000          REPLACE POINTER(UNAME) BY "UNCORRECTED COSINE RESULTS";
742000          READ(K ,<9A6>, FOR I:=0 STEP 1 UNTIL 8 DO CHAR[I]);
743000          READ(K,<9A6>,FOR I:=0 STEP 1 UNTIL 8 DO CHARY[I]);
744000          REPLACE POINTER(XY) BY "UV";
745000          REPLACE POINTER(XZ) BY "UW";
746000          REPLACE POINTER(YZ) BY "VW";
747000          FILL ARRAYNO[0,*] WITH "ORTHOGONAL ARRAY 1 2 3";
748000          FILL ARRAYNO[1,*] WITH "ORTHOGONAL ARRAY 4 5 6";
749000          FILL ARRAYNO[2,*] WITH "ORTHOGONAL ARRAY 7 8 9";
750000          FILL ARRAYNO[3,*] WITH "ORTHOGONAL ARRAY 10 11 12";
751000          FILL ARRAYNO[4,*] WITH "ORTHOGONAL ARRAY 13 14 15";
752000          FILL ARRAYNO[5,*] WITH "ORTHOGONAL ARRAY 16 17 18";
753000          FILL ARRAYNO[6,*] WITH "ORTHOGONAL ARRAY 19 20 21";
754000          FILL ARRAYNO[7,*] WITH "ORTHOGONAL ARRAY 22 23 24";
755000          FILL ARRAYNO[8,*] WITH "ORTHOGONAL ARRAY 25 26 27";
756000          FILL ARRAYNO[9,*] WITH "ORTHOGONAL ARRAY 28 29 30";
757000          FILL ARRAYNO[10,*] WITH "ORTHOGONAL ARRAY 31 32 33";
758000          FILL ARRAYNO[11,*] WITH "ORTHOGONAL ARRAY 34 35 36";
759000          FOR I:=0 STEP 1 UNTIL NOCH/3-1 DO
760000          BEGIN
761000            IF(COMPACTVELANG AND I=0)OR NOT COMPACTVELANG THEN
762000            %     PLOT AVERAGE LONGITUDINAL VELOCITIES AND ANGLES
763000            T7:=*-T;
764000            PLOTVELANG(LABELX,27,CNAME,24,PCMEAN[0,*,*],PCTHETA[0,*,*],NFD,NFL-1,
765000            XDIST,CHAR,ARRAYNO[0,*]);
766000            T7:=*+T;
767000            T8:=*-T;
768000            %     PLOT TURBULENCE INTENSITIES,ONE GRAPH PER ORTHOGONAL ARRAY
769000            PLOTTIXYZ(LABELX,27,COMPACTLBL,54,CPXTI[I,*,*],CPYTI[I,*,*],CPZTI[I,*,*]
770000            ,UPXTI[I,*,*],UPYTI[I,*,*],UPZTI[I,*,*],NFD,NFL-1,XDIST,CHAR,CHARY,ARRAY
771000            NO[I,*]);
772000            %     PLOT REYNOLDS STRESSES,ONE GRAPH PER ORTHOGONAL ARRAY
773000            PLOTREYNOLDSSTRESS(LABELX,27,COMPACTLBL,54,CPREXZ[I,*,*],UPREXZ[I,*,*],
774000            NFD,NFL-1,XDIST,CHAR,XZ,2,ARRAYNO[I,*],CPREXY[I,*,*],UPREXY[I,*,*]
775000            ,CPREYZ[I,*,*],UPREYZ[I,*,*],CHARY[*]);
776000            T8:=*+T;
777000          END;
778000          %     WRITE OUT PROCESSOR TIMES FOR PLOTS
779000          WRITE(L,*/,T7,T8);
780000        END;
781000      END;
782000    END;
783000    FINISHIT:
784000    IF NOPLOTS AND IFTEST=0 THEN
785000    WRITE(L,<"NOPLOTS=T AND IFTEST=0 MEANS NO PRINTOUT"/"BETTER TO HA"
786000    "VE EITHER IFTEST=1 OR NOPLOTS=FALSE">);
787000    WRITE(L,<"END OF PROGRAMME">);
788000 END.
```

```
INPUT STRING WAS
"SEQVELTURBREY STEP 2"
```

APPENDIX F

PROGRAM 'PSAUTCORS'

F.1 Typical WFL For Using This Program

F.1.1 Calculate and Plot all spectra, autocorrelation functions and cross-correlation functions

The source files PSAUTCORS and the FFT package MATHLIBFFT/= are assumed to be on tape A999.

Assume that data has been recorded from four orthogonal arrays on a tower at heights of 3.2,5.3,15.3 and 19.2 m. The data has been formatted and copied using COPYDATA to a library tape called A123. The data file on this tape is called WD and it contains 8192 samples in each of the twelve channels. The scan rate of the data on the tape is 2. The output required after running this program is :

(1) Data corrected for anemometer non-cosine response.

(2) The power spectral densities are required for all three orthogonal components.

(3) The autocorrelation functions are required for all three orthogonal components.

(4) A parabolic trend line is to be removed from all data streams.

(5) All possible cross-correlation functions are required between pairs of like velocity components.

(6) Each power spectral density plot is required on a separate graph, as a function of frequency in Hz.

(7) Each autocorrelation function plot is required on a separate graph.

(8) The data to be cross-correlated is required to have had a parabolic trend line removed from it.

(9) The minimum number of graphs of cross-correlation functions are required.

(10) A cosine taper data window is not required for the spectral estimates.

A JOB to output the results according to the above criteria is given below

```
7
5  JOB PSAUTCORS/WD  HILL DATA;
7
5  PROCESSTIME=600; IOTIME=600;
7
5  USER MECH021/PASSWORD; CLASS=10; BEGIN
7
5  COPY MATHLIBFFT/= FROM A999;
   COPY PSAUTCORS FROM A999;
   COMPILE OBJECTPS ALGOL LIBRARY;
   COMPILER FILE TAPE=PSAUTCORS;
   DATA
$  SET MERGE
$  RESET LIST
7
5  IF FILE OJECTPS ISNT PRESENT THEN GO ENDIT;
7
5  COPY WD AS INFYLE FROM A123;
   RUN OBJECTPS;
   DATA KR;
```

[4 cards with the 101 non-cosine response correction factors on them in 26I3 format. The non-cosine response correction factors are given in the correct order in Appendix A]

[3 cards with the 36 individual anemometer calibration factors on them in F5.4 format. The order of these is triplet 1 - x_1, y_1, z_1, triplet 2 - x_1, y_1, z_1 ... up to triplet 12.]

```
   2,1,1, 8192,4,
   0,
   1,
   0,
   1, 1, 1,
```

```
1,18,1,0,0,1,
1,1,2,
1, /
1,4,1,7,1,10,4,7,4,10,7,10,2,5,2,8,2,11,5,8,5,11,8,11,/
3,6,3,9,3,12,6,9,6,12,9,12,
0,0,0,1,
1,
3.2,10.3,15.3,19.2,
12,
0,2,0,1,1,1,0,
0,2,0,2,1,1,0,
0,2,0,3,1,1,0,
0,2,0,4,1,1,0,
0,2,0,1,1,1,1,
0,2,0,2,1,1,1,
0,2,0,3,1,1,1,
0,2,0,4,1,1,1,
0,2,0,1,1,1,2,
0,2,0,2,1,1,2,
0,2,0,3,1,1,2,
0,2,0,4,1,1,2,
7
5  ENDIT:
7
5  REMOVE (MECH021);
7
5  END JOB
```

F.1.2 Spectra only-calculated from one array and for one of the three orthogonal components

Assume the same data set as in F.1.1, however, it is desired to calculate the lateral component power spectral density of orthogonal array 3 for the three types of trend removal. The spectra from no, linear, and parabolic trend removal are required to be plotted on the same graph. The data is not

required to be corrected for the non-cosine response of the anemometers.

The WFL is the same as for F.1.1. The non-cosine response and calibration factor data cards are the same also as for F.1.1. The data cards required following the calibration cards in F.1.1 for this output are given below

```
2, 1,1, 8192, 4,
0,
0,
1, 3,
0,1,0,
0,
0,
0,
0,1,1,1,
0,
3.2, 10.3, 15.3, 19.2,
1,
1,1,0,3,0,1,1,
```

F.1.3 Spectrum and Autocorrelations required as a function of frequen

Assume that the data in the file WD in F.1.1 is at a scan rate of 16 and contains 32768 samples per channel. Data from four orthogonal arrays are contained in the file.

Power spectral densities and autocorrelation functions of all componen are required to be calculated at scan rates of 8,4,2,1, .5, .25 Hz. The graphical output from each height and from each component is required on separate graphs which show the effect of the different scan rates. All data streams are required to have a linear trend removal, to be corrected for non-cosine response of the anemometers but no cosine taper data windo is required.

The WFL is the same as for F.1.1. The cards required after the calibration factor cards in F.1.1 are given below, to achieve the output required.

```
16,2,6,32768,4,
0,
1,
0,
1,1,1,
0,
0,
0
0,0,1,0,
1,
3.2, 10.3, 15.3, 19.2,
12,
0,1,0,1,1,1,0,
0,1,0,2,1,1,0,
0,1,0,3,1,1,0,
0,1,0,4,1,1,0,
0,1,0,1,1,1,1,
0,1,0,2,1,1,1,
0,1,0,3,1,1,1,
0,1,0,4,1,1,1,
0,1,0,1,1,1,2,
0,1,0,2,1,1,2,
0,1,0,3,1,1,2,
0,1,0,4,1,1,2,
```

F.2. Listing of Program 'PSAUTCORS'

```
PPPP   SSS   AAA  U   U TTTTT  CCC   OOO  RRRR   SSS
P   P S   S A   A U   U   T   C   C O   O R   R S   S
P   P S     A   A U   U   T   C     O   O R   R S
PPPP   SSS  AAAAA U   U   T   C     O   O RRRR   SSS
P         S A   A U   U   T   C     O   O R R        S
P     S   S A   A U   U   T   C   C O   O R  R  S   S
P      SSS  A   A  UUUU   T    CCC   OOO  R   R  SSS
```

2065 RECORDS, CREATED 23/11/78

```
  100 $SET LINEINFO
  200 $BINDFR RESET LIST
  300 $ SET AUTOBIND
  400 %   BIND PLOT PROCEDURES RESIDENT ON DISK,INTO THIS PROGRAMME
  500 %   AT COMPILATION
  600 $BIND= ROM PLOTA/=
  700 BEGIN
  800   %    ECLARE GLOBAL FILES
  900   FIL  VDU(KIND=PRINTER);
 1000   FILE FILE6(KIND=PRINTER);
 1100   FILE LP(KIND=PRINTER);
 1200   FILE FX(KIND=DISK,FILETYPE=7,UNITS=WORDS,MAXRECSIZE=1024,
 1300   BLOCKSIZE=1024,AREASIZE=15,FLEXIBLE=TRUE),
 1400   FC(KIND=DISK,FILETYPE=7,UNITS=WORDS,MAXRECSIZE=1024,
 1500   BLOCKSIZE=1024,AREASIZE=15,FLEXIBLE=TRUE),
 1600   FAUT(KIND=DISK,FILETYPE=7,UNITS=WORDS,MAXRECSIZE=1024,
 1700   BLOCKSIZE=1024,AREASIZE=15,FLEXIBLE=TRUE),
 1800   FAULG(KIND=DISK,FILETYPE=7,UNITS=WORDS,MAXRECSIZE=1024,
 1900   BLOCKSIZE=1024,AREASIZE=15,FLEXIBLE=TRUE),
 2000   FAVSP(KIND=DISK,FILETYPE=7,UNITS=WORDS,MAXRECSIZE=41,
 2100   BLOCKSIZE=41,AREASIZE=300,FLEXIBLE=TRUE),
 2200   FFQAXIS(KIND=DISK,FILETYPE=7,UNITS=WORDS,MAXRECSIZE=
 2300   41,BLOCKSIZE=41,AREASIZE=300,FLEXIBLE=TRUE);
 2400   FILE KR(KIND=READER),
 2500   INFYLE(KIND=DISK,FILETYPE=7,UNITS=WORDS,MAXRECSIZE=256,
 2600   BLOCKSIZE=768,AREASIZE=60,FLEXIBLE=TRUE,PROTECTION=SAVE);
 2700   %   DECLARE PLOT PROCEDURES WHICH HAVE ALREADY BEEN COMPILED AS
 2800   %   EXTERNAL

 2900   PROCEDURE AINIT(L);VALUE L;INTEGER L;EXTERNAL;PROCEDURE AEND;EXTERNAL;

 3000   PROCEDURE ABOX(X,Y,NX,NY,XINC,YINC,THICK);VALUE X,Y,NX,NY,XINC,YINC,
 3100   THICK;INTEGER X,Y,NX,NY,XINC,YINC,THICK; EXTERNAL;

 3200   PROCEDURE AGRID(X,Y,NX,NY,XINC,YINC);VALUE X,Y,NX,NY,XINC,YINC;
 3300   INTEGER X,Y,NX,NY,XINC,YINC; EXTERNAL;

 3400   PROCEDURE ASCA(X,Y,XINC,YINC,LO,INC,N,SIZE,DIREC);VALUE X,Y,XINC,YINC,
 3500   LO,INC,N,SIZE,DIREC;INTEGER X,Y,XINC,YINC,LO,INC,N,SIZE,DIREC;EXTERNAL;

 3600   PROCEDURE ALAB(X,Y,LABLE,N,SIZE,DIREC);VALUE X,Y,N,SIZE,DIREC;
 3700   INTEGER X,Y,N,SIZE,DIREC; REAL ARRAY LABLE[*]; EXTERNAL;

 3800   PROCEDURE AORIG(X,Y);VALUE X,Y;INTEGER X,Y; EXTERNAL;

 3900   PROCEDURE  ATYPE(L,N);VALUE N;INTEGER N;REAL ARRAY L[*]; EXTERNAL;

 4000   PROCEDURE ATYPEG(L,N);VALUE N;INTEGER N;REAL ARRAY L[*]; EXTERNAL;

 4100   PROCEDURE ALINE(X,Y,N,XOR,YOR,XSCAL,YSCAL);VALUE N,XOR,YOR,XSCAL,YSCAL;
 4200   INTEGER N;REAL XOR,YOR,XSCAL,YSCAL;REAL ARRAY X[*],Y[*]; EXTERNAL;

 4300   PROCEDURE ALINED(X,Y,N,XOR,YOR,XSCAL,YSCAL,NLINE,NGAP);VALUE N,XOR,YOR,
 4400   XSCAL,YSCAL,NLINE,NGAP;REAL XOR,YOR,XSCAL,YSCAL;INTEGER N,NLINE,NGAP;
 4500   REAL ARRAY X[*],Y[*];  EXTERNAL;

 4600   PROCEDURE ALINEC(X,Y,N,XOR,YOR,XSCAL,YSCAL,CHAR,XOFF,YOFF,SIZE,DIREC);
 4700   VALUE N,XOR,YOR,XSCAL,YSCAL,CHAR,XOFF,YOFF,SIZE,DIREC;
 4800   REAL CHAR,XOR,YOR,XSCAL,YSCAL;      INTEGER N,XOFF,YOFF,SIZE,DIREC;
 4900   REAL ARRAY X[*],Y[*]; EXTERNAL;

 5000   PROCEDURE ALINEX(XINIT,XINC,Y,N,YOR,YSCAL);VALUE XINIT,XINC,N,YOR,YSCAL;
 5100   INTEGER XINIT,XINC,N;REAL YOR,YSCAL;REAL ARRAY Y[*]; EXTERNAL;

 5200   PROCEDURE ASPEED(N); VALUE N; INTEGER N; EXTERNAL;

 5300   PROCEDURE ASUBP(N); VALUE N; INTEGER N; EXTERNAL;

 5400   PROCEDURE AENDP; EXTERNAL;

 5500   PROCEDURE AONP(N); VALUE N; INTEGER N; EXTERNAL;

 5600   PROCEDURE AOFFP(N); VALUE N; INTEGER N; EXTERNAL;

 5700   PROCEDURE ADELP(N); VALUE N; INTEGER N; EXTERNAL;

 5800   PROCEDURE ASECT(N); VALUE N; INTEGER N; EXTERNAL;

 5900   PROCEDURE AFLASH(N); VALUE N; INTEGER N; EXTERNAL;

 6000   PROCEDURE ANTENS(N); VALUE N; INTEGER N; EXTERNAL;
```

```
6100    PROCEDURE ASEND; EXTERNAL;

6200    PROCEDURE ASCALE(IX,IY,IXINC,IYINC,X0,XINC,N,ISIZE,IDIREC,FMT,NC);
6300    VALUE IX,IY,IXINC,IYINC,X0,XINC,N,ISIZE,IDIREC,NC;
6400    REAL IX,IY,IXINC,IYINC,X0,XINC,N,ISIZE,IDIREC,NC;
6500    ARRAY FMT[*];EXTERNAL;
6600    %   INCLUDE THE NUMERALS PACKAGE FAST FOURIER TRANSFORM
6700    %   PROCEDURES WHICH ARE IN THE LIBRARY *MATHLIB/SYMBOL
6800    %   ON COMPUTER CENTRE LIBRARY TAPE E32.THEY ARE BETWEEN
6900    %   RECORD NUMBERS 12903000-13235000 INCLUSIVE,AND THEIR
7000    %   LISTING IS INCLUDED ELSEWHERE.
7100    $ INCLUDE "MATHLIBFFT/SFFTF."
7200    $ INCLUDE "MATHLIBFFT/SFFTR."
7300    $ INCLUDE "MATHLIBFFT/SSINCOS."
7400    $ INCLUDE "MATHLIBFFT/SBITREV2."
7500    %   DECLARE GLOBAL VARIABLES. READ IN CORRECTION FACTORS FOR
7600    %   NON-COSINE RESPONSE CORRECTION AND PROPELLOR ANEMOMETER
7700    %   CORRECTION FACTORS,IN THE ORDER CHANNEL 1,2---N.
7800    INTEGER CTR,I;ARRAY HORCOR[1:101);
7900    ARRAY CORFCTR[1:36];
8000    INTEGER PT;ARRAY AY[0:5];
8100    PT:=0;
8200    READ(KR,<26I3>,FOR I:=1 STEP 1 UNTIL 101 DO HORCOR[I));
8300    WRITE(LP,<"THE NON-COSINE CORRECTION RESPONSE CORRECTION"
8400    " FACTORS ARE CONTAINED IN HORCOR">);
8500    WRITE(LP,<"HORCOR ARRAY"/(25I5)>,FOR I:=1 STEP 1 UNTIL 101 DO HORCOR
8600    [I]);
8700    FOR I:=1 STEP 1 UNTIL 101 DO HORCOR[I]:=*/100;
8800    READ(KR,<16F5.4>,FOR I:=1 STEP 1 UNTIL 36 DO CORFCTR[I]);
8900    WRITE(LP,<"PROPELLOR ANEMOMETER CORECTION FACTORS RPS TO M/S"/
9000    "IN THE ORDER ANEMOMETER (CHANNEL) NUMBER 1 TO 36 RESPECTIVELY"/
9100    (10F13.4)>,FOR I:=1 STEP 1 UNTIL 36 DO CORFCTR[I]);
9200    BEGIN
9300      %   NON-COSINE RESPONSE CORRECTION PROCEDURE AFTER HORST(1973)
9400      %   CONVERTED TO ALGOL AND MODIFIED SLIGHTLY

9500      PROCEDURE HORSTCORRECTION(NOARRAYS,NIN,HGHTCTR,BL,AC);
9600      INTEGER NOARRAYS,NIN,HGHTCTR;BOOLEAN BL;
9700      INTEGER AC;
9800      BEGIN
9900        INTEGER NN,I,J,K,II,JJ,KK,IA,AI,HG3,AI3NA;
10000       REAL T1,T2,T3;
10100       REAL U,V,W,GU,GV,GW,S;
10200       LABEL L1,L4,L7,L9,EF;BOOLEAN BL;
10300       ARRAY X[0:2,0:255];
10400       LABEL LAB;
10500       I:=J:=75;K:=50;HG3:=HGHTCTR*3;
10600       T1:=AC/32*CORFCTR[HG3+1];
10700       T2:=AC/32*CORFCTR[HG3+2];
10800       T3:=AC/32*CORFCTR[HG3+3];
10900       FOR AI:=0 STEP 1 UNTIL NIN/256-1 DO
11000       BEGIN
11100         AI3NA:=AI*3*NOARRAYS;
11200         FOR J:=0,1,2 DO
11300         READ(INFYLE[AI3NA+HG3+J],256,X[J,*])[EF];
11400         FOR IA:=0 STEP 1 UNTIL 255 DO
11500         BEGIN NN:=0;
11600           GU:=X[0,IA]*T1;GV:=X[1,IA]*T2;GW:=X[2,IA]*T3;
11700           L1:
11800           U:=GU*HORCOR[I];V:=GV*HORCOR[J];W:=GW*HORCOR[K];
11900           S:=SQRT(U*U+V*V+W*W)+.01;
12000           II:=U*50/S+51;
12100           JJ:=V*50/S+51;
12200           KK:=W*50/S+51;
12300           IF(ABS(II-I)-1)GTR 0 THEN GO TO L4;
12400           IF(ABS(JJ-J)-1)GTR 0 THEN GO TO L4;
12500           IF(ABS(KK-K)-1)LEQ 0 THEN GO TO L7;
12600           L4:IF(NN:=*+1)GEQ 6 THEN GO TO L9;
12700           I:=II;J:=JJ;K:=KK; GO TO L1;
12800           L9:
12900           IF(CTR:=*+1)<50 THEN
13000           WRITE(LP,<"6 ITS IN HORST I=",I3," J=",I3," K=",I3," II=",
13100           I3," JJ=",I3," KK=",I3," GU=",F9.4," GV=",F9.4," GW=",F9.4,
13200           " HGHTCTR=",I3," AI=",I5," IA=",I3>,I,J,K,II,JJ,KK,GU,GV,GW,
13300           HGHTCTR,AI,IA);
13400           L7:X[0,IA]:=U;X[1,IA]:=V;X[2,IA]:=W;
13500         END OF IA LOOP;
13600         FOR J:=0,1,2 DO
13700         WRITE(INFYLE[AI3NA+HG3+J],256,X[J,*])[EF];
13800       END OF AI LOOP;
13900       GO TO LAB;
14000       EF:BL:=TRUE;WRITE(LP,<3(/"END OF FILE ON READ OR"
14100       " WRITE STATEMENT IN HORSTCORRECTION"/)>);
14200       LAB:
14300     END;%E N D   O F   H O R S T C O R R E C T I O N;
14400     %
14500     %
14600     %   PLOTS THE AUTOCORRELATION FUNCTION AS A FUNCTION OF
14700     %   (1) POSITION OF EACH ARRAY OF ANEMOMETERS,
14800     %   (2)FREQUENCY DATA PROCESSED AT,
14900     %   (3)TREND REMOVAL

15000     PROCEDURE PLOTAUTO(HEIGHT,NOARRAYS,ACTFREQ1516,NOFRQS,
15100     SAMPFRQS,HEIGHTS,FREQS,TRENDS,DIRECTION,TRENDCTR,FRQCTR,HGHTCTR,NOPTSOUT
```

```
15200     ,STARTFRQ);
15300     VALUE NOARRAYS,ACTFREQ1516,NOFRQS,DIRECTION,TRENDCTR,FRQCTR,
15400     HGHTCTR,HEIGHTS,FREQS,TRENDS,STARTFRQ;
15500     INTEGER STARTFRQ;
15600     ARRAY HEIGHT,SAMPFRQS,NOPTSOUT[0];
15700     INTEGER NOARRAYS,NOFRQS,DIRECTION,TRENDCTR,FRQCTR,HGHTCTR;
15800     BOOLEAN HEIGHTS,FREQS,TRENDS;
15900     REAL ACTFREQ1516;
16000     BEGIN
16100       ARRAY X,Y[0:1023];INTEGER AS,BS,CS;
16200       ARRAY TRENDLBL[0:10],DIRNLBL[0:3],HEIGHTLBL[0:5+NOARRAYS],
16300       FRQLBL[0:5+NOFRQS],PLOTLABEL[0:8];
16400       INTEGER I,J;
16500       POINTER P;
16600       ARRAY FMT[0:0];
16700       OWN BOOLEAN FIRSTTIME;
16800       FILE KARDS(KIND=READER),LINE(KIND=PRINTER);
16900       OWN ARRAY L1[0:2],L2[0:4];
17000       AS:=NOARRAYS*(STARTFRQ-1+NOFRQS)*3;
17100       BS:=NOARRAYS*(STARTFRQ-1+NOFRQS);
17200       CS:=NOARRAYS;
17300       REPLACE POINTER(FMT) BY "F4.1";
17400       IF NOT FIRSTTIME THEN
17500       BEGIN
17600         REPLACE POINTER(L1) BY "TIME LAG (SEC.)";
17700         REPLACE POINTER(L2) BY "CORRELATION COEFFICIENT    ";
17800         FIRSTTIME:=TRUE;
17900       END;
18000       AINIT(1400);
18100       ASPEED(3);
18200       AORIG(300,200);
18300       PT:=*+1;REPLACE POINTER(AY) BY "PLOT NUMBER ",PT FOR 3 NUMERIC;
18400       ALAB(-275,410,AY,15,2,4);
18500       ABOX(0,0,14,15,75,50,1);
18600       ABOX(0,0,14,1,75,250,1);
18700       ASCA(-35,-25,75,0,0,10,14,1,2);
18800       ASCALE(-60,-5,0,50,-.5,.1,16,1,2,FMT,4);
18900       ALAB(360,-65,L1,15,1,2);
19000       ALAB(-70,100,L2,27,1,4);
19100       %
19200       %  THE ABOVE LABELS AND SCALES ARE THE SAME FOR ALL AUTOCORRELATION
19300       %  GRAPHS
19400       %  WRITE LABELS FOR EACH SPECIAL CASE
19500       %
19600       IF HEIGHTS THEN
19700       %   PLOT AS A FUNCTION OF POSITION
19800       BEGIN
19900         CASE TRENDCTR OF
20000         BEGIN
20100           0:REPLACE POINTER(TRENDLBL) BY "NO TREND REMOVAL";
20200           1:REPLACE POINTER(TRENDLBL) BY "LINEAR TREND REMOVAL";
20300           2:REPLACE POINTER(TRENDLBL) BY "PARABOLIC TREND REMOVAL";
20400         END;
20500         CASE DIRECTION OF
20600         BEGIN
20700           0:REPLACE POINTER(DIRNLBL) BY "LONGITUDINAL DIRECTION";
20800           1:REPLACE POINTER(DIRNLBL) BY "LATERAL DIRECTION";
20900           2:REPLACE POINTER(DIRNLBL) BY "VERTICAL DIRECTION";
21000         END;
21100         REPLACE P:POINTER(HEIGHTLBL) BY " HEIGHTS OF ANEMOMETERS ARE= ";
21200         FOR I:=0 STEP 1 UNTIL NOARRAYS-1 DO
21300         REPLACE P:P BY HEIGHT[I] FOR 4 NUMERIC,", ";
21400         REPLACE P-2 BY ".";
21500         REPLACE POINTER(FRQLBL) BY "SAMPLING FREQUENCY= ",ACTFREQ1516
21600         /(2**(FRQCTR-1))  FOR 5 NUMERIC," HZ";
21700         REPLACE POINTER(PLOTLABEL) BY "AUTOCORRELATION AS A FUNCTION OF
21800         HEIGHT";
21900         %  NOW WRITE THE LABELS
22000         ALAB(-280,20,PLOTLABEL,39,1,4);
22100         ALAB(-260,20,HEIGHTLBL,28+6*NOARRAYS,1,4);
22200         ALAB(-240,20,FRQLBL,28,1,4);
22300         ALAB(-220,20,TRENDLBL,22,1,4);
22400         ALAB(-200,20,DIRNLBL,22,1,4);
22500         %   LAG ARRAY STORED IN FILE FAULG
22600         READ(FAULG[FRQCTR-1],1024,X);
22700         FOR I:=0 STEP 1 UNTIL NOARRAYS-1 DO
22800         %   AUTOCORRELATION DATA ARRAY STORED IN FILE FAUT
22900         BEGIN READ(FAUT[AS*TRENDCTR+BS*DIRECTION+CS*
23000           (FRQCTR-1)+I],1024,Y);
23100           ALINED(X[*],Y[*],
23200           NOPTSOUT[FRQCTR-1],0,-.5,100,.2,2*I+4,2*I+4);END;
23300       END OF HEIGHTS BLOCK;
23400       %
23500       %
23600       IF FREQS THEN
23700       %   PLOT AS A FUNCTION OF PROCESSING FREQUENCY
23800       BEGIN
23900         CASE TRENDCTR OF
24000         BEGIN
24100           0:REPLACE POINTER(TRENDLBL) BY "NO TREND REMOVAL";
24200           1:REPLACE POINTER(TRENDLBL) BY "LINEAR TREND REMOVAL";
24300           2:REPLACE POINTER(TRENDLBL) BY "PARABOLIC TREND REMOVAL";
24400         END;
24500         %
24600         CASE DIRECTION OF
```

```
24700         BEGIN
24800           0:REPLACE POINTER(DIRNLBL) BY "LONGITUDINAL DIRECTION";
24900           1:REPLACE POINTER(DIRNLBL) BY "LATERAL DIRECTION";
25000           2:REPLACE POINTER(DIRNLBL) BY "VERTICAL DIRECTION";
25100         END;
25200         P:=POINTER(FRQLBL[0]);
25300         REPLACE P:POINTER(FRQLBL) BY "SAMPLING FREQUENCIES ARE= ";
25400         FOR I:=STARTFRQ-1 STEP 1 UNTIL STARTFRQ-1+NOFRQS-1 DO
25500         REPLACE P:P BY SAMPFRQS[I] FOR 5 NUMERIC,", ";
25600         REPLACE P-2 BY " ";
25700         REPLACE P:P BY "HZ";
25800         REPLACE POINTER(HEIGHTLBL) BY "HEIGHT OF ORTHOGONAL ARRAY= ",
25900         HEIGHT[HGHTCTR-1] FOR 4 NUMERIC," METRES";
26000         REPLACE POINTER(PLOTLABEL) BY "AUTOCORRELATION AS A FUNCTION OF
26100         SAMPLING FREQUENCY";
26200         ALAB(-280,20,PLOTLABEL,51,1,4);
26300         ALAB(-260,20,FRQLBL,28+7*NOFRQS,1,4);
26400         ALAB(-240,20,HEIGHTLBL,39,1,4);
26500         ALAB(-220,20,TRENDLBL,23,1,4);
26600         ALAB(-200,20,DIRNLBL,22,1,4);
26700         FOR I:=STARTFRQ-1 STEP 1 UNTIL STARTFRQ-1+NOFRQS-1 DO
26800         BEGIN READ(FAULG[I],1024,X);
26900           READ(FAUT[AS*TRENDCTR+BS*DIRECTION+CS*I+HGHTCTR-1],
27000           1024,Y);
27100           ALINED(X[*],Y[*],
27200           NOPTSOUT[I],0,-.5,100,.2,2*I+5,2*I+5);END;
27300       END OF FREQS BLOCK;
27400       %
27500       %
27600       %  TREND REMOVAL BLOCK;
27700       %
27800       IF TRENDS THEN
27900       %   PLOT AS A FUNCTION OF TYPE OF TREND REMOVAL
28000       BEGIN
28100         CASE DIRECTION OF
28200         BEGIN
28300           0:REPLACE POINTER(DIRNLBL) BY "LONGITUDINAL DIRECTION";
28400           1:REPLACE POINTER(DIRNLBL) BY "LATERAL DIRECTION";
28500           2:REPLACE POINTER(DIRNLBL) BY "VERTICAL DIRECTION";
28600         END;
28700         REPLACE POINTER(FRQLBL) BY "SAMPLING FREQUENCY= ",
28800         ACTFREQ1516/(2**(FRQCTR-1)) FOR 5 NUMERIC," HZ";
28900         REPLACE POINTER(HEIGHTLBL) BY "HEIGHT OF ORTHOGONAL ARRAY= ",
29000         HEIGHT[HGHTCTR-1] FOR 4 NUMERIC," METRES";
29100         REPLACE POINTER(TRENDLBL) BY "TREND REMOVALS ARE- NONE LINEAR, PAR
29200         ABOLIC BY LEAST SQUARES";
29300         REPLACE POINTER(PLOTLABEL) BY "AUTOCORRELATION AS A FUNCTION OF
29400         TREND REMOVAL";
29500         ALAB(-280,20,PLOTLABEL,46,1,4);
29600         ALAB(-260,20,FRQLBL,28,1,4);
29700         ALAB(-240,20,HEIGHTLBL,39,1,4);
29800         ALAB(-220,20,TRENDLBL,60,1,4);
29900         ALAB(-200,20,DIRNLBL,22,1,4);
30000         READ(FAULG[FRQCTR-1],1024,X);
30100         FOR I:=0,1,2 DO
30200         BEGIN READ(FAUT[AS*I+BS*DIRECTION+CS*(FRQCTR-1)
30300           +HGHTCTR-1],1024,Y);
30400           ALINED(X[*],Y[*],
30500           NOPTSOUT[FRQCTR-1],0,-.5,100,.2,3*I+5,3*I+5);END;
30600       END OF TRENDS BLOCK;
30700       AEND;

30800     END OF PROCEDURE P L O T A U T O ;
30900     %   THIS PROCEDURE SELECTS THE AUTOCORRELATION DATA FOR THE
31000     %   FIRST 135 SECONDS OF LAG,AVERAGES IT AND STORES IT
31100     %   IN FILE FAUT.THE CORRESPONDING LAG VALUES ARE STORED
31200     %   IN FILE FAULG.THE DATA IS ORGINALLY CONTAINED IN
31300     %   ARRAYS AINR,AINI FROM AN INVERSE FOURIER TRANSFORM
31400     %   OF THE POWER SPECTRUM

31500     PROCEDURE AVERAGEAUTO(AINR,AINI,TEMPFRQ,NUM,TRENDCTR,DIRNCTR,
31600     FRQCTR1,HGHTCTR1,NOARRAYS,STARTFRQ,NOFRQS,TEMPNIN);
31700     VALUE TEMPFRQ,TRENDCTR,DIRNCTR,FRQCTR1,HGHTCTR1,
31800     NOARRAYS,STARTFRQ,NOFRQS;
31900     REAL NUM;
32000     REAL TEMPFRQ;
32100     ARRAY AINR,AINI[*];
32200     INTEGER TRENDCTR,DIRNCTR,FRQCTR1,HGHTCTR1,NOARRAYS,
32300     STARTFRQ,NOFRQS,TEMPNIN;
32400     BEGIN
32500       REAL TOT;
32600       ARRAY AUTOOUT,LAGAXIS[0:1023];
32700       INTEGER AS,BS,CS;
32800       OWN INTEGER SFQ;
32900       INTEGER I,J;
33000       INTEGER SMALL,BIG,XINCR,TEMP;
33100       % CALCULATE COUNTERS FOR ADDRESSING DATA FILE
33200       AS:=NOARRAYS*(STARTFRQ-1+NOFRQS)*3;
33300       BS:=NOARRAYS*(STARTFRQ-1+NOFRQS);
33400       CS:=NOARRAYS;
33500       % CORRECT VALUES BECAUSE FFT AVERAGES OVER TEMPNIN, NOT TEMPNIN
33600       % -LAG
33700       FOR I:=0 STEP 2 UNTIL TEMPFRQ*180 DO BEGIN
33800         AINR[I/2]:=**TEMPNIN/(TEMPNIN-I);
33900         AINI[I/2]:=**TEMPNIN/(TEMPNIN-I-1);
```

```
34000       END;
34100       IF TEMPFRQ>8 THEN
34200       BEGIN  ARRAY SAVE[0:128*TEMPFRQ];
34300         FOR I:=0 STEP 2 UNTIL 128*TEMPFRQ-1 DO BEGIN
34400           SAVE[I]:=AINR[I/2];  SAVE[I+1]:=AINI[I/2];  END;
34500         TEMP:=TEMPFRQ/8;
34600         SMALL:=TEMP/2;BIG:=3*TEMP/2-1;
34700         AUTOOUT[0]:=AINR[0];
34800         FOR I:=1 STEP 1 UNTIL 1023 DO
34900         FOR J:=SMALL STEP 1 UNTIL BIG DO
35000         AUTOOUT[I]:=*+SAVE[(I-1)*TEMP +J]/TEMP;
35100         FOR I:=0 STEP 1 UNTIL 1023 DO LAGAXIS[I]:=I;
35200         NUM:=1024;
35300       END
35400       ELSE
35500       BEGIN
35600         XINCR:=8/TEMPFRQ;
35700         TEMP:=1024/XINCR-1;
35800         FOR I:=0 STEP 2 UNTIL TEMP-1 DO  BEGIN
35900           AUTOOUT[I]:=AINR[I/2];  AUTOOUT[I+1]:=AINI[I/2]; END;
36000         FOR I:=0 STEP 1 UNTIL TEMP DO LAGAXIS[I]:=XINCR*I;
36100         NUM:=1024/XINCR;
36200       END;
36300       % WRITE DATA TO A FILE TO SAVE FOR PLOTTING
36400       WRITE(FAUT[AS*TRENDCTR+BS*DIRNCTR+CS*FRQCTR1+HGHTCTR1],
36500       1024,AUTOOUT);
36600       IF SFQ=0 OR SFQ NEQ FRQCTR1 THEN BEGIN
36700         WRITE(FAULG[FRQCTR1],1024,LAGAXIS);
36800         SFQ:=FRQCTR1;END;
36900       %   INTEGRATE THE AREA UNDER THE AUTOCORRELATION CURVE
37000       I:=0;TOT:=0; DO BEGIN
37100         TOT:=*+AINR[I]+AINI[I];I:=*+1; END
37200       %   INTEGRATE UNTIL THE CORRELATION IS 5%
37300       UNTIL AINR[I] <.05  OR AINI[I] <.05;
37400       WRITE(LP,<"AUTOCORRELATION INTEGRATED TO 5 %",F10.5," WHICH OCCURRS"
37500       " AT",F10.5," SECS LAG">,TOT*16/(TEMPFRQ*15),2*I*16/(TEMPFRQ*15
37600       ));
37700       DO BEGIN TOT:=*+AINR[I]+AINI[I]; I:=*+1;END UNTIL
37800       %   INTEGRATE TO FIRST CROSSING OF LAG AXIS
37900       AINR[I] <-.001 OR AINI[I] <-.001;
38000       WRITE(LP,<"AUTOC TO FIRST CROSSING",F10.5," AT",F10.5," SECS LAG">,
38100       TOT*16/(TEMPFRQ*15),2*I*16/(TEMPFRQ*15));
38200       DO BEGIN TOT:=*+AINR[I]+AINI[I];I:=*+1;END UNTIL
38300       %   INTEGRATE TO SECOND CROSSING OF LAG AXIS
38400       AINR[I]>.001 OR AINI[I] >.001;
38500       WRITE(LP,<"AUTOC TO 2ND CROSSING",F10.5," AT",F10.5," SECS LAG">,
38600       TOT*16/(TEMPFRQ*15),2*I*16/(TEMPFRQ*15));
38700       DO BEGIN TOT:=*+AINR[I]+AINI[I];I:=*+1; END UNTIL
38800       %   INTEGRATE TO THIRD CROSSING OF LAG AXIS
38900       AINR[I]<-.001 OR AINI[I] < -.001;
39000       WRITE(LP,<"AUTOC TO 3RD CROSSING",F10.5," AT",F10.5," SECS LAG">,
39100       TOT*16/(TEMPFRQ*15),2*I*16/(15*TEMPFRQ));
39200       DO BEGIN TOT:=*+AINR[I]+AINI[I];I:=*+1;END UNTIL
39300       I>TEMPNIN*(.1)/2;
39400       %   INTEGRATE TO 10% OF THE FILE LENGTH
39500       WRITE(LP,<"AUTOC TO 10% OF THE RECORD LENGTH=",F10.5," AT",F10.5,
39600       " SECS LAG">,TOT*16/(15*TEMPFRQ),2*I*16/(15*TEMPFRQ));

39700     END OF PROCEDURE A V E R A G E A U T O ;
39800     %
39900     %   THIS PROCEDURE PLOTS THE POWER SPECTRAL DENSITY AS A FUNCTION
40000     %   OF (1) POSITION OF EACH ARRAY OF ANEMOMETERS,
40100     %   (2) FREQUENCY AT WHICH THE DATA WAS PROCESSED,
40200     %   (3) TYPE OF TREND REMOVAL

40300     PROCEDURE PLOTPOWER(NOPTSOUT,HEIGHT,NOARRAYS,
40400     ACTFREQ1516,NOFRQS,SAMPFRQS,HEIGHTS,FREQS,TRENDS,DIRECTION,TRENDCT
40500     R,FRQCTR,HGHTCTR,VSNFRQ,STARTFRQ);
40600     VALUE NOARRAYS,ACTFREQ1516,NOFRQS,DIRECTION,TRENDCTR,FRQCTR,
40700     HGHTCTR,STARTFRQ;
40800     INTEGER STARTFRQ;
40900     ARRAY NOPTSOUT,HEIGHT,
41000     SAMPFRQS[*];
41100     INTEGER NOARRAYS,NOFRQS,DIRECTION,TRENDCTR,FRQCTR,HGHTCTR;
41200     BOOLEAN HEIGHTS,FREQS,TRENDS,VSNFRQ;
41300     REAL ACTFREQ1516;
41400     BEGIN
41500       INTEGER AS,BS,CS;ARRAY X,Y[0:40];
41600       ARRAY TRENDLBL[0:10],DIRNLBL[0:3],HEIGHTLBL[0:5+NOARRAYS],
41700       FRQLBL[0:5+NOFRQS],PLOTLABEL[0:8];
41800       INTEGER I,J;
41900       POINTER P;
42000       OWN BOOLEAN FIRSTTIME;
42100       FILE KARD(KIND=READER),LINE(KIND=PRINTER);
42200       OWN ALPHA ARRAY L1[0:0],L2[0:5,0:1],L3[0:4],L4[0:3],L5[0:5];
42300       ARRAY P1,Q[0:5],START[2:9];
42400       ARRAY TYPELBL[0:5];
42500       %
42600       AS:=NOARRAYS*(STARTFRQ-1+NOFRQS)*3;
42700       BS:=NOARRAYS*(STARTFRQ-1+NOFRQS);
42800       CS:=NOARRAYS;
42900       AINIT(1500);
43000       IF NOT FIRSTTIME THEN
43100       BEGIN
43200         REPLACE POINTER(TYPELBL) BY "USE WET INK, .3MM NIB PLEASE";
```

```
43300         ATYPE(TYPELBL,29);
43400         FOR I:=0 STEP 1 UNTIL 5 DO
43500         REPLACE POINTER(L2[I,*]) BY " 10**",-4+I FOR 2 NUMERIC;
43600         REPLACE POINTER(L3) BY "FREQUENCY IN CYCLES/SECOND";
43700         REPLACE POINTER(L4) BY "POWER*FREQUENCY/RMS**2";
43800         REPLACE POINTER(L5) BY "NON-DIMENSIONALISED FREQUENCY NZ/U";
43900         REPLACE POINTER(L1) BY "I";
44000         FIRSTTIME:=TRUE;
44100       END;
44200       %  CALCULATE SOME NUMBERS FOR SCALES AND LABELS. PLOT THEM.
44300       FOR I:=0 STEP 1 UNTIL 5 DO BEGIN P1[I]:=I;Q[I]:=0;END;
44400       FOR I:=2 STEP 1 UNTIL 9 DO START[I]:=-LOG(I);
44500       ASPEED(3);
44600       AORIG(300,300);
44700       PT:=*+1;REPLACE POINTER(AY) BY "PLOT NUMBER ",PT FOR 3 NUMERIC;
44800       ALAB(-275,410,AY,15,2,4);
44900       ABOX(0,0,5,3,200,200,1);
45000       ALINEC(P1,Q,6,0,0,.5,1,L1[0],-5,-5,1,2);
45100       FOR I:=2 STEP 1 UNTIL 9 DO
45200       ALINEC(P1,Q,5,START[I],0,.5,1,L1[0],-5,-5,1,2);
45300       FOR I:=1 STEP 1 UNTIL 9 DO
45400       BEGIN
45500         J:=ENTIER(LOG(I)*200-45);
45600         ASCA(J,-20,200,0,I,0,5,1,2);
45700       END;
45800       FOR I:=0 STEP 1 UNTIL 5 DO
45900       ALAB(200*I-35,-35,L2[I,*],7,1,2);
46000       IF VSNFRQ THEN ALAB(230,-65,L5,34,2,2)   ELSE
46100       ALAB(240,-65,L3,26,2,2);
46200       FOR I:=0,1,2,3 DO BEGIN P1[I]:=0;Q[I]:=I;END;
46300       ALINEC(P1,Q,4,0,0,1,.5,L1[0],-5,5,1,0);
46400       FOR I:=2 STEP 1 UNTIL 9 DO
46500       ALINEC(P1,Q,3,0,START[I],1,.5,L1[0],-5,5,1,0);
46600       FOR I:=1 STEP 1 UNTIL 9 DO
46700       BEGIN
46800         J:=ENTIER(LOG(I)*200);
46900         ASCA(-60,J,0,200,I,0,3,1,2);
47000       END;
47100       FOR I:=1 STEP 1 UNTIL 4 DO
47200       ALAB(-95,200*(I-1),L2[I,*],7,1,2);
47300       ALAB(-105,80,L4,22,2,4);
47400       %
47500       %   THE AXES, SCALES AND LABELS ARE NOW DRAWN
47600       %  DECIDE WHAT TO PLOT. DRAW GRAPH.
47700       %
47800       IF HEIGHTS THEN
47900       %   PLOT AS A FUNCTION OF POSITION OF ARRAY
48000       BEGIN
48100         CASE TRENDCTR OF
48200         BEGIN
48300           0:REPLACE POINTER(TRENDLBL) BY "NO TREND REMOVAL";
48400           1:REPLACE POINTER(TRENDLBL) BY "LINEAR TREND REMOVAL";
48500           2:REPLACE POINTER(TRENDLBL) BY "PARABOLIC TREND REMOVAL";
48600         END;
48700         CASE DIRECTION OF
48800         BEGIN
48900           0:REPLACE POINTER(DIRNLBL) BY "LONGITUDINAL DIRECTION";
49000           1:REPLACE POINTER(DIRNLBL) BY "LATERAL DIRECTION";
49100           2:REPLACE POINTER(DIRNLBL) BY "VERTICAL DIRECTION";
49200         END;
49300         REPLACE P:POINTER(HEIGHTLBL) BY " HEIGHTS OF ANEMOMETERS ARE= ";
49400         FOR I:=0 STEP 1 UNTIL NOARRAYS-1 DO
49500         REPLACE P:P BY HEIGHT[I] FOR 4 NUMERIC,", ";
49600         REPLACE P-2 BY ".";
49700         REPLACE POINTER(FRQLBL) BY "SAMPLING FREQUENCY= ",ACTFREQ1516
49800         /(2**(FRQCTR-1))  FOR 5 NUMERIC," HZ";
49900         REPLACE POINTER(PLOTLABEL) BY "POWER SPECTRA AS A FUNCTION OF HEIG
50000         HT";
50100         %  NOW WRITE THE LABELS
50200         ALAB(-280,20,PLOTLABEL,37,1,4);
50300         ALAB(-260,20,HEIGHTLBL,28+6*NOARRAYS,1,4);
50400         ALAB(-240,20,FRQLBL,25,1,4);
50500         ALAB(-220,20,TRENDLBL,23,1,4);
50600         ALAB(-200,20,DIRNLBL,22,1,4);
50700         %   SPECTRA DATA STORED IN FILE FAVSP,FREQUENCY AXIS DATA
50800         %   STORED IN FILE FFQAXIS
50900         FOR I:=0 STEP 1 UNTIL NOARRAYS-1 DO
51000         BEGIN READ(FAVSP[AS*TRENDCTR+BS*DIRECTION
51100           +CS*(FRQCTR-1)+I],41,Y);
51200           READ(FFQAXIS[CS*(FRQCTR-1)+I],41,X);
51300           ALINED(X(*),Y[*],NOPTSOUT[FRQCTR-1],-4,-3,.5,.5,
51400           2*I+4,2*I+4);END;
51500       END OF HEIGHTS BLOCK;
51600       %
51700       %
51800       IF FREQS THEN
51900       %   PLOT AS A FUNCTION OF PROCESSING FREQUENCY
52000       BEGIN
52100         CASE TRENDCTR OF
52200         BEGIN
52300           0:REPLACE POINTER(TRENDLBL) BY "NO TREND REMOVAL";
52400           1:REPLACE POINTER(TRENDLBL) BY "LINEAR TREND REMOVAL";
52500           2:REPLACE POINTER(TRENDLBL) BY "PARABOLIC TREND REMOVAL";
52600         END;
52700         CASE DIRECTION OF
```

```
52800         BEGIN
52900           0:REPLACE POINTER(DIRNLBL) BY "LONGITUDINAL DIRECTION";
53000           1:REPLACE POINTER(DIRNLBL) BY "LATERAL DIRECTION";
53100           2:REPLACE POINTER(DIRNLBL) BY "VERTICAL DIRECTION";
53200         END;
53300         P:=POINTER(FRQLBL[0]);
53400         REPLACE P:POINTER(FRQLBL) BY "SAMPLING FREQUENCIES ARE= ";
53500         FOR I:=STARTFRQ-1 STEP 1 UNTIL STARTFRQ-1+NOFRQS-1 DO
53600         REPLACE P:P BY SAMPFRQS[I] FOR 5 NUMERIC,", ";
53700         REPLACE P-2 BY " ";
53800         REPLACE P:P BY "HZ";
53900         REPLACE POINTER(HEIGHTLBL) BY "HEIGHT OF ORTHOGONAL ARRAY= ",
54000         HEIGHT[HGHTCTR-1] FOR 4 NUMERIC," METRES";
54100         REPLACE POINTER(PLOTLABEL) BY "POWER SPECTRA AS A FUNCTION OF SAMP
54200         LING FREQUENCY";
54300         %  NOW WRITE THE LABELS
54400         ALAB(-280,20,PLOTLABEL,49,1,4);
54500         ALAB(-260,20,FRQLBL,28+7*NOFRQS,1,4);
54600         ALAB(-240,20,HEIGHTLBL,32,1,4);
54700         ALAB(-220,20,TRENDLBL,23,1,4);
54800         ALAB(-200,20,DIRNLBL,22,1,4);
54900         FOR I:=STARTFRQ-1 STEP 1 UNTIL STARTFRQ-1+NOFRQS-1 DO
55000         BEGIN READ(FFQAXIS[CS*I+HGHTCTR-1],41,X);
55100           READ(FAVSP[AS*TRENDCTR+BS*DIRECTION+CS*I
55200           +HGHTCTR-1],41,Y);
55300           ALINED(X[*],Y[*],NOPTSOUT[I],-4,-3,.5,.5,
55400           2*I+4,2*I+4);END;
55500       END OF FREQS BLOCK;
55600       %
55700       %
55800       %  TREND REMOVAL BLOCK;
55900       %
56000       IF TRENDS THEN
56100       %   PLOT AS A FUNCTION OF TYPE OF TREND REMOVAL
56200       BEGIN
56300         CASE DIRECTION OF
56400         BEGIN
56500           0:REPLACE POINTER(DIRNLBL) BY "LONGITUDINAL DIRECTION";
56600           1:REPLACE POINTER(DIRNLBL) BY "LATERAL DIRECTION";
56700           2:REPLACE POINTER(DIRNLBL) BY "VERTICAL DIRECTION";
56800         END;
56900         REPLACE POINTER(FRQLBL) BY "SAMPLING FREQUENCY= ",
57000         ACTFREQ1516/(2**(FRQCTR-1)) FOR 5 NUMERIC," HZ";
57100         REPLACE POINTER(HEIGHTLBL) BY "HEIGHT OF ORTHOGONAL ARRAY= ",
57200         HEIGHT[HGHTCTR-1] FOR 4 NUMERIC," METRES";
57300         REPLACE POINTER(PLOTLABEL) BY "POWER SPECTRA AS A FUNCTION OF TREN
57400         D REMOVAL";
57500         %  WRITE THE LABELS ON THE PLOT
57600         ALAB(-280,20,PLOTLABEL,44,1,4);
57700         REPLACE POINTER(TRENDLBL) BY "TREND REMOVALS ARE- NONE, LINEAR, PA
57800         RABOLIC BY LEAST SQUARES";
57900         ALAB(-260,20,TRENDLBL,60,1,4);
58000         ALAB(-240,20,FRQLBL,28,1,4);
58100         ALAB(-220,20,HEIGHTLBL,39,1,4);
58200         ALAB(-200,20,DIRNLBL,22,1,4);
58300         READ(FFQAXIS[CS*(FRQCTR-1)+HGHTCTR-1],41,X);
58400         FOR I:=0,1,2 DO
58500         BEGIN READ(FAVSP[AS*I+BS*DIRECTION+CS*(FRQCTR-1)
58600           +HGHTCTR-1],41,Y);
58700           ALINED(X[*],Y[*],NOPTSOUT[FRQCTR-1],-4,-3,.5,.5,
58800           3*I+5,3*I+5);END;
58900       END OF TRENDS BLOCK;
59000       AEND;
59100
59200     END OF PPROCEDURE P L O T P O W E R ;
59300     %
59400     %   THIS PROCEDURE NORMALISES THE DATA BY REMOVING THE MEAN AND
59500     %   DIVIDING BY THE STANDARD DEVIATION OF THE DATA
59600     %   IT WILL ALSO APPLY A DATA WINDOW TO THE DATA,THE DATA
59700     %   WINDOW BEING A RAISED COSINE BELL ON THE FIRST 10% OF
59800     %   THE DATA, AND THE LAST 10%. ANY OTHER TYPE OF TAPER COULD
59900     %   BE INSERTED HERE IF DESIRED.

60000     PROCEDURE COSINETAPER(ARYR,ARYI,TEMPNIN,COSTAPER,
60100     IFAUTO,STDDEV,XM,J);
60200
60300     VALUE TEMPNIN; INTEGER TEMPNIN;
60400
60500     ARRAY STDDEV,XM[*];
60600     INTEGER J;
60700     BOOLEAN COSTAPER,IFAUTO;
60800     ARRAY ARYR,ARYI[*];
60900     BEGIN
61000       INTEGER I,MAX;
61100       INTEGER TEMPNIN1,T2,T2M1;REAL R1,R2;
61200       REAL TEMP;
61300       T2:=TEMPNIN/2;  T2M1:=T2-1;
61400       TEMPNIN1:=TEMPNIN-1;
61500       MAX:= ENTIER(TEMPNIN/10)-1;
61600       IF (MAX MOD 2)=0 THEN ELSE MAX:=*+1;
61700       BEGIN
61800         IF STDDEV[J]=0 THEN  BEGIN
61900           REPLACE POINTER(ARYR[0]) BY 0 FOR T2 WORDS;
62000           REPLACE POINTER(ARYI[0]) BY 0 FOR T2 WORDS; END ELSE
62100         FOR I:=0 STEP 1 UNTIL T2M1 DO BEGIN
```

```
62200           ARYR[I]:=(ARYR[I]-XM[J])/STDDEV[J];
62300           ARYI[I]:=(ARYI[I]-XM[J])/STDDEV[J];  END;
62400       END;
62500       IF IFAUTO AND COSTAPER THEN
62600       FOR I:=0 STEP 1024 UNTIL T2M1 DO BEGIN
62700         WRITE(FAULG[12+I/1024],1024,ARYR[I]);
62800         WRITE(FAULG[13+I/1024+T2/1024],1024,ARYI[I]);
62900       END;
63000       IF COSTAPER THEN
63100       %   THIS IS THE COSINE TAPER BLOCK
63200       FOR I:=0 STEP 2 UNTIL  MAX-1 DO
63300       BEGIN
63400         R1:=(COS(1.570796*(1-I/MAX)))**2;
63500         ARYR[I/2]:=**R1;ARYI[T2M1-I/2]:=**R1;
63600         R2:=(COS(1.570796*(1-(I+1)/MAX)))**2;
63700         ARYI[I/2]:=**R2;
63800         ARYR[T2M1-I/2]:=**R2;
63900       END;

64000     END OF PROCEDURE C O S I N E T A P E R ;
64100     COMMENT
64200     THIS PROCEDURE PUTS THE SPECTRAL COMPONENT DATA CONTAINED
64300     IN THE FORMAL PARAMETER "INARY" INTO A FORM SUITABLE FOR P
64400     PLOTTING. THE DC COMPONENT IS NOT PLOTTED. THE 1ST 4 COMPONENTS
64500     HAVE NO AVEAGING. THE REST OF THE SPECTRAL COMPONENTS ARE
64600     AVERAGED INTO EQUAL PARTIAL OCTAVE BANDWIDTHS WITH
64700     F-UPPER/F-LOWER =1.3333.              ;

64800     PROCEDURE AVSPECTRA(INARY,HGHT,VEL,SR,N,VSNFRQ,NOPTSOUT,
64900     TRENDCTR,DIRNCTR,FRQCTR1,HGHTCTR1,NOARRAYS,STARTFRQ,NOFRQS);
65000     VALUE SR,N,HGHT,VEL,VSNFRQ,TRENDCTR,DIRNCTR,FRQCTR1,
65100     HGHTCTR1,NOARRAYS,STARTFRQ,NOFRQS;
65200     ARRAY INARY[*];
65300     REAL HGHT,VEL,SR;
65400     BOOLEAN VSNFRQ;
65500     INTEGER N,NOPTSOUT,TRENDCTR,DIRNCTR,FRQCTR1,HGHTCTR1,NOARRAYS,
65600     STARTFRQ,NOFRQS;
65700     BEGIN
65800       ARRAY OUTARY,FRQOUT[0:40];
65900       INTEGER AS,BS,CS;
66000       REAL T,FUND,LGSR2,RE,R,X,X1;
66100       INTEGER N2,I,NO,J,CP,NO1;
66200       ARRAY C[0:41]; OWN INTEGER FIRST,OF,OH;
66300       IF FIRST=0 THEN BEGIN FIRST:=OF:=OH:=100;END;
66400       % CALCULATE COUNTERS FOR ADDRESSING DATA FILE
66500       CS:=NOARRAYS;
66600       BS:=CS*(STARTFRQ-1+NOFRQS);
66700       AS:=BS*3;
66800       % CALCULATE LENGTH OF RECORDING
66900       T:=N/SR;     % T IS LENGTH IN SECS
67000       % CALC FUNDAMENTAL FREQUENCY
67100       FUND:=1/T;
67200       % CALC POWER*FREQUENCY
67300       N2:=N/2;
67400       FOR I:=0 STEP 1 UNTIL N2 DO INARY[I]:=**I*FUND;
67500       % CALC THE CUT OFF ARRAY ELEMENT NOS FOR AVERAGING OVER
67600       % FREQUENCY
67700       % FIRST 4 POINTS NO AVERAGING
67800       LGSR2:=LOG(SR/2); X:=LOG(4*FUND); R:=LGSR2-X;
67900       RE:=0; I:=0;
68000       DO BEGIN
68100         C[I]:=ENTIER(4*10**RE);
68200         I:=*+1; RE:=*+.125;
68300       END UNTIL RE>R;
68400       C[I]:=N/2;
68500       NO:=I-1;
68600       NOPTSOUT:=4+1+NO;
68700       % PERFORM AVERAGING OVER FREQUENCY
68800       FOR I:=0 STEP 1 UNTIL NO DO
68900       BEGIN
69000         CP:=C[I+1]-C[I];
69100         FOR J:=C[I]+1 STEP 1 UNTIL C[I+1] DO
69200         OUTARY[I+4]:=*+INARY[J]/CP;
69300         OUTARY[I+4]:=LOG(OUTARY[I+4]);   END;
69400       % FIRST 4 POINTS HAVE NO AVERAGING
69500       FOR I:=1,2,3,4 DO
69600       OUTARY[I-1]:=LOG(INARY[I]);
69700       % CALC FREQ SCALE
69800       FOR I:=1,2,3,4 DO FRQOUT[I-1]:=LOG(I*FUND);
69900       % FREQ SCALE NOW INCREMENTED IN CONSTANT AMOUNTS
70000       %OF .125
70100       X1:=X+.0625; NO1:=NO-1;
70200       FOR I:=0 STEP 1 UNTIL NO1 DO
70300       FRQOUT[4+I]:=X1+.125*I;
70400       FRQOUT[4+NO]:=(FRQOUT[3+NO]+.0625+LGSR2)/2;
70500       %   IF VSNFRQ IS TRUE THE SPECTRUM WILL BE PLOTTED AGAINST
70600       %   DIMENSIONLESS FREQUENCY FREQ*HEIGHT/AV.VELOCITY
70700       %   ALTER FREQ SCALE ONLY IS VSNFRQ TRUE BY ALLOWING FOR
70800       % FACT THAT POWER SPECTRA VS NON-DIMENSIONALISED FREQUENCY
70900       % IS PLOTTED VS LOG(FREQ*HEIGHT/VEL)
71000       IF VSNFRQ THEN BEGIN
71100         RE:=LOG(HGHT/VEL);  NO1:=NO+4;
71200         FOR I:=0 STEP 1 UNTIL NO1 DO
71300         FRQOUT[I]:=*+RE;
71400       END;
```

```
71500       % WRITE DATA TO A FILE FOR LATER PLOTTING
71600       %   SPECTRUM ARRAY WRITTEN TO FILE FAVSP
71700       WRITE(FAVSP[AS*TRENDCTR+BS*DIRNCTR+CS*FRQCTR1+
71800       HGHTCTR1],41,OUTARY);
71900       IF FRQCTR1 NEQ OF OR HGHTCTR1 NEQ OH THEN BEGIN
72000         %   FREQ AXIS ARRAY WRITTEN TO FILE FFQAXIS
72100         WRITE(FFQAXIS[CS*FRQCTR1+HGHTCTR1],41,FRQOUT);
72200         OF:=FRQCTR1;OH:=HGHTCTR1;   END;

72300     END OF PROCEDURE A V S P E C T R A;
72400     %
72500     %
72600     %
72700     %
72800     %
72900     %   THIS PROCEDURE PLOTS CROSS-CORRELATIONS. THERE IS ONE GRAPH
73000     %   FOR EVERY PAIR OF DATA STREAMS CORRELATED,BUT THE ONE
73100     %   GRAPH MAY HAVE CURVES FROM ALL TYPES OF TREND REMOVAL
73200     %   WHICH HAVE BEEN USED FOR THE SAME CORRELATION PAIR.
73300     %   CORRELATIONS ARE PLOTTED FOR MAXIMUM LAGS OF +OR-68 SECS

73400     PROCEDURE PLOTCROSSCOR(CSR,CSI,CORFRQ,CROSS,ACTFREQ1516,
73500     TRENDCTR,ACTFRQ,NIN,LX,CNTRD,CLTRD,CPTRD);
73600     %
73700     %
73800     VALUE CORFRQ,ACTFREQ1516,TRENDCTR,ACTFRQ,NIN,LX;
73900     INTEGER CORFRQ,TRENDCTR,ACTFRQ,NIN,LX;
74000     REAL ACTFREQ1516;
74100     ARRAY CSR,CSI,CROSS[*];
74200     BOOLEAN CNTRD,CLTRD,CPTRD;
74300     BEGIN
74400       INTEGER NO,NUM,TEMP,SMALL,BIG,I,J,XINCR  ;
74500       REAL SAM,ISAM;
74600       ARRAY CROSSOUT[0:1024],TRENDLBL[0:3],CORLBL1[0:6],FR1[0:8],
74700       FR2[0:8],L1[0:2],L2[0:4];
74800       ARRAY CORLBL2[0:9];
74900       POINTER P;
75000       ARRAY FMT[0:0];
75100       INTEGER T2;
75200       REAL REEL;
75300       ARRAY XD[0:1024]; LABEL LAB;
75400       % CALCULATE NUMBER OF POINTS IN THE ARRAYS CSR,CSI
75500       NO:=NIN/2**(CORFRQ-1);
75600       T2:=NO/2;
75700       REPLACE POINTER(FMT) BY "F4.1";
75800       % CALCULATE THE GENERATED SAMPLING FREQUENCY
75900       SAM:=ACTFREQ1516/2**(CORFRQ-1);
76000       % CALCULATE APPROX INTEGER SAMPLING FREQUENCY
76100       ISAM:=ACTFRQ/2**(CORFRQ-1);
76200       TEMP:=ISAM/8;
76300       %   SET UP A DATA ARRAY FOR PLOTTING. THE DATA TO BE PLOTTED, FOR
76400       %   THE SHORT LAGS CONSIDERED, IS CONTAINED IN THE EXTREME
76500       %   ENDS OF THE ARRAYS CSR AND CSI.
76600       IF ISAM>8 THEN
76700       BEGIN
76800         ARRAY S1[NO-512*TEMP:NO],S2[0:513*TEMP);
76900         SMALL:=TEMP/2;BIG:=3*TEMP/2-1;
77000         FOR I:=0 STEP 2 UNTIL 512*TEMP-TEMP/2-2 DO BEGIN
77100           S1[NO-512*TEMP+TEMP/2+I]:=CSR[NO/2-256*TEMP+TEMP/4+I/2];
77200           S1[NO-512*TEMP+TEMP/2+I+1]:=CSI[NO/2-256*TEMP+TEMP/4+I/2];END;
77300         FOR I:=0 STEP 1 UNTIL 512.5*TEMP DO BEGIN
77400           S2[I]:=CSR[I/2];   S2[I+1]:=CSI[I/2]; END;
77500         FOR I:=0 STEP 1 UNTIL 510 DO
77600         FOR J:=SMALL STEP 1 UNTIL BIG DO
77700         CROSSOUT[I]:=*+S1[NO-(512-I)*TEMP+J]/TEMP;
77800         FOR J:=SMALL STEP 1 UNTIL TEMP-1 DO
77900         CROSSOUT[511]:=*+S1[NO-TEMP+J]/TEMP;
78000         FOR J:=TEMP STEP 1 UNTIL BIG DO
78100         CROSSOUT[511]:=*+S2[J-TEMP]/TEMP;
78200         FOR I:=0 STEP 1 UNTIL 511 DO
78300         FOR J:=SMALL STEP 1 UNTIL BIG DO
78400         CROSSOUT[512+I]:=*+S2[I*TEMP+J]/TEMP;
78500         NUM:=1024;XINCR:=1;
78600         FOR I:=0 STEP 1 UNTIL 1024 DO XD[I]:=I;
78700       END
78800       ELSE
78900       BEGIN
79000         XINCR:=8/ISAM;
79100         TEMP:=1024/XINCR;
79200         FOR I:=0 STEP 2 UNTIL TEMP/2-1 DO BEGIN
79300           CROSSOUT[I]:=CSR[T2-(TEMP/4-I/2)];
79400           CROSSOUT[I+1]:=CSI[T2-(TEMP/4-I/2)];  END;
79500         FOR I:=0 STEP 2 UNTIL TEMP/2-1 DO     BEGIN
79600           CROSSOUT[I+TEMP/2):=CSR[I/2];
79700           CROSSOUT[I+1+TEMP/2]:=CSI[I/2];END;
79800         NUM:=1024/XINCR;
79900         FOR I:=0 STEP XINCR UNTIL 1024 DO XD[I/XINCR]:=I;
80000       END;
80100       REEL:=NO;
80200       FOR I:=0 STEP 1 UNTIL NUM-1 DO CROSSOUT[I]:=*/REEL;
80300       WRITE(LP,</"CROSS-CORRELATION BETWEEN DIRECTION",I6," AND",I6>,
80400       CROSS[LX],CROSS[LX+1]);
80500       WRITE(LP,*/,CSR[0]);
80600       WRITE(LP,<"ZERO LAG CROSS-CORRELATION VALUE-CSR[0]/NO=",
80700       F10.6>,CSR[0]/NO);
```

```
80800       WRITE(LP,*/,ACTFRQ,ACTFREQ1516,NIN,CORFRQ,NO,TRENDCTR,LX);
80900       % NOW GRAPH RESULTS
81000       REPLACE POINTER(CORLBL1)BY "CROSS-CORRELATION AS A FUNCTION"
81100       " OF TIME";
81200       REPLACE P:POINTER(CORLBL2)BY "BETWEEN DIRECTION NUMBER";
81300       REPLACE P:P BY CROSS[LX] FOR 2 NUMERIC," AND DIRECTION NUMBER",
81400       CROSS[LX+1] FOR 2 NUMERIC;
81500       REPLACE P BY ".";
81600       REPLACE POINTER(FR1) BY "GRAPH CALCULATED USING A SAMPLING"
81700       " FREQUENCY OF",SAM FOR 5 NUMERIC;
81800       REPLACE POINTER(FR2) BY "WHEREAS THE PHYSICAL SAMPLING"
81900       " FREQUENCY WAS=",ACTFREQ1516 FOR 5 NUMERIC;
82000       IF (TRENDCTR GTR 0) AND CNTRD  THEN GO TO LAB;
82100       IF (TRENDCTR GTR 1) AND CLTRD THEN GO TO LAB;
82200       AINIT(1500);
82300       ASPEED(3);
82400       AORIG(300,200);
82500       PT:=*+1;REPLACE POINTER(AY) BY "PLOT NUMBER ",PT FOR 3 NUMERIC;
82600       ALAB(-275,410,AY,15,2,4);
82700       ABOX(0,0,14,15,75,50,1);
82800       ABOX(0,0,14,1,75,250,1);
82900       ABOX(0,0,1,15,525,50,1);
83000       ASCA(-30,-30,75 ,0,-70,10,14,1,2);
83100       REPLACE POINTER(L1) BY "TIME LAG(SEC.)";
83200       REPLACE POINTER(L2)BY "CORRELATION COEFFICIENT   ";
83300       ALAB(360,-65,L1,14,2,2);
83400       ALAB(-70,100,L2,26,2,4);
83500       ALAB(-280,20,CORLBL1,39,1,4);
83600       ALAB(-260,20,CORLBL2,50,1,4);
83700       ALAB(-240,20,FR1,51,1,4);
83800       ALAB(-220,20,FR2,49,1,4);
83900       LAB:
84000       IF CSR[0]<0 THEN
84100       BEGIN
84200         ASCALE(460,-11,0,50,.5,-.1,15,1,2,FMT,4);
84300         REEL:=-1;
84400       END ELSE
84500       BEGIN
84600         ASCALE(460,-11,0,50,-.5,.1,15,1,2,FMT,4);
84700         REEL:=1;
84800       END;
84900       CASE TRENDCTR OF
85000       BEGIN
85100         0:REPLACE POINTER(TRENDLBL)BY "NO TREND REMOVAL";
85200         1:REPLACE POINTER(TRENDLBL)BY "LINEAR TREND REMOVAL";
85300         2:REPLACE POINTER(TRENDLBL)BY"PARABOLIC TREND REMOVAL";
85400       END;
85500       ALAB(-200+TRENDCTR*20,20,TRENDLBL,23,1,2);
85600       ALINED(XD[*],CROSSOUT[*],NUM,-13,-.5*REEL,100,.2*REEL,
85700       5+5*TRENDCTR,1+5*TRENDCTR);
85800       IF TRENDCTR=0 AND NOT CLTRD AND NOT CPTRD THEN AEND;
85900       IF TRENDCTR=1 AND NOT CPTRD THEN AEND;
86000       IF TRENDCTR=2 THEN AEND;

86100     END OF PROCEDURE P L O T C R O S S C O R ;
86200     %   THIS PROCEDURE PLOTS CROSS-CORRELATIONS EXACTLY THE SAME WAY
86300     %   AS THE PROCEDURE ABOVE, EXCEPT THAT THIS PROCEDURE PRODUCES
86400     %   FEWER GRAPHS, THE INPUT TO THE PROGRAMME TO PRODUCE CROSS-
86500     %   CORRELATION PLOTS IS PAIRS OF NUMBERS INDICATING THE
86600     %   DATA STREAMS TO BE CROSS-CORRELATED. WHENEVER THE
86700     %   FIRST NUMBER OF THE NEXT PAIR IS THE SAME AS THE
86800     %   FIRST NUMBER OF THE PREVIOUS PAIR, THE CURVES WILL
86900     %   BE PLOTTED ON THE SAME GRAPH.
87000     %         ONLY ONE KIND OF TREND REMOVAL MAY BE PLOTTED
87100     %   ON THESE GRAPHS, AND THIS IS NOMINATED AS AN INPUT
87200     %   PARAMETER ON A DATA CARD.

87300     PROCEDURE PL(CSR,CSI,CORFRQ,CROSS,ACTFREQ1516,
87400     TRENDCTR,ACTFRQ,NIN,LX,CNTRD,CLTRD,CPTRD,NUMCORS,TR);
87500     %
87600     %
87700     VALUE CORFRQ,ACTFREQ1516,TRENDCTR,ACTFRQ,NIN,LX;
87800     INTEGER CORFRQ,TRENDCTR,ACTFRQ,NIN,LX;
87900     INTEGER NUMCORS,TR;
88000     REAL ACTFREQ1516;
88100     ARRAY CSR,CSI,CROSS[*];
88200     BOOLEAN CNTRD,CLTRD,CPTRD;
88300     BEGIN
88400       INTEGER NO,NUM,TEMP,SMALL,BIG,I,J,XINCR  ;
88500       REAL SAM,ISAM;
88600       ARRAY CROSSOUT[0:1024],TRENDLBL[0:3],CORLBL1[0:6],FR1[0:8],
88700       FR2[0:8],L1[0:2],L2[0:4];
88800       ARRAY CORLBL2[0:9];
88900       POINTER P;
89000       ARRAY FMT[0:0];
89100       INTEGER T2;
89200       REAL REEL;
89300       ARRAY XD[0:1024]; LABEL LAB;
89400       OWN INTEGER REF,CT,CTT,RL;
89500       % CALCULATE NUMBER OF POINTS IN THE ARRAYS CSR,CSI.
89600       NO:=NIN/2**(CORFRQ-1);
89700       T2:=NO/2;
89800       REPLACE POINTER(FMT) BY "F4.1";
89900       % CALCULATE THE GENERATED SAMPLING FREQUENCY
90000       SAM:=ACTFREQ1516/2**(CORFRQ-1);
```

```
90100       % CALCULATE APPROX INTEGER SAMPLING FREQUENCY
90200       ISAM:=ACTFRQ/2**(CORFRQ-1);
90300       TEMP:=ISAM/8;
90400       IF ISAM>8 THEN
90500       BEGIN
90600         ARRAY S1[NO-512*TEMP:NO],S2[0:513*TEMP];
90700         SMALL:=TEMP/2;BIG:=3*TEMP/2-1;
90800         FOR I:=0 STEP 2 UNTIL 512*TEMP-TEMP/2-2 DO BEGIN
90900           S1[NO-512*TEMP+TEMP/2+I]:=CSR[NO/2-256*TEMP+TEMP/4+I/2];
91000           S1[NO-512*TEMP+TEMP/2+I+1]:=CSI[NO/2-256*TEMP+TEMP/4+I/2];END;
91100         FOR I:=0 STEP 1 UNTIL 512.5*TEMP DO BEGIN
91200           S2[I]:=CSR[I/2];   S2[I+1]:=CSI[I/2]; END;
91300         FOR I:=0 STEP 1 UNTIL 510 DO
91400         FOR J:=SMALL STEP 1 UNTIL BIG DO
91500         CROSSOUT[I]:=*+S1[NO-(512-I)*TEMP+J]/TEMP;
91600         FOR J:=SMALL STEP 1 UNTIL TEMP-1 DO
91700         CROSSOUT[511]:=*+S1[NO-TEMP+J]/TEMP;
91800         FOR J:=TEMP STEP 1 UNTIL BIG DO
91900         CROSSOUT[511]:=*+S2[J-TEMP]/TEMP;
92000         FOR I:=0 STEP 1 UNTIL 511 DO
92100         FOR J:=SMALL STEP 1 UNTIL BIG DO
92200         CROSSOUT[512+I]:=*+S2[I*TEMP+J]/TEMP;
92300         NUM:=1024;XINCR:=1;
92400         FOR I:=0 STEP 1 UNTIL 1024 DO XD[I]:=I;
92500       END
92600       ELSE
92700       BEGIN
92800         XINCR:=8/ISAM;
92900         TEMP:=1024/XINCR;
93000         FOR I:=0 STEP 2 UNTIL TEMP/2-1 DO BEGIN
93100           CROSSOUT[I]:=CSR[T2-(TEMP/4-I/2)];
93200           CROSSOUT[I+1]:=CSI[T2-(TEMP/4-I/2)];  END;
93300         FOR I:=0 STEP 2 UNTIL TEMP/2-1 DO     BEGIN
93400           CROSSOUT[I+TEMP/2]:=CSR[I/2];
93500           CROSSOUT[I+1+TEMP/2]:=CSI[I/2];END;
93600         NUM:=1024/XINCR;
93700         FOR I:=0 STEP XINCR UNTIL 1024 DO XD[I/XINCR]:=I;
93800       END;
93900       WRITE(LP,</"CROSS-CORRELATION BETWEEN DIRECTION",I6," AND",I6>,
94000       CROSS[LX],CROSS[LX+1]);
94100       WRITE(LP,*/,CSR[0]);
94200       WRITE(LP,<"ZERO LAG CROSS-CORRELATION VALUE-CSR[0)/NO=",F10.6>,
94300       CSR[0]/NO);
94400       REEL:=NO;
94500       FOR I:=0 STEP 1 UNTIL NUM-1 DO CROSSOUT[I]:=*/REEL;
94600       WRITE(LP,*/,CORFRQ,TRENDCTR,ACTFRQ,NIN,LX,ACTFREQ1516);
94700
94800       IF CROSS[LX]=REF THEN GO TO LAB ELSE BEGIN
94900         IF REF=0 THEN BEGIN AINIT(1500);REF:=CROSS[LX]; END
95000         ELSE BEGIN AEND; AINIT(1500);CTT:=0; REF:=CROSS[LX];
95100         END;
95200       END;
95300       ASPEED(3); AORIG(300,200);
95400       PT:=*+1;REPLACE POINTER(AY) BY "PLOT NUMBER ",PT FOR 3 NUMERIC;
95500       ALAB(-275,410,AY,15,2,4);
95600       ABOX(0,0,14,15,75,50,1);ABOX(0,0,14,1,75,250,1);
95700       ABOX(0,0,1,15,525,50,1);
95800       ASCA(-30,-30,75 ,0,-70,10,14,1,2);
95900       REPLACE POINTER(L1) BY "TIME LAG(SEC.)";
96000       REPLACE POINTER(L2)BY "CORRELATION COEFFICIENT   ";
96100       ALAB(360,-65,L1,14,2,2);
96200       ALAB(-70,100,L2,26,2,4);
96300       IF TR=0 THEN REPLACE POINTER(CORLBL1) BY "NO TREND REMOVAL       ";
96400       IF TR=1 THEN REPLACE POINTER(CORLBL1) BY "LINEAR TREND REMOVAL   ";
96500       IF TR=2 THEN REPLACE POINTER(CORLBL1)BY "PARABOLIC TREND REMOVAL";
96600       ALAB(-280,20,CORLBL1,23,1,4);
96700       IF CSR[0]<0 THEN BEGIN
96800         ASCALE(460,-11,0,50,.5,-.1,16,1,2,FMT,4);
96900         RL:=-1; END ELSE BEGIN
97000         ASCALE (460,-11,0,50,-.5,.1,16,1,2,FMT,4);
97100         RL:=1; END;
97200       LAB:
97300       REPLACE POINTER(CORLBL2)BY "DIRECTIONS",CROSS[LX) FOR 5
97400       NUMERIC, " AND",CROSS[LX+1] FOR 5 NUMERIC;
97500       ALAB(-260+20*CTT,20,CORLBL2,24,1,4);
97600       ALINED(XD[*],CROSSOUT[*],NUM,-13,-.5*RL,
97700       100,.2*RL,5+7*CTT,1+2*CTT);
97800       CTT:=*+1; CT:=*+1;
97900       IF CT=NUMCORS THEN AEND;
98000       %

98100     END OF PROCEDURE P L ;
98200     %   THIS PROCEDURE IS USED IN CONJUNCTION WITH FAST FOURIER
98300     %   TRANSFORM PACKAGE. THE FFT PACKAGE ALLOWS FOR COMPLEX
98400     %   INPUT AND OUTPUT. SINCE THE TIME SERIES DATA IS REAL,
98500     %   USE OF THIS PROCEDURE ALLOWS A 2-N POINT REAL DATA
98600     %   STREAM TO BE FOURIER TRANSFORMED WITH AN N POINT FFT. IT
98700     %   MAKES USE OF ONE ARRAY WHICH IS NORMALLY RESERVED FOR
98800     %   THE IMAGINARY NUMBERS.
98900     %   AN INVERSE FFT MAY ALSO BE TAKEN OF HERMITTIAN DATA
99000     %   TO HAVE REAL DATA RETURNED.

99100     PROCEDURE RRDR(XR,XI,M,DIRN);VALUE M,DIRN;
99200     INTEGER M,DIRN;ARRAY XR,XI[0];
99300     BEGIN
```

```
 99400       INTEGER I,N,N2;REAL T1,T2,T3,T4,ARG;
 99500       REAL RE,S,C;
 99600       N:=2**M;        N2:=N/2;
 99700       RE:=3.1415926536/N;
 99800       I:=0;
 99900       DO   BEGIN
100000         C:=COS(ARG:=RE*I);        S:=SIN(ARG);
100100         T1:=(XR[I]+XR[N-I])/2;
100200         T2:=(XR[I]-XR[N-I])/2;
100300         T3:=(XI[I]+XI[N-I])/2;
100400         T4:=(XI[I]-XI[N-I])/2;
100500         XR[I]:=T1+(ARG:=C*T3*DIRN+S*T2);
100600         XR[N-I]:=T1-ARG;
100700         XI[I]:=T4-(ARG:=C*T2*DIRN-S*T3);
100800         XI[N-I]:=-T4-ARG;
100900       END UNTIL I:=*+1 GTR N2;

101000     END OF PROCEDURE R R D R ;
101100     %
101200     %
101300     %     **********      MAINLINE       **********
101400     %
101500     INTEGER TRDIRN;BOOLEAN COMPRESS;
101600     INTEGER DIRN;
101700     BOOLEAN CROSSCOR,CNTRD,CLTRD,CPTRD;
101800     INTEGER NUMCORS,CORFRQ,INT,LX;
101900     INTEGER ACTFRQ,NOFRQS,NIN,NOARRAYS;
102000     INTEGER STARTFRQ;
102100     BOOLEAN NOTREND,LINTREND,PARTREND;
102200     BOOLEAN PSVSNFQ;
102300     BOOLEAN IFAUTO;
102400     BOOLEAN ONEHT;  INTEGER ONEHEIGHT;
102500     ARRAY X[0:255];
102600     INTEGER KK,AS,BS,CS;
102700     INTEGER K;
102800     %   TIME(12) IS A SYSTEM CLOCK GIVING THE ELAPSED PROCESSOR
102900     %   TIME. USED TO TIME PARTS OF THE PROGRAMME
103000     DEFINE T=TIME(12)*2.4@-6#;
103100
103200
103300     BOOLEAN LNG,LAT,VER;
103400     %
103500     %                       READ IN CONTROL PARAMETERS
103600     %
103700     %  STARTFRQ IS THE HIGHEST FREQ REQD FOR PROCESSING
103800     %  STARTFRQ=1 MEANS THAT THE HIGHEST FREQ IS ACTFRQ
103900     %  READ IN AS STARTFRQ=2 MEANS ACTFRQ/2,=3  ACTFRQ/4 ETC
104000     %   WHEN RUN FROM CANDE PUT FILE VDU(REMOTE), FILE KR(REMOTE)
104100     %   AND PROGRAMME ASKS FOR INPUT FROM CANDE TERMINAL
104200     WRITE(VDU,<"INPUT ACTFRQ,STARTFRQ,NOFRQS,NIN_ENOARRAYS">);
104300     %
104400     %
104500     %
104600     READ(KR,/,ACTFRQ,STARTFRQ,NOFRQS,NIN,NOARRAYS);
104700     %
104800     %
104900     %
105000     WRITE(LP,*/,ACTFRQ,STARTFRQ,NOFRQS,NIN,NOARRAYS);
105100     WRITE(LP,<"THE DATA IS STORED ON TAPE WITH A SCAN RATE OF",I3," OR A"
105200     " SAMPLING FREQUENCY OF",F9.4," HZ"/"THE HIGHEST FREQUENCY FOR"
105300     " PROCESSING IS",F9.4," HZ. THE PROCESSING IS TO BE DONE AT",I4,
105400     /" DIFFERENT FREQUENCIES, EACH ONE HALF THE PREVIOUS FREQUENCY"/
105500     "THE NUMBER OF SAMPLES PER CHANNEL IN THE INPUT DATA FILE"
105600     " IS",I7,/"DATA FROM",I4," ORTHOGONAL ARRAYS OF"
105700     " ANEMOMETERS IS CONTAINED IN THE FILE">,
105800     ACTFRQ,ACTFRQ*15/16,ACTFRQ*15/(16*2**(STARTFRQ-1)),
105900     NOFRQS,NIN,NOARRAYS);
106000     WRITE(VDU,*/,ACTFRQ,STARTFRQ,NOFRQS,NIN,NOARRAYS);
106100     WRITE(VDU,<"INPUT PSVSNFQ TRUE OR FALSE">);
106200     %
106300     %
106400     %
106500     READ(KR,/,PSVSNFQ); WRITE(LP,*/,PSVSNFQ);
106600     %
106700     %
106800     %
106900     IF PSVSNFQ THEN WRITE(LP,<"POWER STPECTRA WILL BE"
107000     " PLOTTED VERSUS DIMENSIONLESS FREQUENCY FREQ*HEIGHT/"
107100     "(AVERAGE VELOCITY AT THAT HEIGHT)">) ELSE WRITE(LP,
107200     <"SPECTRA WILL BE PLOTTED VERSUS FREQUENCY IN HZ">);
107300     WRITE(VDU,*/,PSVSNFQ);
107400     WRITE(VDU,<"INPUT IFAUTO TRUE OR FALSE">);
107500     %
107600     %
107700     %
107800     READ(KR,/,IFAUTO);
107900     %
108000     %
108100     %
108200     WRITE(VDU,*/,IFAUTO);
108300     WRITE(LP,*/,IFAUTO);
108400     IF IFAUTO THEN WRITE(LP,<//"THE AUTOCORRELATIONS WILL BE CALCULATE
108500     D ALONG WITH THE POWER SPECTRA">) ELSE WRITE(LP,<//"NO AUTOCORRELATIONS
108600     WILL BE CALCULATED">);
108700     %   ONEHEIGHT=1 IS THE FIRST ARRAY, 2 THE SECOND ETC
```

```
108800      WRITE(VDU,<"INPUT ONEHT, IF ONEHT THEN ONEHEIGHT">);
108900      %
109000      %
109100      %
109200      READ(KR,/,ONEHT,IF ONEHT THEN ONEHEIGHT);
109300      %
109400      %
109500      %
109600      WRITE(VDU,*/,ONEHT,IF ONEHT THEN ONEHEIGHT);
109700      IF ONEHT THEN WRITE(LP,</"ONLY ONE ORTHOGONAL ARRAY OF ANEMOM"
109800      "ETERS IS BEING CONSIDERED"/"FOR ANY"
109900      " ANALYSIS WHICH IS ARRAY NO",I3/>,ONEHEIGHT) ELSE
110000      WRITE(LP,<"DATA FROM ALL ORTHOGONAL ARRAYS OF ANEMOMETERS"
110100      " WILL BE PROCESSED">);
110200      %
110300      WRITE(VDU,<"INPUT LNG,LAT,VER TRUE OR FALSE TO INDICATE"
110400      " DIRECTION FOR PROCESSING">);
110500      %
110600      %
110700      %
110800      READ(KR,/,LNG,LAT,VER);
110900      %
111000      %
111100      %
111200      WRITE(LP,*/,LNG,LAT,VER);
111300      IF LNG THEN WRITE(LP,<"LONGITUDINAL DATA WILL BE"
111400      " PROCESSED">);
111500      IF VER THEN WRITE(LP,<"VERTICAL DATA WILL BE PROCESSED">);
111600      IF LAT THEN WRITE(LP,<"LATERAL DATA WILL BE PROCESSED">);
111700      WRITE(VDU,*/,LNG,LAT,VER);
111800      %
111900      WRITE(VDU,<"INPUT CROSSCOR,NUMCORS,CORFRQ,CNTRD,CLTRD,CPTRD">);
112000      %
112100      %
112200      %
112300      READ(KR,/,CROSSCOR,IF CROSSCOR THEN NUMCORS,IF CROSSCOR THEN CORFRQ,
112400      %
112500      %
112600      IF CROSSCOR THEN CNTRD,IF CROSSCOR THEN CLTRD,IF CROSSCOR
112700      %
112800      %
112900      THEN CPTRD);
113000      WRITE(LP,*/,CROSSCOR,IF CROSSCOR THEN NUMCORS,IF
113100      CROSSCOR THEN CORFRQ, IF CROSSCOR THEN CNTRD, IF
113200      CROSSCOR THEN CLTRD, IF CROSSCOR THEN CPTRD);
113300      IF CROSSCOR THEN WRITE(LP,<"THE NUMBER OF CROSS-CORRELATIONS REQD"
113400      " IS",I4," WITH CORFRQ=",I4,/"THE CROSS-CORRELATIONS WILL BE"
113500      " CALCULATED AT A SAMPLING FREQUENCY OF ACTFRQ*15/(16*2**(CORFRQ"
113600      "-1))=",F9.4>,NUMCORS,CORFRQ,ACTFRQ*15/(16*2**(CORFRQ-1)));
113700      %
113800      %
113900      WRITE(VDU,<"INPUT CROSSCOR, IF CROSSCOR TRUE THEN "
114000      "-COMPRESS,T OR F,TRDIRN-0 FOR NO TREND REMOVAL"/
114100      "1 FOR LINEAR, 2 FOR PARABOLIC">);
114200      %
114300      %
114400      %
114500      READ(KR,/,CROSSCOR,IF CROSSCOR THEN COMPRESS,
114600      IF CROSSCOR THEN TRDIRN);
114700      %
114800      %
114900      %
115000      WRITE(LP,*/,CROSSCOR);IF CROSSCOR THEN WRITE(LP,*/,
115100      COMPRESS,TRDIRN);
115200      IF CROSSCOR AND COMPRESS THEN BEGIN
115300        IF TRDIRN=0 AND NOT CNTRD THEN BEGIN WRITE(LP,<"TRDIRN=0"
115400          " BUT CNTRD FALSE, HENCE"/"CNTRD WILL BE MADE TRUE"
115500          " PROGRAMMATICALLY">);CNTRD:=TRUE;END;
115600        IF TRDIRN=1 AND NOT CLTRD THEN BEGIN WRITE(LP,<
115700          "TRDIRN=1 BUT CLTRD FALSE,HENCE CLTRD"/" WILL BE MADE"
115800          " TRUE PROGRAMMATICALLY">); CLTRD:=TRUE; END;
115900        IF TRDIRN=2 AND NOT CPTRD THEN BEGIN WRITE(LP,<
116000          "TRDIRN=2 BUT CPTRD FALSE,HENCE CPTRD"/" WILL BE MADE"
116100          " TRUE PROGRAMMATICALLY">); CPTRD:=TRUE; END;
116200      END;
116300      IF CROSSCOR THEN BEGIN
116400        IF CNTRD THEN WRITE(LP,<"CROSS-CORRELATIONS WILL BE CALCULATED WITH"
116500        " NO TREND REMOVAL">);
116600        IF CLTRD THEN WRITE(LP,<"CROSS-CORRELATIONS WILL BE CALCULATED"
116700        " WITH LINEAR TREND REMOVAL">);
116800        IF CPTRD THEN WRITE(LP,<"CROSS-CORRELATIONS WILL BE"
116900        " CALCULATED WITH PARABOLIC TREND REMOVAL">);
117000        IF COMPRESS THEN WRITE(LP,<"WHERE CONSECUTIVE PAIRS OF"
117100        " NUMBERS INDICATING DATA STREAMS TO BE CORRELATED HAVE THE"
117200        " FIRST NUMBER IN EACH PAIR IDENTICAL,"/"THEY WILL BE PLOTTED"
117300        " ON THE SAME GRAPH">);
117400        IF COMPRESS THEN BEGIN
117500          IF TRDIRN=0 THEN WRITE(LP,<"WITH NO TREND REMOVAL">);
117600          IF TRDIRN=1 THEN WRITE(LP,<"WITH LINEAR TREND REMOVAL">);
117700          IF TRDIRN=2 THEN WRITE(LP,<"WITH PARABOLIC TREND REMOVAL">);
117800        END COMPRESS BLOCK; END CROSSCOR BLOCK;
117900      %
118000      %
118100      BEGIN
118200        %
```

```
118300        %          DECLARATIONS,DYNAMICCALLY DIMENSION SOME ARRAYS
118400        %
118500        INTEGER ARRAY CROSS[1:IF CROSSCOR THEN 2*NUMCORS ELSE 1];
118600        ARRAY NUM[0:STARTFRQ-1+NOFRQS-1];
118700        BOOLEAN CSCRTN;
118800        LABEL PLOTLOOPLBL,ERRORCOND,OVERLBL;
118900        INTEGER LOOPCOUNTER,NOOFLOOPS;
119000        ARRAY AV,SV,ST2,STV,ST3,ST4,ST2V,ST,XM,
119100        RMS,STDDEV[0:2],A0,A1,C1,C2,C3,C4,B0,B1,B2[0:2];
119200        REAL ACTFREQ1516,SI,CO;
119300        INTEGER TEMPNIN,HGHTCTR,FRQCTR,I,J,HGHTCTR1,TEMPNIN1,FRQCTR1;
119400        REAL TEMPFRQ;
119500        REAL SACTFRQ;
119600        REAL ARG;
119700        ARRAY
119800        HEIGHT[0:NOARRAYS-1],VEL[0:NOARRAYS-1],NOPTSOUT[0:
119900        STARTFRQ-1+NOFRQS-1];
120000        INTEGER FRQAV;
120100        BOOLEAN COSTAPER;
120200        REAL TEMPSTORE1,TEMPSTORE2;
120300        INTEGER M,T2,T2P1,T2M1;
120400        INTEGER PQ;
120500        REAL TREAD,TALTFQ,TRES,TSUMS,TNRMS,TCOS,TFHR,TMAG,TAREA,TAVS,TNAUTO,TAVA
120600        ,TLIN,TLTR,TLAVRMS,TLINNORM,TPAR,TPPWRH,TPAUTH,TPPWRF,TPATF,TNOTRD;
120700        REAL TTIME;
120800        REAL TH,TR;
120900        REAL THCPU,THIO;
121000        LABEL FRQLABL,PLOTLBL;
121100        LABEL LOOPHOLE;
121200        INTEGER DIRECTION,TRENDCTR;
121300        ARRAY SAMPFRQS[0:STARTFRQ-1+NOFRQS-1];
121400        BOOLEAN HEIGHTS,FREQS,TRENDS;
121500        REAL FACTOR;
121600        ARRAY AREA[0:2];
121700        TTIME:=T;
121800        WRITE(LP,<"START EXECUTION TIME=",F13.4>,T);
121900        WRITE(VDU,<"INPUT CRSCR &PAIRS OF NOS FOR CROSS CORRELATIONS">);
122000        %
122100        %
122200        %
122300        READ(KR,/,CROSSCOR,IF CROSSCOR THEN FOR I:=1 STEP 1 UNTIL
122400        2*NUMCORS DO CROSS[I]);
122500        %
122600        %
122700        %
122800        IF CROSSCOR THEN WRITE(LP,</"THE NUMBER OF CROSS-CORRELATIONS",
122900        "REQD IS=",X2,I5,/,"AND ARE BETWEEN THE FOLLOWING PAIRS OF",
123000        "DIRECTIONS"/8(I3,X1,I3,X6)>,NUMCORS,FOR I:=1 STEP 1 UNTIL
123100        2*NUMCORS DO CROSS[I]) ELSE
123200        WRITE(LP,</"NO CROSS-CORRELATIONS WILL BE CALCULATED",
123300        " OR GRAPHED"/>);
123400        WRITE(VDU,<"INPUT COSTAPER,NOTREND,LTRD,PTRD">);
123500        %
123600        %
123700        %
123800        READ(KR,/,COSTAPER,NOTREND,LINTREND,PARTREND);
123900        %
124000        %
124100        %
124200        WRITE(VDU,*/,COSTAPER,NOTREND,LINTREND,PARTREND);
124300        WRITE(LP,*/,COSTAPER,NOTREND,LINTREND,PARTREND);
124400        IF COSTAPER THEN WRITE(LP,<"A COSINE TAPER DATA WINDOW WILL"
124500        " BE USED">) ELSE WRITE(LP,<"A BOXCAR DATA WINDOW WILL"
124600        " BE USED">);
124700        IF NOTREND THEN WRITE(LP,<"PROCESSING WILL BE DONE WITH NO"
124800        " TREND REMOVAL">);
124900        IF LINTREND THEN WRITE(LP,<"PROCESSING WILL BE DONE WITH"
125000        " LINEAR TREND REMOVAL">);
125100        IF PARTREND THEN WPITE(LP,<"PROCESSING WILL BE"
125200        " DONE WITH PARABOLIC TREND REMOVAL">);
125300        %
125400        %
125500        IF CNTRD AND NOT NOTREND THEN BEGIN WRITE(LP,<"CNTRD IS"
125600          " TRUE BUT NOTREND FALSE. NOTREND WILL BE MADE TRUE PROGRAMMATICALLY">);
125700          NOTREND:=TRUE; END;
125800        IF CLTRD AND NOT LINTREND THEN BEGIN WRITE(LP,<"CLTRD IS"
125900          " TRUE BUT LINTREND FALSE.LINTREND WILL BE MADE TRUE PROGRAMMATICALLY">)
126000          ;LINTREND:=TRUE; END;
126100        IF CPTRD AND NOT PARTREND THEN BEGIN WRITE(LP,<"CPTRD IS TRUE"
126200          " BUT PARTREND IS FALSE. PARTREND WILL BE MADE TRUE PROGRAMMATICALLY">);
126300          PARTREND:=TRUE; END;
126400        %
126500        %
126600        %
126700        WRITE(VDU,<"INPUT CSCRTN T OR F">);READ(KR,/,CSCRTN);WRITE(LP,*/,
126800        CSCRTN);WRITE(VDU,*/,CSCRTN);
126900        IF CSCRTN THEN WRITE(LP,<"DATA WILL BE CORRECTED FOR"
127000        " NON-COSINE RESPONSE OF THE ANEMOMETERS">) ELSE
127100        WRITE(LP,<"THE DATA WILL NOT BE CORRECTED FOR THE"
127200        " NON-COSINE RESPONSE OF THE ANEMOMETERS">);
127300        %
127400        %
127500        WRITE(VDU,<"INPUT HEIGHTS OF ANEMOMETERS">);
127600        %
127700        %
```

```
127800        %
127900        READ(KR,/,FOR I:=0 STEP 1 UNTIL NOARRAYS-1 DO HEIGHT[I]);
128000        %
128100        %
128200        %
128300        WRITE(LP,</"THE HEIGHTS OF THE ORTHOGONAL ARRAYS OF ANEMOMETERS"
128400        /"ARE RESPECTIVELY">);
128500        WRITE(LP,*/,FOR I:=0 STEP 1 UNTIL NOARRAYS-1 DO HEIGHT[I]);
128600        FOR I:=0 STEP 1 UNTIL STARTFRQ-1+NOFRQS-1 DO
128700        SAMPFRQS[I]:=ACTFRQ*15/(16*2**I);
128800        WRITE(LP,*/,FOR I:=0 STEP 1 UNTIL NOFRQS-1 DO SAMPFRQS[I]);
128900        FRQCTR:=STARTFRQ-1;
129000        SACTFRQ:=ACTFRQ*15/16;
129100        %      THIS LABEL IS USED WHEN THE DATA IS TO BE PROCESSED
129200        %      AGAIN BUT THIS TIME THE DATA IS PROCESSED AT HALF THE PREVIOUS
129300        %      SAMPLING FREQUENCY
129400        FRQLABL:
129500        TTIME:=T;WRITE(LP,*/,FRQCTR,TTIME);
129600        TTIME:=T;WRITE(VDU,*/,FRQCTR,TTIME);
129700        IF ONEHT THEN HGHTCTR:=ONEHEIGHT-1 ELSE HGHTCTR:=0;
129800        FRQCTR:=*+1;
129900        IF FRQCTR>NOFRQS+STARTFRQ-1 THEN GO TO PLOTLBL;
130000        FRQCTR1:=FRQCTR-1;
130100        TEMPNIN:=NIN/(2**FRQCTR1);
130200        IF TEMPNIN<2048 THEN BEGIN
130300          WRITE(LP,<"PROGRAMME WILL NOT RUN WITH LESS THAN 2048 DATA SAMPLE"
130400          "S, TEMPNIN=",I6>,TEMPNIN);
130500          GO TO PLOTLBL;END;
130600        IF TEMPNIN>16384 THEN BEGIN
130700          WRITE(LP,<"IF MORE THAN 16384 SAMPLES ARE BEING USED THE WORD LON"
130800          "G IN LINE NUMBER 132300 "/"WILL HAVE TO BE REMOVED. ALSO THE DEAL"
130900          "LOCATE STATEMENTS WILL HAVE TO BE CHANGED TO"/"%DEALLOCATE. THIS"
131000          " IS BEST DONE ON CANDE WITH A REPLACE STATEMENT">);
131100          GO TO PLOTLBL;END;
131200        TEMPNIN1:=TEMPNIN-1;
131300        TEMPFRQ:=ACTFRQ/2**FRQCTR1;
131400        ACTFREQ1516:=TEMPFRQ*15/16;
131500        T2:=TEMPNIN/2; T2M1:=T2-1; T2P1:=T2+1;
131600        %
131700        %
131800        BEGIN
131900          %
132000          %      MORE DECLARATIONS AND DYNAMICALLY DIMENSIONED ARRAYS
132100          %
132200          LABEL INLAB,OUTLAB;
132300          LONG
132400          ARRAY XR,XI,AR,AI[0:T2P1];
132500          BOOLEAN BL;
132600          BOOLEAN BOO;
132700          ARRAY S,C[0:T2/2+1];
132800          LABEL HGHTLABL;
132900          LABEL LABEL3,LABEL4;
133000          BL:=FALSE;
133100          M:=LOG(TEMPNIN)/LOG(2)-1;
133200          SINCOS(S,C,M);
133300          %
133400          %      THIS LABEL IS USED WHEN A NEW ORTHOGONAL ARRAY OF DATA IS TO
133500          %      BE PROCESSED.EACH ORTHOGONAL ARRAY IS PROCESSED IN ORDER,
133600          %      PROVIDING ONLY ONE IS NOT BEING PROCESSED,THE ORDER IS
133700          %      ORTHOGONAL ARRAY 1,ORTHOGONAL ARRAY 2,3,4 ETC UP TO
133800          %      THE NUMBER OF ORTHOGONAL ARRAYS OF ANEMOMETERS
133900          HGHTLABL:
134000          IF CSCRTN AND FRQCTR=STARTFRQ THEN BEGIN
134100            %    CORRECTING FOR NON-COSINE RESPONSE IS DONE IF CSCRTN IS TRUE,
134200            %    AND IS ONLY DONE AT THE HIGHEST FREQUENCY PROCESSING IS DONE AT
134300            %    THE DATA IS READ OFF THE DISK FILE,CORRECTED,AND WRITTEN BACK
134400            %    TO IT.
134500            THCPU:=*-T;THIO:=*-TIME(13);
134600            HORSTCORRECTION(NOARRAYS,NIN,HGHTCTR,BL,ACTFRQ);
134700            THCPU:=*+T; THIO:=*+TIME(13);
134800            WRITE(LP,<"TIME FOR NON-COSINE RESPONSE CORRECTION IS-CPU=",F8.3,
134900            " IO=",F8.3," FOR ORTHOGONAL ARRAY NUMBER",I4>,THCPU,THIO*2.40-6,
135000            HGHTCTR+1);END;
135100          FOR I:=0,1,2 DO AV[I]:=0;
135200          FOR I:=0,1,2 DO SV[I]:=ST2[I]:=ST3[I]:=ST4[I]:=ST2V[I]:=STV[I]:=0;
135300          HGHTCTR:=*+1;
135400          HGHTCTR1:=HGHTCTR-1;
135500          FRQAV:=2**FRQCTR1;
135600          BEGIN

135700            PROCEDURE PROC(BOO,J,TRENDCTR);
135800            BOOLEAN BOO;INTEGER J,TRENDCTR;
135900            BEGIN
136000              LABEL SKIP;
136100              %    NO  OF REAL POINTS =2**(M+1)
136200              M:=LOG(TEMPNIN)/LOG(2)-1;
136300              %      SET DIRN=1 FOR FORWARD TRANSFORM
136400              DIRN:=1;
136500              IF CROSSCOR AND CORFRQ=FRQCTR AND COSTAPER AND BOO AND NOT
136600              IFAUTO THEN BEGIN
136700                %DATA IS NORMALISED BY REMOVING MEAN AND DIVIDING BY STANDARD DEVIATION
136800                %   FORWARD FFT IS TAKEN AND RESULT SAVED IN FILE FC FOR
136900                %   CROSS-CORRELATIONS.
137000                FOR LX:=1 STEP 1 UNTIL 2*NUMCORS DO
137100                IF CROSS[LX]=HGHTCTR1*3+J+1 THEN
```

```
137200              BEGIN
137300                FOR I:=0 STEP 1 UNTIL T2M1 DO BEGIN
137400                  AR[I]:=(XR[I]-XM[J])/STDDEV[J];
137500                  AI[I]:=(XI[I]-XM[J])/STDDEV[J]; END;
137600                FFTF(AR[*],AI[*],S,C,M); BITREV2(AR[*],AI[*],M);
137700                RRDR(AR[*],AI[*],M,DIRN);
137800                FOR I:=0 STEP 1024 UNTIL T2 DO BEGIN
137900                  WRITE(FC[AS*TRENDCTR+BS*(LX-1)+I/1024],1024,AR[I]);
138000                  WRITE(FC[AS*TRENDCTR+BS*(LX-1)+KK+I/1024],1024,AI[I]);
138100                END;
138200                WRITE(LP,<"SINCE THE MEAN IS REMOVED THE AREA UNDER THE GRAPH"
138300                " SHOULD BE SMALL">);
138400                WRITE(LP,<"TRENDCTR=",I3,"   J=",I6," AR[0]:=",E10.4>,TRENDCTR,
138500                J,AR[0]);
138600                DEALLOCATE(AR);DEALLOCATE(AI);
138700              END;
138800            END OF IF CROSSCOR BLOCK;
138900            TNRMS:=*-T;
139000            % NORMALISE DATA
139100            % TEST TO SEE WHETHER COSINE TAPER IS REQUIRED
139200            COSINETAPER(XR[*],XI[*],TEMPNIN,COSTAPER,IFAUTO,
139300            STDDEV[*],XM[*],J);
139400            %   CHECK TIMES FOR FOURIER TRANSFORM
139500            TNRMS:=*+T;
139600            TFHR:=TH:=TR:=TALTFQ:=0;
139700            TFHR:=*-T;
139800            DIRN:=1;
139900            %  PERFORM FORWARD TRANSFORM
140000            TH:=TH-T;
140100            FFTF(XR[*],XI[*],S,C,M);
140200            TH:=*+T; TALTFQ:=*-T;
140300            BITREV2(XR[*],XI[*],M);
140400            TALTFQ:=*+T;
140500            TR:=TR-T;
140600            RRDR(XR[*],XI[*],M,DIRN);
140700            TR:=TR+T;
140800            TFHR:=*+T;
140900            WRITE(LP,</"TIME TAKEN FOR FFTF,BITREV2,RRDR WITH",I8,
141000            " POINTS IS",F9.3," SECONDS"/>,2**(M+1),TFHR);TFHR:=0;
141100            WRITE(LP,<"FFTF=",F9.4,"BITREV2=",F9.4," RRDR=",F9.4>,
141200            TH,TALTFQ,TR);  TH:=TR:=TALTFQ:=0;
141300            IF NOT COSTAPER AND IFAUTO THEN   BEGIN
141400              FOR I:=0 STEP 1024 UNTIL T2 DO BEGIN
141500                %   DATA SAVED IN FILE FAULG FOR AUTOCORRELATION
141600                WRITE(FAULG[12+I/1024],1024,XR[I]);
141700                WRITE(FAULG[13+I/1024+T2/1024],1024,XI[I]);
141800              END;  END;
141900            IF NOT COSTAPER AND CROSSCOR AND CORFRQ=FRQCTR AND BOO
142000            THEN BEGIN
142100              FOR LX:=1 STEP 1 UNTIL 2*NUMCORS DO
142200              IF CROSS[LX]=HGHTCTR1*3+J+1 THEN  BEGIN
142300                FOR I:=0 STEP 1024 UNTIL T2 DO BEGIN
142400                  %   DATA SAVED AGAIN IN FILE FC FOR CROSS-CORRELATIONS
142500                  WRITE(FC[AS*TRENDCTR+BS*(LX-1)+I/1024],1024,XR[I]);
142600                  WRITE(FC[AS*TRENDCTR+BS*(LX-1)+KK+I/1024],1024,XI[I]);
142700                END;
142800              END;
142900            END;
143000            WRITE(LP,<"XR[0] SHOULD BE SMALL BECAUSE MEAN REMOVED">);
143100            WRITE(LP,<"J=",I6," XR[0]=",E13.4>,J,XR[0]);
143200            %  CALCULATE MAGNITUDE AND MULTIPLY BY SCALE FACTOR
143300            %
143400            %  THE MAGNITUDE HAS TO BE SCALED BECAUSE THE FINITE FOURIER TRANSFORM
143500            %  IS ONLY AN APPROXIMATION TO THE THE CONTINUOUS FOURIER TRANSFORM
143600            %
143700            %   IF A COSINE TAPER IS USED THEN FACTOR IS 2*1.143*DELTAT/NO OF DATA
143800            %  POINTS
143900            %  IF NO TAPER IS USED THEN THE FACTOR IS 2/(SAMPLING FREQUENCY*NO OF
144000            %  DATA POINTS)
144100            %  BECAUSE DELTAT=1/SAMPLING FREQUENCY
144200            %
144300            IF COSTAPER THEN FACTOR:=2*1.143/(TEMPFRQ*TEMPNIN) ELSE
144400            FACTOR:=2/(TEMPFRQ*TEMPNIN);
144500            %
144600            TMAG:=*-T;
144700            %   CALCULATE POWER SPECTRAL DENSITY
144800            FOR I:=0 STEP 1 UNTIL T2 DO
144900            BEGIN
145000              XR[I]:=FACTOR*(XR[I]**2+XI[I]**2);
145100              AREA[J]:=*+XR[I];
145200            END;
145300            TMAG:=*+T;
145400            % CALL AVERAGING PROCEDURE
145500            %   TO SAVE THE SPECTRUM IN A FORM SUITABLE FOR PLOTTING
145600            TAVS:=*-T;
145700            AVSPECTRA(XR[*],HEIGHT[HGHTCTR1],VEL[HGHTCTR1],ACTFREQ1516,
145800            TEMPNIN,PSVSNFQ,NOPTSOUT[FRQCTR1],TRENDCTR,J,FRQCTR1,
145900            HGHTCTR1,NOARRAYS,STARTFRQ,NOFRQS);
146000            TAVS:=*+T;
146100            AREA[J]:=AREA[J]*TEMPFRQ/TEMPNIN;
146200            WRITE(LP,<"THE AREA UNDER THE SPECTRUM, FOR A NORMALISED BY RMS**2, CORR
146300            ECT GRAPH  SHOULD=1"/"J=",I3," AREA[J]=",E13.5
146400            >,J,AREA[J]);
146500            AREA[J]:=XM[J]:=RMS[J]:=0;
146600            IF IFAUTO THEN
```

```
146700            %   THIS BLOCK CALCULATES THE AUTOCORRELATION
146800            BEGIN
146900              TNAUTO:=*-T;
147000              DIRN:=1;
147100              IF NOT COSTAPER THEN GO TO SKIP;
147200              FOR I:=0 STEP 1024 UNTIL T2M1 DO BEGIN
147300                READ(FAULG[12+I/1024],1024,XR[I]);
147400                READ(FAULG[13+I/1024+T2/1024],1024,XI[I]);
147500              END;
147600              %   FORWARD TRANSFORM
147700              FFTF(XR[*],XI[*],S,C,M);
147800              BITREV2(XR[*],XI[*],M);
147900              RRDR(XR[*],XI[*],M,DIRN);
148000              SKIP:
148100              IF NOT COSTAPER THEN
148200              FOR I:=0 STEP 1024 UNTIL T2 DO BEGIN
148300                READ(FAULG[12+I/1024],1024,XR[I]);
148400                READ(FAULG[13+I/1024+T2/1024],1024,XI[I]);
148500              END;
148600              IF CROSSCOR AND CORFRQ=FRQCTR AND COSTAPER AND BOO
148700              THEN BEGIN
148800                FOR LX:=1 STEP 1 UNTIL 2*NUMCORS DO
148900                IF CROSS[LX]=HGHTCTR1*3+J+1 THEN BEGIN
149000                  FOR I:=0 STEP 1024 UNTIL T2 DO BEGIN
149100                    %   SAVE IN FILE FC FOR CROSS-CORRELATIONS
149200                    WRITE(FC[AS*TRENDCTR+BS*(LX-1)+I/1024],1024,XR[I]);
149300                    WRITE(FC[AS*TRENDCTR+BS*(LX-1)+KK+I/1024],1024,XI[I]);
149400                  END;
149500                END;
149600              END;
149700              FOR I:=0 STEP 1 UNTIL T2 DO
149800              BEGIN
149900                XR[I]:=(XR[I]**2+XI[I]**2)/TEMPNIN;
150000                XI[I]:=0;
150100              END OF I LOOP;
150200              WRITE(LP,<"XR[0] SHOULD BE SMALL AFTER FORD XFRM BECAUSE MEAN"
150300              " REMOVED, J=",I3," XR[0]= ",E13.5>,J,XR[0]);
150400              XR[0]:=0;
150500              %   INVERSE TRANSFORM
150600              DIRN:=-1;
150700              RRDR(XR[*],XI[*],M,DIRN);
150800              BITREV2(XR[*],XI[*],M);
150900              FFTR(XR[*],XI[*],S,C,M);
151000              WRITE(LP,<"XR[0] SHOULD BE =1 AFTER INV XFRM BECAUSE DIVIDED"
151100              " BY RMS, J=",I3," XR[0]=",E13.4>,J,XR[0]);
151200              %   CALL AVERAGING PROCEDURE FOR AUTOCORRELATIONS AND
151300              %   SAVE IN A FORM SUITABLE FOR PLOTTING
151400              TAVA:=*-T;
151500              AVERAGEAUTO(XR[*],XI[*],TEMPFRQ,NUM[FRQCTR1],TRENDCTR,J,
151600              FRQCTR1,HGHTCTR1,NOARRAYS,STARTFRQ,NOFRQS,TEMPNIN);
151700              TAVA:=*+T;
151800              TNAUTO:=*+T;
151900            END OF IF IFAUTO BLOCK;
152000            TNOTRD:=*+T;

152100          END OF PROCEDURE PROC;
152200          LABEL IN,OUT,L1,EOF;
152300          TREAD:=*-T;
152400          REPLACE POINTER(XR) BY 0 FOR T2P1 WORDS;
152500          REPLACE POINTER(XI) BY 0 FOR T2P1 WORDS;
152600          REPLACE POINTER(AR) BY 0 FOR T2P1 WORDS;
152700          REPLACE POINTER(AI) BY 0 FOR T2P1 WORDS;
152800          TEMPSTORE1:=ACTFRQ/32*CORFCTR[3*HGHTCTR1+1];
152900          TEMPSTORE2:=ACTFRQ/32*CORFCTR[3*HGHTCTR1+2];
153000          FOR I:=0 STEP 1 UNTIL NIN/256-1 DO
153100          BEGIN
153200            %   READ HORIZONTAL ANEMOMETER DATA FOR ONE ARRAY.CONVERT TO
153300            %   M/S,CALCULATE MEANS,CONVERT TO DESIRED SCAN RATE BY
153400            %   ADDING CONSECUTIVE SAMPLES TOGETHER.
153500            READ(INFYLE[I*3*NOARRAYS+3*HGHTCTR1],256,X)[EOF];
153600            FOR KK:=0 STEP 2*FRQAV UNTIL 255 DO  BEGIN
153700              FOR K:=0 STEP 1 UNTIL FRQAV-1 DO BEGIN
153800                XR[INT:=((I*128+KK/2)/FRQAV)]:=*+X[K+KK]/FRQAV;
153900                XI[INT]:=*+X[K+FRQAV+KK]/FRQAV; END K;
154000              IF CSCRTN THEN AV[0]:=*+XR[INT]+XI[INT] ELSE
154100              AV[0]:=*+(XR[INT]:=**TEMPSTORE1)+(XI[INT]:=**TEMPSTORE1);END KK;
154200            READ(INFYLE[I*3*NOARRAYS+1+3*HGHTCTR1],256,X)[EOF];
154300            FOR KK:=0 STEP 2*FRQAV UNTIL 255 DO        BEGIN
154400              FOR K:=0 STEP 1 UNTIL FRQAV-1 DO BEGIN
154500                AR[INT:=((I*128+KK/2)/FRQAV)]:=*+X[K+KK]/FRQAV;
154600                AI[INT]:=*+X[K+FRQAV+KK]/FRQAV;  END K;
154700              IF CSCRTN THEN AV[1]:=*+AR[INT]+AI[INT] ELSE
154800              AV[1]:=*+(AR[INT]:=**TEMPSTORE2)+(AI[INT]:=**TEMPSTORE2);END KK;
154900          END E N D   I   L 0 0 P ;
155000          TREAD:=*+T;
155100          GO TO L1;
155200          EOF:
155300          %   END OF INPUT FILE.FINISH.
155400          WRITE(LP,<"END OF FILE ON READ STATEMENT",/,"HGHTCTR1=",
155500          I4,X2,"FRQCTR1=",I4,X2,"I=",I3,X2,"J=",I3>,HGHTCTR1,FRQCTR1,
155600          I,J);
155700          CLOSE(INFYLE,*);
155800          GO TO LOOPHOLE;
155900          L1:
156000          WRITE(LP,</>);
```

```
156100          WRITE(LP,<"NUMBER OF ORTHOGONAL ARRAY=",I4,X2,"FREQUENCY OF DATA",
156200          F8.5,X2,"NUMBER OF DATA POINTS=",I7>,HGHTCTR,ACTFRQ/2**FRQCTR1,
156300          TEMPNIN);
156400          WRITE(LP,</>);
156500          ARG:=ARCTAN2(AV[1],AV[0]);
156600          SI:=SIN(ARG);
156700          CO:=COS(ARG);
156800          AV[0]:=AV[0]/TEMPNIN;AV[1]:=AV[1]/TEMPNIN ;
156900          VEL[HGHTCTR1]:=AV[0]*CO+
157000          AV[1]*SI;
157100          %
157200          %   RESOLVE THE HORIZONTAL ANEMOMETER DATA INTO COMPONENTS
157300          %   PARALLEL AND PERPINDICULAR TO AVERAGE WIND DIRECTION
157400          %   FOR THAT PARTICULAR ANEMOMETER ARRAY
157500          %
157600          %
157700          %  RESOLVE LOOP ALSO CALCULATE ROOT MEAN SQUARE
157800          TRES:=*-T;
157900          FOR I:=0 STEP 1 UNTIL T2M1 DO
158000          BEGIN
158100            TEMPSTORE1:=XR[I];
158200            TEMPSTORE2:=XI[I];
158300            XR[I]:=**CO+AR[I]*SI;
158400            XI[I]:=**CO+AI[I]*SI;
158500            RMS[0]:=*+XR[I]*XR[I]+XI[I]*XI[I] ;
158600            AR[I]:=**CO-TEMPSTORE1*SI;
158700            AI[I]:=**CO-TEMPSTORE2*SI;
158800            RMS[1]:=*+AR[I]*AR[I]+AI[I]*AI[I];
158900          END;
159000          %   WRITE RESOLVED DATA TO A TEMPORARY DISK FILE FOR LATER USE
159100          TRES:=*+T;
159200          FOR I:=0 STEP 1024 UNTIL T2M1 DO
159300          WRITE(FX[I/1024],1024,XR[I]);% XR LONG DATA
159400          FOR I:=0 STEP 1024 UNTIL T2M1 DO
159500          WRITE(FX[(T2+I)/1024],1024,XI[I]);%XI LONG DATA
159600          FOR I:=0 STEP 1024 UNTIL T2M1 DO
159700          WRITE(FX[(TEMPNIN+I)/1024],1024,AR[I]);% AR LAT DATA
159800          FOR I:=0 STEP 1024 UNTIL T2M1 DO
159900          WRITE(FX[(TEMPNIN+T2+I)/1024],1024,AI[I]);
160000          % AI IN FOURTH CHUNK LAT DATA
160100          %   REMOVE ARRAYS AR AND AI FROM MEMORY
160200          DEALLOCATE(AR);DEALLOCATE(AI);
160300          WRITE(LP,<"AVERAGE VELOCITY IN LONGITUDINAL DIRECTION IS",F10.5,X2,
160400          "METRES PER SECOND">,VEL[HGHTCTR1]);
160500          WRITE(LP,<"BEFORE RESOLVING, AV ON X ANEMOM=",F10.5,"  AV ON Y ANE
160600          MOM=",F10.5,"  METRES PER SECOND"
160700          ,/,"AVERAGE ANGLE OF ATTACK OF WIND VECTOR TO X ANEM=",F10.5,
160800          X2"DEGREES">,AV[0],
160900          AV[1],
161000          ARG*180/3.14159);
161100          %
161200          %   START DETAILED PROCESSING,EACH ARRAY HAS THE DATA
161300          %   PROCESSED IN THE ORDER LONGITUDINAL,LATERAL,VERTICAL,
161400          %   DEPENDING ON THE STATE OF THE BOOLEANS LNG,LAT,VER
161500          FOR J:=0,1,2 DO BEGIN
161600            IF J=0 AND LNG THEN GO TO IN;
161700            IF J=1 AND LAT THEN GO TO IN;
161800            IF J=2 AND VER THEN GO TO IN;
161900            GO TO OUT;
162000            IN:
162100            WRITE(LP,<//>);
162200            %
162300            % NOW THE BOOLEANS ARE TESTED AND THE VARIOUS TYPES OF TREND
162400            % REMOVAL DONE
162500            %   VERTICAL DATA IS READ OFF THE DATA FILE,CONVERTED TO THE
162600            %   DESIRED SCAN RATE,CONVERTED TO M/S AND THE MEAN AND
162700            %   MEAN SQUARE CALCULATED
162800            IF J=2 THEN BEGIN
162900              REPLACE POINTER(XR) BY 0 FOR T2P1 WORDS;
163000              REPLACE POINTER(XI) BY 0 FOR T2P1 WORDS;
163100              AV[2]:=RMS[2]:=0;
163200              TEMPSTORE1:=ACTFRQ/32*CORFCTR[3*HGHTCTR1+3];
163300              FOR I:=0 STEP 1 UNTIL NIN/256-1 DO
163400              BEGIN
163500                READ(INFYLE[I*3*NOARRAYS+2+3*HGHTCTR1],256,X)[EOF];
163600                FOR KK:=0 STEP 2*FRQAV UNTIL 255 DO BEGIN
163700                  FOR K:=0 STEP 1 UNTIL FRQAV-1 DO BEGIN
163800                    XR[INT:=((I*128+KK/2)/FRQAV)]:=*+X[K+KK]/FRQAV;
163900                    XI[INT]:=*+X[K+FRQAV+KK]/FRQAV; END K;
164000                  IF CSCRTN THEN AV[2]:=*+XR[INT]+XI[INT] ELSE
164100                  AV[2]:=*+(XR[INT]:=**TEMPSTORE1)+(XI[INT]:=**TEMPSTORE1);
164200                  RMS[2]:=*+XR[INT]*XR[INT]+XI[INT]*XI[INT];
164300                END KK;
164400              END;
164500              FOR I:=0 STEP 1024 UNTIL T2M1 DO
164600              WRITE(FX[(2*TEMPNIN+I)/1024],1024,XR[I]);
164700              FOR I:=0 STEP 1024 UNTIL T2M1 DO
164800              WRITE(FX[(2*TEMPNIN+T2+I)/1024],1024,XI[I]);
164900              XM[2]:=AV[2]/TEMPNIN; RMS[2]:=*/TEMPNIN       ;
165000              WRITE(LP,<"AV VEL ON Z ANEMOM=",F10.5," METRES PER"
165100              " SECOND">,XM[2]);
165200              STDDEV[2]:=SQRT(RMS[2]-XM[2]*XM[2]);
165300              WRITE(LP,<"VERTICAL MS=",F10.5,"VERTICAL RMS=",F10.5,"VERTICAL"
165400              " STDDEV=",F10.5," M/S">,RMS[2],SQRT(RMS[2]),STDDEV[2]);
165500              WRITE(LP,<"VERTICAL STTDEV=",F10.5," M/S">,STDDEV[2]);
```

```
165600              END OF J EQ 2 BLOCK;
165700              IF J=0 THEN BEGIN
165800                %   LONGITUDINAL DIRECTION,THE DATA IS STILL RETAINED IN
165900                %   THE ARRAYS XR,XI.
166000                RMS[0]:=*/TEMPNIN; XM[0]:=AV[0]*CO+AV[1]*SI;
166100                STDDEV[0]:=SQRT(RMS[0]-XM[0]*XM[0]);
166200                WRITE(LP,<"WITH NO TREND REMOVAL LONG MEAN=",F10.5,
166300                " M/S"/"LONG MS=",F14.4,"LONG RMS=",F10.5,"LONG"
166400                " STDDEV=",F10.5>,XM[0],RMS[0],SQRT(RMS[0]),STDDEV[0]);
166500              END OF J EQ 0 BLOCK  ;
166600              IF J=1 THEN BEGIN
166700                %   LATERAL DIRECTION DATA READ OFF TEMPORARY DISK FILE
166800                FOR I:=0 STEP 1024 UNTIL T2M1 DO
166900                READ(FX[(TEMPNIN+I)/1024],1024,XR[I]);%READ LAT DATA
167000                FOR I:=0 STEP 1024 UNTIL T2M1 DO
167100                READ(FX[(TEMPNIN+T2+I)/1024],1024,XI[I]);
167200                XM[1]:=AV[1]*CO-AV[0]*SI;
167300                RMS[1]:=*/TEMPNIN; STDDEV[1]:=SQRT(RMS[1]-XM[1]*XM[1]);
167400                WRITE(LP,<"WITH NO TREND REMOVAL LAT MEAN=",F10.5," M/S"/
167500                "LAT MS=",F10.5,"LAT RMS=",F10.5,"LAT STDDEV=",F10.5," M/S"
167600                >,XM[1],RMS[1],SQRT(RMS[1]),STDDEV[1]);
167700              END OF J EQ 1 BLOCK;
167800              KK:=T2/1024+1; %NO OF RECORDS PER ARRAY OF CROSSCOR DATA
167900              AS:=4*KK*NUMCORS; BS:=2*KK;
168000              IF NOTREND THEN
168100              %   THIS BLOCK IS ENTERED ONLY IF THE DATA IS TO BE PROCESSED WITH NO
168200              %   TREND REMOVAL
168300              BEGIN
168400                TRENDCTR:=0;
168500                TNOTRD:=*-T;
168600                % THE MEAN IS ALREADY CALCULATED FROM RESOLVING
168700                %
168800                BOO:=CNTRD;
168900                PROC(BOO,J,TRENDCTR);
169000                %
169100              END OF NO TREND REMOVAL BLOCK;
169200              % TEST FOR LINEAR TREND REMOVAL
169300              %
169400              %
169500              %
169600              IF LINTREND THEN
169700              %
169800              %   THIS BLOCK IS ENTERED ONLY IF THE DATA IS TO BE PROCESSED
169900              %   WITH A LINEAR TREND REMOVAL
170000              BEGIN
170100                TRENDCTR:=1;
170200                XM[J]:=RMS[J]:=0;
170300                TLIN:=*-T;
170400                %   READ REQUIRED DATA FROM FILE FX
170500                IF J=0 THEN
170600                FOR I:=0 STEP 1024 UNTIL T2M1 DO BEGIN
170700                  READ(FX[I/1024],1024,XR[I]);
170800                  READ(FX[(T2+I)/1024),1024,XI[I]); END;
170900                IF J=1 THEN
171000                FOR I:=0 STEP 1024 UNTIL T2M1 DO BEGIN
171100                  READ(FX[(TEMPNIN+I)/1024],1024,XR[I]);
171200                  READ(FX[(TEMPNIN+T2+I)/1024],1024,XI[I]);  END;
171300                IF J=2 THEN
171400                FOR I:=0 STEP 1024 UNTIL T2M1 DO BEGIN
171500                  READ(FX[(2*TEMPNIN+I)/1024],1024,XR[I]);
171600                  READ(FX[(2*TEMPNIN+T2+I)/1024],1024,XI[I]);END;
171700                TSUMS:=*-T;
171800                %   CALCULATE LINEAR TREND LINE BY LEAST SQUARES
171900                ST[J]:=(TEMPNIN1)*TEMPNIN/2;
172000                FOR I:=0 STEP 2 UNTIL TEMPNIN1 DO
172100                BEGIN
172200                  SV[J]:=*+XR[I/2]+XI[I/2];
172300                  ST2[J]:=*+I*I+(I+1)*(1+1);
172400                  STV[J]:=*+I*XR[I/2]+(I+1)*XI[I/2];
172500                END;
172600                TSUMS:=*+T;
172700                % OUTPUT TREND PARAMETERS
172800                BEGIN
172900                  A0[J]:=(STV[J]*ST[J]-ST2[J]*SV[J])/(ST[J]*ST[J]-
173000                  TEMPNIN*ST2[J]);
173100                  A1[J]:=(SV[J]/TEMPNIN-STV[J]/ST[J])/(ST[J]/TEMPNIN-ST2[J]/
173200                  ST[J]);
173300                END;
173400                IF J=0 THEN
173500                WRITE(LP,</"LONGITUDINAL DIRECTION LINEAR TREND REMOVAL VALUES">);
173600                WRITE(LP,<"THE LINEAR TREND LINE IS OF THE FORM X(T)=X(T)-"
173700                "A0-A1*T">);
173800                IF J=1 THEN WRITE(LP,</"LAT DIRN LINEAR TREND REMOVAL"/>);
173900                IF J=2 THEN WRITE(LP,</"VERT DIRN LINEAR TREND REMOVAL"/>);
174000                WRITE(LP,<"A0 THE VEL AXIS INTERCEPT=",E13.5,X2,"A1 AN INDICATIO"
174100                "N OF THE SLOPE=",E13.5,/,"A0+A1*TEMPNIN/2, THE AVERAGE=",E13.5,
174200                X2,"A0+A1*TEMPNIN1, THE FINAL VALUE=",E13.5>,A0[J],A1[J],
174300                A0[J]+A1[J]*TEMPNIN/2,A0[J]+A1[J]*TEMPNIN1);
174400                TLTR:=*-T;
174500                %   REMOVE TREND,CALCULATE MEAN AND MEAN SQUARE
174600                FOR I:= 0 STEP 2 UNTIL TEMPNIN1 DO
174700                BEGIN
174800                  XR[I/2]:=XR[I/2]-A0[J]-A1[J]*I;
174900                  XI[I/2]:=XI[I/2]-A0[J]-A1[J]*(I+1);
175000                  XM[J]:=*+XR[I/2]+XI[I/2];
```

```
175100              RMS[J]:=*+XR[I/2]*XR[I/2]+XI[I/2]*XI[I
175200              /2];
175300            END;
175400            TLTR:=*+T;
175500            TLAVRMS:=*-T;
175600            XM[J]:=XM[J]/TEMPNIN;RMS[J]:=RMS[J]/TEMPNIN;
175700            STDDEV[J]:=SQRT(RMS[J]-XM[J]*XM[J]);
175800            WRITE(LP,<"MEAN OF DATA AFTER LIN TREND REM (XM) =",E13.5,X5,
175900            "STD DEV DITTO=",E13.5," M/S">,XM[J],STDDEV[J]);
176000            BOO:=CLTRD;
176100            PROC(BOO,J,TRENDCTR);
176200          END OF LINEAR TREND REMOVAL BLOCK;
176300          % TEST FOR PARABOLIC TREND REMOVAL
176400          %
176500          %
176600          %
176700          IF PARTREND THEN
176800          %
176900          %   THIS BLOCK IS ENTERED ONLY IF THE DATA IS TO BE PROCESSED
177000          %   WITH A PARABOLIC TREND REMOVAL
177100          BEGIN
177200            TRENDCTR:=2;
177300            XM[J]:=RMS[J]:=0;
177400            TPAR:=*-T;
177500            %   READ REQUIRED VELOCITY DATA FROM FILE FX
177600            IF J=0 THEN
177700            FOR I:=0 STEP 1024 UNTIL T2M1 DO BEGIN
177800              READ(FX[I/1024],1024,XR[I]);
177900              READ(FX[(T2+I)/1024],1024,XI[I]); END;
178000            IF J=1 THEN
178100            FOR I:=0 STEP 1024 UNTIL T2M1 DO BEGIN
178200              READ(FX[(TEMPNIN+I)/1024],1024,XR[I]);
178300              READ(FX[(TEMPNIN+T2+I)/1024],1024,XI[I]);  END;
178400            IF J=2 THEN
178500            FOR I:=0 STEP 1024 UNTIL T2M1 DO BEGIN
178600              READ(FX[(2*TEMPNIN+I)/1024],1024,XR[I]);
178700              READ(FX[(2*TEMPNIN+T2+I)/1024],1024,XI[I]);END;
178800            %   CALCULATE PARABOLIC TREND LINE BY LEAST SQUARES
178900            IF NOT LINTREND THEN
179000            BEGIN
179100              ST[J]:=(TEMPNIN1)*TEMPNIN/2;
179200              FOR I:=0 STEP 2 UNTIL TEMPNIN1 DO
179300              BEGIN
179400                SV[J]:=*+XR[I/2]+XI[I/2];
179500                ST2[J]:=*+I*I+(I+1)*(I+1);
179600                STV[J]:=*+I*XR[I/2]+(I+1)*XI[I/2];
179700              END;
179800            END;
179900            FOR I:=0 STEP 2 UNTIL TEMPNIN1 DO
180000            BEGIN
180100              ST3[J]:=*+I**3+(I+1)**3;
180200              ST4[J]:=*+I**4+(I+1)**4;
180300              ST2V[J]:=*+I*I*XR[I/2]+(I+1)*(I+1)*XI[I/2];
180400            END;
180500            % CALCULATE VARIABLES TO BE USED IN THE TREND REMOVAL
180600            C1[J]:=(SV[J]*ST3[J]-STV[J]*ST2[J])/(ST[J]*ST3[J]-ST2[J]**2)
180700            ;
180800            C2[J]:=(STV[J]*ST4[J]-ST2V[J]*ST3[J])/(ST2[J]*ST4[J]
180900            -ST3[J]**2);
181000            C3[J]:=(TEMPNIN*ST3[J]-ST[J]*ST2[J])/(ST[J]*ST3[J]-ST2[J]**2
181100            );
181200            C4[J]:=(ST[J]*ST4[J]-ST2[J]*ST3[J])/(ST2[J]*ST4[J]
181300            -ST3[J]**2);
181400            B0[J]:=(C1[J]-C2[J])/(C3[J]-C4[J]);
181500            B1[J]:=C1[J]-B0[J]*C3[J];
181600            B2[J]:=(SV[J]-B1[J]*ST[J]-B0[J]*TEMPNIN)/ST2[J];
181700            WRITE(LP,<"VALUES OF PARAMETERS FOR PARABOLIC TREN"
181800            "D REMOVAL">);
181900            IF J=0 THEN WRITE(LP,</"LONGITUDINAL DIRECTION"/>);
182000            IF J=1 THEN WRITE(LP,</"LATERAL DIRECTION"/>);
182100            IF J=2 THEN WRITE(LP,</"VERTICAL DIRECTION"/>);
182200            WRITE(LP,<"THE PARABOLIC TREND LINE IS IN THE FORM X(T)=X(T)-"
182300            "B0-B1*T-B2*T**2">);
182400            WRITE(LP,<"B0, THE VEL AXIS INTERCEPT=",E13.5,X2,"B1=",E1
182500            3.5,/,"B0+B1*TEMPNIN1+B2*TEMPNIN1**2, THE FINAL VALUE=",E13.5,X2,/,"THE
182600            TREND REMOVAL HAS A TURNING POINT WHEN -B1/(2*B2)=",I7,X2,
182700            "WHICH IS=",E13.5>,B0[J],B1[J],B0[J]+B1[J]*TEMPNIN1+B2[J]*TEMPNIN1**2,
182800            -B1[J]/(2*B2[J]),B0[J]-B1[J]**2/(4*B2[J]));
182900            WRITE(LP,<"B2=",E13.5>,B2[J]);
183000            % REMOVE TREND
183100            FOR I:=0 STEP 2 UNTIL TEMPNIN1 DO
183200            BEGIN
183300              XR[I/2]:=XR[I/2]-B0[J]-B1[J]*I-B2[J]*I*I;
183400              XI[I/2]:=XI[I/2]-B0[J]-B1[J]*(I+1)-B2[J]*(I+1)
183500              *(I+1);
183600              XM[J]:=*+XR[I/2]+XI[I/2];
183700              RMS[J]:=*+XR[I/2]*XR[I/2]+XI[I/2]*XI[I
183800              /2];
183900            END;
184000            XM[J]:=XM[J]/TEMPNIN;
184100            RMS[J]:=RMS[J]/TEMPNIN;
184200            STDDEV[J]:=SQRT(RMS[J]-XM[J]**2);
184300            WRITE(LP,<"MEAN AFTER PARABOLIC TREND REMOVAL=",E13.5,
184400            "  STD DEV DITTO=",E13.5," M/S">,XM[J],STDDEV[J]);
184500            BOO:=CPTRD;
```

```
184600              PROC(BOD,J,TRENDCTR);
184700            END OF PARTREND LOOP;
184800            OUT:
184900          END OF J LOOP;
185000          %
185100          % THE TREND REMOVAL PARTS HAVE NOW ALL BEEN GONE THROUGH
185200          % THE PROGRAMME NOW REQUIRES TO LOOP BACK TO THE HEIGHT LOOP
185300          % LABEL SO THAT THE PROCESS CAN BE REPEATED FOR A NEW HEIGHT
185400          % WHEN ALL THE HEIGHTS HAVE BEEN DONE THE SAMPLING FREQUENCY
185500          % CAN BE DECREASED
185600          %
185700          IF ONEHT THEN HGHTCTR:=HGHTCTR+NOARRAYS;
185800          IF HGHTCTR<NOARRAYS THEN GO TO HGHTLABL;
185900          %
186000        END OF NEW PROC BLOCK;
186100        %
186200        IF CROSSCOR AND CORFRQ=FRQCTR THEN BEGIN
186300          %
186400          % IF CROSS-CORRELATIONS ARE BEING PRODUCED THEY NEED NOW
186500          % TO BE FORMED-MULTIPLIED TOGETHER AND PLOTTED
186600          DIRN:=-1;
186700          TEMPNIN:=NIN/2**(CORFRQ-1);
186800          M:=LOG(TEMPNIN)/LOG(2)-1;
186900          FOR I:=1 STEP 2 UNTIL 2*NUMCORS DO BEGIN
187000            FOR INT:=0,1,2 DO BEGIN
187100              %   DO THE CROSS-CORRELATION WITH THE RIGHT KIND OF TREND REMOVAL
187200              IF CNTRD AND INT=0 THEN GO TO INLAB;
187300              IF CLTRD AND INT=1 THEN GO TO INLAB;
187400              IF CPTRD AND INT=2 THEN GO TO INLAB;
187500              GO TO OUTLAB;
187600              INLAB:
187700              %   IF COMPRESS IS TRUE,THE PROCEDURE PL IS USED WHICH PLOTS SEVERAL
187800              %   CURVES ON ONE GRAPH.IT PLOTS THE CURVE FOR ONLY ONE KIND
187900              %   OF TREND REMOVAL
188000              IF COMPRESS THEN
188100              IF INT NEQ TRDIRN THEN GO TO OUTLAB;
188200              %   READ REQUIRED DATA
188300              FOR PQ:=0 STEP 1024 UNTIL T2 DO BEGIN
188400                READ(FC[AS*INT+BS*(I-1)+PQ/1024),1024,XR[PQ]);
188500                READ(FC[AS*INT+BS*(I-1)+KK+PQ/1024],1024,XI[PQ]);
188600                READ(FC[AS*INT+BS*I+PQ/1024],1024,AR[PQ]);
188700                READ(FC[AS*INT+BS*I+KK+PQ/1024],1024,AI[PQ]);
188800              END;
188900              %   MULTIPLY THE TWO COMPLEX SPECTRAL DATA STREAMS TOGETHER
189000              %   THE MULTIPLICATION ALSO MAKES THE XR,XI DATA INTO THE COMPLEX
189100              %   CONJUGATE,IE IT MAKES XI=-XI
189200              FOR J:=0 STEP 1 UNTIL T2 DO
189300              BEGIN
189400                TEMPSTORE1:=XR[J];
189500                XR[J]:=**AR[J]+XI[J]*AI[J];
189600                XI[J]:=TEMPSTORE1*AI[J]-XI[J]*AR[J];
189700              END;
189800              %   TAKE INVERSE FOURIER TRANSFORM
189900              RRDR(XR[*],XI[*],M,DIRN);
190000              BITREV2(XR[*],XI[*],M);
190100              FFTR(XR[*],XI[*],S,C,M);
190200              %   XR AND XI NOW CONTAIN THE CROSS-CORRELATION DATA
190300              %   IT IS PLOTTED EITHER IN PL OR PLOTCROSSCOR
190400              IF COMPRESS THEN
190500              PL(XR[*],XI[*],CORFRQ,CROSS[*],SACTFRQ,INT,ACTFRQ,NIN,I,CNTRD,
190600              CLTRD,CPTRD,NUMCORS,TRDIRN) ELSE
190700              PLOTCROSSCOR(XR[*],XI[*],CORFRQ,CROSS[*],SACTFRQ,
190800              INT      ,ACTFRQ,NIN,I,CNTRD,CLTRD,CPTRD);
190900              OUTLAB:
191000            END;
191100          END;
191200        END;
191300      END OF HGHTCTR BLOCK;
191400      %   ALL PROCESSING FOR THIS SCAN RATE OR SAMPLING FREQUENCY
191500      %   IS FINISHED. THE PROGRAMME LOOPS BACK TO THE LABEL FRQLBL
191600      %   WHERE PROCESSING MAY CONTINUE, THE NEXT PROCESSING
191700      %   IS DONE AT HALF THE PRESENT SCAN RATE
191800      GO TO FRQLABL;
191900      %
192000      %   THIS LABEL IS USED WHEN NUMBER CRUNCHING HAS FINISHED
192100      %   AND THE POWER SPECTRAL DENSITY AND AUTOCORRELATION
192200      %   FUNCTIONS ARE TO BE PLOTTED
192300      PLOTLBL:
192400      %
192500      COMMENT
192600      THE SPECTRAL AND AUTOCORRELATION OUTPUT CAN BE PLOTTED IN A
192700      VARIETY OF WAYS. THE PLOTTING OUTPUT WILL DEPEND ON THE PREVIOUS
192800      CONTROL PARAMETERS USED. THE AUTOCORRELATION CORRESPONDING
192900      TO THE SPECTRUM WILL ALWAYS BE PLOTTED IF IFAUTO IS
193000      TRUE.
193100      TO PLOT. A SERIES OF DATA CARDS IS READ. THE FIRST
193200      CARD CONTAINS AN INTEGER WHICH IS THE NUMBER OF CARDS TO BE
193300      READ NEXT WITH PLOTTING CONTROL INFORMATION ON
193400      THEM. EACH CARD HAS 7 NUMBERS ON IT WHICH ARE
193500      READ INTO THE VARIABLES -
193600      TRENDS,TRENDCTR,HEIGHTS,HGHTCTR,FREQS,FRQCTR,DIRECTION
193700      TRENDS,HEIGHTS,FREQS ARE BOOLEANS. ONLY ONE CAN BE
193800      TRUE(=1) PER CARD. IF TRUE THE PLOTS WILL BE FUNCTIONS
193900      OF TYPE OF TREND REMOVAL, POSITION, OR PROCESSING FREQUENCY
194000      RESPECTIVELY.
```

```
194100        TRENDCTR,HGHTCTR,FRQCTR,DIRECTION ARE INTEGERS
194200        TRENDCTR=0 FOR NO TREND REMOVAL,1 FOR LINEAR, 2 FOR PARABOLIC
194300        HGHTCTR IS THE NUMBER OF THE ARRAY TO BE PLOTTED, IE HAS
194400        A VALUE BETWEEN 1 AND THE NUMBER OF ORTHOGONAL ARRAYS.
194500        FRQCTR IS THE FREQUENCY THE DATA IS TO BE PLOTTED AT, HAS
194600        A VALUE BETWEEN STARTFRQ AND STARTFRQ + NOFRQS-1
194700        DIRECTION IS THE DIRECTION TO BE PLOTTED
194800        =0 FOR LONGITUDINAL, 1 LATERAL, 2 VERTICAL.
194900        E.G. IF 1 PLOT OF THE LONGITUDINAL DIRECTION WAS
195000        DESIRED AS A FUNCTION OF TREND REMOVAL, THE 6TH ARRAY
195100        AND AT THE HIGHEST SCAN RATE PROCESSED AT, THE DATA
195200        CARDS WOULD BE
195300        1,
195400        1,1,0,6,0,1,0,
195500        2 PLOTS AS FUNCTIONS OF POSITION WITH PARABOLIC TREND
195600        REMOVAL AND AT HALF THE HIGHEST SCAN RATE, FOR THE
195700        LATERAL AND VERTICAL DIRECTIONS WOULD BE
195800        2,
195900        0,2,1,1,0,2,1,
196000        0,2,1,1,0,2,2,
196100        IN BOTH THE ABOVE EXAMPLES, STARTFRQ WAS SET TO 1 BY
196200        PREVIOUS DATA CARDS. IF STARTFRQ WERE=3, THE TWO
196300        EXAMPLES BECOME
196400        1,
196500        1,1,0,6,0,3,0,
196600        2,
196700        0,2,1,1,0,4,1,
196800        0,2,1,1,0,4,2,
196900        OBVIOUSLY, IF ONLY ONE ORTHOGONAL ARRAY IS BEING PROCESSED
197000        THE BOOLEAN HEIGHTS HAS TO BE FALSE FOR ANY PLOTS.;
197100        %
197200        READ(KR,/,NOOFLOOPS); LOOPCOUNTER:=0;
197300        WRITE(LP,<//"NUMBER OF TIMES PLOT PROCEDURES CALLED=",I6//>,NOOFLOOPS);
197400        PLOTLOOPLBL: LOOPCOUNTER:=*+1;
197500        IF LOOPCOUNTER>NOOFLOOPS THEN GO TO LOOPHOLE;
197600        READ(KR,/,TRENDS,TRENDCTR,HEIGHTS,HGHTCTR,FREQS,FRQCTR,DIRECTION);
197700        WRITE(LP,*/,LOOPCOUNTER,TRENDS,TRENDCTR,HEIGHTS,HGHTCTR,FREQS,FRQCTR,
197800        DIRECTION);
197900        IF ONEHT THEN BEGIN
198000          IF HGHTCTR NEQ ONEHEIGHT THEN BEGIN
198100            WRITE(LP,<"HGHTCTR IS NOT EQUAL TO ONEHEIGHT,HGHTCTR=",I6
198200            ,"ONEHEIGHT=",I6>,HGHTCTR,ONEHEIGHT); GO TO ERRORCOND; END;
198300          IF HEIGHTS THEN BEGIN WRITE(LP,<"HEIGHTS SHOULD BE FALSE SINCE"
198400            " ONEHT IS TRUE">); GO TO ERRORCOND; END; END;
198500        IF TRENDS THEN
198600        IF HEIGHTS OR FREQS THEN BEGIN
198700          WRITE(LP,<"FREQS OR HEIGHTS TRUE WHEN TRENDS IS TRUE">);
198800          WRITE(LP,*/,FREQS,HEIGHTS); GO TO ERRORCOND; END;
198900        IF FREQS THEN
199000        IF TRENDS OR HEIGHTS THEN BEGIN
199100          WRITE(LP,<"TRENDS OR HEIGHTS TRUE WHEN FREQS IS TRUE">);
199200          WRITE(LP,*/,TRENDS,HEIGHTS); GO TO ERRORCOND; END;
199300        IF TRENDS OR HEIGHTS OR FREQS THEN ELSE BEGIN
199400          WRITE(LP,<"TRENDS=HEIGHTS=FREQS=FALSE MEANS NO OUTPUT">);
199500          GO TO ERRORCOND; END;
199600        IF HGHTCTR<1 OR HGHTCTR >12 THEN BEGIN
199700          WRITE(LP,<"ERROR IN HGHTCTR,HGHTCTR=",I7>,HGHTCTR);
199800          GO TO ERRORCOND; END;
199900        IF FRQCTR<STARTFRQ OR FRQCTR>(STARTFRQ+NOFRQS-1)
200000        THEN BEGIN WRITE(LP,<"ERROR IN FRQCTR,FRQCTR=",I6>,FRQCTR);
200100          GO TO ERRORCOND; END;
200200        IF TRENDCTR<0 OR TRENDCTR>2 THEN BEGIN
200300          WRITE(LP,<"ERROR IN TRENDCTR,TRENDCTR=",I6>,TRENDCTR);
200400          GO TO ERRORCOND; END;
200500        IF DIRECTION<0 OR DIRECTION>2 THEN BEGIN
200600          WRITE(LP,<"ERROR IN DIRECTION,DIRECTION=",I6>,DIRECTION);
200700          GO TO ERRORCOND; END;
200800        IF DIRECTION=0 THEN
200900        IF NOT LNG THEN BEGIN
201000          WRITE(LP,<"DIRECTION=0 BUT LNG IS FALSE">);
201100          GO TO ERRORCOND; END;
201200        IF DIRECTION=1 THEN
201300        IF NOT LAT THEN BEGIN WRITE(LP,<"DIRECTION=1 BUT"
201400          " LAT FALSE">); GO TO ERRORCOND; END;
201500        IF DIRECTION=2 THEN
201600        IF NOT VER THEN BEGIN
201700          WRITE(LP,<"DIRECTION=2 BUT VER FALSE">);
201800          GO TO ERRORCOND; END;
201900        IF TRENDCTR=0 THEN
202000        IF NOT NOTREND THEN BEGIN
202100          WRITE(LP,<"TRENDCTR=0 BUT NOTREND IS FALSE">);
202200          GO TO ERRORCOND; END;
202300        IF TRENDCTR=1 THEN
202400        IF NOT LINTREND THEN BEGIN
202500          WRITE(LP,<"TRENDCTR=1 BUT LINTREND IS FALSE">);
202600          GO TO ERRORCOND; END;
202700        IF TRENDCTR=2 THEN
202800        IF NOT PARTREND THEN BEGIN
202900          WRITE(LP,<"TRENDCTR=2 BUT PARTREND IS FALSE">);
203000          GO TO ERRORCOND; END;
203100        WRITE (LP,<2("PLOTTING PARAMETERS APPEAR OK DATA WILL"
203200        " BE PLOTTED          ")//>);
203300
203400        BEGIN
203500
```

```
203600          TPPWRF:=*-T;
203700          %   PLOT THE POWER SPECTRAL DENSITY
203800          PLOTPOWER(NOPTSOUT[*],HEIGHT[*],
203900          NOARRAYS,ACTFREQ1516,NOFRQS,SAMPFRQS[*],HEIGHTS,FREQS,TRENDS,
204000          DIRECTION,TRENDCTR,FRQCTR,HGHTCTR,PSVSNFQ,STARTFRQ);
204100          TPPWRF:=*+T;
204200
204300          TPATF:=*-T;
204400          IF IFAUTO THEN
204500          %   PLOT THE AUTOCORRELATION FUNCTION
204600          PLOTAUTO(HEIGHT[*],NOARRAYS,
204700          ACTFREQ1516,NOFRQS,SAMPFRQS[*],HEIGHTS,FREQS,TRENDS,DIRECTION,
204800          TRENDCTR,FRQCTR,HGHTCTR,NUM[*],STARTFRQ);
204900          TPATF:=*+T;
205000        END;
205100        GO TO OVERLBL;
205200        ERRORCOND:
205300        WRITE(LP,<70("*")," ERROR IN PLOT PARAMETERS AS ABOVE"//>);
205400        OVERLBL:
205500        GO TO PLOTLOOPLBL;
205600        LOOPHOLE:
205700        %   ELAPSED PROCESSOR TIMES FOR VARIOUS PARTS
205800        WRITE(LP,*/,TREAD,TALTFQ,TRES,TSUMS,TNRMS,TCOS,TFHR,TMAG,TAREA,TAVS,TNAU
205900        TO,TAVA,TLIN,TLTR,TLAVRMS,TLINNORM,TPAR,TPPWRH,TPAUTH,    TPPWRF,TPATF,T
206000        NOTRD);
206100        %
206200        WRITE(LP,<"END OF PROGRAMME">);
206300      END;
206400    END;
206500 END.
```

INPUT STRING WAS
"PSAUTCORS STEP 2"

FLOWCHART OF PROGRAM 'PSAUTCORS'

START

Declare global files, plot procedures compiled externally, include the source FFT procedures in Algol which are on computer centre tape in the MATHLIB library package. Declare variables global to the procedures.

Read in correction factors for non-cosine response correction, propeller anemometer calibration factors.

Declare variables global to mainline

Read ACTFRQ, the scan rate of the data in the input data file.
STARTFRQ[1], the highest scan rate for processing to start at
NOFRQS, the number of different scan rates for processing
NIN, the number of samples in each channel in the input file
NOARRAYS, the number of orthogonal anemometer arrays in the data file.

PSVSNFQ, if true, power spectra are plotted against dimensionless frequency, $f \times Z/\bar{V}$, otherwise against frequency in Hz

IFAUTO, if true all autocorrelations corresponding to power spectra calculated will be plotted

ONEHT, if true, only one orthogonal anemometer array will be processed, number ONEHEIGHT

LNG, if true, all longitudinal component data will be processed
LAT, if true, all lateral component data will be processed
VER, if true, all vertical component data will be processed

---

(1) These are integers representing the scan rate, e.g.
STARTFRQ, CORFRQ = 1 means processing at ACTFRQ/2^0
STARTFRQ, CORFRQ = 3 means processing at ACTFRQ/2^2 etc.

Cont'd

CROSSCOR, if true cross-correlations will be calculated, the number calculated being NUMCORS, and calculated at a frequency CORFRQ(1)

CNTRD, if true, cross-correlation will be calculated with no trend removal.

CLTRD, if true, cross-correlations will be calculated with linear trend removal.

CPTRD, if true, cross-correlations will be calculated with parabolic trend removal.

CROSSCOR, if true,read (COMPRESS, if true, the cross-correlations will be plotted in a compressed format, with a trend removal corresponding to TRDIRN - 0 - none, 1 - linear, 2 - parabolic).

Declare variables. Dynamically dimension some arrays.

If CROSSCOR true, read pairs of numbers corresponding to the data streams to be cross-correlated, into the array CROSS.

Read COSTAPER, if true a raised cosine taper will be applied to the first and last 10% of the time series data.

NOTREND, if true all analysis will be carried out with no trend removal.

LINTREND, if true, all analysis will be carried out with linear trend removal.

PARTREND, if true, all analysis will be carried out with parabolic trend removal.

Read CSCRTN, if true, data will be corrected for anemometer non-cosine response.

Read the heights of each orthogonal anemometer array into array HEIGHTS.

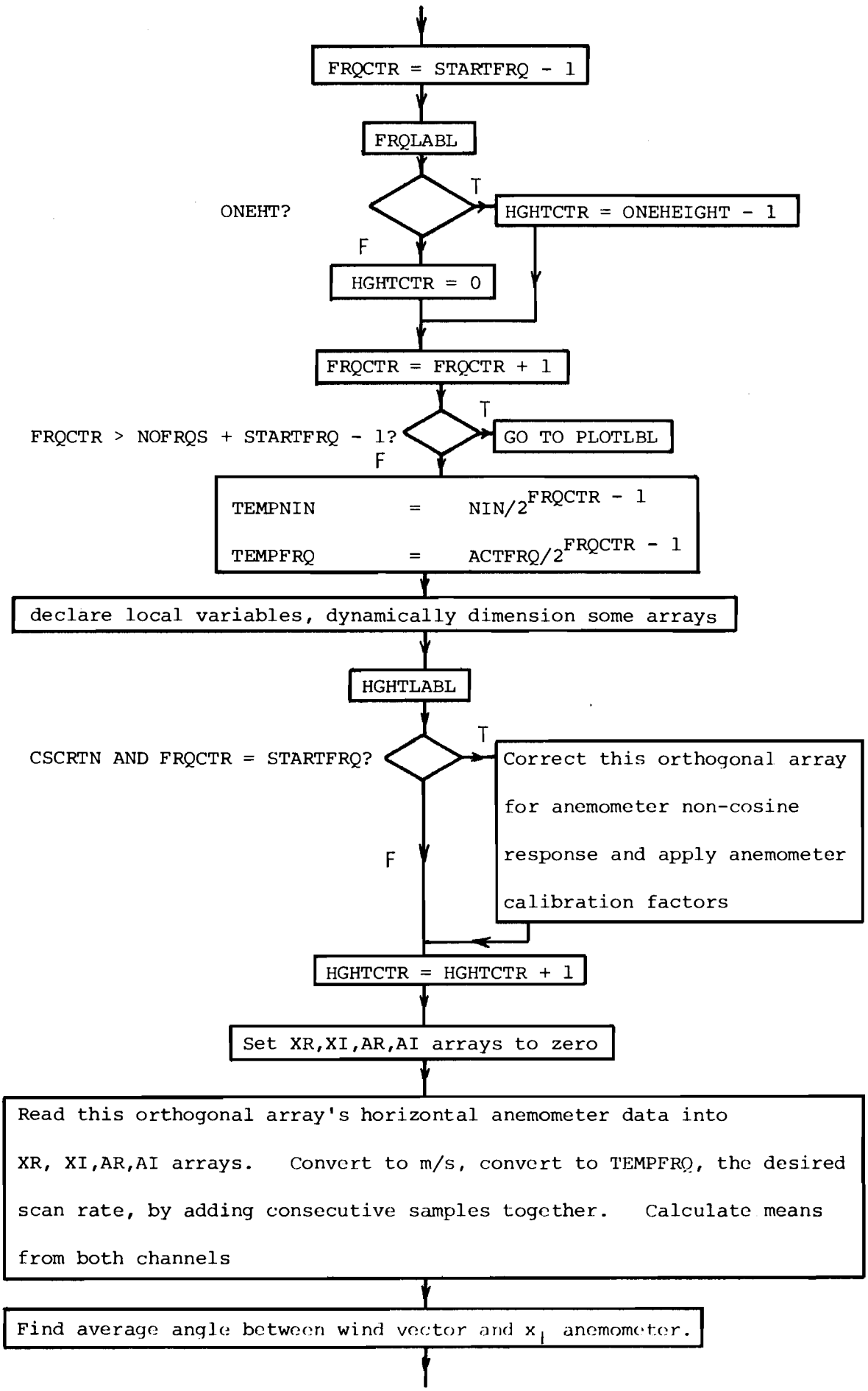
FRQCTR = STARTFRQ - 1
FRQLABL
ONEHT?
T
HGHTCTR = ONEHEIGHT - 1
F
HGHTCTR = 0
FRQCTR = FRQCTR + 1
FRQCTR > NOFRQS + STARTFRQ - 1?
T
GO TO PLOTLBL
F
TEMPNIN = NIN/2^FRQCTR - 1
TEMPFRQ = ACTFRQ/2^FRQCTR - 1
declare local variables, dynamically dimension some arrays
HGHTLABL
CSCRTN AND FRQCTR = STARTFRQ?
T
Correct this orthogonal array for anemometer non-cosine response and apply anemometer calibration factors
F
HGHTCTR = HGHTCTR + 1
Set XR,XI,AR,AI arrays to zero
Read this orthogonal array's horizontal anemometer data into XR, XI,AR,AI arrays. Convert to m/s, convert to TEMPFRQ, the desired scan rate, by adding consecutive samples together. Calculate means from both channels
Find average angle between wind vector and x1 anemometer.

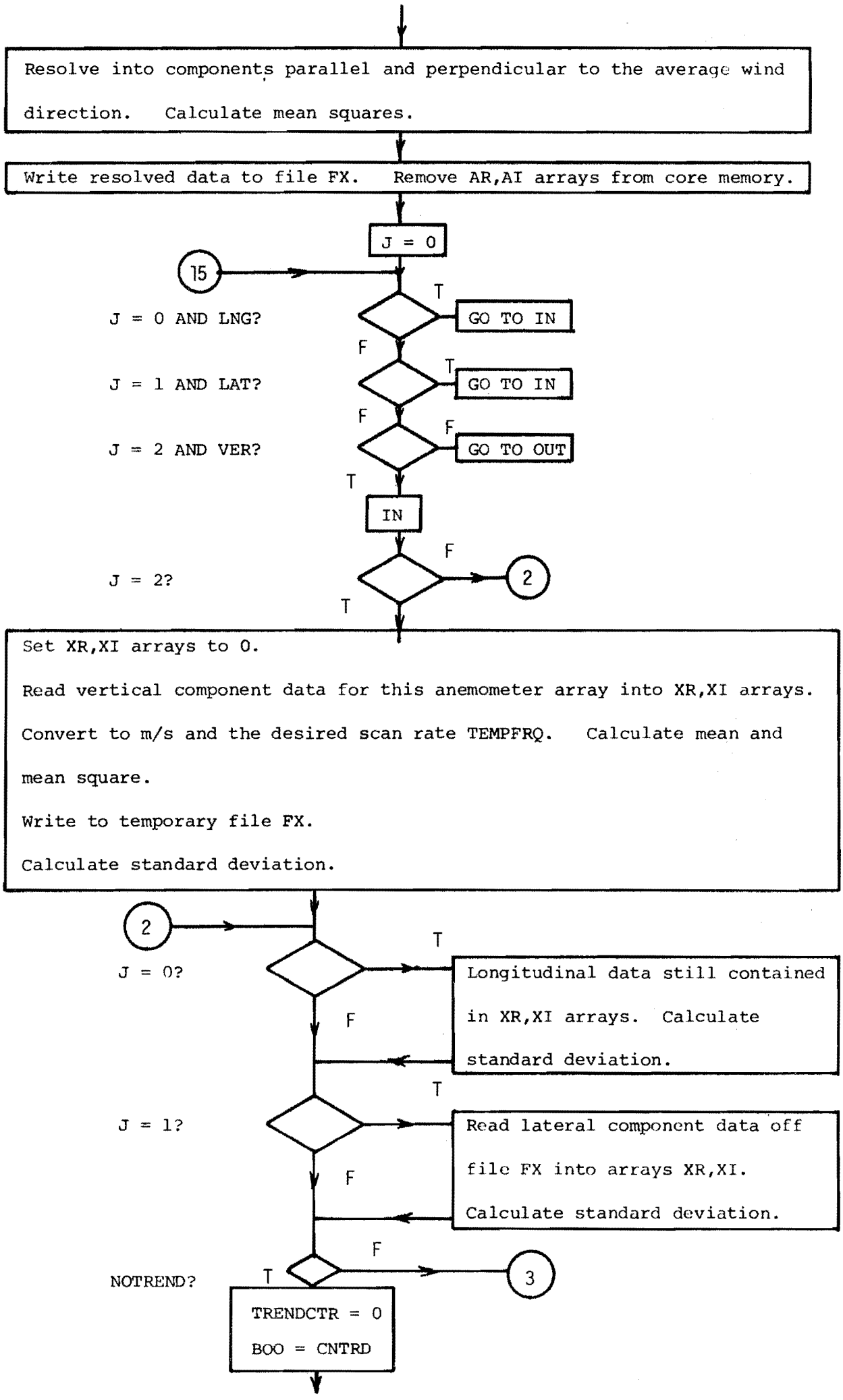
Resolve into components parallel and perpendicular to the average wind direction. Calculate mean squares.
Write resolved data to file FX. Remove AR,AI arrays from core memory.
J = 0
15
J = 0 AND LNG?
T
GO TO IN
F
J = 1 AND LAT?
T
GO TO IN
F
J = 2 AND VER?
F
GO TO OUT
T
IN
J = 2?
F
2
T
Set XR,XI arrays to 0.
Read vertical component data for this anemometer array into XR,XI arrays.
Convert to m/s and the desired scan rate TEMPFRQ. Calculate mean and mean square.
Write to temporary file FX.
Calculate standard deviation.
2
J = 0?
T
Longitudinal data still contained in XR,XI arrays. Calculate standard deviation.
F
J = 1?
T
Read lateral component data off file FX into arrays XR,XI.
Calculate standard deviation.
F
NOTREND?
F
3
T
TRENDCTR = 0
BOO = CNTRD

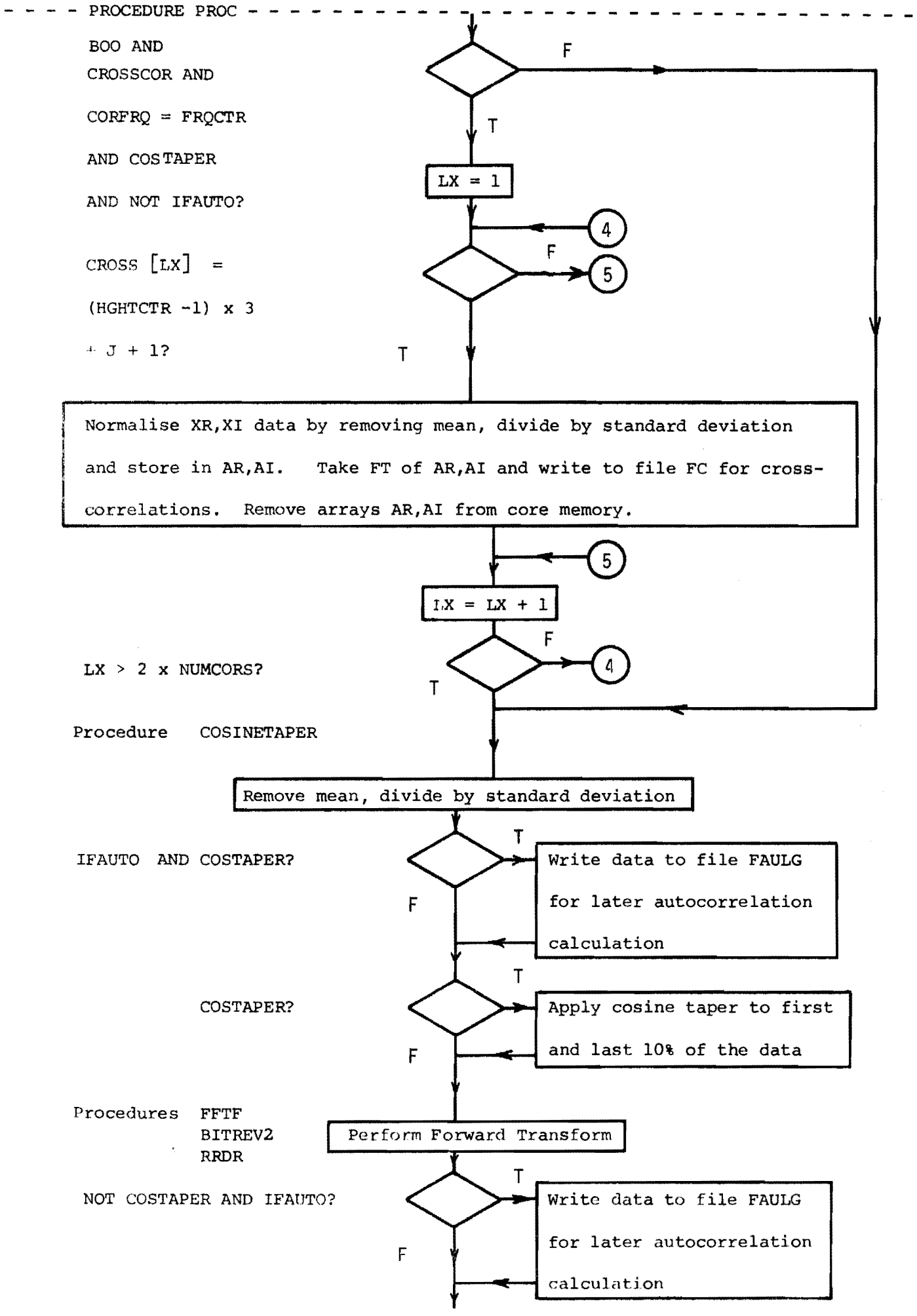
PROCEDURE PROC
BOO AND
CROSSCOR AND
CORFRQ = FRQCTR
AND COSTAPER
AND NOT IFAUTO?
F
T
LX = 1
4
CROSS [LX] =
(HGHTCTR -1) x 3
+ J + 1?
F
5
T
Normalise XR,XI data by removing mean, divide by standard deviation and store in AR,AI. Take FT of AR,AI and write to file FC for cross-correlations. Remove arrays AR,AI from core memory.
5
LX = LX + 1
F
LX > 2 x NUMCORS?
4
T
Procedure COSINETAPER
Remove mean, divide by standard deviation
T
IFAUTO AND COSTAPER?
F
Write data to file FAULG for later autocorrelation calculation
T
COSTAPER?
F
Apply cosine taper to first and last 10% of the data
Procedures FFTF
BITREV2
RRDR
Perform Forward Transform
T
NOT COSTAPER AND IFAUTO?
F
Write data to file FAULG for later autocorrelation calculation

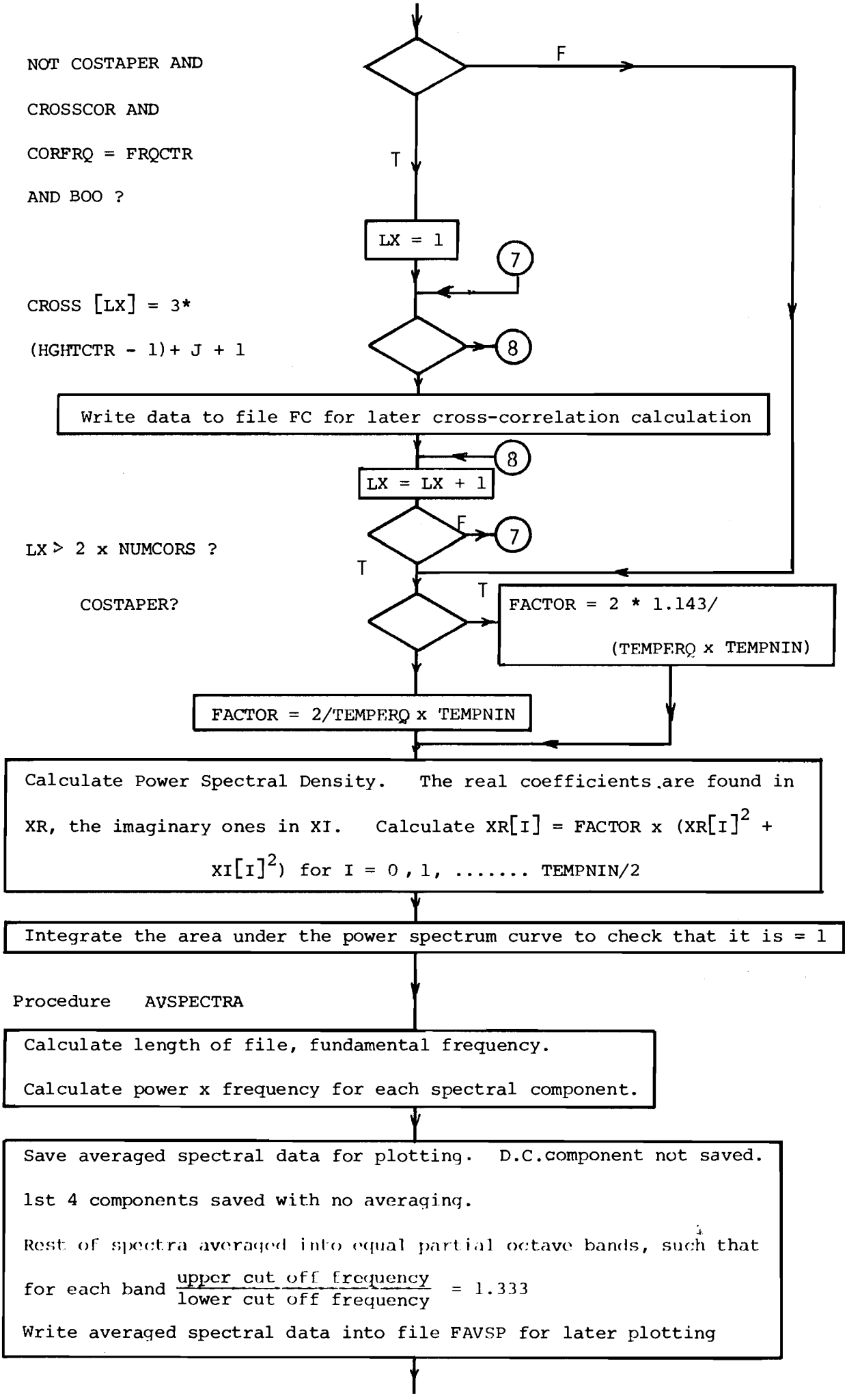
NOT COSTAPER AND
CROSSCOR AND
CORFRQ = FRQCTR
AND BOO ?
F
T
LX = 1
7
CROSS [LX] = 3*
(HGHTCTR - 1)+ J + 1
8
Write data to file FC for later cross-correlation calculation
8
LX = LX + 1
F
7
LX > 2 x NUMCORS ?
T
COSTAPER?
T
FACTOR = 2 * 1.143/
(TEMPERQ x TEMPNIN)
FACTOR = 2/TEMPERQ x TEMPNIN
Calculate Power Spectral Density. The real coefficients are found in XR, the imaginary ones in XI. Calculate XR[I] = FACTOR x (XR[I]2 + XI[I]2) for I = 0 , 1, ... TEMPNIN/2
Integrate the area under the power spectrum curve to check that it is = 1
Procedure AVSPECTRA
Calculate length of file, fundamental frequency.
Calculate power x frequency for each spectral component.
Save averaged spectral data for plotting. D.C.component not saved.
1st 4 components saved with no averaging.
Rest of spectra averaged into equal partial octave bands, such that
for each band upper cut off frequency / lower cut off frequency = 1.333
Write averaged spectral data into file FAVSP for later plotting

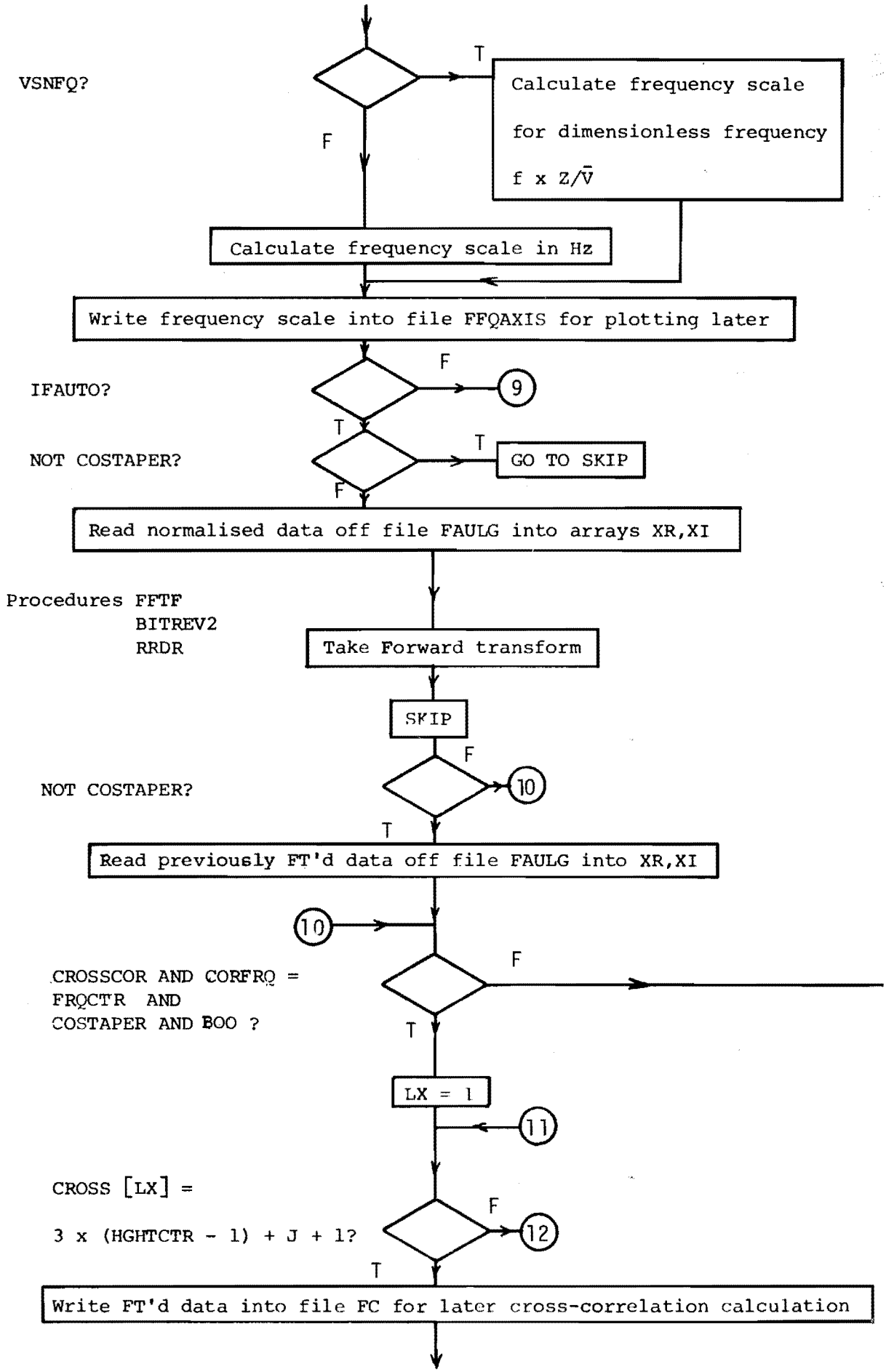
VSNFQ?
T
Calculate frequency scale
for dimensionless frequency
f x Z/V̄
F
Calculate frequency scale in Hz
Write frequency scale into file FFQAXIS for plotting later
IFAUTO?
F
9
T
NOT COSTAPER?
T
GO TO SKIP
F
Read normalised data off file FAULG into arrays XR,XI
Procedures FFTF
BITREV2
RRDR
Take Forward transform
SKIP
NOT COSTAPER?
F
10
T
Read previously FT'd data off file FAULG into XR,XI
10
CROSSCOR AND CORFRQ =
FRQCTR AND
COSTAPER AND BOO ?
F
T
LX = 1
11
CROSS [LX] =
3 x (HGHTCTR - 1) + J + 1?
F
12
T
Write FT'd data into file FC for later cross-correlation calculation

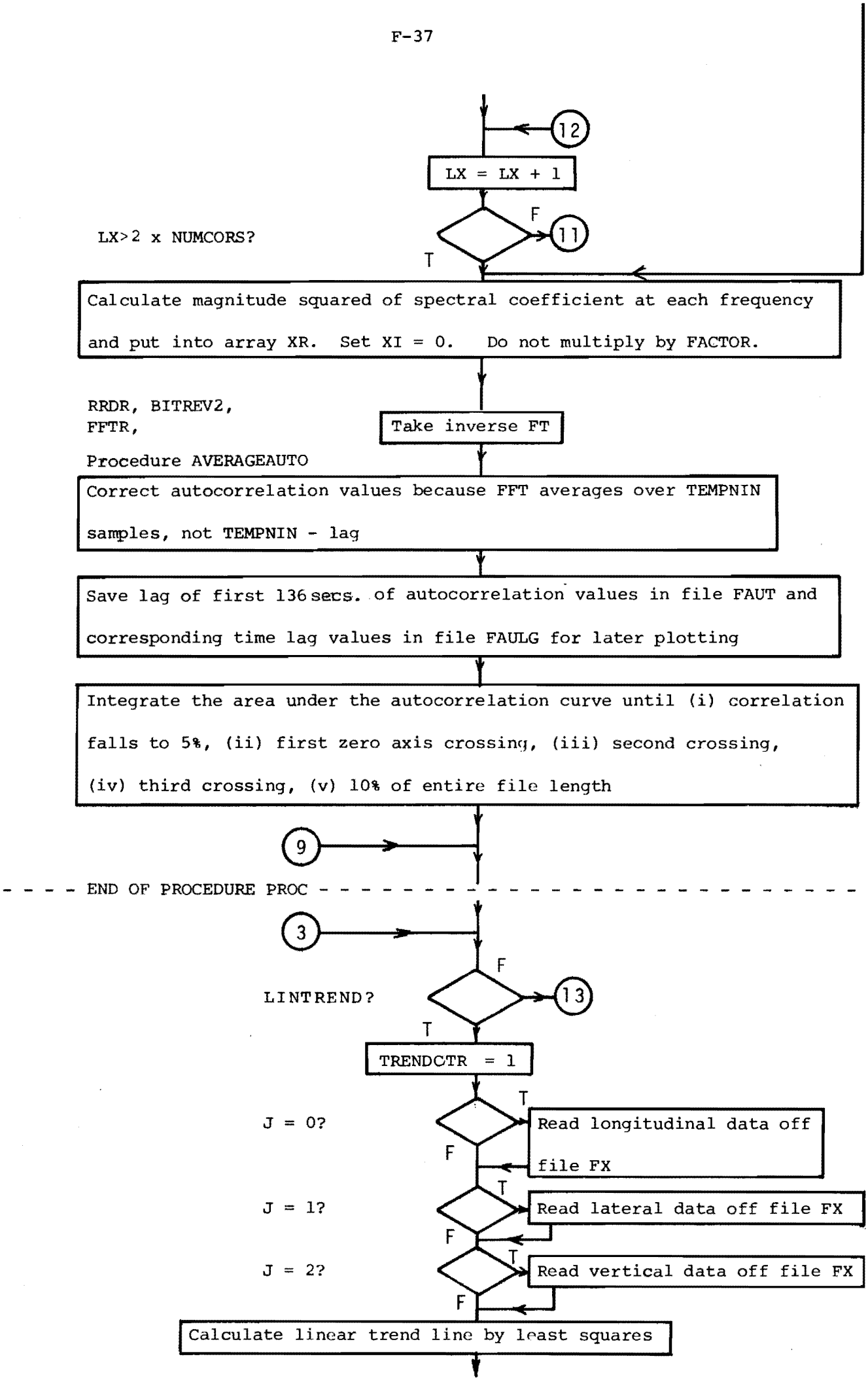
12
LX = LX + 1
F
LX>2 x NUMCORS?
11
T
Calculate magnitude squared of spectral coefficient at each frequency and put into array XR. Set XI = 0. Do not multiply by FACTOR.
RRDR, BITREV2, FFTR,
Take inverse FT
Procedure AVERAGEAUTO
Correct autocorrelation values because FFT averages over TEMPNIN samples, not TEMPNIN - lag
Save lag of first 136 secs. of autocorrelation values in file FAUT and corresponding time lag values in file FAULG for later plotting
Integrate the area under the autocorrelation curve until (i) correlation falls to 5%, (ii) first zero axis crossing, (iii) second crossing, (iv) third crossing, (v) 10% of entire file length
9
END OF PROCEDURE PROC
3
F
LINTREND?
13
T
TRENDCTR = 1
T
J = 0?
Read longitudinal data off file FX
F
T
J = 1?
Read lateral data off file FX
F
T
J = 2?
Read vertical data off file FX
F
Calculate linear trend line by least squares

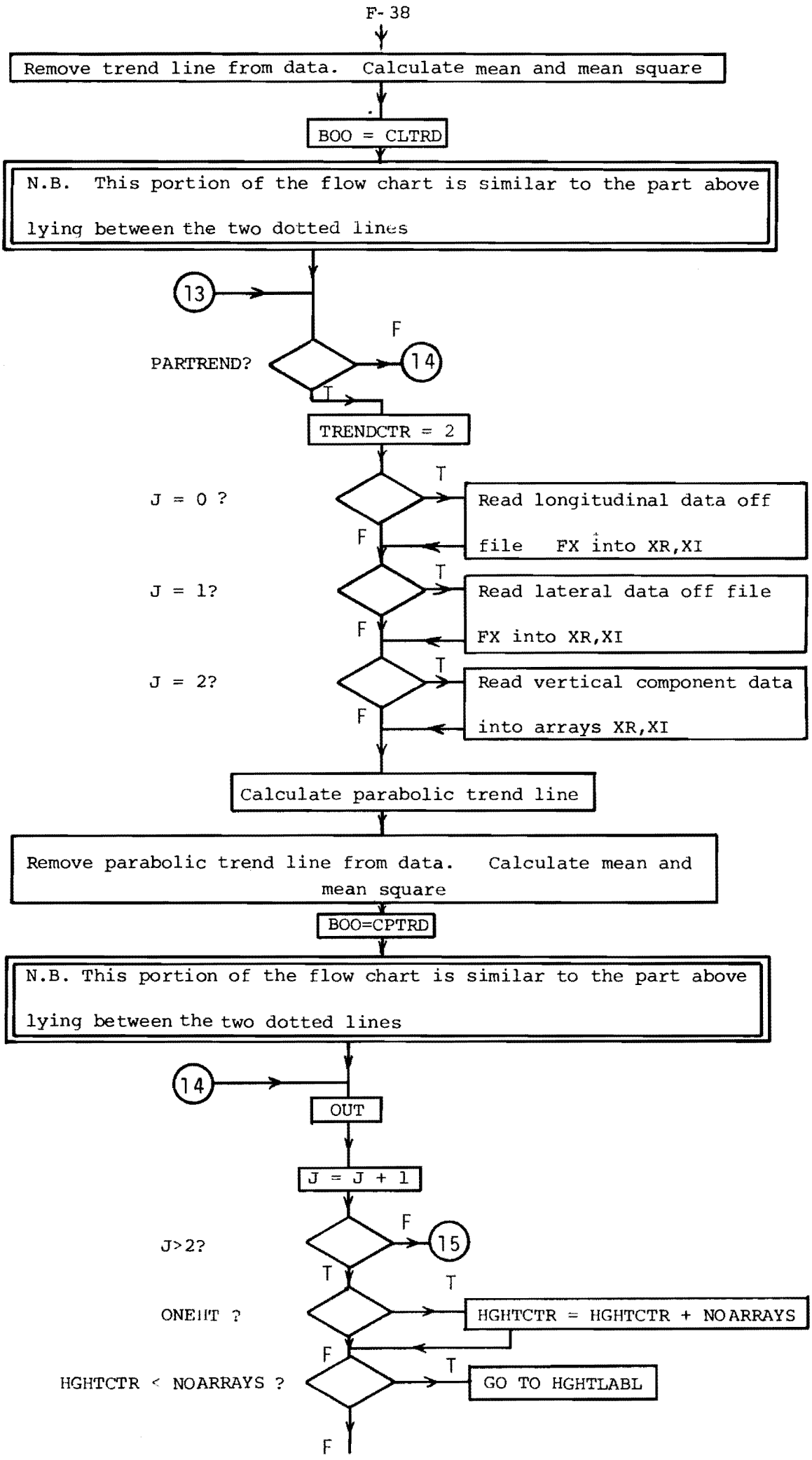
Remove trend line from data. Calculate mean and mean square
BOO = CLTRD
N.B. This portion of the flow chart is similar to the part above lying between the two dotted lines
13
PARTREND?
F
14
T
TRENDCTR = 2
J = 0 ?
T
Read longitudinal data off file FX into XR,XI
F
J = 1?
T
Read lateral data off file FX into XR,XI
F
J = 2?
T
Read vertical component data into arrays XR,XI
F
Calculate parabolic trend line
Remove parabolic trend line from data. Calculate mean and mean square
BOO=CPTRD
N.B. This portion of the flow chart is similar to the part above lying between the two dotted lines
14
OUT
J = J + 1
J>2?
F
15
T
ONEHT ?
T
HGHTCTR = HGHTCTR + NOARRAYS
F
HGHTCTR < NOARRAYS ?
T
GO TO HGHTLABL
F

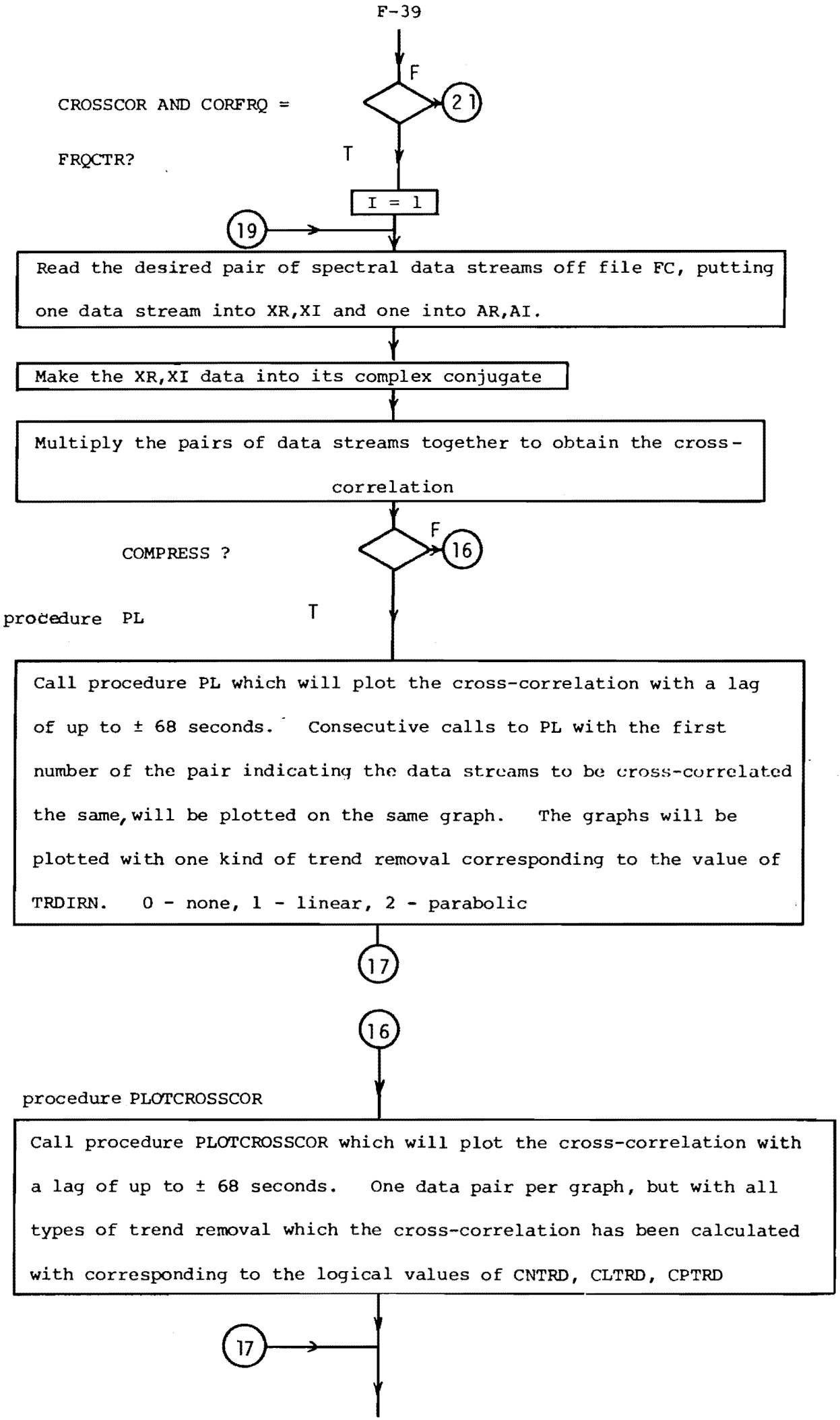
CROSSCOR AND CORFRQ =
FRQCTR?
F
T
21
I = 1
19
Read the desired pair of spectral data streams off file FC, putting one data stream into XR,XI and one into AR,AI.
Make the XR,XI data into its complex conjugate
Multiply the pairs of data streams together to obtain the cross-correlation
COMPRESS ?
F
T
16
procedure PL
Call procedure PL which will plot the cross-correlation with a lag of up to ± 68 seconds. Consecutive calls to PL with the first number of the pair indicating the data streams to be cross-correlated the same, will be plotted on the same graph. The graphs will be plotted with one kind of trend removal corresponding to the value of TRDIRN. 0 - none, 1 - linear, 2 - parabolic
17
16
procedure PLOTCROSSCOR
Call procedure PLOTCROSSCOR which will plot the cross-correlation with a lag of up to ± 68 seconds. One data pair per graph, but with all types of trend removal which the cross-correlation has been calculated with corresponding to the logical values of CNTRD, CLTRD, CPTRD
17

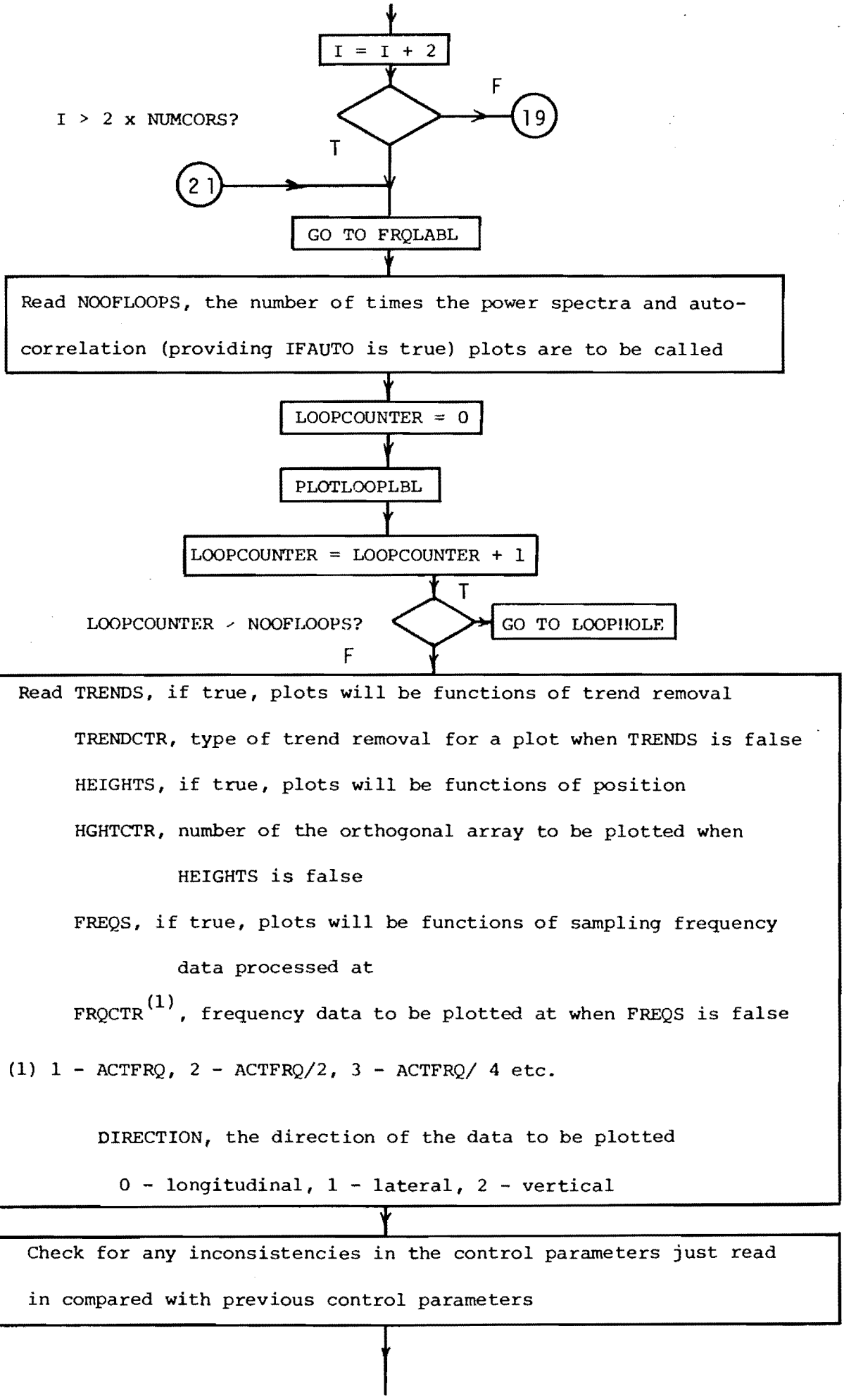
I = I + 2
I > 2 x NUMCORS?
F
19
T
21
GO TO FRQLABL
Read NOOFLOOPS, the number of times the power spectra and auto-correlation (providing IFAUTO is true) plots are to be called
LOOPCOUNTER = 0
PLOTLOOPLBL
LOOPCOUNTER = LOOPCOUNTER + 1
T
LOOPCOUNTER > NOOFLOOPS?
GO TO LOOPHOLE
F
Read TRENDS, if true, plots will be functions of trend removal
TRENDCTR, type of trend removal for a plot when TRENDS is false
HEIGHTS, if true, plots will be functions of position
HGHTCTR, number of the orthogonal array to be plotted when HEIGHTS is false
FREQS, if true, plots will be functions of sampling frequency data processed at
FRQCTR(1), frequency data to be plotted at when FREQS is false
(1) 1 - ACTFRQ, 2 - ACTFRQ/2, 3 - ACTFRQ/ 4 etc.
DIRECTION, the direction of the data to be plotted
0 - longitudinal, 1 - lateral, 2 - vertical
Check for any inconsistencies in the control parameters just read in compared with previous control parameters

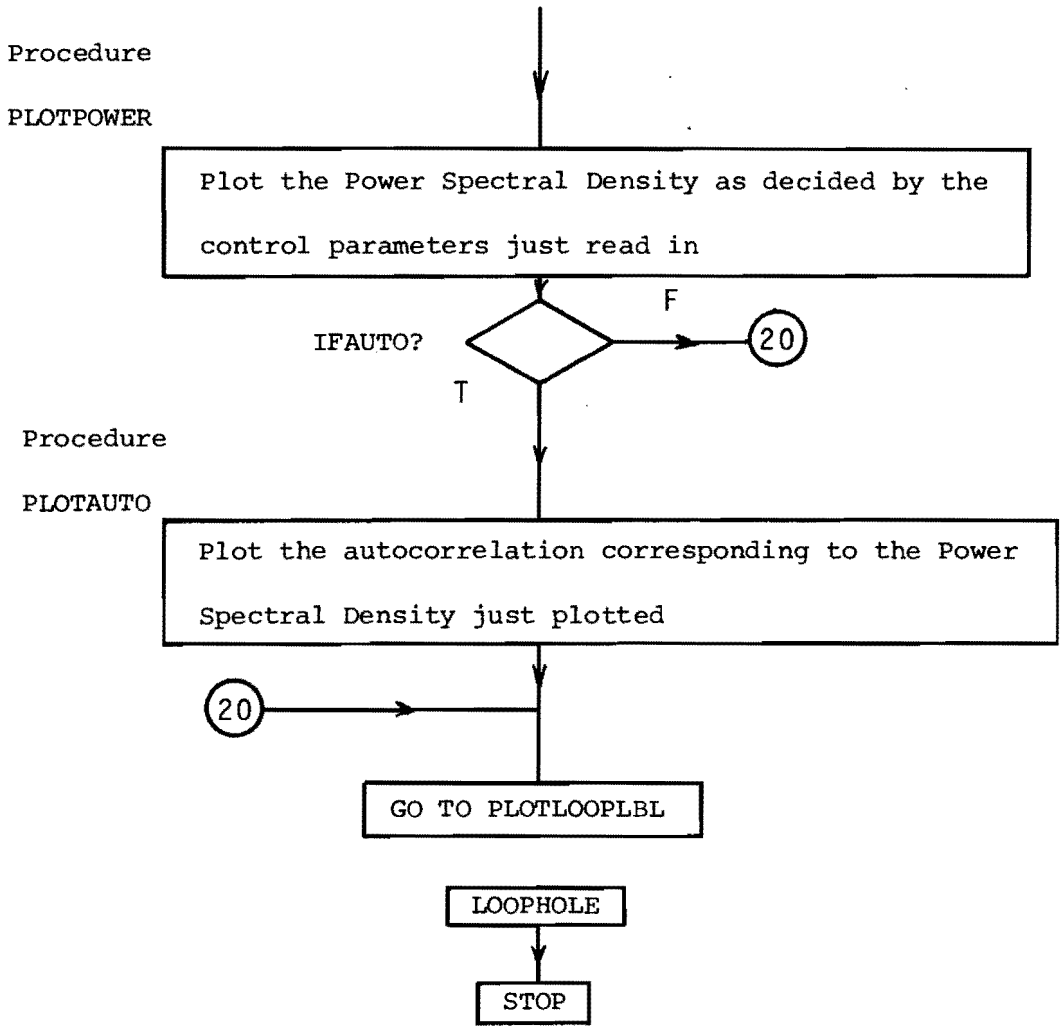
Procedure
PLOTPOWER
Plot the Power Spectral Density as decided by the control parameters just read in
IFAUTO?
F
20
T
Procedure
PLOTAUTO
Plot the autocorrelation corresponding to the Power Spectral Density just plotted
20
GO TO PLOTLOOPLBL
LOOPHOLE
STOP

APPENDIX G

PROGRAM 'JOINFILES'

G.1. Typical WFL for Using This Program

G.1.1 Reduce scan rate and join two files

Assume that the source file JOINFILES is on tape A999. Also the file F1 is on tape D986. It contains 16384 samples at a scan rate of 8 and has data from five orthogonal arrays. The file F2 on the same tape contains 8192 samples at a scan rate of 16 and also has data from five orthogonal arrays.

It is desired to join file F2 onto the end of file F1 and to reduce the scan rate of the resultant file to two and call it F3. The three files F1, F2 and F3 are required to be written back to the same tape.

The JOB to do this is given below.

```
7
5  JOB JOINFILES F1 AND F2;
   PROCESSTIME=300;
   USER MECH021/PASSWORD; CLASS=6; BEGIN
7
5  COPY JOINFILES FROM A999;
   COMPLILE JOINTHERM ALGOL LIBRARY
   COMPILER FILE TAPE=JOINFILES;
   DATA
$  SET MERGE
$  RESET LIST
$  SET LINEINFO
7
5  IF FILE JOINTHEM ISNT PRESENT THEN GO HOME;
7
5  COPY F1, F2, FROM D986;
7
5  RUN JOINTHEM;
   FILE IN=F1;  FILE OUT=F3;
7
5  DATA KR;
```

```
   5,16384, 8,2,
7
5  RUN JOINTHEM;

   FILE IN=F2; FILE OUT=F3;
7
5  DATA KR;

   5, 8192, 16,2,
7
5  COPY F1, F2, F3 TO D986;
7
5  HOME:
7  END JOB
5
```

G.2. Listing of Program 'JOINFILES'.

```
JJJJJ  000  IIIII N   N FFFFF IIIII L     EEEE   SSS
  J   0   0   I   N   N F       I   L     E     S   S
  J   0   0   I   NN  N F       I   L     E     S
  J   0   0   I   N N N FFF     I   L     EEE    SSS
J J   0   0   I   N  NN F       I   L     E         S
J J   0   0   I   N   N F       I   L     E     S   S
 J     000  IIIII N   N F     IIIII LLLLL EEEEE  SSS


81 RECORDS, CREATED 22/11/78

 1000 BEGIN
 2000   %
 3000   %                      DECLARE FILES INTEGERS
 4000   %
 5000   FILE IN(KIND=DISK,FILETYPE=7),OUT(KIND=DISK,FILETYPE
 6000   =7,UNITS=WORDS,MAXRECSIZE=256,BLOCKSIZE=768,
 7000   AREASIZE=60,FLEXIBLE=TRUE,PROTECTION=SAVE),
 8000   LP(KIND=PRINTER),KR(KIND=READER);
 9000   INTEGER NOOFARRAYS,OUTPUTSCANRATE,NOOFSCANS,COUNT,
10000   INPUTSCANRATE,AA,AA1,NA3,NA1,BB,INT1,INT2,INT3,HT,I,J,CC;
11000   READ(KR,/,NOOFARRAYS,NOOFSCANS,INPUTSCANRATE,OUTPUTSCANRATE);
12000   WRITE(LP,*/,NOOFARRAYS,NOOFSCANS,INPUTSCANRATE,OUTPUTSCANRATE);
13000   IF OUT.PRESENT THEN COUNT:=OUT.LASTRECORD ELSE COUNT:=-1;
14000   IF COUNT=-1 THEN WRITE(LP,<"THIS RUN OF THE PROGRAMME PRODUCES"
15000   " THE FIRST FILE">) ELSE
16000   WRITE(LP,<"THE NUMBER OF THE LAST RECORD OF THE "/
17000   "OUTPUT FILE BEFORE HAVING THIS FILE ADDED TO IT "
18000   "IS=",I7>,COUNT);
19000   AA:=ENTIER(INPUTSCANRATE/OUTPUTSCANRATE);
20000   BEGIN
21000     %       DECLARE AND DYNAMICALLY DIMENSION ARRAYS
22000     ARRAY X[0:2,0:AA*256];
23000     % DECLARE LABELS
24000     LABEL E,FINI;
25000     IF AA>1 THEN BEGIN
26000       %     THIS BLOCK IS ONLY ENTERED IF THE DATA IS BEING COMPRESSED
27000       %     EVERY AA SAMPLES ARE ADDED TOGETHER
28000       WRITE(LP,<"THE OUTPUT SCANRATE WILL BE REDUCED BY ADDING "
29000       "EVERY",I5,"  CONSECUTIVE SAMPLES FROM EACH CHANNEL">
30000       ,AA);
31000       NOOFSCANS:=(NOOFSCANS DIV (AA*256))*256;
32000       WRITE(LP,<"NUMBER OF POINTS IN OUTPUT FILE=",I7>,NOOFSCANS);
33000       WRITE(LP,<"LENGTH OF FILE=",F10.6," MINUTES">,NOOFSCANS*16/
34000       (OUTPUTSCANRATE*15*60));
35000       AA1:=AA-1;NA3:=3*NOOFARRAYS;NA1:=NOOFARRAYS-1;
36000       FOR BB:=0 STEP 1 UNTIL NOOFSCANS/256-1 DO BEGIN      %LOOP 1
37000         INT3:=BB*3*NOOFARRAYS;INT1:=INT3*AA;
38000         FOR HT:=0 STEP 1 UNTIL NA1 DO BEGIN INT2:=3*HT;     %LOOP 2
39000           FOR J:=0,1,2 DO BEGIN                               %LOOP 3
40000             FOR I:=0 STEP 1 UNTIL AA1 DO
41000             READ(IN[J+INT2+I*NA3+INT1],256,X[J,I*256])[E];
42000             FOR I:=1 STEP 1 UNTIL AA1 DO
43000             X[J,0]:=*+X[J,I];
44000             FOR I:=1 STEP 1 UNTIL 255 DO BEGIN X[J,I]:=0;       %LOOP 4
45000               FOR CC:=0 STEP 1 UNTIL AA1 DO
46000               X[J,I]:=*+X[J,I*AA+CC];
47000             END;                                                %END LOOP 4
48000             WRITE(OUT[COUNT+1+J+INT2+INT3],256,X[J,0]);
49000           END;                                                %END LOOP 3
50000         END;                                                %END LOOP 2
51000       END;                                                %END LOOP 1
52000     END OF AA GTR 1 BLOCK;
53000     IF AA=1 THEN BEGIN
54000       %     THIS BLOCK IS ONLY ENTERED IF DATA IS NOT BEING COMPRESSED
55000       IF OUT.PRESENT THEN
56000       IF (COUNT:=OUT.LASTRECORD) GEQ 0 THEN
57000       READ(OUT[COUNT],<A1>,COUNT);%POSITIONS READ/WRITE POINTER
58000       WRITE(LP,<"NO DATA COMPRESSION USED">);
59000       WRITE(LP,<"LENGTH OF FILE=",F10.6," MINUTES">,(NOOFSCANS
60000       DIV 256)*256*16/(OUTPUTSCANRATE*15*60));
61000       WRITE(LP,<"NUMBER OF POINTS IN OUTPUT FILE=",I7>,
62000       (NOOFSCANS DIV 256)*256);
63000       FOR I:=0 STEP 1 UNTIL NOOFSCANS/256-1 DO
64000       FOR HT:=0 STEP 1 UNTIL NOOFARRAYS-1 DO
65000       FOR J:=0,1,2 DO BEGIN
66000         READ(IN,256,X[J,*])[E];
67000         WRITE(OUT,256,X[J,*]);
68000       END OF I HT J LOOPS;
69000     END OF AA EQ 1 BLOCK;
70000     IF AA<1 THEN        %ERROR IN INPUT CONTROL PARAMETERS
71000     WRITE(LP,<"CHECK INPUT PARAMETERS"/
72000     "REMEMBER OUTPUT SCANRATE=<INPUT SCANRATE"/
73000     "BY A POWER OF 2">);
74000     GO TO FINI;
75000     E:WRITE(LP,<"END OF INPUT FILE BEFORE"
76000     " EXPECTED - PARAMATER VALUES BELOW">);
77000     WRITE(LP,*/,AA,AA1,NA3,NA1,BB,INT3,INT1,HT,J,I,CC);
78000     FINI:
79000     WRITE(LP,<"PROGRAM FINISHED">);
80000   END;
81000 END.
```

APPENDIX H

LISTING OF THE PROCEDURES USED FOR THE FAST FOURIER TRANSFORM

The calling sequence and the input/output of the procedures listed below have been discussed in detail in Section 5.6.2.3, and are also well described within the listings themselves.

```
M   M  AAA  TTTTT H   H L      IIIII BBB   FFFFF FFFFF TTTTT      /  SSS  FFFFF FFFFF TTTTT FFFFF
MM MM A   A   T   H   H L        I   B  B  F     F        T       /  S   S F     F       T   F
M M M A   A   T   H   H L        I   B  B  F     F        T      /   S     F     F       T   F
M M M AAAAA   T   HHHHH L        I   BBBB  FFF   FFF      T     /     SSS  FFF   FFF     T   FFF
M   M A   A   T   H   H L        I   B   B F     F        T    /         S F     F       T   F
M   M A   A   T   H   H L        I   B   B F     F        T   /      S   S F     F       T   F
M   M A   A   T   H   H LLLLL IIIII BBBB  F     F        T  /       SSS  F     F       T   F

123 RECORDS, CREATED 29/07/77

    1000 COMMENT@@@@@      UCSD/FFTPAK.              ;
    2000 COMMENT
    3000 COMMENT*XXXX
    4000 PURPOSE.
    5000 A SET OF FOUR PROCEDURES FOR COMPUTING FOURIER TRANSFORMS
    6000 BY THE COOLEY-TUKEY METHOD (FAST FOURIER TRANSFORMS):
    7000 FFTF     : COMPUTES FAST FOURIER TRANSFORM
    8000 FFTR     : COMPUTES THE INVERSE FOURIER TRANSFORM
    9000 SINCOS   : GENERATES TABLES OF SINES AND COSINES FOR
   10000 USE BY FFTF AND FFTR
   11000 BITREV2 : ARRANGES ARRAYS INTO BIT REVERSED ORDER FOR
   12000 USE BY FFTF AND FFTR
   13000 COMMENT*YYYY
   14000 COMMENT*ZZZZ;
   15000 COMMENT@@@@@      FFTF.                     ;

   16000 PROCEDURE FFTF(XR,XI,S,C,M);    % FORWARD TRANSFORM
   17000 COMMENT*XXXX
   18000 PURPOSE. COMPUTES FAST FOURIER TRANSFORM USING COOLEY-TUKEY METHOD
   19000 COMMENT*YYYY
   20000 INPUT.
   21000 XR - REAL PART OF THE INPUT ARRAY
   22000 XI - IMAGINARY PART OF THE INPUT ARRAY
   23000 S  - ARRAY OF SINES PRODUCED BY SINCOS
   24000 M  - INTEGER SPECIFYING THE SIZE OF XR AND XI TO BE 2**M
   25000 OUTPUT.
   26000 XR - REAL PART OF TRANSFORMED ARRAY (BIT REVERSED ORDER)
   27000 XI - IMAG. PART OF TRANSFORMED ARRAY (BIT REVERSED ORDER)
   28000 METHOD.
   29000 LET Z(0),Z(1),...,Z(2**M-1) BE 2**M COMPLEX NUMBERS.
   30000 FFTF COMPUTES THE COMPLEX NUMBWERS W(0),W(1),..,W(2**M-1)
   31000 GIVEN BY:
   32000 W(L) = SUM OVER J FROM 0 TO 2**M-1 OF
   33000 Z(J) EXP(2*P*I*J*K/2**M)
   34000 WHERE:
   35000 P = THE CONSTANT PI,
   36000 K = TAKES VALUES FROM 0 TO 2**M-1,
   37000 L = BIT REVERSED REPRESENTATION OF K IN A FIELD
   38000 OF LENGTH M,
   39000 I = SQUARE ROOT OF -1.
   40000 REMARK.
   41000 THE OUTPUT IS NOT NORMALIZED. A CALL TO FFTF FOLLWED
   42000 IMMEDIATELY BY FFTR REPRODUCES THE ORIGINAL
   43000 DATA MULTIPLIED BY 2**M.
   44000 REFERENCES.
   45000 1. SINGLETON, R. C."ON COMPUTING THE FAST FOURIER
   46000 TRANSFORM", CACM, VOL. 10, NO. 10, OCT 1967, PP.647-654
   47000 2. BRACEWELL, R. "THE FOURIER TRANSFORM AND ITS
   48000 APPLICATIONS", MCGRAW HILL, 1965.
   49000 COMMENT*ZZZZ;
   50000 %%%%
```

```
 82000          (WI1:=(XI1:=XI[J1])+(XI3:=XI[J3]));
 83000          XR[J1]:=(WR3:=(WR0-WR1))*(C2:=C[P2]) -(WI3:=(WI0-WI1))*
 84000          (S2:=S[P2]);
 85000          XI[J1]:=(WR3*S2+WI3*C2);
 86000          XR[J2]:=(WR3:=(WR0:=(XR0-XR2))-(WI1:=(XI1-XI3)))*(C1:=C[P1])
 87000          -(WI3:=(WI0:=(XI0-XI2))+(WR1:=(XR1-XR3)))*(S1:=S[P1]);
 88000          XI[J2]:=(WR3*S1+WI3*C1);
 89000          XR[J3]:=(WR3:=(WR0+WI1))*(C3:=(IF P3 LSS NH THEN C[P3] ELSE
 90000          C[NR:=NZ-P3]))
 91000          -(WI3:=(WI0-WR1))*(S3:=(IF P3 LSS NH THEN S[P3]
 92000          ELSE -S[NR]));
 93000          XI[J3]:=(WR3*S3+WI3*C3);
 94000        END UNTIL JJ:=*+1 GEQ NQ;  % LOOP 1
 95000      END UNTIL L:=*+N GEQ NZ;  % LOOP 2
 96000      N:=N.[38:37];  % DIV 4
 97000    END UNTIL NQ:=N.[38:37] LEQ 1;  % LOOP 3
 98000    IF NQ EQL 0 THEN  % HAVE AN ODD POWER OF 2 - - FINISH WITH BASE 2
 99000    BEGIN
100000      J:=0; L:=1;
101000      DO BEGIN
102000        XR[J]:=(XR1:=XR[J])+(XR2:=XR[L]);
103000        XI[J]:=(XI1:=XI[J])+(XI2:=XI[L]);
104000        XR[L]:=XR1-XR2;
105000        XI[L]:=XI1-XI2;
106000        L:=*+2;
107000      END UNTIL J:=*+2 GEQ NZ;
108000    END ELSE       % HAVE AN EVEN POWER OF 2 -- FINISH WITH BASE 4
109000    BEGIN
110000      J:=0;
111000      DO BEGIN
112000        J3:=(J2:=(J1:=J+1)+1)+1;
113000        XR[J]:=(XR0:=XR[J])+(XR1:=XR[J1])+(XR2:=XR[J2])+(XR3:=XR[J3]);
114000        XI[J]:=(XI0:=XI[J])+(XI1:=XI[J1])+(XI2:=XI[J2])+(XI3:=XI[J3]);
115000        XR[J1]:=XR0-XR1+XR2-XR3;
116000        XI[J1]:=XI0-XI1+XI2-XI3;
117000        XR[J2]:=XR0-XI1-XR2+XI3;
118000        XI[J2]:=XI0+XR1-XI2-XR3;
119000        XR[J3]:=XR0+XI1-XR2-XI3;
120000        XI[J3]:=XI0-XR1-XI2+XR3;
121000      END UNTIL J:=*+4 GEQ NZ;
122000    END;
123000  END F F T F;

INPUT STRING WAS
"MATHL1BFFT/SFFTF STEP 2"
```

```
M    M  AAA  TTTTT H   H L      IIIII BBB   FFFFF FFFFF TTTTT      /  SSS  FFFFF FFFFF TTTTT RRRR
MM MM A   A   T   H   H L        I   B  B  F     F       T       /  S   S F     F       T   R   R
M M M A   A   T   H   H L        I   B  B  F     F       T      /   S     F     F       T   R   R
M M M AAAAA   T   HHHHH L        I   BBBB  FFF   FFF     T     /     SSS  FFF   FFF     T   RRRR
M   M A   A   T   H   H L        I   B   B F     F       T    /         S F     F       T   R R
M   M A   A   T   H   H L        I   B   B F     F       T   /      S   S F     F       T   R  R
M   M A   A   T   H   H LLLLL IIIII BBBB  F     F       T  /       SSS  F     F       T   R   R


111 RECORDS, CREATED 13/03/78

    1000 COMMENT@@@@@      FFTR.                      ;

    2000 PROCEDURE FFTR(XR,XI,S,C,M);     % REVERSE FAST FOURIER TRANSFORM
    3000 COMMENT*XXXX
    4000 PURPOSE. COMPUTES INVERSE FOURIER TRANSFORM (COOLEY-TUKEY METHOD)
    5000 COMMENT*YYYY
    6000 INPUT.
    7000 XR - REAL PART OF THE INPUT ARRAY (BIT REVERSED ORDER)
    8000 XI - IMAG. PART OF THE INPUT ARRAY (BIT REVERSED ORDER)
    9000 S  - ARRAY OF SINES PRODUCED BY SINCOS
   10000 M  - INTEGER SPECIFYING THE SIZE OF XR AND XI TO BE 2**M
   11000 OUTPUT.
   12000 XR - REAL PART OF TRANSFORMED ARRAY
   13000 XI - IMAG. PART OF TRANSFORMED ARRAY
   14000 METHOD.
   15000 FOR A COMPLEX ARRAY W IN BIT REVERSED ORDER,
   16000 FFTR COMPUTES THE COMPLEX NUMBZERS Z(0),Z(1),..,W(2**M-1)
   17000 GIVEN BY:
   18000 Z(K) = SUM OVER J FROM 0 TO 2**M-1 OF
   19000 W(L) EXP(-2*P*I*J*K/2**M)
   20000 WHERE:
   21000 P = THE CONSTANT PI,
   22000 K = TAKES VALUES FROM 0 TO 2**M-1,
   23000 L = BIT REVERSED REPRESENTATION OF K IN A FIELD
   24000 OF LENGTH M,
   25000 I = SQUARE ROOT OF -1.
   26000 REMARK.
   27000 THE OUTPUT IS NOT NORMALIZED. A CALL TO FFTF FOLLWED
   28000 IMMEDIATELY BY FFTR REPRODUCES THE ORIGINAL
   29000 DATA MULTIPLIED BY 2**M.
   30000 REFERENCES.
   31000 1. SINGLETON, R. C."ON COMPUTING THE FAST FOURIER
   32000 TRANSFORM", CACM, VOL. 10, NO. 10, OCT 1967, PP.647-654
   33000 2. BRACEWELL, R. "THE FOURIER TRANSFORM AND ITS
   34000 APPLICATIONS", MCGRAW HILL, 1965.
   35000 COMMENT*ZZZZ;
   36000 %%%%
```

```
 82000       J:= L-1;  JJ:=0;
 83000       DO BEGIN       %  LOOP  1
 84000         J3:=(J2:=(J1:=(J:=*+1)+NQ)+NQ)+NQ;
 85000         P3:=(P2:=(P1:=JJ*D)+P1)+P1;
 86000         XR[J]:=(WR0:=XR[J])
 87000         +(WR1:=(XR1:=XR[J1])*(C2:=C[P2])+(XI1:=XI[J1])*(S2:=S[P2]))
 88000         +(WR2:=(XR2:=XR[J2])*(C1:=C[P1])+(XI2:=XI[J2])*(S1:=S[P1]))
 89000         +(WR3:=(XR3:=XR[J3])*(C3:=(IF P3 LSS NH THEN C[P3]
 90000         ELSE C[NR:=NZ-P3])))
 91000         +(XI3:=XI[J3])*(S3:=(IF P3 LSS NH THEN S[P3]
 92000         ELSE  -S[NR]))  );
 93000         XI[J]:=(WI0:=XI[J])
 94000         +(WI1:=XI1*C2 - XR1*S2)
 95000         +(WI2:=XI2*C1 - XR2*S1)
 96000         +(WI3:=XI3*C3 - XR3*S3);
 97000         XR[J1]:= WR0 - WR1 + WI2 - WI3;
 98000         XI[J1]:= WI0 - WI1 - WR2 + WR3;
 99000         XR[J2]:= WR0 + WR1 - WR2 - WR3;
100000         XI[J2]:= WI0 + WI1 - WI2 - WI3;
101000         XR[J3]:= WR0 - WR1 - WI2 + WI3;
102000         XI[J3]:= WI0 - WI1 + WR2 - WR3;
103000       END  UNTIL  JJ:=*+1  GEQ NQ ;     %  LOOP  1
104000     END UNTIL  L:= * + N  GEQ  NZ;      % LOOP 2
105000     NQ:=NQ*4;
106000   END UNTIL  N:=N*4 GTR NZ;    %  LOOP 3
106040   % NEXT TWO LINES INSERTED BY R FLAY 27/2/70 TO NORMALISE
106045   % OUTPUT WHEN FORWARD AND INVERSE TRANSFORMS BOTH CALLED
106050   I:=0; THRU NZ DO BEGIN XR[I]:=*/NZ;       XI[I]:=*/NZ;
106060     I:=*+1;          END;
107000 END   F  F  T R ;
```

```
INPUT STRING WAS
"MATHLIBFFT/SFFTR STEP 2"
```

M A T H L I B F F T / S B I T R E V 2

```
69 RECORDS, CREATED 29/07/77

    1000 COMMENT@@@@@      BITREV2.

    2000 PROCEDURE BITREV2(XR,XI,N);
    3000 COMMENT*XXXX
    4000
    5000 PURPOSE.
    6000 REORDERS THE CONTENTS OF ARRAYS XR,XI BY BIT REVERSAL --
    7000 FOR USE WITH FAST FOURIER TRANSFORM PROCEDURES FFTF & FFTR
    8000 N SPECIFIES THE LENGTH OF XR AND XI TO BE 2**N
    9000 FOR N = 13,14,15 OR 16 THE SEQUENCE OF EXCHANGES IS DESIGNED
   10000 TO MINIMIZE OVERLAYS
   11000 COMMENT*YYYY
   12000 INPUT.
   13000 XR - INPUT ARRAY FOR BIT REVERSED ARRANGEMENT
   14000 XI - INPUT ARRAY FOR BIT REVERSAL
   15000 N  - SPECIFIES LENGTH OF XR AND XI TO 2**N
   16000 OUTPUT.
   17000 XR - BIT REVERSED ARRANGEMENT OF INPUT XR
   18000 XI - BIT REVERSED ARRANGEMENT OF INPUT XI
   19000
   20000 COMMENT*ZZZZ;
   21000 VALUE N; INTEGER N;
   22000 ARRAY XR,XI[0];
   23000 BEGIN
   24000   REAL  J,R,M,TR,TI,DJ;
   25000   LABEL QUIT;
   26000   VALUE ARRAY  A3(0,4,2,6,1,5,3,7);
   27000   VALUE ARRAY  A4(0,8,4,12,2,10,6,14,1,9,5,13,3,11,7,15);
   28000   VALUE ARRAY  A5(0,16,8,24,4,20,12,28,2,18,10,26,6,22,14,30,
   29000   1,17, 9,25,5,21,13,29,3,19,11,27,7,23,15,31);
   30000   VALUE ARRAY  A6(0,32,16,48,8,40,24,56,4,36,20,52,12,44,28,60,
   31000   2,34,18,50,10,42,26,58,6,38,22,54,14,46,30,62,
   32000   1,33,17,49,9,41,25,57,5,37,21,53,13,45,29,61,
   33000   3,35,19,51,11,43,27,59,7,39,23,55,15,47,31,63);

   34000   PROCEDURE LOOP;
   35000   DO BEGIN
   36000     CASE N OF
   37000     BEGIN  ; ; ; % 0,1,2  NOT IMPLEMENTED
   38000       R:=A3[J.[2:3]];  %3
   39000       R:=A4[J.[3:4]];  %4
   40000       R:=A5[J.[4:5]];  %5
   41000       R:=A6[J.[5:6]];  %6
   42000       R:=(A3[J.[6:3 ]])&A4[J.[3:4]][6:3:4]; % 7
   43000       R:=(A4[J.[7:4]])&A4[J.[3:4]][7:3:4]; % 8
   44000       R:=(A5[J.[8:5]])&A4[J.[3:4]][8:3:4]; % 9
   45000       R:=(A5[J.[9:5]])&A5[J.[4:5]][9:4:5]; % 10
   46000       R:=(A6[J.[10:6]])&A5[J.[4:5]][10:4:5]; % 11
   47000       R:=(A6[J.[11:6]])&A6[J.[5:6]][11:5:6]; % 12
   48000       R:=(A4[J.[12:4]])&A5[J.[8:5]][8:4:5]&A4 [J.[3:4]][12:3:4]; % 13
   49000       R:=(A4[J.[13:4]])&A6[J.[9:6]][9:5:6]&A4 [J.[3:4]][13:3:4]; % 14
   50000       R:=(A5[J.[14:5]])&A5[J.[9:5]][9:4:5]&A5[J.[4:5]][14:4:5]; % 15
   51000       R:=(A5[J.[15:5]])&A6[J.[10:6]][10:5:6]&A5[J.[4:5]][15:4:5];% 16
   52000     END C A S E S;
   53000     IF R GTR J THEN
   54000     BEGIN
   55000       TR:= XR[J];   TI:= XI[J];
   56000       XR[J]:=XR[R]; XI[J]:=XI[R];
   57000       XR[R]:=TR;    XI[R]:=TI;
   58000     END;
   59000   END UNTIL J:=*+DJ  GEQ M;
   60000   IF N GTR 16 THEN GO QUIT;
   61000   M:=0 &1[N:0:1];  %  2**N
   62000   IF N LEQ 12 THEN BEGIN DJ:=1; J:=1; LOOP; END ELSE
   63000   BEGIN
   64000     DJ:=0&1[N-4:0:1];
   65000     J:=1;
   66000     DO LOOP UNTIL J:=J.[N-5:N-4]+1 EQL 1;
   67000   END;
   68000   QUIT:
   69000 END B I T R E V 2;


INPUT STRING WAS
"MATHLIBFFT/SBITREV2 STEP 2"
```

M A T H L I B F F T / S S I N C O S

```
34 RECORDS, CREATED 29/07/77

    1000
    2000 COMMENT@@@@@      SINCOS.

    3000 PROCEDURE SINCOS(S,C,M);
    4000 COMMENT*XXXX
    5000 PURPOSE.
    6000 USED TO SET UP SIN & COS TABLES FOR FAST FOURIER TRANSFORM
    7000 COMMENT*YYYY
    8000 INPUT.
    9000 M - INTEGER SPECIFYING LENGTH OF S AND C TO BE 2**(M-1)
   10000 OUTPUT.
   11000 S - ARRAY OF SINES NEEDED BY FFTF AND FFTR
   12000 C - ARRAY OF COSINES NEEDED BY FFTF AND FFTR
   13000 REMARK.
   14000 S,C SHOULD EACH BE  DECLARED ARRAY[0:2**(M-1)]
   15000
   16000 COMMENT*ZZZZ;
   17000 VALUE M;
   18000 INTEGER M;
   19000 ARRAY S,C[0];
   20000 BEGIN
   21000   REAL DPHI,ARG;
   22000   INTEGER I,L;
   23000   L:=0&1[M-1:0:1];  %  2**(M-1)
   24000   DPHI:=3.1415926536/L;
   25000   S[0]:=0;
   26000   C[0]:=1;
   27000   S[L]:=0;
   28000   C[L]:=-1;
   29000   I:=1;
   30000   DO BEGIN
   31000     S[I]:=SIN(ARG:=I*DPHI);
   32000     C[I]:=COS(ARG);
   33000   END UNTIL I:=*+1 GEQ L;
   34000 END;


INPUT STRING WAS
"MATHLIBFFT/SSINCOS STEP 2"
```